Catalytic Asymmetric Alkylation of Olefins with Alcohol Derivatives

Inaugural-Dissertation

zur

Erlangung des Doktorgrades

der Mathematisch-Naturwissenschaftlichen Fakultät

der Universität zur Köln

vorgelegt von

Luc Maxime Debie

aus Nijmegen, (den Niederlanden)

Köln, 2025

Table of contents

ABSTRACT

For over a century, chemists have sought to replicate nature's efficient synthesis of complex hydrocarbon terpenes, which are valued for their bioactivity. In nature, enzymes catalyze this process through selective alkylation reactions between olefins and alcohol derivatives. Despite significant advances in synthetic methodology over the past decades, biomimetic versions of this reactivity remain underrepresented in the literature.

This thesis aims to describe our efforts toward the development of a catalytic asymmetric alkylation of olefins with alcohol derivatives. The developed methodology uses a range of benzylic- and allylic acetates as alkylating agents in nucleophilic reactions of olefins. A scope of each of these components was established, demonstrating remarkable substrate generality of the reaction with a single fluorinated imidodiphosphorimidate catalyst. X-ray crystallographic analysis revealed the critical role of the fluorinated catalyst motif in achieving high enantioselectivity. Further mechanistic studies elucidated the complex cationic nature of the discovered reaction, which proceeds via an S_N1 pathway, and exhibits characteristics of a dynamic kinetic resolution. Finally, attempts at derivatization of the obtained products were carried out, yielding several prospective pathways toward useful bioactive compounds.

KURZZUSAMENFASSUNG

Seit über einem Jahrhundert versuchen Chemiker, die effiziente Synthese komplexer Kohlenwasserstoffterpene, die wegen ihrer Bioaktivität geschätzt werden, nachzubilden. In der Natur katalysieren Enzyme diesen Prozess durch selektive Alkylierungsreaktionen zwischen Olefinen und Alkoholderivaten. Trotz bedeutender Fortschritte in der Synthesemethodik in den letzten Jahrzehnten sind biomimetische Versionen dieser Reaktivität in der Literatur nach wie vor unterrepräsentiert.

Diese Arbeit beschreibt unsere Bemühungen zur Entwicklung einer katalytischen asymmetrischen Alkylierung von Olefinen mit Alkoholderivaten. Die entwickelte Methodik verwendet eine Reihe von Benzyl- und Allylacetaten als Alkylierungsmittel in nukleophilen Reaktionen von Olefinen. Der Anwendungsbereich jeder dieser Komponenten wurde ermittelt, wodurch die bemerkenswerte Substratgeneralität der Reaktion mit einem einzigen fluorierten Imidodiphosphorimidat-Katalysator nachgewiesen wurde. Durch Röntgenkristallographische Analyse wurde die entscheidende Rolle des fluorierten Katalysatormotivs für das Erzielen einer hohen Enantioselektivität aufgezeigt. Weitere mechanistische Untersuchungen klärten die komplexe kationische Beschaffenheit der entdeckten Reaktion auf, die über einen S_N1-Weg abläuft und Merkmale einer dynamischen kinetischen Auflösung aufweist. Schließlich wurden Versuche zur Derivatisierung der erhaltenen Produkte durchgeführt, die mehrere vielversprechende Wege zu nützlichen bioaktiven Verbindungen ergaben.

LIST OF ABBREVIATIONS

9-BBN	9-(9-borabicyclo[3.3.1]nonan)yl
Ac	acetyl
ACDC	asymmetric counteranion-directed catalysis
acetyl-CoA	acetyl-coenzyme A
BALT	binaphthyl-allyl-tetrasulfone
bbbpy	4,4’-di-tert-butyl-2,2’-dipyridyl
BINOL	1,1′-Bi-2-naphthol
BINSA	1,1′-binaphthyl-2,2′-disulfonic acid
Bn	benzyl
Boc	*tert*-butyloxycarbonyl
Bpin	pinacolboryl
BPTM	phosphoryl bis((trifluoromethyl)sulfonyl) methane
CoA	coenzyme A
COD	1,5-cyclooctadiene
CPA	chiral phosphoric acid
CyH	cyclohexane
CyMe	methylcyclohexane
dba	dibenzylideneacetone
DCE	1,2-dichloroethane
DMAP	4-(dimethylamino)pyridine
DMAPP	dimethylallyl pyrophosphate
DMSO	dimethyl sulfoxide
DSI	disulfonimide
DKR	dynamic kinetic resolution
EDG	electron-donating group
e.e.	enantiomeric excess
e.r.	enantiomeric ratio
Et	ethyl
EWG	electron-withdrawing group
FCC	flash column chromatography
FPP	farnesyl pyrophosphate
G3P	glyceraldehyde 3-phosphate
GC (GC-MS)	gas chromatography (gas chromatography coupled with mass detection)
GGPP	geranylgeranyl pyrophosphate

GPP	geranyl pyrophosphate
HCP	hexachlorobisphosphazonium
HIA	hydride ion affinity
HMDS	hexamethyldisilazane
HMG-CoA	β-hydroxy-β-methylglutaryl-CoA
HOMO	highest occupied molecular orbital
IDP	imidodiphosphate
IDPi	imidodiphosphorimidates
iIDP	imino-imidodiphosphates
Int	intermediate
IPP	isopentyl pyrophosphate
IPPS	isoprenyl pyrophosphate synthases
i-Pr	isopropyl
JINGLE	1,1'-Binaphthyl-2,2'-bis(sulfuryl)imide
KR	kinetic resolution
LA	Lewis acid
LPP	linalyl pyrophosphate
LUMO	lowest unoccupied molecular orbital
M	molar
Me	methyl
MeCN	acetonitrile
MEP	methylerythrol phosphate
MS	mass spectrometry
Ms	molecular sieves
MVA	mevalonic acid
N/A	not applicable
NADPH	nicotinamide adenine dinucleotide phosphate
Naphth	naphthyl
NBD	norbornadiene
NPP	neryl pyrophosphate
NPPA	*N*-phosphinyl phosphoramide
NSAID	non-steroidal anti-inflammatory drugs
NTPA	*N*-triflyl phosphoramide
PADi	*N*,*N*′-bistriflylphosphoramidimidate
PCCP	1,2,3,4,5-pentacarboxycyclopentadiene
Ph	phenyl
Phen	phenanthryl

PhH	benzene
PhMe	toluene
PMB	*para*-methoxybenzyl
PSQPP	presqualene pyrophosphate
PTLC	preparative thin layer chromatography
p-TsOH	*para*-toluenesulfonic acid
quant.	quantitative (yield)
BINAP	2,2’-bis(diphenylphosphino)-1,1’-binaphthyl
r.r.	regiomeric ratio
$SiO_2/AgNO_3$	silica impregnated with 10% $AgNO_3$
SPINOL	1,1′-spirobiindane-7,7′-diol
SQS	squalene synthase
TADDOL	α,α,α',α'-tetraaryl-2,2-disubstituted 1,3-dioxolane-4,5-dimethanol
Tf	trifluoromethylsulfonyl, triflyl
TFA	trifluoroacetic acid
TfOH	triflic acid
THF	tetrahydrofuran
TRIP	3,3'-bis(2,4,6-triisopropylphenyl)-1,1'-binaphthyl-2,2'-diyl hydrogenphosphate
Triphen	triphenylenyl
Ts	*para*-toluenesulfonyl, tosyl
TS	transition state
TTP	1,1,3,3-tetratriflylpropene
VANOL	3,3'-diphenyl-[2,2'-binaphthalene]-1,1'-diol
VAPOL	2,2'-diphenyl-[3,3'-biphenanthrene]-4,4'-diol
VTNA	variable time normalization analysis

1. INTRODUCTION

Humankind has an innate tendency to find beauty in symmetry. This propensity strongly influences forms of human expression such as art, architecture and science. Perhaps the most striking example of the latter was the long-standing privileged status of the theory of supersymmetry in physics. However, efforts to validate the theory of supersymmetry have been largely in vain, and the theory has been all but abandoned, leading physicists to conclude that asymmetry permeates the physical world so thoroughly that even the standard model of particle physics is not left untouched.[1,2] These findings underscore the importance of asymmetry as a natural phenomenon that must be considered when performing scientific research, a fact that is well-understood by chemists.

Chirality is a property of asymmetry that can be defined as the inability of an object or system to be superimposed onto its mirror image. Chirality in the physical world shows itself most notably in the homochirality of biological life. Living organisms rely on a uniformly chiral subset of building blocks to assemble their molecular components. The origin of the homochirality of life has been the subject of spirited debate since van ‘t Hoff and Le Bel published their theory of organic stereochemistry in 1874, which identified the tetrahedral carbon atom as an underlying reason for biological chirality.[3,4] Without homochirality, potentially unfavorable interactions of racemates in chiral environments would likely have prevented the chiral tetrahedral carbon from becoming a viable basis for life. This phenomenon is best exemplified in modern medicine, where it is appreciated that the administration of opposite enantiomers of a drug can lead to a difference in pharmacological and toxicological outcomes.[5] It is therefore unsurprising that biological systems have evolved complex biochemical machinery to prevent the inadvertent formation of racemates.

Enzymes are nature’s most powerful catalytic machinery, demonstrating unparalleled reactivity and selectivity in the synthesis of countless natural products by virtue of their three-dimensional structure.[6] Enzymes have long been an inspiration for synthetic chemists, who continuously attempt to mimic enzymatic reactivity by expanding their synthetic toolbox. The resulting maturation of various branches of organic chemistry over the last century has left virtually no synthetic target out of reach.

The field of asymmetric organocatalysis represents arguably the purest attempt at mimicking the natural reactivity and stereoselectivity of enzymes. A 1912 publication by Bredig

and Fiske reporting the quinidine-catalyzed hydrocyanation of benzaldehyde demonstrated the potential of small purely organic molecules to act as asymmetric catalysts.[7] However, the consensus through the end of the 20th century remained that effective asymmetric catalysis could only be achieved by enzymes and transition metals.[8] In 2000, List expanded the available asymmetric methodologies with his seminal report on enamine catalysis, using L-proline—an essential amino acid—to catalyze the intermolecular aldol reaction.[9] Soon after, MacMillan reported his iminium-catalyzed Diels–Alder reaction.[10] These discoveries finally kickstarted the field of organocatalysis, the importance of which was recognized when the pair was awarded the 2021 Nobel prize in chemistry "*for the development of asymmetric organocatalysis*".

In chemical synthesis, the most attractive synthetic routes start from commonly available, simple building blocks and build complexity as desired in the fewest possible number of steps.[11] Terpene biosynthesis represents an idealized example of expedient synthesis, in which complex hydrocarbon skeletons are constructed out of oligomeric prenyl pyrophosphates through terpene cyclization.[12] Translating terpene biosynthesis to small-molecule catalysis remains a standing challenge to this day, although a number of efforts have been made toward chemical terpene- and polyene cyclization strategies.[13]

Yet more challenging is the design of intermolecular catalytic asymmetric alkylation reactions of unactivated olefins with alcohol derivatives. The olefin alkylation reaction comprises the *in situ* generation of a carbocation equivalent, followed by C–C bond formation through nucleophilic attack by an olefin. Deprotonation of the resulting intermediate delivers the product, which itself is an olefin. Olefins are ideal substrates for synthetic chemistry, on account of their versatility as a synthetic handle and abundance. The same qualities apply broadly to alcohols and their derivatives. Consequently, these functional groups are ideally suited for generating the requisite carbocation equivalents in the olefin alkylation reaction.

The following chapters will contain: first, an overview of asymmetric organocatalysis, up to the current state of the art in Brønsted- and Lewis acid-catalysis; second, a section will be devoted to the biosynthesis of aliphatic and aromatic terpene natural products; third, the challenges in designing olefin alkylation reactions will be discussed, contextualized by existing methods for the alkylation of olefins and other π-nucleophiles using alcohol derivatives; and finally, our design of a general intermolecular catalytic asymmetric alkylation reaction of olefins with alcohol derivatives will be detailed.

2. BACKGROUND

2.1. Asymmetric Organocatalysis

2.1.1. *Conceptualization of Catalysis*

Although earlier hints at catalytic processes can be found in the literature,[14,15] it was not until a 1835 annual report on the progress of chemistry by Jöns Jacob Berzelius that the term "catalysis" was coined. Berzelius introduced the term when contemplating earlier reported reactions that were accelerated by substances that themselves remained unchanged. Referring to the catalytic ability of these substances he stated:

"*This is a new power to produce chemical activity belonging to both inorganic and organic nature, which is surely more widespread than we have hitherto believed and the nature of which is still concealed from us… I shall therefore, using a derivation well-known in chemistry, call it the catalytic power of the substances, and the decomposition by means of this power catalysis.*"[16] (*translated from Swedish*[17])

Interestingly, Berzelius also applied this newfound concept to living organisms. Writing to Justus von Liebig in 1835 he speculated that it is probable that these catalytic forces also play a major role in the mechanisms of life.[18] However, von Liebig and the broader chemical society were not immediately convinced by these ideas, as Berzelius did not provide a theoretical framework for the concept.

The establishment of the modern field of catalysis is most commonly accredited to Wilhelm Ostwald. Ostwald took an interest in Berzelius' writings on catalysis in 1883, and dedicated two decades to providing insights into reaction dynamics and energetics, especially the relation between reaction rates and the strength of acids and bases.[19,20] Through his studies of catalytic processes, he was able to develop a process for the synthesis of nitric acid,[21] which alleviated German fears of remaining dependent on the import of nitrate fertilizers from Chile. Ostwald defined catalysis as the "*acceleration of a slow chemical process by the presence of a foreign material which is not consumed and leaves the equilibrium of the reaction unchanged*", and received the Nobel prize in chemistry in 1909 "*for his work on catalysis and for his investigations into the fundamental principles governing chemical equilibria and rates of reaction.*" The foundational principles of catalysis that Ostwald established laid the groundwork for the development of one of its most impactful subfields: asymmetric catalysis.

2.1.2. *An introduction to asymmetric catalysis*

The preparation of enantiopure chiral substances has long attracted attention from chemists, because of the difference in biological activity frequently exhibited by enantiomers of the same substance.[5,22] Obtaining enantiopure compounds through non-asymmetric catalysis places a limit of 50% yield of a single enantiomer, and long and costly procedures are often required to separate the enantiomers. Therefore, asymmetric catalysis is a worthwhile pursuit as it doubles the theoretical yield, and has the potential to simplify the purification of enantiopure samples.

Molecules and their functionalities colliding with each other can lead to a chemical reaction. The spontaneity of a reaction is a thermodynamic quality described by the change in Gibbs free energy *G*. Reactions under thermal conditions will always tend toward the minimization of *G*. The change in free energy ΔG for a set of reactants as it relates to the equilibrium constant K_{eq} is given by:

$$\Delta G = -RT\ln\left(K_{eq}\right) \tag{2.1}$$

where K_{eq} is the ratio of products to reactants at equilibrium. Accordingly, $K_{eq} > 1$ will result in $\Delta G < 0$, meaning that the reaction can occur spontaneously. To assess whether a reaction will take place, its kinetic parameters also have to be considered. The kinetics of a given reaction are governed by the Gibbs free activation energy $\Delta G^{\ddagger}$, which is the difference in free energy between the reactants and the transition state (TS) of a given reaction coordinate (Figure 2.1, left).

Catalysis has no influence over ΔG, as the catalyst itself is not consumed during a given reaction. Therefore, the energetic contributions of the catalyst before and after the reaction cancel each other out. Instead, performing an otherwise uncatalyzed reaction A + B → C in the presence of a suitable catalyst alters the kinetic profile of the reaction by lowering $\Delta G^{\ddagger}$ (Figure 2.1, left). In many catalytic reactions, the high-lying concerted pathway of an uncatalyzed process is replaced by a lower-lying stepwise pathway which proceeds through intermediates (Int1, Int2), each with their own preceding TS.

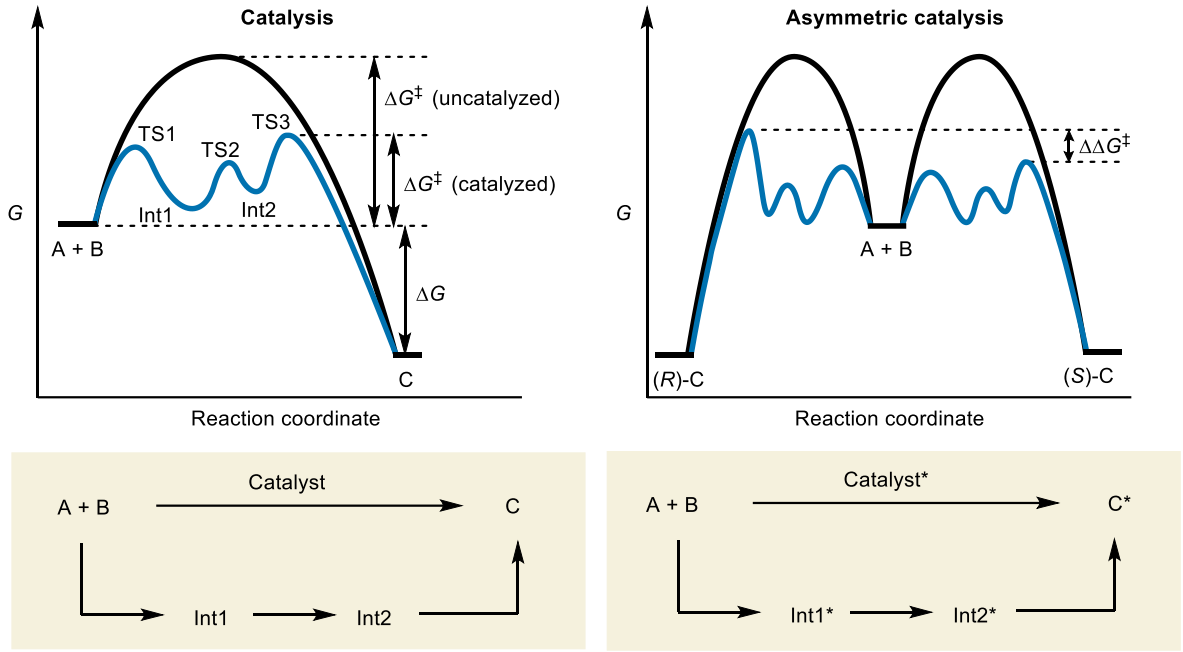

Figure 2.1 Gibbs free energy landscapes of catalysis (left) and asymmetric catalysis (right).

Asymmetric catalysis similarly does not alter the ΔG of the reaction forming chiral product C*. Enantiomers (*R*)-C and (*S*)-C are equal in Gibbs free energy and would therefore be formed as a racemate at thermodynamic equilibrium. To influence the distribution of enantiomers resulting from a stereocenter-forming reaction, asymmetric catalysis exploits diastereomeric transition states with distinct values for $\Delta G^{\ddagger}$ in the reaction pathways toward each enantiomer of C*, causing a difference in their rate of formation. This difference in $\Delta G^{\ddagger}$ is expressed as $\Delta\Delta G^{\ddagger}$, and is the result of the interactions of achiral substrates A and B with the chiral catalyst. The ratio of the resulting molecular fractions F_{R} and F_{S} of enantiomers (*R*)-C and (*S*)-C is defined as the enantiomeric ratio (e.r.), which is also commonly expressed as the enantiomeric excess (e.e.) of one enantiomer over the other:

$$\mathrm{e.e.} = |F_{\mathrm{R}} - F_{\mathrm{S}}| \tag{2.2}$$

The e.r. is directly dictated by the relative rate constants of the formation of each enantiomer k_{R} and k_{S}, and the relation of e.r. to $\Delta\Delta G^{\ddagger}$ is given by the Arrhenius equation:

$$\mathrm{e.r.} = \frac{F_{\mathrm{R}}}{F_{\mathrm{S}}} = \frac{k_{\mathrm{R}}}{k_{\mathrm{S}}} = e^{-\frac{\Delta\Delta G^{\ddagger}}{RT}} \tag{2.3}$$

The principle of using a chiral catalyst to create a difference in activation energies recently found practical application in the rise of asymmetric organocatalysis.

2.1.3. *The Emergence of Asymmetric Organocatalysis*

Asymmetric organocatalysis is defined by the use of small chiral organic molecules as catalysts. Early examples of organocatalytic reactions can be found in the literature as far back as 1860. However, it was not until the pioneering discoveries by List[9] and MacMillan[10] in 2000 that organocatalysis gained recognition as a third branch of asymmetric catalysis. List and MacMillan would go on to define the field through their significant work, introduce numerous classes of organocatalysts, and coin the term organocatalysis itself.[23] Their contributions would ultimately be recognized in 2021 when they were awarded the Nobel prize in chemistry "*for the development of asymmetric organocatalysis*".

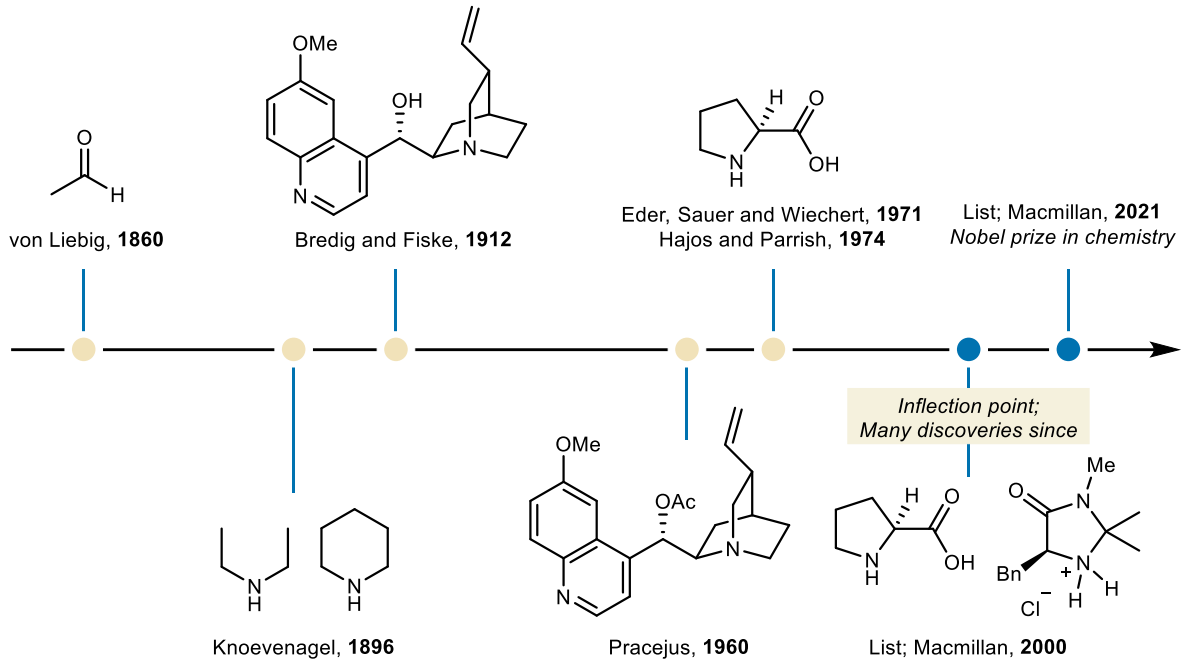

Figure 2.2 Timeline of significant organocatalytic discovery.

In 1900, Ostwald first speculated on the possible existence of "organische Katalysatoren" (engl., *organic catalysts*) which would be stable and active at elevated temperatures. His speculation contrasted the known activity of "Fermente" (engl., *ferments*) from living organisms that catalyze reactions essential to life; the topic of a book by C. Oppenheimer he was reviewing.[24] As is often the case, the nomenclature lagged behind the phenomenon, as the first known example of a non-asymmetric reaction involving an organic catalyst had already been reported by von Liebig in 1860, who described the hydrolysis of cyanogen to oxamide (Figure 2.2).[25] The role of substoichiometric acetaldehyde in accelerating the rate of the reaction was unknown at the time, but it was described in 1928 as an example of an organic catalyst by Langenbeck,[26] who just one year earlier had pointed to

the modest catalytic activity of organic molecules compared to enzymes, accompanied by the following provocation:

"*Vielleicht geling es der synthetischen Chemie, die Eigenschaften der organischen Katalysatoren allmählich so zu verbessern, daß sie den Enzymen in ihrer Wirkung immer ähnlicher werden.*"[27] (engl., "Perhaps synthetic chemistry will gradually succeed in improving the properties of organic catalysts to such an extent that they become increasingly similar to enzymes in their effect."[17])

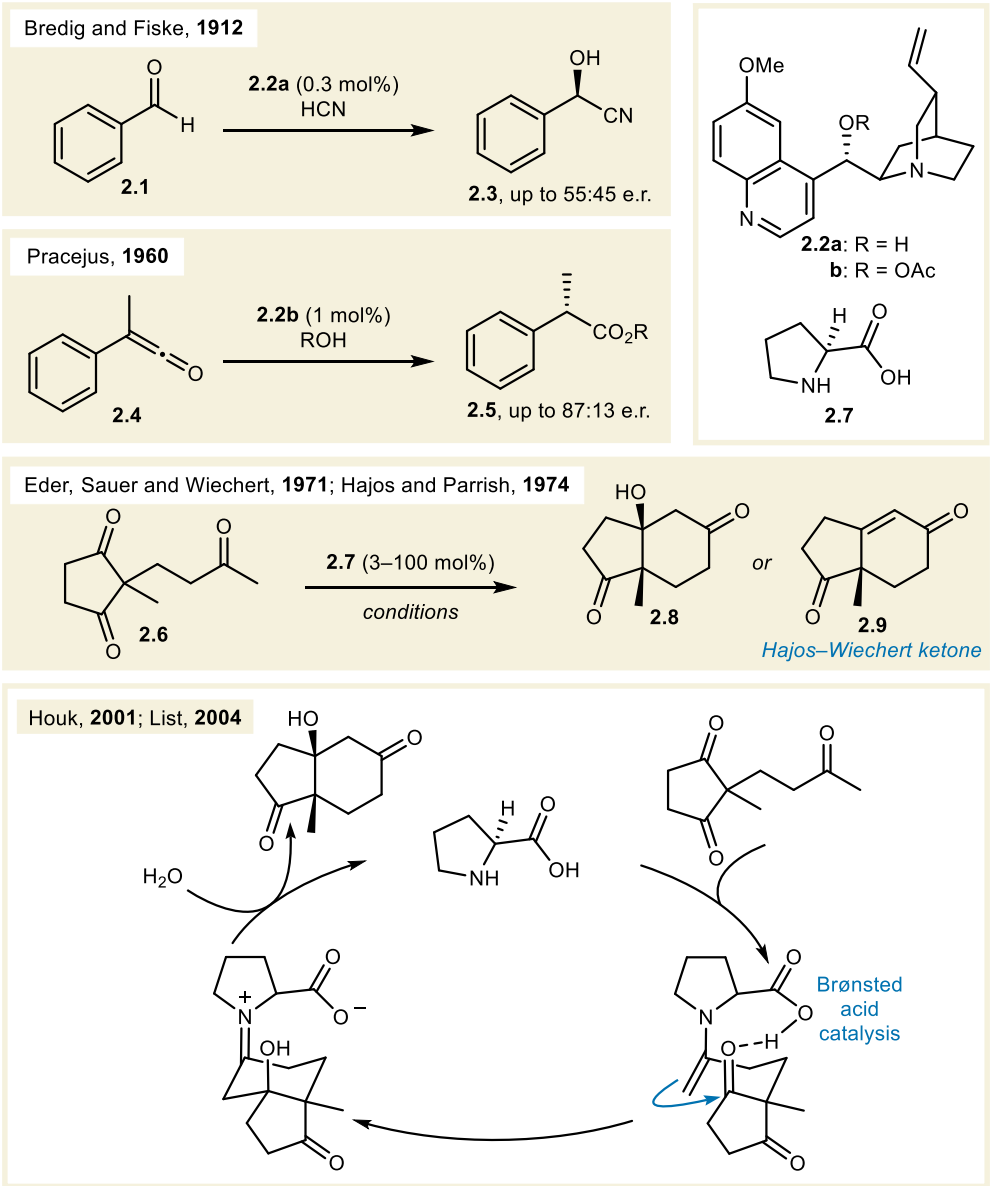

Scheme 2.1 Early developments in asymmetric organocatalysis (top), and the mechanism of the Hajos–Parrish–Eder–Sauer–Wiechert reaction (bottom).

In 1896, a publication by Knoevenagel on the condensation of benzaldehyde with acetoacetate represented a second entry into non-asymmetric organocatalysis. The reaction was catalyzed by secondary amines and represents an early example of iminium catalysis.[28]

It took until 1912 for the first example of asymmetric organocatalysis to be published by Bredig and Fiske (Scheme 2.1, top).[7] Their hydrocyanation of benzaldehyde (**2.1**) employed cinchona alkaloids **2.2a** as catalysts, achieving modest, yet reproducible enantioinduction for **2.3** (up to 55:45 e.r.). Forty-eight years later, Pracejus expanded on this alkaloid catalysis by reporting an *O*-acetyl-cinchona alkaloid (**2.2b**)-catalyzed addition of alcohols to methyl phenyl ketene, obtaining the corresponding ester products **2.5** with significant enantioinduction (up to 87:13 e.r.).

The proline (**2.7**)-catalyzed Hajos–Parrish–Eder–Sauer–Wiechert intramolecular aldol reaction, developed in the 1970s, marked the first use of an amino acid in asymmetric organocatalysis (Scheme 2.1, top).[29,30] The bicyclic products of the reaction were typically obtained with high levels of optical purity, and both the aldol addition (**2.8**) and condensation (**2.9**) products could be obtained by the addition of an additional acid mediator. The condensation product is known as the "Hajos–Wiechert ketone", and its 6,6-fused bicycle analog as the "Wieland–Miescher ketone". Both bicycles have found applications in steroid- and other natural product syntheses.[31] The origin of stereoselectivity in the Hajos–Parrish–Eder–Sauer–Wiechert reaction was elucidated in the early 2000s by Houk and List through computational and experimental methods, respectively.[32–34] The reaction proceeds via an enamine intermediate, wherein the Brønsted acidic carboxylic acid moiety of proline preferentially coordinates to one ketone on the cyclopentane-1,3-dione, thereby activating it for nucleophilic attack (Scheme 2.1, bottom).

A pioneering discovery in 2000 by List et al. underlined the importance of generality in organocatalytic asymmetric aldol reactions (Scheme 2.2, top).[9] In their publication, the authors demonstrated that L-proline could act as a powerful catalyst for intermolecular aldol reactions between acetone (**2.10**) and a range of aldehydes. Most notably, when isobutyraldehyde (**2.11**) was used, aldol product **2.12** was obtained in excellent yield and enantioselectivity. In the same year, MacMillan reported a Diels–Alder reaction of enals catalyzed by the phenylalanine-derived imidazolidinone salt **2.15** (Scheme 2.2, bottom). The reaction tolerated fairly unbiased substrates such as acrolein (**2.13**) and isoprene (**2.14**), affording products **2.16** in very good yields and excellent enantioselectivities. In the same publication, the authors went on to coin

the term “organocatalysis”, to adequately term their discovery. List and MacMillan’s complementary reports defined the fields of enamine and iminium catalysis, and generalized the concept of asymmetric catalysis using small chiral organic molecules. These publications demonstrated the potential of chiral secondary amine catalysts, sparking widespread interest and a surge in subsequent research.[35–37]

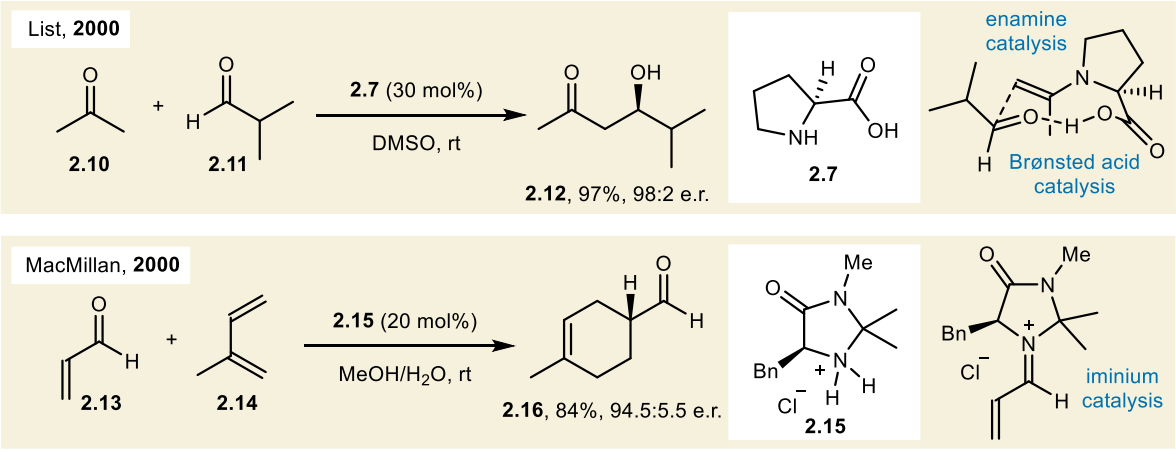

Scheme 2.2 Seminal publications by List (top) and MacMillan (bottom) on enamine- and iminium catalysis, respectively.

The rapid expansion of the field of organocatalysis in the early 2000s necessitated a rigorous classification of activation modes. Enamine catalysis employs a secondary amine to transform a carbonyl group into a nucleophilic enamine intermediate with a raised highest occupied molecular orbital (HOMO). In iminium catalysis, the amine catalyst condenses with the carbonyl electrophile, which lowers the lowest unoccupied molecular orbital (LUMO). In these examples the Lewis basicity of secondary amines is leveraged for substrate activation. Mechanistic studies by Houk and List revealed that the Brønsted acidity of proline is integral to its reactivity and enantioinduction, indicating that a classification based on acidity and basicity could be sensible. In 2005, List categorized asymmetric organocatalysis into four parts: Lewis base, Lewis acid, Brønsted base, and Brønsted acid catalysis (Figure 2.3).[38] However, this categorization is not exhaustive, as many catalysts are bifunctional in their activation mode. One such instance is proline, which contains Lewis basic lone pairs on nitrogen and the carbonyl oxygen, as well as a Brønsted acidic proton.

Organocatalytic activation principles can also be subdivided into covalent and non-covalent modes. Enamine and iminium catalysis are examples of the former, while Lewis/Brønsted acid catalysis are found in the latter category.[39–41] To illustrate this dichotomy,

the LUMO-lowering effect observed in iminium catalysis can be compared to carbonyl activation by coordination of the same enal to a Lewis- or Brønsted acid (Figure 2.4).

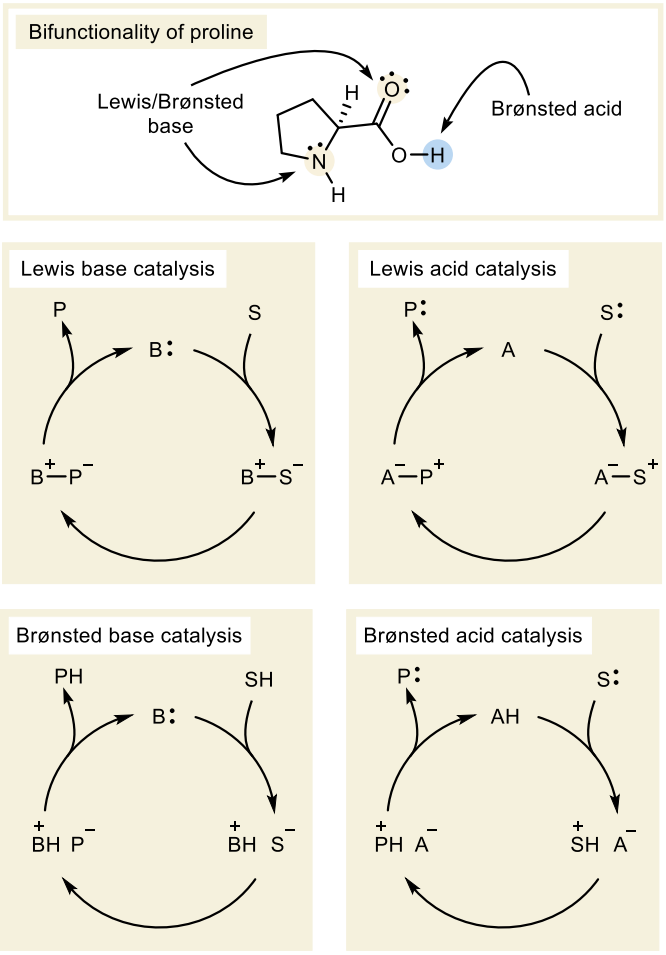

Figure 2.3 Proline as a bifunctional catalyst (top), and the categorization of organocatalysis by List (bottom). S = substrate, P = product.

The categorization of organocatalysts according to their activation modes is helpful in describing their modes of substrate activation. In addition to the above categorizations, alternative categorizations have been proposed.[23]

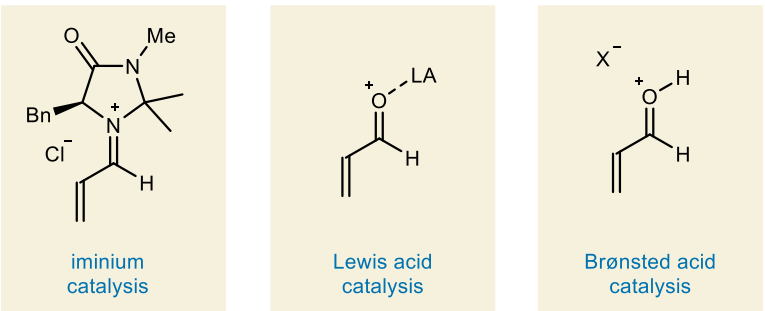

Figure 2.4 Iminium ion-, Lewis acid-, and Brønsted acid activation of acrolein. LA = Lewis acid.

2.1.4. *Asymmetric Brønsted Acid Organocatalysis*

Acid catalysis arguably represents the most general activation mode in organocatalysis, as any substrate that has electron density can theoretically be activated by an acid.[42] It is therefore no surprise that the number of available acid catalysts has grown exponentially since organocatalysis became recognized as a third pillar of asymmetric catalysis.

The ability of acids to accept electron density is best described by Lewis' theory of acids and bases. A Lewis acid is defined by IUPAC as "a molecular entity (and the corresponding chemical species) that is an electron-pair acceptor and therefore able to react with a Lewis base to form a Lewis adduct", its Lewis base counterpart consequently being an electron-pair donor.[43] In Lewis' definition of acids and bases, Brønsted acids are a special form of Lewis acid, in which the electron-pair acceptor is the simplest possible Lewis acid: a hydron (informally: proton). In Brønsted acid catalysis, the acidic proton of the catalyst coordinates to an electron pair of the substrate, priming it for transformation by lowering its LUMO.

Substrate activation by Brønsted acid catalysis can be subdivided into *general Brønsted acid catalysis* and *specific Brønsted acid catalysis*. A specific acid is defined as the protonated form of the reaction solvent.[44] Thus, specific acid catalysis is catalysis by the protonated reaction solvent, which is brought about by full dissociation of a given acid in the reaction medium. In specific acid catalysis, the concentration of the Brønsted acid only serves to establish the pH of the medium, and is not involved in the rate-determining step of the reaction. Conversely, full dissociation of the acid does not take place in general acid catalysis, and the acid in its H-form is involved in the rate determining step. To illustrate this difference, the observed overall rate constant (k_{obs}) for a hypothetical acid-catalyzed pseudo-first order reaction in aqueous media can be broken up into three components according to:[45]

$$k_{\mathrm{obs}} = k_{\mathrm{H_3O^+}}[\mathrm{H_3O^+}] + k_{\mathrm{HA}}[\mathrm{HA}] + k_{\mathrm{H_2O}}[\mathrm{H_2O}] \qquad (2.4)$$

In specific acid catalysis, complete dissociation of the acid catalyst to its conjugate base and a hydronium ion causes $k_{\mathrm{H_3O^+}}[\mathrm{H_3O^+}]$ to be the sole contributor to the overall rate constant—aside from the (often minor) uncatalyzed term $k_{\mathrm{H_2O}}[\mathrm{H_2O}]$. On the other hand, the incomplete acid dissociation in general catalysis means there is a significant concentration of the H-form (HA) present in the reaction medium, which results in a significant contribution of $k_{\mathrm{HA}}[\mathrm{HA}]$ to the overall rate constant.[46]

This kinetic definition of general- and specific Brønsted acid catalysis can be extended to include complete or incomplete protonation of a Lewis basic functionality on the electrophilic component of a reaction, as opposed to protonation of the solvent. In this case, the difference between the acid dissociation constants (pK_a) of the protonated catalyst and the conjugate acid of the substrate determines whether full dissociation of the acid catalyst occurs.[47] This causes the classification of general and specific Brønsted acid catalysts to be flexible between acid-catalyzed reactions—not just between solvents—meaning the type of catalysis must be established independently for each system of acid catalysts and substrates.[48] Nevertheless, trends can be observed in the types of catalysts that are used in either case (Figure 2.5):[49]

- *General Brønsted acid catalysis* relies on comparatively weak acid-base interactions, commonly termed hydrogen bonds (H-bonds). Examples of chiral H-bond donor catalysts include thioureas (**2.17**)[50]; chiral diols such as α,α,α',α'-tetraaryl-2,2-disubstituted 1,3-dioxolane-4,5-dimethanol (TADDOL, **2.18**)[51] and 1,1′-bi-2-naphthol (BINOL)-derived scaffolds (**2.19**)[52]; bisamidines (HQuin-BAM, **2.20**)[53]; and squaramides (**2.21**).[54]
- *Specific Brønsted acid catalysis* employs comparatively strong acid-base interactions to achieve full substrate protonation. Strong Brønsted acids commonly used to this effect include mineral acids such as hydrochloric acid, fluoroboric acid and sulfuric acid; and sulfonic acids such as triflic acid (TfOH, **2.22**) and *para*-toluenesulfonic acid (*p*-TsOH, **2.23**). Chiral phosphoric acids (CPAs, **2.24**) are a frequently used class of chiral specific Brønsted acid catalysts derived from chiral diols, and a number of next-generation strong chiral Brønsted acid catalysts have been prepared based on similar design principles (*vide infra*).

General Brønsted acid catalysis has immensely advanced the field of asymmetric organocatalysis following a seminal publication by Jacobsen on peptide-derived thiourea catalysts in 1998.[55,56] However, catalysis based on hydrogen bonding has inherent limitations. The activation of weakly Lewis basic substrates cannot be achieved by most hydrogen bond donors. Therefore, strong acids are required to protonate these relatively unbiased substrates. The next section will discuss known types of strong chiral Brønsted acid catalysts.

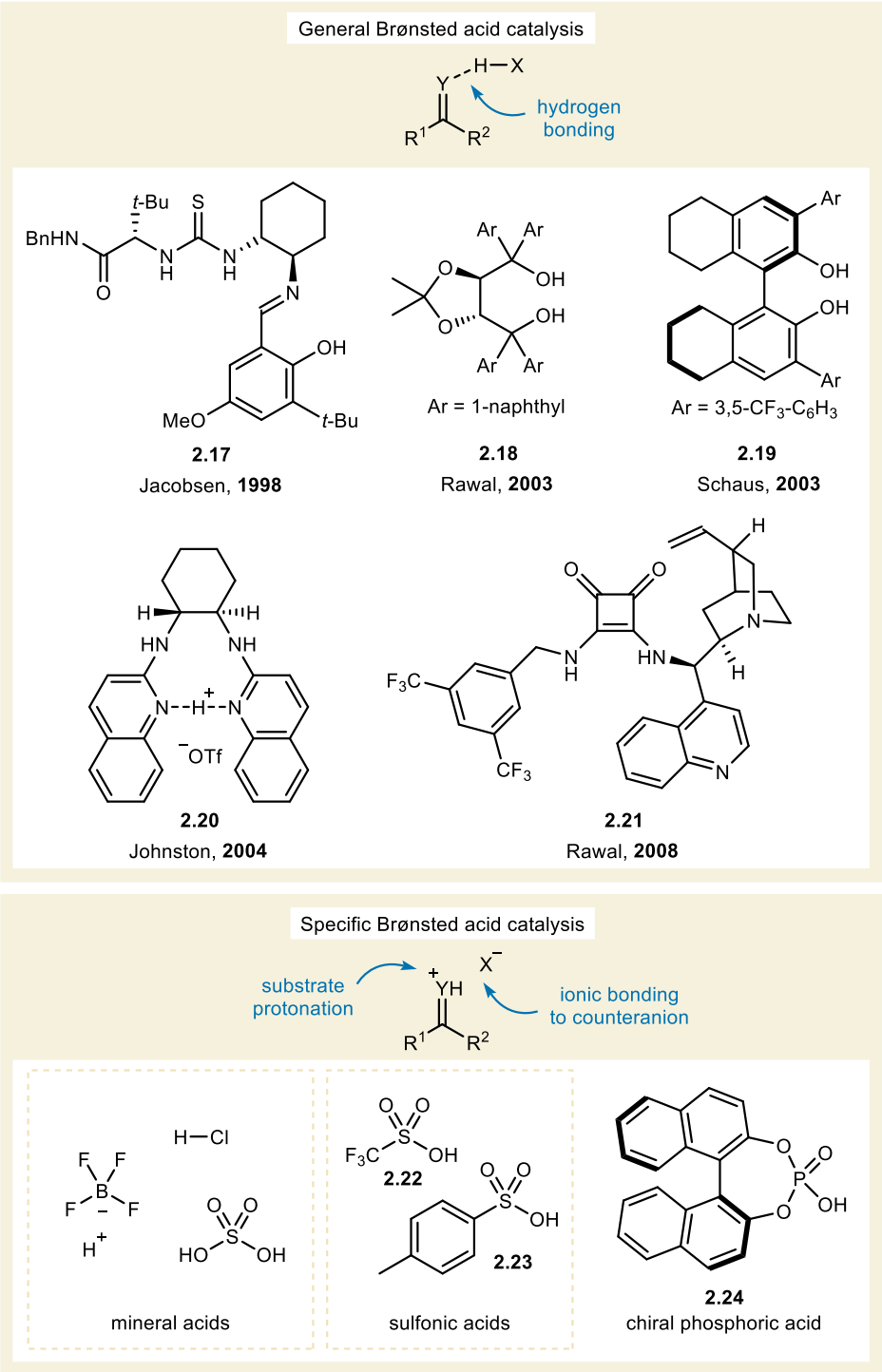

Figure 2.5 General and specific Brønsted acid catalysis.

2.1.5. *Strongly Acidic Chiral Organocatalysts*

To activate unbiased substrates via asymmetric specific Brønsted acid catalysis, strong acid-base interactions must be established by sufficiently strong chiral organic acids. In 2004,

Akiyama and Terada independently took inspiration from the high catalytic activity exhibited by asymmetric rhodium- and rare earth metal-complexes with BINOL-derived organophosphate ligands.[57–61] They reported that 3,3'-substituted CPAs (**2.27**) acted as competent Brønsted acid catalysts in Mannich-type reactions with *N*-protected imine electrophiles **2.25** and **2.29**, which reacted with silyl ketene acetal (SKAs, **2.26**) and acetylacetone (**2.30**) nucleophiles (Scheme 2.3).[62,63] It is worth noting that the calcium salt of **2.27b** was later found to be the active catalyst in Terada's publication. The salt and the Brønsted acid were both competent catalysts, but yielded opposite stereochemical outcomes.[64] Both authors speculated that CPAs could have broader applications in Mannich-type reactions due to the highly modular nature of the employed BINOL-backbone. This sentiment was echoed by the community, and soon numerous publications employing CPAs appeared.[65] One particularly privileged CPA catalyst containing 3,3'-(2,4,6-triisopropylphenyl)-substituents (TRIP, **2.27c**) was reported by List in 2005 and has found applications in a variety of reactions.[65–67]

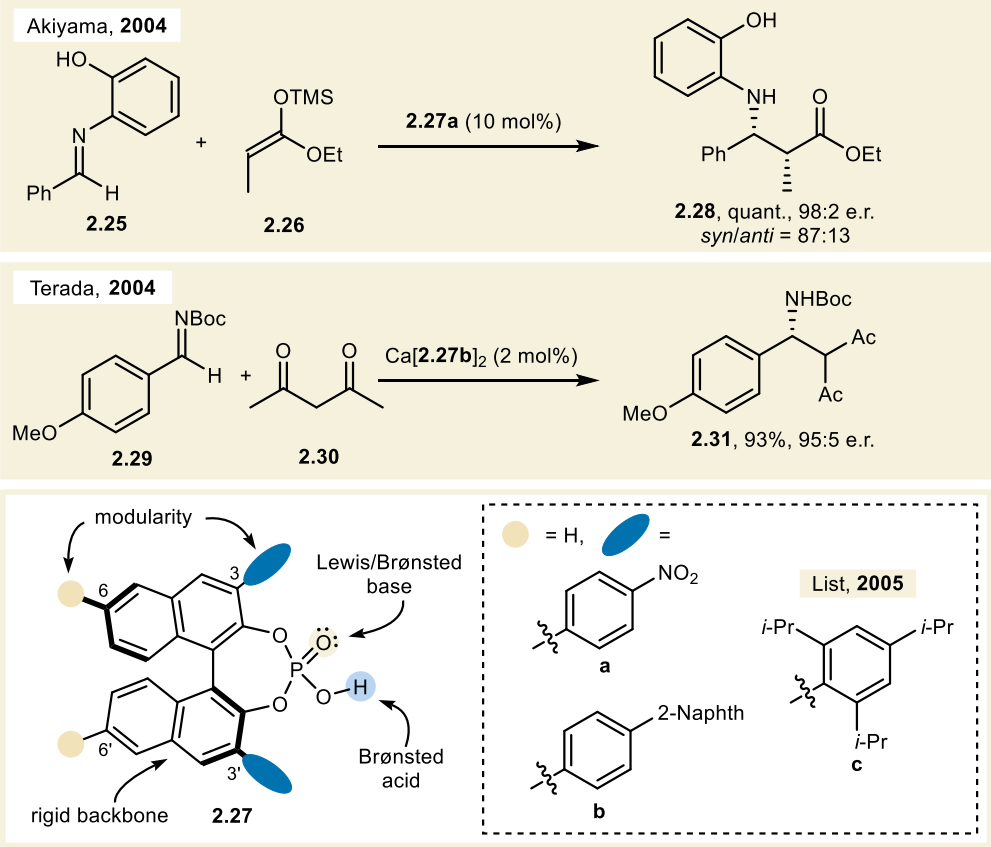

Scheme 2.3 Seminal contributions to CPA catalysis.

The BINOL (**2.32**) backbone of CPA catalysts is a common design feature of chiral organocatalysts. BINOL provides a rigid and well-defined stereochemical environment for

asymmetric transformations. Furthermore, the introduction of moieties with variable steric and electronic properties in the 3,3'- and 6,6' positions allows for facile modulation of those properties in the catalyst. Phosphoric acids are bifunctionally Brønsted acidic and Lewis/Brønsted basic, which enables strong binding to substrates that contain the complementary functional groups. Often, two reactants are simultaneously engaged, ensuring maximum leverage of the chiral BINOL environment.[68] Besides BINOL-based CPAs, a number of chiral diols have similarly been used as backbones for CPA catalysts. Among them are TADDOL (**2.33**), H_8-BINOL (**2.34**), 1,1′-spirobiindane-7,7′-diol (SPINOL, **2.35**), 3,3'-diphenyl-[2,2'-binaphthalene]-1,1'-diol (VANOL, **2.36**) and 2,2'-diphenyl-[3,3'-biphenanthrene]-4,4'-diol (VAPOL, **2.37**) (Figure 2.6).[67,69]

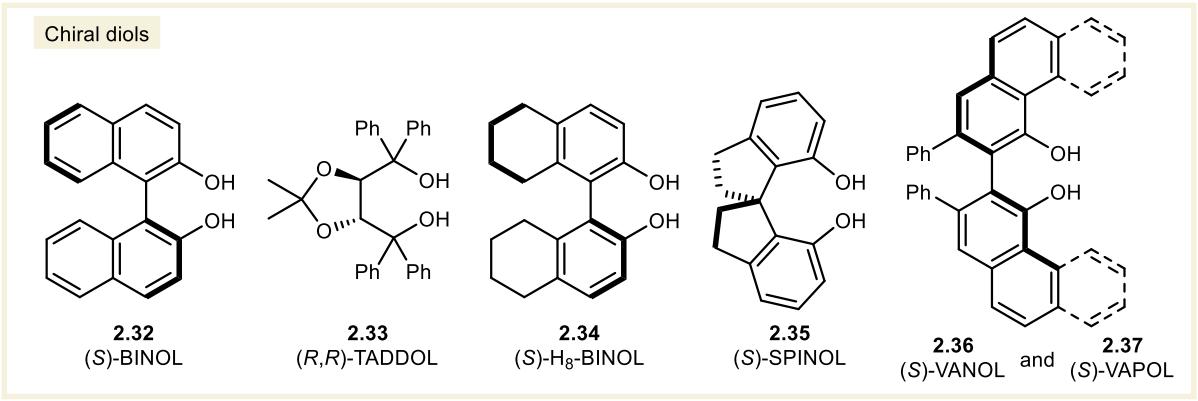

Figure 2.6 Examples of chiral diol backbones used in the synthesis of CPA catalysts.

Despite the high activity of CPAs in transfer hydrogenation and addition reactions of imines, their moderate acidity (**2.27**, pK_a = 13.6 in MeCN)[70] precludes them from activating less Lewis basic functionalities such as carbonyl compounds and olefins. These limitations prompted chemists to develop alternative strategies to improve the reactivity of chiral Brønsted acids. One such approach was metal-Lewis acid-assisted CPA catalysis first reported by Ishihara,[71] which led to improved reactivity in a number of transformations.[72–76] However, this strategy carries the inherent risk of achiral Lewis acid-catalyzed background reactivity. An aromatic 1,2,3,4,5-pentacarboxycyclopentadiene (PCCP) catalyst bearing menthyl esters type of chiral Brønsted acid was reported in 2016 by Lambert. This catalyst was capable of replicating the Mukaiyama–Mannich-type reactivity reported by Akiyama.[77] However, this motif has not seen much application since its introduction.

While the aforementioned strategies offer interesting approaches to the design of chiral acid catalysts, the field has primarily focused on developing more acidic chiral diol-based

catalysts to activate unbiased substrates. A key strategy for enhancing acidity is the application of the "Yagupolskii principle". In 2001, the Yagupolskii group observed a significant increase in acidity when replacing the oxo substituents of *p*-toluenesulfonamide (**2.38**, pK_a = 16.3 in DMSO) with *N*-trifluoromethylsulfonyl (*N*-triflyl, *N*-Tf) substituents. These substitutions led to an increase in pK_a of the resulting *N*-(triflyl)sulfonimidamide (**2.39**, pK_a = 8.0 in DMSO) and *N*,*N*-bis(triflyl)sulfondiimidamide (**2.40**, pK_a = 3.3 in DMSO) of up to 13 orders of magnitude compared to the parent sulfonamide (Figure 2.7).[78] The same group reported a similar effect for the *N*-triflyl substitution of carboxylic acids. Replacing the oxygen atoms of benzoic acid (**2.41**, pK_a = 20.7 in MeCN) led to an increase in acidity of the resulting amide (**2.42**, pK_a = 11.06 in MeCN) and amidine (**2.43**, pK_a = 6.17 in MeCN) compounds of up to 14.5 orders of magnitude.[79] The acidifying effect of the triflyl substituent, which is central to the Yagupolskii principle, is twofold. First, the negative charge of the conjugate base is delocalized via resonance over the nitrogen and two oxygen atoms of the sulfonyl group. Second, the strong inductive electron-withdrawing effect of the trifluoromethyl substituent provides additional charge stabilization. The latter can be demonstrated by comparing the pK_a values of methylsulfonamide (**2.44**, pK_a = 17.5 in DMSO) and trifluoromethylsulfonamide (**2.45**, pK_a = 9.7 in DMSO), where the presence of three additional fluorine atoms on carbon provides a strong electron withdrawing effect without additional resonance stabilization.[80]

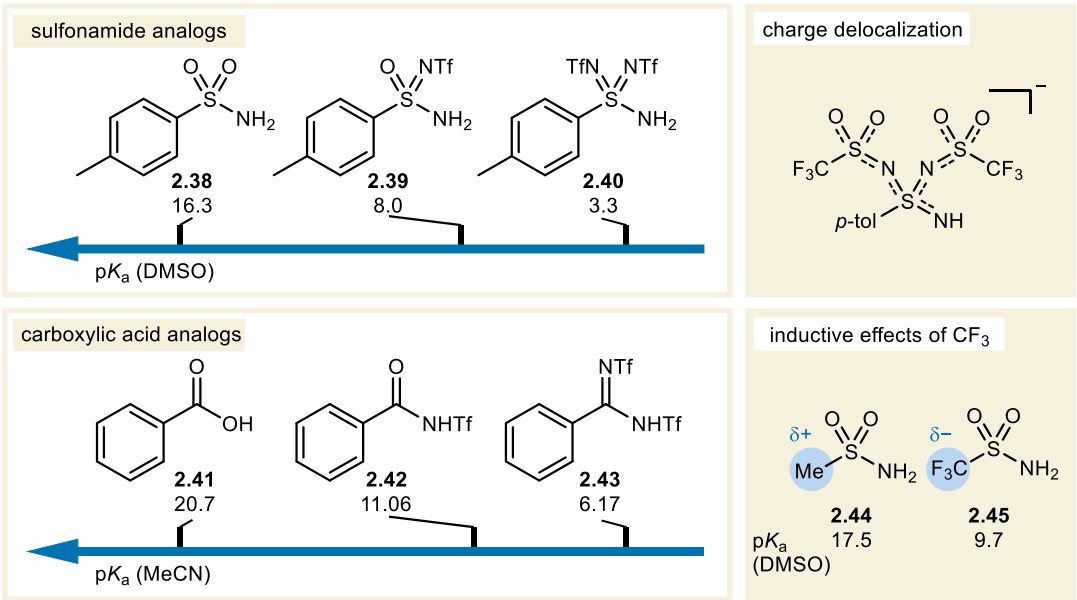

Figure 2.7 pK_a values of compounds demonstrating the Yagupolskii principle.

Yagupolskii's discovery paved the way for the synthesis of chiral organic superacids. These are acids that have a higher acid strength than sulfuric acid, or more precisely defined by

Olah; acidic mediums with a Hammett acidity value (H_0) lower than that of 100% sulfuric acid ($H_0 < -12$), although superacids are more commonly compared to sulfuric acid (H_2SO_4, pK_a = 7.6 in MeCN) by their measured pK_a values in a given solvent.[81,82] The acidity of a number of chiral acids has been determined in MeCN, meaning they can be directly compared (Figure 2.8). For very strong acids, reliable pK_a measurements in MeCN cannot be performed. However, estimated pK_a values based on measurements in 1,2-dichloroethane (DCE) or computed pK_a values have been reported.[83,84]

In 2006, Yamamoto synthesized the first chiral organic superacid by applying the Yagupolskii principle to phosphate-based Brønsted acid catalysts. The resulting *N*-triflyl phosphoramide (NTPA, **2.46**, pK_a = 6.4 in MeCN)[70] catalysts successfully catalyzed a Diels–Alder reaction between electron rich dienes and enones, where CPAs had previously failed to do so.[85] In 2016, List performed a second Yagupolskii substitution of the same catalyst to furnish the even more strongly acidic *N*,*N*′-bistriflylphosphoramidimidate (PADi, pK_a unknown) catalysts. PADis were used by the authors to synthesize α-tocopherol, yielding the product with moderate stereoselectivity.[86] Independently, Blanchet, Toste, and Yamamoto later modified the structures of CPA and NTPA catalysts by substituting the oxygen atoms on phosphorus by sulfur- or selenium atoms, leading to better charge stabilization by virtue of their larger atomic radii.[87–89]

A number of attempts at modifying the reactivity of chiral organic acids incorporated sulfur(VI) centers directly into the binaphthalene backbone of the catalyst. Independent reports by List and Ishihara in 2008 described 1,1′-binaphthyl-2,2′-disulfonic acid (BINSA, pK_a unknown) catalysts, which were successfully employed in numerous addition reactions of imines.[90–92] Chiral disulfonimides (DSIs, **2.47**, pK_a = 8.4 in MeCN)[93] were reported one year later in consecutive publications by List and Giernoth.[94,95] These powerful catalysts showed high activity in C–C bond forming transformations such as Mukaiyama-aldol and Hosomi–Sakurai reactions. This reactivity resulted from their ability to undergo rapid deprotosilylation, granting access to reactivity as a "silylium" Lewis acid catalyst similar to Me_3SiNTf_2.[92,94,96–99] At that time, silylium Lewis acid catalysis had not been broadly established for other chiral acids, with only a few niche examples of silylated CPA-catalyzed transformations existing in the literature.[100,101] Moreover, Yamamoto had reported that the deprotosilylated form of NTPAs was not able to act as an effective catalyst, despite the relatively high acidity of NTPAs compared to DSIs.[85] A report by Berkessel in 2010 subsequently described 1,1'-Binaphthyl-

2,2'-bis(sulfuryl)imide (JINGLE, **2.48**, pK_a = 5.0 in MeCN)[70] superacids. Although the structure and reactivity of JINGLEs is similar to that of DSIs, their application has been limited to a small number of Diels–Alder- and aza-semipinacol reactions.[102,103]

The List group further exploited charge stabilization by triflyl substituents in their 2016 report on Binaphthyl-allyl-tetrasulfone (BALT, **2.49**, estimated pK_a ≈ 2.8 in MeCN) catalysts.[104] These superacidic C–H acid analogs of CPAs acted as effective silylium Lewis acid catalysts for Diels–Alder reactions of cinnamates. The structure of BALTs was inspired by the high Lewis acidity of the deprotosilylated form of the C–H acid Tf_3CH, which had been employed as a silylium Lewis acid catalyst by Yamamoto.[105] The BALT structure bears resemblance to 1,1,3,3-tetratriflylpropene (TTP, **2.50**, estimated pK_a ≈ −2.8 in MeCN), an achiral C–H superacid reported by List in the same year, which similarly exhibited high silylium Lewis acidity.[106] In 2022, the Zhao group introduced phosphoryl bis((trifluoromethyl)sulfonyl) methane (BPTM, **2.51**, calculated pK_a ≈ 1.3 in MeCN) catalysts; C–H acid derivatives of CPAs containing a bis(triflyl)methyl substituent.[84] Their design principle relied on the relative estimated pK_a values of TfOH (0.7), Tf_2NH (0.3), and Tf_3CH (−3.7) in MeCN.[83]

Shifting our focus to a different structural motif, List had already reported on N-phosphinyl phosphoramide (NPPA, pK_a unknown) catalysts in 2010.[107] These acids replaced the acidic hydroxy group of CPA with an *N*-phosphinyl substituent, analogously to the *N*-triflyl substituent in NTPAs. NPPAs performed well in the asymmetric *N*,*O*-acetalization of aldehydes compared to CPAs and NTPAs, but did not see further application. However, the introduction of the imide-like structure of NPPAs containing two P(V) centers foreshadowed the advent of "confined" acids, which came two years later.

List established the concept of asymmetric "confined" acid catalysis in 2012 with the introduction of C_2-symmetric, BINOL-derived imidodiphosphate (IDP, **2.52**, estimated pKa ≈ 11.5 in MeCN)[108] catalysts.[109] In their landmark publication, the authors utilized IDPs to catalyze an asymmetric acetalization toward olean, a fruit fly pheromone which had until then only been synthesized enantiospecifically from chiral starting materials. Although only moderately more acidic than CPAs,[108] the potential of confined chiral acids was immediately recognized. Soon after, single and double Yagupolskii substitutions of the confined IDP scaffold were realized, resulting in imino-imidodiphosphates (iIDPs, **2.53**, pK_a ≈ 9.1 in MeCN)[108] and superacidic imidodiphosphorimidates (IDPis, **2.54**, pKa = 4.5–≤2 in MeCN).[93,108,110,111] iIDPs are strong Brønsted acids that have enabled many transformations with unprecedented reactivity

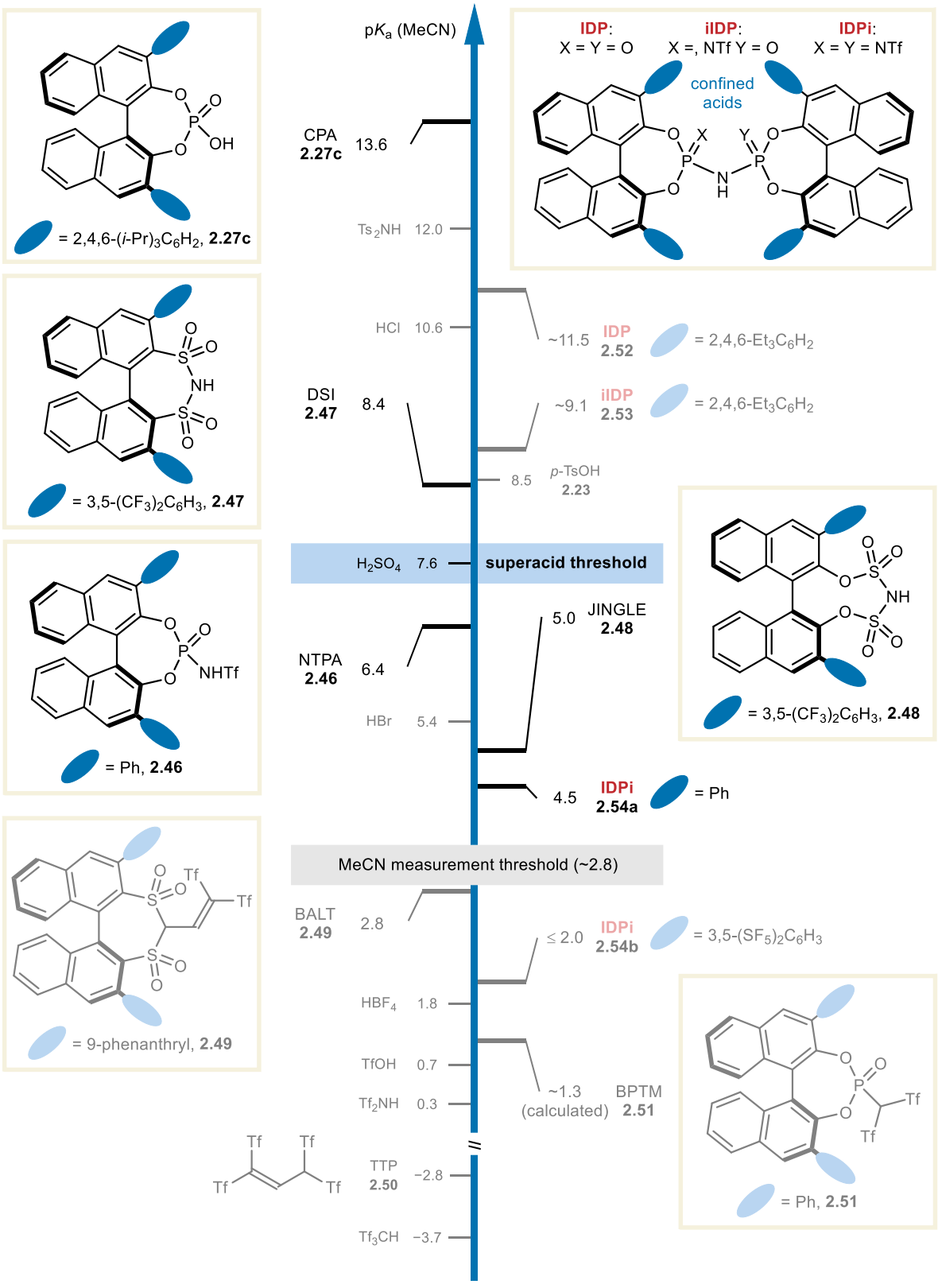

Figure 2.8 pK_a values in MeCN of selected BINOL-based Brønsted acids, achiral organic acids, and mineral acids.[70,82,83,93,106,108,112–114] The pK_a of BPTM is calculated in MeCN at the B3LYP level of theory.[84] pK_a values < ~2.8 are estimated in MeCN ± 1.5 pK_a units.[83]

and selectivity, including Prins reactions, Friedel–Crafts additions, and carbonyl-ene cyclizations.[115–117] Furthermore, IDPi catalysts exhibit reactivity very similar to that of DSIs and BALTs. Their high acidity allows for efficient deprotosilylation, leading to their reactivity as highly confined silylium Lewis acids. The unprecedented combination of confinement and reactivity exhibited by IDPis has given rise to a multitude of high-level publications featuring the activation of unbiased substrates, and currently represents the state of the art in asymmetric organocatalysis.[108] The synthesis of confined acid catalysts was generalized by the List group in 2021 with their development of hexachlorobisphosphazonium (HCP) salts, reagents that provide facile and modular access to these powerful catalysts.[118]

2.1.6. *Asymmetric Counteranion Directed Catalysis*

In acid catalysis, a (partial) positive charge is induced in the electrophile through its coordination to the acid catalyst, which in turn gains anionic character. In specific Brønsted acid catalysis featuring full protonation of the substrate, the induced formal positive charge on the electrophile must necessarily be accompanied by a closely bound counteranion, given that the reaction occurs in a sufficiently non-polar solvent.[119] Consequently, the use of a chiral acid catalyst leads to the formation of a chiral ion pair intermediate, in which stereochemical information is communicated from the chiral catalyst anion to the activated achiral electrophile cation. This chiral environment results in the existence of diastereomeric transition states in the chiral center-forming reaction with a nucleophile, leading to enantioenriched products. Achieving enantioinduction through chiral ion pairing with an enantiomerically pure counteranion has been termed *Asymmetric Counteranion-Directed Catalysis* (ACDC) by List.[98]

A proof of concept for ACDC was established by the List group in 2006. Their publication reported the asymmetric Hantzsch ester reduction of enals through iminium catalysis. The catalyst for this transformation was a salt composed of an achiral morpholinium cation and a (*R*)-TRIP anion. Whereas previous reports of asymmetric iminium catalysis relied on enantioinduction by covalent attachment of a chiral amine to the electrophile, this report showed that ACDC could provide a sufficiently chiral environment to yield the products with excellent enantioinduction (Figure 2.9).[120] This method decoupled the mode of enantioinduction from the mode of substrate activation; a significant advantage in terms of modular catalyst design.

Toste and coworkers subsequently employed ACDC in their Au-catalyzed reaction of allenes toward 5-membered heterocycles.[121] Their method used Ag-salts of CPAs to generate the strongly π-acidic cationic Au(I) catalysts *in situ*, establishing a chiral ion pair. The authors reasoned that employing a chiral counteranion, as opposed to a chiral ligand, improved the stereochemical outcome of the reaction, due to the linear coordination geometry of Au(I), which places chiral ligands far away from the emerging stereocenter in the relevant transition states.

The concept of ACDC is not limited to strong chiral Brønsted acid catalysis. Although unrecognized at the time, weaker acids such as chiral thiourea H-bond donors reported by Jacobsen engage in ACDC by strong coordination to the chloride anion, thereby generating a composite chiral "counteranion".[122,123]

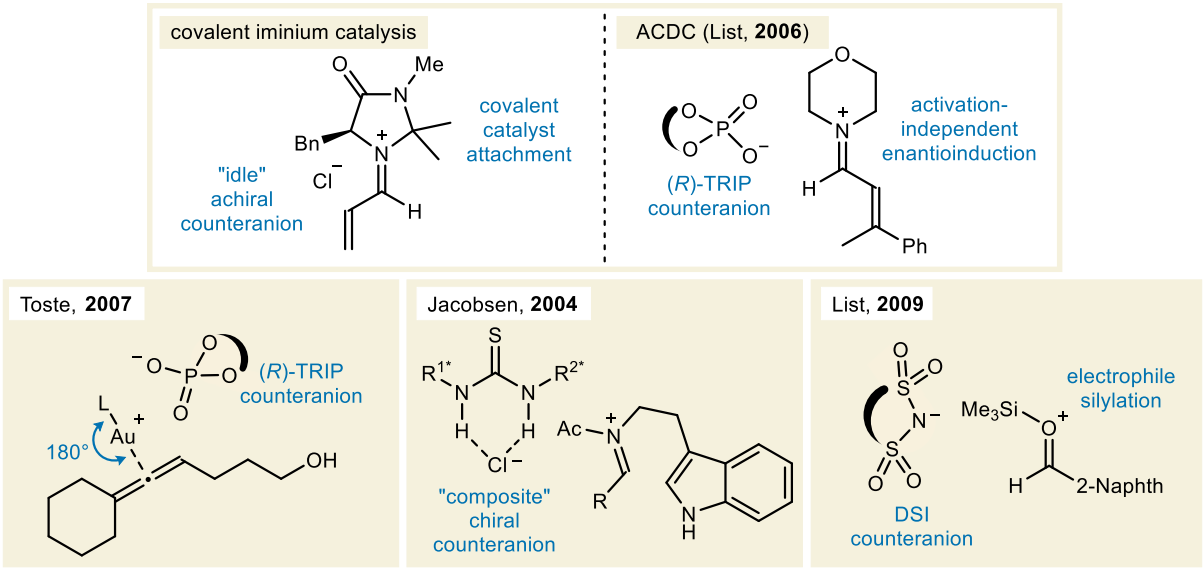

Figure 2.9 The principle of ACDC and examples of enantioinduction by ion-pairing.

Strong chiral Brønsted acids such as DSIs, BALTs, and IDPis (*vide supra*) can participate in *silylium-ACDC*, a form of Lewis acid catalysis characterized by rapid deprotosilylation of the catalyst in the presence of a silylated nucleophile or other silylating agent (Scheme 2.4). The resulting silylium Lewis acid provides access to transformations such as Mukaiyama-aldol reactions and Lewis acid-catalyzed Diels–Alder reactions. Silylium-ACDC has several distinct advantages over "traditional" (transition) metal-based asymmetric Lewis acid catalysis. Most notably, weakly coordinating achiral anionic ligands in metal-based catalysts can dissociate from the metal center and become silylated, causing non-asymmetric silylium Lewis acid background catalysis. This background reactivity is suppressed in silylium-ACDC, due to the absence of such ligands. Furthermore, metal-based

systems frequently feature Lewis basic chiral ligands, which reduce the Lewis acidity of the metal center and impede catalysis. Conversely, the distinct activation mode of silylium-ACDC, which precludes interaction of the acid backbone with the Lewis acidic site, leads to catalysts with enhanced Lewis acidity. Lastly, silylium-ACDC possesses a self-repairing and self-drying catalytic cycle, in which the silylated catalyst can scavenge water molecules present in the system before being re-silylated. This self-repair leads to highly anhydrous reaction conditions with a relatively simple reaction setup. These combined advantages have led to a rapid expansion of the field in recent years.[108]

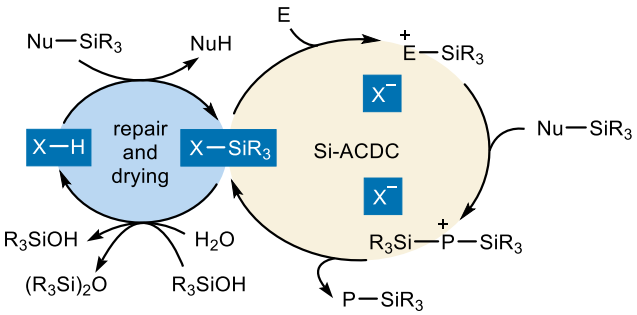

Scheme 2.4 A general mechanism of silylium-ACDC.

2.2. Hydrocarbon Biosynthesis

The maturing of the fields of enzymology and organic chemistry over more than a century has allowed for the meticulous study of the (bio)synthesis of natural products. Among these efforts, hydrocarbon synthesis has been one of the most studied interfaces between chemistry and biology. The study of hydrocarbons has largely been driven by the hydrocarbon-rich nature of many essential oils, which have been cherished by ancient cultures for millennia, due to their therapeutic and aromatic qualities.[124] Over the decades, chemists have found ways to mimic, and even expand upon, the reactivity of enzymes involved in the synthesis of natural hydrocarbons. Early, moderately successful, attempts by Lerner focused on the use of monoclonal antibodies as highly modifiable proteins which could induce reactivity in a small number of substrates.[125,126] Later, development of the field of directed evolution granted access to tailor-made enzymes for chemical transformations.[127] However, the simplest, and arguably the most effective approach has come from the field of organocatalysis. The development of small molecule organocatalysts has allowed chemists to contribute significantly to the synthesis of hydrocarbon-derived natural products.[128] While it is still a relatively young field,

organocatalysis returns to the inspiration of enzymes as natural catalysts, a connection that chemists have made since the beginning of the 20th century.[24,27]

The biosynthesis of hydrocarbons presents an idealized form of the olefin alkylation reaction. Olefin alkylation reactions initiate with carbocation formation (herein referring specifically to *carbenium ions*; trivalent carbocations with a vacant p-orbital), followed by the attack of an alkene nucleophile. Next, optional cationic rearrangements take place, and finally the reaction is terminated by selective deprotonation. Enzymes can perform these transformations with unrivaled selectivity, typically producing the product as a single enantiomer of a single diastereomer. The reactivity and selectivity of enzymes makes them an exemplary blueprint for the design of asymmetric olefin alkylation reactions. In the following subchapters, the origin of terpene chemistry and the mechanisms of hydrocarbon biosynthesis through olefin alkylation will be discussed.

2.2.1. *The Inception of Terpene Chemistry*

In 1866, August Kekulé coined the term "terpene" to describe hydrocarbons of the formula $C_{10}H_{16}$, which naturally occurred in turpentine oils obtained by the distillation of resin from living trees.[129] This definition was later expanded to any natural compound of the formula $C_{5n}H_{8n}$, based on the formal derivatives of isoprene (Figure 2.10).[130] The broader umbrella of "terpenoids" came into widespread use in 1955 to describe terpenes and terpene-derived structures with additional, most commonly oxygen-containing, functional groups.[131,132]

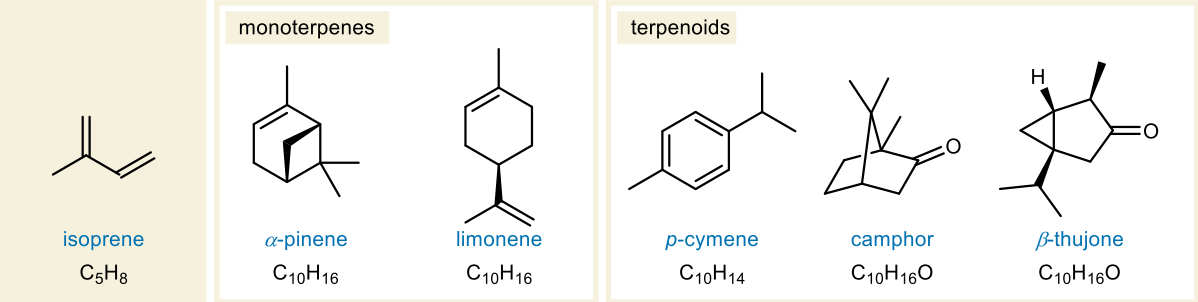

Figure 2.10 Isoprene and selected monoterpene and monoterpenoid examples.

It was the diligent work of Kekulé's student, Otto Wallach, that laid the groundwork for the modern understanding and categorization of terpenes. Up until the 1880s, research on terpenes had lacked a systematic approach. Although reports were abundant, the literature on the subject did not carry a common theme.[133] Wallach characterized and catalogued a number

of terpenes and their origins by combing through this literature, and supplemented the field through his own studies of terpene derivatization, crystallization and isolation. In 1887, he established that terpenes are oligomers composed of C_5 units originating from isoprene.[134–136] For his contributions, Wallach was awarded the 1910 Nobel prize in chemistry "*for his services to organic chemistry and the chemical industry by his pioneer work in the field of alicyclic compounds.*"

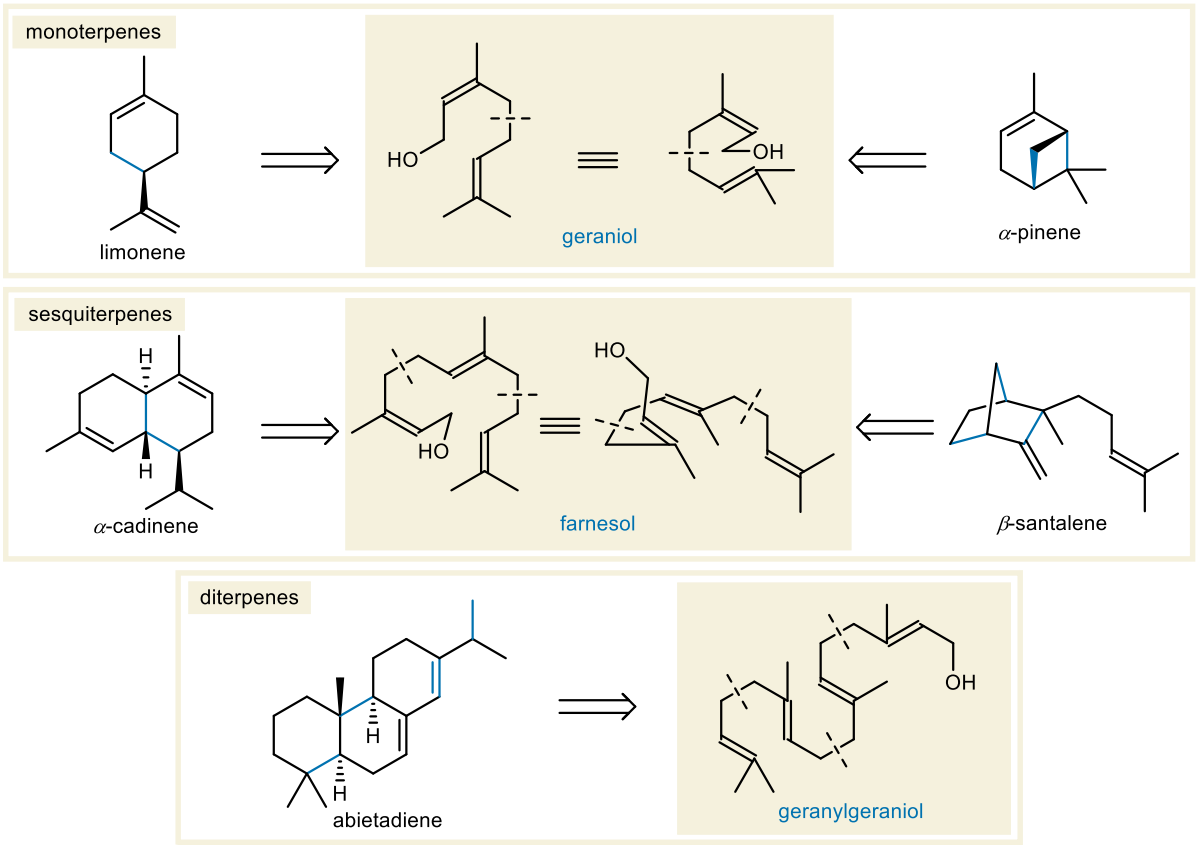

Scheme 2.5 Biosynthetic prenols and their enzyme-induced conformations in the synthesis of monoterpenes, sesquiterpenes and diterpenes, as imagined by Ružička. Individual isoprene units are indicated with dashed lines in the prenols.

Leopold Ružička resumed the systematic study of terpenes in 1922, focusing mostly on the higher terpenes. His work provided mechanistic insight into the formation of terpenes through his structural assignment and synthesis of several sesquiterpenes (C_{15}), diterpenes (C_{20}) and triterpenes (C_{30}). Ružička also coined the term "*isoprene rule*" to describe the C_5-oligomeric constitution of terpenes observed by Wallach. Further investigation of natural terpene structures led him to propose that simple prenols such as geraniol, farnesol and geranylgeraniol were likely the biological precursors of terpenic compounds (Scheme 2.5); a phenomenon which he termed the "*biogenetic isoprene rule*". Moreover, he suggested that enzymes promote certain "constellations" (conformations) of terpene precursors, giving rise to

the observed structural diversity of terpenes following a series of selective cationic cyclizations and rearrangements.[137] Ružička's critical insights greatly expedited structural elucidation efforts of natural compounds, leading to his 1939 awarding of the Nobel prize in chemistry "*for his work on polymethylenes and higher terpenes.*"

2.2.2. *The Origin of Biological C_5 Building Blocks*

Publications by various groups in the 1950s unveiled isopentyl pyrophosphate (IPP) and dimethylallyl pyrophosphate (DMAPP) as the true biological C_5 building blocks of terpenoids.[138,139] IPP and DMAPP are products of the mevalonic acid (MVA) pathway, which is present in most organisms (Scheme 2.6). This pathway starts from acetyl coenzyme A (acetyl-CoA), which serves as the carbon source for IPP and DMAPP. Two enzymatic condensations of three total molecules of acetyl-CoA yield acetoacetyl-CoA and β-hydroxy-β-methylglutaryl-CoA (HMG-CoA), respectively. A subsequent nicotinamide adenine dinucleotide phosphate (NADPH)-mediated enzymatic reduction results in the formation of mevalonic acid (MVA). These reactions constitute the "upper mevalonate pathway", which is conserved in all eukaryotes, archaea and eubacteria. The "lower mevalonate pathway" proceeds from MVA, with a number of phosphorylation steps and a decarboxylation step leading to the formation of IPP, which is then isomerized to DMAPP. The sequence of these enzymatic steps toward IPP and DMAPP varies between organisms.[138] Key in the elucidation of IPP and DMAPP biosynthesis were the discoveries of Bloch and Lynen, who independently demonstrated that mevalonic acid is an essential and committed intermediate in the biosynthesis of terpenes and sterols.[140] Their discoveries were awarded with the 1964 Nobel prize in Physiology or Medicine "*for their discoveries concerning the mechanism and regulation of the cholesterol and fatty acid metabolism*".

An alternative pathway to IPP and DMAPP was discovered in bacteria, algae and higher plants in the 1990s. The driving force behind this discovery was the incomplete inhibition of terpenoid synthesis by known strong MVA pathway inhibitors in higher plants, especially for terpenoids contained in plastid organelles. Subsequent metabolic studies revealed the methylerythrol phosphate (MEP) pathway, often simply called the non-mevalonate pathway, which is located in these organelles. The MEP pathway uses pyruvate and glyceraldehyde 3-phosphate (G3P) as alternative carbon sources to acetyl-CoA.[141,142]

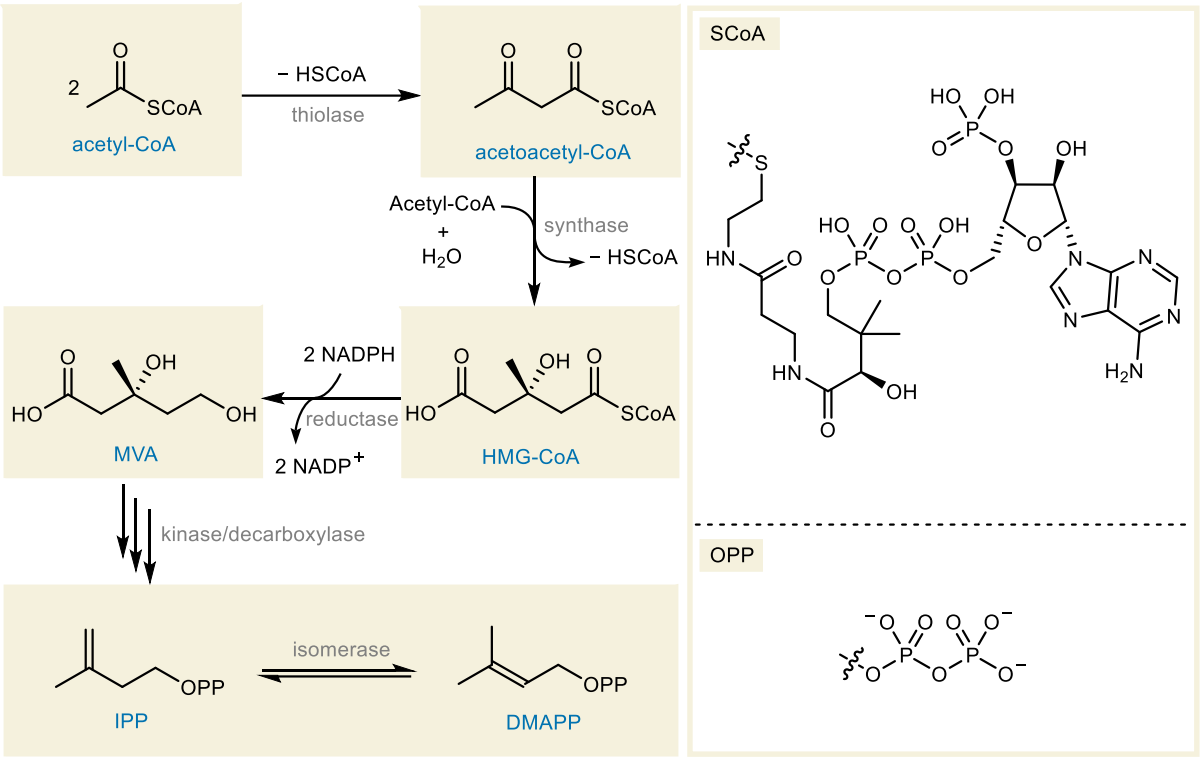

Scheme 2.6 Biosynthesis of IPP and DMAPP via the MVA pathway. Enzyme names are simplified to their function. The lower mevalonate pathway is simplified due to variations between organisms.

2.2.3. *The Head and Tail of Terpene Precursors*

DMAPP serves as a prenyl donor to IPP in enzyme-catalyzed, so-called "head-to-tail" reactions. Some confusion around the terms "head" and "tail" exists in the nomenclature of terpene (bio)synthesis, because of differences in nomenclature between the fields of biology and chemistry, and a distinction between inter- and intramolecular reactions. The following set of rules, which merge the nomenclature of both fields, and provide guidelines for terpenoid "head and tail" reactivity, will be adhered to in this thesis (Scheme 2.7):

1. When referring to intermolecular chain elongations of prenyl pyrophosphates, the electrophilic prenyl donor containing the pyrophosphate moiety (DMAPP or another prenyl pyrophosphate) is referred to as the "head", and the nucleophile (IPP) serves as the "tail" end of the reaction. In this nomenclature, head and tail refer to the entire molecule, and the distinction is based on which precursor molecule will form the "head", and which will form the "tail" of the elongated product; *i.e.* DMAPP will become the "head" of geranyl pyrophosphate (GPP), and IPP will become the "tail". Thus, in chain elongation reactions, "head" and "tail" represent a state of *becoming*.

2. This nomenclature carries over to non-conventional biosyntheses of linear terpenes like squalene. Squalene is synthesized in a reductive "head-to-head" coupling of two molecules of farnesyl pyrophosphate (FPP), and therefore contains two "heads". Again, the two "heads" of the reaction are named so because they *become* the "heads" of squalene.
3. In cyclization reactions, "head" and "tail" refer to the two ends of the cyclization substrate as they originate from the molecule's precursors; *e.g.* the "head" of FPP is the prenyl end, and the "tail" is the pyrophosphate end. This nomenclature is based on the carbon skeleton of the substrate of a cyclization reaction. Modification by, for example, epoxidation of a "head" alkene does not change its designation. Thus, in cyclization reactions, "head" and "tail" refer to a state of *being*.
4. The electrophile, or electron sink, is referred to first, and the nucleophile last; *i.e.* a "head-to-tail" cyclization refers to an electrophilic head, and a nucleophilic tail. This nomenclature refers to charge propagation from the cationic species generated on the electrophilic end toward the nucleophilic end by a series of cascading nucleophilic attacks.
5. "Middle" is sometimes used to refer to an isoprene unit in the middle of the molecule. This results in terms like "head-to-middle" cyclizations, which can refer to a cationic intermediate in which a prenyl unit performed nucleophilic attack on the electrophilically activated "head" group, or to an incomplete cyclization product of a reaction where the "tail" did not participate.

This working definition is based on convention and has obvious flaws that would be best addressed with a more rigorous and systematic naming based on atom numbering.[143] However, such nomenclature can be equally confusing in the sense that it does not imply the type of reactivity of a molecule or functional group, which cannot always be instinctively derived from chemical structure, especially in enzymatic reactions.

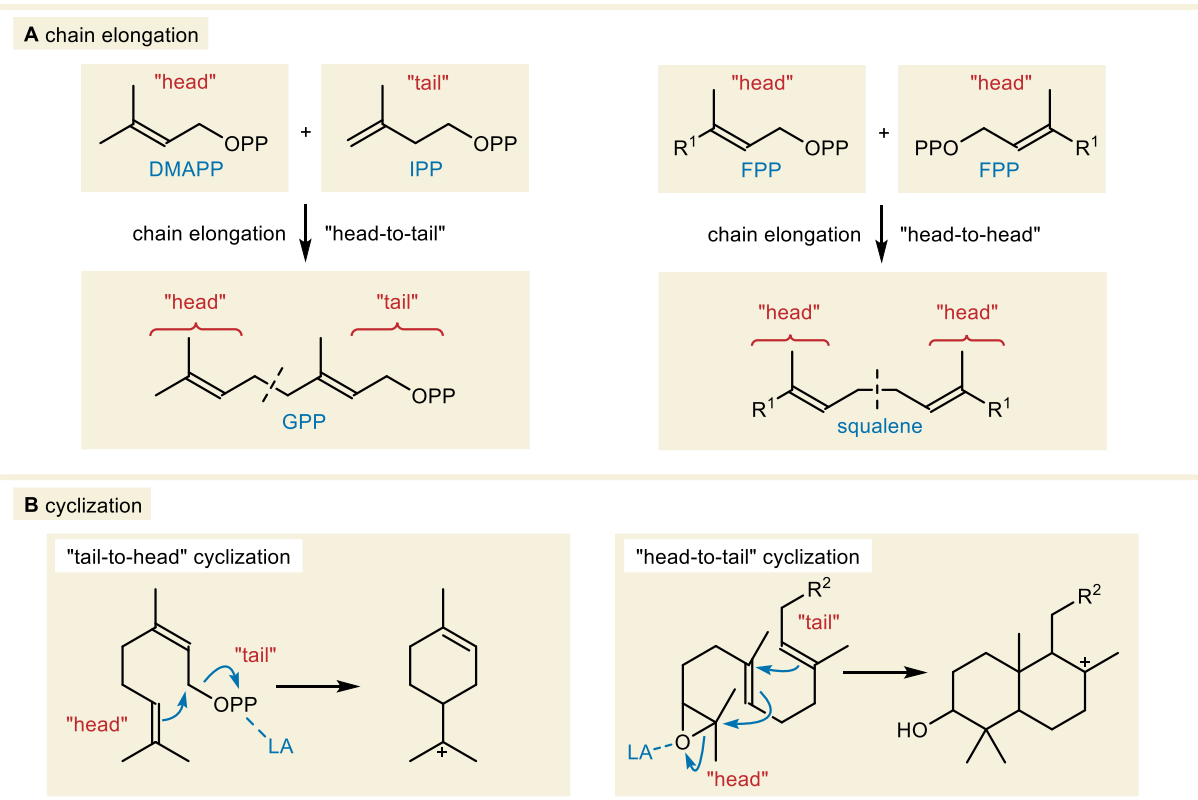

Scheme 2.7 "Head" and "tail" nomenclature of chain elongation reactions (A) and cyclization reactions (B) in terpene (bio)synthesis. R^1 = geranyl, R^2 = tail moiety. Dashed lines indicate C–C bond-formation between the "head" and "tail" reaction partners.

2.2.4. *Biosynthesis of Prenyl Pyrophosphates*

The C_5 building blocks IPP and DMAPP are enzymatically converted into oligomeric prenyl pyrophosphates, the direct precursors of terpenes.[144,145] The pyrophosphate moiety in these compounds serves as a more suitable leaving group than the alcohols initially proposed in the biogenetic isoprene rule. However, it is worth noting that Ružička was remarkably close in his hypothesis.

The head-to-tail reaction between DMAPP and IPP is catalyzed by a class of prenyltransferases called isoprenyl pyrophosphate synthases (IPPSs). This reaction leads to the formation of GPP, which itself serves as a prenyl donor to IPP to produce FPP. Further prenylations yield geranylgeranyl pyrophosphate (GGPP) and higher prenyl pyrophosphate oligomers. The chain length of these oligomers is determined by sterically demanding amino acid residues in the active site of IPPS enzymes, leading to a distributions of prenyl pyrophosphate oligomers which varies based on the IPPS enzyme types present in different organisms.[146]

IPPSs provide a principal example of an intermolecular biochemical reaction between a carbocation and an unactivated alkene (Scheme 2.8). IPPSs are Mg^{2+}-dependent enzymes containing two Mg^{2+} binding sites to bind the pyrophosphate moieties of IPP and the prenyl donor. The metal center bound to the prenyl donor is used by the enzyme as a Lewis acidic site for the electrophilic activation of the pyrophosphate moiety. Departure of this nucleofuge generates an allylic carbocation, which is attacked by the electron-rich C=C bond of IPP. Subsequent selective deprotonation of the resulting tertiary cation leads to the formation of predominantly *E*-alkene products.[146–149] *Cis*-type IPPSs are also known and well-documented.[150] However, they share few structural similarities in the active site with *trans*-type IPPSs beyond their Mg^{2+}- dependent activation site. In *trans*-type IPPSs, deprotonation of the cation after IPP attack is performed by the Mg^{2+}-bound pyrophosphate nucleofuge of the prenyl donor. In *cis*-type IPPSs, a basic histidine or aspartate residue of the enzyme assumes this role.[146,148–151]

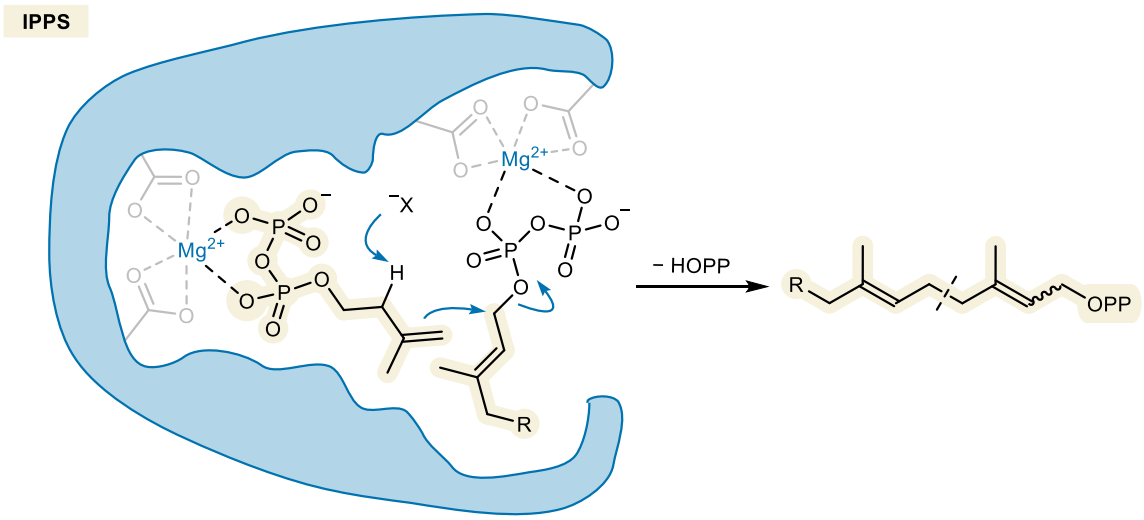

Scheme 2.8 Head-to-tail biosynthesis of prenyl pyrophosphates by IPPSs. X^- = pyrophosphate (*trans*-type IPPSs), aspartate/histidine (*cis*-type IPPSs); R = H, (poly)prenyl. The newly formed C–C bond is indicated with a dashed line in the product.

2.2.5. *Biosynthesis of Terpenes*

The oligomeric products of IPPSs are transformed into terpenic compounds by cyclase enzymes, which are subdivided into two classes. Class I cyclases catalyze tail-to-head cyclization reactions, and class II cyclases catalyze head-to-tail cyclizations. Class I cyclases are more commonly associated with terpene biosynthesis, as they effectuate the activation of the pyrophosphate group, resulting in cyclization to hydrocarbon products (Scheme 2.8). Like

IPPSs, class I cyclases are Mg^{2+}-dependent enzymes, and the steps of the cyclization reaction are nearly identical to those of prenyl pyrophosphate synthesis, although there is no external IPP nucleophile in cyclases. Instead, these enzymes promote a privileged conformer of the precursor, which primes one or more of the alkene moieties of the substrate to act as an intramolecular π-nucleophile.[146] Furthermore, the three-dimensional structure of cyclases can induce selective hydride- or alkyl shifts, granting access to structurally diverse carbon skeletons.[152,153]

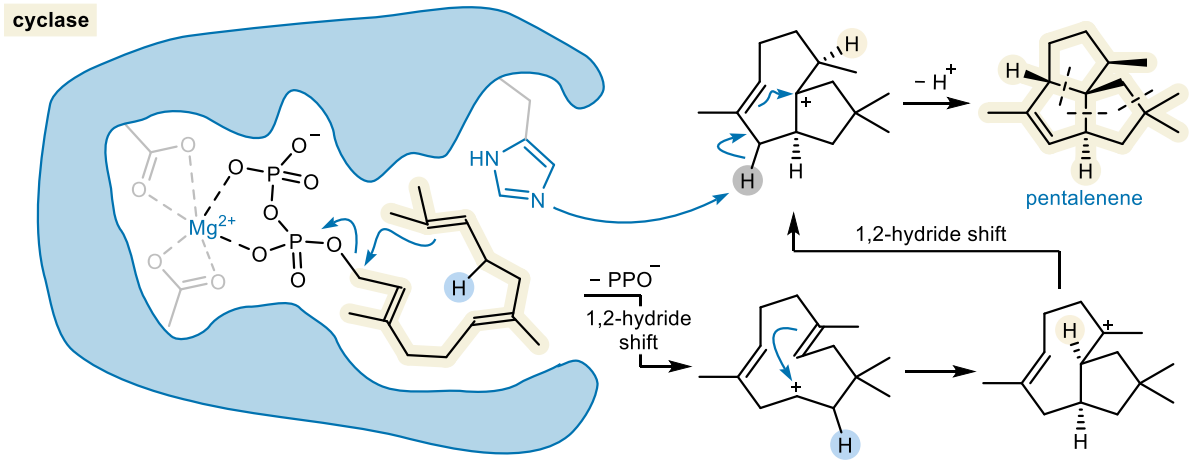

Scheme 2.9 Pentalenene synthase-catalyzed tail-to-head biosynthesis of the sesquiterpene pentalenene;[154] an example of the reactivity of class I cyclases. Newly formed C–C bonds are indicated with dashed lines in the product.

Among class I cyclase-catalyzed terpene biosyntheses, monoterpenes constitute a special case. The *E*-alkene geometry of GPP prevents it from undergoing direct cyclization upon cation formation due to the high rotational barrier of allylic cations. Class I monoterpene cyclases accept GPP as a substrate, but do not directly convert it to the desired terpenic product. Instead, GPP is first isomerized to linalyl pyrophosphate (LPP), which adopts the desired conformation (Scheme 2.10). LPP is then re-activated and cyclizes to the α-terpinyl cation, which is a common intermediate of many monoterpene skeleton types. Interestingly, the *Z*-alkene form of GPP, neryl pyrophosphate (NPP), was shown to be a less suitable substrate than GPP for most of these cyclases, suggesting a high level of substrate specificity.[155–157] Similar isomerization activity has been proposed for sesquiterpene- and higher terpene cyclases that could catalyze cyclizations via nerolidol and its higher oligomers. However, FPP and higher prenyl pyrophosphate activation modes require more elucidation due to discrepancies between enzymes. Furthermore, tail-to-head cyclizations forming medium-sized ring or macrocyclic intermediates do not always require initial isomerization.[158]

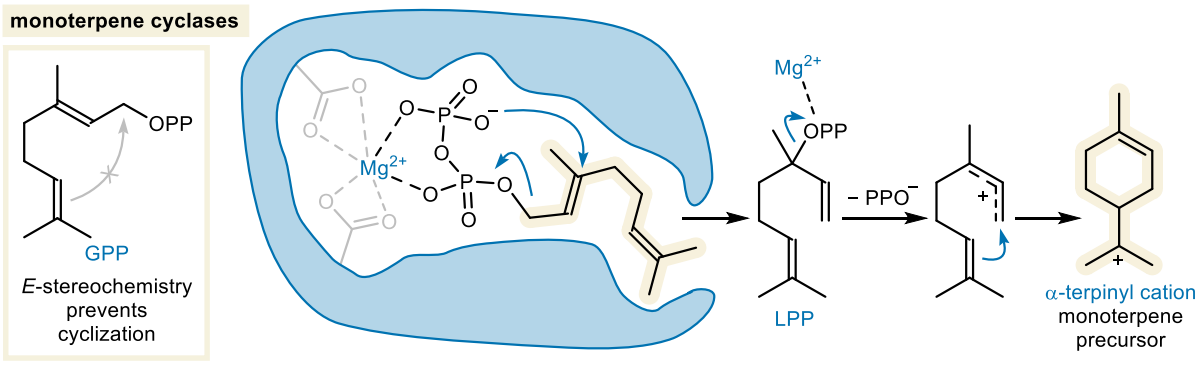

Scheme 2.10 Isomerization of GPP to LPP catalyzed by monoterpene cyclases, and subsequent formation of the α-terpinyl cation; an intermediate in the biosynthesis of many monoterpenes.

The biosynthesis of the triterpene squalene represents a unique example of a reductive head-to-head coupling. Squalene synthase (SQS) dimerizes FPP with the loss of two pyrophosphate moieties in a two-step reaction (Scheme 2.11).

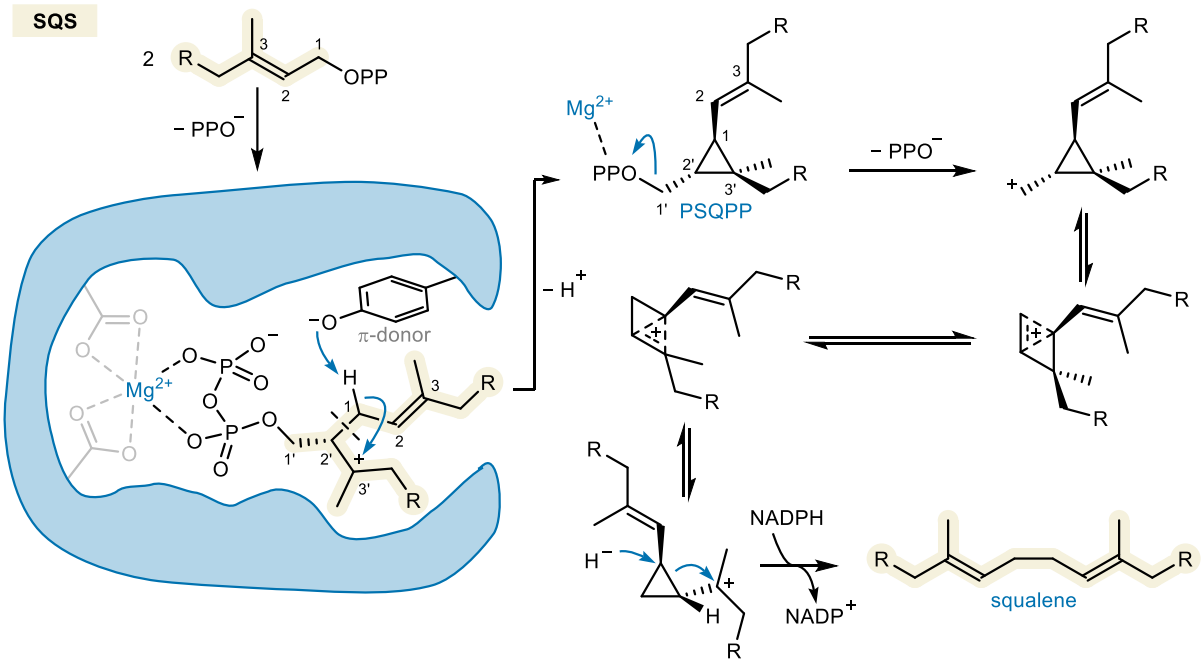

Scheme 2.11 Squalene synthesis over two SQS-catalyzed steps. The newly formed C–C bond in the initial condensation between two molecules of FPP is indicated with a dashed line in the intermediate. R = geranyl.

Mechanistically, the first step of the reaction deviates from the head-to-tail reactivity of IPPSs. In addition to a Mg^{2+} binding site for each FPP molecule, SQS possesses a conserved tyrosine residue that aids in the activation of the pyrophosphate of the prenyl donor by acting as a Brønsted acid. After leaving group activation, the resulting tyrosine phenolate stabilizes the allylic cation through cation-π interactions, which primes the cation for attack from the 2'-position of the second FPP equivalent. Next, an unusual deprotonation β to the cation by the

tyrosine phenolate causes ring closure toward the cyclopropane intermediate presqualene pyrophosphate (PSQPP). PSQPP remains bound to the enzyme, but moves to a different active site, where it is re-activated to generate a primary non-classical cyclopropylcarbinyl cation, which rearranges to a tertiary cyclopropylcarbinyl cation through bicyclobutonium cation intermediates. Finally, NADPH bound to the enzyme delivers a hydride to open the cyclopropane ring and liberate squalene.[159–162]

Reactions of squalene themselves have been the subject of intensive study, as squalene is the precursor of many biologically relevant compounds across all branches of evolution. Notable squalene-derived products include lanosterol (precursor of cholesterol) and steroid hormones in humans, as well as hopanoids in bacteria.[163,164] Biosynthesis of the latter is catalyzed by the class II cyclase squalene-hopene cyclase (SHC), and starts with the protonation of one of squalene's terminal prenyl moieties. A series of selective intramolecular C–C bond-forming olefin alkylation reactions and alkyl shifts then establish an extensive fused-ring network. Finally, the reaction is terminated by deprotonation of the terminal *Z*-methyl group (Scheme 2.12).[165,166] Initiation by C=C bond protonation is performed by an aspartic acid residue with an *anti*-oriented proton, a conformation which is stabilized by H-bonding interactions to other amino acid residues and water molecules in the active site. This *anti*-orientation greatly enhances the acidity of the carboxylic acid, and allows the class II cyclase to activate the substrate in the absence of a suitable leaving group such as pyrophosphate.[167]

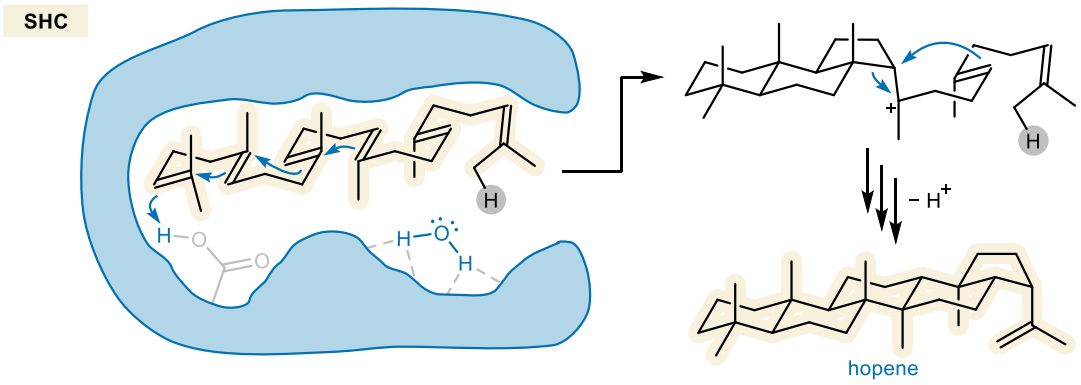

Scheme 2.12 Simplified mechanism of hopene synthesis by SHC. The second cyclization–ring expansion sequence is omitted for the sake of brevity. The site of deprotonation is highlighted in gray, with the enzyme-bound water responsible for deprotonation displayed in proximity.

The preceding section provide a glimpse into olefin alkylation reactivity that has been discovered by the study of natural hydrocarbon synthesis. The reactivity displayed by the different enzyme classes involved in terpene biosynthesis can deepen our understanding of the necessary design elements of chemical catalytic asymmetric alkylation reactions of olefins. Of

special note are the intermolecular reaction between IPP and DMAPP, and the synthesis of PSQPP, catalyzed by IPPS and SQS, respectively. The former features activation of a suitable leaving group by a Lewis acid, regioselective addition of an external alkene nucleophile, and selective deprotonation. The latter utilizes Brønsted acid activation to deliver a stereochemically pure product possessing multiple stereocenters. These features embody the ideals of olefin alkylation reactivity, and will be key to the design of reactivity within this thesis.

2.3. Carbocation Electrophiles and Olefin Nucleophiles

Intermolecular catalytic asymmetric olefin alkylation reactions are characterized by the nucleophilic attack of an alkene group onto an *in situ* generated carbocation electrophile, followed by deprotonation of the resulting carbocation. This type of reactivity has sparingly been referred to as the "aliphatic Friedel–Crafts" reaction in the context of carbocations generated from alkyl- or acyl halides by action of a Lewis acid catalyst.[168,169] However, the Friedel–Crafts reaction has become synonymous with electrophilic aromatic substitution reactions of arenes over time. Furthermore, "aliphatic Friedel–Crafts"-type reactions more commonly result in termination by halide addition, and acylations appear more frequently than alkylations. Therefore, the preferred nomenclature in this thesis remains the olefin alkylation reaction.

As shown in the previous section, substrates of class I cyclases commonly feature C(sp^3)–O bonds that can be activated by an acid moiety on the enzyme. By extension, the organocatalytic versions of olefin alkylation reactions can take advantage of the same motif, and employ ACDC to yield enantioenriched products (Scheme 2.13). In the following sections, the feasibility of certain electrophile–nucleophile combinations will be discussed.

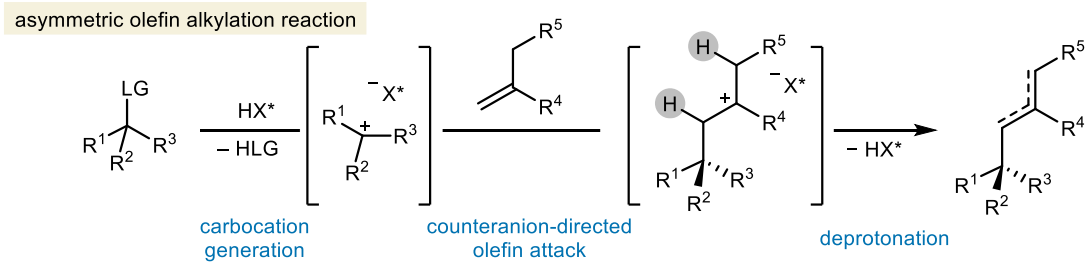

Scheme 2.13 The general concept of the asymmetric alkylation of an olefin with a C(sp^3) electrophile using ACDC.

2.3.1. *Generating Carbocations*

The first observation of a carbocation is often credited to Norris, who in 1902 described the formation of colored solutions upon the ionization of compounds in sulfuric acid, and speculated on the existence of a trivalent carbon species in this reaction.[170,171] Similar work was carried out independently by Gomberg, Kehrman and Wentzel in the same year.[172,173] Their findings are now understood to have been the observation of the triphenylmethylium cation. Twenty years later, Meerwein and van Emster published their studies on the cationic rearrangement of camphene hydrochloride to isobornyl chloride, which significantly advanced chemists' understanding of the mechanistic underpinnings of carbocation chemistry.[174] A subsequent 1928 publication by Ingold and Rothstein proposed the existence of the S_N1 subclass of substitution reactions.[175] The concept of heterolytic bond cleavage was introduced by Whitmore in 1932, who would go on to describe the role of alkene protonation in acid-catalyzed polymerization reactions.[176,177] The following decades were characterized by an abundance of publications deepening chemists' understanding of carbocation chemistry. Key to understanding the reactivity of carbocations was Olah, who used superacids to generate cations with lifetimes long enough to be studied.[178] Olah's work was widely recognized as pivotal to the field, and he was awarded the 1994 Nobel prize in chemistry "*for his contribution to carbocation chemistry.*"

The modest proton affinity of alkene functional groups necessitates harsh conditions for their use as carbocation precursors under Brønsted acid catalysis. The strong Brønsted acids required to activate alkenes may lead to the formation of isomeric- or other by-products during a given reaction. As a consequence, a limited number of asymmetric hydrofunctionalizations reactions have been reported that feature the protonation of an alkene by a strong chiral Brønsted acid.[179–182] Conversely, more basic functional groups—such as imines and carbonyl compounds—have seen wide application in organocatalytic transformations in the presence of relatively weakly acidic CPAs.[67] The 4-fluorophenol H-bond basicity scale (pK_{BHX}) provides a comprehensive way to assess the basicity of compounds bearing various functional groups, which can give a sense of their susceptibility to activation by an acid (Figure 2.11).[183]

Enzymatic olefin alkylation reactions (*vide supra*) achieve carbocation generation by the activation of a suitable nucleofuge (*e.g.*, pyrophosphate), or by the selective protonation of one C=C bond of a hydrocarbon polyene substrate (*e.g.*, squalene). The selectivity of the latter case relies to a large extent on the three-dimensional structure of the enzyme. The enzyme

selectively binds to a single substrate, and orients an acidic moiety toward one C=C bond of the substrate in an induced conformer (see section 2.2.5). Such regioselective protonations are not trivial using small molecule Brønsted acid catalysts, due to the lack of a well-defined three-dimensional environment. Furthermore, many alkene groups have comparable pK_{BHX} values, which can complicate the selective protonation of the intended electrophilic alkene over the nucleophilic alkene. Moreover, the products of olefin alkylation reactions are themselves olefins, meaning that they could re-enter the catalytic cycle. Cationic polymerizations of alkenes are also well documented.[184] This phenomenon further increases the likelihood of side-reactivity and complicates selective reaction termination.

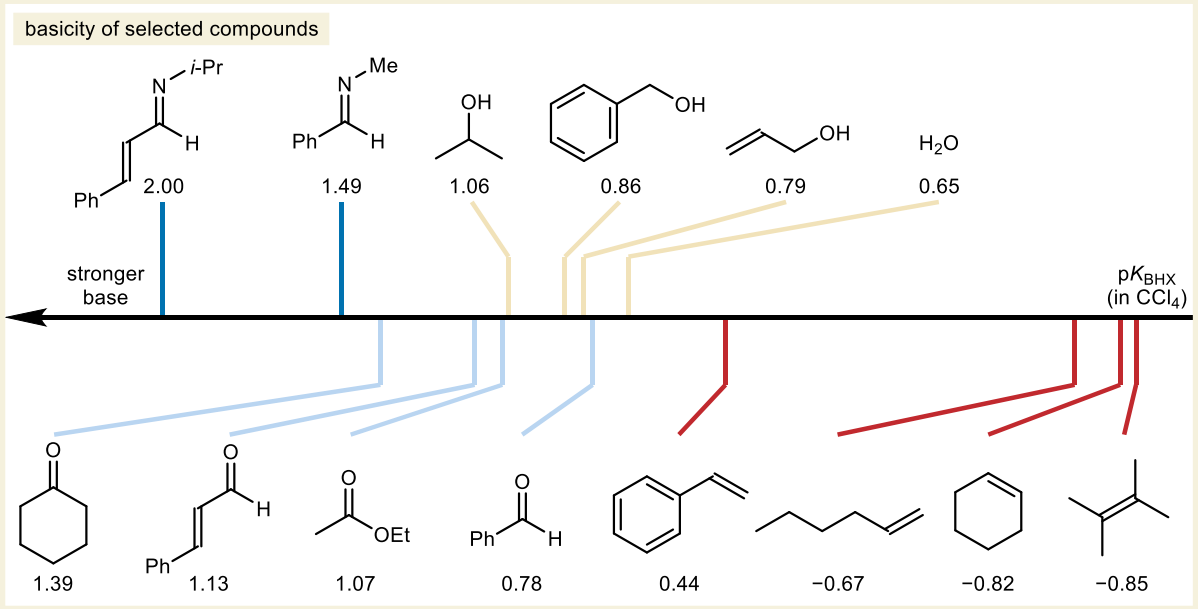

Figure 2.11 The pK_{BHX} values (in CCl_4) of selected imines (blue), carbonyl compounds (light blue), hydroxy compounds (yellow), and olefins (red).[183]

To improve the selectivity of cation generation, acid-catalyzed olefin alkylation reactions can benefit from the installation of heteroatom-containing leaving groups on the electrophile. The higher pK_{BHX} of such leaving groups compared to alkenes causes preferential coordination to the more basic functionality, allowing for more selective activation. Additionally, Lewis acid catalysis may be employed instead of Brønsted acids to suppress side-reactions of the olefin. The weak carbophilicity of most conventional Lewis acids prevents their coordination to carbon–carbon π-bonds (coordination of this type is largely exclusive to late transition metals), instead favoring the formation of σ-complexes with heteroatoms.[185,186]

Departure of a nucleofuge leaving group from an organic compound results the formation of a carbocation. Carbocations bearing no α-heteroatom substituents are

comparatively high energy intermediates, due to the lack of resonance stabilization from adjacent atoms with lone pairs. However, hyperconjugation from neighboring alkyl groups, and charge delocalization to conjugated alkenyl- and aryl substituents, can somewhat increase carbocation stability. The stability of a give carbocation can be assessed by its hydride ion affinity (HIA); the negative of $\Delta H°$ for the reaction of H^- with a carbocation in the gas phase (Figure 2.12).[187]

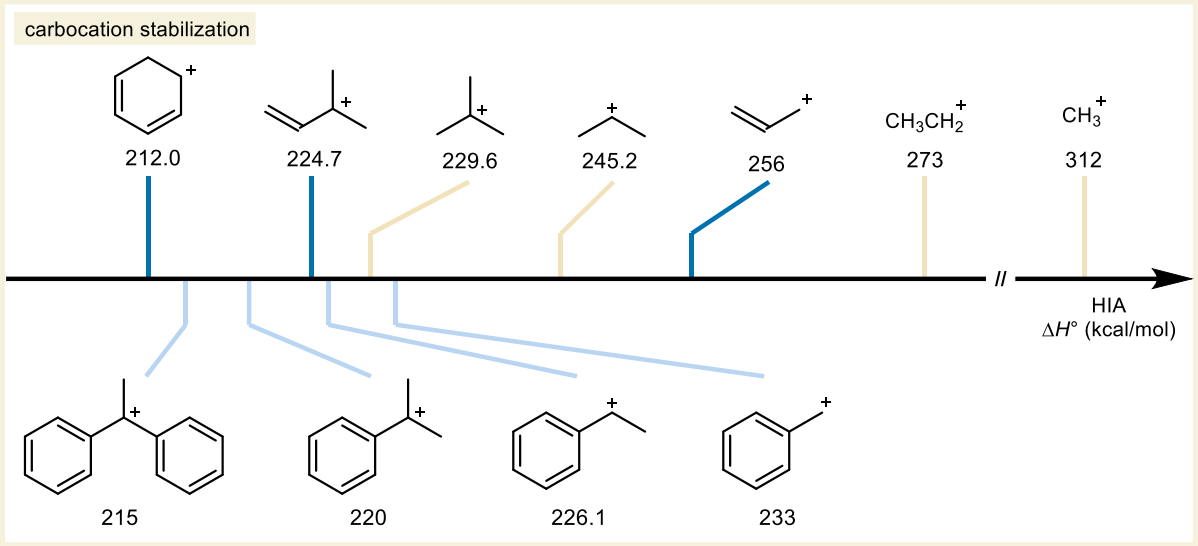

Figure 2.12 The HIAs of selected carbocations: the unstabilized methenium cation, and cations with alkyl stabilization (yellow), alkenyl stabilization (blue), and aryl stabilization (light blue).[187]

The challenge of generating poorly stabilized carbocations can be overcome by installing a nucleofuge with superior leaving group ability. Such a leaving group provides a thermodynamic driving force for the reaction through the formation of a stable by-product. For example, the pyrophosphate leaving group in terpene biosynthesis is stabilized by charge delocalization, and contains strong P–O single and double bonds. Similarly, the formation of a strong Si–O bond can be exploited by the activation of an oxygen-containing leaving group using silylium-ACDC.

2.3.2. *Olefins as Nucleophiles*

Olefins have found applications in a wide variety of reactions, many of which have been recognized as important contributions to the field of organic chemistry, leading to their inventors being awarded the Nobel prize in chemistry. In chronological order, examples of such reactions include: the Diels–Alder reaction (1950); the Ziegler–Natta polymerization (1963);

the asymmetric hydrogenation reactions of Knowles and Noyori, and the asymmetric oxidation reactions of Sharpless (2001); the olefin metathesis reactions developed by Chauvin, Grubbs, and Schrock (2005); and the Pd-catalyzed Heck reaction (2010).

In addition to these milestone applications of olefins, their use has received attention in a number of (asymmetric) C–C bond-forming reactions (Scheme 2.14, top). Examples include the Prins reaction,[110,115,188,189] the carbonyl–ene and imine–ene reactions,[190–192] the inverse electron-demand oxa- and aza-Diels–Alder reactions,[193,194] and the carbonyl–olefin metathesis reaction.[195] These reactions involve the nucleophilic addition of an alkene to a C=O or C=N bond, or an concerted (asynchronous) breaking of multiple π-bonds while forming new σ-bonds. The carbonyl- or imine groups present in these transformations can exert control over the C–C bond-forming step of the reaction by remaining coordinated to the acid catalyst, ensuring its proximity to the site of bond formation. Therefore, a heteroatom moiety can act as a directing group (Scheme 2.14, bottom), which can be a useful quality in asymmetric catalysis. Moreover, positive charge on protonated oxygen and nitrogen atoms is stabilized by resonance effects from the resonant π-bond. Conversely, the nucleophilic attack of an unactivated olefin nucleophile onto a heteroatom-free carbocation features no such directing- or stabilizing groups.

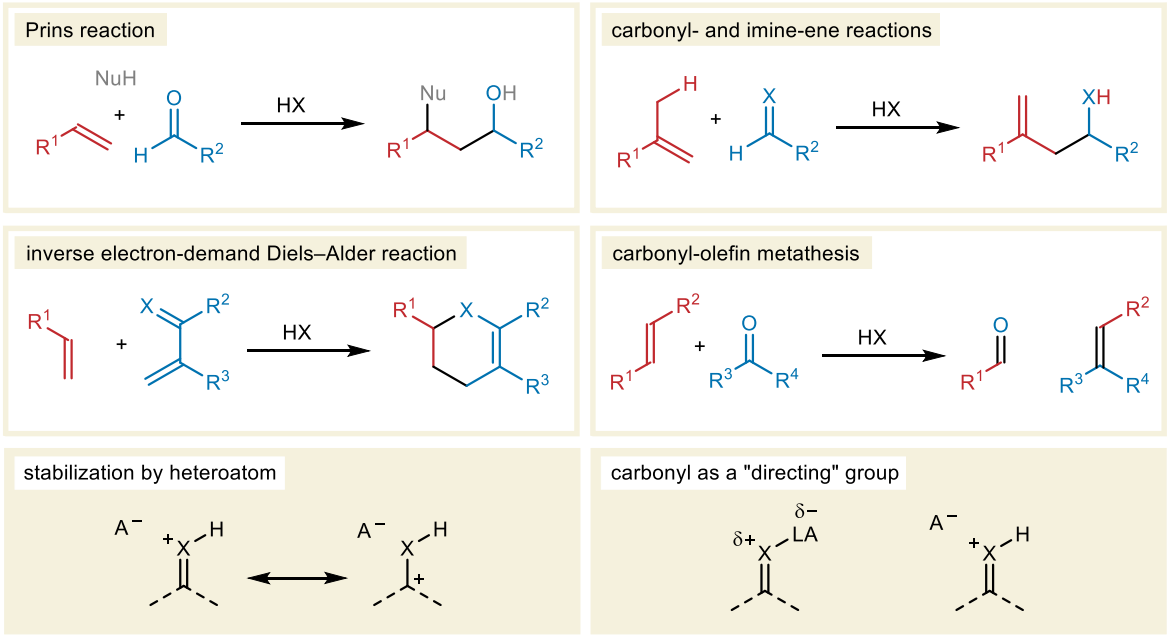

Scheme 2.14 Schematic representation of the Prins; carbonyl–ene and imine–ene; inverse electron-demand Diels–Alder; and carbonyl–olefin metathesis reactions (top), and the stabilizing- and directing group capabilities of carbonyl/imine groups (bottom). X = O, NR.

Olefins are ideal π-nucleophiles in many respects. They are widely available as a primary product of petroleum refining and cracking, and are a likely hub chemical in the

transition to sustainable feedstocks.[196,197] Olefins are often bench-stable, easy to handle, neutral compounds. Conversely, commonly used C(sp^3) nucleophiles such as organometallic reagents (R–MgX, R–Li, etc.) and C(sp^2) nucleophiles (silyl ketene acetals, enamines, metal enolates, etc.) often have to be freshly prepared before use or require several steps to synthesize. Furthermore, the alkene is a versatile functional group that is readily transformed into a plethora of other moieties. However, the lack of directing groups on aliphatic olefins and their poor nucleophilicity (*vide infra*) have led to their infrequent use as nucleophiles in intermolecular asymmetric alkylation reactions.

2.3.3. *Mayr's Reactivity Parameters*

The high electrophilicity of carbocations causes them to undergo nucleophilic addition with most nucleophiles, even weakly nucleophilic olefins. Empirical quantification of the electrophilicity and nucleophilicity of several carbocations and π-nucleophiles has been performed by Mayr (Figure 2.13, A and B).[198–200] The resulting electrophilicity and nucleophilicity scales can provide a sense of the expected reaction kinetics of several electrophile–nucleophile combinations.

The reactivity parameters on Mayr's scales are arbitrarily referenced to the bis(4-methoxyphenyl)methylium cation ($E = 0.00$) and 2-methylpent-1-ene ($s = 1.00$). The scales are logarithmic, *e.g.* methylenecyclohexane ($N = 1.16$) can be expected to react approximately one thousand times faster than 1-hexene ($N = -2.25$) with a given electrophile. The rate constant of a reaction between a given electrophile–nucleophile pair can be derived from the Mayr–Patz equation:

$$\log k_{20\,^\circ C} = s(N + E) \tag{2.5}$$

where N and E represent the nucleophilicity and electrophilicity parameters, respectively, and s is the nucleophile-specific slope parameter, which corrects for steric factors and other relevant interactions. As a general rule, reactions with a $\log k_{20\,^\circ C} < -6$ do not occur at appreciable rates. Furthermore, deviation from linear correlation of the reaction parameters is observed as the diffusion limit (5×10^9 M^{-1} s^{-1}) is approached, leading to unreliable values for $\log k > 8$.

Remarkably, carbocation electrophiles with the highest electrophilicity parameters can be expected to undergo reactions at significant rates even with extremely non-nucleophilic

compounds such as α-olefins. For example, the reaction of the 1-mesitylethan-1-ylium cation (E = 6.04) with 1-hexene, a log $k_{20\,°C}$ of 3.75 is expected. However, reactivity parameter measurements by Mayr most frequently employ BF_4^- salts of the electrophile in stoichiometric quantities under a set of standard conditions. When designing a reaction, differences in concentration, temperature, and solvent inevitably lead to changes in the reaction rate. Most importantly, in a reaction featuring catalytic activation of the electrophile, the maximum concentration of the activated electrophile is dictated by the concentration of the catalyst; a kinetic hallmark of specific acid catalysis. In acid-catalyzed reactions with weakly basic substrates, this necessitates strongly acidic catalysts to sufficiently activate the electrophile and generate significant quantities of the cationic intermediate.

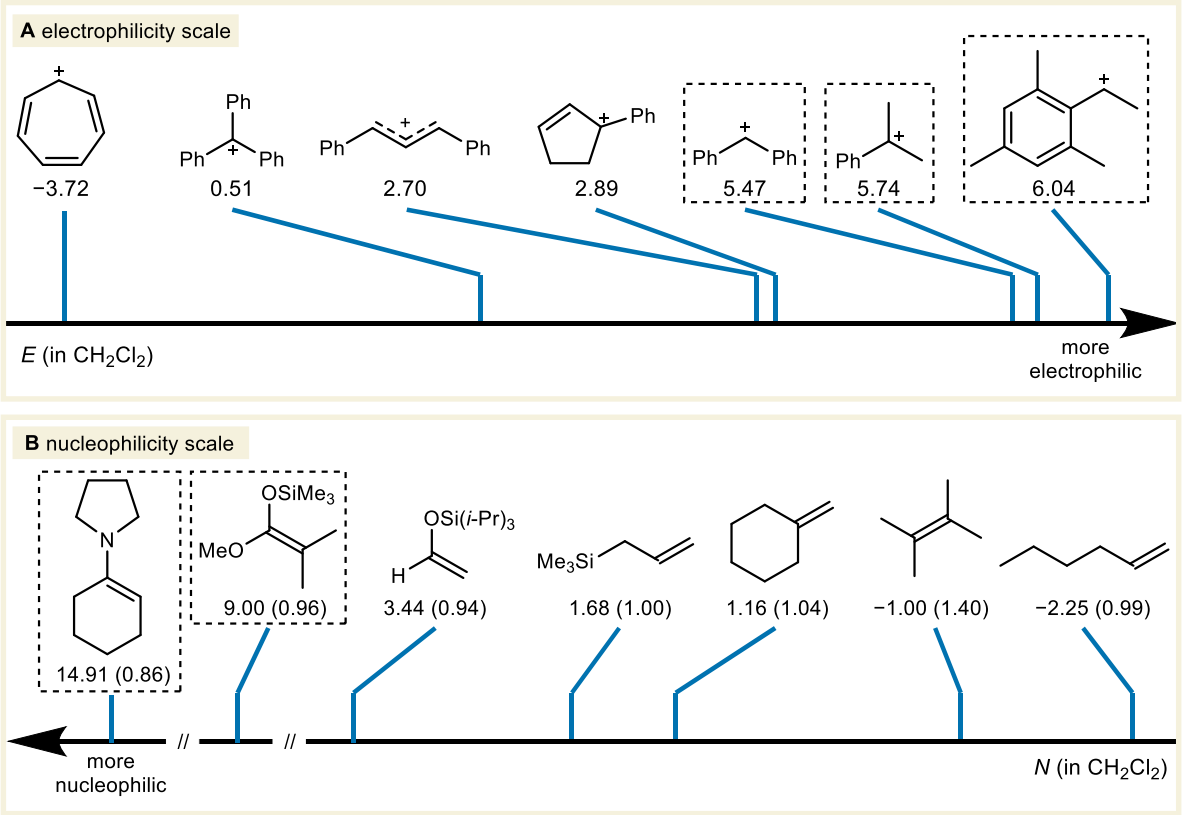

Figure 2.13 Mayr's electrophilicity (A) and nucleophilicity (B) scales. Nucleophile values in brackets represent the nucleophile-specific slope parameter s. Examples of electrophile–nucleophile pairs that react with diffusion control are highlighted in dashed squares.[198–200]

2.4. Alkylation of π-Nucleophiles with Alcohol Derivatives

Over the past decades, various reports have described the alkylation of π-nucleophiles with alcohol derivatives. In these reactions, a carbocation is generated from a substrate containing a C(sp^3)–O bond, often by action of an acid catalyst. The leaving group can be an alcohol, silyl ether, or acetate, which departs from the substrate via heterolytic dissociation. This carbocation is then attacked by the π-nucleophile, forming a C–C bond. Subsequent deprotonation by the conjugate base of the catalyst yields an olefinic product (Scheme 2.15A). Formally, these are substitution reactions where the C–O bond of the electrophile is substituted for a C–C bond, and, depending on the mechanism can be uni- or bimolecular. Epoxides participate in similar heterolysis reactivity, as they also contain C(sp^3)–O bonds. This is a useful generalization when assessing certain polyene cyclizations (*vide infra*).

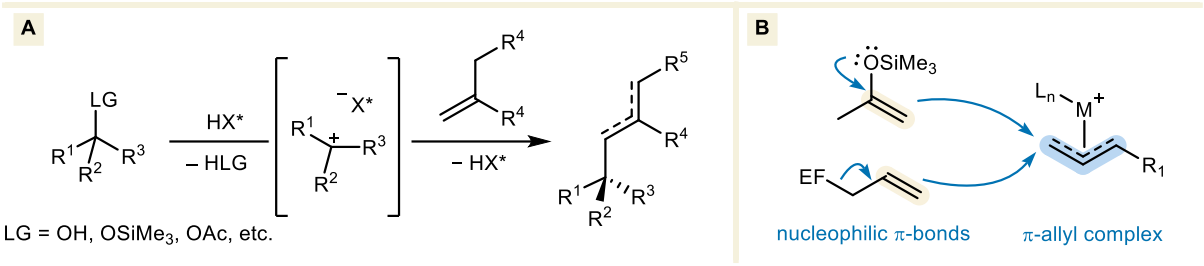

Scheme 2.15 (A) Overview of the acid-catalyzed asymmetric olefin alkylation reaction. (B) Strategies to enhance the nucleophilicity of π-nucleophiles, and stabilize allylic cations by π-allyl complex formation. EF = electrofuge.

To circumvent the challenges that come with the direct alkylation of olefins with alcohol derivatives, two main strategies have been successfully employed (Scheme 2.15B). First, more reactive π-nucleophiles have been leveraged to construct the desired C–C bonds. Examples of such nucleophiles include derivatives of carbonyl compounds— such as *O*-silylated enol ethers or metal-stabilized enolates—and olefins containing a metal or electropositive main group atom (B, Mg, Zn, Si, Sn, etc.) in the allylic position to the nucleophilic alkene moiety. In the latter two cases, the allylic heteroatom acts as a competent electrofuge, enhancing the π-nucleophilic character of the alkene (Figure 2.14B). Second, transition metals have been employed to stabilize an allylic carbocation intermediate, forming a stable π-allyl complex. The formation of a π-allyl complex is a common feature of Tsuji–Trost-type reactivity, in which a Pd π-allyl complex acts as the effective electrophile. In the following sections, notable examples of alkylation reactions of π-nucleophiles with alcohol derivatives that employed these strategies will be discussed, followed by an overview of the known olefin alkylation methodology.

2.4.1. *Intermolecular Alkylation of Allylsilane Nucleophiles*

In a 1982 publication, Cella remarked that there was a gap in the literature for direct "reductive alkylation reactions of carbinols", referring to a form of the C–O → C–C substitution reaction mentioned above. His report disclosed the first non-asymmetric synthesis of hydrocarbons **2.57** by the allylation reaction of benzylic alcohols and benzhydrols (**2.55**) with allyltrimethylsilane **2.56**, mediated by stoichiometric gaseous BF_3 (Scheme 2.16).[201] Interestingly, the authors noted that the olefinic decomposition product in some cases acted as a competent nucleophile, generating the dimeric condensation product. This reactivity foreshadowed the ability of olefins to act as π-nucleophiles in alkylation reactions with alcohol

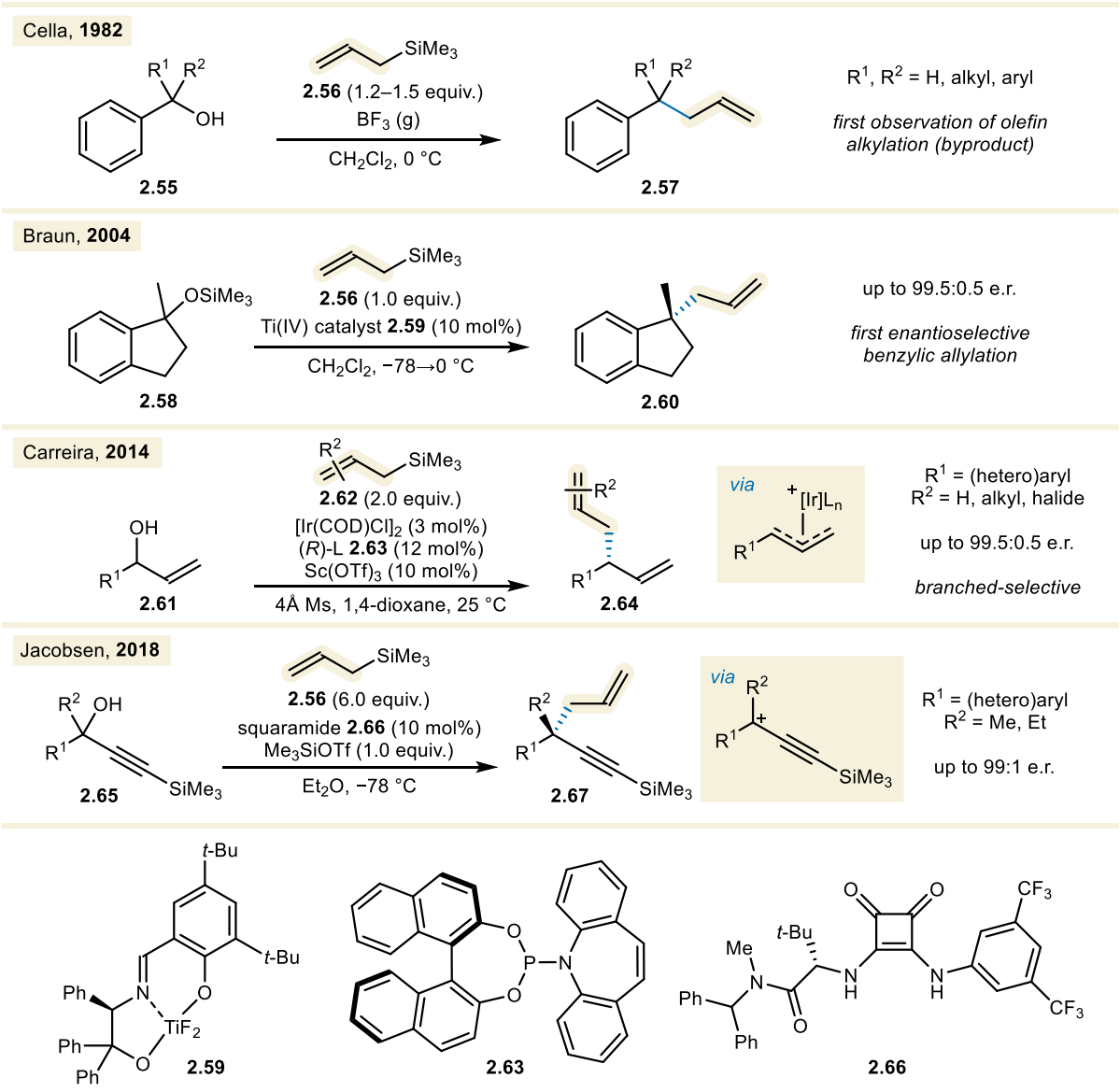

Scheme 2.16 Examples of non-asymmetric and asymmetric intermolecular alkylation reactions of allylsilane nucleophiles with alcohol derivatives. COD = 1,5-cyclooctadiene.

derivatives. Catalytic versions of Cella's method were subsequently developed using a variety of Lewis acids, such as trityl perchlorate,[202] bis(fluorosulfuryl)imide (which is deprotosilylated in the presence of allylsilane),[203] $B(C_6F_5)_3$,[204] $BiCl_3$,[205] $InCl_3/Me_3SiBr$ or $InCl_3/I_2$,[206,207] $[Rh(COD)_2]SbF_6/P(OPh)_3$,[208] and $FeCl_3$.[209,210]

A number of efforts have been made to produce catalytic asymmetric versions of allylations using allylsilanes. In a first example of its kind, Braun used Ti(IV)-based Lewis acid catalyst **2.59** to allylate benzylic silyl ethers **2.58** in a dynamic kinetic resolution, leading to hydrocarbon products **2.60** containing tertiary and quaternary stereocenters with excellent enantioselectivity.[211] A second example came from Carreira, who used Ir-catalysis in conjunction with his phosphoramidite ligand **2.63** to elaborate allylic alcohols **2.61** into the corresponding 1,5-dienes **2.64** with excellent regio- and enantioselectivity.[212] The reaction was initiated by allylic alcohol activation with a $Sc(OTf)_3$ Lewis acid promoter, followed by the formation of an Ir(III) π-allyl complex, a species which is known to yield branched products with high selectivity. The reaction tolerated allylsilanes **2.62** with various substituents. Most recently, Jacobsen published an organocatalytic allylation of tertiary acetates **2.65** using allylsilane **2.56**.[213] In this method, a Me_3SiOTf promoter was employed to generate carbocation intermediates, which were stabilized by an additional alkynyl moiety. In this reaction, chiral squaramide catalyst **2.66** facilitated facial discrimination during nucleophilic addition of the allylsilane, yielding products **2.67** containing a quaternary stereocenter.

2.4.2. *Intermolecular Alkylation of Allylboron Nucleophiles*

Allylboranes and allylboronic esters have been used as π-nucleophiles in alkylations with alcohol derivatives in analogous fashion to allylsilanes (Scheme 2.17). Organoboron compounds can be transformed into the corresponding borate complexes *in situ* by coordination of an oxygen (or other) nucleophile, which greatly enhances their nucleophilicity. The first, non-asymmetric example of an allylboronic ester alkylation reaction was published by the Kobayashi group in 2009. The authors reported a $Ni(PPh_3)_4$- or $Pd(PPh_3)_4$-catalyzed allyl–allyl coupling of allyl carbonates **2.68** and allylboronic esters **2.69** proceeding through Ni- or Pd π-allyl complexes, yielding linear 1,5-dienes **2.70**.[214] One year later, the same group employed InOTf as a simple Lewis acid catalyst to couple 9-allyl-9-borabicyclo[3.3.1]nonane (allyl-9-BBN, **2.72**) to benzylic methyl ethers **2.71**, affording allylated products **2.73**.[215] In a third report, this time on the $Ni(PPh_3)_4$-catalyzed allyl–allyl coupling between allylic alcohols and

allylboronic esters, Kobayashi highlighted a scope entry where the nucleophile contained geminal silane and borane groups. In this reaction, the borane took precedent as the electrofuge in a highly chemoselective transformation yielding the vinylsilane product.[216]

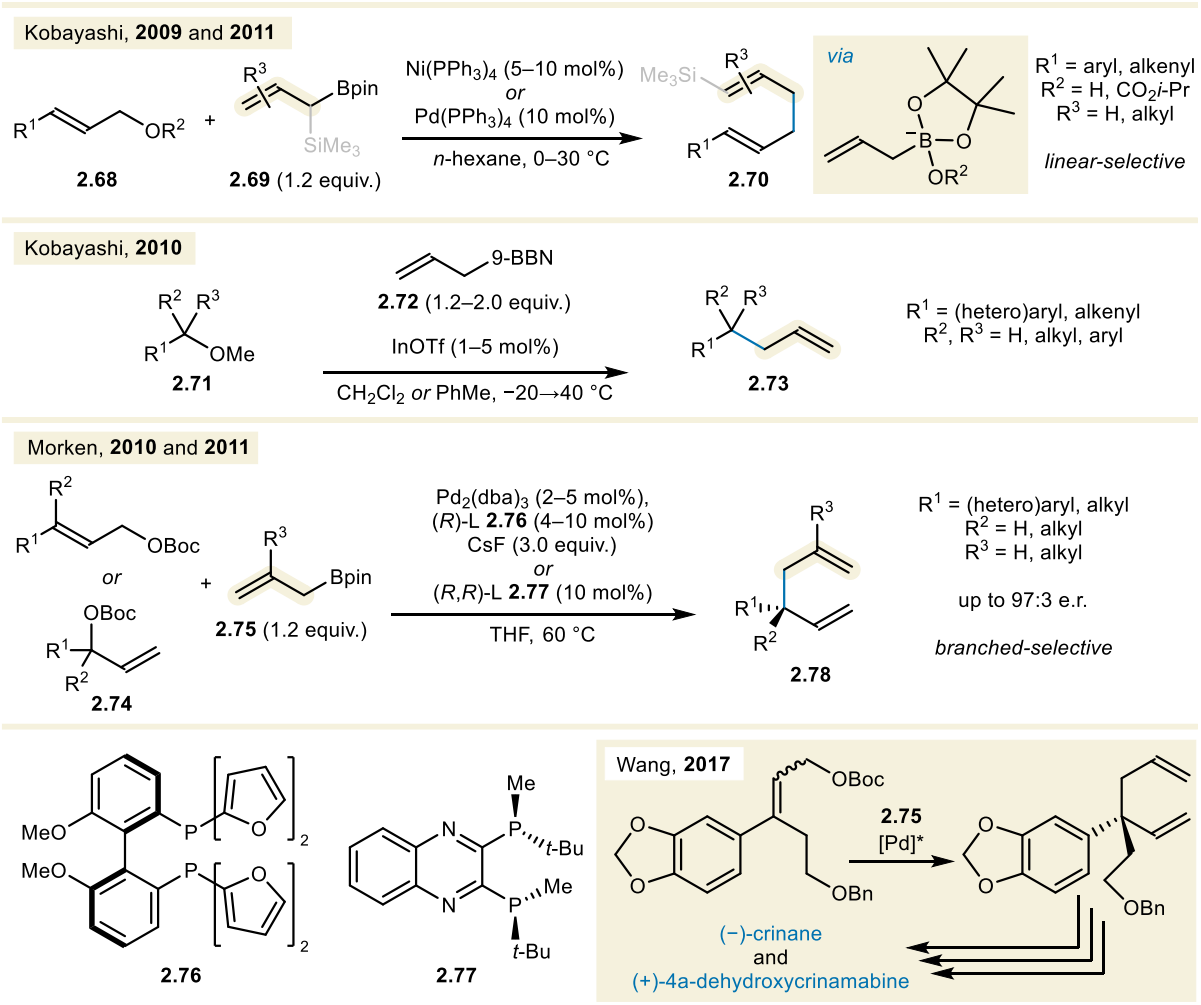

Scheme 2.17 Examples of non-asymmetric and asymmetric intermolecular alkylation reactions of allylborane and allylboronic ester nucleophiles with alcohol derivatives. Bpin = pinacolboryl, 9-BBN = 9-(9-borabicyclo[3.3.1]nonan)yl, dba = dibenzylideneacetone.

Concurrently, the Morken group developed a highly regioselective Pd-catalyzed allyl-allyl cross-coupling chemistry of allylboronic esters **2.75** and *tert*-butyloxycarbonyl (Boc)-protected alcohols **2.74**. Their method provided access to highly enantioenriched 1,5-dienes **2.78** bearing tertiary and quaternary stereocenters using chiral phosphine ligands **2.76** and **2.77**, and showed high regioselectivity for the branched 1,5-diene products.[217,218] This powerful methodology was applied by the Wang group for the installation of a quaternary stereocenter in the key step of their total synthesis of (−)-crinane and (+)-4a-dehydroxycrinamabine.[219] The scope of this Tsuji–Trost-type reaction was later expanded to include esters on the electrophile, and multi-substituted allylboronic ester nucleophiles by Ding and Yang, respectively.[220,221]

Morken later discovered that the reaction occurs in a stereospecific manner with enantioenriched acetate starting materials, supplanting the need for chiral ligands.[222] Another, somewhat niche stereospecific allylation of the tropylium cation was published by Aggarwal in 2017.[223] This reaction proceeded through the addition of phenyllithium to allylboronic esters, generating highly nucleophilic allylboronate intermediates which were alkylated without a catalyst present.

2.4.3. *Intermolecular Alkylation of Other Nucleophiles with Allylic Electrofuges*

Only a few alkylations of allylmagnesium halides (allyl-Grignard reagents) with alcohol derivatives have been reported (Scheme 2.18). First, a report from Yamamoto in 1994 detailed the CuCN•2LiCl-catalyzed allyl–allyl coupling between substituted allylmagnesium chloride reagents **2.80** and allyl diphenyl phosphates **2.79**. 1,5-Diene products **2.81** were obtained with a moderate preference for the branched regioisomer.[224] In a 2001 publication, Bäckvall reported the opposite regioselectivity for a similar, CuBr•SMe_2-mediated allyl–allyl coupling between acetates **2.82** and (γ-alkyl)allylmagnesium chlorides **2.83**, leading to linear 1,5-diene products **2.84**.[225] The authors performed mechanistic studies that provided strong evidence for a Cu(III) π-allyl intermediate in the reaction, in which the Cu center contained three pseudo-equivalent allyl groups.

Enantioselective alkylations of allyl-Grignard reagents with alcohol derivatives remain elusive to this date. However, Feringa reported an enantioselective version of a copper-catalyzed, moderately branched-selective allyl–allyl coupling in 2013.[226] The authors used Cu•SMe_2, ligated by their phosphoramidite ligand **2.87** to couple allylmagnesium bromide **2.86** to allyl bromides **2.85**. Allyl halides are frequently employed in Tsuji–Trost-type reactions, but are generally considered undesirable substrates compared to allylic alcohol derivatives, owing to the relatively low commercial availability and high toxicity of many allyl halide compounds compared to their allylic alcohol counterparts.

A rather unusual nucleophile design was employed by Yorimitsu and Oshima in their 2008 publication on the allyl–allyl coupling between Boc-protected alcohols **2.89** and homoallylic alcohols **2.90**. In their method, the authors described a fragmentation of the tertiary homoallylic alcohol nucleophile after deprotonation of the hydroxy group and coordination to the metal center, forming the ketone as a side product. This fragmentation enhanced

π-nucleophilicity in similar fashion to allylic metal-electrofuges, and allowed for efficient nucleophilic attack onto the *in situ* formed Ni(II) π-allyl complex. This allylation reaction led to linear 1,5-dienes **2.91** with high regioselectivity. Moderate regioselectivities on the nucleophile side were observed when substituents were introduced β to the oxygen atom. Interestingly, homoallylic alcohols bearing a β-silane moiety exclusively underwent fragmentation of the homoallylic alcohol, leading to the vinylsilane products similar to those observed by Kobayashi.[227]

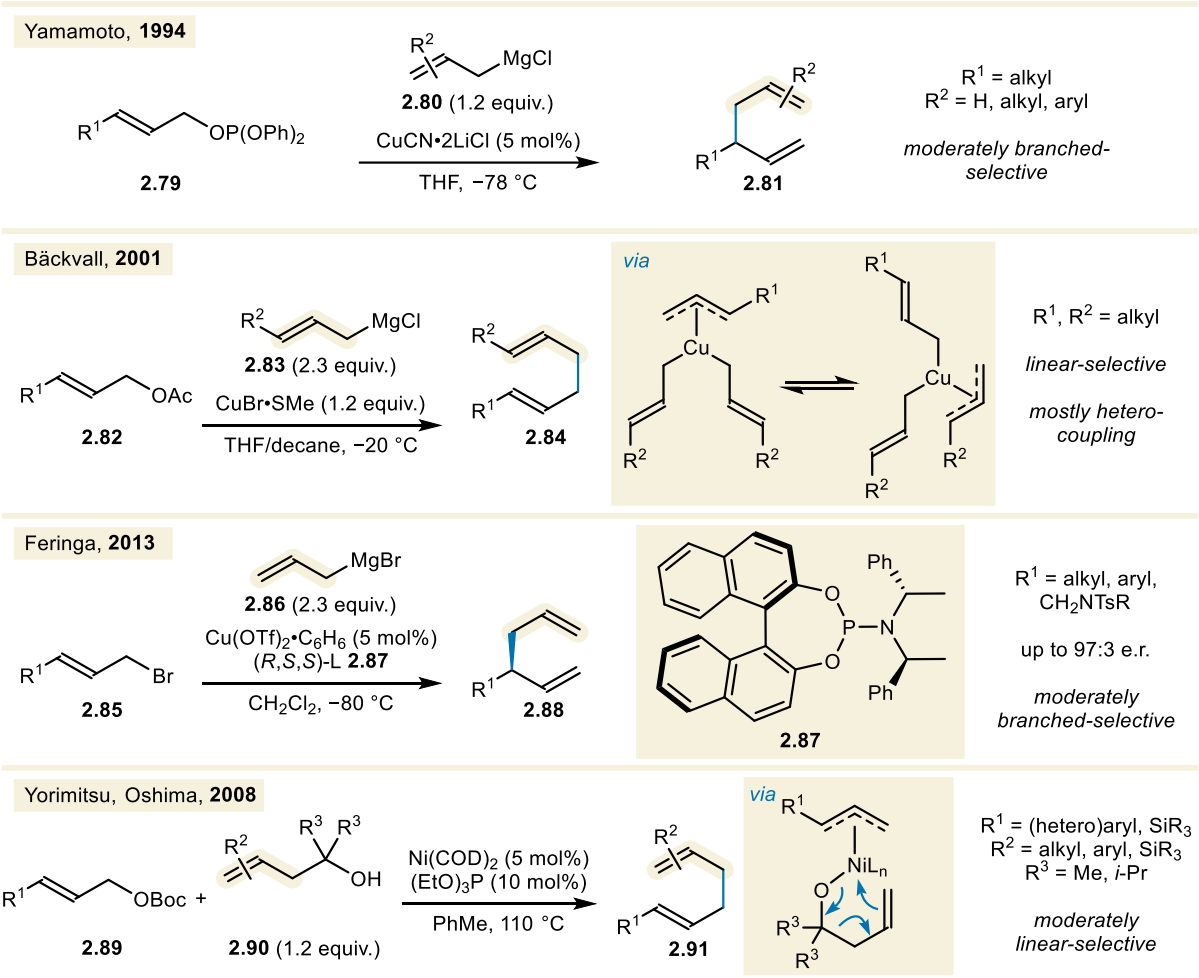

Scheme 2.18 Examples of non-asymmetric and asymmetric intermolecular alkylation reactions of allylmagnesium halide and homoallylic alcohol nucleophiles with alcohol derivatives.

2.4.4. *Intermolecular Alkylation of Enolate and Enol Silane Nucleophiles*

Despite their notably higher nucleophilicity, enolates and enol silanes often react similarly to other π-nucleophiles from a mechanistic perspective. This is especially true for

silylated carbonyl derivatives, which can have analogous reactivity to allylsilanes under (silylium) Lewis acidic conditions.

The best known example of an alkylation reaction of enolates and enol silanes is the Pd(0)-catalyzed Tsuji–Trost allylation, which was initially developed using enamines and 1,3-dicarbonyl compounds as nucleophiles (Scheme 2.19).[228,229] Since its debut, numerous nucleophiles have been coupled to allylic alcohol derivatives in non-asymmetric and asymmetric Tsuji–Trost reactions.[230–233] Asymmetric Tsuji–Trost-type reactivity has been extended to other transition metals that can form π-allyl complexes (*vide supra*). Examples are the Ir-, and Cu-catalyzed reactions from Carreira and Feringa mentioned above. Despite the large number of reports over the decades, this area of research remains active. Recent reports of asymmetric Tsuji–Trost-type reactions have focused on the use of abundant (transition) metals. For example, a report by Stoltz detailed an asymmetric Mo(0)-catalyzed allylation of malonates, leading to the branched products with moderate regioselectivities.[234] Furthermore, branched allylation products of α-benzothiazyl acetamides were obtained by Feng and Liu using Ir/Mg-dual catalysis.[235] These examples serve to illustrate the diversity of Tsuji–Trost-type allylation reactions of carbonyl-derived nucleophiles.

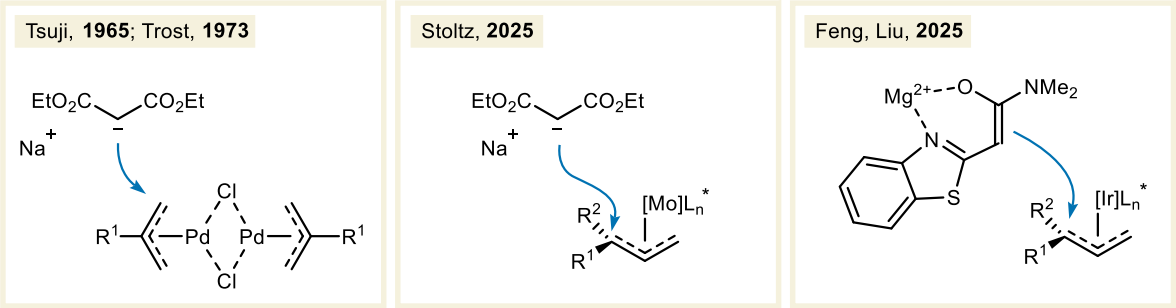

Scheme 2.19 Examples of the reactivity of Tsuji–Trost-type π-allyl intermediates with enolate nucleophiles.

Reports on transition metal-free alkylations of enolates and enol silanes with alcohol derivatives are scarce in comparison to Tsuji–Trost-type reactions proceeding through π-allyl intermediates. Nonetheless, Lewis acid catalysis has successfully been applied in this context, akin to the alkylation reactions of allylsilanes and allylboronic esters (Scheme 2.20). In 2005, Bach reported that benzylic cations generated from benzylic alcohol derivatives by the action of stoichiometric HBF_4 underwent highly diastereoselective nucleophilic attack, leading primarily to *syn* products.[236] The scope of this reaction primarily encompassed heteroarene nucleophiles, making this a Friedel–Crafts reaction. However, one scope entry showed the $ZnCl_2$-mediated alkylation of the trimethylsilyl enol ether derived from acetophenone (**2.93**)

with benzylic acetate **2.92**, leading to the formation of ester product **2.94** with excellent diastereoselectivity. One year later, Baba reported a more general $InCl_3$-catalyzed direct alkylation of 1,3-dicarbonyl compounds **2.97** with allylic alcohols **2.95** and benzylic alcohols **2.96**.[237] The non-symmetrical allylic cations generated through this method showed a preference for the reaction toward linear products **2.98** with moderate regioselectivity. Benzylation led to compounds **2.99** as the sole products of the reaction.

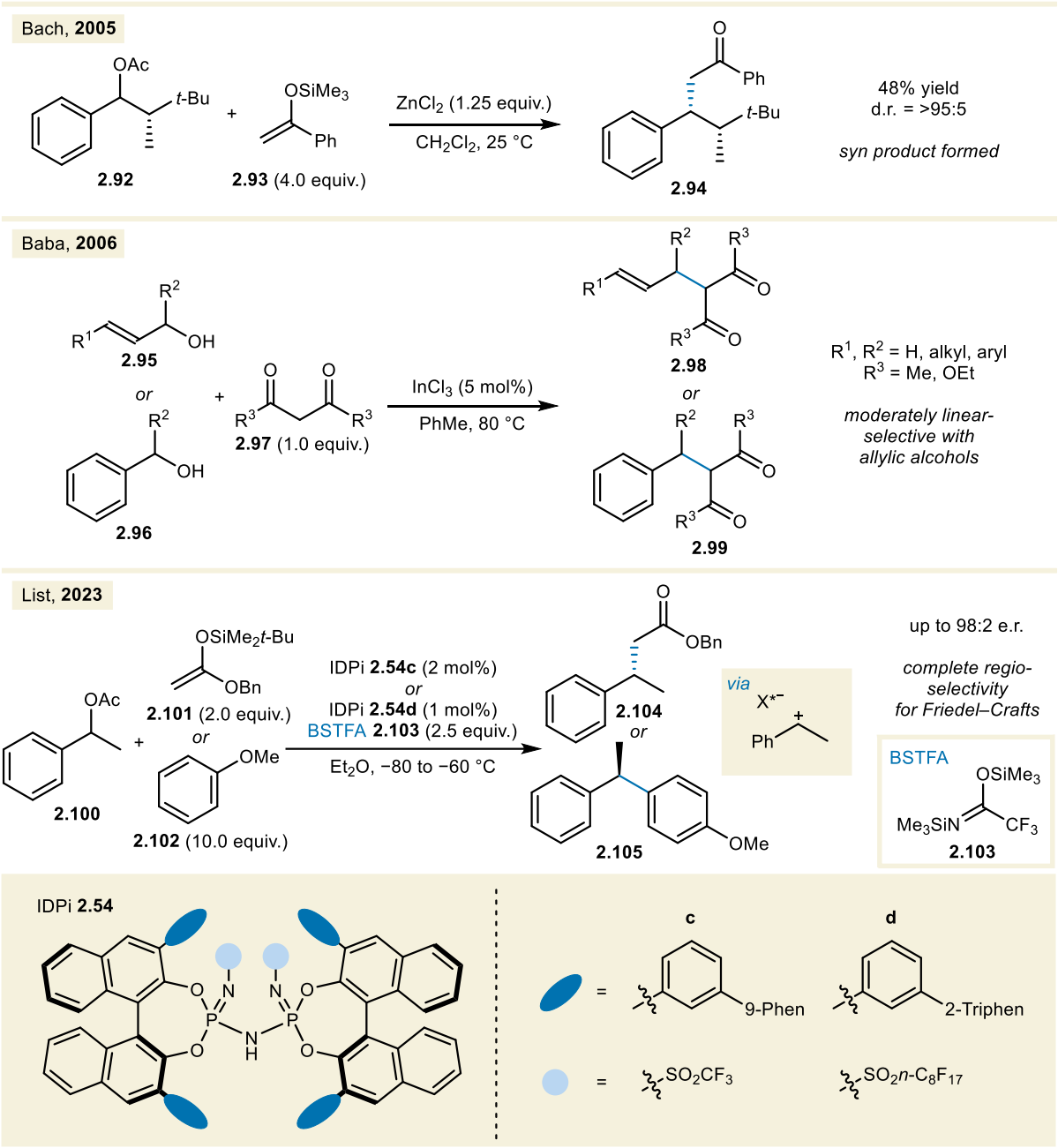

Scheme 2.20 Examples of intermolecular alkylation reactions of enol silane, 1,3-dicarbonyl, and arene nucleophiles with alcohol derivatives. Phen = phenanthryl, Triphen = triphenylenyl.

In 2023, List reported the first asymmetric benzylation reaction of SKA **2.101** and electron-rich arenes **2.102** using silylium-ACDC with IDPi catalysts.[238] Using their method, ester products **2.104** were obtained with excellent enantioselectivities. Furthermore, the use of *N*,*O*-Bis(trimethylsilyl)trifluoroacetamide (BSTFA, **2.103**) as an external silylium source in the Friedel–Crafts alkylation reaction led to the formation of diarylethane products **2.105** with excellent regioselectivities. The authors reported that the lifetime of the benzylic cation was long enough for observation using NMR spectroscopy when 1-(2,4,6-trimethoxyphenyl)ethyl acetate was used as the carbocation precursor, allowing the authors to observe the "naked" benzylic cation paired with the Tf_2N^- anion.

2.4.5. *Biomimetic Polyene Cyclizations*

Biomimetic polyene cyclizations seek to replicate the enzymatic processes at the heart of terpene biosynthesis. A number of biomimetic polyene cyclizations have been reported that employ cascade alkene cyclizations onto epoxide or alcohol-derived electrophiles. These reactions typically occur according to the Stork–Eschenmoser postulate in the absence of a well-defined three-dimensional stereochemical environment akin to enzymatic polyene cyclizations. Furthermore, terminating groups are often used that allow the synthesis of the cyclized products with good chemo- and regioselectivities.

In 1968, Johnson successfully employed an allylic alcohol electrophile in a biomimetic polyene-like cyclization (Scheme 2.21).[239] Activation of the cyclopentenol group of the polyene substrate with trifluoroacetic acid (TFA) resulted in a selective tricyclization reaction, in which a terminal alkene moiety served as the terminating group. The product was obtained with a surprisingly high yield of 30% and nearly complete selectivity for the desired product, which could be elaborated into racemic 16,17-dehydroprogesterone in five additional steps. Similar polyene cyclizations featuring activation of an allylic alcohol by simple Brønsted- or Lewis acids have been published more recently by Qu[240] and Siegel.[241] Qu employed highly stabilized cation intermediates alongside electron-rich arene terminating groups to achieve bi- and tricyclization in a H_2O/hexafluoroisopropanol (HFIP) solvent mixture. Siegel used $FeCl_3$ as a Lewis acid catalyst to substrate activation and selective cyclization, followed by termination with an electron-rich arene moiety to furnish a tetracyclic intermediate in his total synthesis of celastrol.

Substantial contributions to polyene cyclizations of allylic alcohols were made using Carreira's Ir/phosphoramidite catalysis in the presence of an acid promoter. The Ir(III) π-allyl intermediates formed in these reactions are highly reactive toward intramolecular nucleophilic attack by alkene moieties, and show a strong preference for branched product formation. Furthermore, the products are usually obtained with an e.r. >95.5:0.5. In 2012, the Carreira group used this catalytic system in conjunction with a $Zn(OTf)_2$ promoter to catalyze bi- and tricyclizations terminated by various electron-rich (hetero)arene substituents.[242] Development of this strategy allowed the same group to accomplish the enantioselective total synthesis of asperolide C, in which a bicyclic system was formed after termination by an allylsilane moiety.[243] The same catalytic system was applied by the Li group in 2014, in their total synthesis of the highly complex taiwaniadducts B, C and D.[244] These syntheses featured two Ir-catalyzed polyene cyclization steps: one bicyclization terminated by an electron-rich arene, and one tricyclization terminated by a hydroxy group. The same group published a second total synthesis employing Ir-catalyzed tricyclization in 2015.[245] Again, this publication featured a polyene cyclization terminated by an electron-rich arene, this time yielding a tetracyclic intermediate in their synthesis of mycoleptodiscin A.

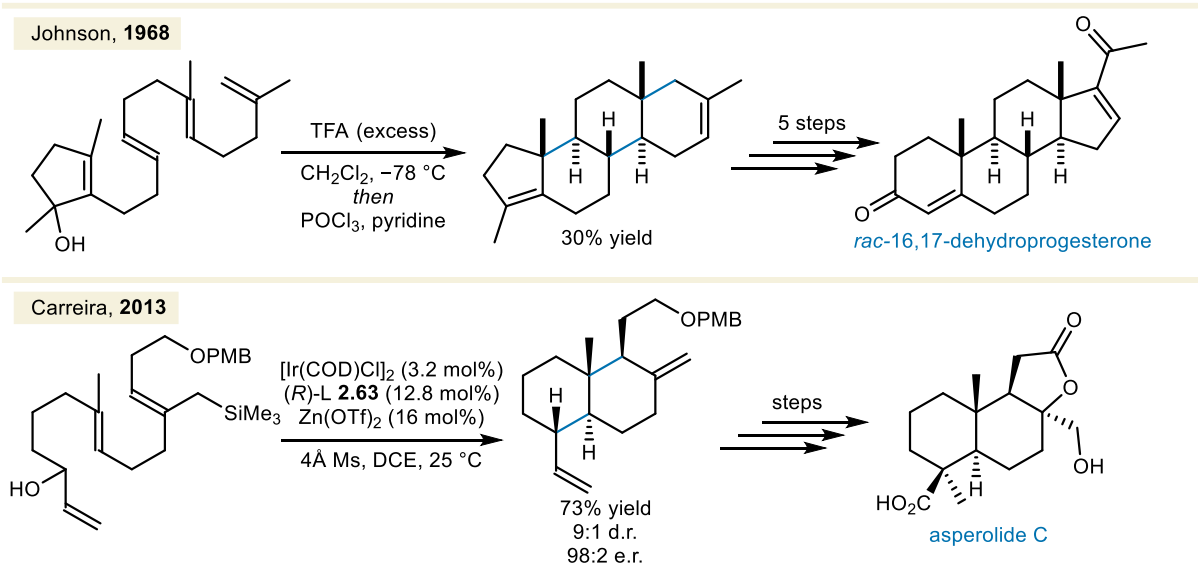

Scheme 2.21 Examples polyene cyclizations featuring allylic alcohol activation. PMB = *p*-methoxybenzyl, DCE = 1,2-dichloroethane.

In the same year as Johnson's seminal publication, van Tamelen reported head-to-tail polyene cyclizations of epoxide compounds in his efforts to elucidate the mechanism of lanosterol biosynthesis.[246] At the time, limited knowledge about the biosynthesis of steroid hormones was available, but the authors made a case for the presence of biological epoxide

intermediates, and provided evidence for their hypothesis by performing analogous Lewis acid catalyzed polyene cyclization reactions starting from epoxides (Scheme 2.22).

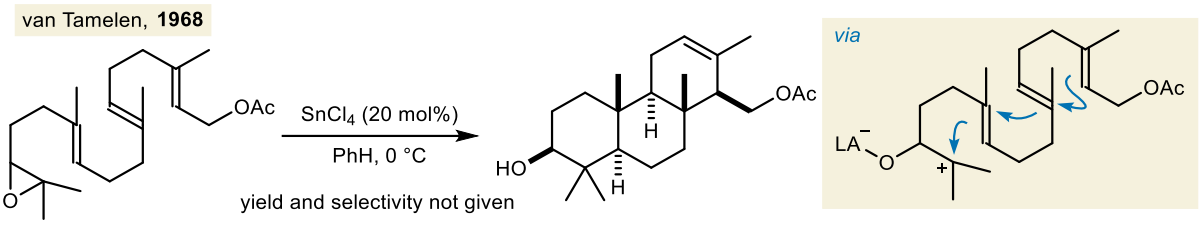

Scheme 2.22 van Tamelen's head-to-tail Lewis acid-mediated epoxide polyene cyclization.

Lewis acid-mediated polyene cyclizations of epoxides received considerable attention from chemists in the following years, but the most significant advances in the head-to-tail polyene cyclizations of epoxides came in the 1990s and early 2000s, when the Corey group published the total syntheses of multiple triterpenoid natural products (Scheme 2.23). In their 1993 synthesis of aegiceradienol and triterpenes derived thereof, a polyene cyclization furnished three 6-membered rings in one step from the epoxide precursor. In this tricyclization, $MeAlCl_2$ was used as the Lewis acid mediator, which served to open the epoxide and generate a carbocation equivalent.[247] The terminating group in this polyene cyclization was a 1,3-diene, which formed an allylic cation intermediate after the final cyclization. After deprotonation, a mixture of two constitutional isomers was obtained that could be selectively consolidated into a single product by HCl/AcOH-catalyzed isomerization. A second tricyclization strategy was employed in the Corey group's 1996 synthesis of dammarenediol II. This synthesis featured a similar $MeAlCl_2$-mediated epoxide opening and threefold cyclization, this time featuring termination by an enol silane. The ketone product of the reaction was elaborated into the natural product in seven additional steps.[248] Analogous tricyclization strategies were employed in their 1997 and 1998 syntheses of scalarenedial and Eocene Messel shale polyprenoids (which both featured tetracyclization steps),[249,250] their 1999 synthesis of aegiceradienol,[251] and their 2008 synthesis of germanicol.[252] In their germanicol synthesis, the authors explored an alternative route to the pentacyclic structure of the natural product, which involved the construction of an electron rich 3,4-dihydronaphthalene moiety as a terminating group. Treatment of this compound with $MeAlCl_2$ led to a mixture of the bi- and tricyclized intermediates, the former of which could be converted to the latter by simple treatment with TfOH. In Corey's 2002 synthesis of (+)-α-onocerin, the authors employed a $MeAlCl_2$-mediated tetracyclization as the final step toward the natural product.[253] (+)-α-Onocerin is a dimeric compound containing two identical bicycles, which the authors leveraged by performing a double epoxide opening of the

symmetrical precursor. The bicyclization that followed featured allylsilane termination to yield the product containing two terminal alkenes.

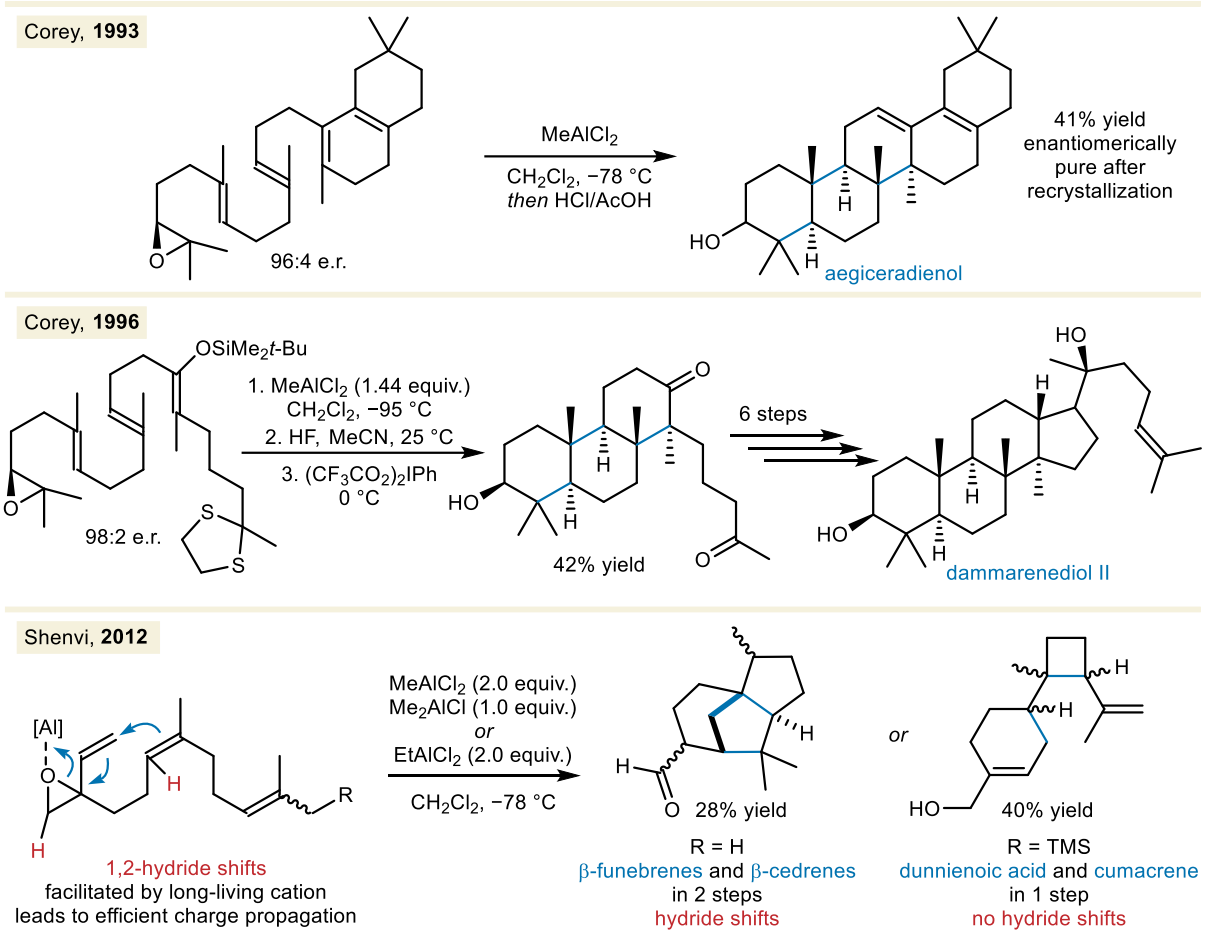

Scheme 2.23 Examples of head-to-tail (Corey) and tail-to-head (Shenvi) polyene cyclizations featuring epoxide activation.

In 2012, Shenvi assessed the selectivity of acid-mediated tail-to-head cyclizations of vinyl epoxides containing alkene- and allylsilane terminating groups upon treatment with a variety of Lewis acids (Scheme 2.23).[254] The authors found that "non-dissociating ligands"—such as Lewis acids that remain bound to the nucleofuge after electrophile activation—promote efficient charge propagation throughout the molecule. Interestingly, this is reminiscent of how the pyrophosphate moiety remains coordinated to the Mg^{2+} center in enzyme-catalyzed terpene cyclizations. The authors speculated that this effect is caused by the inability of the oxygen-associated anion to deprotonate the propagating cation, leading to more complete cyclization products. The best results were obtained using $MeAlCl_2/Me_2AlCl$ to activate the substrate with an alkene terminating group, and $EtAlCl_2$ for the allylsilane terminating group. These conditions were very similar those employed in Corey polyene cyclizations, which provides an explanation

for the high selectivities obtained in Corey's head-to-tail cyclizations toward triterpenoid natural products. Although a mixture of products was obtained using Shenvi's cyclization strategy, a clear preference for a reaction pathway toward a given carbon skeleton was observed based on the terminating group. Termination by an alkene led to β-funebrene and β-cedrene scaffolds containing a *trans*-bicyclo[3.3.0]octane framework. Conversely, allylsilane termination led to dunnienoic acid and cumacrene scaffolds containing vicinal cyclohexane and cyclobutene rings. The total synthesis of these four natural products could be completed from the cyclized intermediates in a small number of steps, yielding the products as mixtures of diastereomers.

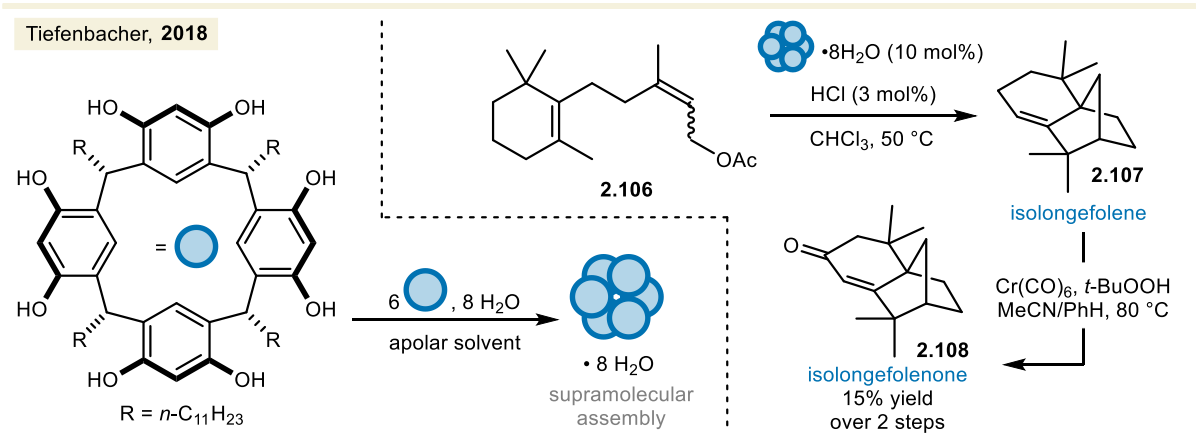

Scheme 2.24 Tiefenbacher's synthesis of isolongefolenone from cyclofarnesyl acetate, catalyzed by a supramolecular assembly.

A number of biomimetic polyene cyclizations have also been performed by the Tiefenbacher group. Their group developed resorcin[4]arenes-based catalysts which formed a supramolecular assembly with water in an apolar medium. These assemblies functioned as capsule-like Brønsted acid catalyst in the presence of substoichiometric HCl, and were employed in the tail-to-head cyclization of cyclofarnesyl acetate (**2.106**) to isolongefolene (**2.107**) (Scheme 2.24). Subsequent allylic oxidation of the product afforded the natural product isolongefolenone (**2.108**) in 15% yield over two steps.[255] Their protocol of supramolecular assembly catalysis has also been applied to a number of other tail-to-head cyclizations.[256] Although cyclization products are often obtained with moderate yields and selectivities, these supramolecular assemblies present an interesting approach to mimicking the reactivity of enzymes. Furthermore, recent work by the Tiefenbacher group has featured supramolecular assemblies which can produce terpenoid products with high enantioselectivities.[257]

The above discussed literature survey of polyene cyclizations is non-exhaustive, as the literature on this topic is vast, and many further activation modes exist. However, it provides an overview of relevant intramolecular activation modes for the alkylation of olefins with alcohol derivatives. Notably, polyene cyclizations through formal hydroalkoxylation reactions have been excluded from our survey. This form of reactivity is not applicable to our system, as demonstrated by the following examples.

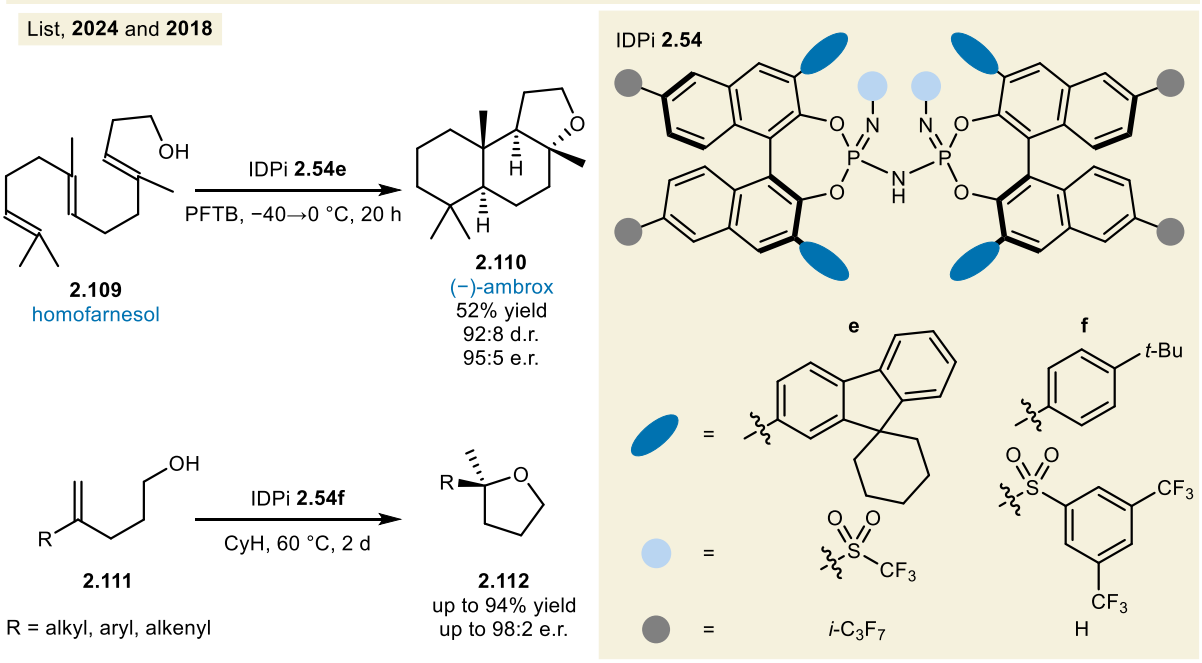

Scheme 2.25 Examples of intramolecular hydroalkoxylation reactions catalyzed by strongly acidic IDPi catalysts.

In 2024, the List group demonstrated that IDPi catalyst **2.54e** catalyzes the asymmetric polyene cyclization of (3*E*,7*E*)-homofarnesol (**2.109**) to (−)-ambrox (**2.110**) (Scheme 2.25).[258] In this transformation, the Brønsted acid catalyst—aided by a perfluorinated alcohol solvent—mimics the action of a class II terpene cyclase. Protonation of the terminal alkene moiety led to a head-to-tail cyclization, which is terminated by the hydroxy group. An analogous monocyclization reaction had been previously explored by the List group in their 2018 publication on intramolecular hydroalkoxylation reactions of olefins **2.111** toward substituted tetrahydrofuran products **2.112** catalyzed by IDPi **2.54f**.[180]

Formally, the hydroalkoxylation reactivity is complementary to the olefin alkylation reaction in some respect. In a hydroalkoxylation reaction, one C–C (π-)bond and one O–H bond are broken, and a C–H bond and C–O bond are formed. Conversely, one C–O bond and a C–H bond are broken during the olefin alkylation reaction, and a C–C (σ-)bond and O–H bond are

formed. Both reactivity types are represented in polyene cyclizations, and the selectivity of the reaction depends on the stability of the intermediates and products. Hence, an adequate driving force (see section 2.3.1) may potentially overturn the above-mentioned hydroalkoxylation reactivity of IDPi catalysts.

2.4.6. *Intermolecular Alkylation of Olefins*

As highlighted in the previous section, many of the reported allyl–allyl couplings with allyl-electrofuge-containing π-nucleophiles employ transition metals to generate transition metal π-allyl complexes in Tsuji–Trost-type reactions. Conversely, benzylations of π-nucleophiles mainly employ Lewis acids to achieve activation of the electrophile. In the latter case, electron-donating substituents are often installed on the arene to stabilize the benzylic carbocation intermediate, while electron poor arenes are poorly tolerated. Friedel–Crafts-type reactions with benzylic alcohol derivatives containing electron donating substituents are especially common in the literature.[259–264] Common stabilized intermediates include quinone methides and 2-indolyl-substituted carbocations. These intermediates aid in substrate activation, and often contribute to higher enantioselectivities through H-bonding to the Brønsted acid catalyst.

Only a handful of olefin alkylation reactions with alcohol derivatives have been published to date. Most known examples employ π-allyl complexes, which can react with olefin nucleophiles through migratory insertion, followed by β-hydride elimination. A first such reaction was reported by Tsukada in 2001, and featured a Rh-catalyzed activation of allyl tosylates (**2.113**), which reacted with styrenes **2.114** to yield primarily linear 1,4-dienes **2.115** (Scheme 2.26).[265] The authors reported that various Pd-based catalysts and Lewis acids were ineffective in this transformation, highlighting the need for efficient cation stabilization in a reaction with such a weak nucleophile. Furthermore, the reaction proceeded without an additional acid promoter, but higher yields were achieved when a substoichiometric allyl iodide additive was introduced. These findings could indicate that the leaving groups of either allylic species formed an acid promoter *in situ*, which could help facilitate leaving group activation. A similar strategy was employed by Jamison and coworkers, in their 2010 and 2011 Ni-catalyzed olefin allylation reactions yielding 1,4-dienes.[266,267] This report focused primarily on the alkylation reactions of light olefins (ethylene, propene) and higher α-olefins. The authors leveraged the high propensity for migratory insertion of Ni(II) π-allyl complexes in their

method. Interestingly, the products of aliphatic olefin allylation were obtained with anti-Markovnikov regioselectivity, whereas the allylation of styrenes led to the formation of Markovnikov products. The authors argued that this regioselectivity originates from steric hindrance between aliphatic residues and the ligand during side-on coordination. The method was compatible with unprotected allylic alcohols and a large variety of allylic alcohol derivatives, including ethers, silyl ethers, acetates and carbonates. The activation of these functional groups was achieved by action of the superstoichiometric Lewis acid promoter Me_3SiOTf. In 2014, de Bruin and Reek published a Pd-catalyzed alkylation of styrenes with allylic alcohols yielding linear 1,4-dienes.[268] This reaction showed mechanistic similarities to the above examples, and featured a catalytic 1,3-diethylurea H-bond promoter to activate the allylic alcohols.

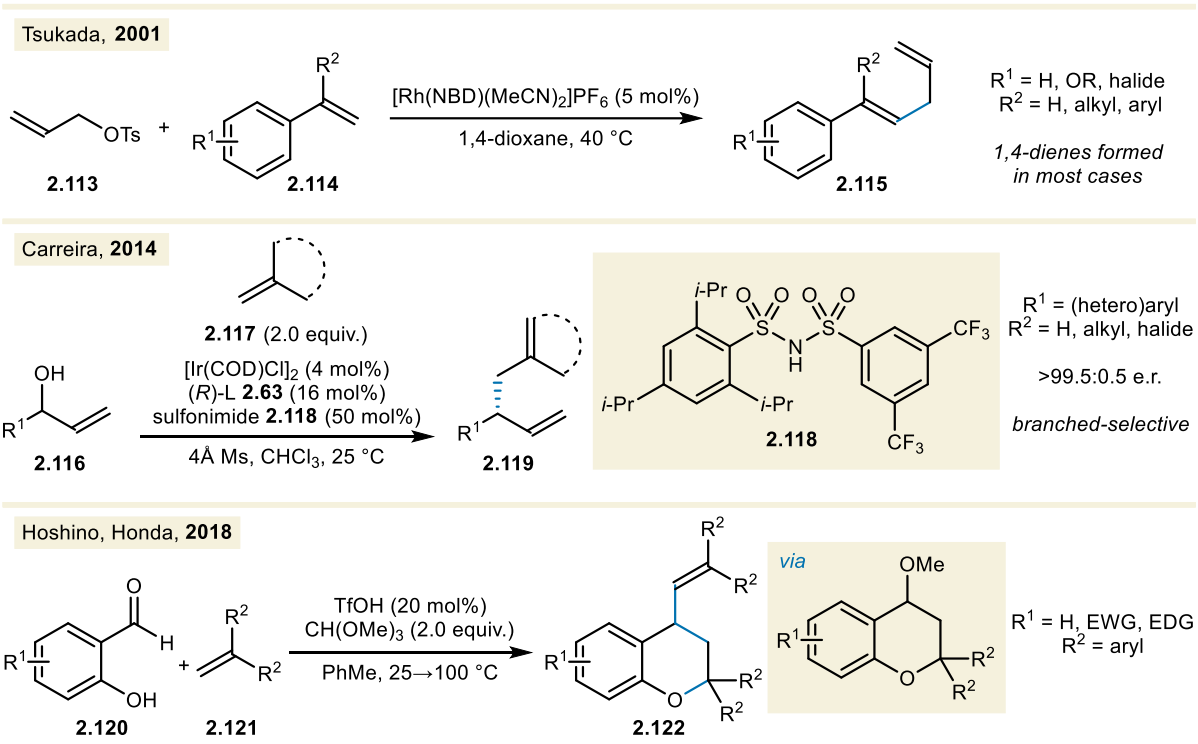

Scheme 2.26 Examples of non-asymmetric and asymmetric intermolecular alkylation reactions of olefins with alcohol derivatives. EWG = electron-withdrawing group, EDG = electron-donating group, NBD = norbornadiene.

To the best of our knowledge, only one intermolecular asymmetric alkylation reaction of olefins with alcohols exists to date. This 2014 method published by Carreira and coworkers used Ir/phosphoramidite catalysis in the presence of a strongly Brønsted acidic sulfonimide promoter (**2.118**) to activate allylic alcohols **2.116**, followed by nucleophilic attack from unactivated 1,1-disubstituted olefins **2.117**.[269] 1,5-Diene products **2.119** were obtained with excellent regio- and enantioselectivities, as was the case for previous methods employing

Ir/phosphoramidite catalysis. The authors employed 4Å molecular sieves (Ms) to scavenge water liberated from the reaction, indicating that the backward reaction might outcompete the addition of the olefin in the presence of water. While the method yielded impressive results, it relied on dual catalysis by and expensive/toxic transition metal and a high catalyst loading of the Brønsted acid promoter. The development of an organocatalytic transformation of this kind could mitigate these drawbacks. Furthermore, the method only tolerated substrates bearing a 1-aryl-substituent on the allylic alcohol, and no additional substituents on the vinyl group. Moreover, the scope of the olefin component was limited to 1,1-disubstituted alkenes.

Asymmetric organocatalytic versions of the olefin alkylation reaction with alcohol derivatives have not yet been reported to the best of our knowledge. Only one example of a non-asymmetric organocatalytic alkylation of 1,1-diarylethylenes **2.121** with silycilaldehydes **2.120** has been reported by Hoshino and Honda in 2018.[270] The method featured a somewhat niche TfOH-catalyzed, $CH(OMe)_3$-mediated inverse electron-demand oxa-Diels–Alder reaction of salicylaldehyde and 1,1-diphenylethylene, leading to the bicyclic methyl ether product. Upon heating of the reaction mixture, activation of the methyl ether occurred, which caused the addition of a second equivalent of **2.121**, yielding products **2.122**. Both reactions proceeded through an *o*-quinone methide-type intermediate by virtue of the electron-donating hydroxy group on salicylaldehyde. Furthermore, $CH(OMe)_3$ served as a dehydrating agent for the equivalent of water released during the reaction. The highly engineered substrates used in this reaction highlight the difficulty in designing organocatalytic alkylation reactions of alkenes with alcohol derivatives, as these systems cannot take advantage of transition metal-stabilization by the formation of a π-allyl complex intermediate.

2.5. Summary and Outlook

The previous subchapters provide an overview of the current state of the art of alkylation reactions of π-nucleophiles. Relevant enzymatic reactions in terpene biosynthesis were highlighted in sections 2.2.4 and 2.2.5, and intermolecular and intramolecular alkylation reactions of π-nucleophiles with alcohol derivatives were discussed throughout section 2.4. Despite the impressive progress that has been made in this field—especially over the last decades—a unifying principle that ties together olefin alkylation reactivity has yet to be established. Olefin alkylations that have been published consistently fall into other categories of reactivity, such as Tsuji–Trost-type reactions and polyene cyclizations. The literature survey

above highlights a gap in the known reactivity of alkenes and alcohol derivatives in the form of a general organocatalytic asymmetric intermolecular alkylation reaction of unactivated olefin nucleophiles with alcohol derivatives.

Our literature survey has also revealed the impressive contributions from the field of organocatalysis to nearly every subsection of the highlighted reactivity. This third pillar of asymmetric synthesis has provided protocols for the synthesis of enantioenriched, biologically relevant compounds, frequently rivaling the reactivity and selectivity of transition metal- and enzyme-catalyzed reactions. Organocatalytic protocols inch ever closer to mimicking the reactivity of natural enzymes, and in some respects already contend with enzymes in terms of substrate generality, reactivity and selectivity.

The recent development of strong and confined acid catalysts by List has greatly increased the chemical space which is accessible by organocatalytic methods. In particular, IDPi catalysts have been shown to facilitate a plethora of previously inaccessible transformation of small, unbiased substrates through ACDC and silylium-ACDC.[108] Due to their strong acidity and ability to act as Lewis acid catalysts, we proposed that IDPi catalysts could be used to facilitate a general catalytic asymmetric olefin alkylation reaction. Our efforts toward this goal will be presented in chapter 4 of this thesis.

3. OBJECTIVES

The goal of this doctoral work is to design an intermolecular organocatalytic asymmetric alkylation reaction of unactivated olefins with alcohol derivatives. As highlighted in the previous chapter, the use of olefins as π-nucleophiles in catalytic reactions with *in situ* generated carbocation equivalents is underrepresented in the literature. Our desired reactivity should deviate from transition metal-stabilized cationic intermediates, and should not employ activating groups on the olefin such as an allylic electrofuge.

Our inspiration for the design of such a reaction is twofold (Scheme 3.1). First, the natural reactivities of IPPS and SQS enzymes, which achieve efficient and chemoselective activation of prenyl pyrophosphates, and facilitate intermolecular reactions of the resulting cations with unactivated olefins with unrivaled selectivity. Second, Braun and Carreira's intermolecular alkylations of allylsilanes and olefins, respectively. These methods achieve the activation of unbiased alcohol substrates using acid catalysis, and delivered hydrocarbon products with high enantio- and regioselectivities.

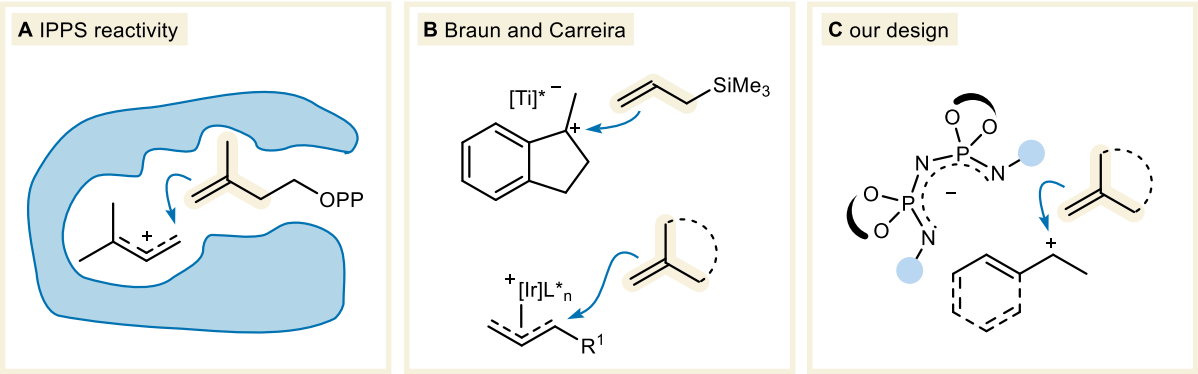

Scheme 3.1 Parallels between IPPS reactivity (A), the intermolecular reactions developed by Braun and Carreira (B), and our reaction design for an IDPi-catalyzed alkene alkylation reaction (C).

Based on literature precedents employing silylated nucleophiles,[211,212,238] we suspected that silylium-ACDC would be well-suited to activate alcohol derivatives. The high oxophilicity of silicon could serve as a strong driving force for electrophile activation, overturning the previously observed hydroalkoxylation reactivity in IDPi-catalyzed reactions of alcohols and olefins.[180,258] Furthermore, capture of the oxygen-containing leaving group by a stoichiometric silylium source would serve to suppress backward reactivity. Alternatively, molecular sieves could be used to capture water liberated after carbocation generation from unprotected alcohols, as demonstrated by Carreira.[269] Molecular sieves have also been shown to be compatible with

IDPi catalysis in Diels–Alder reactions.[271,272] The silylation or removal of water or another oxygen-containing leaving group would also serve to reduce hydration- or hydroalkoxylation side-reactivity.

We envisioned that the strong and confined acids developed by List could serve as a platform for developing an alkylation reaction of alkenes. These catalysts have induced unprecedented reactivity and enantioselectivity in unbiased substrates that were previously inaccessible by any other means.[108] The strong acidity of IDPi catalysts should sufficiently activate alcohol derivatives with minimal stabilization, and we speculated that their confined reactive site could produce enantioenriched hydrocarbon products even in the absence of directing groups on the substrate (Scheme 3.2).

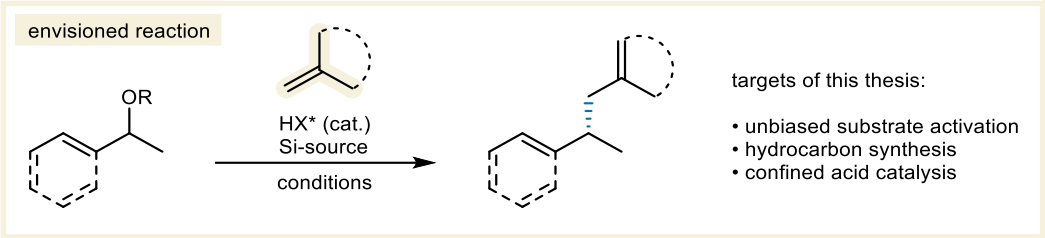

Scheme 3.2 Our envisioned reaction, and the conditions this intermolecular catalytic asymmetric alkylation of olefins with alcohol derivatives should fulfill.

4. RESULTS AND DISCUSSION

This chapter details our investigation of an intermolecular organocatalytic asymmetric alkylation reaction of unactivated olefins with alcohol derivatives. Our efforts encompassed: 1) the identification of a reactive system that could be optimized; 2) the synthesis of catalysts with sufficient acidity to activate C(sp3)–O bonds, while providing the products with high levels of enantioinduction; 3) the exploration of a substrate scope, product derivatization, and the development of a two-step, one-pot olefin alkylation with benzylic alcohols; and 4) experimental studies to probe the mechanism of the reaction.

4.1. Reaction Discovery and Optimization

4.1.1. *Initial Screening of Substrates and Conditions*

We initiated our investigations by studying the reactivity profile of an alcohol and an olefin in the presence of a strong Brønsted acid (Scheme 4.1). We chose 1-phenylethanol (**4.1**) as a model substrate, because the phenyl group provides a UV-active functional handle that is useful for analysis, and the aromatic substituent moderately stabilizes the presumed carbocation intermediate. Methylenecyclohexane (**4.2**) was chosen as the olefin nucleophile, due to its commercial availability, and because it is a 1,1-disubstituted olefin with a fairly average nucleophilicity parameter (N = 1.16) according to Mayr's database.[200] Furthermore, we speculated that the tertiary cation formed upon nucleophilic attack of the alkene might exhibit a strong bias for deprotonation toward internal olefin **4.4**, and forgo the formation of the exocyclic olefin **4.5**. IDPi catalyst **4.3** was selected as a model catalyst due to its high acidity as a consequence of the strongly electron-withdrawing trifluoromethyl substituents on both the 3,3' "wings" of the BINOL backbone and within the sulfonamide "core". The reaction was performed in $CDCl_3$, allowing for facile analysis of reaction mixtures by ^1H NMR spectroscopy.

The crude mixture after this first reaction showed a mixture of newly formed compounds. However, only traces of the desired hydrocarbon products **4.4** and **4.5** were found. Somewhat expectedly, subjecting **4.1** to Brønsted acid catalysis yielded primarily the dehydration products. Ether **4.6** was obtained in 23% yield as a mixture of diastereomers, and traces of styrene (**4.7**) were present. Furthermore, **4.2** was completely converted to the more stable internal olefin **4.8**. The mass balance of the reaction did not add up for all identifiable starting materials and products, leading us to believe that oligomerization of the elimination

by-product **4.7** could have taken place. The addition of 4Å molecular sieves did not facilitate the reaction toward **4.4**, and no conversion of **4.1** was observed. Furthermore, the isomerization of **4.2** to **4.8** was significantly reduced in the presence of molecular sieves, indicating potential de-activation of the acid catalyst.

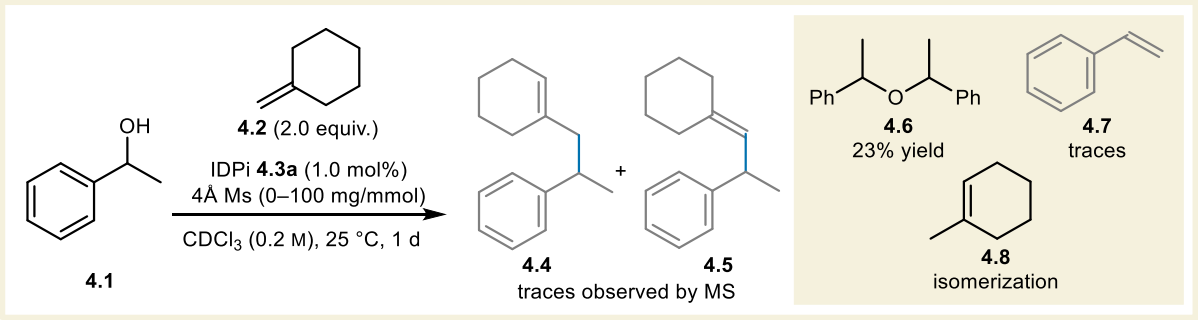

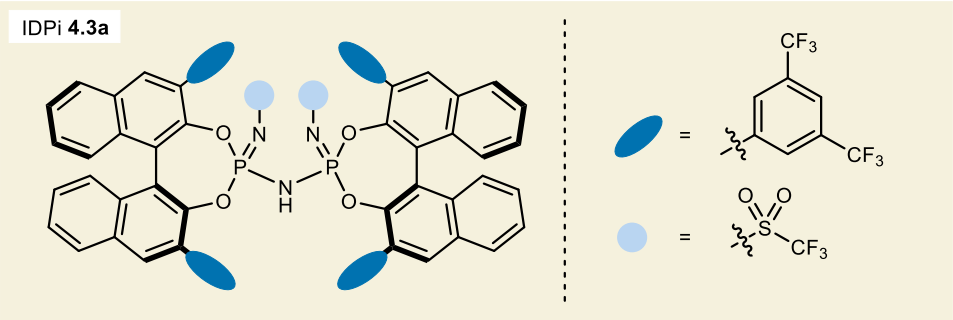

Scheme 4.1 Initial investigation of a Brønsted acid-catalyzed reaction. Yields of all screening reactions in this subchapter are determined by ^{1}H NMR spectroscopy, using mesitylene as an internal standard after reaction quenching with Et_3N. Ms = molecular sieves, M = molar, MS = mass spectrometry.

Next, we investigated whether silylium Lewis acid catalysis could have a positive effect on the reaction outcome by overturning the etherification reaction. BSTFA (**4.9**) was selected as a silylium source, due to its lack of a nucleophilic π-bond. Furthermore, we speculated that *O*-desilylation of the reagent would provide a strong driving force for the deprotosilylation of the catalyst by generating a strong C=O bond. Additionally, we expected negligible nucleophilic character for the expected by-product *N*-(trimethylsilyl)trifluoroacetamide (**4.10**). BSTFA was added as a superstoichiometric reagent, as we anticipated that one equivalent would be used to produce silyl ether **4.11**, after which a second silylation would lead to ion pair formation, alongside $(Me_3Si)_2O$ (**4.12**) as an innocuous by-product (Scheme 4.2).

The reaction afforded desired product **4.4** with a yield of 41%, and a negligible amount of product isomer **4.5**. Substantial formation of **4.7** was also observed, indicating a competing elimination pathway. Isomerization toward **4.8** was negligible under the reaction conditions, confirming our hypothesis that Lewis acid catalysis selectively activates the oxygen-containing

leaving group. The racemate of **4.4** was synthesized using 5 mol% of Tf_2NH instead of the IDPi catalyst, after which analysis of the IDPi-catalyzed reaction by gas chromatography (GC) revealed an e.r. of 63:37 in the reaction containing BSTFA.

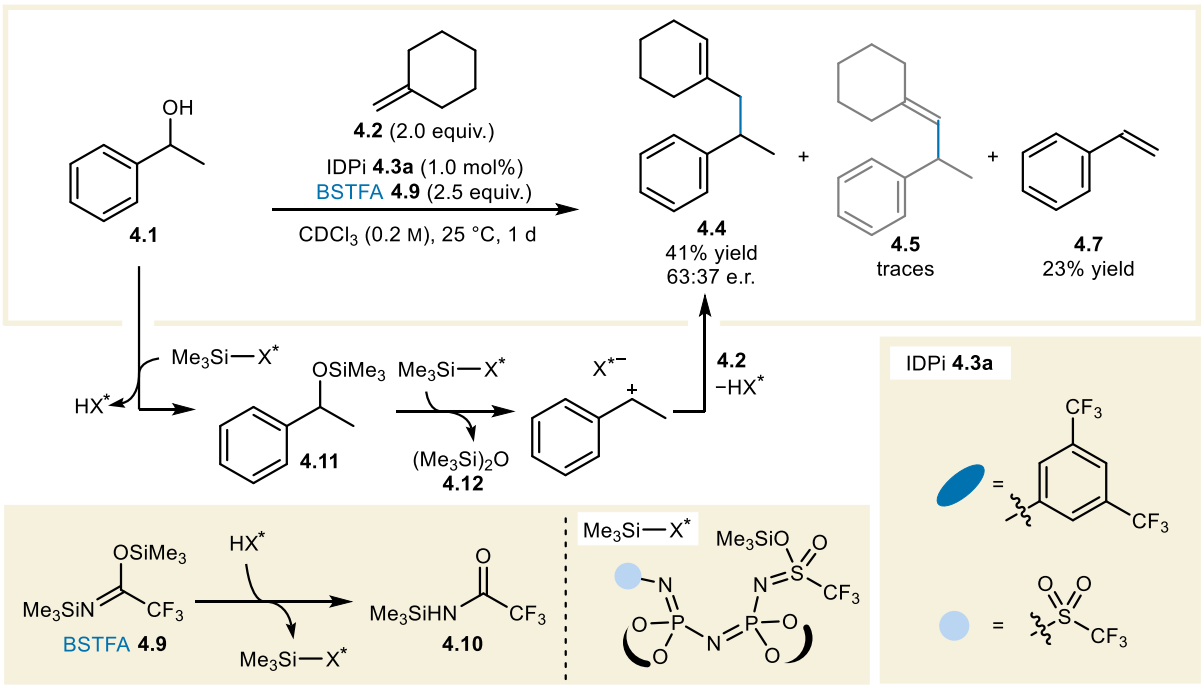

Scheme 4.2 Initial investigation of a Lewis acid-catalyzed reaction.

To gain a sense of the effect of acid catalysts bearing different wing- and core substituents on the reaction outcome, a number of iIDP and IDPi catalysts were applied to the reaction conditions (Scheme 4.3A). We found that iIDP catalysts **4.13a** and **4.13b** were unable to catalyze the reaction toward **4.4**, despite the electron-withdrawing substituents on the wings. IDPi catalysts bearing electron-neutral or moderately electron-rich wings were similarly ineffective in yielding significant quantities of **4.4**. Nevertheless, a small amount of the product was obtained using catalysts **4.3b**–**4.3e**, allowing us to evaluate the enantioselectivity of these reactions. The reaction with catalyst **4.3b** bearing a pentafluorophenyl core yielded less than 5% of the product, demonstrating the importance of the inductive effect of the electron-withdrawing trifluoromethyl core substituent. A significant amount (26–34%) of **4.7** was formed using catalysts **4.3c**–**4.3e**. The lower acidity of these catalysts compared to **4.3a** ostensibly favors the elimination pathway. IDPi **4.3f** provided **4.4** in good yield, and the reaction showed negligible formation of **4.7**. However, the resulting hydrocarbon product was obtained as a racemate, indicating an unfavorable effect of polar substituents on enantioinduction. Of the assessed catalysts, only **4.3e** led to a modest increase in enantioselectivity. However, this came

at the cost of a near complete loss in yield, prompting us to continue screening catalysts with substitution patterns similar to **4.3a**.

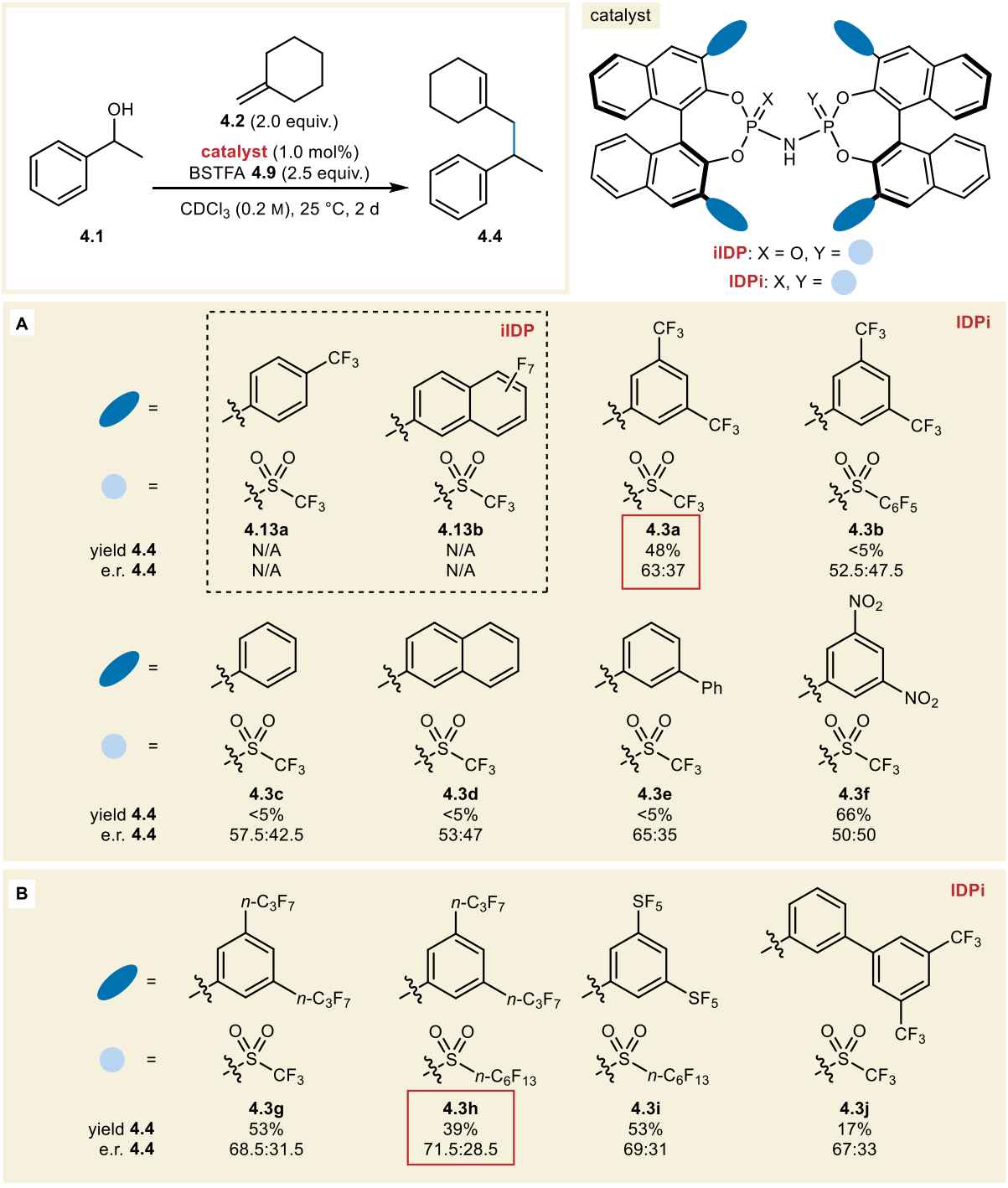

Scheme 4.3 Initial screening of iIDP and IDPi catalysts (A), followed by screening of IDPi catalysts bearing perfluorinated substituents (B) for the model olefin alkylation reaction. N/A = not applicable.

A number of IDPi catalysts bearing perfluorinated substituents on the wings were evaluated (Scheme 4.3B). These reactions led to the formation of **4.4** in modest to good yields. IDPis **4.3g** and **4.3h** demonstrated that the introduction of longer *n*-perfluoroalkyl substituents

on the wing and in the core substantially increased the enantioselectivity, as did the introduction of 3,5-bis(pentafluorosulfanyl)-substituents in **4.3i**. IDPi **4.3j** performed only marginally better than its non-perfluoroalkylated analog, **4.3e** in terms of yield and enantioselectivity.

Next, solvent effects were evaluated in the presence of IDPi **4.3a** (Scheme 4.4A). Screening several solvents revealed that non-polar solvents such as cyclohexane (CyH) and methylcyclohexane (CyMe) led to an increase in enantioselectivity, while more polar solvents such as Et_2O and MeCN provided decreased enantioselectivity, or were wholly unsuitable as reaction mediums. We chose CyMe as the reaction solvent for further screening, because of its low melting point compared to CyH.

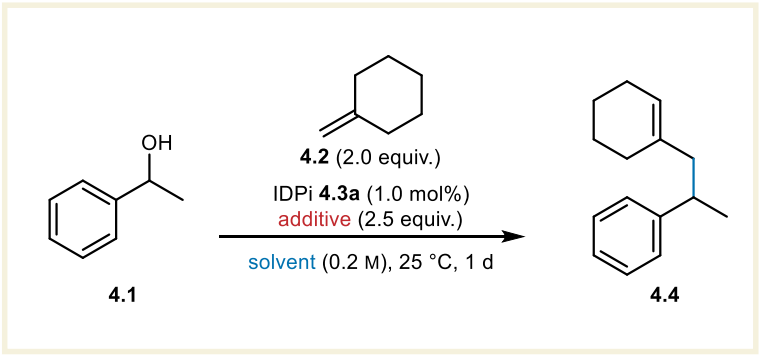

A

entry[a]	solvent	yield **4.4**	e.r. **4.4**
1	CH_2Cl_2	63%	58:42
2	PhMe	49%	59:41
3	Et_2O	35%	57:43
4	MeCN	<5%	N/A
5	CyH	39%	66:34
6	CyMe	43%	66:34

B additive[b]

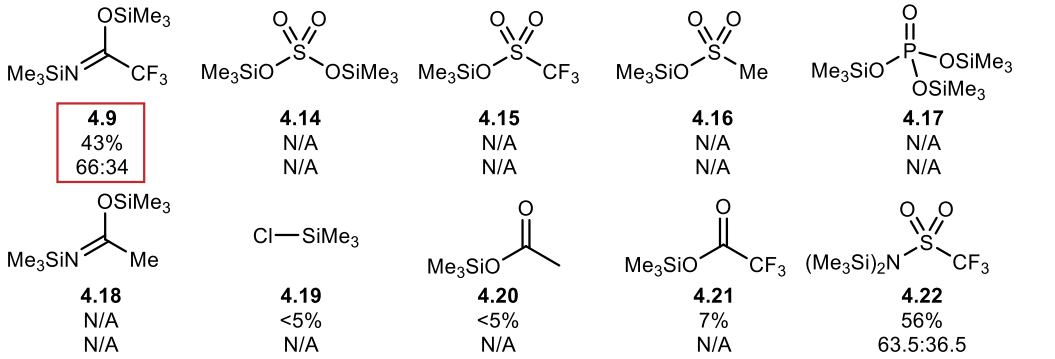

	4.9	**4.14**	**4.15**	**4.16**	**4.17**
yield **4.4**	43%	N/A	N/A	N/A	N/A
e.r. **4.4**	66:34	N/A	N/A	N/A	N/A

	4.18	**4.19**	**4.20**	**4.21**	**4.22**
yield **4.4**	N/A	<5%	<5%	7%	56%
e.r. **4.4**	N/A	N/A	N/A	N/A	63.5:36.5

Scheme 4.4 Screening solvents (A) and silylating agents (B) for the synthesis of **4.4** with catalyst **4.3a**. [a]With BSTFA. [b]in CyMe.

Various commercially available non-nucleophilic silylating agents were tested under the reaction conditions to assess their performance compared to BSTFA (Scheme 4.4B). Use of silylating agents **4.14**–**4.18** did not lead to appreciable product formation. Complete decomposition of the starting material was observed with trimethylsilyl sulfonates **4.14**–**4.16**. A small amount of **4.4** was observed with trimethylsilyl chloride (**4.19**) as the silylating agent. However, the reaction led to the formation of a complex mixture. Reactions with trimethylsilyl acetate (**4.20**) and trimethylsilyl trifluoroacetate (**4.21**) produced a small amount of **4.4**, and a significant amount of silyl ether **4.11**, indicating low potency of these silylating agents

compared to BSTFA. The reaction with *N*,*N*-bis(trimethylsilyl)-trifluoromethansulfonamide (**4.22**) yielded the hydrocarbon product with a significant yield of 56%. However, the higher yield came at a cost of a moderate loss of enantioinduction, and the moisture-sensitive nature of the reagent compared to BSTFA led us to proceed with the latter in further screenings.

Evaluating the e.r. of **4.4** in reactions with catalysts bearing progressively longer perfluoroalkyl chains on the wings (**4.3a**, **4.3k** and **4.3g**) revealed an optimal chain length of two carbons for these substituents (Scheme 4.5). Interestingly, longer chain core substituents led to a slight decrease in the enantioselectivity in CyMe, as we observed a higher e.r. with IDPi **4.3g** than with **4.3l** and **4.3h**. This trend was the inverse of our findings in $CDCl_3$, where longer core substituents led to a slight increase in enantioselectivity.

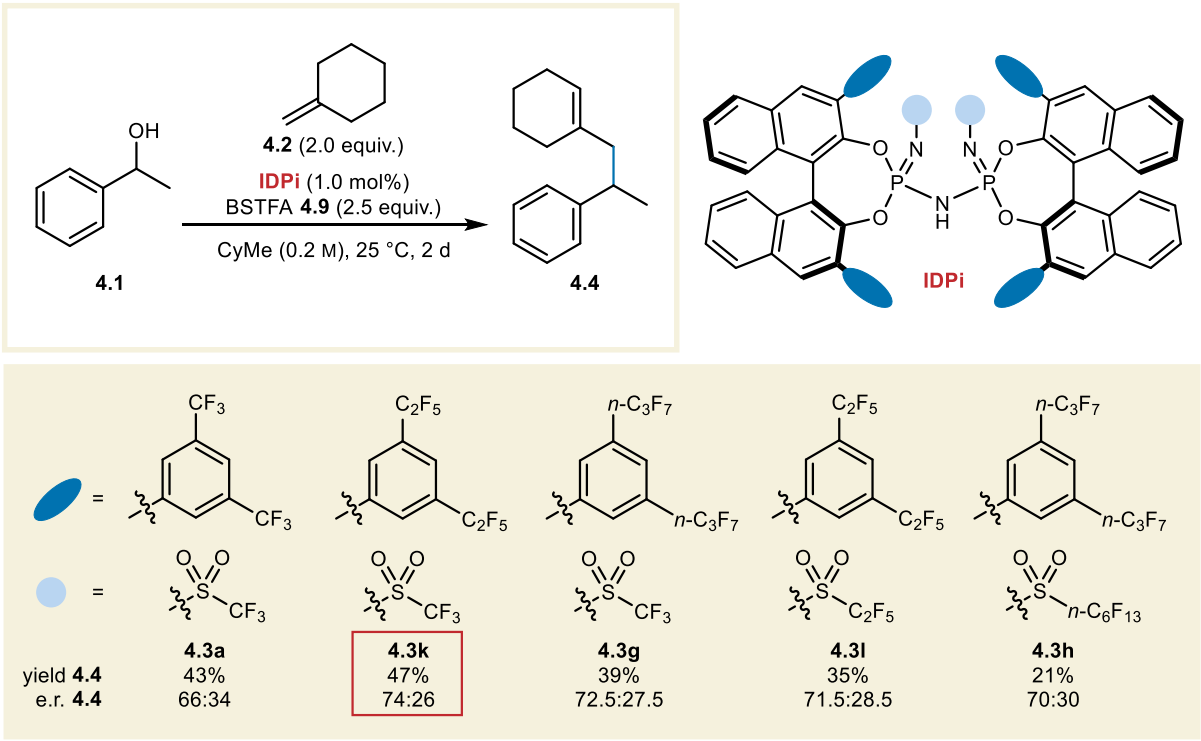

Scheme 4.5: Screening of perfluoroalkylated IDPi catalysts.

4.1.2. *Temperature Effects and Substrate Screening*

The temperature sensitivity of the model reaction was investigated to establish whether a lower reaction temperature could lead to significant gains in enantioselectivity without the loss of reactivity (Scheme 4.6A). Significant product formation was observed at temperatures down to 0 °C, albeit with a substantial loss in yield. Reactions at and below −20 °C afforded

only traces of **4.4**, and at −60 °C, no measurable product was formed. Reliable measurements of the e.r. of **4.4** could be performed down to −40 °C, revealing that the enantioselectivity of the reaction strongly depended on the temperature. We hypothesized that the shutdown in reactivity at lower temperatures could be a consequence of the weak basicity and sterically encumbered nature of silyl ether intermediate **4.11**. These factors combined might hinder activation of the intermediate by obstructing the approach of the silylated catalyst. This decreased reactivity at lower temperatures impeded our ability to take advantage of beneficial temperature effects. We speculated that this obstacle could be overcome by installing a suitable leaving group containing a more Lewis basic, less sterically hindered activation site.

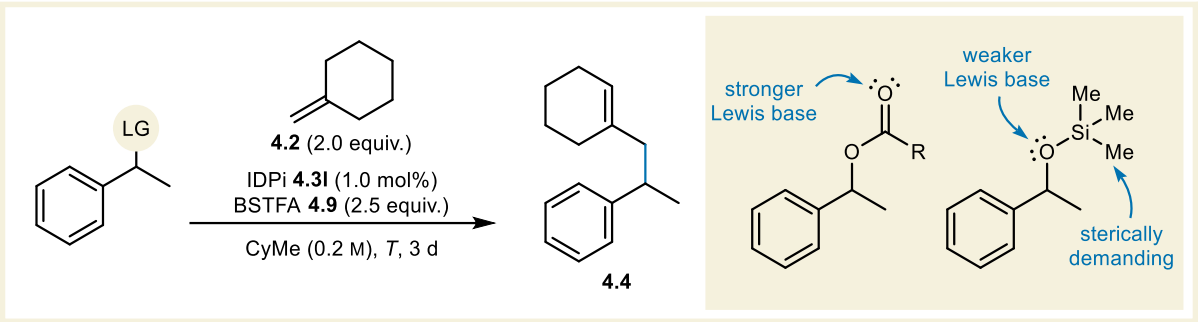

A

entry[a]	*T*	yield **4.4**	e.r. **4.4**
1	25 °C	43%	66:34
2	0 °C	23%	69:31
3	−20 °C	<5%	74:26
4	−40 °C	<5%	78:22
5	−60 °C	N/A	N/A

B

entry[b]	LG =		yield **4.4**	e.r. **4.4**
1	OH	**4.1**	N/A	N/A
2	OAc	**4.23**	42%	89.5:10.5
3	OCO_2Me	**4.24**	68%	90:10
4	OBz	**4.25**	<5%	92:8
5	OC(O)*n*-Bu	**4.26**	74%	88.5:11.5
6	OPiv	**4.27**	<5%	88:12
7	$OC(O)CF_3$	**4.28**	N/A	N/A
8	$OC(O)CCl_3$	**4.29**	<5%	50:50
9	$OC(NH)CCl_3$	**4.30**	61%	81:19

Scheme 4.6: Screening different temperatures for the model reaction with the free alcohol substrate (A), and screening different leaving groups at −60 °C (B). [a]with **4.1**. [b]at −60 °C.

A number of alcohol derivatives were screened at −60 °C to test this hypothesis (Scheme 4.6B). Compared to the free alcohol, reactions using ester leaving groups led to significant formation of the desired product. Acetate **4.23** delivered hydrocarbon **4.4** in 43% yield, and with a significantly improved e.r. of 89.5:10.5. An even higher yield of 68% and a somewhat improved e.r. of 90:10 were observed with methylcarbonate **4.24**. Low conversion was observed with benzoate **4.25**, and the reaction yielded only a minor amount of **4.4**, reflecting its decreased basicity compared to the acetate.[183] However, an even higher e.r. of 92:8 was observed, indicating that the leaving group influenced the stereoselectivity of the reaction to some extent. Valerate **4.26** performed similarly to the methylcarbonate in terms of yield, but the product was obtained with a slightly reduced e.r. of 88.5:11.5. Pivaloate **4.27** yielded a trivial amount of **4.4**,

possibly a consequence of the sterically encumbered nature of the leaving group. The enantioselectivity of the reaction with **4.27** was also significantly reduced compared to the other ester substrates, potentially due to unfavorable steric interactions with the catalyst. Reactions with trifluoroacetate **4.28** and trichloroacetate **4.29** both led to negligible product formation. A reliable value could not be obtained for the enantioselectivity of the former reaction. However, the latter substrate yielded the product as the racemate, possibly due to background reactivity catalyzed by the trichloroacetic acid by-product. Finally, the reaction with trichloroacetimidate **4.30** led to a good yield of **4.4**, albeit with a reduced e.r. of 81:19, possibly due to the polarizing effect of the leaving group on the overall reaction mixture, which could unfavorably affect ion pairing between the catalyst anion and the cation intermediate.

Interestingly, parasitic elimination pathway toward **4.7** was negligible at −60 °C in the reaction employing all of the above derivatives of **4.1**. We therefore speculated that formation of the C–C bond by nucleophilic attack of the alkene is kinetically favored, allowing us to convert these alcohol derivatives to the desired product cleanly at low temperatures. We decided to continue our screening efforts with acetate **4.23**, as it delivered the desired hydrocarbon product with a promising yield and enantioselectivity. The acetate is a particularly attractive leaving group due to its facile synthesis from the alcohol and Ac_2O in the presence of catalytic 4-(dimethylamino)pyridine (DMAP) or catalytic acid (Scheme 4.7, right).[273]

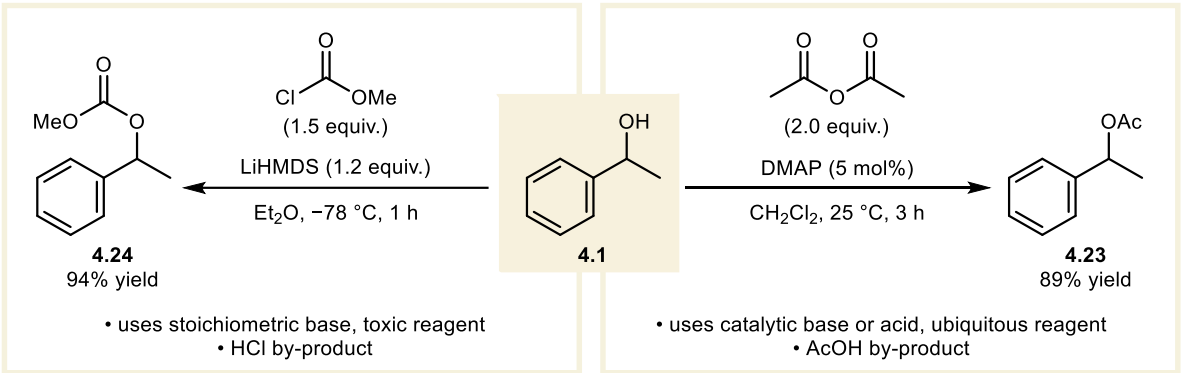

Scheme 4.7 Synthesis of methylcarbonate (left) and acetate (right) derivatives of alcohols.

Conversely, the synthesis of methylcarbonates requires the toxic and sensitive reagent methyl chloroformate alongside a stoichiometric base, and generates HCl as a byproduct (Scheme 4.7, left). We envisioned that the innocuous by-products of acylating reagents such as Ac_2O (AcOH by-product) and isopropenyl acetate (acetone by-product) could provide an opportunity for the development of a one-pot process toward hydrocarbon product **4.4**, starting from the alcohol. Our efforts toward such a process will be described in section 4.3 of this thesis.

4.1.3. *Fine-Tuning of the IDPi Catalyst*

Early efforts to fine-tune the IDPi catalyst structure included the synthesis of perfluoroethyl-substituted catalyst **4.3l**, which indicated a key role for the electron-withdrawing groups in the wings in the enantioinduction of the model reaction. Due to the privileged nature of derivatives of IDPi **4.3a** in the model reaction, we considered various modification sites of this catalyst motif. The highly substituted wings of **4.3a** present a challenge for catalyst optimization: if both *m*-positions are dedicated to a perfluoroalkyl substituent, only the *p*-position would be available for the installation of a functional group that could positively affect the reaction outcome (Figure 4.1A). The *o*-positions of confined acid catalysts are typically unsuitable for derivatization, due to the high steric demand of *o*-substituents. While these steric effects are often beneficial in CPA catalysis—as has been demonstrated by the success of TRIP (*vide supra*)—the dimerization of the BINOL motif during IDPi synthesis is impeded by this high steric demand. Consequently, only a few IDPi catalysts bearing *o*-substituents have been reported to date.[118]

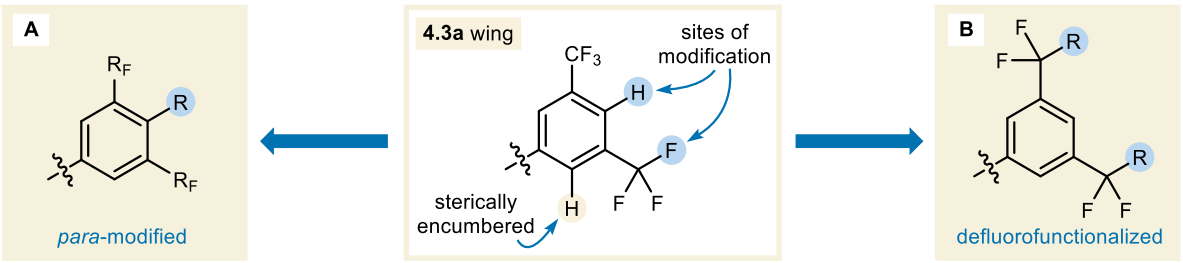

Figure 4.1 Assessment of modifiable sites in the structural motif of IDPi **4.3a** by *p*-substitution (A) and defluorofunctionalization (B). R_F = perfluoroalkyl.

These synthetic constraints on the derivatization of IDPi **4.3a** led us to explore alternative strategies for catalyst modification. Early on in our investigations, we speculated that the *m*-trifluoromethyl groups in the wings of **4.3a** might lend themselves to modification through formal defluorofunctionalization (Figure 4.1B). We speculated that a modular approach toward structurally diverse motifs of this kind would facilitate our screening efforts. Motivated by this prospect, we sought to establish a synthesis of wing substituents containing $–CF_2R$ moieties. Our synthesis of these wings relied on a deoxofluorination strategy (Scheme 4.8A).

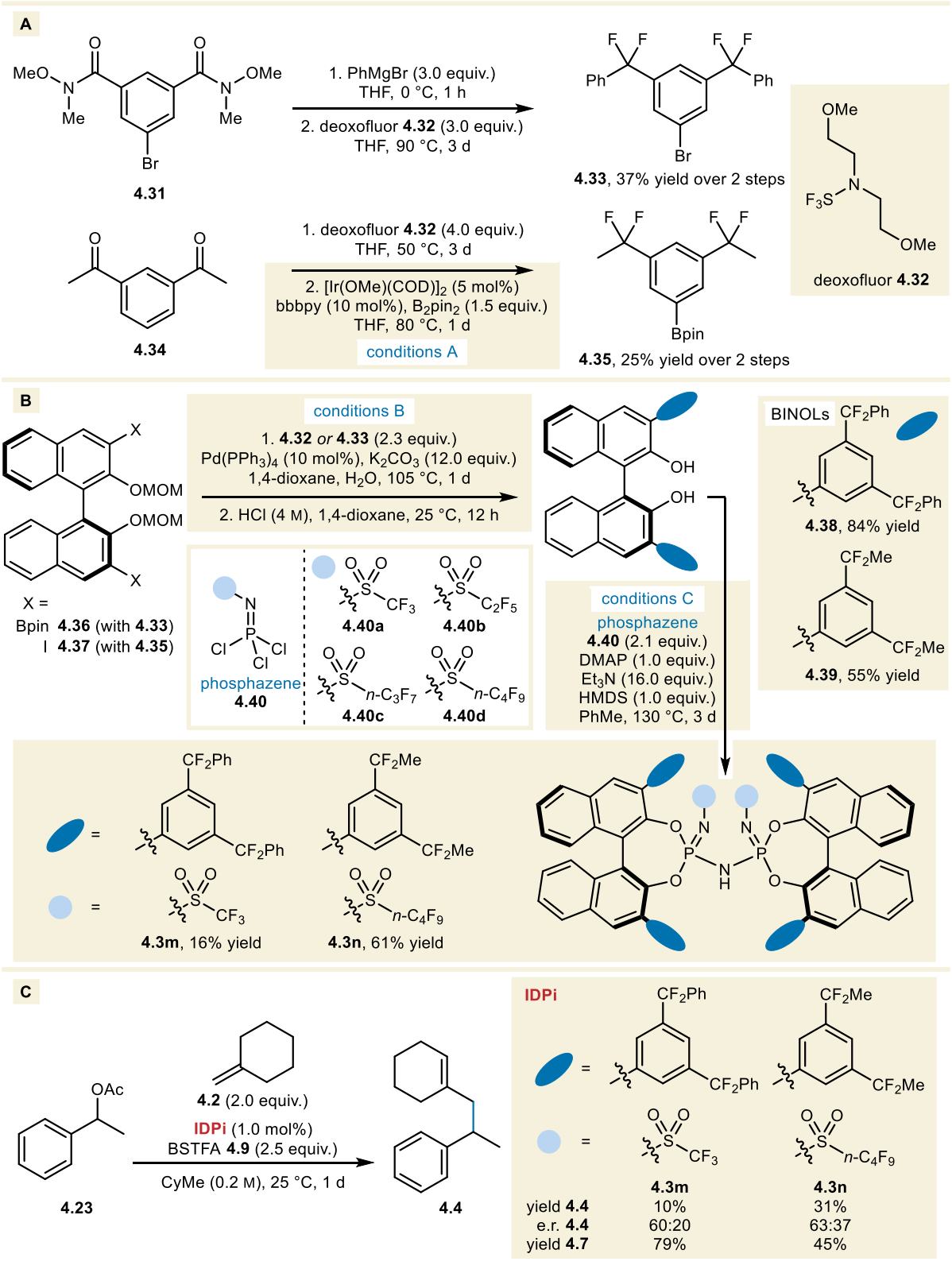

Scheme 4.8 Synthesis of *m*-modified analogs of **4.3a** and their application: synthesis of wing substituents through deoxofluorination coupled with Grignard addition to a Weinreb amide, or Hartwig borylation (A), and IDPi synthesis according to established strategies using phosphazene reagents. Phosphazenes **4.40a** and **4.40d** were used, **4.40b** and **4.40c** are shown for later reference (B); and the application of the synthesized catalysts in the model reaction toward hydrocarbon product **4.4** (C). bbbpy = 4,4'-di-tert-butyl-2,2'-dipyridyl.

Weinreb amide **4.31** was subjected to a Grignard reaction, followed by deoxofluor (**4.32**)-mediated deoxofluorination to yield aryl bromide **4.33**. Arylboronic ester **4.35** was synthesized by deoxofluorination of 1,3-diacetylbenzene (**4.34**), followed by Hartwig borylation (conditions A). These arenes were subjected to a Suzuki–Miyaura coupling (conditions B) with methoxymethyl (MOM)-protected 3,3'-Bpin-BINOL, or its 3,3'-iodo analog (**4.36** or **4.37**), followed by deprotection. The resulting chiral diols **4.38** and **4.39** were subjected to established conditions for IDPi synthesis (conditions C)[274] using phosphazene reagents **4.40** and hexamethyldisilazane (HMDS), yielding catalysts **4.3m** and **4.3n** (Scheme 4.8B).

These two analogs of **4.3a** were applied in the model reaction (Scheme 4.8C). We found that both catalysts, although able to catalyze the reaction at 25 °C, showed significantly reduced yields of hydrocarbon product **4.4**. Instead, a significant increase in the elimination toward **4.7** was observed, possibly as a consequence of the reduced acidity of the catalysts brought about by the substitution of an electron-withdrawing fluorine atom. Moreover, these catalysts underperformed in terms of enantioselectivity compared to **4.3a**. These lackluster results, as well as the unreliable and dangerous nature of the deoxofluorination reaction (resulting in a hospital trip over fears of hydrofluoric acid poisoning), led us to abandon this route.

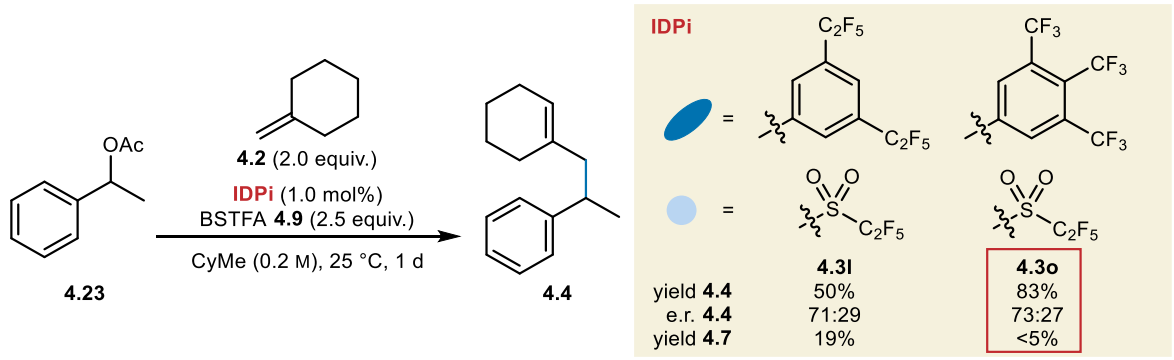

Scheme 4.9 Comparison of IDPis **4.3l** and **4.3o** in the model reaction.

Parallel to the above efforts, we explored *p*-functionalization of the wing substituent. We started by adding an additional *p*-trifluoromethyl substituent to the analog of IDPi **4.3a** containing a perfluoroethyl core. Catalyst **4.3o** was accessible from commercially available tris(trifluoromethyl)benzene after Hartwig borylation (conditions A), followed by Suzuki–Miyaura coupling (conditions B) and IDPi synthesis (conditions C) with *N*-(perfluoroethyl)phosphazene **4.40b**. Application of this catalyst in the model reaction led to a significant leap in enantioselectivity compared to **4.3a**, and provided a slight increase in the e.r. of **4.4** compared to catalysts **4.3l** bearing 3,5-perfluoroethyl wing substituents (Scheme 4.9).

Furthermore, the additional electron-withdrawing group led to near complete inhibition of the elimination pathway toward **4.7**, even at 25 °C, leading to a significant increase in yield of the desired product.

This positive result encouraged us to continue screening catalysts with *p*-substituted wings. Unfortunately, our attempt at a modular synthesis of *para*-aryl-substituted analogs of **4.3a** was unsuccessful (Scheme 4.10A). A lack of dimerization of the *p*-phenyl BINOL during IDPi synthesis (conditions C) led to exclusive formation of NTPA **4.41**, which was unable to catalyze the model reaction. We speculated that the sterically encumbered nature of larger *p*-substituents obstructs the synthesis of these IDPi derivatives of **4.3a**. Unwilling to abandon *p*-substitution at this time, we investigated the modification of the chain length of the perfluoroalkyl substituents of catalyst **4.3o**. Synthesis of these perfluoroalkylated catalysts took place through a common route involving Ullmann coupling (conditions D), followed by Hartwig borylation (conditions A) to yield arylboronic acids **4.42**–**4.44** (Scheme 4.10B), which were transformed into IDPis **4.3p**–**4.3r** by successive Suzuki–Miyaura coupling (conditions B) and dimerization (conditions C) with phosphazene **4.40b**.

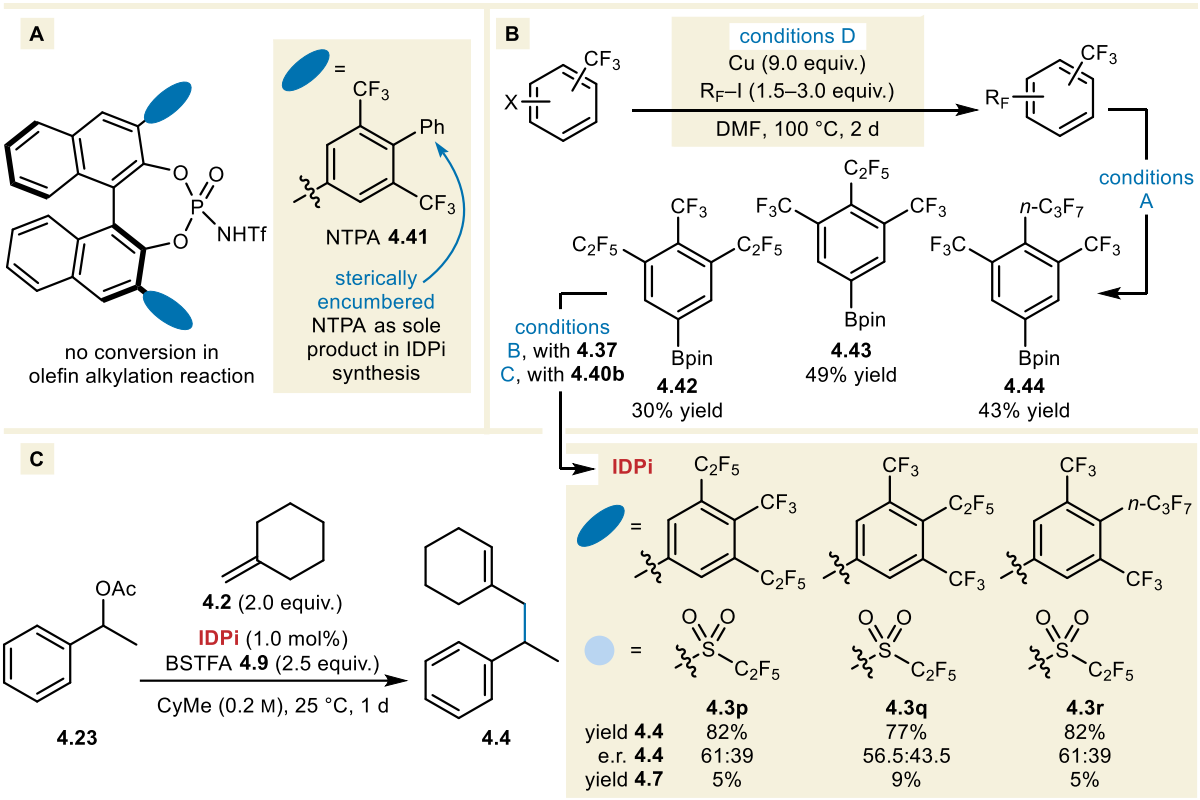

Scheme 4.10 Sterically encumbered *p*-Ph-substituted NTPA **4.41** (A), the synthesis of perfluoroalkyl-wing substituents toward analogs of IDPi **4.3o** (B), and application of these catalysts in the model reaction (C).

Upon applying these analogs of **4.3o** to the model reaction, we regrettably did not find a direct synergistic effect between substituents that individually affected the reaction outcome positively. In fact, installing longer perfluoroalkyl substituents in both the *m*- and *p*-positions on 3,4,5-tris(perfluoroalkyl)arene wings led to a significant decrease in the enantioselectivity of the reaction in each case (Scheme 4.10C). However, the high yields of these reactions corroborated our earlier observation that the addition of more electron-withdrawing substituents on the wings led to increased product formation.

We speculated that the decrease in enantioselectivity using IDPis **4.3p**–**4.3r** could be caused by the increased steric demand of the perfluoroalkyl substituents. To test this hypothesis, we were keen to synthesize catalysts with smaller *p*-substituents than a trifluoromethyl group. In this category, only the introduction of halogen atoms would lead to catalysts with similar electronic properties. Therefore, we set out to synthesize *p*-halogenated analogs of IDPi **4.3l** (Scheme 4.11A). The installation of iodo-, bromo-, and chloro-substituents was achieved by a Sandmeyer reaction from the MOM-protected BINOL containing *p*-amino-substituted wings (**4.47**). This BINOL was synthesized in two steps from 4-Bpin-aniline (**4.45**) by photochemical *o*-(bis)perfluoroalkylation to yield **4.46**,[275] followed by Suzuki–Miyaura coupling. The *p*-fluoro analog of **4.3l** was synthesized from the commercially available 1,3-dibromo-2-fluorobenzene (**4.51**) through consecutive Ullmann coupling (conditions D), Hartwig borylation (conditions A), and Suzuki–Miyaura coupling (conditions B). The resulting BINOLs **4.48**–**4.52** containing *p*-halo substituents were transformed into IDPis **4.3s**–**4.3v** (conditions C) with phosphazene **4.40b**.

Application of IDPis **4.3s**–**4.3v** in the model reaction at 25 °C yielded the desired product with good to very good yield (Scheme 4.11B). We observed an increase in the yield and enantioselectivity of the reaction with decreasing size and increasing electronegativity of the halo-substituent. Furthermore, the reaction with catalyst **4.3v** yielded the smallest amount of **4.7**, indicating that the increased electronegativity of fluorine aided the suppression of the elimination pathway. Almost identical results were obtained with *p*-chloro IDPi **4.3u** and *p*-fluoro IDPi **4.3v**, which both led to a substantial increase in enantioselectivity compared to the previous best result obtained with **4.3o**. Upon lowering the reaction temperature to −60 °C, a sharp increase in enantioselectivity was observed for reactions with IDPis **4.3u** and **4.3v**, yielding **4.4** with near-excellent enantioselectivities. IDPis **4.3s** and **4.3t** were unable to catalyze the model reaction at this temperature. Additionally, these catalysts showed signs of

decomposition over a period of one month, leading to the formation of significant amounts of the protodehalogenated catalysts (~10% in both cases). Decomposition was not observed for IDPis **4.3u** and **4.3v**.

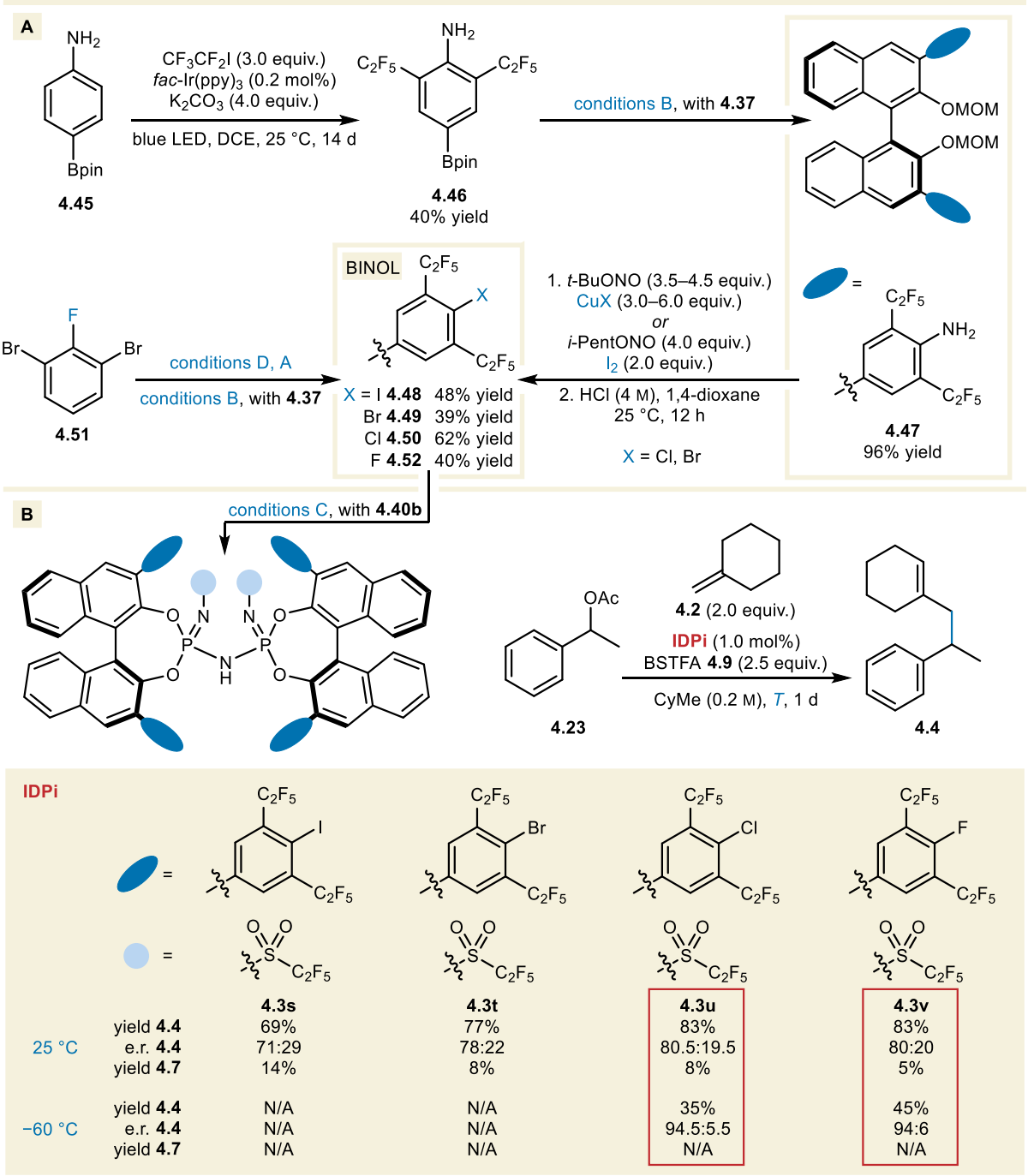

Scheme 4.11 Synthesis of *p*-halo-substituted analogs of **4.3l** (A), and screening of the synthesized catalysts in the model reaction at 25 °C and −60 °C (B).

We decided to screen for the length of the perfluoroalkyl core, to exclude the possibility that a significantly better core substituent was overlooked. Synthesis of the trifluoromethyl- and

n-perfluoropropyl core analogs of **4.3v** was performed from BINOL **4.52** (conditions C) with phosphazenes **4.40a** and **4.40c**. Comparison of the resulting IDPis **4.3w** and **4.3x** to IDPi **4.3v** at −60 °C demonstrated that the perfluoroethyl core outperformed catalysts with both smaller and larger perfluoroalkyl cores (Scheme 4.12).

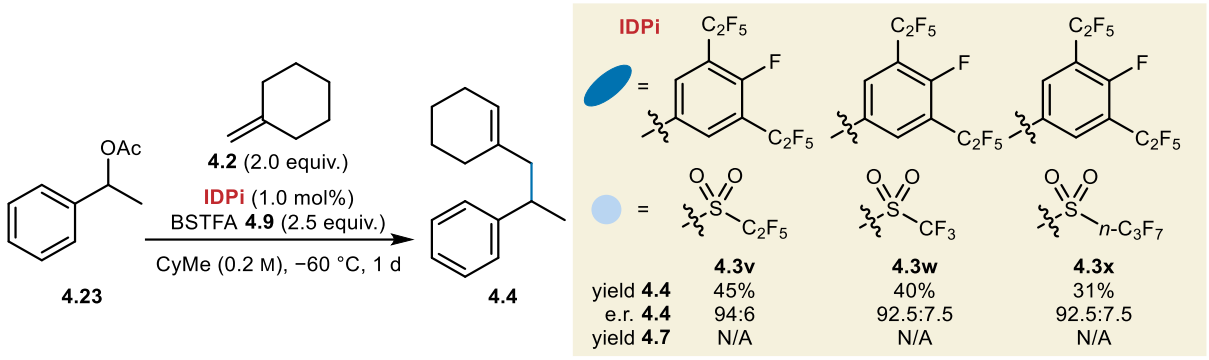

Scheme 4.12 Direct comparison of the lengths of perfluoroalkyl core substituents through synthesis of analogs of IDPi **4.3v**, and their application in the model reaction.

As a final screening effort, we investigated the effect of the reaction concentration with respect to acetate **4.23** in reactions with IDPis **4.3u** and **4.3v** (Scheme 4.13). Using a catalyst loading of 2.5 mol% and maintaining the concentration of olefin **4.2** allowed us to obtain very good yields even at lower concentrations. Interestingly, no concentration dependence of the enantioselectivity was observed with **4.3u**, leaving this catalyst unable to pass the "excellence"

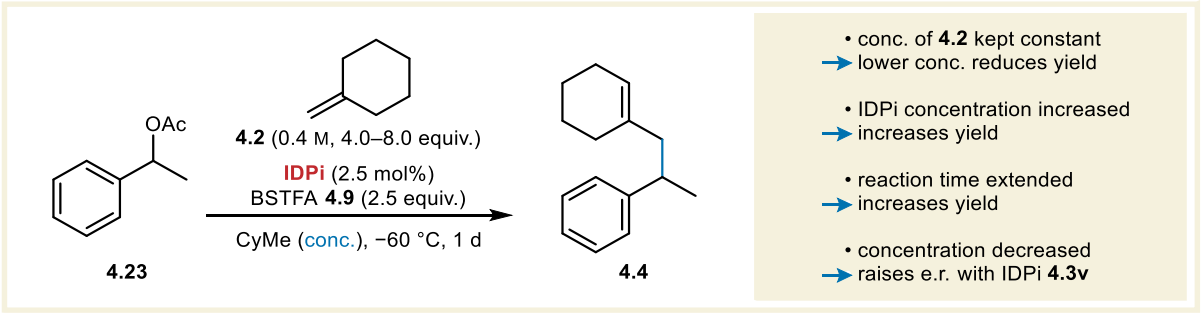

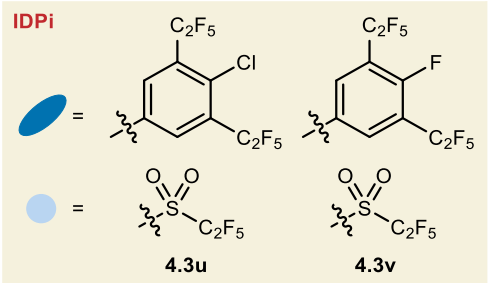

entry	IDPi	conc. **4.23**	yield **4.4**	e.r. **4.4**	yield **4.7**
1[a]	**4.3u**	0.1 M	89%	94:6	N/A
2[a]	**4.3u**	0.05 M	74%	94:6	N/A
3	**4.3v**	0.1 M	60%	95:5	N/A
4	**4.3v**	0.05 M	61%	96:4	N/A
5[b]	**4.3v**	0.05 M	79%	96:4	N/A

Scheme 4.13 Screening of the reaction concentration with respect to **4.23**, using catalysts **4.3u** and **4.3v**. [a]reaction time = 2 d. [b]reaction time = 3 d.

threshold. Gratifyingly, a moderate concentration dependence was observed with **4.3v**, which provided **4.4** in a yield of 61%, and with a satisfactory e.r. of 96:4 at a concentration of 0.05 M. Extending the reaction time to three days increased the yield of the desired product to 79%, while maintaining excellent enantioselectivity.

With the identification of IDPi **4.3v**, our search for the optimal catalyst was complete. The reaction uses a highly acidic IDPi catalyst featuring perfluoroethyl substituents on the wings and in the core. The installation of *p*-fluoro substituents on the wings of the catalyst led to a significant breakthrough in terms of enantioselectivity. This catalyst provided excellent enantioinduction in the reaction toward hydrocarbon **4.4**, even in the absence of directing groups on the carbocationic intermediate and the unactivated olefin nucleophile. The solid-state structure of IDPi **4.3v** was determined by single-crystal X-ray diffraction (Figure 4.2). This structure revealed that two *p*-fluoro substituents directly flank the active site of the catalyst. Assuming that the observed solid-state conformation translates to the solution phase, and the silylated IDPi is structurally similar, this observation provides an explanation as to why these fluorine atoms contribute so strongly to the reaction outcome with respect to enantioselectivity.

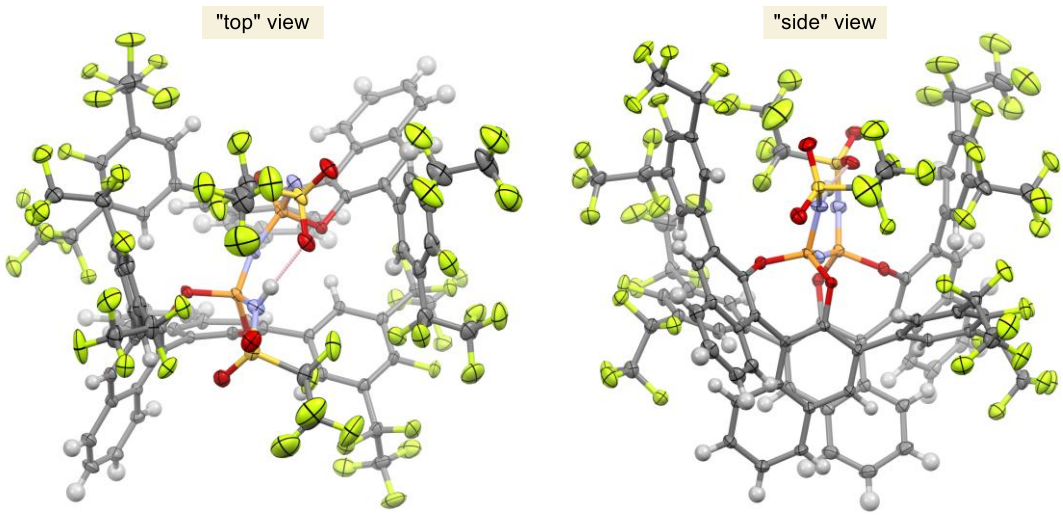

Figure 4.2 Solid-state structure of IDPi **4.3v**. The "top" view shows the catalyst active site. The "side" view shows wings containing *p*-fluoro substituents positioned near the active site. Thermal ellipsoids are drawn at the 50% probability level. Solvent molecules (PhMe) and disordered parts (CF_3-fluorine atoms) are omitted for clarity. Color code: white, H; black, C; cyan, N; red, O; light green, F; orange, P; yellow, S. *Crystal obtained by Dr. Jiaxiang Lu.*

Furthermore, the use of BSTFA as a non-nucleophilic silylating agent suppressed the formation of undesired by-products, while enabling strong Lewis-acidic activation of the acetate. With the optimal catalyst and conditions in hand, we turned our attention toward exploring the substrate scope of the reaction.

4.2. Scope of the Olefin Alkylation Reaction

Isolation-scale experiments for the reaction scope were performed in cooperation with the undergraduate student Thibault Gotta.

The exploration of the reaction scope featured four parts: 1) the evaluation of sterically and electronically diverse substituents on the aryl substituent of acetate **4.23**, 2) the evaluation of olefins with various alkene substitution patterns, 3) combinations of the former two points, yielding products that we attempted to derivatize into (analogs of) biologically active compounds, and 4) the expansion of our developed olefin alkylation reaction to allylic acetates, to access formal organocatalytic Tsuji–Trost-type reactivity. In each part, a scope of successful substrate combinations is highlighted. Additionally, a number of substrates which were not successfully converted to the desired product, or did not produce satisfactory results is shown.

4.2.1. *Benzylic Acetate Scope*

First, we explored the model reaction's tolerance to arene substitution (Scheme 4.14). In addition to the model substrate leading to **4.4**, *m*-methyl substituents were well-tolerated, yielding hydrocarbons **4.54a** and **4.54b** with good to excellent yields and excellent enantioselectivities. Acetate **4.53c**, containing a sterically bulky *m*-isopropyl-substituent was transformed into corresponding hydrocarbon product **4.54c** with excellent enantioselectivity upon lowering of the reaction temperature to −70 °C. A slightly reduced yield was observed for products **4.54d** and **4.54e** bearing *p*-phenyl and *p*-(1-propynyl) substituents, respectively. This decrease in yield can be explained by the reduced solubility of the substrates at the reaction temperature. The acetates visibly agglomerated on the walls of the reaction vial, but nonetheless yielded the desired products with moderate yields. A slight decrease of the e.r. was observed for product **4.54d**, which featured additional stabilization of the carbocation intermediate through resonance effects. Products **4.54f** and **4.54g** containing electron-withdrawing *m*-methoxy substituents were obtained with good yields and (near-) excellent enantioselectivities. Interestingly, a small amount of the spirocyclic indane products was obtained in these reactions, indicating a competing cyclization process before deprotonation in the case of nucleophilic *o*-positions on the arene. Substrates bearing *p*-halo substituents led to products **4.54h** and **4.54i** in excellent yields and enantioselectivities. Co-crystallization of **4.54i** with a 1,3,5,7-tetrakis(2-

fluoro-4-methoxyphenyl)-adamantane (TFM) chaperone developed by Richerd and coworkers unambiguously revealed that the products were obtained in the (*S*)-configuration.[276]

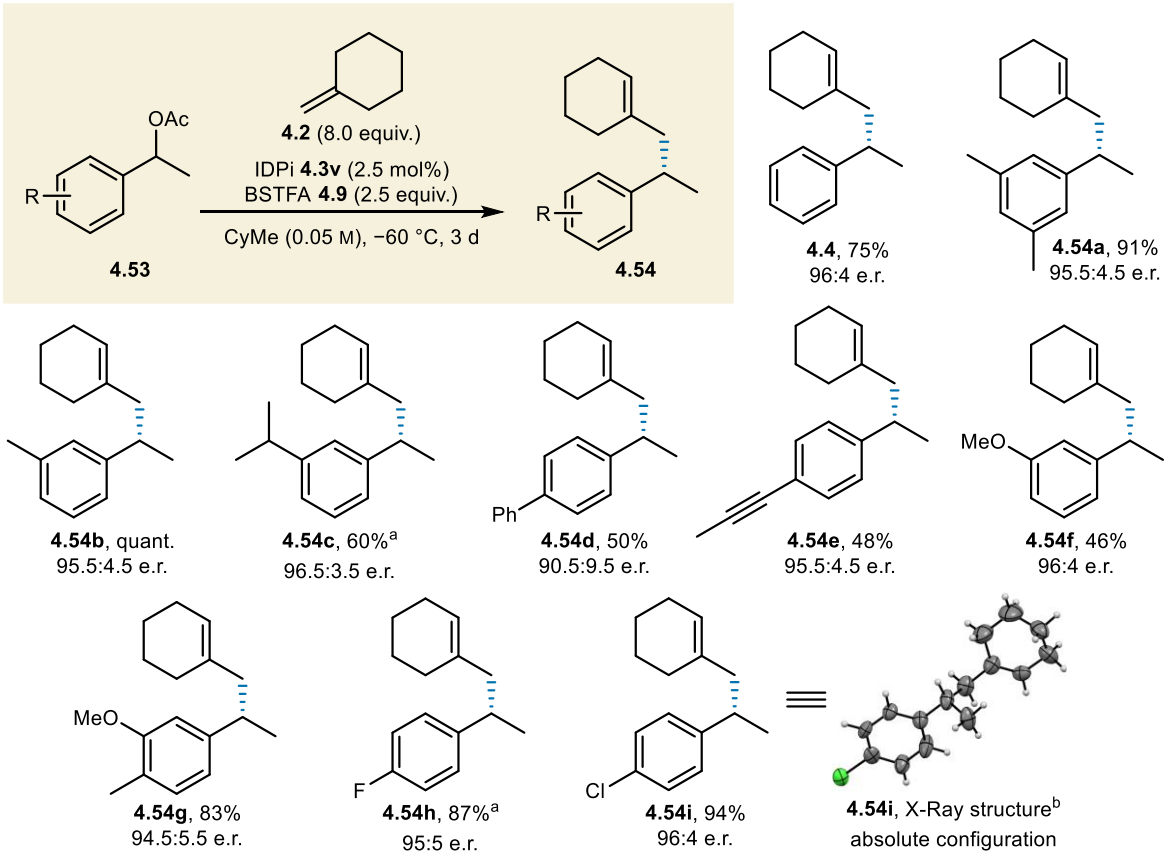

Scheme 4.14 Exploration of the benzylic acetate scope, yielding products with various aryl-substituents. Yields of the isolated compounds are given. [a]reaction performed at −70 °C. [b]thermal ellipsoids are drawn at the 50% probability level, and two TFM molecules are omitted for clarity. Color code: white, H; black, C; green, Cl.

A number of acetates led to unsatisfactory outcomes under the optimized conditions (Scheme 4.15). Strongly electron-withdrawing substituents, such as the trifluoromethyl group of **4.53j**, led to negligible product formation. The cation-destabilizing effect of strongly electron-withdrawing substituents is likely too great to allow for efficient substrate activation. Conversely, reactions with substrates containing electron-donating substituents in the *p*- and *o*-positions led to quantitative formation of products **4.54k**–**4.54m**. However, the enantioselectivity of these reactions was significantly reduced compared to the model reaction. We speculate that the higher degree of stabilization of the respective carbocationic intermediates diminishes ion pairing interactions with the catalyst, resulting in reduced enantioinduction during the C–C bond forming step. Similarly, substrate **4.53n** led to the formation of the 2-thiophenyl-substituted product with poor enantioselectivity, possibly due to the highly electron-donating nature of the heterocycle. Modification of the methyl substituent on the parent

acetate, such as its replacement by an ethyl substituent in **4.54o**, led to decreased reactivity and enantioselectivity, which we attributed to steric effects. The catalyst shows a high degree of substrate specificity for 1-substituted ethyl acetate substrates. A requirement of substrates containing a methyl substituent is described in organocatalysis and enzymology as the catalyst or enzyme containing a "methyl hole"; *i.e.* a binding pocket for a methyl substituent.[277] When primary benzyl acetate **4.54p** was used as the electrophile, hydrocarbon product **4.54p** formed in near-quantitative yield at 25 °C. However, no stereocenter was formed during the reaction. Therefore, the reaction simply demonstrates the capability of the catalyst to activate primary benzylic acetates. Likewise, we wanted to test whether our optimal catalyst can be used to furnish quaternary stereocenters. Indeed, when tertiary acetate **4.53q** was subjected to the reaction conditions, the desired hydrocarbon product **4.54q** was obtained with moderate yield despite the poor nucleophilicity of the olefin and the potentially sterically encumbered nature of the carbocationic intermediate. However, the product was nearly racemic, which we attributed to a combination of steric factors similarly to the reaction with **4.53o**, and additional stabilization of the cationic intermediate akin to electron-rich substrates **4.53k**–**4.53n**.

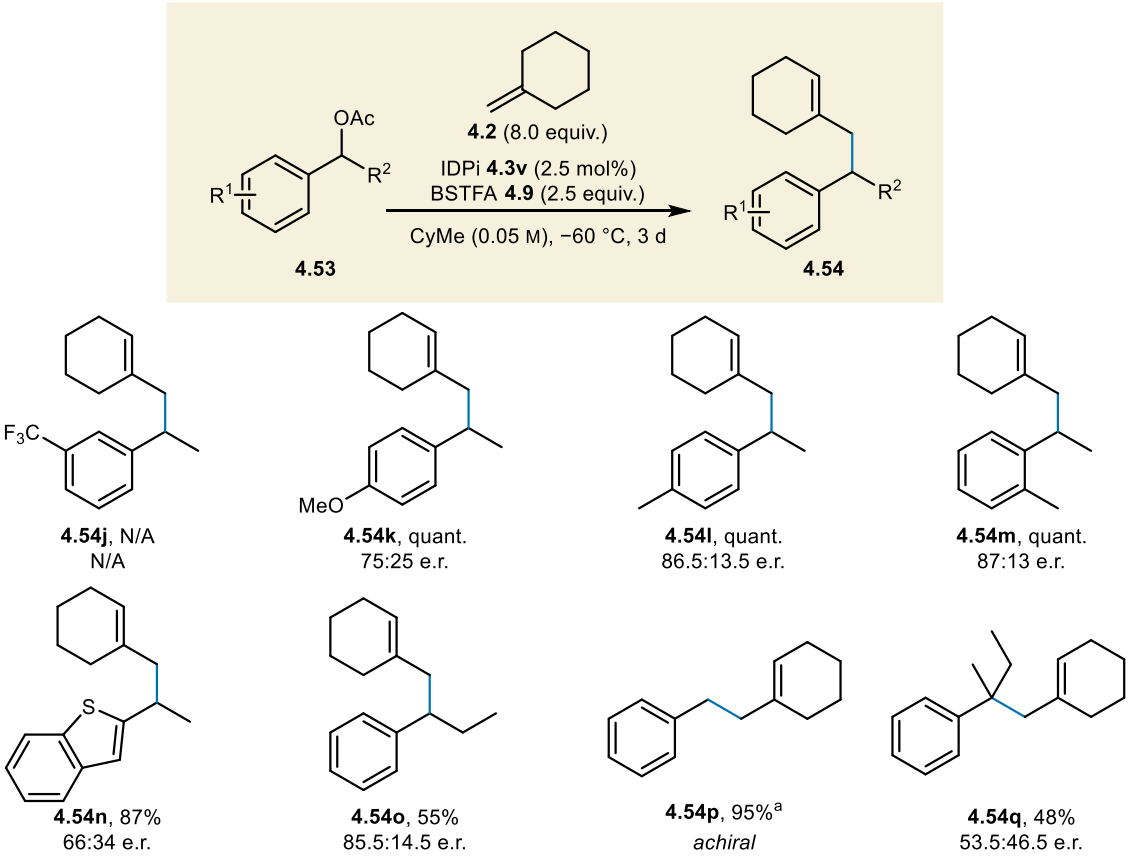

Scheme 4.15 Reactions with acetate substrates that yielded unsatisfactory results. Yields were determined by ^{1}H NMR spectroscopy using mesitylene as the internal standard. [a]reaction performed at 25 °C.

4.2.2. *Olefin Scope*

Next, we explored the reaction scope with respect to the olefin nucleophile (Scheme 4.16). Replacing methylenecyclohexane (**4.2**, $N = 1.16$) with the significantly more nucleophilic methylenecyclopentane (**4.55a**, $N = 2.82$), or methylenecycloheptane (**4.55b**, $N = 2.24$) led to the formation of hydrocarbon products **4.56a** and **4.56b** in good yields and (near-) excellent enantioselectivities. Tetramethylethylene (**4.55c**, $N = -1.00$) surprisingly provided hydrocarbon product **4.56c** containing vicinal quaternary and tertiary centers with very good yield and excellent enantioselectivity despite its low *N*-parameter. This observation demonstrated that the alkene substitution pattern had very little influence on the transition state of the enantiodetermining step. Another interesting result came from the reaction with 1,1-diphenylethylene (**4.55d**), which lacks protons in the allylic position of the nucleophilic site. Consequently, the compound **4.57d** bearing a vinyl substituent was obtained as the sole product of the reaction. The excellent e.r. of **4.57d** indicated that the site of deprotonation has a negligible effect on enantioinduction during C–C bond formation, indicating a stepwise reaction mechanism. To evaluate the selectivity of the reaction with respect to alkene geometry, we tested olefins **4.55e** and **4.55f**. These olefins led to the formation of isomeric mixtures **4.56e** and **4.56f**, which showed a slight preference for deprotonation toward the sterically favored alkene geometry. Application of α-cyclohexylstyrene (**4.55g**) to the reaction conditions yielded tetrasubstituted olefin **4.56g** with excellent regioselectivity. The use of gaseous isobutene (**4.55h**) led to a slight preference for trisubstituted product **4.47h**, although a substantial amount of terminal olefin product **4.56h** was formed as well, likely due to the kinetic preference for terminal deprotonation. Interestingly, using a large excess of isobutene led to the formation of a considerable amount (~23%) of the double addition product, where a second equivalent of isobutene adds to the tertiary carbocation intermediate after the enantiodetermining, C–C bond forming step. All three of the product isomers could be separated by flash column chromatography (FCC) on silica impregnated with 10% $AgNO_3$ ($SiO_2/AgNO_3$). Unfortunately, the e.r. of the double addition product could not be determined. Trisubstituted alkene **4.55i** led to the formation of a mixture of terminal olefin diastereomers **4.56i** with a slight preference for the *anti*-configuration. Both diastereomers were obtained with very high enantioselectivity, corroborating our earlier hypothesis that the alkene substitution pattern does not strongly influence the enantiodetermining step. This reaction was also accompanied by the formation of a minor amount of tetrasubstituted olefin isomer **4.57i**, for which we were unable to obtain a reliable e.r. value. Gratifyingly, increasing the steric bulk of the alkyl substituent on the

nucleophilic position of the alkene fully suppressed the formation of the tetrasubstituted olefin product, leading to diastereomeric mixture **4.56j** bearing an ethyl substituent. The diastereoselectivity of this reaction was slightly enhanced compared to **4.56i**. Lastly, ethylidenecyclohexane (**4.55k**) led to the formation of **4.56k** as the sole constitutional isomer, and with moderate diastereoselectivity. Surprisingly, storage of **4.56k** at 0 °C over a period of a month led to crystallization of the major diastereomer. We attempted to analyze these crystals by single-crystal X-ray diffraction, but were unable to definitively assign the absolute configuration, due to the poor scattering behavior of the purely hydrocarbon compound. However, this X-ray analysis confirmed the formation of the desired product.

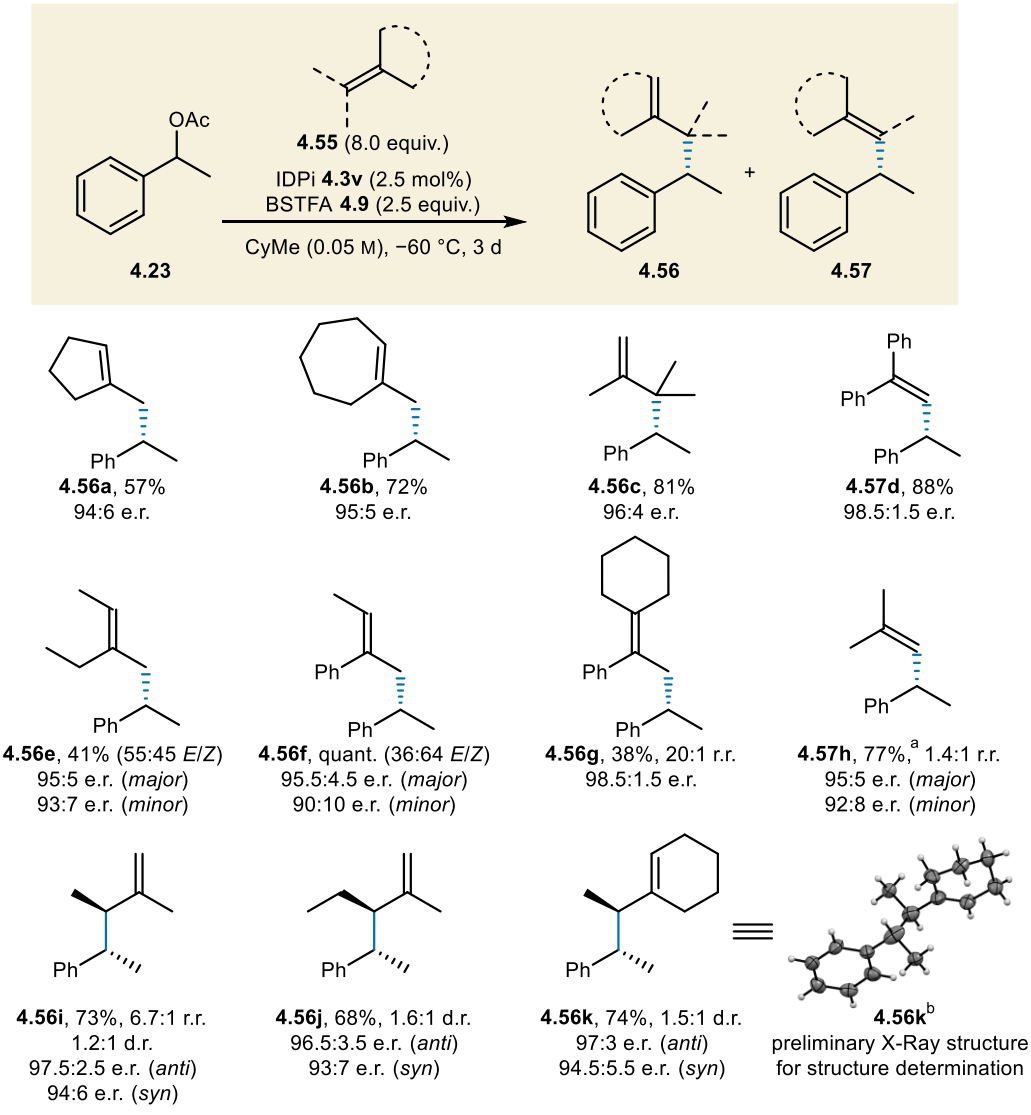

Scheme 4.16 Exploration of the olefin scope. Yields of the isolated compounds are given. Regioselectivity not shown for products with a r.r. >20:1. [a]excess isobutene was condensed into the reaction mixture at −60 °C. [b]the absolute configuration of the product could not be assigned based on this preliminary crystal structure. Thermal ellipsoids are drawn at the 50% probability level. Color code: white, H; black, C.

A number of olefins yielded undesirable reaction outcomes under the optimized conditions (Figure 4.3). Most prominently, α-olefins such as 1-octene (**4.55l**) were unreactive, due to their poor nucleophilicity. Somewhat surprisingly, methylenecyclobutane (**4.55m**) was similarly unreactive, despite its high nucleophilicity parameter (N = 1.65) compared to **4.2**. The reaction with olefin **4.55n** led to the formation of a complex mixture of products. In addition to the three expected products after deprotonation, two addition isomers of the same molecular weight were formed, alongside several oligomeric products. The products of the reaction were inseparable, leaving us unable to identify the unexpected by-products. We speculate that cyclization may have caused the formation of additional isomers. Furthermore, double addition may have taken place, akin to the reaction with isobutene. Complex mixtures were also observed with styrene (**4.55o**), and 1,3-dienes **4.55p** and **4.55q**. We hypothesize that resonance stabilization of the carbocationic species after C–C bond formation could facilitate oligomerization in these cases. Lastly, reactions with olefins **4.55r** and **4.55s**, bearing inductively electron-withdrawing groups, led to negligible product formation.

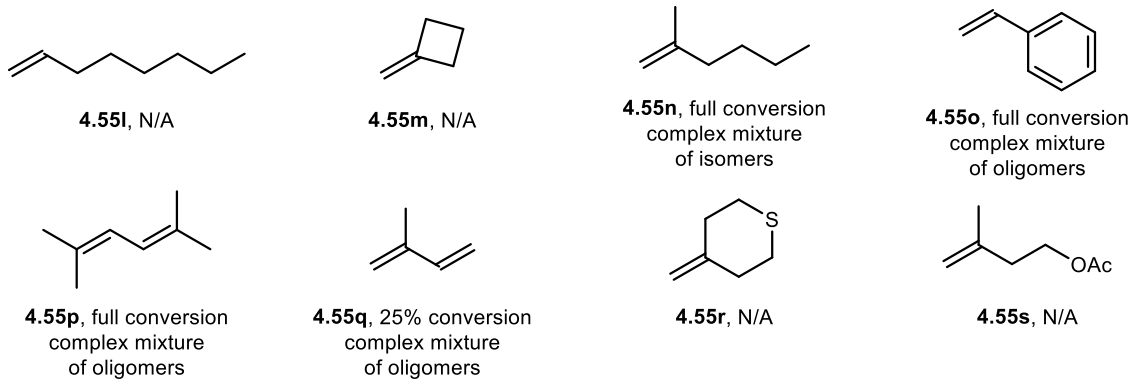

Figure 4.3 Olefin substrates that led to unsatisfactory outcomes under the model reaction conditions. Reactions were evaluated by ^{1}H NMR spectroscopy using mesitylene as the internal standard.

4.2.3. *Mixed Scope and Product Derivatization*

We decided to explore mixed combinations of substrates to more thoroughly establish the limitations of the reaction, and to obtain products that could be transformed into biologically active molecules (Scheme 4.17). Acetates bearing electron-withdrawing substituents in the *p*-position reacted readily with **4.55a**, yielding the corresponding *p*-brominated and *p*-ethynylated products **4.59a** and **4.59b** with good yields and (near-)excellent enantioselectivities. Similarly, the *p*-brominated acetate reacted well with **4.55c**, yielding product **4.59c** with good yield and excellent enantioselectivity. Gratifyingly, a benzylic acetate

bearing a *m*-(allyloxy)methyl group was transformed to product **4.59d** in very good yield and excellent enantioselectivity. Furthermore, no by-product formation was observed despite the presence of the potentially reactive allyl benzyl ether. We identified that formal vinylation using **4.55d** could lead to precursors of non-steroidal anti-inflammatory drugs (NSAIDs), such as flurbiprofen (**4.61**) and ibuprofen (**4.62**). Indeed, **4.55d** in combination with the corresponding acetates led to products **4.60e** and **4.60f** in moderate to good yields, and with excellent enantioselectivities. Oxidative C=C bond cleavage of **4.60e** according to known methodology yielded flurbiprofen with moderate yield and with almost complete stereoretention.[278] The poor yield of the reaction was likely a consequence of the small scale, leading to product loss upon acid–base extraction.

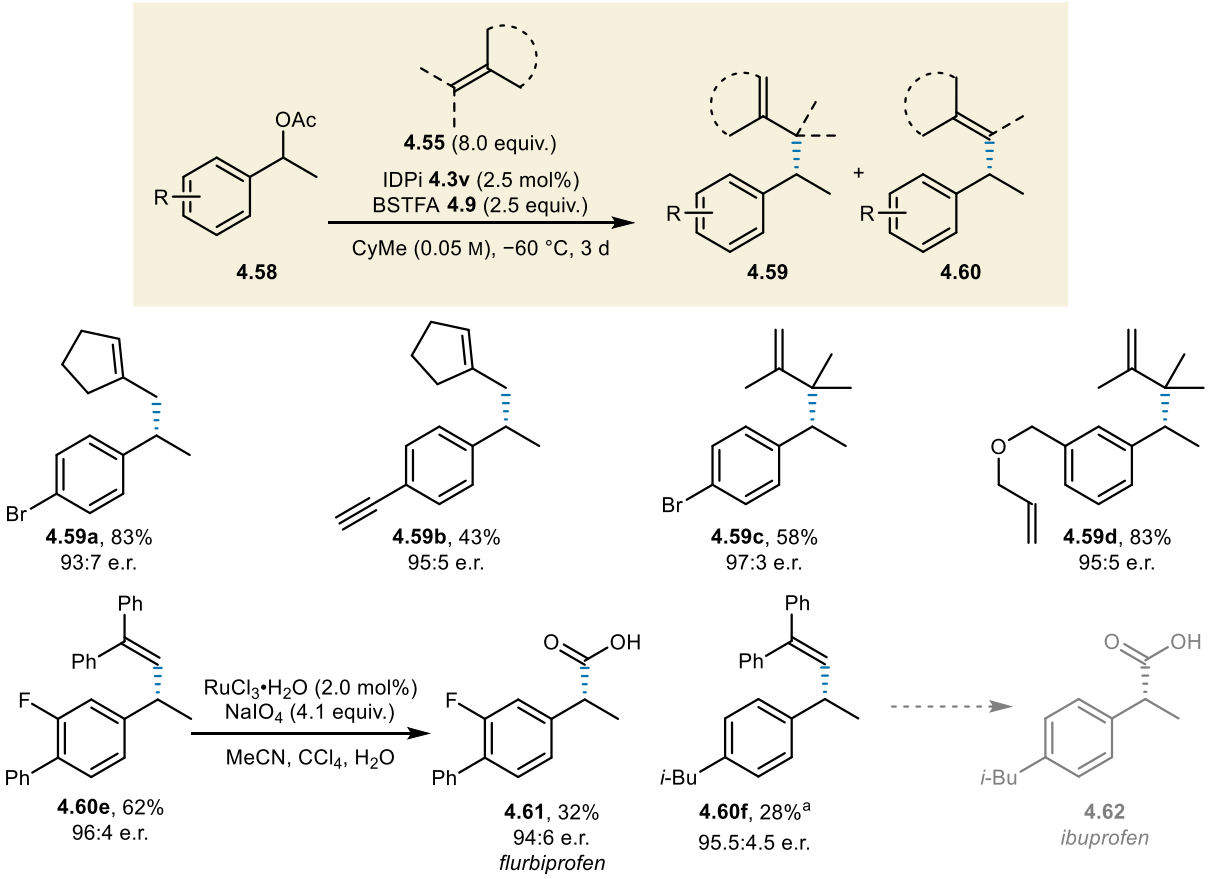

Scheme 4.17 Exploration of a mixed scope using diverse acetate- and olefin substrates and flurbiprofen synthesis. [a]reaction performed at −85 °C.

Efforts were made to transform allyl benzyl ether **4.59d** into an analog of galaxolide (**4.63**), a well-known synthetic musk odorant used as a common ingredient in consumer products such as perfumes, cosmetics and personal hygiene products. Due to concerns about its environmental persistence and toxicity to aquatic life, galaxolide use is slowly being phased out

in favor of non-polycyclic musk odorants by the European Union.[279] We hoped to develop a synthesis of an analog of galaxolide that contains one less quaternary benzylic carbon center; a motif which is often associated with high environmental persistence.[280] Developing a stereoselective synthesis of such a compound might alleviate toxicity concerns related to complex mixtures of racemic polycyclic compounds. Furthermore, previous stereoselective syntheses of galaxolide (Scheme 4.18A) demonstrated that the (4*S*)-diastereomers contribute most strongly to the odor profile, while changing the configuration at the C(7)-position provides diastereomers with different odor facets.[281,282] Therefore, we were most interested in developing a diastereoselective cyclization of the allyl benzyl ether.

We hoped that a double cyclization of **4.59d** would yield the desired compound in a single step. Monocyclization toward indane **4.64** was expected to be facile, due to the Thorpe–Ingold effect, which favors cyclization of compounds bearing *gem*-dimethyl groups. Furthermore, we hypothesized that the electron-rich nature of the arene could facilitate electrophilic aromatic substitution. We speculated that the second cyclization would be more challenging, due to the relatively high Lewis basicity of oxygen compared to the allyl substituent, and the potential for formation of stabilized allylic- and benzylic carbocations. The difficulty of this transformation is reflected in a lack of literature precedents reporting 6-membered ring formations from allyl benzyl ethers. However, the formation of 5- and 6-membered carbacycles and oxygen-containing heterocycles using common acid catalysts or radical initiation has been previously reported.[283–286]

We started our investigation by subjecting **4.59d** to a number of acid catalysts (Scheme 4.18B). Dual catalysis by $RuCl_3•H_2O$ and AgOTf led to the formation of a complex mixture, in which the only identifiable product was a minor amount of indane product **4.64**. Low conversion of the starting material was observed with $Y(OTf)_3$ and $Sc(OTf)_3$, yielding no noteworthy products. Using $Bi(OTf)_3$, a significant amount of **4.64** was obtained, alongside minor by-products, but no formation of **4.63** was observed. Interestingly, **4.64** was obtained in excellent yield as the sole product of the reaction when Tf_2NH was used as a Brønsted acid catalyst.

Realizing the inherent limitations of cationic cyclizations, we attempted to achieve the desired cyclization reaction using Co-salen catalysis in the presence of silane and an oxidant (Scheme 4.18C). Upon subjecting **4.59d** to these conditions, complex mixtures were obtained containing several isomers of the desired molecular weight. Fragmentation patterns in MS indicated that a small amount of the desired product may have formed. However, these data

corresponded to a minor constituent of the reaction mixture. Furthermore, deallylation was observed, as well as the formation of several other side products. We speculated that cyclization

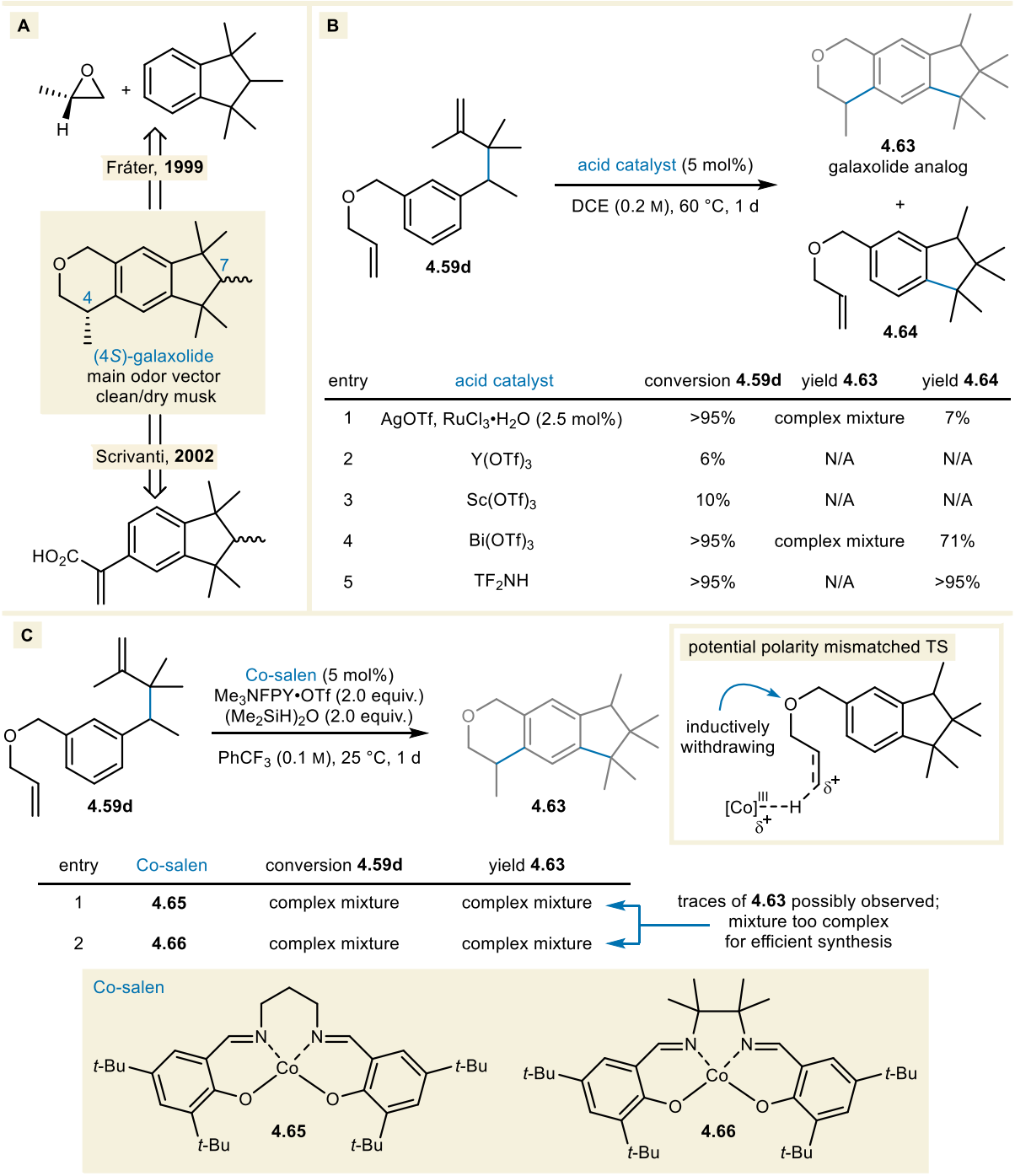

entry	acid catalyst	conversion **4.59d**	yield **4.63**	yield **4.64**
1	AgOTf, $RuCl_3$•H_2O (2.5 mol%)	>95%	complex mixture	7%
2	$Y(OTf)_3$	6%	N/A	N/A
3	$Sc(OTf)_3$	10%	N/A	N/A
4	$Bi(OTf)_3$	>95%	complex mixture	71%
5	TF_2NH	>95%	N/A	>95%

entry	Co-salen	conversion **4.59d**	yield **4.63**
1	**4.65**	complex mixture	complex mixture
2	**4.66**	complex mixture	complex mixture

Scheme 4.18 Previous stereoselective syntheses of galaxolide (A), attempts to derivatize **4.59d** into an analog of the odorant galaxolide using an acid catalysis (B), and a radical cyclization strategy with Co-salen catalysts (C).

of the (allyloxy)methyl substituent failed due to polarity mismatching between the cobalt hydride species and the alkene during hydrogen atom transfer (HAT).[287,288] Although HAT transfer to *O*-allyl groups has been reported,[289] the alkene moiety on the allyl group is electron

poor due to the inductive effect from the neighboring oxygen atom, which impedes HAT from metal hydride species. Furthermore, *O*-deallylation and alkene isomerization using Co-salen hydrides under very similar conditions has been reported, which explains the formation of complex mixtures.[290] Because of these challenges, we decided to abandon this synthesis. Nevertheless, we were pleased to have discovered a highly selective monocyclization toward indane **4.64** using Tf_2NH.

4.2.4. *Allylic Acetate Scope and Product Derivatization*

We were eager to investigate whether our model reaction conditions could be applied to olefin alkylation reactions with allylic alcohol derivatives. Upon subjecting allylic acetate **4.67a** to the standard conditions, we found that the desired 1,5-diene formed as the sole product in excellent yield and a promising e.r. of 88.5:11.5 at −60 °C (Scheme 4.19A). Simply tuning the reaction temperature allowed us to obtain desired hydrocarbon product **4.68a** in good yield and excellent enantioselectivity.

Next, we explored the reaction scope with respect to allylic acetates **4.67** (Scheme 4.19B). Due to limitations of the equipment, the reaction temperature could not be reduced beyond −90 °C at isolation scale. Nevertheless, **4.68a** was obtained in moderate yield and near-excellent enantioselectivity. Interestingly, acetate **4.67b** bearing a 3-methyl substituent led to significantly improved enantioinduction, affording 1,5-diene **4.68b** with very good yield and excellent enantioselectivity at −80 °C. This temperature was subsequently adopted as the standard temperature of the reaction. During the reaction with **4.67b**, a small amount (~7%) of the spirocyclic by-product was also formed, which could be easily separated from **4.68b** by $SiO_2/AgNO_3$ FCC. Similarly, 3-phenyl-substituted acetate **4.67c** yielded 1,5-diene **4.68c** in good yield and with a remarkable e.r. of 99.5:0.5. The high enantioselectivity of the reaction is somewhat counterintuitive, as a phenyl substituent on **4.53d** previously led to decreased enantioinduction. This result can be rationalized by examining the allylic cation intermediate furnished from **4.67c**, which is not stabilized through resonance by the adjacent phenyl substituent, in contrast to the benzylic cation from **4.53d**. Furthermore, we speculated that additional π-π interactions between the catalyst and the substrate could play a role in increasing the enantioselectivity of the reaction.

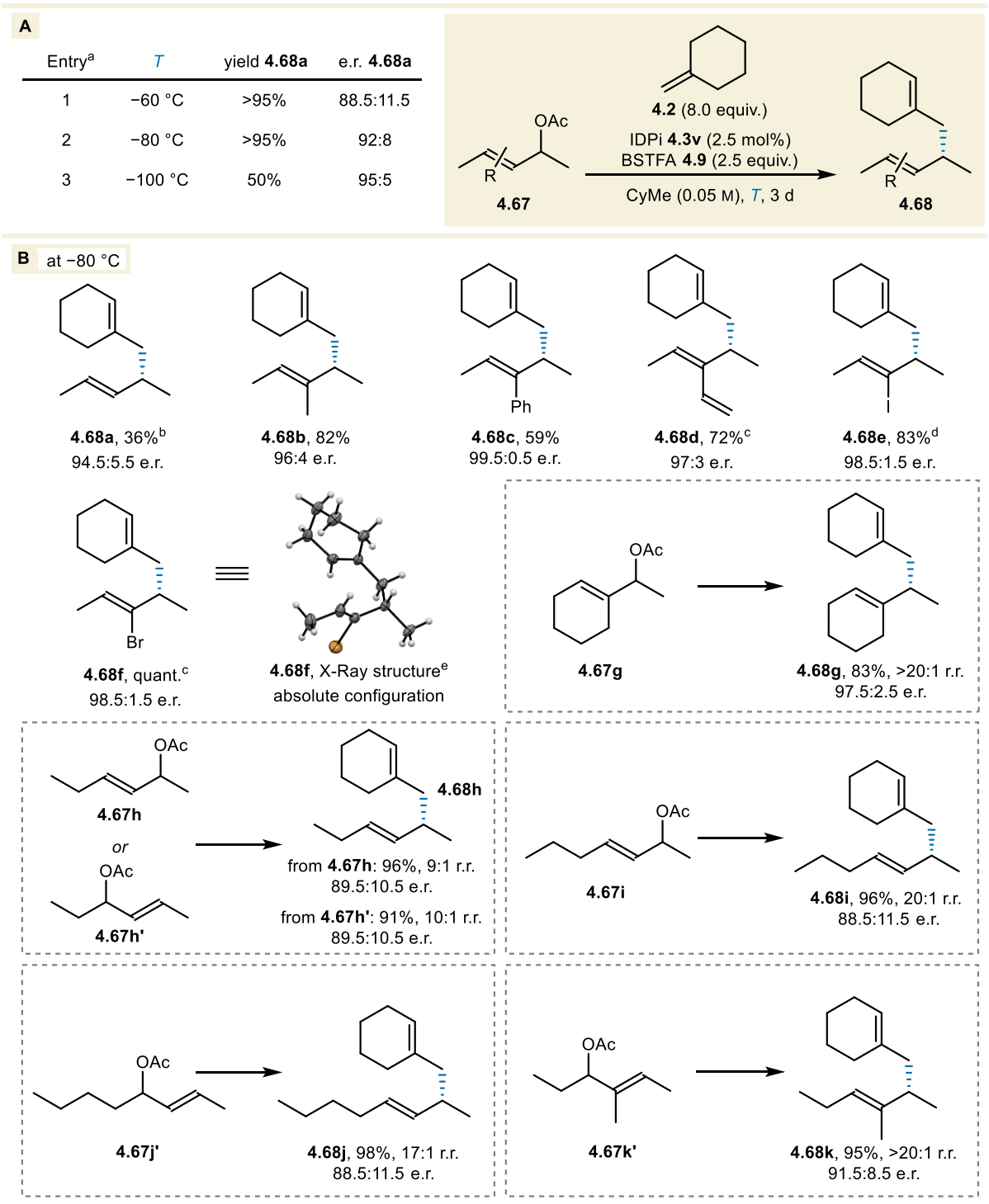

Scheme 4.19 (A) Temperature screening of allylic acetate substrate **4.67a**. Yields were obtained by ^{1}H NMR spectroscopy using mesitylene as the internal standard. (B) Allylic acetate scope. Yields of isolated products are given. All products were obtained with *E*/*Z* >20:1. [a]with **4.67a**. [b]reaction performed at −90 °C. [c]reaction performed at −50 °C. [d]reaction performed at −60 °C. [e]thermal ellipsoids are drawn at the 50% probability level. Two TFM molecules and one molecule of **4.68f** are omitted for clarity. Color code: white, H; black, C; brown, Br.

High enantioselectivity was also observed in the synthesis of triene **4.68d**. Dienyl acetate **4.67d** underwent conversion to the desired product at −50 °C, and only traces of product were formed at temperatures below −60 °C. Interestingly, this reaction was accompanied by the

formation of a complex mixture of cyclized by-products (<20%), which could be separated from **4.68d** by $SiO_2/AgNO_3$ FCC. Analysis of the mixture revealed the formation of 5- and 6-membered spirocycles, presumably through 5-*endo-trig*- or 6-*endo-trig*-cyclizations of the cationic intermediate after the addition of **4.2** (Scheme 4.20). Analysis by NMR spectroscopy indicated that these intermediates either underwent deprotonation toward 1,3-diene products, or a second addition of **4.2** followed by deprotonation toward 1,4- or 1,5-diene products. Due to the complexity of the by-product mixture, full characterization could not be completed. However, the high selectivity for the desired triene product **4.68d** indicated a strong preference for deprotonation after initial addition of **4.2**.

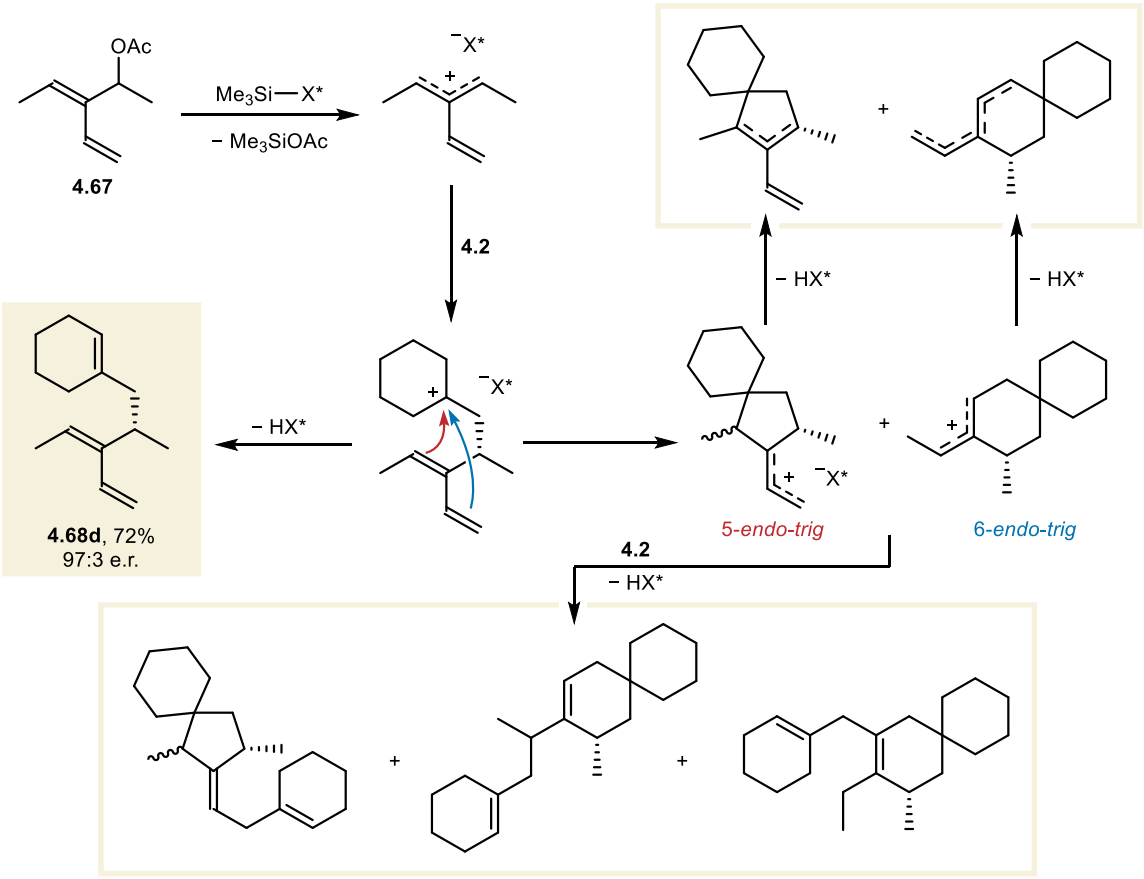

Scheme 4.20 Plausible mechanism of by-product formation in the reaction with **4.67d**.

Upon further exploration of the substrate scope, we were delighted to observe smooth transformation of 3-halo-substituted allylic acetates into products **4.68e** and **4.68f** with very good to quantitative yields and excellent enantioselectivities. Furthermore, co-crystallization of **4.68f** with TFM allowed us to definitively determine the absolute configuration of the product. Akin to **4.67d**, these acetates required higher temperatures for their effective activation. The high enantioselectivity of these reactions led us to conclude that electron-withdrawing

substituents in the 3-position are beneficial for the enantioselectivity of the reaction. However, the electron-donating methyl substituent in **4.67b** similarly induced high enantioselectivity. Thus, other substrate–catalyst interactions should be considered, such as halogen bonding, dispersive interactions, or even the limitation of degrees of rotational freedom by the introduction of these substituents. The latter might be corroborated by the reaction of cyclohexenyl-containing allylic acetate **4.67g**, which yielded hydrocarbon product **4.68g** with even higher enantioselectivity than **4.68b**.

We were keen to investigate the reactivity of acetates yielding non-symmetrical allylic cation upon leaving group departure. Non-symmetrical allylic carbocations can undergo nucleophilic addition at the two non-equivalent positions, leading to two possible regioisomeric products. The formation of **4.68g** provided a promising first example in this regard, as nucleophilic addition of the alkene was exclusively observed on the least sterically hindered carbon. Furthermore, only a small amount (~7%) of the spirocyclic by-product was observed, a comparable result to the reaction with **4.67b**. High regioselectivity was also observed in the reactions of **4.67h** and its allylic transposition isomer, **4.67h'**, proving that the IDPi catalyst could effectively differentiate between methyl- and ethyl substituents; a phenomenon that had previously only been observed in the IDPi-catalyzed cyanosilylation reaction of butanone.[291] Product **4.68h** was obtained with excellent yield and very good enantioselectivity in both cases. We speculated that the decrease in e.r. of **4.68h** compared to **4.68a** could be caused by unfavorable steric interactions between the substrate and the catalyst. The additional degrees of rotational freedom brought about by longer *n*-alkyl chains may lead to a decrease in $\Delta\Delta G^{\ddagger}$ of the enantiodetermining step. The reactions with **4.67h** and **4.67h'** led to nearly identical outcomes. These data indicate an S_N1 reaction where carbocation formation precedes nucleophilic attack by the alkene. Linear substrates **4.67i** and **4.67j'** bearing longer *n*-alkyl substituents yielded corresponding 1,5-dienes **4.68i** and **4.68j** in excellent yields and very good regio- and enantioselectivities. Lastly, adding a methyl substituent in the 4-position of **4.67k'** led to a substantial increase in the regioselectivity of the reaction, and a moderate increase in the e.r. of product **4.68k** compared to **4.67h** and **4.67h'**.

A number of allylic acetates led to unsatisfactory reaction outcomes when subjected to the standard conditions (Figure 4.4). Acetate **4.67l**, the *Z*-isomer of **4.67b**, led to reduced product formation and enantioselectivity. Furthermore, the product was obtained as a mixture of double bond isomers, and a number of inseparable by-products were formed, which

prevented accurate determination of the e.r. of the *Z*-product. We speculated that an *E*/*Z*-mixture was observed because of the high energetic barrier for spontaneous rotation along the conjugated bonds of the allylic cation, leading to non-equivalent electrophilic sites.[292] Nucleophilic addition of the alkene preferentially takes place at the site leading to the *E*-product. We speculated that the geometry of the intermediate during this addition could lead to unfavorable steric interactions during C–C bond formation. Similarly unfavorable steric interactions might play a role in the decreased enantioselectivity of the reaction with acetate **4.67m**. However, the additional methyl group compared to **4.67a** could also cause a decrease in enantioinduction through cation stabilization similar to that observed in electron-rich benzylic acetates. Akin to reactions with benzylic acetates **4.54o** and **4.54q**, we observed that deviations from the 1-substituted ethyl acetate motif led to a decrease in enantioselectivity, as evidenced by acetates **4.67n** and **4.67o**. Lastly, we attempted to entirely remove resonance stabilization by subjecting *sec*-butyl acetate (**4.67p**) to the reaction conditions. The desired product was not obtained. However, at 25 °C, full elimination toward a 1:1 mixture of (*E*)- and (*Z*)-2-butene was observed when using IDPi **4.3v**. Interestingly, neither IDPi **4.3a** nor Tf_2NH were able to facilitate the elimination reaction, evidencing the remarkably high catalytic activity of **4.3v**.

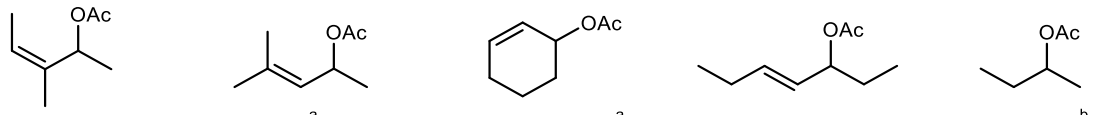

4.67l, 43%
E:*Z* = 3.6:1
91:9 e.r. (*E*)

4.67m, 95%,[a] >20:1 r.r.
73.5:26.5 e.r.

4.67n, quant.[a]
62.5:37.5 e.r.

4.67o, 51%
66.5:33.5 e.r.

4.67p, N/A[b]

Figure 4.4 Allylic acetates and sec-butyl acetates; substrates that led to unsatisfactory outcomes under the standard reaction conditions. Reactions were performed at −80 °C, and evaluated by ^{1}H NMR spectroscopy using mesitylene as an internal standard. [a]reaction performed at −60 °C. [b]reaction performed at 25 °C.

We were keen to explore the derivatization of product **4.68e**, given the versatility of vinyl halide groups in organic transformations. In the interest of continuing the theme of hydrocarbon synthesis, we attempted to develop an intramolecular Heck reaction toward 5,6-fused ring compound **4.70**. However, subjecting **4.68e** to Pd-catalyzed Heck conditions using $Pd(OAc)_2$ and *rac*-2,2'-bis(diphenylphosphino)-1,1'-binaphthyl (*rac*-BINAP, **4.69**) did not afford the desired product (Scheme 4.21). This observation is congruent with the difficult nature of 5-*endo* Heck cyclizations, a reaction which typically precludes unactivated olefin substrates from participation.[293]

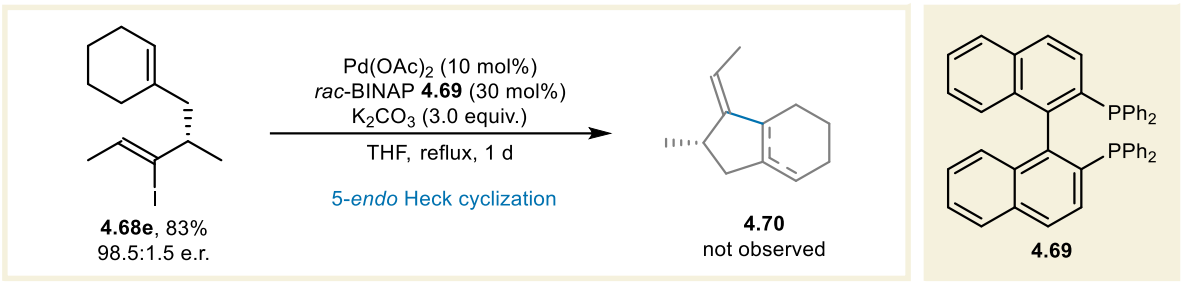

Scheme 4.21 Attempt at a 5-*endo* Heck cyclization of **4.68e**.

Therefore, we altered our approach to that of a carbonylative Heck reaction, hoping to facilitate the more common 5-*exo*- and 6-*endo*-cyclizations (Scheme 4.22). Using $Pd(PPh_3)_4$, we observed the formation of two distinct cyclized products, which were confirmed by NMR spectroscopy and MS to be 6-*endo* product **4.72** and 5-*exo* product **4.73**. Due to the formation of a number of unidentifiable by-products, we were unable to isolate these compounds and accurately determine the yield and enantiospecificity of the reaction. Interestingly, the 5-*exo* product **4.71** could not be detected in the reaction mixture. We speculated that after 5-*exo*-cyclization, the resulting organopalladium species preferentially underwent a second CO-insertion reaction. Under the basic reaction conditions, deprotonation of the enone, followed by coordination of the enolate to the acyl palladium complex then led to ring closure by reductive elimination, yielding **4.73** as the major product. We hypothesized that **4.72** was formed through 6-*endo*-cyclization, followed by *syn*-β-hydride elimination toward the β,γ-unsaturated ketone. However, this product isomerized to the more stable enone product under the basic reaction conditions, and base-catalyzed isomerization of the exocyclic double bond led to the formation of an *E*/*Z*-mixture. Screening additional ligands such as *rac*-BINAP (**4.69**), cataCXium (**4.74**), and Xantphos (**4.75**) yielded complex mixtures in which the desired products could not be identified. However, the reaction showed a slight preference for the formation of 6-*endo* product **4.72** with 1,1'-bis(diphenylphosphino)ferrocene (dppf, **4.76**). This preference was enhanced when we switched to PEPPSI-IPr (**4.77**) as the Pd-source. These results demonstrated that **4.68e** could undergo carbonylative Heck cyclization towards two different products, and that the choice of catalytic system could be leveraged in a divergent synthesis of 6-*endo* product **4.72** and the unexpected 5-*exo* double carbonylation product **4.73**.

The preceding subchapter demonstrated the broad applicability of our developed alkylation reaction of unactivated olefins with benzylic- and allylic acetates, and the use of the resulting products in follow-up transformations. Thorough exploration of the substrate scope

allowed us to turn our attention back to the prospective direct alkylation of olefins using alcohols.

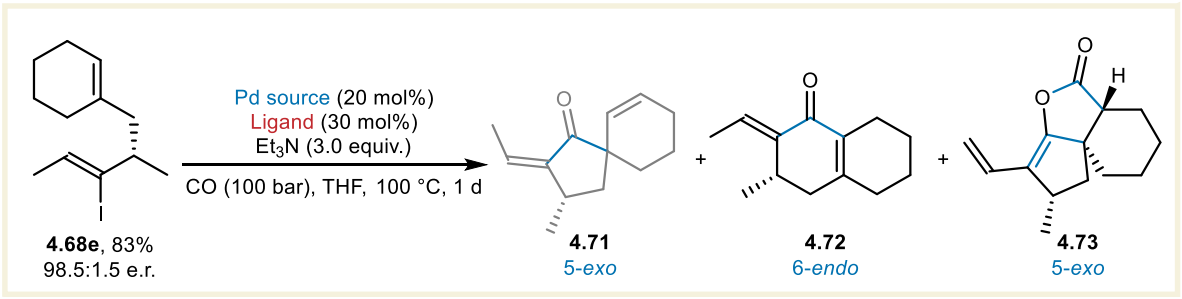

entry	Pd source	Ligand	ratio **4.72**:**4.73**	*E*:*Z* **4.72**[a]	d.r. **4.73**[a]
1[b]	$Pd(PPh_3)_4$	-	1:1.6	1.4:1	5:1
2	$Pd(OAc)_2$	*rac*-BINAP **4.69**	complex mixture	N/A	N/A
3	$Pd(OAc)_2$	cataCXium **4.74**	complex mixture	N/A	N/A
4	$Pd(OAc)_2$	Xantphos **4.75**	complex mixture	N/A	N/A
5	$Pd(OAc)_2$	dppf **4.76**	1.1:1	1.2:1	2.8:1
6	PEPPSI-IPr **4.77**	-	5.4:1	1.6:1	3:1

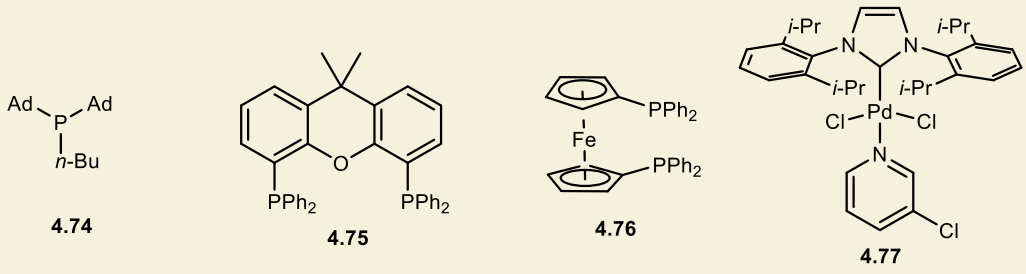

Scheme 4.22 Attempts at 5-*exo*- and 6-*endo* Heck cyclizations of **4.68e**. [a]major product isomers are shown. [b]reaction performed with 50 mol% $Pd(PPh_3)_4$, 50 bar of CO, at 80 °C.

4.3. Developing a Two-Step, One-Pot Process and Upscaling the Reaction

The two-step, one-pot process was developed in cooperation with the undergraduate student Thibault Gotta.

In section 4.1.2, we proposed the development of a two-step, one-pot process for the alkylation of olefins with alcohols (Scheme 4.23). Our proposal relied on the innocuous nature of the by-products of acid-catalyzed acylation reactions; most notably AcOH when using Ac_2O, and acetone when using isopropenyl acetate. Therefore, we decided to explore the acylation reaction of benzylic alcohol **4.1** using common acylation reagents in the presence of an IDPi catalyst, under the standard reaction conditions of our model olefin alkylation reaction.

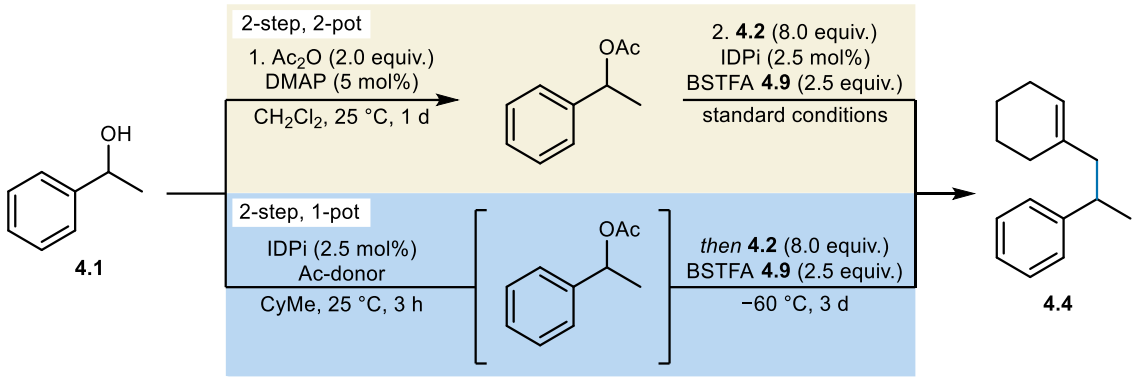

Scheme 4.23 Conceptualization of a two-step, one-pot olefin alkylation reaction with benzylic alcohol **4.1**.

Our screening of three acylating reagents revealed that IDPi **4.3a** efficiently catalyzed the acylation of **4.1** at 25 °C (Scheme 4.24A). The reaction with Ac_2O afforded **4.23** with excellent yield, and with negligible by-product formation. Conversely, reactions with isopropenyl acetate and AcCl as acyl-donors provided **4.23** with poor yields, and the formation of significant quantities of ether **4.6** was observed. Formation of styrene (**4.7**) was not observed in all three reactions. Switching to IDPi **4.3v** led to the formation of near-quantitative **4.23** in only three hours.

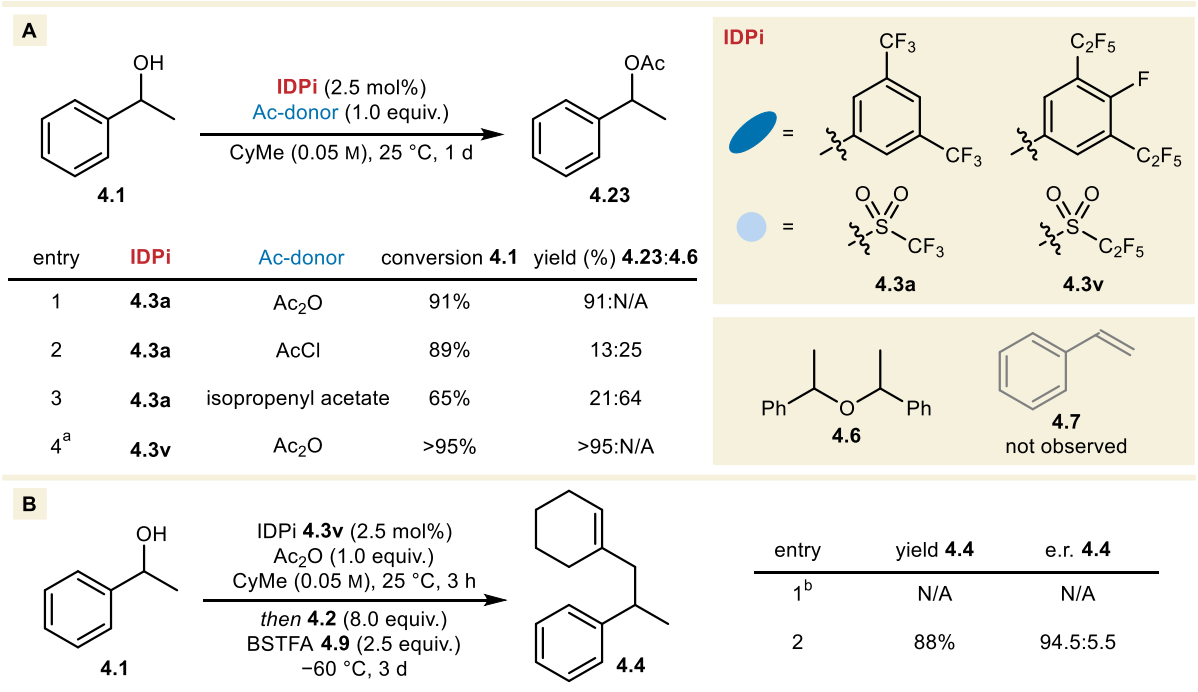

entry	IDPi	Ac-donor	conversion **4.1**	yield (%) **4.23**:**4.6**
1	**4.3a**	Ac_2O	91%	91:N/A
2	**4.3a**	AcCl	89%	13:25
3	**4.3a**	isopropenyl acetate	65%	21:64
4[a]	**4.3v**	Ac_2O	>95%	>95:N/A

entry	yield **4.4**	e.r. **4.4**
1[b]	N/A	N/A
2	88%	94.5:5.5

Scheme 4.24 Screening of acylation reagents in the IDPi-catalyzed acylation of **4.1** (A), and application of the acylation reaction in a two-step, one-pot process (B). Yields were determined by ^{1}H NMR spectroscopy using CH_2Br_2 as an internal standard. [a]reaction time = 3 h. [b]reaction vessel improperly sealed.

These conditions were applied to a two-step, one-pot reaction. After the three-hour acylation reaction with Ac_2O, the reaction mixture was cooled to −60 °C, and olefin **4.2**

and BSTFA were added (Scheme 4.24B). We discovered that under these conditions, the reaction was very sensitive to residual water. The olefin alkylation reaction did not take place when the reaction vessel was improperly sealed, and only acetate **4.23** was obtained. When the reaction was performed in a properly dried reaction vessel, hydrocarbon **4.4** was obtained in 88% yield, and a slightly reduced e.r. of 94.5:5.5; a comparable result to the established model reaction starting from acetate **4.23**.

The developed two-step, one-pot process was applied to the synthesis of **4.4** on a larger scale. We aimed to perform the two-step, one-pot reaction at 13.00 mmol scale. However, due to limitations of the equipment, water entered the reaction vessel on our initial attempt, which led to stalling of the reaction at the acylation stage. Fortunately, we were able to re-isolate the catalyst, which showed negligible decomposition after being subjected to the reaction conditions. In our second attempt, we were able to establish dry reaction conditions, allowing us to perform the reaction at 8.59 mmol scale. The product was obtained with a yield of 1.17 g (68%) and 95.5:4.5 e.r.; a comparable result to the above screening reaction, as well as the previously established model olefin alkylation reaction.

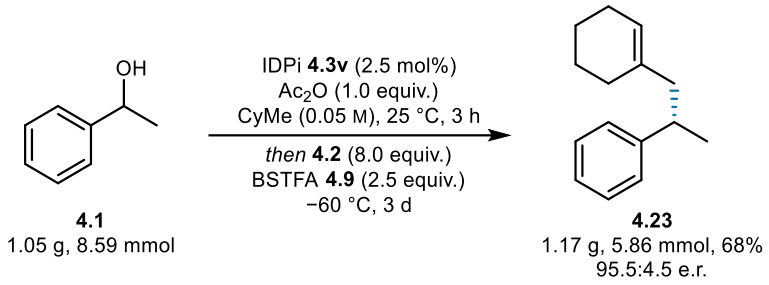

Scheme 4.25 The two-step, one-pot reaction scaled up by a factor of 430.

Demonstrating that our developed two-step, one-pot olefin alkylation can be scaled up by a factor of at least 430 simultaneously established the scalability of the developed methodology starting from acetate **4.23**. Having optimized this process, we turned our attention toward elucidating the mechanism of the reaction.

4.4. Experimental Investigation of the Olefin Alkylation Reaction Mechanism

Mechanistic experiments were performed to build a better understanding of the developed reaction on a molecular level. Our experimental design was informed by previous observations with regard to the yield and enantioselectivity of the model reaction and select

scope entries. One key observation was a seemingly reduced reaction rate over time when performing our optimization studies (see section 4.1.3). We hypothesized that by-product inhibition might result in a slower reaction rate as conversion of the acetate increased. Furthermore, the stereoablative substrate activation made us were eager to establish whether the developed olefin alkylation was an S_N1 reaction featuring kinetic resolution (KR).

A general mechanistic hypothesis of the model reaction was established based on our observations during development of the reaction and exploration of the substrate scope (Scheme 4.26). We envisioned that initial silylation of the catalyst with BSTFA furnishes the silylated IDPi. Due to the formation of a stereogenic S(VI) center, the silylated catalyst could exist as a mixture of (rapidly interchanging) diastereomers. However, a previous report by our group suggested that one diastereomer of the silylated catalyst dominates, as evidenced by the instantaneous formation of two dd signals in ^{31}P NMR upon addition of a triisopropylsilyl donor to the IDPi.[294] Next, coordination of the catalyst to the acetate **4.23** results in substrate activation to afford the ion pair, accompanied by the loss of Me_3SiOAc. Subsequent nucleophilic attack of olefin **4.2** onto the benzylic carbocation constitutes the enantiodetermining, C–C bond-forming step. Finally, deprotonation of the tertiary cation completes the cycle, delivering hydrocarbon product **4.4** and the Brønsted acid catalyst.

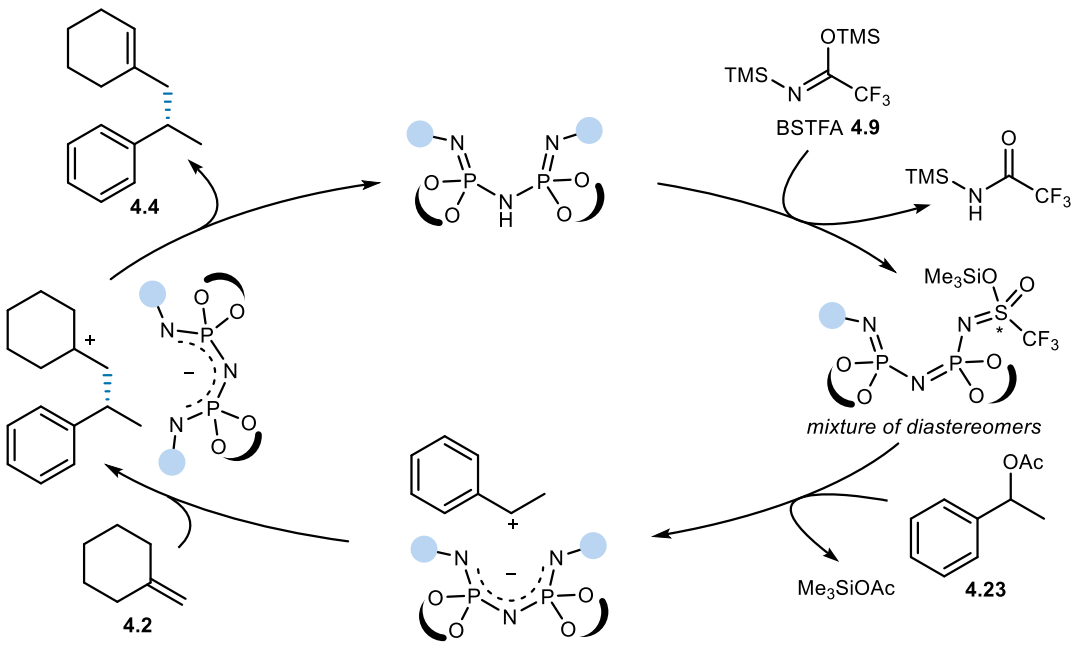

Scheme 4.26 Mechanistic hypothesis for the model IDPi-catalyzed olefin alkylation reaction of methylenecyclohexane **4.2** with benzylic acetate **4.23**.

4.4.1. *Reaction Monitoring and Inhibition Studies*

We started our mechanistic investigations by studying the concentration profile and e.e. of the starting material and product over time. A reaction monitoring experiment of the model reaction was performed using catalyst **4.3a** (Figure 4.5). Data on the reactivity of **4.23** toward **4.4** were obtained by taking aliquots of the reaction mixture containing DCE as an internal standard over three days. The aliquots were subsequently analyzed by ^{1}H NMR and chiral GC.

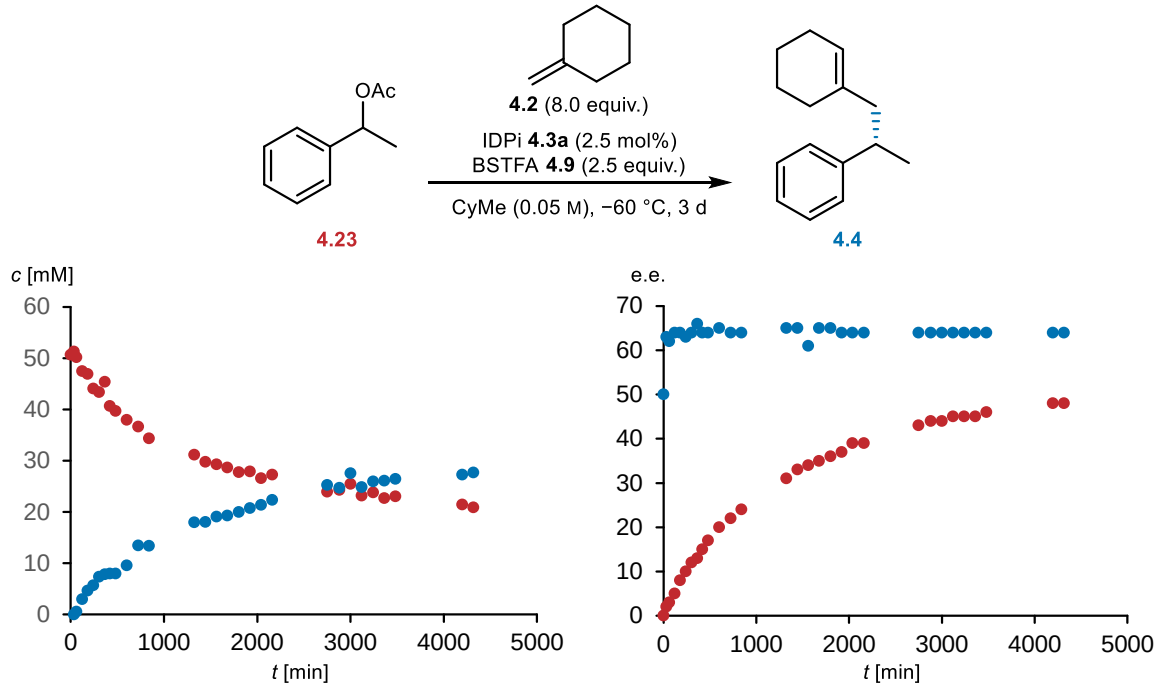

Figure 4.5 Monitoring of the concentration profile and e.e. of **4.23** and **4.4** in the model reaction with **4.3a**.

The concentration profile revealed a significant decrease of the reaction rate over time; an expected result for an S_N1 reaction with first-order dependence on the electrophile. However, the stark decrease of the reaction rate at higher conversions is incompletely explained by a decrease in the concentration of **4.23**. This led us to suspect an inhibitory effect caused by a by-product of the reaction. This suspicion was strengthened by the observed e.e. values of the starting material and product over time. The constant e.e. of **4.4** strongly suggested an S_N1 reaction pathway. Mechanistically, an S_N1 process funnels both enantiomers of **4.23** through a common carbocation intermediate before undergoing nucleophilic attack. Consequently, the enantioselectivity of the reaction is not influenced by the relative concentrations of the enantiomers of **4.23**. A steep increase in the e.e. of **4.23** was observed at low conversion, which leveled off over the duration of the reaction. The preferential consumption of one enantiomer of the acetate indicates a KR. However, the stabilization of e.e. and incomplete consumption of

one enantiomer implies *in situ* racemization of the acetate, hinting at a dynamic kinetic resolution (DKR). We suspected that racemization of **4.23** could be a consequence of reversible substrate activation. In this scenario, the liberated Me_3SiOAc would add back onto the common carbocationic intermediate, with the loss of the trimethylsilyl group. Reversible substrate activation would also rationalize the decreased reaction rate at higher conversions. In this scenario, Me_3SiOAc competes with olefin **4.2** in the nucleophilic addition to the common carbocation intermediate, and acts as a concentration-dependent inhibitor.

To probe the potential inhibitory effect of the by-product, we performed the model reaction in the presence of variable quantities of Me_3SiOAc (Figure 4.6, left). These experiments revealed a decrease in the reaction rate in the presence of higher initial concentrations of Me_3SiOAc. From these measurements, we aimed to establish the partial order of the reaction with respect to Me_3SiOAc. Assuming an S_N1 reaction, the rate equation of the catalytic model reaction including an inhibitor may take the form of:

$$v = k[\mathbf{4.23}]^{\alpha}[\mathrm{Me_3SiOAc}]^{\beta}[\mathrm{IDPi}]^{\gamma} \tag{4.1}$$

Where v is the rate of the reaction, k is the rate constant, and α, β, and γ are the partial orders with respect to each reaction component. Using variable time normalization analysis (VTNA) allowed us to determine the partial order of the reaction with respect to the inhibitor by simple graphical analysis, independently of the other reaction components.[295] In VTNA, the time axis of the concentration profile is replaced by the approximated time integral of the analyte raised to the correct power. Normalization of the time axis with respect to the time integral of Me_3SiOAc was performed according to:

$$\int_{t=0}^{t=n} [\mathrm{Me_3SiOAc}]^{\beta} dt \approx \sum_{i=1}^{n} \left(\frac{[\mathrm{Me_3SiOAc}]_i + [\mathrm{Me_3SiOAc}]_{i-1}}{2} \right)^{\beta} (t_i - t_{i-1}) \tag{4.2}$$

To determine partial order β, the concentration profiles of three separate measurements are plotted against the time integral of Me_3SiOAc (Figure 4.6, right). By incrementally varying the value of β, the correct value for this exponent can be visually estimated. Our VTNA analysis with respect to Me_3SiOAc revealed a value of β of approximately −0.5. This partial order relates the rate of the model reaction to the concentration of Me_3SiOAc according to:

$$v \propto [\mathrm{Me_3SiOAc}]^{-0.5} \tag{4.3}$$

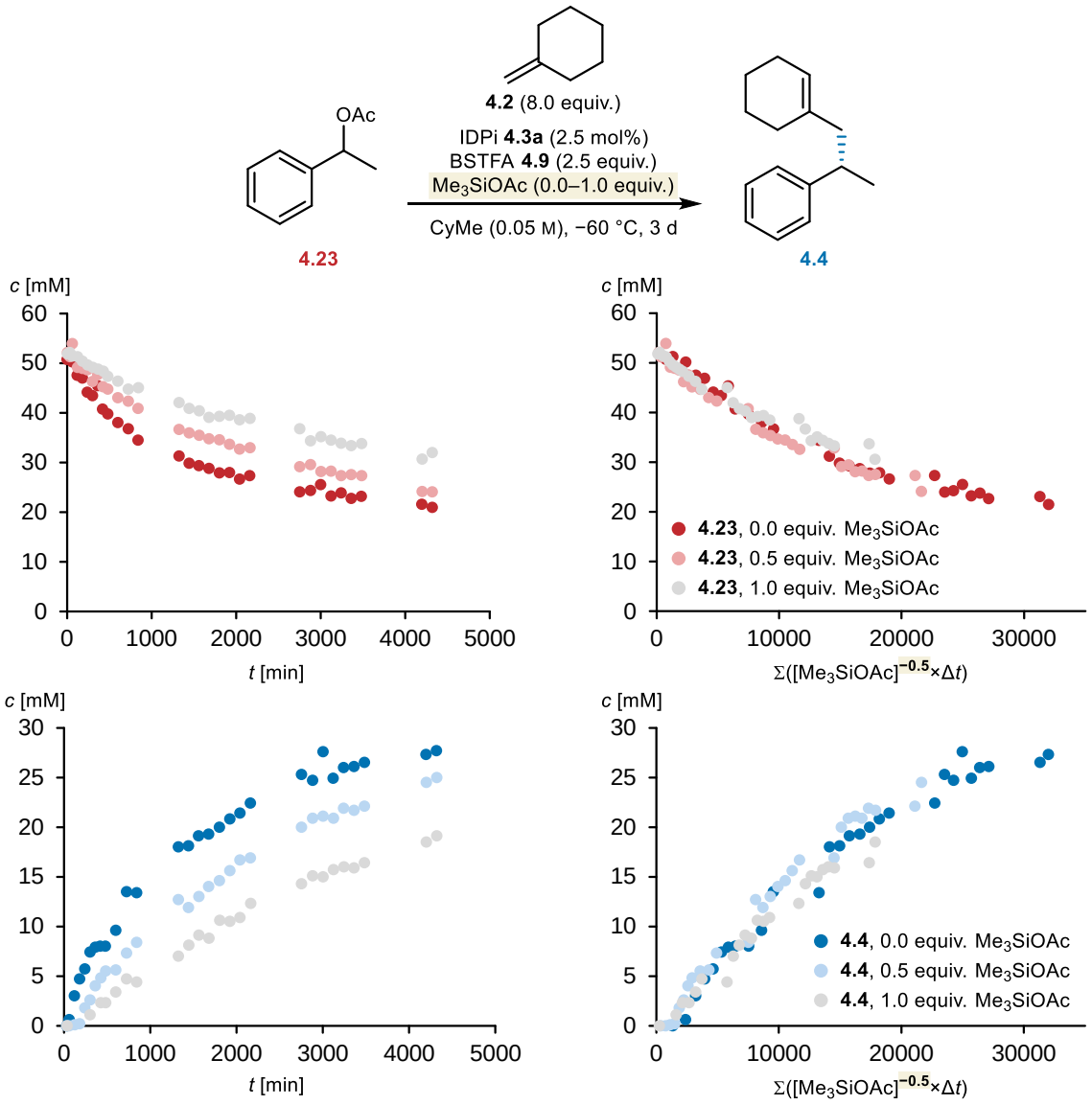

Figure 4.6 The model olefin alkylation reaction performed with variable concentrations of Me_3SiOAc and IDPi **4.3a** (left), and VTNA analysis of these experiments (right).

A fractional partial order can be indicative of a complex reaction mechanism. In the case of our model reaction, the common carbocationic intermediate leading to both racemization and C–C bond formation could be the cause of this complexity. The observed DKR characteristics of the reaction corroborate this hypothesis. In typical reactions featuring a DKR, racemization is a fast process, resulting in effectively racemic starting materials being present throughout the reaction.[296] Conversely, our developed model reaction shows enantioenrichment of the starting material, albeit tending to a maximum. This observation indicates that racemization occurs with a slower rate than the reaction toward **4.4** at low concentrations of Me_3SiOAc, but the rates of racemization and C–C bond formation equalize as the concentration of Me_3SiOAc increases. This experiment led us to conclude that Me_3SiOAc is a semi-competitive nucleophile toward

the benzylic cation, which exhibits a weak inhibitory effect at higher concentrations. This observation explains incomplete conversion in the reactions of **4.23** with some weakly nucleophilic olefin substrates.

4.4.2. *Leaving Group Scrambling Studies*

To further assess the reversibility of benzylic cation formation, a leaving group scrambling experiment was performed (Figure 4.7). Acetate **4.23** was subjected to the standard reaction conditions in the presence of IDPi **4.3a** and equimolar deuterium-labeled $Me_3SiOAc\text{-}d_3$, while the olefin nucleophile was excluded.

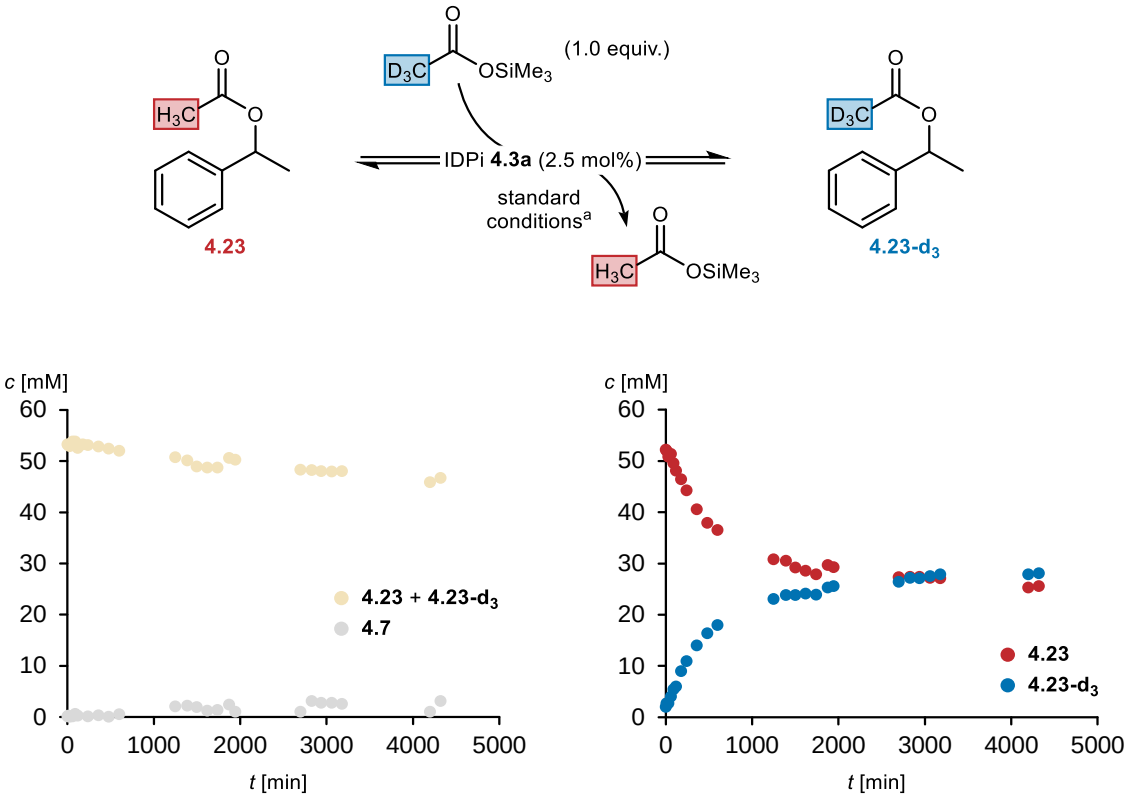

Figure 4.7 Leaving group scrambling experiment with IDPi **4.3a**. [a]standard conditions: BSTFA **4.9** (2.5 equiv.), CyMe (0.05 M), −60 °C, 3 d.

Monitoring of the total concentration of **4.23** + **4.23-d3** and styrene (**4.7**) revealed that elimination remained limited over the course of the reaction, allowing us to assess the isotopic distribution of the starting material with reasonable confidence. We found that after approximately two days, near-complete scrambling of the leaving group had occurred, leading to the formation of a roughly 1:1 mixture of **4.23** and **4.23-d3**. This observation confirmed our suspicion that activation of **4.23** is reversible, and provided additional evidence that Me_3SiOAc

acts as a competitive nucleophile toward the benzylic cation. Interestingly, leaving group scrambling occurs at a similar rate to the observed formation of **4.4** during our earlier reaction monitoring experiment, indicating that the elementary step of carbocation formation is likely the rate-determining step of the reaction.

4.4.3. *Kinetic Isotope Effect Studies*

Exploration of the allylic acetate scope of the model reaction revealed that allylic acetate **4.67h** and its allylic transposition isomer **4.67h'** react in an enantioconvergent manner toward product **4.68h** with similar regio- and enantioselectivities (section 4.2.4). These observations strongly suggested that our developed methodology is an S_N1 reaction where carbocation formation precedes C–C bond formation. Additionally, the above leaving group scrambling experiment suggested that carbocation formation from **4.23** could be the rate determining step of the reaction. To rule out an S_N2 pathway and investigate the rate-determining step of the reaction, we performed intermolecular competition H/D kinetic isotope effect (KIE) studies. To this end, 1-phenylethyl-1-*d* acetate (**4.23-d$_1$**) was synthesized (Scheme 4.27).

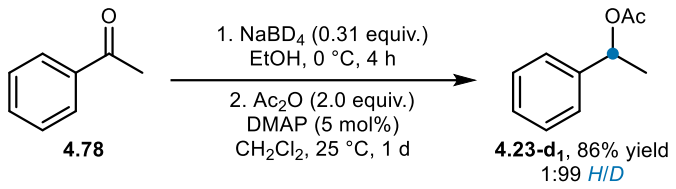

Scheme 4.27 Synthesis of **4.23-d$_1$** for intermolecular competition H/D KIE experiment. H/D-labeled carbon indicated in blue.

In conventional intermolecular competition KIE experiments, the KIE value of the product (KIE_P) is calculated by simply taking the ratio of light/heavy isotope-labeled product.[297] However, this method neglects the changing ratio of light/heavy isotope-containing starting material in a reaction where the KIE ≠ 1. To take these changes in relative concentrations into account, the conversion-dependent KIE_P can be calculated according to:[298]

$$\mathrm{KIE_P} = \frac{\ln\left(1-F\right)}{\ln\left[1-\left(\frac{FR_P}{R_0}\right)\right]} \tag{4.4}$$

where F is the conversion with respect to the total amount of consumed starting material, R_P is the isotope ratio of the product, and R_0 is the isotope ratio of the starting material at $t = 0$. The

isotope ratios are calculated by dividing the fraction of heavy isotope compound by the fraction of light isotope compound (X_D/X_H). Conversion of the starting material and the ratio R_P/R_0 for the intermolecular competition experiment with **4.23** and **4.23-d$_1$** are given by:[299,300]

$$F = 1 - \frac{[\mathbf{4.23} + \mathbf{4.23\text{-}d_1}]}{[\mathbf{4.23} + \mathbf{4.23\text{-}d_1}]_0} \tag{4.5}$$

$$\frac{R_P}{R_0} = \frac{\left(\frac{[\mathbf{4.4\text{-}d_1}]}{[\mathbf{4.4}]}\right)}{\left(\frac{[\mathbf{4.23\text{-}d_1}]}{[\mathbf{4.23}]}\right)} = \frac{[\mathbf{4.4\text{-}d_1}] \times [\mathbf{4.23}]}{[\mathbf{4.23\text{-}d_1}] \times [\mathbf{4.4}]} \tag{4.6}$$

Furthermore, the uncertainty of the calculated KIE$_P$ (ΔKIE) with respect to F and R_P/R_0 in each experiment can be calculated according to equations (4.7) and (4.8), and combined uncertainty ΔKIE$_P$ is given by equation (4.9).[298,299]

$$\Delta\mathrm{KIE_F} = \left\{ \frac{\left(\frac{R_P}{R_0}\right) ln(1-F)}{\left[1 - F\left(\frac{R_P}{R_0}\right)\right] ln^2\left[(1-F)\frac{R_P}{R_0}\right]} - \frac{1}{(1-F)ln\left[1 - F\left(\frac{R_P}{R_0}\right)\right]} \right\} \Delta F \tag{4.7}$$

$$\Delta\mathrm{KIE_R} = \left\{ \frac{-Fln(1-F)}{\left[1 - F\left(\frac{R_P}{R_0}\right) ln^2\left[1 - F\left(\frac{R_P}{R_0}\right)\right]\right]} \right\} \Delta\left(\frac{R_P}{R_0}\right) \tag{4.8}$$

$$\Delta\mathrm{KIE_P} = \sqrt{\Delta\mathrm{KIE_F}^2 + \Delta\mathrm{KIE_R}^2} \tag{4.9}$$

The intermolecular competition study between non-deuterated **4.23** and deuterated **4.23-d$_1$** was performed in the presence of catalyst **4.3a** under the standard olefin alkylation conditions. The reaction was performed in duplicate to minimize the potential for measurement error (Table 4.1, entries 1 and 2). Conversion of **4.23** and **4.23-d$_1$** were determined by ^{1}H NMR spectroscopy, and the isotope ratios of the 1:1 starting mixture of **4.23**:**4.23-d$_1$**, and product **4.4** were determined by GC-MS. These measurements yielded values for F, R_P, and R_0 summed up in Table 4.1. Applying equations (4.4)–(4.9) to the obtained data yielded values for KIE$_P$ and ΔKIE$_P$ for each of the duplicate experiments. Taking the average of these KIE values, and the

root mean square of their respective ΔKIE_P values yielded a final KIE of 1.30 ± 0.05 for this intermolecular competition experiment.

Table 4.1 Data analysis for intermolecular competition KIE experiment. H/D-labeled carbon indicated in blue.

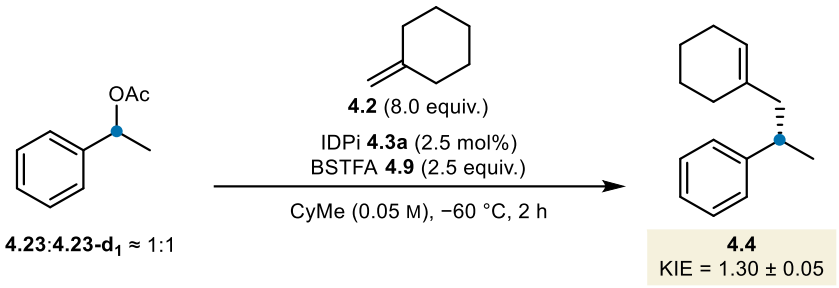

entry	R_P	R_0	F	$KIE_P \pm \Delta KIE_P$
1	0.741 ± 0.01	0.951 ± 0.01	9.9% ± 2.0%	1.30 ± 0.03
2	0.727 ± 0.04	0.938 ± 0.01	4.2% ± 2.0%	1.30 ± 0.07

Since no bond is broken or formed to the isotopically labeled atom, only to the adjacent carbon atom (C_α), the observed KIE is secondary in nature. The largest contributor to an observable secondary KIE is the change in zero-point energy (ZPE) of the out-of-plane bending modes for C_α–H and C_α–D bonds going from C(sp^3)–H/D to C(sp^2)–H/D. The higher ZPE of C(sp^3)–H bonds compared to C(sp^3)–D bonds results in a lower relative activation energy of the former toward the C(sp^2) intermediate, in which the out-of-plane bending vibration is weakened. Consequently, compounds containing lighter isotopes have comparatively high reaction rates in reactions where C(sp^3) to C(sp^2) rehybridization takes place as the rate-determining step. For such a reaction, KIE >1, which is classified as a "normal" KIE. Accordingly, inverse KIEs (KIE < 1) are observed in reactions with C(sp^2) to C(sp^3) rehybridization as the rate-determining step.[301]

Our observed secondary normal KIE of 1.30 ± 0.05 thus suggests rate-determining formation of a benzylic carbocation after departure of the leaving group from substrate **4.23**. Attribution of the KIE to this elementary step is definitive within our mechanistic hypothesis, because there is no upstream rehybridization event involving the substrate, and downstream C(sp^2) to C(sp^3) rehybridization during C–C bond formation would lead to an inverse KIE.[297] Furthermore, catalyst deprotosilylation does not involve the isotopically labeled substrate, and we can assume deprotosilylation of IDPi **4.3a** to be fast based on previous studies.[294] The observed negligible isomerization of alkene **4.2** under the reaction conditions—and even at room temperature (see section 4.1.1)—also suggests that the resting state of the catalyst is the silylated form.

KIE measurements can also be used to distinguish between S_N1 and S_N2 reactions. Secondary large normal isotope effects are atypical for S_N2 pathways, because the trigonal bipyramidal transition state during Walden inversion leads to relatively small changes in the frequencies of out-of-plane bending vibrations, resulting in small normal or inverse KIEs of ~1.[302] Significant secondary normal KIEs have a theoretical maximum value of 1.4. However, values of 1.1–1.2 are more commonly found, because the full difference between the sp^3 and sp^2 carbon upon rehybridization is usually not felt at the transition state.[301] The found large secondary normal KIE of 1.30 ± 0.05 in our experiment therefore establishes that substantial $C(sp^3)$ to $C(sp^2)$ rehybridization occurs, indicating strong S_N1 character.

4.4.4. *Reactions with Enantiopure Starting Materials*

To further rule out an S_N2 mechanism, and provide additional evidence for the existence of a DKR in the model reaction, we performed the model reaction starting from enantiopure acetates (*R*)-**4.23** and (*S*)-**4.23** in parallel with racemic **4.23** (Figure 4.8). As expected from our earlier observations pointing to a DKR, different levels of conversion were observed for each enantiomer of **4.23** after a one-day reaction time. Furthermore, the reactions were enantioconvergent, producing (*S*)-enriched **4.4** as the sole product with nearly the same enantiomeric ratio in all cases. This result supports our hypothesis of an S_N1 reaction proceeding through a common benzylic carbocation intermediate, corroborating our earlier observations in the convergent synthesis of **4.68h** from **4.67h** and **4.67h'** (section 4.2.4), and the above KIE studies. Moreover, chiral GC analysis of the recovered starting material reveals that **4.23** is enriched for the (*S*)-enantiomer, regardless of the absolute configuration of the starting material. These data are in line with our observation that an equilibrium of (*R*)/(*S*)-**4.23** is reached over time. A higher reaction rate for (*R*)-**4.23** toward (*S*)-**4.4** is additionally indicative of an S_N1 reaction, because Walden inversion during the S_N2 reaction of (*R*)-**4.23** with **4.2** would lead to the formation of (*R*)-**4.4**.

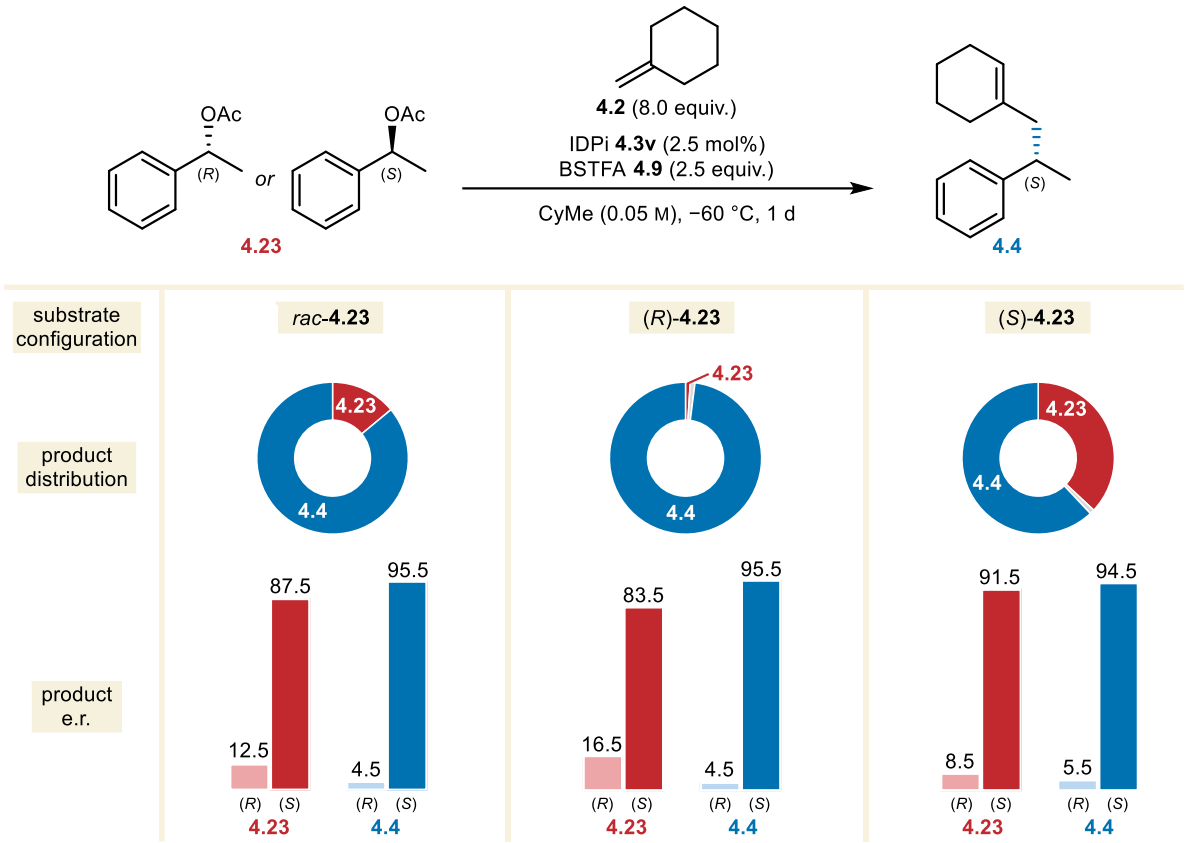

Figure 4.8 Data analysis for reactions with racemic and enantiopure **4.23** in the presence of IDPi **4.3v**. Yields were determined by ^{1}H NMR spectroscopy using mesitylene as an internal standard.

4.4.5. *Evaluation of the Role of BSTFA*

Lastly, the role of BSTFA (**4.9**) in the model reaction was more closely examined. Since BSTFA possesses two trimethylsilyl groups, we were keen to determine whether both trimethylsilyl groups could engage in the reaction. To test this, we performed the model reaction in the presence of varying amounts of BSTFA. The reactions were performed in dried glassware under an argon atmosphere to minimize the hydrolysis of the reagent due to the self-drying and self-repair cycle of silylium-ACDC.

As previously described, no product was formed in the absence of BSTFA. Interestingly, even at 0.25 equivalents of BSTFA, a minor amount of **4.4** was formed. As expected, increasing the equivalents of BSTFA used led to an increase in yield. Under the dry reaction conditions, we observed the formation of 77% of **4.4** with only 0.5 equivalents of BSTFA. This high yield confirms our suspicion that both trimethylsilyl groups of BSTFA can be used in the reaction. Assumedly, residual water in the vessel or the reagents causes the sub-quantitative yield in this

reaction. The use of 1.0 equivalent of BSTFA led to near-quantitative product formation. Given the water-sensitivity of the reaction, we speculate that using 2.5 equivalents of BSTFA provides a "cushion" of robustness for the developed methodology, as the excess of silylating reagent facilitates the self-drying- and self-repair cycles of the catalyst.

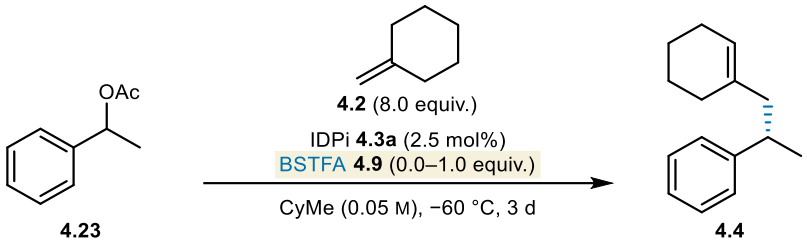

entry	equiv. **4.9**	yield **4.4**	e.r. **4.4**
1	0.0	N/A	N/A
2	0.25	16%	95:5
3	0.5	77%	95.5:4.5
4	1.0	>95%	95.5

Scheme 4.28 Evaluation of the stoichiometry of BSTFA (**4.9**) under dry reaction conditions. Yields were determined by ^{1}H NMR spectroscopy using mesitylene as an internal standard.

4.4.6. *Updated Mechanistic Hypothesis*

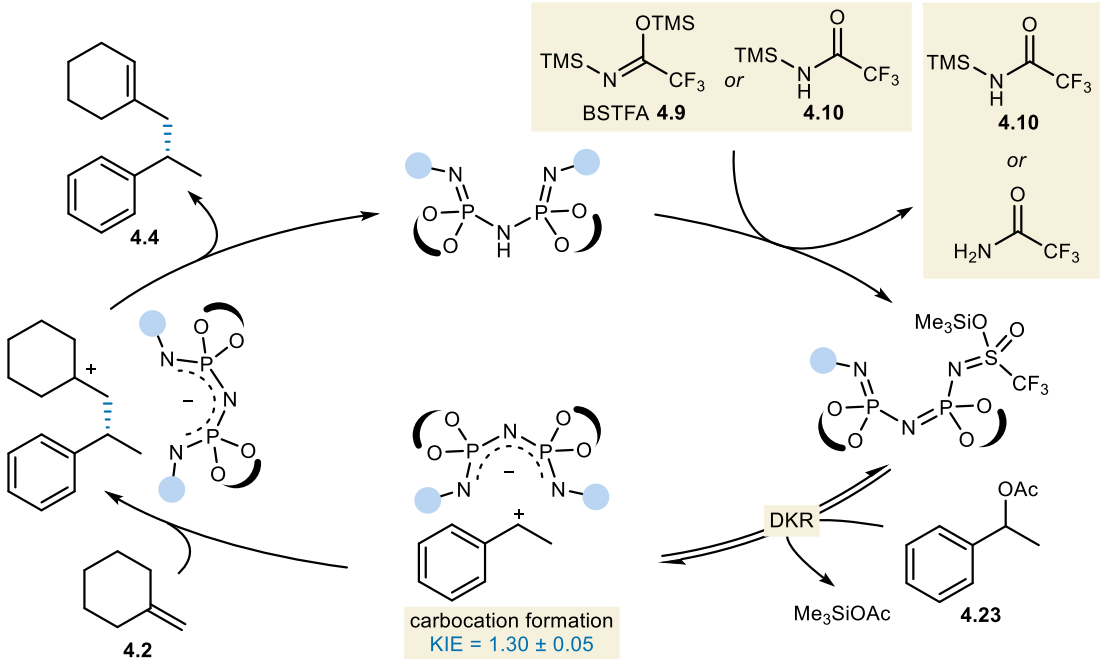

Scheme 4.29 Updated mechanistic hypothesis for the model IDPi-catalyzed olefin alkylation reaction of methylenecyclohexane **4.2** with benzylic acetate **4.23**.

The above mechanistic experiments allowed us to update our mechanistic hypothesis (Scheme 4.29) by including the observed phenomena of: 1) catalyst deprotosilylation using both trimethylsilyl groups of BSTFA; 2) reversible leaving group activation, leading to a DKR where Me_3SiOAc acts as a weakly competitive nucleophile to the olefin, causing a degree of racemization; 3) carbocation formation preceding C–C bond formation with the nucleophilic alkene moiety.

In summary, our experimental mechanistic studies elucidated important kinetic aspects of the developed catalytic asymmetric olefin alkylation reaction. These findings allowed us to propose a plausible reaction mechanism, which strongly implies the formation of an ion pair between a benzylic cation and the catalyst anion, brought about by activation of the acetate substrate by the highly Lewis acidic silylium-IDPi.

5. SUMMARY

Inspired by the biosynthesis of terpenoids, we established an intermolecular catalytic asymmetric alkylation of olefins with alcohol derivatives (Scheme 5.1). A niche of reactivity was discovered for highly acidic IDPi catalysts with benzylic acetates in the presence of an appropriate silylating agent. Activation of acetates with silylated IDPis bearing strongly electron-withdrawing groups in the wings and core furnished minimally stabilized carbocations. These highly electrophilic species were leveraged to alkylate unactivated olefins.

Installing *p*-fluoro substituents on the wings of the IDPi proved crucial to the design of our optimal catalyst. These fluorine substituents provided a breakthrough in enantioselectivity of our model reaction when exhaustive screening of *m*- and *p*-fluorinated substituents did not yield the desired results. We attributed this previous lack of success to the sterically encumbered environment at the active site of the catalyst brought about by more sterically demanding substituents. Halide substituents therefore provided a narrow "steric window of opportunity" to reach the desired enantioselectivity in our model reaction. The solid-state structure of the optimal catalyst corroborated our hypothesis by revealing that the key fluorine substituents directly flanked the active site of the catalyst (Figure 5.1).

During our exploration of the substrate scope, we initially branched out in two directions. First, we explored substitution of the model substrate's arene moiety, and successfully incorporating a number of electron-donating and electron-withdrawing groups. Second, we investigated a range of unactivated olefin nucleophiles. To our delight, we were able to employ di-, tri-, and even tetrasubstituted alkenes, despite the non-nucleophilic nature of highly substituted alkenes. The regioselectivity of the deprotonation step could be controlled by the choice of olefin, affording the allylation- and vinylation products with generally excellent regioselectivities.

Pushing further, we expanded the substrate scope to allylic acetates; substrates which are underrepresented as alkyl donors in asymmetric organocatalytic reactions with unactivated olefin nucleophiles. In fact, only one previous report of an asymmetric olefin alkylation reaction with alcohols had been reported to the best of our knowledge.[269] This prior report used Ir-catalysis to selectively furnish branched products. Our exploration of the allylic acetate scope revealed that our method was complementary to the existing report, yielding the 1,5-diene products with highly regio- and enantioinduction in a reaction under steric control.

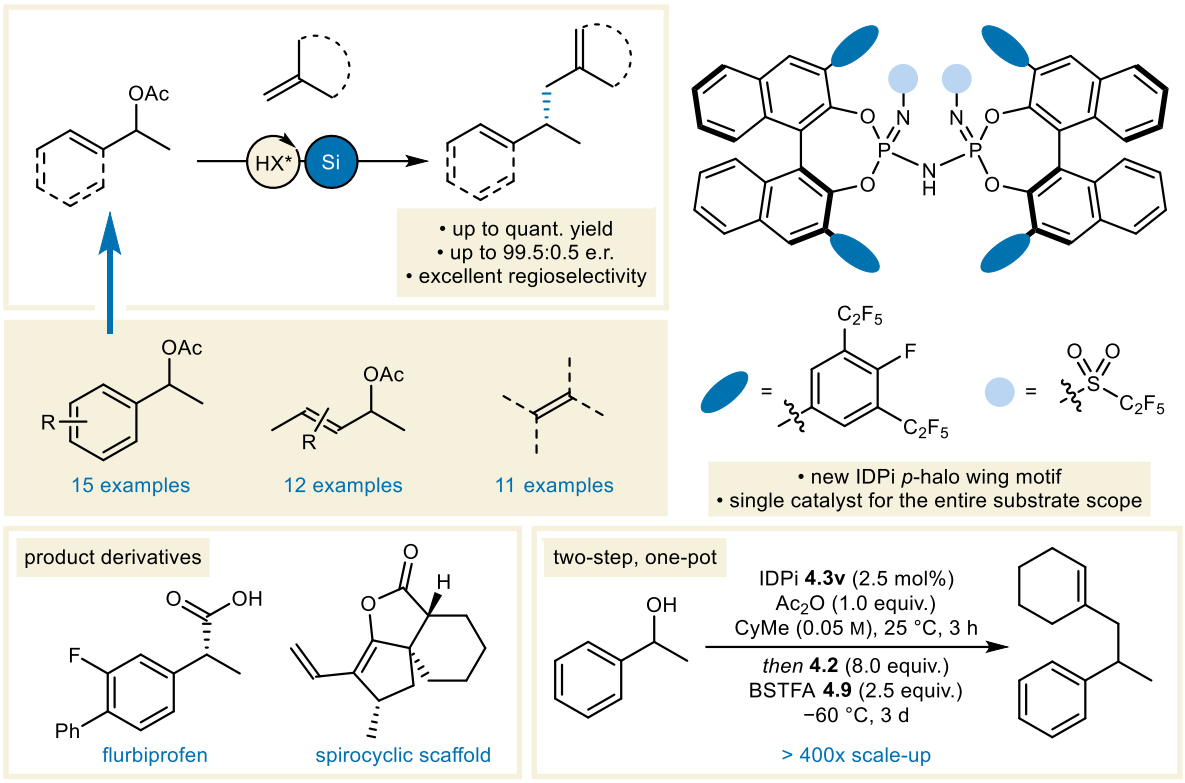

Scheme 5.1 Summary of the developed catalytic asymmetric alkylation of olefins with alcohol derivatives. A broad substrate scope was accessed with a single IDPi catalyst. Relevant product derivatives are shown, as well as the developed scalable two-step, one-pot process.

Derivatization of the products obtained using our developed method was achieved with varying degrees of success. We were able to synthesize the anti-inflammatory drug flurbiprofen from a scope entry featuring formal vinylation of a benzylic acetate; methodology that may be extended to an enantioselective synthesis of ibuprofen and other NSAIDs. Efforts toward the synthesis of galaxolide analogs proved semi-successful. We were able to affect a highly selective monocyclization toward an indane product, but the cyclization of the allyl benzyl ether moiety remained unsolved. Furthermore, we were able to access fused- and spirocyclic carbon frameworks using intramolecular carbonylative Heck coupling of a vinyl iodide-containing scope entry. The product distribution in this reaction could be controlled by the choice of Pd catalyst.

In the interest of using unprotected alcohols as alkylation reagents in our developed methodology, we established a two-step, one-pot process starting from 1-phenylethanol. This process featured acylation of the unprotected alcohol in the presence of our optimal IDPi catalyst in its Brønsted acid form. Acylation proved vital for maintaining the reactivity of the alkyl donor at the low temperatures required for high enantioinduction. Subsequent, application of the standard alkylation conditions by cooling of the reaction mixture and addition of the

olefin and silylating agent afforded the hydrocarbon product by silylium-ACDC. In this process, the IDPi catalyst gratifyingly facilitated both reactions with high efficiency, proving its utility as both a Brønsted acid- and Lewis acid catalyst. Furthermore, the reaction was demonstrated to be highly scalable.

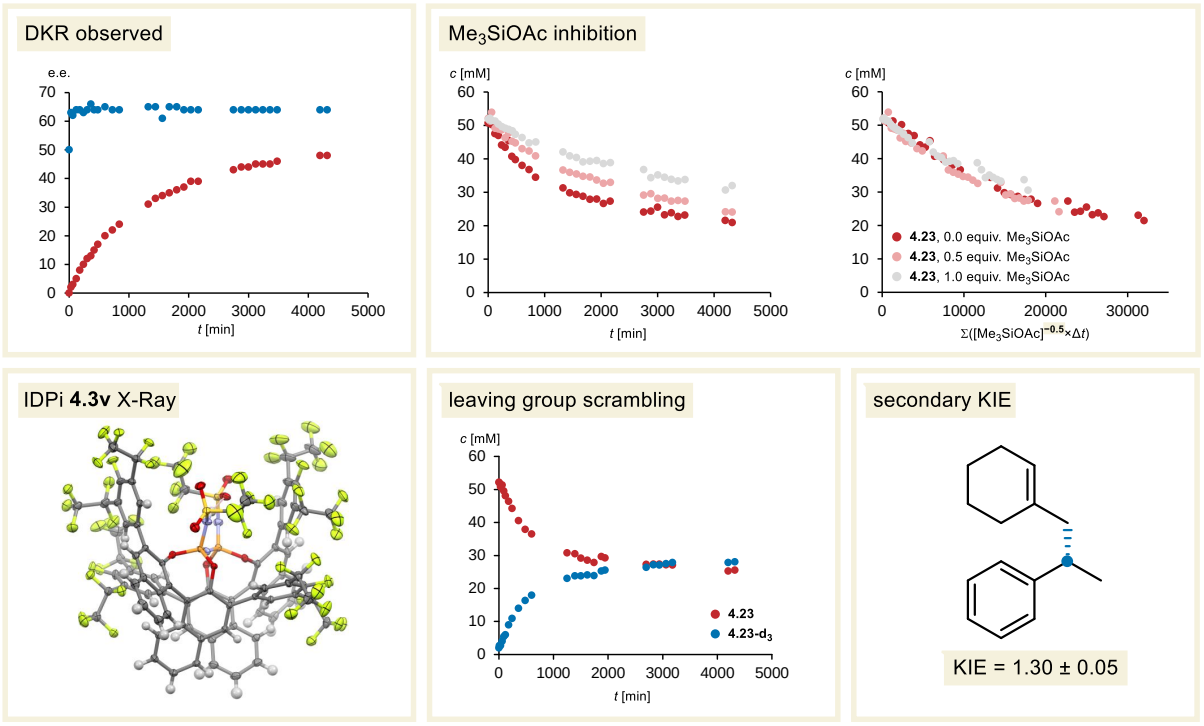

Figure 5.1 Summary of the experimental mechanistic studies of the developed model catalytic asymmetric alkylation of olefins with benzylic acetate.

Experimental studies were performed to elucidate the mechanism of the developed olefin alkylation reaction (Figure 5.1). Through reaction monitoring, inhibition studies, KIE studies, and experiments with enantiopure starting materials, we established that the developed methodology was an S_N1 reaction with characteristics of a DKR. Furthermore, the Me_3SiOAc by-product acted as a competitive inhibitor of the reaction, and facilitated racemization of the starting acetate. The proposed reaction mechanism starts from the IDPi catalyst in its Brønsted acidic form, which is silylated by the *N*- or *O*-trimethylsilyl groups of BSTFA. Subsequent activation of the acetate by the silylium-IDPi causes the formation of a catalyst–carbocation ion pair with the loss of Me_3SiOAc. Ion pair formation opens up two reaction pathways. First, C–C bond formation with the alkene can take place, leading to a tertiary cation which yields the desired hydrocarbon product after deprotonation. Second, Me_3SiOAc can attack the carbocation, inhibiting the forward reaction and causing a degree of racemization.

6. OUTLOOK

Despite our succes in developing a catalytic asymmetric alkylation reaction of unactivated olefins with benzylic- and allylic acetates, a few avenues of improvement remain underexplored.

First, a more thorough investigation of the direct alkylation of olefins with alcohols could be launched (Scheme 6.1, left). In lieu of alcohol reactivity at lower temperatures, we established a two-step, one-pot process. However, future development of more acidic catalysts motifs with modular synthetic routes similar to IDPis could facilitate provide stronger activation of substrates bearing free hydroxy groups, or their silyl ether derivatives that are formed *in situ* during silylium-ACDC.

Second, the substrate scope could be broadened to include alcohol derivatives and olefins with even less stabilizing substituents (Scheme 6.1, right). Although the current methodology generates highly reactive benzylic- and allylic cations, our optimal IDPi catalyst failed to provide the desired olefin alkylation products when using saturated substrates such as *sec*-butyl acetate. More acidic catalyst motifs may provide a solution to this problem as well, and sufficiently acidic catalysts may even be able to generate carbocations with lifetimes long enough to alkylate α-olefins.

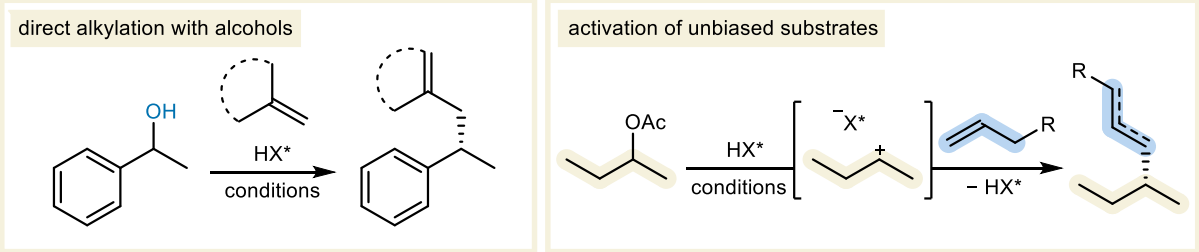

Scheme 6.1 "Ideal" direct alkylation of olefins with unprotected alcohols (left), and activation of unbiased substrates (right).

Exploration of the substrate scope of our developed method revealed that only derivatives of 1-substituted ethanol were tolerated as the electrophilic component of the reaction. Future development of catalyst motifs deviating from the IDPi structures explored in this thesis may resolve these constraints, which arise from the "methyl hole" observed in our optimal catalyst (Scheme 6.2, top left). Expansion of the functional group tolerance in this direction might also extend to the enantioselective alkylation of olefins with tertiary benzylic acetates. Our optimal catalyst demonstrated that quaternary stereocenters can be created using

tertiary benzylic acetates as alkyl donors in reactions with poorly nucleophilic olefins. However, the product of our preliminary attempt toward this goal was nearly racemic. Efforts toward an enantioselective alkylation of π-nucleophiles with tertiary acetates are currently being carried out in our laboratory.

One fairly straightforward extension of the current methodology would be to investigate electrophiles bearing a triple bond. While the developed methodology has been demonstrated to tolerate alkyne-containing electrophiles, derivatives of propargylic alcohols could be directly tested as electrophiles. Such a reaction might lead to the selective propargylation or allenylation of olefins (Scheme 6.2, top right).

We also performed preliminary studies toward a catalytic asymmetric alkylation of 1,3-diene nucleophiles (see section 4.2.2). In these trials, we observed the formation of oligomeric species in the presence of our strongly acidic optimal IDPi catalyst. Interestingly, using IDPis with less electron-poor wings yielded better product distributions, and high yields of the 1,3-diene products were obtained when the achiral catalyst Tf_2NH was used. Tuning the acidity of the catalyst and the reaction conditions could lead to the development of a catalytic asymmetric alkylation reaction of 1,3-dienes with alcohol derivatives (Scheme 6.2, bottom). Moreover, the stabilized nature of the allylic cation intermediates obtained after initial C–C bond formation between a carbocation and a 1,3-diene nucleophile may be leveraged to form cyclopentane- or cycloheptane rings when combined with an allylic acetate alkyl donor.

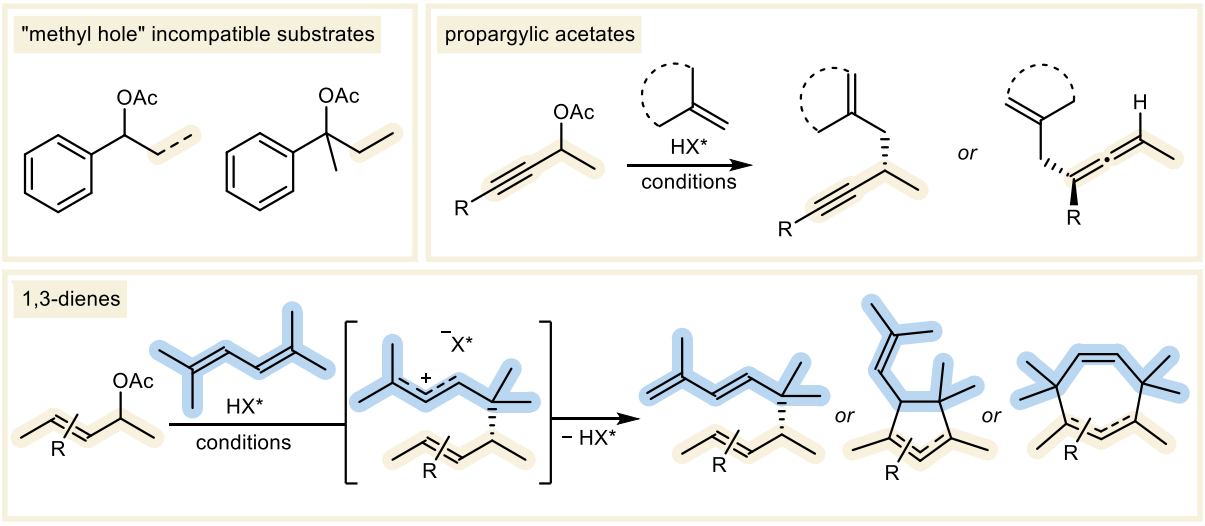

Scheme 6.2 Substrates that are methyl hole-incompatible (top left), and possible reactions of propargylic acetates (top right), and 1,3-dienes (bottom).

Lastly, our product derivatization efforts were moderately successful. We believe that the development of a catalytic- or radical cyclization of allyl benzyl ethers could lead to the synthesis of galaxolide analogs, which could have favorable biological activities (Figure 6.1, top). Furthermore, our efforts toward an intramolecular carbonylative Heck reaction showed that the developed methodology can grant access complex polycyclic products in a small number of steps from simple starting materials. Further optimization of this process could lead to its application in the synthesis of biologically relevant fused ring- or spirocyclic carbacycles; scaffolds which are commonly found in terpenoid odorants (Figure 6.1, bottom).[303]

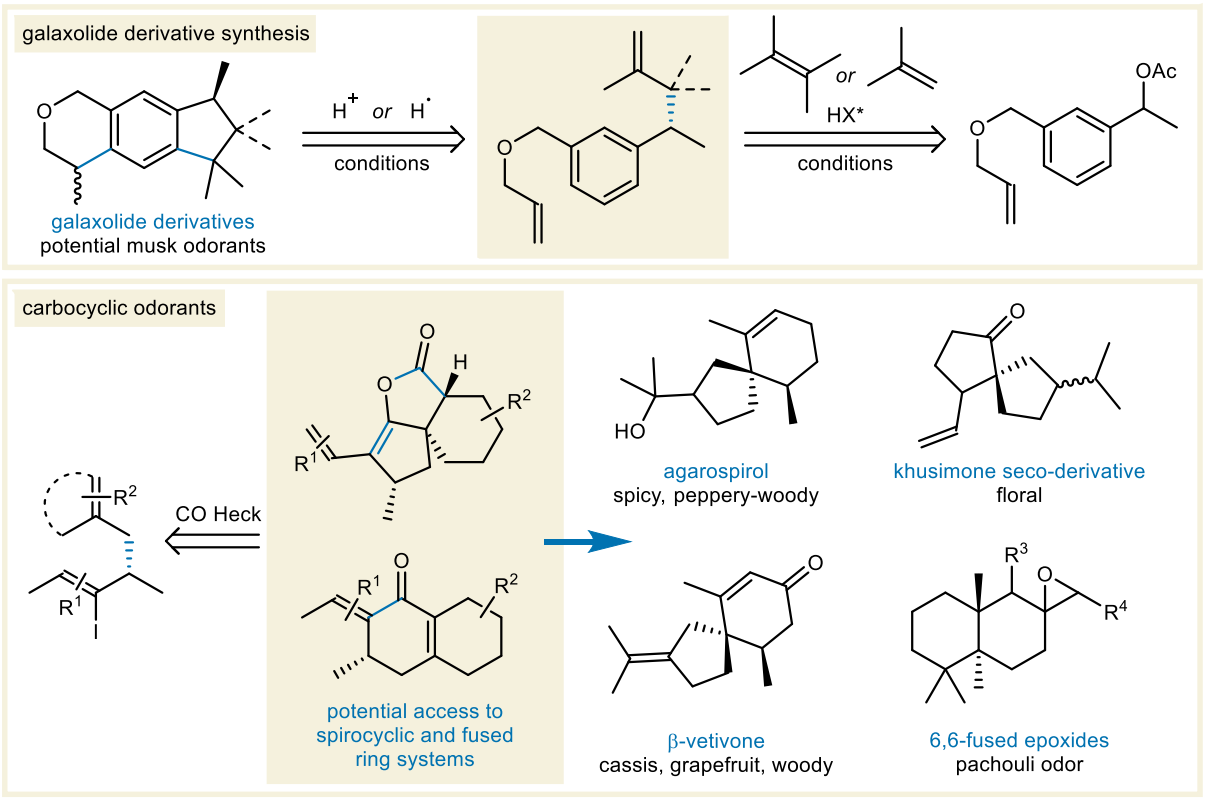

Figure 6.1 Envisioned synthesis of galaxolide derivatives (top), and odorants with related structures to cyclic compounds that could be accessed through intramolecular carbonylative Heck couplings of vinyl iodides (bottom).

7. EXPERIMENTAL SECTION

7.1. General Working Methods and Materials

Chemicals: Unless otherwise indicated, starting materials were obtained from Sigma-Aldrich, ABCR-GmbH, TCI, Acros Co. Ltd., Fluorochem or Deutero GmbH. Commercially available substances were used without further purification.

Solvents: Solvents (*n*-pentane, acetone, Et_2O, THF, 1,4-Dioxane, Cyclohexane, CH_2Cl_2, $CHCl_3$, PhH and PhMe) were dried by distillation from appropriate drying agents in the technical department of the Max-Plack-Institut für Kohlenforschung and obtained in Schlenk flasks under argon atmosphere. Further solvents (CyMe, oxylene, *n*-hexanes) were obtained from commercial suppliers and stored under an atmosphere of argon in a Schlenk tube.

Inert Gas: Anhydrous argon was purchased from Air Liquide with >99.5% purity.

Thin Layer Chromatography: Thin layer chromatography (TLC) was performed using silica gel precoated plastic sheets (Polygram SIL G/UV254, 0.2 mm, with fluorescent indicator; Macherey-Nagel) which was visualized with a UV lamp (254 nm) and/or phosphomolybdic acid (PMA), and/or Cerium Ammonium Molybdate (CAM), and/or $KMnO_4$. PMA stain: PMA (20 g) in EtOH (200 mL). CAM stain: Ammonium molybdate tetrahydrate (2.5 g), Cerium ammonium sulfate dihydrate (1 g) and Sulfuric acid (10 mL) in Water (90 mL). $KMnO_4$ stain: $KMnO_4$ (1.5 g), K_2CO_3 (10 g) and 10% NaOH (1.25 mL) in water (200 mL).

Column Chromatography: Column chromatography was carried out using Merck silica gel (60 Å, 230–400 mesh, particle size 0.040–0.063 mm) using technical grade solvents. Elution was accelerated using compressed air. All reported yields, unless otherwise specified, refer to spectroscopically and chromatographically pure compounds.

Nomenclature: Nomenclature follows the suggestions proposed by the computer program ChemBioDraw (23.1.1) of Revvity Signals.

Nuclear Magnetic Resonance Spectroscopy: ^{1}H, ^{13}C, ^{19}F, ^{31}P Nuclear magnetic resonance (NMR) spectra for compound characterization were recorded on a Bruker Avance III 500 or a Bruker Avance Neo 600 MHz NMR spectrometer in a suitable deuterated solvent unless specified otherwise. The solvent employed and the respective measuring frequency are indicated for each experiment. ^{1}H chemical shifts (δ) are reported in ppm relative to the protonated solvent resonance employed as the internal standard ($CDCl_3$ δ = 7.26, CD_2Cl_2 δ =

5.32, THF-d_8 δ = 3.58, 1.72). The resonance multiplicity is described as s (singlet), d (doublet), t (triplet), q (quadruplet), p (pentet), sext (sextet), h (heptet), m (multiplet), and br (broad). All spectra were recorded at 298 K unless otherwise specified, processed with the computer program MNova 14.2.0 of Mestrelab, and coupling constants are reported as observed. Signals are reported as follows: chemical shift δ in ppm (multiplicity, coupling constant *J* in Hz, number of protons). All X-nuclei spectra were acquired proton decoupled unless otherwise stated. $^{13}C\{^{1}H, ^{19}F\}$ NMR spectra were acquired with a Bruker TBO probe (^{1}H, ^{19}F, BB) with inverse gated decoupling. For ^{1}H waltz16 was used for decoupling. For ^{19}F the decoupling scheme bi_p5m4sp_4sp.2 with adiabatic chirp pulses with an offset at -105 ppm was used to ensure the broadband decoupling on ^{19}F.

Mass Spectrometry: Electrospray ionization (ESI) mass spectrometry was conducted on a Bruker ESQ 3000 spectrometer. High resolution mass spectrometry (HRMS) was performed on a Finnigan MAT 95 (EI) or Bruker APEX III FTMS (7 T magnet, ESI). The ionization method and mode of detection employed is indicated for the respective experiment and all masses are reported in atomic units per elementary charge (m/z) with an intensity normalized to the most intense peak.

Specific Rotations: Specific rotations ($[\alpha]_D^T$)were measured using a Rudolph Research Analytics Autopol IV automatic polarimeter at the indicated temperature with a sodium lamp (sodium D line, λ = 589 nm). Measurements were performed in an acid resistant 1 mL cell (50 mm length) with concentrations (g/(100 mL)) reported in the corresponding solvent.

Enantiomeric Ratios: Enantiomeric ratios (e.r.) were determined by GC or HPLC analysis using a chiral stationary phase column, indicated in each experiment, by comparing the samples with the corresponding racemic mixtures.

X-Ray Crystallography: Single crystals suitable for X-ray diffraction were grown as specified in the respective experiment. The X-ray crystal structure analyses were performed in the X-ray department of the Max-Planck-Institut für Kohlenforschung. Crystal structures were visualized and rendered using the program Mercury using version 4.2.0 developed by The Cambridge Crystallographic Data Centre (CCDC).

7.2. Synthesis of Substrates and Reagents

7.2.1. *Synthesis of Olefins*

methylenecycloheptane (4.55b)

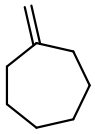

In a flame-dried Schlenk flask under an argon atmosphere, $MePPh_3Br$ (9.55 g, 26.75 mmol, 1.5 equiv.) was suspended in anhydrous Et_2O (34 mL) and the mixture was cooled to 0 °C. *t*-BuOK (3.00 g, 26.75 mmol, 1.5 equiv.) was added and the suspension was stirred at 25 °C for 1 h. Cycloheptanone (2.10 mL, 2.00 g, 17.83 mmol, 1.0 equiv.) was then added dropwise, and the reaction was stirred at the same temperature for 16 h. The reaction was then quenched with water, the mixture was transferred to an extraction funnel and extracted with Et_2O (3x). The combined organic phases were washed with brine, dried over Na_2SO_4, filtered and concentrated in vacuo. The residue was subjected to FCC (pentane) to yield the title compound as a colorless oil (1.94 mg, 14.65 mmol, 82%). The spectroscopic data were in accordance with the literature.[304]

^{1}H NMR (501 MHz, $CDCl_3$) δ 4.68 (p, *J* = 1.0 Hz, 2H), 2.31 – 2.24 (m, 4H), 1.63 – 1.48 (m, 8H).

but-1-en-2-ylbenzene (4.55f)

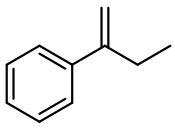

In a flame-dried Schlenk flask under an argon atmosphere, *t*-BuOK (501.8 mg, 4.47 mmol, 1.2 equiv.) was suspended in anhydrous THF (7.4 mL), after which $MePPh_3Br$ (1.60 g, 4.47 mmol, 1.2 equiv.) was added and the suspension was stirred at 25 °C for 1 h. Propiophenone (0.50 mL, 0.50 g, 3.73 mmol, 1.0 equiv.) was then added dropwise, and the reaction was stirred at the same temperature for 1 h. The mixture was then filtered through a short pad of silica gel with subsequent washing of the silica gel with hexanes (100 mL). The filtrate was concentrated in vacuo and subjected to FCC (hexanes/EtOAc, 99:1) to yield the title compound as a colorless oil (380.2 mg, 2.88 mmol, 77%). The spectroscopic data were in accordance with the literature.[305]

^{1}H NMR (501 MHz, $CDCl_3$) δ 7.45 – 7.39 (m, 2H), 7.36 – 7.30 (m, 2H), 7.29 – 7.24 (m, 1H), 5.28 (q, *J* = 1.0 Hz, 1H), 5.06 (q, *J* = 1.5 Hz, 1H), 2.52 (q, *J* = 7.4 Hz, 2H), 1.11 (t, *J* = 7.4 Hz, 3H).

(1-cyclohexylvinyl)benzene (4.55g)

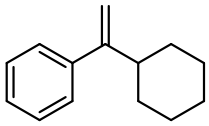

In a flame-dried Schlenk flask under an argon atmosphere, $MePPh_3Br$ (4.92 g, 13.78 mmol, 1.5 equiv.) was suspended in anhydrous Et_2O (35 mL) and the mixture was cooled to 0 °C. *n*-BuLi (2.5 M in hexanes, 5.15 mL, 12.86 mmol, 1.4 equiv.) was added and the suspension was stirred at the same temperature for 1 h. Cyclohexyl phenyl ketone (1.73 g, 9.19 mmol, 1.0 equiv.) in Et_2O (10 mL) was then added dropwise, and the reaction was stirred at 25 °C for 16 h. The reaction was then quenched with water, the mixture was transferred to an extraction funnel and extracted with Et_2O (3x). The combined organic phases were washed with brine, dried over Na_2SO_4, filtered and concentrated in vacuo. The residue was subjected to FCC (pentane) to yield the title compound as a colorless oil (1.62 g, 8.70 mmol, 95%). The spectroscopic data were in accordance with the literature.[306]

^{1}H NMR (501 MHz, $CDCl_3$) δ 7.37 – 7.23 (m, 5H), 5.13 (d, *J* = 1.4 Hz, 1H), 5.01 (t, *J* = 1.4 Hz, 1H), 2.42 (ttd, *J* = 11.6, 3.2, 1.2 Hz, 1H), 1.93 – 1.66 (m, 5H), 1.41 – 1.10 (m, 5H).

7.2.2. *Synthesis of Acetates*

General procedure 1 (GP1): Synthesis of acetates from alcohols

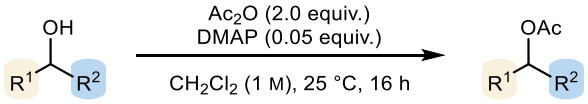

In a round bottom flask under ambient conditions, the respective alcohol (1.0 equiv.) was dissolved in CH_2Cl_2 (1.0 M). Ac_2O (2.0 equiv.) was then added in one portion, followed by DMAP (0.05 equiv.). The reaction was stirred at 25 °C overnight or until monitoring by TLC (pentane/acetone, 19:1) indicated full conversion of the starting material. Excess MeOH was added and the reaction was stirred for a further 30 minutes. The mixture was then diluted with pentane, transferred to an extraction funnel and washed with water (2x) and saturated $NaHCO_3$ solution (2x). The organic phase was then dried over Na_2SO_4, filtered and concentrated in vacuo. The crude residue was subjected to FCC (pentane/acetone, 19:1, unless otherwise indicated) to afford the corresponding acetate.

General procedure 2 (GP2): synthesis of alcohols from aldehydes

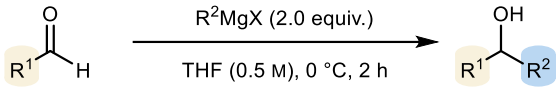

In a flame-dried Schlenk flask under an argon atmosphere, the respective aldehyde (1.0 equiv.) was dissolved in THF (0.5 M) and the mixture was cooled to 0 °C. The corresponding Grignard reagent (1.05–2.0 equiv.) was then added dropwise, and the reaction was stirred for 2 h at the same temperature. After monitoring by TLC (pentane/acetone, 9:1) indicated full conversion of the starting material, the reaction was quenched by addition of a saturated ammonium chloride solution. The mixture was extracted with Et_2O (3x), the combined organic phases were dried over Na_2SO_4, filtered and concentrated in vacuo. The corresponding crude residues were then subjected to acetylation via GP1 assuming quantitative yield.

General procedure 3 (GP3): synthesis of alcohols from ketones

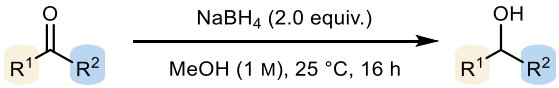

In a round bottom flask under ambient conditions, the respective ketone (1.0 equiv.) was dissolved in EtOH (1.0 M). $NaBH_4$ (2.0 equiv.) was then added portionwise. The reaction was stirred at 25 °C overnight or until monitoring by TLC (pentane/acetone, 9:1) indicated full conversion of the starting material. The reaction was quenched by addition of water. Brine was then added, and the mixture was extracted with EtOAc (3x). The combined organic phases were dried over Na_2SO_4, filtered and concentrated in vacuo. The corresponding crude residues were then subjected to acetylation via GP1 assuming quantitative yield.

1-phenylethyl acetate (4.23)

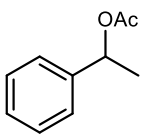

Preparation from 1-phenylethanol (10.00 g, 81.86 mmol, 1.0 equiv.) according to GP1 afforded the title compound as a colorless oil (8.88 g, 81.86 mmol, 66%). The spectroscopic data were in accordance with the literature.[307]

^{1}H NMR (501 MHz, $CDCl_3$) δ 7.38 – 7.33 (m, 4H), 7.32 – 7.27 (m, 1H), 5.88 (q, J = 6.6 Hz, 1H), 2.08 (s, 3H), 1.54 (d, J = 6.6 Hz, 3H).

1-(3,5-dimethylphenyl)ethyl acetate (4.53a)

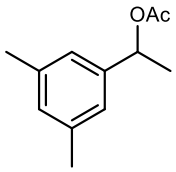

Preparation from 1-(3,5-dimethylphenyl)ethan-1-one (889.2 mg, 6.00 mmol, 1.0 equiv.) according to GP3 and GP1 afforded the title compound as a light yellow oil (1.16 g, 6.00 mmol, quant.).

^{1}H NMR (501 MHz, $CDCl_3$) δ 6.99 – 6.96 (br s, 2H), 6.94 – 6.92 (br s, 1H), 5.82 (q, *J* = 6.6 Hz, 1H), 2.32 (br s, 6H), 2.08 (s, 3H), 1.52 (d, *J* = 6.6 Hz, 3H).

^{13}C NMR (126 MHz, $CDCl_3$) δ 170.5, 141.7, 138.2, 129.7, 124.0, 72.5, 22.3, 21.5, 21.4.

HRMS (ESI) (m/z): calculated for $C_{12}H_{16}O_2Na$ $[M+Na]^+$: 215.104249; found: 215.104090.

1-(*m*-tolyl)ethyl acetate (4.53b)

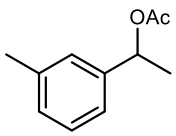

Preparation from 1-(m-tolyl)ethan-1-ol (612.9 mg, 4.50 mmol, 1.0 equiv.) according to GP1 afforded the title compound as a colorless oil (719.8 mg, 4.04 mmol, 90%).

^{1}H NMR (501 MHz, $CDCl_3$) δ 7.24 (t, *J* = 7.4 Hz, 1H), 7.18 – 7.07 (m, 3H), 5.85 (q, *J* = 6.6 Hz, 1H), 2.36 (s, 2H), 2.07 (s, 3H), 1.52 (d, *J* = 6.6 Hz, 3H).

^{13}C NMR (126 MHz, $CDCl_3$) δ 170.7, 142.0, 138.5, 129.0, 128.8, 127.2, 123.5, 72.7, 22.5, 21.8, 21.7.

HRMS (GC-EI) (m/z): calculated for $C_{11}H_{14}O_2$ $[M]^+$: 178.098830; found: 178.098880.

1-(3-isopropylphenyl)ethyl acetate (4.53c)

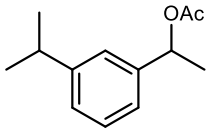

Preparation from 1-(3-isopropylphenyl)ethan-1-one (2.85 g, 17.57 mmol, 1.0 equiv.) according to GP3 and GP1 afforded the title compound as a colorless oil (3.62 g, 17.57 mmol, quant.).

^{1}H NMR (501 MHz, $CDCl_3$) δ 7.28 (t, *J* = 7.6 Hz, 1H), 7.22 – 7.14 (m, 3H), 5.88 (q, *J* = 6.6 Hz, 1H), 2.92 (h, *J* = 6.9 Hz, 1H), 2.08 (s, 3H), 1.54 (d, *J* = 6.6 Hz, 3H), 1.26 (d, *J* = 6.9 Hz, 6H).

^{13}C NMR (126 MHz, $CDCl_3$) δ 170.5, 149.3, 141.7, 128.6, 126.1, 124.5, 123.7, 72.6, 34.3, 24.1, 22.4, 21.5.

HRMS (GC-EI) (m/z): calculated for $C_{13}H_{18}O_2$ $[M]^+$: 206.130130; found: 206.130170.

1-([1,1'-biphenyl]-4-yl)ethyl acetate (4.53d)

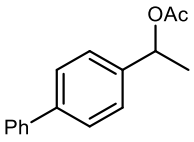

Preparation from 1-([1,1'-biphenyl]-4-yl)ethan-1-ol (892.2 mg, 4.50 mmol, 1.0 equiv.) according to GP1 afforded the title compound as a colorless oil (987.2 mg, 4.11 mmol, 91%).

^{1}H NMR (501 MHz, $CDCl_3$) δ 7.62 – 7.55 (m, 4H), 7.44 (dd, *J* = 8.3, 6.6 Hz, 4H), 7.39 – 7.32 (m, 1H), 5.94 (q, *J* = 6.6 Hz, 1H), 2.10 (s, 3H), 1.58 (d, *J* = 6.6 Hz, 3H).

^{13}C NMR (126 MHz, $CDCl_3$) δ 170.7, 141.2, 141.1, 141.0, 129.1, 127.7, 127.6, 127.5, 126.9, 72.4, 22.5, 21.7.

HRMS (GC-EI) (m/z): calculated for $C_{16}H_{16}O_2$ $[M]^+$: 240.114480; found: 240.114270.

1-(4-(prop-1-yn-1-yl)phenyl)ethyl acetate (4.53e)

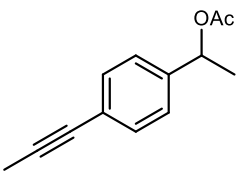

Preparation from 1-(4-(prop-1-yn-1-yl)phenyl)ethan-1-one (**7.1**, 181.4 mg, 1.15 mmol, 1.0 equiv.) according to GP3 and GP1 afforded the title compound as a yellow oil (160.3 mg, 0.79 mmol, 69%).

^{1}H NMR (501 MHz, $CDCl_3$) δ 7.39 – 7.33 (m, 2H), 7.29 – 7.22 (m, 2H), 5.85 (q, *J* = 6.6 Hz, 1H), 2.07 (s, 3H), 2.04 (s, 3H), 1.51 (d, *J* = 6.6 Hz, 3H).

^{13}C NMR (126 MHz, $CDCl_3$) δ 170.4, 141.1, 131.8, 126.1, 123.8, 86.2, 79.6, 72.1, 22.2, 21.5, 4.5.

HRMS (GC-EI) (m/z): calculated for $C_{13}H_{14}O_2$ $[M]^+$: 202.098830; found: 202.098800.

1-(3-methoxyphenyl)ethyl acetate (4.53f)

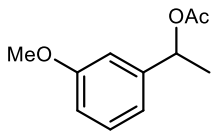

Preparation from 1-(3-methoxyphenyl)ethan-1-one (1.50 g, 9.99 mmol, 1.0 equiv.) according to GP3 and GP1 afforded the title compound as a colorless oil (1.20 g, 6.19 mmol, 62%).

^{1}H NMR (501 MHz, $CDCl_3$) δ 7.27 (t, *J* = 7.9 Hz, 1H), 6.94 (dt, *J* = 7.6, 1.3 Hz, 1H), 6.90 (t, *J* = 2.1 Hz, 1H), 6.83 (ddd, *J* = 8.2, 2.6, 0.9 Hz, 1H), 5.85 (q, *J* = 6.6 Hz, 1H), 3.82 (s, 3H), 2.08 (s, 3H), 1.53 (d, *J* = 6.6 Hz, 3H).

^{13}C NMR (126 MHz, $CDCl_3$) δ 170.4, 159.8, 143.5, 129.7, 118.5, 113.2, 112.0, 72.3, 55.4, 22.4, 21.5.

HRMS (GC-EI) (m/z): calculated for $C_{11}H_{14}O_3$ $[M]^+$: 194.093745; found: 194.093830.

1-(3-methoxy-4-methylphenyl)ethyl acetate (4.53g)

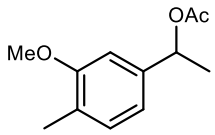

Preparation from 1-(3-methoxy-4-methylphenyl)ethan-1-one (1.00 g, 6.09 mmol, 1.0 equiv.) according to GP3 and GP1 afforded the title compound as a colorless oil (1.27 g, 6.09 mmol, quant.).

^{1}H NMR (501 MHz, $CDCl_3$) δ 7.15 – 7.08 (m, 1H), 6.87 (dd, *J* = 7.6, 1.7 Hz, 1H), 6.82 (d, *J* = 1.7 Hz, 1H), 5.86 (q, *J* = 6.6 Hz, 1H), 3.85 (s, 3H), 2.21 (s, 3H), 2.07 (s, 3H), 1.54 (d, *J* = 6.6 Hz, 3H).

^{13}C NMR (126 MHz, $CDCl_3$) δ 170.4, 157.7, 140.5, 130.6, 126.4, 117.9, 108.0, 72.5, 55.3, 22.2, 21.4, 16.0.

HRMS (GC-EI) (m/z): calculated for $C_{12}H_{16}O_3$ $[M]^+$: 208.109395; found: 208.109510.

1-(4-fluorophenyl)ethyl acetate (4.53h)

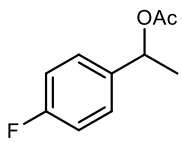

Preparation from 1-(4-fluorophenyl)ethan-1-one (1.00 g, 7.13 mmol, 1.0 equiv.) according to GP3 and GP1 afforded the title compound as a light yellow oil (970.6 mg, 5.33 mmol, 75%).

^{1}H NMR (501 MHz, $CDCl_3$) δ 7.37 – 7.29 (m, 2H), 7.07 – 6.99 (m, 2H), 5.86 (q, *J* = 6.6 Hz, 1H), 2.06 (s, 3H), 1.52 (d, *J* = 6.6 Hz, 3H).

^{13}C NMR (126 MHz, $CDCl_3$) δ 170.4, 163.4, 161.5, 137.6, 137.6, 128.1, 128.0, 115.6, 115.4, 71.8, 22.3, 21.5.

^{19}F NMR (471 MHz, $CDCl_3$) δ -114.44.

HRMS (GC-EI) (m/z): calculated for $C_{10}H_{11}FO_2$ $[M]^+$: 182.073758; found: 182.073880.

1-(4-chlorophenyl)ethyl acetate (4.53i)

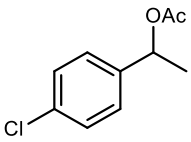

Preparation from 1-(4-chlorophenyl)ethan-1-ol (704.7 mg, 4.50 mmol, 1 equiv.) according to GP1 afforded the title compound as a pale yellow oil (791.0 mg, 3.98 mmol, 88%).

^{1}H NMR (501 MHz, $CDCl_3$) δ 7.34 – 7.26 (m, 5H), 5.84 (q, *J* = 6.6 Hz, 1H), 2.07 (s, 3H), 1.51 (d, *J* = 6.7 Hz, 3H).

^{13}C NMR (126 MHz, $CDCl_3$) δ 170.5, 140.6, 134.0, 129.0, 127.9, 71.9, 22.5, 21.6.

HRMS (GC-EI) (m/z): calculated for $C_{10}H_{11}ClO_2$ $[M]^+$: 198.044208; found: 198.044240.

1-(4-bromophenyl)ethyl acetate (4.58a)

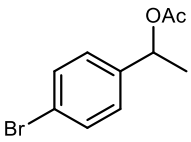

Preparation from 1-(4-bromophenyl)ethan-1-ol (904.8 mg, 4.50 mmol, 1.0 equiv.) according to GP1 afforded the title compound as a colorless oil (647.0 mg, 2.53 mmol, 56%).

^{1}H NMR (501 MHz, $CDCl_3$) δ 7.49 – 7.45 (m, 2H), 7.24 – 7.20 (m, 2H), 5.82 (q, *J* = 6.6 Hz, 1H), 2.07 (s, 3H), 1.51 (d, *J* = 6.6 Hz, 3H).

^{13}C NMR (126 MHz, $CDCl_3$) δ 170.5, 141.1, 132.0, 128.2, 122.1, 72.0, 22.5, 21.6.

HRMS (GC-EI) (m/z): calculated for $C_{10}H_{11}BrO_2$ $[M]^+$: 241.993705; found: 241.993610.

1-(4-ethynylphenyl)ethyl acetate (4.58b)

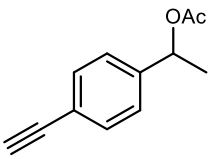

Preparation from 4-ethynylbenzaldehyde (415.6 mg, 2.84 mmol, 1.0 equiv.) and MeMgCl (3 M in THF, 1.05 equiv.) according to GP2 and GP1 afforded the title compound as a pale yellow oil (449.6 mg, 2.39 mmol, 84%).

^{1}H NMR (501 MHz, $CDCl_3$) δ 7.50 – 7.44 (m, 2H), 7.33 – 7.27 (m, 2H), 5.86 (q, *J* = 6.6 Hz, 1H), 3.06 (s, 1H), 2.08 (s, 3H), 1.52 (d, *J* = 6.6 Hz, 3H).

^{13}C NMR (126 MHz, $CDCl_3$) δ 170.4, 142.6, 132.4, 126.2, 121.8, 83.5, 77.5, 72.0, 22.3, 21.4.

HRMS (GC-EI) (m/z): calculated for $C_{12}H_{12}O_2$ $[M]^+$: 188.083180; found: 188.083160.

1-(2-fluoro-[1,1'-biphenyl]-4-yl)ethyl acetate (4.58e)

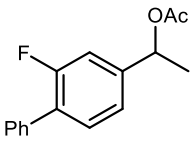

Preparation from 1-(2-fluoro-[1,1'-biphenyl]-4-yl)ethan-1-ol (**7.2**, 330.4 mg, 1.53 mmol, 1.0 equiv.) according to GP1 afforded the title compound as a yellow oil (336.4 mg, 1.30 mmol, 85%). The spectroscopic data were in accordance with the literature.[308]

^{1}H NMR (501 MHz, $CDCl_3$) δ 7.53 (dt, *J* = 8.1, 1.5 Hz, 2H), 7.48 – 7.33 (m, 4H), 7.23 – 7.13 (m, 2H), 5.89 (q, *J* = 6.6 Hz, 1H), 2.11 (s, 3H), 1.57 (d, *J* = 6.6 Hz, 3H).

^{13}C NMR (126 MHz, $CDCl_3$) δ 170.4, 159.8 (d, *J* = 248.4 Hz), 143.4 (d, *J* = 7.4 Hz), 135.6, 131.0 (d, *J* = 3.9 Hz), 129.1 (d, *J* = 2.9 Hz), 128.7, 128.6, 127.9, 122.1 (d, *J* = 3.5 Hz), 113.9 (d, *J* = 24.1 Hz), 71.6, 22.3, 21.4.

^{19}F NMR (471 MHz, $CDCl_3$) δ -117.51.

HRMS (GC-EI) (m/z): calculated for $C_{16}H_{15}FO_2$ $[M]^+$: 258.105058; found: 258.104920.

1-(4-isobutylphenyl)ethyl acetate (4.58f)

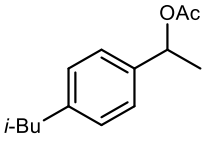

Preparation from 1-(4-isobutylphenyl)ethan-1-ol (131.7 mg, 0.74 mmol, 1.0 equiv.) according to GP1 afforded the title compound as a colorless oil (117.4 mg, 0.53 mmol, 72%).

^{1}H NMR (501 MHz, $CDCl_3$) δ 7.26 (d, *J* = 8.0 Hz, 2H), 7.12 (d, *J* = 8.1 Hz, 2H), 5.87 (q, *J* = 6.6 Hz, 1H), 2.46 (d, *J* = 7.1 Hz, 2H), 2.06 (s, 3H), 1.85 (h, *J* = 6.7 Hz, 1H), 1.53 (d, *J* = 6.5 Hz, 3H), 0.90 (d, *J* = 6.6 Hz, 6H).

^{13}C NMR (126 MHz, $CDCl_3$) δ 170.5, 141.6, 139.0, 129.3, 126.1, 72.4, 45.3, 30.3, 22.5, 22.2, 21.6.

HRMS (GC-EI) (m/z): calculated for $C_{14}H_{20}O_2$ $[M]^+$: 220.145780; found: 220.145590.

pent-3-en-2-yl acetate (4.67a)

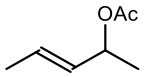

Preparation from (*E*)-pent-3-en-2-ol (430.7 mg, 5.00 mmol, 1.0 equiv., *E*/*Z*≈92:8) according to GP1 afforded the title compound as a colorless oil (559.8 mg, 1.88 mmol, 38%, *E*/*Z*≈92:8).

^{1}H NMR (501 MHz, $CDCl_3$) δ 5.72 (dqd, *J* = 14.1, 6.6, 1.0 Hz, 1H), 5.48 (ddq, *J* = 15.4, 6.9, 1.7 Hz, 1H), 5.34 – 5.26 (m, 1H), 2.03 (s, 3H), 1.71 – 1.67 (m, 3H), 1.28 (d, *J* = 6.4 Hz, 3H).

^{13}C NMR (126 MHz, $CDCl_3$) δ 170.5, 130.9, 128.3, 71.3, 21.5, 20.4, 17.8.

HRMS (GC-EI) (m/z): calculated for $C_7H_{12}O_2$ $[M]^+$: 128.083180; found: 128.083260.

(*E*)-3-methylpent-3-en-2-yl acetate (4.67b)

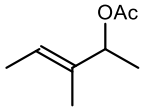

Preparation from tiglic aldehyde (163.0 mg, 1.94 mmol, 1.0 equiv.) and MeMgCl (3 M in THF, 1.5 equiv.) according to GP2 and GP1 afforded the title compound as a colorless oil (148.6 mg, 1.05 mmol, 54%).

^{1}H NMR (501 MHz, $CDCl_3$) δ 5.57 – 5.49 (m, 1H), 5.26 (q, *J* = 6.5 Hz, 1H), 2.03 (s, 3H), 1.64 – 1.58 (m, 6H), 1.28 (d, *J* = 6.4 Hz, 3H).

^{13}C NMR (126 MHz, $CDCl_3$) δ 170.6, 135.2, 121.7, 75.6, 21.5, 19.2, 13.2, 11.8.

HRMS (ESI) (m/z): calculated for $C_8H_{14}O_2Na$ $[M+Na]^+$: 165.088599; found: 165.088770.

(*E*)-3-phenylpent-3-en-2-yl acetate (4.67c)

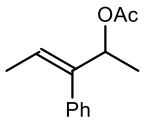

Preparation from (*E*)-2-phenylbut-2-enal (**7.3**, 475.0 mg, 3.25 mmol, 1.0 equiv.) and MeMgCl (3 M in THF, 2.0 equiv.) according to GP2 and GP1 afforded the title compound as a colorless oil (442.4 mg, 2.17 mmol, 67%).

^{1}H NMR (501 MHz, $CDCl_3$) δ 7.39 – 7.32 (m, 2H), 7.30 – 7.25 (m, 1H), 7.20 – 7.14 (m, 2H), 5.83 (qd, *J* = 6.9, 1.1 Hz, 1H), 5.55 (qt, *J* = 6.6, 1.0 Hz, 1H), 2.05 (s, 3H), 1.53 (dd, *J* = 6.9, 0.8 Hz, 3H), 1.24 (d, *J* = 6.5 Hz, 3H).

^{13}C NMR (126 MHz, $CDCl_3$) δ 170.4, 141.8, 138.0, 129.5, 128.2, 127.1, 124.0, 74.4, 21.6, 19.8, 14.4.

HRMS (ESI) (m/z): calculated for $C_{13}H_{16}O_2Na$ $[M+Na]^+$: 227.10425; found: 227.10416.

(*Z*)-3-iodopent-3-en-2-yl acetate (4.67e)

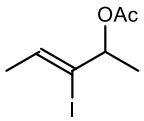

Preparation from (*Z*)-3-iodopent-3-en-2-ol (**7.5**) (1.72 g, 8.11 mmol, 1.0 equiv.) according to GP1 afforded the title compound as a red oil (1.78 g, 7.01 mmol, 86%).

^{1}H NMR (501 MHz, $CDCl_3$) δ 6.06 (qd, *J* = 6.4, 0.8 Hz, 1H), 5.09 (q, *J* = 6.4 Hz, 1H), 2.07 (s, 3H), 1.78 (d, *J* = 6.4 Hz, 3H), 1.35 (d, *J* = 6.4 Hz, 3H).

^{13}C NMR (126 MHz, $CDCl_3$) δ 170.0, 133.3, 111.3, 75.6, 21.6, 21.5, 21.4.

HRMS (ESI) (m/z): calculated for $C_7H_{11}IO_2Na$ $[M+Na]^+$: 276.96960; found: 276.96965.

(*Z*)-3-bromopent-3-en-2-yl acetate (4.67f)

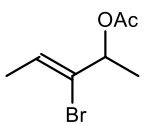

Preparation from (*Z*)-3-bromopent-3-en-2-ol (**7.4**) (2.02 g, 12.27 mmol, 1.0 equiv.) according to GP1 afforded the title compound as a colorless oil (1.97 g, 9.51 mmol, 78%) which was used without FCC purification.

^{1}H NMR (501 MHz, CD_2Cl_2) δ 6.13 (qd, *J* = 6.6, 0.7 Hz, 1H), 5.38 (q, *J* = 6.4 Hz, 1H), 2.03 (s, 3H), 1.75 (dd, *J* = 6.5, 0.5 Hz, 3H), 1.38 (d, *J* = 6.4 Hz, 3H).

^{13}C NMR (126 MHz, CD_2Cl_2) δ 170.0, 128.6, 127.1, 74.0, 21.3, 19.9, 16.6.

HRMS (ESI) (m/z): calculated for $C_7H_{11}BrO_2Na$ $[M+Na]^+$: 228.983474; found: 228.983560.

1-(cyclohex-1-en-1-yl)ethyl acetate (4.67g)

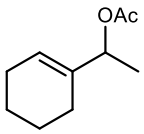

Preparation from cyclohex-1-ene-1-carbaldehyde (500.0 mg, 4.54 mmol, 1.0 equiv.) and MeMgCl (3 M in THF, 1.5 equiv.) according to GP2 and GP1 afforded the title compound as a colorless oil (763.3 mg, 4.54 mmol, quant.).

^{1}H NMR (501 MHz, $CDCl_3$) δ 5.69 (qd, *J* = 2.9, 1.3 Hz, 1H), 5.23 (q, *J* = 6.6 Hz, 1H), 2.04 (s, 3H), 2.06 – 1.93 (m, 4H), 1.71 – 1.48 (m, 4H), 1.29 (d, *J* = 6.5 Hz, 3H).

^{13}C NMR (126 MHz, $CDCl_3$) δ 170.6, 137.2, 123.8, 74.3, 25.0, 24.3, 22.6, 22.5, 21.5, 19.0.

HRMS (ESI) (m/z): calculated for $C_{10}H_{16}O_2Na$ $[M+Na]^+$: 191.104249; found: 191.104340.

(*E*)-hex-3-en-2-yl acetate (4.67h)

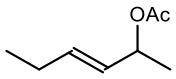

Preparation from (*E*)-pent-2-enal (322.2 mg, 3.83 mmol, 1.0 equiv.) and MeMgCl (3 M in THF, 1.5 equiv.) according to GP2 and GP1 afforded the title compound as a colorless oil (125.3 mg, 0.88 mmol, 23%).

^{1}H NMR (501 MHz, $CDCl_3$) δ 5.74 (dtd, *J* = 15.5, 6.3, 1.1 Hz, 1H), 5.45 (ddt, *J* = 15.4, 6.8, 1.7 Hz, 1H), 5.31 (pd, *J* = 6.5, 1.0 Hz, 1H), 2.03 (s, 3H), 1.29 (d, *J* = 6.5 Hz, 3H), 0.99 (t, *J* = 7.4 Hz, 3H).

^{13}C NMR (126 MHz, $CDCl_3$) δ 170.5, 135.0, 128.6, 71.3, 25.3, 21.6, 20.5, 13.3.

HRMS (ESI) (m/z): calculated for $C_8H_{14}O_2Na$ $[M+Na]^+$: 165.088599; found: 165.088730.

(*E*)-hex-4-en-3-yl acetate (4.67h')

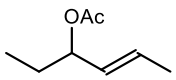

Preparation from (*E*)-but-2-enal (416.6 mg, 5.94 mmol, 1.0 equiv.) and EtMgBr (3 M in Et_2O, 1.5 equiv.) according to GP2 and GP1 afforded the title compound as a colorless oil (437.9 mg, 3.08 mmol, 52%).

^{1}H NMR (501 MHz, $CDCl_3$) δ 5.77 – 5.66 (m, 1H), 5.40 (ddq, *J* = 15.4, 7.5, 1.6 Hz, 1H), 5.11 (q, *J* = 6.9 Hz, 1H), 2.04 (s, 3H), 1.70 (dd, *J* = 6.5, 1.7 Hz, 3H), 1.67 – 1.52 (m, 2H), 0.87 (t, *J* = 7.4 Hz, 3H).

^{13}C NMR (126 MHz, $CDCl_3$) δ 170.6, 129.6, 129.4, 76.4, 27.6, 21.5, 17.9, 9.7.

HRMS (ESI) (m/z): calculated for $C_8H_{14}O_2Na$ $[M+Na]^+$: 165.088599; found: 165.088700.

(*E*)-hept-3-en-2-yl acetate (4.67i)

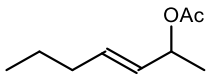

Preparation from (*E*)-hex-2-enal (423.0 mg, 4.31 mmol, 1.0 equiv.) and MeMgCl (3 M in THF, 1.5 equiv.) according to GP2 and GP1 afforded the title compound as a colorless oil (479.9 mg, 3.07 mmol, 71%).

^{1}H NMR (501 MHz, $CDCl_3$) δ 5.69 (dtd, *J* = 15.4, 6.8, 1.0 Hz, 1H), 5.45 (ddt, *J* = 15.4, 6.8, 1.5 Hz, 1H), 5.31 (pd, *J* = 6.4, 0.9 Hz, 1H), 2.03 (s, 3H), 2.02 – 1.95 (m, 2H), 1.39 (sext, *J* = 7.3 Hz, 2H), 1.29 (d, *J* = 6.4 Hz, 3H), 0.89 (t, *J* = 7.4 Hz, 3H).

^{13}C NMR (126 MHz, $CDCl_3$) δ 170.5, 133.3, 129.8, 71.3, 34.4, 22.2, 21.6, 20.6, 13.8.

HRMS (ESI) (m/z): calculated for $C_9H_{16}O_2Na$ $[M+Na]^+$: 179.104249; found: 179.104330.

(*E*)-oct-2-en-4-yl acetate (4.67j')

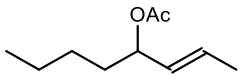

Preparation from (*E*)-but-2-enal (302.1 mg, 4.31 mmol, 1.0 equiv.) and *n*-BuMgCl (2 M in THF, 1.5 equiv.) according to GP2 and GP1 afforded the title compound as a colorless oil (529.9 mg, 3.11 mmol, 72%).

^{1}H NMR (501 MHz, $CDCl_3$) δ 5.71 (dqd, *J* = 15.3, 6.6, 1.0 Hz, 1H), 5.40 (ddq, *J* = 15.3, 7.5, 1.7 Hz, 1H), 5.17 (q, *J* = 7.0 Hz, 1H), 2.03 (s, 3H), 1.69 (dd, *J* = 6.5, 1.7 Hz, 3H), 1.66 – 1.58 (m, 1H), 1.57 – 1.47 (m, 1H), 1.37 – 1.19 (m, 4H), 0.89 (t, *J* = 7.1 Hz, 3H).

^{13}C NMR (126 MHz, $CDCl_3$) δ 170.6, 129.9, 129.2, 75.2, 34.4, 27.5, 22.6, 21.6, 17.9, 14.1.

HRMS (ESI) (m/z): calculated for $C_{10}H_{18}O_2Na$ $[M+Na]^+$: 193.119899; found: 193.120070.

(*E*)-4-methylhex-4-en-3-yl acetate (4.67k')

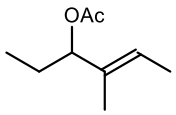

Preparation from tiglic aldehyde (221.0 mg, 2.63 mmol, 1.0 equiv.) and EtMgCl (3 M in THF, 1.5 equiv.) according to GP2 and GP1 afforded the title compound as a colorless oil (283.7 mg, 1.82 mmol, 69%).

^{1}H NMR (501 MHz, $CDCl_3$) δ 5.51 (qt, *J* = 6.7, 1.2 Hz, 1H), 5.04 (t, *J* = 7.1 Hz, 1H), 2.04 (s, 3H), 1.72 – 1.52 (m, 8H), 0.82 (t, *J* = 7.4 Hz, 3H).

^{13}C NMR (126 MHz, $CDCl_3$) δ 170.6, 133.6, 123.1, 81.1, 25.7, 21.5, 13.2, 11.5, 10.0.

HRMS (ESI) (m/z): calculated for $C_9H_{17}O_2$ $[M+H]^+$: 179.104249; found: 179.104400.

1-(4-(prop-1-yn-1-yl)phenyl)ethan-1-one (7.1)

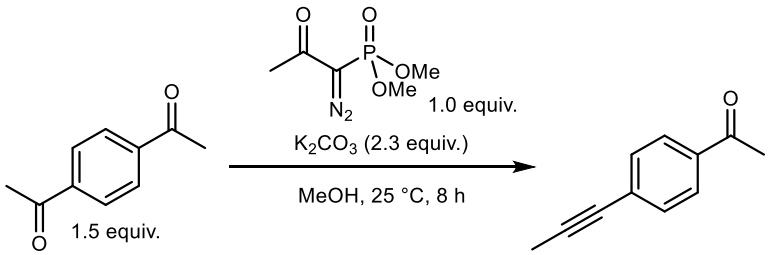

In a round bottom flask under ambient conditions, 1,4-diacetylbenzene (400.0 mg, 2.47 mmol, 1.5 equiv.) was dissolved in MeOH (25 mL). K_2CO_3 (516.3 mg, 3.74 mmol, 2.3 equiv.) and dimethyl-1-diazo-2-oxopropylphosphonate (0.39 mL, 315.9 mg, 1.64 mmol, 1.0 equiv.) were then added, and the reaction was stirred at 25 °C for 8 h. The mixture was then diluted with Et_2O, washed with a saturated ammonium chloride solution, dried over Na_2SO_4, filtered and concentrated in vacuo. The residue was subjected to FCC (pentane/acetone, 19:1) to afford the title compound as a colorless oil (201.5 mg, 1.15 mmol, 70%). The spectroscopic data were in accordance with the literature.[309]

^{1}H NMR (501 MHz, $CDCl_3$) δ 7.92 – 7.84 (m, 2H), 7.49 – 7.42 (m, 2H), 2.58 (s, 3H), 2.08 (s, 3H).

1-(3-((allyloxy)methyl)phenyl)ethyl acetate (4.58d)

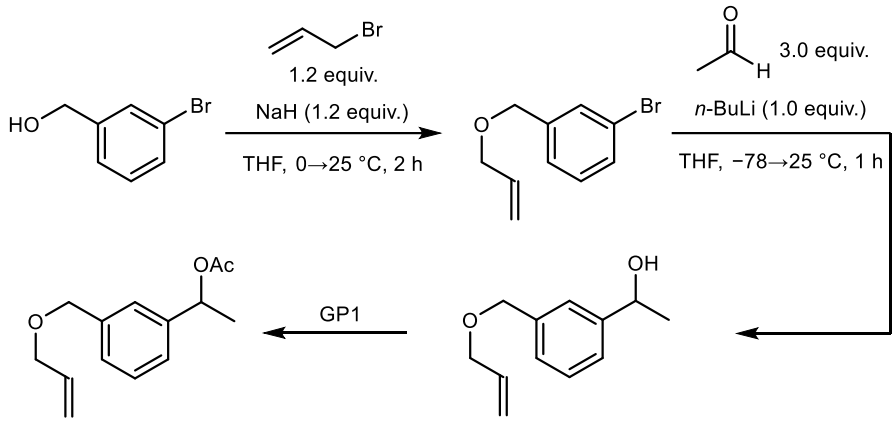

In a flame-dried Schlenk flask under an argon atmosphere, (3-bromophenyl)methanol (748.1 mg, 4.00 mmol, 1.0 equiv.) was dissolved in THF (8 mL) and the mixture was cooled to 0 °C. Allyl bromide (580.7 mg, 4.80 mmol, 1.2 equiv.) and NaH (60% dispersion in mineral oil, 192.0 mg, 4.80 mmol, 1.2 equiv.) were successively added in one portion and the reaction was stirred at 25 °C for 2 h. The reaction was quenched by addition of a saturated ammonium chloride solution, water was added and the mixture was transferred to an extraction funnel and extracted with Et_2O (3x). The combined organic phases were washed with brine, dried over Na_2SO_4, filtered and concentrated in vacuo to afford the crude 1-((allyloxy)methyl)-3-bromobenzene as a viscous oil which was used without further purification assuming quant. yield. The spectroscopic data were in accordance with the literature.[310]

^{1}H NMR (501 MHz, $CDCl_3$) δ 7.51 (t, *J* = 1.8 Hz, 1H), 7.41 (dt, *J* = 7.7, 1.6 Hz, 1H), 7.27 (d, *J* = 7.7 Hz, 1H), 7.21 (t, *J* = 7.7 Hz, 1H), 5.95 (ddt, *J* = 17.3, 10.4, 5.6 Hz, 1H), 5.32 (dq, *J* = 17.2, 1.6 Hz, 1H), 5.23 (dq, *J* = 10.4, 1.4 Hz, 1H), 4.49 (s, 2H), 4.04 (dt, *J* = 5.7, 1.4 Hz, 2H).

In a flame-dried Schlenk flask under an argon atmosphere, the above obtained crude 1-((allyloxy)methyl)-3-bromobenzene was dissolved in THF (15 mL). The mixture was cooled to −78 °C, *n*-BuLi (2.5 M in hexanes, 1.6 mL, 4.00 mmol, 1.0 equiv.) was added dropwise and the reaction was stirred at the same temperature for 1 h. Acetaldehyde (528.6 mg, 12.00 mmol, 3.0 equiv.) was added in one portion, and the reaction was allowed to warm to 25 °C over 2 h. Water was added, the mixture was transferred to an extraction funnel and extracted with EtOAc (3x). The combined organic phases were washed with water, dried over Na_2SO_4, filtered and concentrated in vacuo to afford the crude 1-(3-((allyloxy)methyl)phenyl)ethan-1-ol as a viscous oil which was used without further purification assuming quant. yield.

^{1}H NMR (501 MHz, $CDCl_3$) δ 7.39 – 7.23 (m, 4H), 5.96 (ddt, *J* = 17.3, 10.5, 5.7 Hz, 1H), 5.31 (dq, *J* = 17.2, 1.6 Hz, 1H), 5.21 (dq, *J* = 10.4, 1.4 Hz, 1H), 4.91 (q, *J* = 6.5 Hz, 1H), 4.53 (s, 2H), 4.05 (dt, *J* = 5.7, 1.4 Hz, 2H), 1.50 (d, *J* = 6.4 Hz, 3H).

Subjecting the above obtained crude 1-(3-((allyloxy)methyl)phenyl)ethan-1-ol to GP1 afforded the title compound as a colorless oil (667.6 mg, 2.85 mmol, 71% over 3 steps).

^{1}H NMR (501 MHz, $CDCl_3$) δ 7.38 – 7.25 (m, 4H), 5.96 (ddt, *J* = 17.3, 10.4, 5.6 Hz, 1H), 5.32 (dq, *J* = 17.3, 1.6 Hz, 1H), 5.22 (dq, *J* = 10.4, 1.4 Hz, 1H), 4.53 (s, 2H), 4.04 (dt, *J* = 5.7, 1.4 Hz, 2H), 2.07 (s, 3H), 1.53 (d, *J* = 6.6 Hz, 3H).

^{13}C NMR (126 MHz, $CDCl_3$) δ 170.5, 142.0, 138.8, 134.8, 128.7, 127.4, 125.5, 125.5, 117.4, 72.4, 72.1, 71.5, 22.4, 21.5.

HRMS (ESI) (m/z): calculated for $C_{14}H_{18}O_3Na$ $[M+Na]^+$: 257.11482; found: 257.11463.

1-(2-fluoro-[1,1'-biphenyl]-4-yl)ethan-1-ol (7.2)

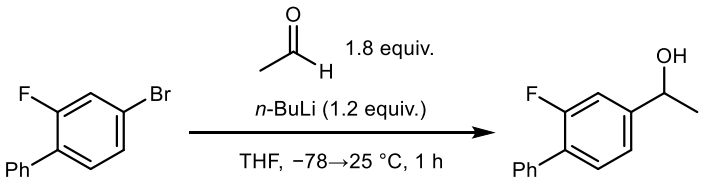

In a flame-dried Schlenk flask under an argon atmosphere, 4-bromo-2-fluoro-1,1'-biphenyl (818.2 mg, 3.26 mmol, 1.0 equiv.) was dissolved in THF (6.3 mL) and the solution was cooled to −78 °C. *n*-BuLi (2.5 M in hexanes, 1.56 mL, 3.91 mmol, 1.2 equiv.) was added dropwise, and the reaction was stirred at the same temperature for 30 minutes. Acetaldehyde (0.26 g, 5.87 mmol, 1.8 equiv.) was added dropwise, and the reaction was allowed to warm to 25 °C over 1 h. The reaction was quenched with MeOH, water was added, the mixture was transferred to an extraction funnel and extracted with Et_2O (3x). The combined organic phases were dried over Na_2SO_4, filtered and concentrated in vacuo. The crude residue was subjected to FCC (pentane/acetone, 9:1) to afford the title compound as a yellow solid (574.5 mg, 2.66 mmol, 82%). The spectroscopic data were in accordance with the literature.[308]

^{1}H NMR (501 MHz, $CDCl_3$) δ 7.55 (dt, *J* = 8.1, 1.6 Hz, 2H), 7.48 – 7.33 (m, 4H), 7.24 – 7.17 (m, 2H), 4.95 (q, *J* = 6.5 Hz, 1H), 1.54 (d, *J* = 6.4 Hz, 3H).

^{13}C NMR (126 MHz, $CDCl_3$) δ 159.8 (d, *J* = 248.2 Hz), 147.5 (d, *J* = 6.9 Hz), 135.6, 130.8 (d, *J* = 3.8 Hz), 129.0 (d, *J* = 3.0 Hz), 128.5, 128.0 (d, *J* = 13.6 Hz), 127.7, 121.3 (d, *J* = 3.3 Hz), 113.1 (d, *J* = 23.5 Hz), 69.6, 25.2.

^{19}F NMR (471 MHz, $CDCl_3$) δ -117.68.

HRMS (GC-EI) (m/z): calculated for $C_{14}H_{13}FO$ $[M]^+$: 216.09449; found: 216.09469.

(*E*)-2-phenylbut-2-enal (7.3)

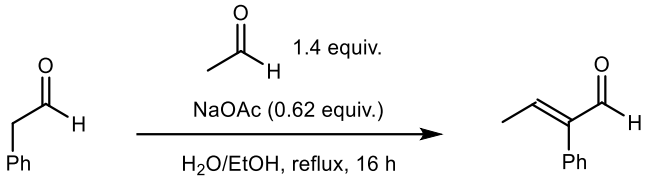

In a round bottom flask under ambient conditions, sodium acetate (846.6 mg, 10.32 mmol, 0.62 equiv.) was dissolved in water (1.7 mL) and EtOH (2.1 mL) and the mixture was cooled to 0 °C. Freshly distilled phenylacetaldehyde (2.00 g, 16.65 mmol, 1 equiv.) and acetaldehyde (1.03 g, 23.30 mmol, 1.4 equiv.) were then added simultaneously in one portion. The reaction was stirred at 25 °C for 1 h, then fitted with a reflux condenser and refluxed for 16 h. After cooling to room temperature, water was added and the mixture was transferred to an extraction funnel and extracted with MTBE (3x). The combined organic phases were washed with water, dried over Na_2SO_4, filtered and concentrated in vacuo. The crude residue was subjected to FCC (pentane/acetone, 9:1) to afford the title compound as a colorless oil (833.6 mg, 5.42 mmol, 33%, *E*/*Z*>99:1). The spectroscopic data were in accordance with the literature.[311]

^{1}H NMR (501 MHz, $CDCl_3$) δ 9.62 (s, 1H), 7.47 – 7.38 (m, 2H), 7.38 – 7.29 (m, 1H), 7.22 – 7.14 (m, 2H), 6.85 (q, *J* = 7.1 Hz, 1H), 2.02 (d, *J* = 7.1 Hz, 3H).

^{13}C NMR (126 MHz, $CDCl_3$) δ 193.7, 151.3, 145.2, 132.4, 129.6, 128.4, 128.1, 16.1.

HRMS (ESI) (m/z): calculated for $C_{10}H_{10}ONa$ $[M+Na]^+$: 169.062384; found: 169.062420.

(*Z*)-3-bromopent-3-en-2-ol (7.4)

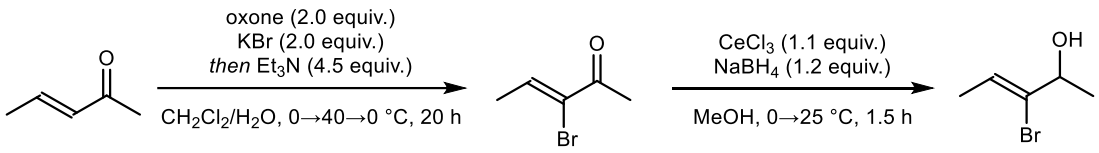

Following a modified procedure by Willis and coworkers.[312] In a round bottom flask under ambient conditions, oxone (29.23 g, 47.55 mmol, 2.0 equiv.) was dissolved in CH_2Cl_2 (120 mL) and water (30 mL). The mixture was cooled to 0 °C, KBr (5.66 g, 47.55 mmol, 2.0 equiv.) was added portionwise over 15 minutes and the reaction was stirred at the same temperature for 40 minutes. (*E*)-3-penten-2-one (2.32 mL, 2.00 g, 23.78 mmol, 1.0 equiv.) was added dropwise, and the reaction was stirred at 25 °C for 16 h and then heated at 40 °C for 4 h. The reaction was then cooled to 0 °C, Et_3N (14.91 mL, 10.83 g, 106.99 mmol, 4.5 equiv.) was added dropwise and stirred at the same temperature for 4 h. Water was added, the mixture was transferred to an extraction funnel and extracted with CH_2Cl_2 (3x). The combined organic phases were washed with water and brine, dried over Na_2SO_4, filtered and concentrated in vacuo. The crude residue was subjected to FCC (pentane/acetone, 9:1) to afford (*Z*)-3-bromopent-3-en-2-one as a white solid (2.33 g, 13.87 mmol, 58%). The spectroscopic data were in accordance with the literature.[313]

^{1}H NMR (501 MHz, $CDCl_3$) δ 7.24 (q, *J* = 6.8 Hz, 1H), 2.45 (s, 3H), 2.02 (d, *J* = 6.8 Hz, 3H).

^{13}C NMR (126 MHz, $CDCl_3$) δ 191.9, 141.1, 129.2, 26.6, 18.5.

HRMS (GC-EI) (m/z): calculated for C_5H_7BrO $[M]^+$: 161.967490; found: 161.967570.

In a round bottom flask under ambient conditions, (*Z*)-3-bromopent-3-en-2-one (2.00 g, 12.27 mmol, 1.0 equiv.) and $CeCl_3 \bullet 7H_2O$ (5.03 g, 13.50 mmol, 1.1 equiv.) were dissolved in MeOH (41 mL), and the mixture was cooled to 0 °C. $NaBH_4$ (557.0 mg, 14.72 mmol, 1.2 equiv.) was added portionwise, and the reaction was stirred at the same temperature for 30 minutes, and then at 25 °C for 1 h. Water was then added, the mixture was transferred to an extraction funnel and extracted with Et_2O (3x). The combined organic phases were washed with water and brine, dried over Na_2SO_4, filtered and concentrated in vacuo to afford the title compound as a yellow oil (2.02 g, 12.27 mmol, quant.) that could be used without further purification. The spectroscopic data were in accordance with the literature.[314]

^{1}H NMR (501 MHz, $CDCl_3$) δ 6.06 (qd, *J* = 6.6, 0.7 Hz, 1H), 4.36 – 4.28 (m, 1H), 1.77 (dd, *J* = 6.5, 0.6 Hz, 3H), 1.37 (d, *J* = 6.3 Hz, 3H).

^{13}C NMR (126 MHz, $CDCl_3$) δ 133.9, 123.8, 72.7, 22.5, 16.5.

HRMS (ESI) (m/z): calculated for C_5H_9BrONa $[M+Na]^+$: 186.972909; found: 186.973040.

(*Z*)-3-iodopent-3-en-2-ol (7.5)

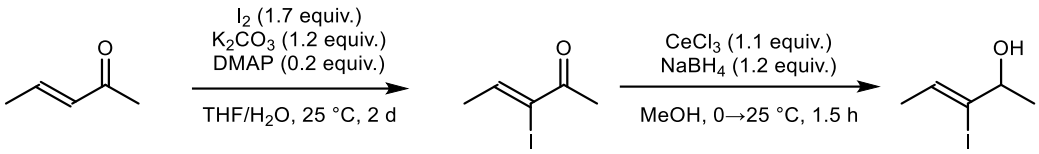

Following a modified procedure by Krafft and coworkers.[315] In a round bottom flask under ambient conditions, (*E*)-pent-3-en-2-one (2.00 g, 23.78 mmol, 1.0 equiv.) was dissolved in THF (60 mL) and water (60 mL). K_2CO_3 (3.94 g, 28.53 mmol, 1.2 equiv.) I_2 (10.26 g, 40.42 mmol, 1.7 equiv.) and DMAP (580.9 mg, 4.76 mmol, 0.2 equiv.) were added and the reaction was stirred at 25 °C for 2 d. Upon completion, the reaction was diluted with EtOAc and the mixture was washed with saturated $Na_2S_2O_3$ and 0.1 M HCl. The organic phase was dried over Na_2SO_4, filtered and concentrated in vacuo to afford the crude (*Z*)-3-iodopent-3-en-2-one as a light pink oil which was used without further purification assuming quant. yield. The spectroscopic data were in accordance with the literature.[316]

^{1}H NMR (501 MHz, $CDCl_3$) δ 7.12 (q, *J* = 6.6 Hz, 1H), 2.51 (s, 3H), 2.09 (d, *J* = 6.6 Hz, 3H).

Following a modified procedure by Willis and coworkers.[312] In a round bottom flask under ambient conditions, the above obtained crude (*Z*)-3-iodopent-3-en-2-one and $CeCl_3$•$7H_2O$ (9.74 g, 26.15 mmol, 1.1 equiv.) were dissolved in MeOH (80 mL), and the mixture was cooled to 0 °C. $NaBH_4$ (1.08 g, 28.53 mmol, 1.2 equiv.) was added portionwise, and the reaction was stirred at the same temperature for 30 minutes, and then at 25 °C for 1 h. Water was then added, the mixture was transferred to an extraction funnel and extracted with Et_2O (3x). The combined organic phases were washed with water and brine, dried over Na_2SO_4, filtered and concentrated in vacuo to afford the title compound as a red oil (3.02 g, 14.27 mmol, 60% over 2 steps) that could be used without further purification.

^{1}H NMR (501 MHz, $CDCl_3$) δ 6.00 (qd, *J* = 6.4, 0.9 Hz, 1H), 3.96 (q, *J* = 6.2 Hz, 1H), 1.79 (d, *J* = 6.4 Hz, 3H), 1.31 (d, *J* = 6.3 Hz, 3H).

^{13}C NMR (126 MHz, $CDCl_3$) δ 130.2, 119.0, 74.6, 24.0, 21.5.

HRMS (GC-EI) (m/z): calculated for C_5H_9IO $[M]^+$: 211.969262; found: 211.969410.

(*Z*)-*tert*-butyl((3-iodopent-3-en-2-yl)oxy)dimethylsilane (7.6)

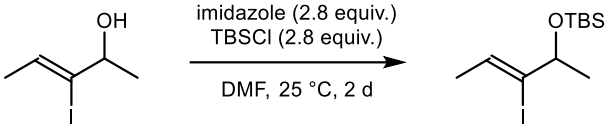

In a round bottom flask under ambient conditions, (*Z*)-3-iodopent-3-en-2-ol (**7.5**, 1.08 g, 5.08 mmol, 1.0 equiv.) was dissolved in DMF (108 mL). Imidazole (970.1 mg, 14.25 mmol, 2.8 equiv.) and TBSCl (2.15 g, 14.25 mmol, 2.8 equiv.) were added, and the reaction was stirred at 25 °C for 3 h. Upon completion, ice was added, the mixture was transferred to an extraction funnel and the mixture was extracted with EtOAc (3x). The combined organic phases were washed with brine, dried over Na_2SO_4, filtered and concentrated in vacuo. The crude residue was subjected to FCC (pentane/Et_2O, 98:2) to afford the title compound as a colorless liquid (1.61 g, 4.95 mmol, 97%).

^{1}H NMR (501 MHz, $CDCl_3$) δ 5.93 (qd, *J* = 6.4, 1.1 Hz, 1H), 4.04 (qt, *J* = 6.1, 0.9 Hz, 1H), 1.77 (dd, *J* = 6.4, 0.8 Hz, 3H), 1.26 (d, *J* = 6.1 Hz, 3H), 0.90 (s, 9H), 0.05 (s, 3H), 0.05 (s, 3H).

^{13}C NMR (126 MHz, $CDCl_3$) δ 128.3, 118.6, 75.2, 26.0, 25.0, 21.4, 18.4, -4.4, -4.7.

HRMS (ESI) (m/z): calculated for $C_{11}H_{23}IOSiNa$ $[M+Na]^+$: 349.045510; found: 349.045560.

(*E*)-*tert*-butyldimethyl((3-vinylpent-3-en-2-yl)oxy)silane (7.7)

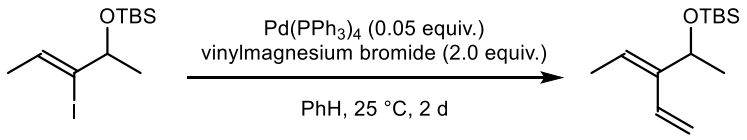

Following a modified procedure by Grubbs and coworkers.[317] In a flame-dried Schlenk flask under an argon atmosphere, $Pd(PPh_3)_4$ (46.9 mg, 0.04 mmol, 0.05 equiv.) was dissolved in

PhH (4.2 mL) and (*Z*)-*tert*-butyl((3-iodopent-3-en-2-yl)oxy)dimethylsilane (**7.6**, 300.0 mg, 0.83 mmol, 1.0 equiv.) was added. Vinylmagnesium bromide (1.0 M in THF, 1.66 mL, 1.66 mmol, 2.0 equiv.) was then added dropwise, and the reaction was stirred at 25 °C for 2 d. The reaction was quenched by addition of a saturated ammonium chloride solution and the mixture was transferred to an extraction funnel and extracted with Et_2O (3x). The combined organic phases were washed with saturated $NaHCO_3$ solution, water, brine, dried over Na_2SO_4, filtered and concentrated in vacuo. The crude residue was subjected to FCC (pentane) to afford the title compound as a colorless liquid (88.0 mg, 0.39 mmol, 47%).

^{1}H NMR (501 MHz, $CDCl_3$) δ 6.56 (dd, *J* = 17.9, 11.5 Hz, 1H), 5.77 (ddd, *J* = 8.4, 7.1, 5.9 Hz, 1H), 5.22 (dd, *J* = 17.9, 1.6 Hz, 1H), 5.12 (dt, *J* = 11.6, 1.7 Hz, 1H), 4.54 – 4.47 (m, 1H), 1.74 (dd, *J* = 7.3, 0.9 Hz, 3H), 1.26 (d, *J* = 6.3 Hz, 3H), 0.89 (s, 9H), 0.04 (s, 3H), 0.01 (s, 3H).

^{13}C NMR (126 MHz, $CDCl_3$) δ 141.5, 131.3, 122.8, 113.9, 69.6, 26.0, 25.0, 18.4, 13.2, -4.7, -4.9.

HRMS (ESI) (m/z): calculated for $C_{13}H_{26}OSiNa$ $[M+Na]^+$: 249.16451; found: 249.16438.

(*E*)-3-vinylpent-3-en-2-yl acetate (4.67d)

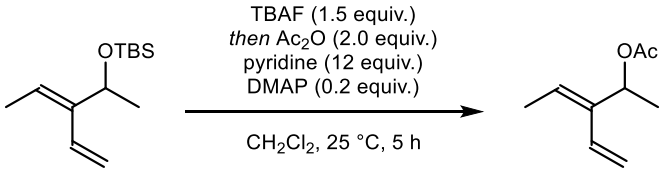

Following a modified procedure by Winterfeldt and coworkers.[318] In a round bottom flask under ambient conditions, (*E*)-*tert*-butyldimethyl((3-vinylpent-3-en-2-yl)oxy)silane (**7.7**, 88.0 mg, 0.39 mmol, 1.0 equiv.) was dissolved in THF (2 mL). TBAF (1.0 M in THF, 0.58 mL, 0.58 mmol, 1.5 equiv.) was added, and the reaction was stirred at 25 °C for 2 h. The solvent was then removed in vacuo, and the residue was dissolved in CH_2Cl_2 (2 mL), after which pyridine (0.38 mL, 4.66 mmol, 12.0 equiv.), Ac_2O (119.0 mg, 1.17 mmol, 3.0 equiv.) and DMAP (9.50 mg, 0.08 mmol, 0.2 equiv.) were added and the reaction was stirred at 25 °C for 5 h. Excess MeOH was added and the reaction was stirred for a further 30 minutes. The mixture was then diluted with pentane, transferred to an extraction funnel and washed with water (2x) and saturated $NaHCO_3$ solution (2x). The organic phase was then dried over Na_2SO_4, filtered and

concentrated in vacuo. The residue was subjected to FCC (pentane/acetone, 19:1) to afford the title compound as a colorless liquid (37.3 mg, 0.24 mmol, 62%).

^{1}H NMR (501 MHz, $CDCl_3$) δ 6.56 (dd, *J* = 18.2, 11.5 Hz, 1H), 5.80 – 5.72 (m, 1H), 5.63 – 5.55 (m, 1H), 5.29 (d, *J* = 17.8 Hz, 1H), 5.18 (dt, *J* = 11.4, 1.5 Hz, 1H), 2.05 (s, 3H), 1.77 (d, *J* = 7.1 Hz, 3H), 1.37 (d, *J* = 6.5 Hz, 3H).

^{13}C NMR (126 MHz, $CDCl_3$) δ 170.5, 137.6, 130.6, 125.2, 114.9, 70.8, 21.5, 20.2, 13.4.

HRMS (GC-EI) (m/z): calculated for $C_9H_{14}O_2$ $[M]^+$: 154.098830; found: 154.098840.

(*Z*)-3-methylpent-3-en-2-yl acetate (4.67l)

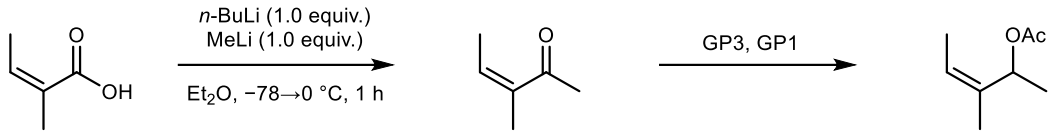

Following a modified procedure by Danheiser and coworkers.[319] In a flame-dried Schlenk flask under an argon atmosphere, angelic acid (1.00 g, 10.00 mmol, 1.0 equiv.) was dissolved in Et_2O (25 mL) and the mixture was cooled to −78 °C. While stirring vigorously, *n*-BuLi (2.5 M in hexanes, 4.0 mL, 10.00 mmol, 1.0 equiv.) and MeLi (1.6 M in THF, 12.5 mL, 10.00 mmol, 1.0 equiv.) were added dropwise successively over 10 minutes. The reaction was stirred at the same temperature for 30 minutes, after which it was allowed to 0 °C over 1 h. Distilled water was added, the mixture was transferred to an extraction funnel and extracted with Et_2O (3x). The combined organic phases were washed with brine, dried over Na_2SO_4 and filtered. Concentration in vacuo maintaining a water bath temperature around 10 °C afforded the crude (*Z*)-3-methylpent-3-en-2-one (*E*/*Z*≈98:2) as a colorless oil which was used without further purification assuming quant. yield. The spectroscopic data were in accordance with the literature.[320]

Note: the product of this reaction readily isomerized to the (E)-enone in the presence of trace acid. ^{1}H NMR spectra were therefore collected in CD_2Cl_2 and contact with silica gel was avoided.

^{1}H NMR (501 MHz, CD_2Cl_2) δ 5.85 (qq, *J* = 7.2, 1.5 Hz, 1H), 2.22 (s, 3H), 1.89 (p, *J* = 1.5 Hz, 3H), 1.85 (dq, *J* = 7.3, 1.5 Hz, 3H).

Subjecting the above obtained crude (*Z*)-3-methylpent-3-en-2-one to GP3 and GP1 afforded the title compound as a colorless oil (406.3 mg, 2.86 mmol, 29% over 3 steps).

^{1}H NMR (501 MHz, $CDCl_3$) δ 5.79 – 5.71 (m, 1H), 5.35 – 5.27 (m, 1H), 2.03 (s, 3H), 1.70 – 1.61 (m, 6H), 1.27 (d, J = 6.6 Hz, 3H).

^{13}C NMR (126 MHz, $CDCl_3$) δ 170.5, 134.9, 122.3, 68.9, 21.4, 18.6, 17.8, 13.0.

HRMS (ESI) (m/z): calculated for $C_8H_{14}O_2Na$ $[M+Na]^+$: 165.08860; found: 165.08868.

7.3. Synthesis of Catalysts

Catalysts **4.13a**, **4.13b**, **4.3a**, **4.3b**, **4.3c**, **4.3d**, **4.3e**, **4.3g**, and **4.3i** were previously reported.[111,115,116,271,274,321,322] Catalysts **4.3f**, **4.3h**, and **4.3j** were previously synthesized by members of our group but not reported. Catalysts **4.3m**, **4.3n**, **4.3s**, and **4.3t** were not fully characterized due to their instability, and catalysts **4.3l**, **4.3o**, **4.3p**, **4.3q**, and **4.3r** were not fully characterized due to limited availability of the material. (S)-2,2'-(2,2'-bis(methoxymethoxy)-[1,1'-binaphthalene]-3,3'-diyl)bis(4,4,5,5-tetramethyl-1,3,2-dioxaborolane) (**4.36**) and (*S*)-3,3'-diiodo-2,2'-bis(methoxymethoxy)-1,1'-binaphthalene (**4.37**) were synthesized according to known literature procedures.[323,324] ((trifluoromethyl)sulfonyl)phosphorimidoyl trichloride (**4.40a**), ((perfluoroethyl)sulfonyl)phosphorimidoyl trichloride (**4.40b**), and ((perfluorobutyl)sulfonyl)phosphorimidoyl trichloride (**4.40d**) were synthesized according to known literature procedures.[111,294,322] ((perfluoropropyl)sulfonyl)phosphorimidoyl trichloride (**4.40c**) analogously synthesized by members of our group but not reported.

7.3.1. *Synthesis of Wing Substituents*

General procedure 4 (GP4): Ullmann perfluoroalkylation

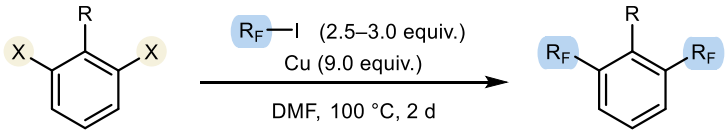

Following a modified procedure by List and coworkers.[322] In a flame-dried J Young Schlenk flask under an argon atmosphere, perfluoroalkyl iodide (2.5–3 equiv.), copper powder (9.0 equiv.) and aryl halide (1.0 equiv.) were dissolved in freshly degassed DMF (0.4 M). The

flask was then sealed, and the reaction was stirred at 100 °C for 4 d, after which it was cooled to 25 °C and full conversion of the starting aryl halide was confirmed by ^{19}F NMR spectroscopy. Water was added, the mixture was filtered thought celite, and the celite was washed with Et_2O. 1.0 M HCl was then added to acidify the mixture, and it was transferred to an extraction funnel and extracted with Et_2O (3x). The combined organic phases were dried over Na_2SO_4, filtered, and concentrated in vacuo. The crude residue was subjected to FCC (pentane, unless otherwise stated) to afford the corresponding perfluoroalkyl arene.

Note 1: perfluoroethyl iodide gas was condensed at −78 °C until the gas cylinder had reduced in weight by the desired amount. The other reagents were then added, the reaction vessel was sealed and heating started.

Note 2: mono-coupled- or protodehalogenated side-products which were inseparable by FCC were removed by precipitated from pentane at −78 °C. Careful decanting of the mother liquor and concentration of the precipitate in vacuo yielded the pure perfluoroalkyl arenes.

Note 3: Due to the volatility of the perfluoroalkyl arenes, mild conditions for concentration in vacuo were applied (water bath temperature: 40 °C, minimum vacuum: 150 mbar). For this reason, the products contained traces of pentane.

1,3-bis(perfluoroethyl)benzene (7.8)

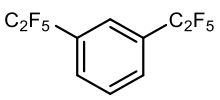

Preparation from 1,3-dibromobenzene (3.84 g, 16.27 mmol, 1.0 equiv.) and pentafluoroethyl iodide (11.20 g, 45.54 mmol, 2.8 equiv.) according to GP4 afforded the title compound as a colorless oil (3.25 g, 10.36 mmol, 64%).

^{1}H NMR (501 MHz, $CDCl_3$) δ 7.86 – 7.81 (m, 3H), 7.73 – 7.66 (m, 1H).

^{13}C{^{1}H} NMR (151 MHz, $CDCl_3$) δ 130.2 (t, *J* = 6.2 Hz), 130.0, 129.7, 124.9 (p, *J* = 6.6 Hz), 119.0 (qt, *J* = 285.9, 38.7 Hz), 112.9 (tq, *J* = 254.6, 38.5 Hz).

^{19}F NMR (471 MHz, $CDCl_3$) δ -84.76, -115.23.

HRMS (GC-EI) (m/z): calculated for $C_{10}H_4F_{10}$ $[M]^+$: 314.014785; found: 314.014790.

1,3-bis(perfluoroethyl)-2-(trifluoromethyl)benzene (7.9)

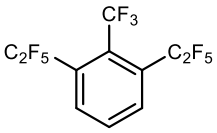

Preparation from 1,3-dichloro-2-(trifluoromethyl)benzene (1.28 g, 5.96 mmol, 1.0 equiv.) and pentafluoroethyl iodide (4.40 g, 17.89 mmol, 3.0 equiv.) according to GP4 afforded the title compound as a colorless oil (721.1 g, 1.83 mmol, 31%) after precipitation from pentane at −78 °C.

^{1}H NMR (501 MHz, $CDCl_3$) δ 8.01 (d, *J* = 8.1 Hz, 2H), 7.88 (t, *J* = 8.1 Hz, 1H).

^{13}C{^{1}H} NMR (126 MHz, $CDCl_3$) δ 133.5 (t, *J* = 9.3 Hz), 131.7, 130.8 (t, *J* = 24.7 Hz), 129.9 (q, *J* = 36.8 Hz), 121.2 (q, *J* = 274.9 Hz), 118.9 (qt, *J* = 287.6, 37.8 Hz), 113.7 (tq, *J* = 257.8, 39.4 Hz).

^{19}F NMR (471 MHz, $CDCl_3$) δ -52.56 (dddd, *J* = 32.3, 22.8, 20.8, 11.3 Hz), -80.56 (q, *J* = 11.7 Hz), -100.61 (q, *J* = 21.2 Hz).

HRMS (GC-EI) (m/z): calculated for $C_{11}H_3F_{13}$ $[M]^+$: 382.002171; found: 382.002340.

2-(perfluoroethyl)-1,3-bis(trifluoromethyl)benzene (7.10)

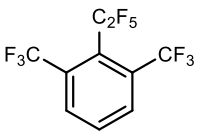

Preparation from 2-bromo-1,3-bis(trifluoromethyl)benzene (1.91 g, 6.51 mmol, 1.0 equiv.) and pentafluoroethyl iodide (4.80 g, 19.52 mmol, 3.0 equiv.) according to GP4 afforded the title compound as a colorless oil (1.56 g, 4.71 mmol, 72%).

^{1}H NMR (501 MHz, $CDCl_3$) δ 8.17 (d, *J* = 8.1 Hz, 2H), 7.88 (t, *J* = 8.1 Hz, 1H).

^{19}F NMR (471 MHz, $CDCl_3$) δ -56.61 (ddt, *J* = 29.6, 20.0, 10.0 Hz), -74.03 (h, *J* = 10.1 Hz), -94.51 (h, *J* = 19.4 Hz).

HRMS (GC-EI) (m/z): calculated for $C_{10}H_3F_{11}$ $[M]^+$: 332.005364; found: 332.005510.

2-(perfluoropropyl)-1,3-bis(trifluoromethyl)benzene (7.11)

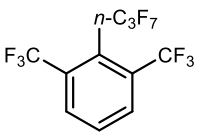

Preparation from 2-bromo-1,3-bis(trifluoromethyl)benzene (1.50 g, 5.12 mmol, 1.0 equiv.) and *n*-heptafluoropropyl iodide (3.79 g, 12.80 mmol, 2.5 equiv.) according to GP4 afforded the title compound as a colorless oil (944.8 mg, 2.47 mmol, 48%).

^{1}H NMR (501 MHz, $CDCl_3$) δ 8.22 (d, *J* = 8.1 Hz, 2H), 7.89 (t, *J* = 8.2 Hz, 1H).

^{19}F NMR (471 MHz, $CDCl_3$) δ -55.84 (p, *J* = 19.8 Hz), -80.33 (dt, *J* = 12.0, 6.4 Hz), -98.26 – -98.55 (m), -118.72 (qt, *J* = 20.4, 10.1 Hz).

HRMS (APCI) (m/z): calculated for $C_{11}H_3F_{13}$ $[M+H]^-$: 382.003271; found: 382.003510.

2-fluoro-1,3-bis(perfluoroethyl)benzene (7.12)

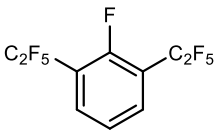

Preparation from 1,3-dibromo-2-fluorobenzene (5.27 g, 20.74 mmol, 1.0 equiv.) and pentafluoroethyl iodide (15.30 g, 62.22 mmol, 3.0 equiv.) according to GP4 afforded the title compound as a colorless oil (3.36 g, 10.13 mmol, 49%) after precipitation from pentane at −78 °C.

^{1}H NMR (600 MHz, $CDCl_3$) δ 7.82 (dd, *J* = 7.9, 6.4 Hz, 2H), 7.46 (tq, *J* = 8.0, 0.9 Hz, 1H).

^{13}C{^{1}H} NMR (151 MHz, $CDCl_3$) δ 158.3 (dp, *J* = 269.4, 3.3 Hz), 133.3 (t, *J* = 7.4 Hz), 124.7 (d, *J* = 4.8 Hz), 118.9 (qt, *J* = 286.7, 37.8 Hz), 118.5 (td, *J* = 24.5, 11.6 Hz), 112.3 (tqd, *J* = 256.8, 40.5, 2.2 Hz).

^{13}C{^{19}F} NMR (151 MHz, $CDCl_3$) δ 158.3 (td, *J* = 9.6, 1.8 Hz), 133.3 (ddd, *J* = 166.9, 9.2, 2.3 Hz), 124.7 (d, *J* = 168.1 Hz), 118.9, 118.5 (d, *J* = 8.6 Hz), 112.4 – 112.3 (m).

^{19}F NMR (565 MHz, $CDCl_3$) δ -84.90 (dt, *J* = 12.2, 2.1 Hz), -111.26 (ddddt, *J* = 27.6, 18.4, 15.6, 12.3, 6.1 Hz), -113.31 (dq, *J* = 21.2, 2.2 Hz).

HRMS (GC-EI) (m/z): calculated for $C_{10}H_3F_{11}$ $[M]^+$: 332.005364; found: 332.005530.

2,6-bis(perfluoroethyl)-4-(4,4,5,5-tetramethyl-1,3,2-dioxaborolan-2-yl)aniline (4.46)

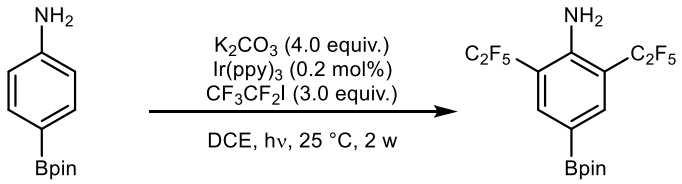

Following a modified procedure by He, Gu and Zhang.[325] In a flame-dried J Young Schlenk flask under an argon atmosphere, 4-(4,4,5,5-tetramethyl-1,3,2-dioxaborolan-2-yl)aniline (250.0 mg, 1.14 mmol, 1.0 equiv.), K_2CO_3 (630.8 mg, 4.56 mmol, 4.0 equiv.) and $Ir(ppy)_3$

(1.5 mg, 2.3 µmol, 0.2 mol%) were dissolved in DCE (11.4 mL). A stock solution of pentafluoroethyl iodide (0.5 M in DCE, 6.8 mL, 3.42 mmol, 3 equiv.) was then added, the flask was sealed, and the reaction was stirred at 25 °C under irradiation by a blue LED (6 W) for 2 w. After monitoring by ^{1}H NMR indicated that conversion had stopped, the reaction was filtered through a pad of celite and washed with EtOAc (3x). The filtrate was concentrated and the crude residue was subjected to FCC (hexanes–hexanes/EtOAc, 9:1) to afford the title compound as a white solid (206.5 mg, 0.45 mmol, 40%).

^{1}H NMR (600 MHz, $CDCl_3$) δ 7.94 (s, 2H), 5.07 (s, 2H), 1.33 (s, 12H).

^{13}C{^{1}H} NMR (151 MHz, $CDCl_3$) δ 147.1 – 146.8 (m), 139.7 (t, *J* = 8.3 Hz), 119.6 (qt, *J* = 287.5, 39.5 Hz), 115.2 (tq, *J* = 254.3, 39.6 Hz), 112.3 (t, *J* = 21.6 Hz), 84.3, 25.0.

^{19}F NMR (471 MHz, $CDCl_3$) δ -84.13, -111.55.

HRMS (ESI) (m/z): calculated for $C_{16}H_{17}BF_{10}NO_2$ $[M+H]^+$: 456.118719; found: 456.118750.

((5-bromo-1,3-phenylene)bis(difluoromethylene))dibenzene (4.33)

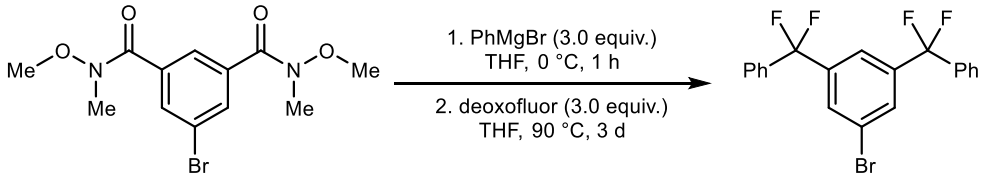

To a solution of 5-bromo-N^1,N^3-dimethoxy-N^1,N^3-dimethylisophthalamide (**4.31**, 400 mg, 1.21 mmol, 1.0 equiv.) in anhydrous THF (24 mL) was added PhMgBr (1 M in Et_2O, 3.62 mL, 3.62 mmol, 3.0 equiv.) at 0 °C. The reaction mixture was stirred at the same temperature for 1 h. The reaction was quenched by addition of a saturated ammonium chloride solution. The mixture was extracted with Et_2O (3x), the combined organic phases were dried over Na_2SO_4, filtered and concentrated in vacuo. The corresponding crude residue containing (5-bromo-1,3-phenylene)bis(phenylmethanone) was used without further purification.

^{1}H NMR (501 MHz, $CDCl_3$) δ 8.14 (d, *J* = 1.5 Hz, 1H), 8.08 (t, *J* = 1.5 Hz, 1H), 7.84 – 7.78 (m, 2H), 7.68 – 7.60 (m, 1H), 7.52 (t, *J* = 7.7 Hz, 2H).

A teflon or polypropylene screw cap vessel was loaded with (5-bromo-1,3-phenylene)bis(phenylmethanone) (474.4 mg, 1.21 mmol, 1.0 equiv.) and deoxofluor (**4.32**, 50% in THF, 1.34 mL, 3.62 mmol, 3.0 equiv.). The vessel was sealed, and the

reaction was stirred at 90 °C for 3 d. The reaction was quenched by addition of a saturated $NaHCO_3$ solution. The mixture was extracted with CH_2Cl_2 (3x), the combined organic phases were dried over Na_2SO_4, filtered and concentrated in vacuo. The crude residue was subjected to FCC (pentane) to afford the title compound as a colorless viscous liquid (185.0 mg, 0.45 mmol, 37%).

^{1}H NMR (501 MHz, $CDCl_3$) δ 7.68 (d, *J* = 1.5 Hz, 2H), 7.65 – 7.64 (m, 1H), 7.50 – 7.40 (m, 10H).

^{19}F NMR (471 MHz, $CDCl_3$) δ -89.24.

HRMS (GC-EI) (m/z): calculated for $C_{20}H_{13}F_4Br$ $[M]^+$: 408.013139; found: 408.013430.

1,3-bis(1,1-difluoroethyl)benzene (7.13)

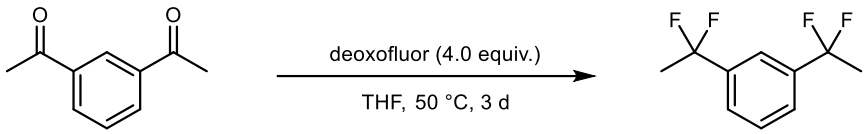

A teflon or polypropylene screw cap vessel was loaded with 1,3-diacetylbenzene (**4.34**, 400 mg, 2.47 mmol, 1.0 equiv.) and deoxofluor (**4.32**, 50% in THF, 3.64 mL, 9.87 mmol, 4.0 equiv.). The vessel was sealed, and the reaction was stirred at 50 °C for 3 d. The reaction was quenched by addition of a saturated $NaHCO_3$ solution. The mixture was extracted with CH_2Cl_2 (3x), the combined organic phases were dried over Na_2SO_4, filtered and concentrated in vacuo. The crude residue was subjected to FCC (pentane) to afford the title compound as a colorless oil (253.5 mg, 1.23 mmol, 50%).

^{1}H NMR (501 MHz, $CDCl_3$) δ 7.67 (s, 1H), 7.62 – 7.57 (m, 2H), 7.55 – 7.48 (m, 1H), 1.96 (t, *J* = 18.2 Hz, 6H).

^{19}F NMR (471 MHz, $CDCl_3$) δ -87.86.

HRMS (GC-EI) (m/z): calculated for $C_{10}H_{10}F_4$ $[M]^+$: 206.071314; found: 206.071630.

General procedure 5 (GP5): Hartwig borylation

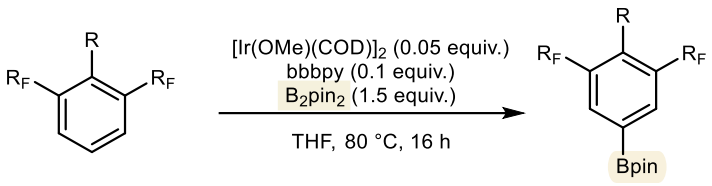

In a flame-dried J Young Schlenk flask under an argon atmosphere, $[Ir(OMe)(COD)]_2$ (0.05 equiv.), 4,4'-di-tert-butyl-2,2'-dipyridyl (bbbpy, 0.1 equiv.), B_2pin_2 (1.5 equiv.) and the respective perfluoroalkylarene (1.0 equiv.) were dissolved in THF (0.17 M), the flask was sealed and the reaction was stirred at 80 °C for 16 h. After monitoring by ^{1}H NMR indicated full conversion, the mixture was concentrated in vacuo. The crude residue was subjected to FCC (pentane) to afford the corresponding boronic esters.

Note: Due to quadripolar relaxation, ^{13}C NMR signals for carbon atoms bonded to boron were not observed in several Bpin esters.

2-(3,5-bis(perfluoroethyl)phenyl)-4,4,5,5-tetramethyl-1,3,2-dioxaborolane (7.14)

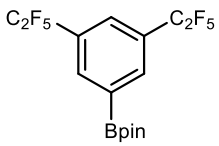

Preparation from 1,3-bis(perfluoroethyl)benzene (**7.8**, 3.06 g, 9.74 mmol, 1.0 equiv.) according to GP5 afforded the title compound as a colorless crystalline solid (4.29 g, 9.74 mmol, quant.).

^{1}H NMR (600 MHz, $CDCl_3$) δ 8.22 (d, *J* = 1.9 Hz, 3H), 7.88 (t, *J* = 2.1 Hz, 2H), 1.37 (s, 18H).

^{13}C{^{1}H} NMR (151 MHz, $CDCl_3$) δ 136.1 (t, *J* = 6.0 Hz), 129.4 (t, *J* = 24.5 Hz), 127.2 (p, *J* = 6.1 Hz), 119.0 (qt, *J* = 285.9, 38.8 Hz), 113.1 (tq, *J* = 254.7, 38.6 Hz), 85.0, 25.0.

^{19}F NMR (471 MHz, $CDCl_3$) δ -84.66, -115.03.

HRMS (APCI) (m/z): calculated for $C_{16}H_{16}BF_{10}O_2$ $[M+H]^+$: 441.10782; found: 441.10803.

2-(3,5-bis(1,1-difluoroethyl)phenyl)-4,4,5,5-tetramethyl-1,3,2-dioxaborolane (4.35)

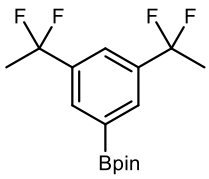

Preparation from 1,3-bis(1,1-difluoroethyl)benzene (**7.13**, 253.5 mg, 1.23 mmol, 1.0 equiv.) according to GP5 afforded the title compound as a colorless crystalline solid (185.6 mg, 0.56 mmol, 45%).

^{1}H NMR (501 MHz, $CDCl_3$) δ 7.98 (s, 2H), 7.74 (s, 1H), 1.94 (t, *J* = 18.2 Hz, 6H), 1.36 (s, 12H).

^{19}F NMR (471 MHz, $CDCl_3$) δ -87.64.

HRMS (GC-CI) (m/z): calculated for $C_{16}H_{25}NBF_4O_2$ $[M+NH_4]^+$: 350.190898; found: 350.190980.

4,4,5,5-tetramethyl-2-(3,4,5-tris(trifluoromethyl)phenyl)-1,3,2-dioxaborolane (7.15)

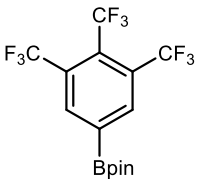

Preparation from 1,2,3-tris(trifluoromethyl)benzene (1.04 g, 3.69 mmol, 1.0 equiv.) according to GP5 afforded the title compound as a colorless crystalline solid (1.22 g, 2.98 mmol, 81%).

^{1}H NMR (501 MHz, $CDCl_3$) δ 8.45 (s, 2H), 1.38 (s, 12H).

^{19}F NMR (471 MHz, $CDCl_3$) δ -54.92 (h, *J* = 15.9 Hz), -57.53 (q, *J* = 15.9 Hz).

HRMS (GC-EI) (m/z): calculated for $C_{15}H_{14}O_2BF_9$ $[M]^+$: 408.093767; found: 408.094440.

2-(3,5-bis(perfluoroethyl)-4-(trifluoromethyl)phenyl)-4,4,5,5-tetramethyl-1,3,2-dioxaborolane (4.42)

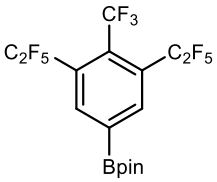

Preparation from 1,3-bis(perfluoroethyl)-2-(trifluoromethyl)benzene (**7.9**, 721.1 mg, 1.83 mmol, 1.0 equiv.) according to GP5 afforded the title compound as a colorless crystalline solid (916.0 mg, 1.80 mmol, 98%).

^{1}H NMR (501 MHz, $CDCl_3$) δ 8.31 (s, 2H), 1.37 (s, 12H).

^{13}C NMR (151 MHz, $CDCl_3$) δ 139.3 (t, *J* = 9.0 Hz), 134.2 (br s), 131.5 (q, *J* = 36.4 Hz), 130.1 (td, *J* = 24.8, 2.4 Hz), 121.5 (q, *J* = 275.1 Hz), 119.1 (qt, *J* = 287.7, 37.8 Hz), 114.1 (tq, *J* = 257.8, 39.3 Hz), 85.5, 25.0.

^{19}F NMR (471 MHz, $CDCl_3$) δ -52.77 (dqt, *J* = 32.8, 21.4, 10.9 Hz), -80.40 (q, *J* = 12.0 Hz), -100.37 (q, *J* = 21.1 Hz).

HRMS (GC-CI) (m/z): calculated for $C_{17}H_{14}O_2BF_{13}$ $[M+H]^+$: 508.087381; found: 508.088360.

4,4,5,5-tetramethyl-2-(4-(perfluoroethyl)-3,5-bis(trifluoromethyl)phenyl)-1,3,2-dioxaborolane (4.43)

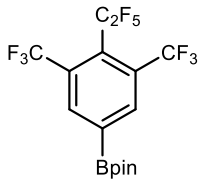

Preparation from 2-(perfluoroethyl)-1,3-bis(trifluoromethyl)benzene (**7.10**, 760.0 mg, 2.29 mmol, 1.0 equiv.) according to GP5 afforded the title compound as a colorless crystalline solid (715.4 mg, 1.56 mmol, 68%).

^{1}H NMR (300 MHz, $CDCl_3$) δ 8.48 (s, 2H), 1.38 (s, 12H).

^{19}F NMR (282 MHz, $CDCl_3$) δ -56.45 (dp, *J* = 29.6, 9.9 Hz), -73.84 (h, *J* = 9.9 Hz), -94.45 (h, *J* = 19.4 Hz).

HRMS (GC-EI) (m/z): calculated for $C_{16}H_{14}O_2BF_{11}$ $[M]^+$: 458.090573; found: 458.090530.

4,4,5,5-tetramethyl-2-(4-(perfluoropropyl)-3,5-bis(trifluoromethyl)phenyl)-1,3,2-dioxaborolane (4.44)

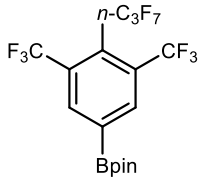

Preparation from 2-(perfluoropropyl)-1,3-bis(trifluoromethyl)benzene (**7.11**, 564.0 mg, 1.48 mmol, 1.0 equiv.) according to GP5 afforded the title compound as a colorless crystalline solid (676.4 mg, 1.33 mmol, 90%).

^{1}H NMR (300 MHz, $CDCl_3$) δ 8.56 (s, 2H), 1.38 (s, 12H).

^{19}F NMR (282 MHz, $CDCl_3$) δ -55.47 – -55.84 (m), -80.31 (dtq, *J* = 9.5, 6.3, 3.1 Hz), -98.16 – -98.80 (m), -118.41 – -118.86 (m).

HRMS (GC-EI) (m/z): calculated for $C_{17}H_{14}O_2BF_{13}$ $[M]^+$: 508.087380; found: 508.088190.

2-(4-fluoro-3,5-bis(perfluoroethyl)phenyl)-4,4,5,5-tetramethyl-1,3,2-dioxaborolane (7.16)

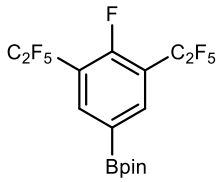

Preparation from 2-fluoro-1,3-bis(perfluoroethyl)benzene (**7.9**, 480.0 mg, 1.45 mmol, 1.0 equiv.) according to GP5 afforded the title compound as a white solid (466.2 mg, 1.02 mmol, 70%).

^{1}H NMR (600 MHz, $CDCl_3$) δ 8.20 (d, *J* = 6.8 Hz, 2H), 1.36 (s, 12H).

^{13}C{^{1}H} NMR (151 MHz, $CDCl_3$) δ 160.2 (dp, *J* = 272.6, 3.3 Hz), 139.6 (t, *J* = 7.1 Hz), 118.9 (qt, *J* = 285.8, 37.9 Hz), 117.9 (td, *J* = 24.5, 11.1 Hz), 112.4 (tq, *J* = 256.8, 40.3 Hz), 85.2, 25.0.

$^{13}C\{^{19}F\}$ NMR (151 MHz, $CDCl_3$) δ 160.2 (t, *J* = 9.7 Hz), 139.6 (dd, *J* = 167.3, 9.5 Hz), 119.0, 117.9, 112.5 – 112.3 (m), 85.2 (dt, *J* = 7.6, 4.0 Hz), 25.0 (qq, *J* = 126.8, 4.2 Hz).

^{19}F NMR (565 MHz, $CDCl_3$) δ -84.73 (dt, *J* = 11.6, 1.9 Hz), -107.67 (tdtt, *J* = 26.2, 20.0, 12.9, 8.0 Hz), -113.02 – -113.10 (m).

HRMS (APCI) (m/z): calculated for $C_{16}H_{15}BF_{11}O_2$ $[M+H]^+$: 459.09840; found: 459.09837.

7.3.2. *Synthesis of BINOLs*

General procedure 6 (GP6): Suzuki-Miyaura coupling of (*S*)-3,3'-diiodo-BINOL

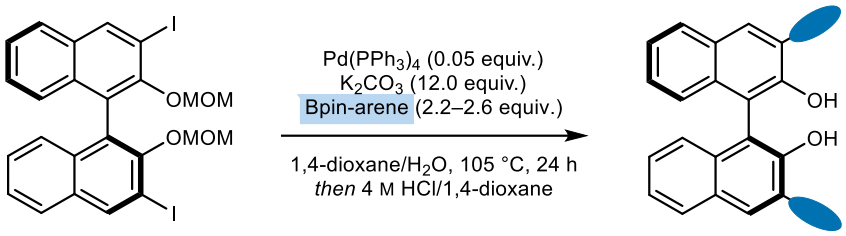

Following a modified procedure by List and coworkers.[274] In an oven-dried crimp cap vial, (*S*)-3,3'-diiodo-2,2'-bis(methoxymethoxy)-1,1'-binaphthalene (**4.37**, 1.0 equiv.), K_2CO_3 (12.0 equiv.) and the respective Bpin-arene (2.2–2.6 equiv.) were dissolved in 1,4-dioxane (0.1 M) and water (0.025 M). The mixture was then degassed by argon sparging for 10 minutes. $Pd(PPh_3)_4$ (0.05 equiv.) was added rapidly, the vessel was sealed and the reaction was stirred at 105 °C for 24 h. After monitoring by TLC (pentane/acetone, 9:1) indicated full conversion, the mixture was diluted with CH_2Cl_2 and water, transferred to an extraction funnel and extracted with CH_2Cl_2 (3x). The combined organic phases were washed with brine, dried over Na_2SO_4, filtered and concentrated in vacuo.

The crude residue was then dissolved in a minimal amount of CH_2Cl_2, HCl (4 M in 1,4-dioxane, 6.0 equiv.) was added and the mixture was stirred at 25 °C for 3 h. After monitoring by TLC (pentane/acetone, 9:1) indicated full conversion, the mixture was concentrated in vacuo. The crude residue was subjected to FCC to yield the corresponding (*S*)-BINOL.

(*S*)-3,3'-bis(3,5-bis(perfluoroethyl)phenyl)-[1,1'-binaphthalene]-2,2'-diol (7.17)

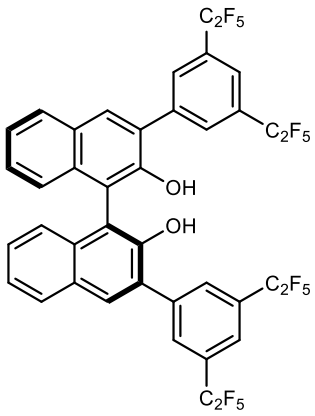

Preparation from 2-(3,5-bis(perfluoroethyl)phenyl)-4,4,5,5-tetramethyl-1,3,2-dioxaborolane (**7.14**, 913.6 mg, 2.08 mmol, 2.6 equiv.) according to GP6 afforded the title compound as a white solid (405.1 mg, 0.45 mmol, 56%) after FCC (hexanes/CH_2Cl_2, 4:1).

^{1}H NMR (600 MHz, $CDCl_3$) δ 8.23 (d, *J* = 1.7 Hz, 4H), 8.11 (s, 2H), 8.01 (ddd, *J* = 8.4, 1.2, 0.6 Hz, 2H), 7.85 (d, *J* = 1.7 Hz, 2H), 7.48 (ddd, *J* = 8.1, 6.8, 1.2 Hz, 2H), 7.43 (ddd, *J* = 8.2, 6.8, 1.3 Hz, 2H), 7.23 (ddt, *J* = 8.4, 1.3, 0.7 Hz, 2H), 5.40 (d, *J* = 0.7 Hz, 2H).

^{13}C{^{1}H} NMR (151 MHz, $CDCl_3$) δ 150.0, 139.6, 133.5, 132.6, 131.4 (t, *J* = 6.1 Hz), 130.1 (t, *J* = 24.5 Hz), 129.6, 129.1, 128.9, 127.7, 125.4, 124.1, 123.8 (p, *J* = 5.7 Hz), 119.0 (qt, *J* = 286.0, 38.7 Hz), 113.0 (tq, *J* = 254.8, 38.6 Hz), 111.9.

^{19}F NMR (565 MHz, $CDCl_3$) δ -84.55, -114.92.

HRMS (ESI) (m/z): calculated for $C_{40}H_{17}F_{20}O_2$ $[M-H]^-$: 909.091475; found: 909.092670.

$[\alpha]_D^{25}$ = 34.5 (c = 0.43, $CHCl_3$)

(*S*)-3,3'-bis(3,5-bis(1,1-difluoroethyl)phenyl)-[1,1'-binaphthalene]-2,2'-diol (4.39)

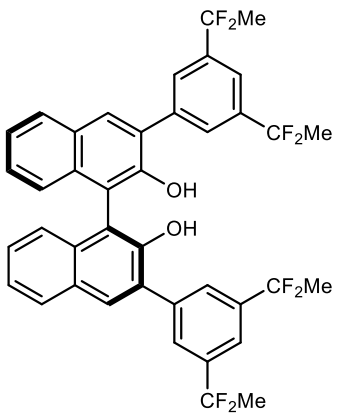

Preparation from 2-(3,5-bis(1,1-difluoroethyl)phenyl)-4,4,5,5-tetramethyl-1,3,2-dioxaborolane (**4.35**, 185.6 mg, 0.56 mmol, 2.3 equiv.) according to GP6 afforded the title compound as a white solid (92.3 mg, 0.13 mmol, 55%) after FCC (hexanes/CH_2Cl_2, 8:2).

^{1}H NMR (501 MHz, CD_2Cl_2) δ 8.11 (s, 2H), 8.02 – 7.96 (m, 6H), 7.69 (s, 2H), 7.45 (ddd, *J* = 8.1, 6.8, 1.2 Hz, 2H), 7.38 (ddd, *J* = 8.2, 6.8, 1.3 Hz, 2H), 7.21 (dd, *J* = 8.4, 1.1 Hz, 2H), 5.46 (s, 2H), 2.00 (t, *J* = 18.4 Hz, 12H).

^{13}C{^{1}H} NMR (126 MHz, CD_2Cl_2) δ 150.6, 139.3, 139.1, 139.1, 138.9, 133.7, 132.4, 130.0, 129.6, 129.1, 128.3, 127.9, 125.1, 124.4, 124.1, 122.2, 120.5, 120.5, 120.3, 112.5, 26.4, 26.2, 26.0.

^{19}F NMR (471 MHz, CD_2Cl_2) δ -87.74.

HRMS (ESI) (m/z): calculated for $C_{40}H_{29}F_8O_2$ $[M-H]^-$: 693.20453; found: 693.20487.

(*S*)-3,3'-bis(3,4,5-tris(trifluoromethyl)phenyl)-[1,1'-binaphthalene]-2,2'-diol (7.18)

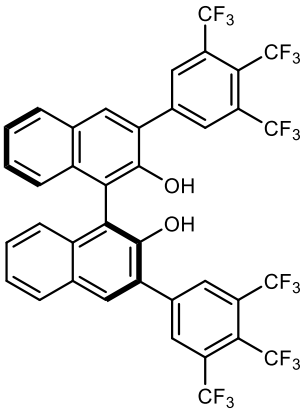

Preparation from 4,4,5,5-tetramethyl-2-(3,4,5-tris(trifluoromethyl)phenyl)-1,3,2-dioxaborolane (**7.15**, 630.0 mg, 1.54 mmol, 2.6 equiv.) according to GP6 afforded the title compound as a white solid (354.1 mg, 0.42 mmol, 70%) after FCC (hexanes/EtOAc, 9:1).

^{1}H NMR (501 MHz, $CDCl_3$) δ 8.49 (s, 4H), 8.15 (s, 2H), 8.05 – 8.01 (m, 2H), 7.51 (ddd, *J* = 8.2, 6.9, 1.3 Hz, 2H), 7.46 (ddd, *J* = 8.3, 6.9, 1.4 Hz, 2H), 7.23 (dd, *J* = 8.5, 1.1 Hz, 2H), 5.39 (d, *J* = 0.7 Hz, 2H).

^{19}F NMR (471 MHz, $CDCl_3$) δ -54.53 (h, *J* = 15.8 Hz), -57.53 (q, *J* = 15.8 Hz).

HRMS (ESI) (m/z): calculated for $C_{38}H_{15}F_{18}O_2$ $[M-H]^-$: 845.07901; found: 845.07972.

(*S*)-3,3'-bis(3,5-bis(perfluoroethyl)-4-(trifluoromethyl)phenyl)-[1,1'-binaphthalene]-2,2'-diol (7.19)

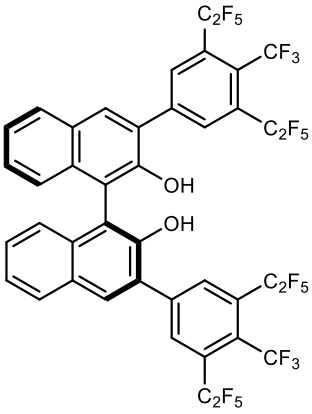

Preparation from 2-(3,5-bis(perfluoroethyl)-4-(trifluoromethyl)phenyl)-4,4,5,5-tetramethyl-1,3,2-dioxaborolane (**4.42**, 328.0 mg, 0.65 mmol, 2.4 equiv.) according to GP6 afforded the title compound as a white solid (179.0 mg, 0.17 mmol, 64%) after FCC (hexanes/CH_2Cl_2, 8:2).

^{1}H NMR (501 MHz, $CDCl_3$) δ 8.40 (s, 4H), 8.15 (s, 2H), 8.08 – 8.03 (m, 2H), 7.53 (ddd, *J* = 8.0, 6.8, 1.2 Hz, 2H), 7.47 (ddd, *J* = 8.3, 6.8, 1.3 Hz, 2H), 7.24 (d, *J* = 8.3 Hz, 2H), 5.42 (s, 2H).

^{19}F NMR (471 MHz, $CDCl_3$) δ -52.38 (dtp, *J* = 33.6, 22.4, 11.1 Hz), -80.42 (q, *J* = 11.9 Hz), -100.51 (q, *J* = 21.0 Hz).

HRMS (ESI) (m/z): calculated for $C_{42}H_{15}F_{26}O_2$ $[M-H]^-$: 1045.066246; found: 1045.066800.

(*S*)-3,3'-bis(4-(perfluoroethyl)-3,5-bis(trifluoromethyl)phenyl)-[1,1'-binaphthalene]-2,2'-diol (7.20)

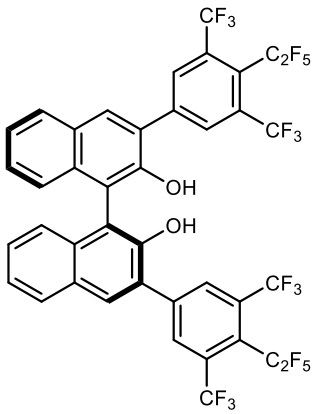

Preparation from 4,4,5,5-tetramethyl-2-(4-(perfluoroethyl)-3,5-bis(trifluoromethyl)phenyl)-1,3,2-dioxaborolane (**4.43**, 388.0 mg, 0.85 mmol, 2.3 equiv.) according to GP6 afforded the title compound as a white solid (185.9 mg, 0.20 mmol, 53%) after FCC (hexanes/CH_2Cl_2, 8:2).

^{1}H NMR (501 MHz, $CDCl_3$) δ 8.53 (s, 4H), 8.17 (s, 2H), 8.03 (d, *J* = 8.1 Hz, 2H), 7.51 (ddd, *J* = 8.2, 6.9, 1.3 Hz, 2H), 7.46 (ddd, *J* = 8.3, 6.8, 1.4 Hz, 2H), 7.23 (d, *J* = 8.4 Hz, 2H), 5.40 (s, 2H).

^{19}F NMR (471 MHz, $CDCl_3$) δ -56.43 (dp, *J* = 29.6, 10.1 Hz), -73.94 (h, *J* = 9.8 Hz), -94.35 (h, *J* = 19.5 Hz).

HRMS (ESI) (m/z): calculated for $C_{40}H_{15}F_{22}O_2$ $[M-H]^-$: 945.07262; found: 945.07365.

(*S*)-3,3'-bis(4-(perfluoropropyl)-3,5-bis(trifluoromethyl)phenyl)-[1,1'-binaphthalene]-2,2'-diol (7.21)

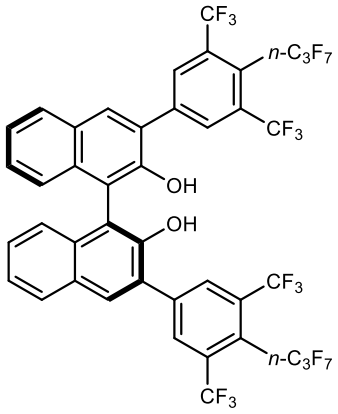

Preparation from 4,4,5,5-tetramethyl-2-(4-(perfluoropropyl)-3,5-bis(trifluoromethyl)phenyl)-1,3,2-dioxaborolane (**4.44**, 360.0 mg, 0.71 mmol, 2.4 equiv.) according to GP6 afforded the title compound as a white solid (199.6 mg, 0.19 mmol, 65%) after FCC (hexanes/CH_2Cl_2, 8:2).

^{1}H NMR (501 MHz, $CDCl_3$) δ 8.62 (s, 2H), 8.18 (s, 1H), 8.04 (d, *J* = 8.2 Hz, 1H), 7.55 – 7.48 (m, 1H), 7.46 (ddd, *J* = 8.2, 6.8, 1.4 Hz, 1H), 7.23 (d, *J* = 8.4 Hz, 1H), 5.41 (s, 1H).

^{19}F NMR (471 MHz, $CDCl_3$) δ -55.67 (p, *J* = 19.8 Hz), -80.29 (d, *J* = 10.6 Hz), -97.97, -118.52 (dq, *J* = 36.8, 18.8 Hz).

HRMS (ESI) (m/z): calculated for $C_{42}H_{15}F_{26}O_2$ $[M-H]^-$: 1045.06624; found: 1045.06767.

(*S*)-3,3'-bis(4-fluoro-3,5-bis(perfluoroethyl)phenyl)-[1,1'-binaphthalene]-2,2'-diol (4.52)

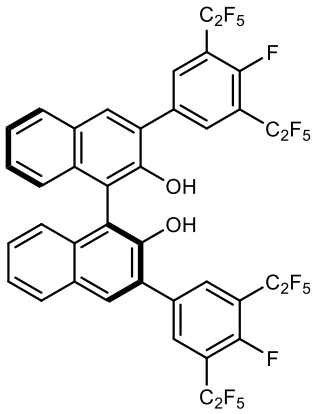

Preparation from 2-(4-fluoro-3,5-bis(perfluoroethyl)phenyl)-4,4,5,5-tetramethyl-1,3,2-dioxaborolane (**7.16**, 760.0 mg, 1.66 mmol, 2.2 equiv.) according to GP6 afforded the title compound as a white solid (612.0 mg, 0.65 mmol, 86%) after FCC (hexanes/EtOAc, 9:1).

^{1}H NMR (600 MHz, $CDCl_3$) δ 8.22 (d, *J* = 5.9 Hz, 4H), 8.09 (s, 2H), 8.04 – 7.99 (m, 2H), 7.50 (ddd, *J* = 8.1, 6.8, 1.2 Hz, 2H), 7.44 (ddd, *J* = 8.3, 6.8, 1.3 Hz, 2H), 7.23 (ddt, *J* = 8.4, 1.3, 0.7 Hz, 2H), 5.39 (br s, 2H).

^{13}C{^{1}H} NMR (151 MHz, $CDCl_3$) δ 157.6 (d, *J* = 267.6 Hz), 149.9, 134.7 (d, *J* = 4.6 Hz), 134.3 (t, *J* = 7.4 Hz), 133.4, 132.4, 129.6, 129.1, 129.0, 126.8, 125.5, 124.1, 119.0 (qt, *J* = 286.6, 37.9 Hz), 118.3 (td, *J* = 24.7, 11.9 Hz), 112.4 (tq, *J* = 258.2, 40.6 Hz), 111.9.

^{13}C{^{19}F} NMR (151 MHz, $CDCl_3$) δ 157.6 (t, *J* = 9.5 Hz), 149.9 (dd, *J* = 9.6, 3.0 Hz), 134.7 (d, *J* = 4.8 Hz), 134.3 (dd, *J* = 167.1, 7.8 Hz), 133.4 (q, *J* = 6.9 Hz), 132.4 (dd, *J* = 158.9, 5.1 Hz), 129.7 – 129.5 (m), 129.7 – 128.5 (m), 129.0 (dd, *J* = 160.8, 8.4 Hz), 126.8 (dq, *J* = 8.5, 4.2 Hz), 125.5 (dd, *J* = 161.9, 8.3 Hz), 124.1 (dd, *J* = 160.2, 7.1 Hz), 119.0, 118.3, 112.5 – 112.3 (m), 111.9 (d, *J* = 4.2 Hz).

^{19}F NMR (565 MHz, $CDCl_3$) δ -84.64 (d, *J* = 11.7 Hz), -113.04 (d, *J* = 20.9 Hz), -113.25 – -113.56 (m).

HRMS (ESI) (m/z): calculated for $C_{40}H_{15}F_{22}O_2$ $[M-H]^-$: 945.072632; found: 945.072900.

$[\alpha]_D^{25}$ = −32.6 (c = 0.47, $CHCl_3$)

(*S*)-3,3'-bis(3,5-bis(difluoro(phenyl)methyl)phenyl)-[1,1'-binaphthalene]-2,2'-diol (4.38)

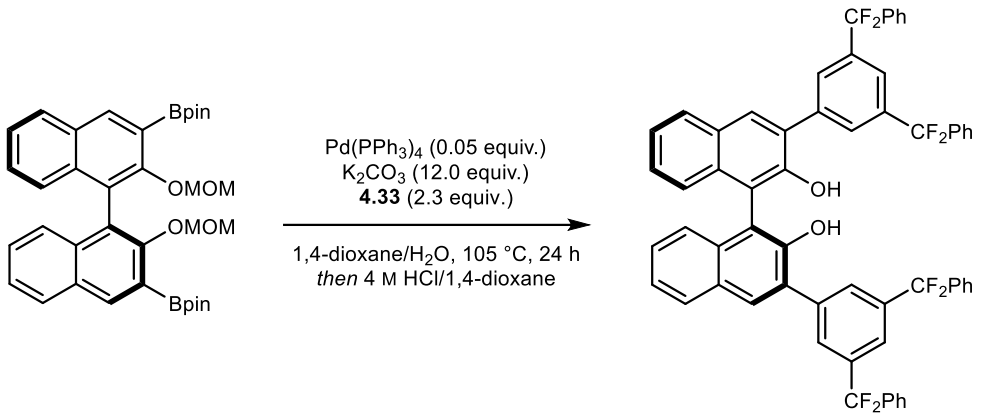

In an oven-dried crimp cap vial, (S)-2,2'-(2,2'-bis(methoxymethoxy)-[1,1'-binaphthalene]-3,3'-diyl)bis(4,4,5,5-tetramethyl-1,3,2-dioxaborolane) (**4.36**, 123.1 mg, 0.20 mmol, 1.0 equiv.), K_2CO_3 (326.0 mg, 2.36 mmol, 12.0 equiv.) and ((5-bromo-1,3-phenylene)bis(difluoromethylene))dibenzene (**4.33**, 185.0 mg, 0.45 mmol, 2.3 equiv.) were dissolved in 1,4-dioxane (2.5 mL) and water (0.6 mL). The mixture was then degassed by argon sparging for 10 minutes. $Pd(PPh_3)_4$ (11.4 mg, 9.8 µmol, 0.05 equiv.) was then added rapidly, the vessel was sealed and the reaction was stirred at 105 °C for 24 h. After monitoring by TLC (hexanes/EtOAc, 9:1) indicated full conversion, the mixture was diluted with CH_2Cl_2 and water, transferred to an extraction funnel and extracted with CH_2Cl_2 (3x). The combined organic phases were washed with brine, dried over Na_2SO_4, filtered and concentrated in vacuo. The crude residue was subjected to FCC (hexanes/EtOAc, 9:1) to afford the title compound as a white crystalline solid (155.6 mg, 0.17 mmol, 84%).

^{1}H NMR (501 MHz, $CDCl_3$) δ 8.11 (s, 6H), 8.00 (d, *J* = 8.1 Hz, 2H), 7.84 (s, 2H), 7.65 – 7.60 (m, 8H), 7.52 – 7.43 (m, 14H), 7.39 (t, *J* = 7.6 Hz, 2H), 7.26 (d, *J* = 8.4 Hz, 2H), 5.68 (br s, 2H).

^{19}F NMR (471 MHz, $CDCl_3$) δ -88.49.

HRMS (ESI) (m/z): calculated for $C_{60}H_{37}F_8O_2$ $[M-H]^-$: 941.26713; found: 941.26685.

(*S*)-4,4'-(2,2'-bis(methoxymethoxy)-[1,1'-binaphthalene]-3,3'-diyl)bis(2,6-bis(perfluoroethyl)aniline) (4.47)

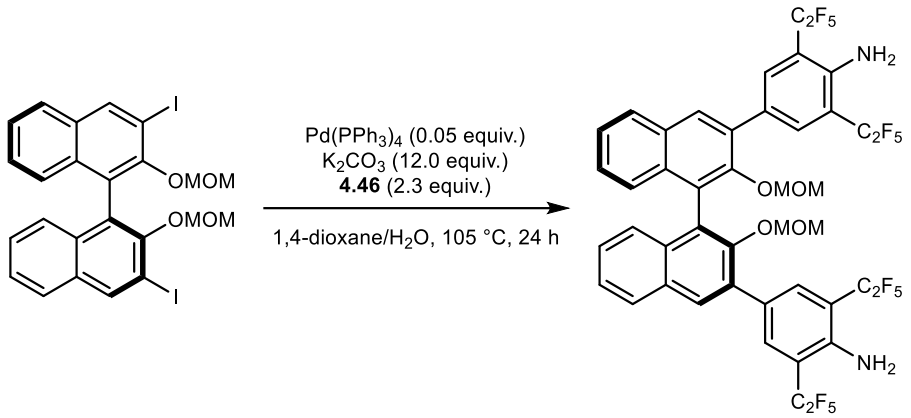

In an oven-dried crimp cap vial, (*S*)-3,3'-diiodo-2,2'-bis(methoxymethoxy)-1,1'-binaphthalene (**4.37**, 189.2 mg, 0.30 mmol, 1.0 equiv.), K_2CO_3 (500.1 mg, 3.63 mmol, 12.0 equiv.) and 2,6-bis(perfluoroethyl)-4-(4,4,5,5-tetramethyl-1,3,2-dioxaborolan-2-yl)aniline (**4.46**, 316.2 mg, 0.69 mmol, 2.3 equiv.) were dissolved in 1,4-dioxane (3.9 mL) and water (1.0 mL). The mixture was then degassed by argon sparging for 10 minutes. $Pd(PPh_3)_4$ (17.5 mg, 15.1 μmol, 0.05 equiv.) was then added rapidly, the vessel was sealed and the reaction was stirred at 105 °C for 24 h. After monitoring by TLC (hexanes/CH_2Cl_2, 3:2) indicated full conversion, the mixture was diluted with CH_2Cl_2 and water, transferred to an extraction funnel and extracted with CH_2Cl_2 (3x). The combined organic phases were washed with brine, dried over Na_2SO_4, filtered and concentrated in vacuo. The crude residue was subjected to FCC (hexanes/CH_2Cl_2, 3:2) to afford the title compound as a yellow solid (251.5 mg, 0.24 mmol, 81%).

^{1}H NMR (600 MHz, $CDCl_3$) δ 7.98 (s, 4H), 7.93 – 7.90 (m, 2H), 7.89 (d, *J* = 0.7 Hz, 2H), 7.45 (ddd, *J* = 8.1, 6.5, 1.5 Hz, 2H), 7.33 – 7.27 (m, 4H), 4.99 (br s, 4H), 4.38 (dd, *J* = 31.4, 5.8 Hz, 4H), 2.45 (s, 6H).

^{13}C{^{1}H} NMR (151 MHz, $CDCl_3$) δ 151.5, 144.0, 134.2 (t, *J* = 8.6 Hz), 133.8, 132.9, 131.0, 130.1, 128.1, 127.8, 126.9, 126.6, 126.5, 125.7, 119.6 (qt, *J* = 287.2, 39.4 Hz), 115.1 (tq, *J* = 254.5, 39.5 Hz), 113.1 (t, *J* = 21.8 Hz), 98.8, 56.1.

^{19}F NMR (565 MHz, $CDCl_3$) δ -84.12 (t, *J* = 2.5 Hz), -111.55 (d, *J* = 20.8 Hz).

HRMS (ESI) (m/z): calculated for $C_{44}H_{27}F_{20}N_2O_4$ $[M-H]^-$: 1027.165703; found: 1027.166230.

$[\alpha]_D^{25}$ = 117.4 (c = 0.45, $CHCl_3$)

(*S*)-3,3'-bis(4-iodo-3,5-bis(perfluoroethyl)phenyl)-[1,1'-binaphthalene]-2,2'-diol (4.48)

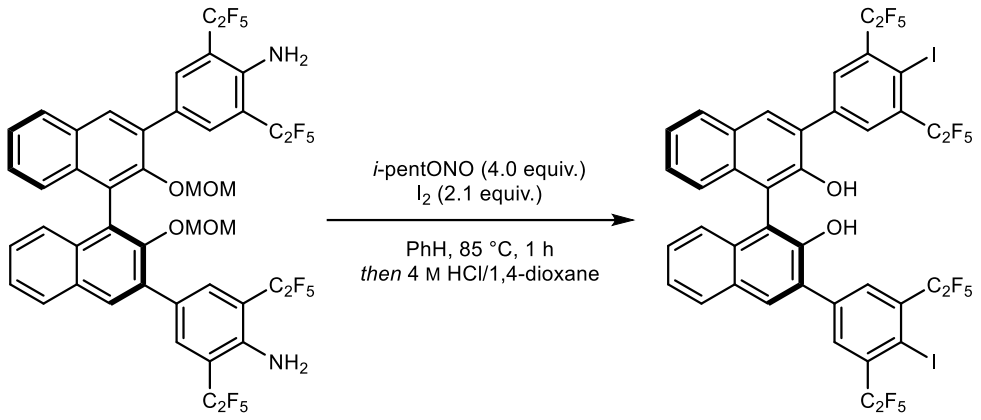

In a flame-dried Schlenk flask under an argon atmosphere, (*S*)-4,4'-(2,2'-bis(methoxymethoxy)-[1,1'-binaphthalene]-3,3'-diyl)bis(2,6-bis(perfluoroethyl)aniline) (**4.47**, 100.0 mg, 0.10 mmol, 1.0 equiv.) and dissolved in PhH (0.5 mL). I_2 (51.8 mg, 0.20 mmol, 2.1 equiv.) and *i*-pentylnitrite (45.6 mg, 0.39 mmol, 4.0 equiv.) were added and the reaction was stirred at 85 °C for 1 h. After monitoring by TLC (hexanes/CH_2Cl_2, 17:3) indicated full conversion, the reaction was quenched by the addition of a saturated $Na_2S_2O_3$ solution. The mixture was transferred to an extraction funnel and extracted with CH_2Cl_2 (3x). The combined organic phases were dried over Na_2SO_4, filtered, and concentrated in vacuo.

The crude residue was then dissolved in a minimal amount of CH_2Cl_2, HCl (4 M in 1,4-dioxane, 145.8 µL, 0.58 mmol, 6.0 equiv.) was added and the mixture was stirred at 25 °C for 3 h. After monitoring by TLC (hexanes/CH_2Cl_2, 17:3) indicated full conversion, the mixture was concentrated in vacuo. The crude residue was subjected to FCC (hexanes/CH_2Cl_2, 17:3) to afford the title compound as a pinkish solid (53.9 mg, 46.0 µmol, 48%).

^{1}H NMR (501 MHz, CD_2Cl_2) δ 8.20 (s, 4H), 8.13 (s, 2H), 8.02 (d, *J* = 8.1 Hz, 2H), 7.51 – 7.45 (m, 2H), 7.41 (ddd, *J* = 8.3, 6.8, 1.3 Hz, 2H), 7.19 (d, *J* = 8.4 Hz, 2H), 5.47 (s, 2H).

^{19}F NMR (471 MHz, CD_2Cl_2) δ -81.76, -105.87.

HRMS (ESI) (m/z): calculated for $C_{40}H_{15}F_{20}I_2O_4$ $[M-H]^-$: 1160.88476; found: 1160.88525.

(*S*)-3,3'-bis(4-bromo-3,5-bis(perfluoroethyl)phenyl)-[1,1'-binaphthalene]-2,2'-diol (4.49)

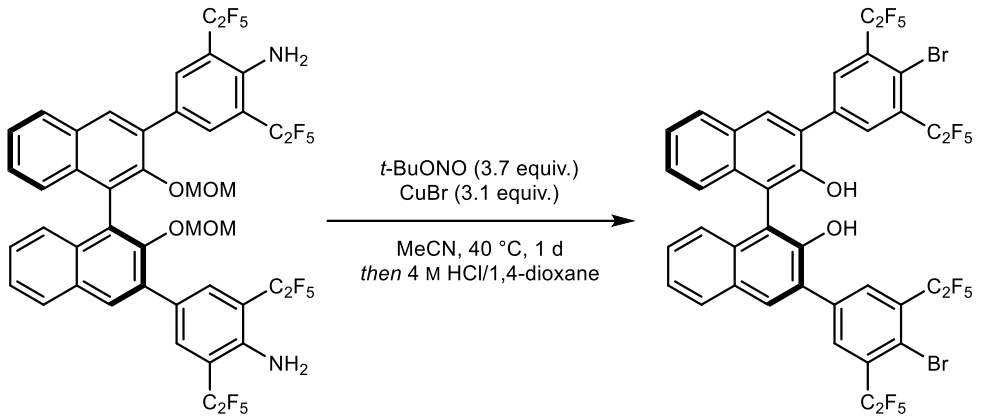

In a flame-dried Schlenk flask under an argon atmosphere, (*S*)-4,4'-(2,2'-bis(methoxymethoxy)-[1,1'-binaphthalene]-3,3'-diyl)bis(2,6-bis(perfluoroethyl)aniline) (**4.47**, 50.0 mg, 48.6 µmol, 1.0 equiv.) and CuBr (21.4 mg, 0.15 mmol, 3.1 equiv.) were dissolved in MeCN (0.6 mL). *t*-Butylnitrite (18.4 mg, 0.18 mmol, 3.7 equiv.) was added and the reaction was stirred at 40 °C for 1 d. After monitoring by TLC (hexanes/CH_2Cl_2, 17:3) indicated full conversion, the mixture was concentrated in vacuo.

The crude residue was then dissolved in a minimal amount of CH_2Cl_2, HCl (4 M in 1,4-dioxane, 72.9 µL, 0.29 mmol, 6.0 equiv.) was added and the mixture was stirred at 25 °C for 3 h. After monitoring by TLC (hexanes/CH_2Cl_2, 17:3) indicated full conversion, the mixture was concentrated in vacuo. The crude residue was subjected to FCC (hexanes/CH_2Cl_2, 17:3) to afford the title compound as a light yellow solid (20.3 mg, 19.0 µmol, 39%).

^{1}H NMR (501 MHz, $CDCl_3$) δ 8.24 (s, 4H), 8.08 (s, 2H), 8.01 (d, *J* = 8.0 Hz, 2H), 7.51 – 7.47 (m, 2H), 7.43 (ddd, *J* = 8.3, 6.8, 1.3 Hz, 2H), 7.21 (d, *J* = 8.4 Hz, 2H), 5.37 (s, 2H).

^{19}F NMR (471 MHz, $CDCl_3$) δ -82.12, -107.75.

(*S*)-3,3'-bis(4-chloro-3,5-bis(perfluoroethyl)phenyl)-[1,1'-binaphthalene]-2,2'-diol (4.50)

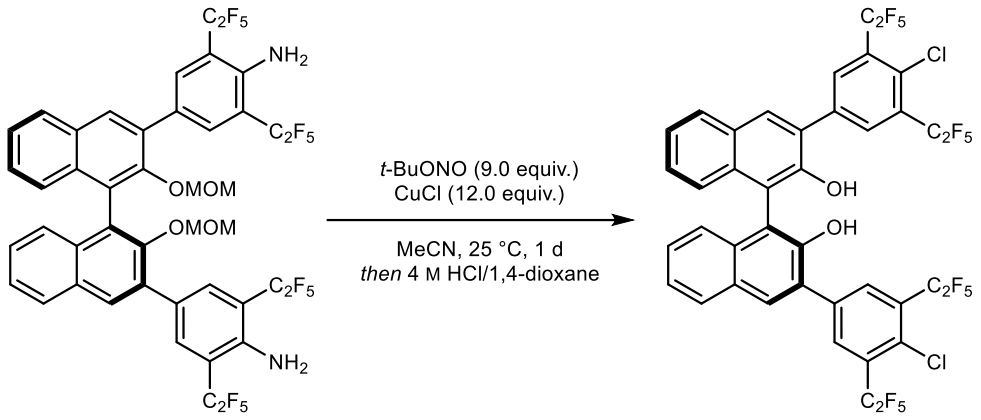

In a flame-dried Schlenk flask under an argon atmosphere, (*S*)-4,4'-(2,2'-bis(methoxymethoxy)-[1,1'-binaphthalene]-3,3'-diyl)bis(2,6-bis(perfluoroethyl)aniline) (**4.47**, 222.4 mg, 0.22 mmol, 1.0 equiv.) and CuCl (256.8 mg, 2.59 mmol, 12.0 equiv.) were dissolved in MeCN (5.7 mL). *t*-Butylnitrite (200.7 mg, 1.95 mmol, 9.0 equiv.) was added and the reaction was stirred at 25 °C for 1 d. After monitoring by TLC (hexanes/CH_2Cl_2, 17:3) indicated full conversion, 1.0 M HCl was added to quench the reaction, the mixture was transferred to an extraction funnel and extracted with CH_2Cl_2 (3x). The combined organic phases were dried over Na_2SO_4, filtered, and concentrated in vacuo.

The crude residue was then dissolved in a minimal amount of CH_2Cl_2, HCl (4 M in 1,4-dioxane, 324.3 µL, 1.30 mmol, 6.0 equiv.) was added and the mixture was stirred at 25 °C for 3 h. After monitoring by TLC (hexanes/CH_2Cl_2, 17:3) indicated full conversion, the mixture was concentrated in vacuo. The crude residue was subjected to FCC (hexanes/CH_2Cl_2, 17:3) to afford the title compound as a white solid (131.8 mg, 135.0 µmol, 62%).

^{1}H NMR (600 MHz, $CDCl_3$) δ 8.26 (s, 2H), 8.08 (s, 1H), 8.01 (ddd, *J* = 8.4, 1.2, 0.5 Hz, 1H), 7.49 (ddd, *J* = 8.1, 6.9, 1.2 Hz, 1H), 7.43 (ddd, *J* = 8.3, 6.8, 1.3 Hz, 1H), 7.21 (ddt, *J* = 8.4, 1.3, 0.7 Hz, 1H), 5.37 (d, *J* = 0.7 Hz, 1H).

^{13}C{^{1}H} NMR (151 MHz, $CDCl_3$) δ 149.9, 137.0, 134.6 (t, *J* = 9.0 Hz), 133.5, 132.4, 132.1 (p, *J* = 2.1 Hz), 129.6, 129.3 (t, *J* = 22.8 Hz), 129.1, 129.0, 126.8, 125.5, 124.1, 119.2 (qt, *J* = 287.5, 38.0 Hz), 113.3 (tq, *J* = 257.8, 40.3 Hz), 111.9.

^{19}F NMR (565 MHz, $CDCl_3$) δ -82.69, -109.26.

HRMS (ESI) (m/z): calculated for $C_{40}H_{15}Cl_2F_{20}O_2$ $[M-H]^-$: 977.013531; found: 977.013830.

$[\alpha]_D^{25} = -15.5$ (c = 0.18, $CHCl_3$)

7.3.3. *Synthesis of IDPis*

General procedure 7 (GP7): Synthesis of (*S*,*S*)-IDPi catalysts

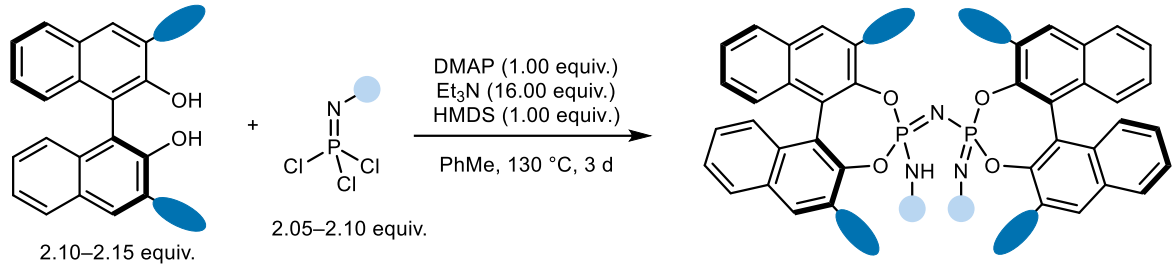

Following a modified procedure by List and coworkers.[274] In a flame-dried J Young Schlenk flask under an argon atmosphere, the respective (*S*)-BINOL (2.10–2.15 equiv.) and DMAP (1.00 equiv.) were loaded. The flask was then put under vacuum (3.4×10^{-2} mbar) and heated in an oil bath at 80 °C for 2 h. The flask was then flushed with argon, after which toluene (0.05 M) was added. The respective phosphazene reagent (2.05–2.10 equiv.) was then added in one portion, followed by anhydrous Et_3N (16.00 equiv.), and the reaction was stirred at 25 °C for 30 minutes. HMDS (1.00 equiv.) was then added, the flask was sealed, and the reaction was stirred at the same temperature for 1 h and then at 130 °C for 3 d. After monitoring by TLC (CH_2Cl_2) indicated full conversion, 1.0 M HCl was added to quench the reaction. The mixture was transferred to an extraction funnel and extracted with CH_2Cl_2 (3x). The combined organic phases were dried over Na_2SO_4, filtered, and concentrated in vacuo. The crude residue was purified by column chromatography (hexanes/CH_2Cl_2, 100:0–0:100).

Acidification of the above obtained IDPi salts was performed by dissolving the salt in a minimal amount of Et_2O and performing slow gravity filtration (3x) over pre-acidified Dowex 50W X8 resin suspended in Et_2O, followed by washing of the resin with Et_2O. The filtrate was then concentrated in vacuo, and acidification was confirmed by ^{1}H- and ^{31}P NMR, yielding the corresponding (*S*,*S*)-IDPis **3** as off-white to yellow solids.

Note 1: Pre-acidification of the resin was performed by washing the commercial solid successively with 0.5 M H_2SO_4, 0.05 M H_2SO_4, water, EtOH, CH_2Cl_2, and Et_2O. The resin may be dried and stored for later use.

Note 2: Acidification using previously reported methods, such as extraction from 6 M HCl or DOWEX 50W X8 filtration in CH_2Cl_2 did not yield fully acidified IDPi catalysts in the case of 3,3'-p-X substituents. We speculate that intimate ion pairing in the IDPi triethylammonium salt obtained after FCC obstructs the acidification of very acidic catalysts. We overcame this issue by using a more polar solvent such as Et_2O during acidification with DOWEX 50W X8.

(*S*,*S*)-IDPi 4.3k

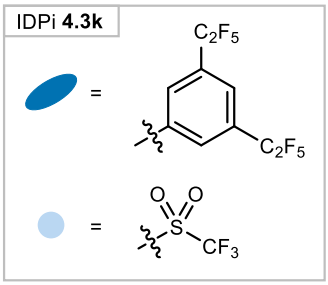

Preparation from (*S*)-3,3'-bis(3,5-bis(perfluoroethyl)phenyl)-[1,1'-binaphthalene]-2,2'-diol (**7.17**, 99.0 mg, 108.7 µmol, 2.1 equiv.) and ((trifluoromethyl)sulfonyl)phosphorimidoyl trichloride (**4.40a**, 30.9 mg, 108.7 µmol, 2.1 equiv.) according to GP7 afforded the title compound as a white solid (77.0 mg, 35 µmol, 68%).

^{1}H NMR (501 MHz, CD_2Cl_2) δ 8.20 (s, 2H), 8.14 (d, *J* = 8.3 Hz, 2H), 7.96 – 7.89 (m, 4H), 7.81 (s, 4H), 7.77 – 7.70 (m, 8H), 7.68 – 7.61 (m, 2H), 7.43 – 7.35 (m, 6H), 7.15 (d, *J* = 8.6 Hz, 2H), 6.61 (s, 2H).

^{13}C{^{1}H} NMR (151 MHz, CD_2Cl_2) δ 144.2, 144.2, 144.2, 142.0, 142.0, 142.0, 138.9, 138.7, 138.5, 133.8, 132.6, 132.6, 132.5, 132.3, 132.3, 131.7, 131.7, 131.6, 131.2, 130.9, 130.9, 130.9, 130.7, 130.6, 130.5, 130.4, 130.3, 130.3, 130.1, 129.5, 129.1, 128.2, 127.5, 127.2, 127.1, 125.0, 124.7, 123.8, 123.8, 123.8, 122.3, 122.1, 122.0, 121.8, 121.6, 120.4, 120.2, 120.2, 119.9, 119.7, 118.5, 118.3, 118.1, 118.0, 117.8, 116.6, 116.4, 116.1, 116.0, 115.9, 115.0, 114.9, 114.8, 114.6, 114.5, 114.4, 114.3, 113.4, 113.3, 113.2, 113.1, 112.9, 112.8, 112.7, 112.6, 111.7, 111.6, 111.5, 111.4, 111.2, 111.1, 111.0, 110.9.

^{19}F NMR (471 MHz, CD_2Cl_2) δ -79.40, -85.08 (d, *J* = 9.5 Hz), -114.46 – -117.15 (m).

^{31}P NMR (203 MHz, CD_2Cl_2) δ -15.19.

HRMS (ESI) (m/z): calculated for $C_{82}H_{32}F_{46}N_3O_8P_2S_2$ $[M-H]^-$: 2186.037726; found: 2186.037570.

$[\alpha]_D^{25}$ = 211.2 (c = 0.43, $CHCl_3$)

(*S*,*S*)-IDPi 4.3l

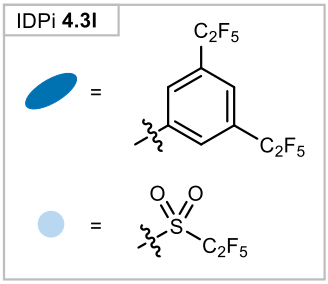

Preparation from (*S*)-3,3'-bis(3,5-bis(perfluoroethyl)phenyl)-[1,1'-binaphthalene]-2,2'-diol (**7.17**, 90.0 mg, 98.8 µmol, 2.1 equiv.) and ((perfluoroethyl)sulfonyl)phosphorimidoyl trichloride (**4.40b**, 33.1 mg, 98.8 µmol, 2.1 equiv.) according to GP7 afforded the title compound as a white solid (30.0 mg, 13 µmol, 28%).

^{1}H NMR (500 MHz, CD_2Cl_2) δ 8.13 – 8.07 (m, 4H), 7.87 (dd, *J* = 4.5, 1.3 Hz, 4H), 7.76 (d, *J* = 1.6 Hz, 4H), 7.75 – 7.70 (m, 6H), 7.69 – 7.64 (m, 2H), 7.63 – 7.57 (m, 2H), 7.39 (d, *J* = 1.6 Hz, 4H), 7.35 (ddd, *J* = 8.3, 6.8, 1.3 Hz, 2H), 7.18 (d, *J* = 8.6 Hz, 2H), 6.54 (s, 2H).

^{19}F NMR (471 MHz, CD_2Cl_2) δ -79.42, -85.08, -114.68 – -117.23 (m).

^{31}P NMR (243 MHz, CD_2Cl_2) δ -9.22.

HRMS (ESI) (m/z): calculated for $C_{84}H_{32}F_{50}N_3O_8P_2S_2$ $[M-H]^-$: 2286.031340; found: 2286.031040.

(*S*,*S*)-IDPi 4.3m

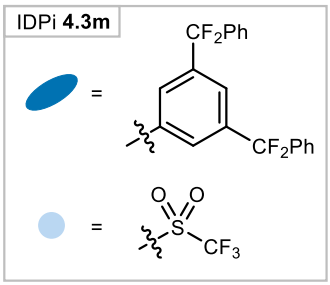

Preparation from (S)-3,3'-bis(3,5-bis(difluoro(phenyl)methyl)phenyl)-[1,1'-binaphthalene]-2,2'-diol (**4.38**, 55.8 mg, 59.2 µmol, 2.10 equiv.) and ((trifluoromethyl)sulfonyl)phosphorimidoyl trichloride (**4.40a**, 16.8 mg, 59.2 µmol, 2.10 equiv.) according to GP7 afforded the title compound as a light brown solid (10.3 mg, 5 µmol, 16%).

^{1}H NMR (501 MHz, CD_2Cl_2) δ 8.15 (s, 2H), 8.05 (d, *J* = 8.3 Hz, 2H), 7.85 (q, *J* = 3.0 Hz, 6H), 7.78 (t, *J* = 7.5 Hz, 2H), 7.67 (d, *J* = 8.5 Hz, 2H), 7.54 (ddd, *J* = 8.1, 6.8, 1.1 Hz, 2H), 7.51 – 7.37 (m, 18H), 7.35 – 7.15 (m, 34H), 7.04 (d, *J* = 8.7 Hz, 2H), 6.53 (s, 2H).

^{19}F NMR (471 MHz, CD_2Cl_2) δ -78.30, -78.56, -78.84, -86.60, -87.15, -87.46 – -88.77 (m), -89.13.

^{31}P NMR (203 MHz, CD_2Cl_2) δ -16.21.

HRMS (ESI) (m/z): calculated for $C_{122}H_{72}F_{22}N_3O_8P_2S_2$ $[M-H]^-$: 2250.38903; found: 2250.39034.

Note: the catalyst was found to decompose upon storage under atmospheric conditions over ~1 week.

(*S*,*S*)-IDPi 4.3n

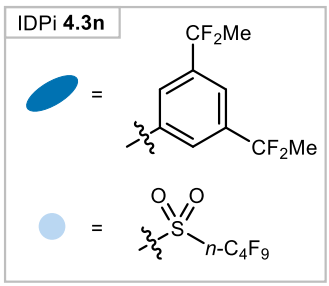

Preparation from (S)-3,3'-bis(3,5-bis(1,1-difluoroethyl)phenyl)-[1,1'-binaphthalene]-2,2'-diol (**4.39**, 70.0 mg, 100.8 µmol, 2.10 equiv.) and ((perfluorobutyl)sulfonyl)phosphorimidoyl trichloride (**4.40d**, 43.8 mg, 100.8 µmol, 2.10 equiv.) according to GP7 afforded the title compound as a light brown solid (60.1 mg, 29 µmol, 61%).

^{1}H NMR (501 MHz, CD_2Cl_2) δ 8.13 (s, 2H), 8.09 (d, *J* = 8.3 Hz, 2H), 7.95 – 7.85 (m, 4H), 7.80 (d, *J* = 8.6 Hz, 2H), 7.67 (ddd, *J* = 8.4, 6.6, 1.4 Hz, 2H), 7.63 – 7.55 (m, 6H), 7.53 (d, *J* = 10.1 Hz, 6H), 7.34 (ddd, *J* = 8.4, 6.8, 1.3 Hz, 2H), 7.13 (d, *J* = 14.2 Hz, 6H), 6.59 (s, 2H), 1.80 (t, *J* = 18.3 Hz, 12H), 1.77 (t, *J* = 18.4 Hz, 12H).

^{19}F NMR (471 MHz, CD_2Cl_2) δ -81.25 (t, *J* = 10.2 Hz), -85.07, -85.60, -87.19, -88.06 (dd, *J* = 256.6, 64.0 Hz), -88.79, -112.68 (q, *J* = 260.9 Hz), -120.92 (d, *J* = 11.7 Hz), -125.39, -126.09 (dt, *J* = 69.0, 12.5 Hz), -126.79.

^{31}P NMR (203 MHz, CD_2Cl_2) δ -16.00.

HRMS (ESI) (m/z): calculated for $C_{88}H_{56}F_{34}N_3O_8P_2S_2$ $[M-H]^-$: 2054.244684; found: 2054.244680.

Note: the catalyst was found to decompose upon storage under atmospheric conditions over ~1 month.

(*S*,*S*)-IDPi 4.3o

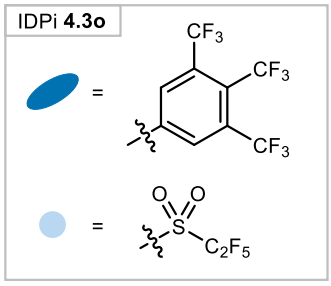

Preparation from (S)-3,3'-bis(3,4,5-tris(trifluoromethyl)phenyl)-[1,1'-binaphthalene]-2,2'-diol (**7.18**, 120.0 mg, 120.5 µmol, 2.10 equiv.) and ((perfluoroethyl)sulfonyl)phosphorimidoyl trichloride (**4.40b**, 40.3 mg, 120.5 µmol, 2.10 equiv.) according to GP7 afforded the title compound as a light yellow solid (58.1 mg, 27 µmol, 47%).

^{1}H NMR (501 MHz, CD_2Cl_2) δ 8.20 (d, *J* = 5.9 Hz, 2H), 8.13 (d, *J* = 8.3 Hz, 2H), 8.02 (s, 4H), 7.89 (dt, *J* = 13.6, 7.6 Hz, 4H), 7.79 – 7.60 (m, 10H), 7.39 (t, *J* = 7.8 Hz, 2H), 7.16 (d, *J* = 8.6 Hz, 2H), 6.72 (s, 2H).

^{19}F NMR (471 MHz, CD_2Cl_2) δ -54.72 – -55.13 (m), -57.54 (q, *J* = 16.1 Hz), -58.46 (q, *J* = 16.8 Hz), -79.65, -117.68.

^{31}P NMR (203 MHz, CD_2Cl_2) δ -12.08.

HRMS (ESI) (m/z): calculated for $C_{80}H_{28}F_{46}N_3O_8P_2S_2$ $[M-H]^-$: 2158.006426; found: 2158.005840.

(*S*,*S*)-IDPi 4.3p

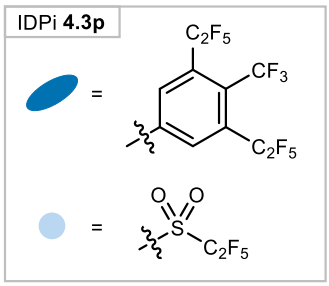

Preparation from (S)-3,3'-bis(3,5-bis(perfluoroethyl)-4-(trifluoromethyl)phenyl)-[1,1'-binaphthalene]-2,2'-diol (**7.19**, 140.0 mg, 133.8 µmol, 2.10 equiv.) and ((perfluoroethyl)sulfonyl)phosphorimidoyl trichloride (**4.40b**, 44.7 mg, 133.8 µmol, 2.10 equiv.) according to GP7 afforded the title compound as a white solid (91.5 mg, 36 µmol, 56%).

^{1}H NMR (501 MHz, CD_2Cl_2) δ 8.10 – 8.04 (m, 4H), 7.96 (s, 4H), 7.84 – 7.74 (m, 4H), 7.66 – 7.55 (m, 6H), 7.51 (s, 4H), 7.32 (ddd, *J* = 8.3, 6.8, 1.3 Hz, 2H), 7.06 (d, *J* = 8.6 Hz, 2H), 6.59 (s, 2H).

^{19}F NMR (471 MHz, $CDCl_3$) δ -52.07 – -52.70 (m), -79.40 (q, *J* = 13.7 Hz), -79.64, -81.10 (q, *J* = 12.1 Hz), -100.31, -101.29, -101.78 – -101.98 (m), -102.56, -117.46, -118.06 (d, *J* = 41.2 Hz), -118.65.

^{31}P NMR (203 MHz, $CDCl_3$) δ -7.87.

HRMS (ESI) (m/z): calculated for $C_{88}H_{28}F_{62}N_3O_8P_2S_2$ $[M-H]^-$: 2557.980882; found: 2557.983120.

(*S*,*S*)-IDPi 4.3q

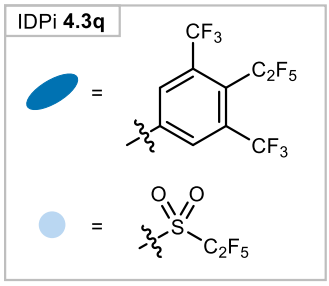

Preparation from (S)-3,3'-bis(4-(perfluoroethyl)-3,5-bis(trifluoromethyl)phenyl)-[1,1'-binaphthalene]-2,2'-diol (**7.20**, 117.4 mg, 124.1 µmol, 2.10 equiv.) and ((perfluoroethyl)sulfonyl)phosphorimidoyl trichloride (**4.40b**, 41.5 mg, 124.1 µmol, 2.10 equiv.) according to GP7 afforded the title compound as a white solid (85.1 mg, 36 µmol, 61%).

^{1}H NMR (501 MHz, CD_2Cl_2) δ 8.20 (s, 2H), 8.16 – 8.01 (m, 6H), 7.91 (ddd, *J* = 8.0, 5.8, 2.0 Hz, 2H), 7.86 (d, *J* = 8.1 Hz, 2H), 7.78 – 7.70 (m, 8H), 7.65 (t, *J* = 7.5 Hz, 2H), 7.39 (ddd, *J* = 8.3, 6.7, 1.3 Hz, 2H), 7.14 (d, *J* = 8.6 Hz, 2H), 6.72 (s, 2H).

^{19}F NMR (471 MHz, CD_2Cl_2) δ -55.75 – -57.65 (m), -74.44 – -74.85 (m), -79.61, -94.63 – -96.85 (m), -116.67 – -118.57 (m).

^{31}P NMR (203 MHz, CD_2Cl_2) δ -11.90.

HRMS (ESI) (m/z): calculated for $C_{84}H_{28}F_{54}N_3O_8P_2S_2$ $[M-H]^-$: 2357.993654; found: 2357.995470.

(*S*,*S*)-IDPi 4.3r

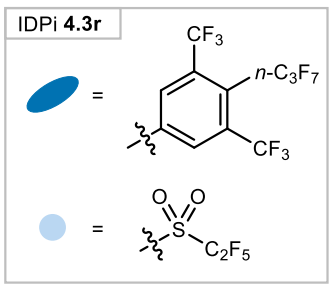

Preparation from (S)-3,3'-bis(4-(perfluoropropyl)-3,5-bis(trifluoromethyl)phenyl)-[1,1'-binaphthalene]-2,2'-diol (**7.21**, 108.3 mg, 103.5 µmol, 2.10 equiv.) and ((perfluoroethyl)sulfonyl)phosphorimidoyl trichloride (**4.40b**, 34.6 mg, 103.5 µmol, 2.10 equiv.) according to GP7 afforded the title compound as a white solid (82.8 mg, 32 µmol, 66%).

^{1}H NMR (501 MHz, CD_2Cl_2) δ 8.25 (s, 2H), 8.15 (d, *J* = 7.9 Hz, 2H), 8.33 – 8.02 (m, 6H), 7.93 (ddd, *J* = 8.1, 6.2, 1.7 Hz, 2H), 7.87 – 7.73 (m, 8H), 7.66 (ddd, *J* = 8.1, 6.8, 1.0 Hz, 2H), 7.41 (ddd, *J* = 8.4, 6.8, 1.3 Hz, 2H), 7.16 (d, *J* = 8.7 Hz, 2H), 6.70 (s, 2H).

^{19}F NMR (471 MHz, CD_2Cl_2) δ -54.12 – -57.02 (m), -79.65, -80.86 (dt, *J* = 40.3, 10.4 Hz), -97.53 – -99.96 (m), -117.63 (d, *J* = 34.6 Hz), -118.95 (dq, *J* = 42.3, 21.1 Hz).

^{31}P NMR (203 MHz, CD_2Cl_2) δ -12.52.

HRMS (ESI) (m/z): calculated for $C_{88}H_{28}F_{62}N_3O_8P_2S_2$ $[M-H]^-$: 2557.98085; found: 2557.98143.

(*S*,*S*)-IDPi 4.3s

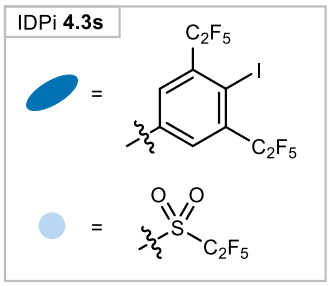

Preparation from (S)-3,3'-bis(4-iodo-3,5-bis(perfluoroethyl)phenyl)-[1,1'-binaphthalene]-2,2'-diol (**4.48**, 53.9 mg, 46.4 µmol, 2.10 equiv.) and ((perfluoroethyl)sulfonyl)phosphorimidoyl trichloride (**4.40b**, 15.5 mg, 46.4 µmol, 2.10 equiv.) according to GP7 afforded the title compound as a brown solid (14.8 mg, 5 µmol, 12%).

^{1}H NMR (501 MHz, CD_2Cl_2) δ 8.19 – 8.07 (m, 4H), 7.94 – 7.79 (m, 4H), 7.76 – 7.56 (m, 10H), 7.39 – 7.30 (m, 4H), 7.28 (s, 2H), 7.05 (d, *J* = 8.6 Hz, 2H), 6.49 (s, 2H).

^{19}F NMR (471 MHz, CD_2Cl_2) δ -78.88 – -79.80 (m), -80.77 – -82.17 (m), -105.06 – -107.76 (m), -115.25 – -118.76 (m).

^{31}P NMR (203 MHz, CD_2Cl_2) δ -14.05.

Note: the catalyst was found to decompose upon storage under atmospheric conditions over ~1 week.

(*S*,*S*)-IDPi 4.3t

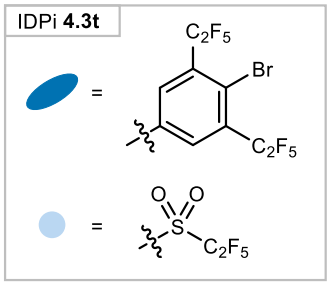

Preparation from (S)-3,3'-bis(4-bromo-3,5-bis(perfluoroethyl)phenyl)-[1,1'-binaphthalene]-2,2'-diol (**4.49**, 20.0 mg, 18.7 µmol, 2.10 equiv.) and ((perfluoroethyl)sulfonyl)phosphorimidoyl trichloride (**4.40b**, 6.3 mg, 18.7 µmol, 2.10 equiv.) according to GP7 afforded the title compound as a brown solid (3.3 mg, 1.3 µmol, 14%).

^{1}H NMR (501 MHz, $CDCl_3$) δ 8.10 – 8.04 (m, 4H), 7.83 (d, *J* = 4.0 Hz, 4H), 7.71 (d, *J* = 11.4 Hz, 6H), 7.59 (t, *J* = 7.6 Hz, 2H), 7.36 (t, *J* = 7.8 Hz, 2H), 7.29 (s, 4H), 7.10 (d, *J* = 8.0 Hz, 4H), 6.46 (s, 2H).

^{19}F NMR (471 MHz, $CDCl_3$) δ -79.15, -81.65, -81.81, -107.70, -109.06, -117.25.

^{31}P NMR (203 MHz, $CDCl_3$) δ -11.99.

HRMS (ESI) (m/z): calculated for $C_{84}H_{28}F_{50}N_3O_8P_2S_2Br_4$ $[M-H]^-$: 2597.673441; found: 2597.670900.

Note: the catalyst was found to decompose upon storage under atmospheric conditions over ~1 month.

(*S*,*S*)-IDPi 4.3u

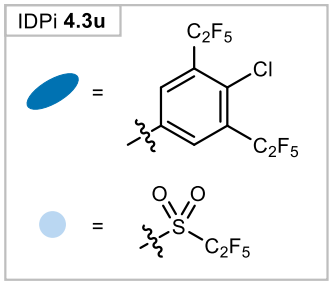

Preparation from (*S*)-3,3'-bis(4-chloro-3,5-bis(perfluoroethyl)phenyl)-[1,1'-binaphthalene]-2,2'-diol (**4.50**, 101.5 mg, 103.6 µmol, 2.1 equiv.) and ((perfluoroethyl)sulfonyl)phosphorimidoyl trichloride (**4.40b**, 34.7 mg, 103.6 µmol, 2.1 equiv.) according to GP7 afforded the title compound as an off-white solid (41.9 mg, 17.3 µmol, 35%).

^{1}H NMR (600 MHz, CD_2Cl_2) δ 8.15 (s, 2H), 8.13 – 8.11 (m, 2H), 7.95 – 7.86 (m, 4H), 7.79 (s, 4H), 7.74 – 7.67 (m, 4H), 7.64 (ddd, *J* = 8.1, 6.8, 1.1 Hz, 2H), 7.42 – 7.35 (m, 6H), 7.12 (dd, *J* = 8.7, 1.0 Hz, 2H), 6.53 (s, 2H).

^{13}C{^{1}H} NMR (151 MHz, CD_2Cl_2) δ 144.0, 144.0, 144.0, 141.9, 141.9, 141.9, 136.4, 136.0, 135.0, 134.9, 134.9, 134.3, 133.7, 133.5, 133.0, 132.6, 132.5, 132.3, 132.2, 131.4, 130.6, 130.0,

129.8, 129.6, 129.5, 129.2, 128.4, 127.6, 127.6, 127.1, 123.9, 123.9, 123.8, 122.6, 122.3, 122.2, 122.1, 121.8, 120.7, 120.4, 120.4, 120.4, 120.2, 120.2, 119.9, 118.8, 118.7, 118.5, 118.5, 118.4, 118.3, 118.2, 118.0, 116.8, 116.8, 116.6, 116.5, 116.4, 116.3, 116.1, 115.4, 115.3, 115.1, 115.1, 114.9, 114.8, 114.6, 114.5, 114.4, 113.9, 113.7, 113.6, 113.4, 113.4, 113.2, 113.1, 112.9, 112.8, 112.0, 111.9, 111.7, 111.6, 111.5, 111.4, 111.2, 111.1, 110.0, 109.7, 109.4, 109.2.

^{19}F NMR (565 MHz, CD_2Cl_2) δ -79.38, -82.89 (d, *J* = 39.2 Hz), -108.38 – -110.17 (m), -110.69, -117.02.

^{31}P NMR (243 MHz, CD_2Cl_2) δ -14.12.

HRMS (ESI) (m/z): calculated for $C_{84}H_{28}Cl_4F_{50}N_3O_8P_2S_2$ $[M-H]^-$: 2421.87543; found: 2421.87629.

$[\alpha]_D^{25}$ = 176.0 (c = 0.13, $CHCl_3$)

(*S*,*S*)-IDPi 4.3v

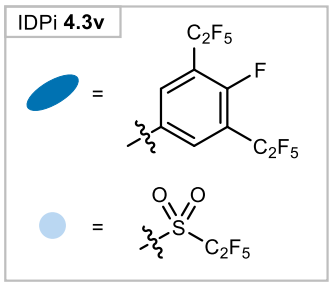

Preparation from (*S*)-3,3'-bis(4-fluoro-3,5-bis(perfluoroethyl)phenyl)-[1,1'-binaphthalene]-2,2'-diol (**4.52**, 448.0 mg, 473.3 µmol, 2.10 equiv.) and ((perfluoroethyl)sulfonyl)phosphorimidoyl trichloride (**4.40b**, 154.5 mg, 462.0 µmol, 2.05 equiv.) according to GP7 afforded the title compound as a yellow solid (283.6 mg, 120.2 µmol, 53%).

^{1}H NMR (600 MHz, CD_2Cl_2) δ 8.14 (s, 2H), 8.11 (ddd, *J* = 8.7, 1.3, 0.6 Hz, 2H), 7.92 – 7.88 (m, 4H), 7.75 (d, *J* = 4.5 Hz, 4H), 7.73 – 7.67 (m, 4H), 7.63 (ddd, *J* = 8.1, 6.8, 1.1 Hz, 2H), 7.40 – 7.36 (m, 2H), 7.33 (d, *J* = 5.5 Hz, 4H), 7.15 (dd, *J* = 8.5, 1.0 Hz, 2H), 6.53 (s, 2H).

^{13}C{^{1}H} NMR (151 MHz, CD_2Cl_2) δ 158.9, 157.1, 144.1, 144.1, 144.1, 142.4, 142.4, 142.3, 134.7, 134.2, 133.9, 133.5, 132.5, 132.2, 132.2, 132.1, 131.4, 130.6, 130.1, 130.0, 129.5, 129.0, 128.2, 127.5, 127.4, 127.1, 127.0, 123.8, 122.4, 122.0, 121.8, 121.5, 120.5, 120.3, 120.1, 119.9, 119.6, 118.8, 118.7, 118.6, 118.4, 118.4, 118.2, 118.0, 117.7, 116.9, 116.7, 116.5, 116.3, 116.1, 114.2, 114.1, 114.0, 113.9, 112.5, 112.4, 112.3, 112.1, 111.9, 111.7, 111.4, 110.8, 110.7, 110.6, 110.4, 109.5.

^{19}F NMR (565 MHz, CD_2Cl_2) δ -79.56, -85.21 (dd, *J* = 21.7, 11.7 Hz), -111.83, -112.61 – -115.20 (m), -117.38.

^{31}P NMR (243 MHz, CD_2Cl_2) δ -13.10.

HRMS (ESI) (m/z): calculated for $C_{84}H_{28}F_{54}N_3O_8P_2S_2$ $[M-H]^-$: 2357.993654; found: 2357.994610.

$[\alpha]_D^{25}$ = 153.5 (c = 0.53, $CHCl_3$)

(*S*,*S*)-IDPi 4.3w

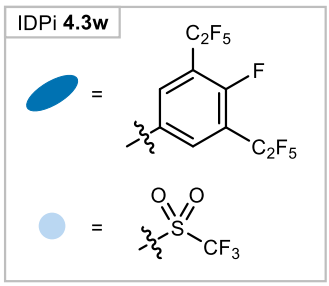

Preparation from (*S*)-3,3'-bis(4-fluoro-3,5-bis(perfluoroethyl)phenyl)-[1,1'-binaphthalene]-2,2'-diol (**4.52**, 92.3 mg, 97.5 µmol, 2.15 equiv.) and ((trifluoromethyl)sulfonyl)phosphorimidoyl trichloride (**4.40a**, 27.1 mg, 95.2 µmol, 2.10 equiv.) according to GP7 afforded the title compound as a yellow solid (69.3 mg, 31 µmol, 68%).

^{1}H NMR (600 MHz, THF) δ 8.18 (s, 2H), 8.12 – 8.07 (m, 2H), 7.96 (dd, *J* = 8.3, 1.2 Hz, 2H), 7.91 (d, *J* = 5.9 Hz, 4H), 7.84 (ddd, *J* = 8.0, 6.7, 1.1 Hz, 2H), 7.72 (d, *J* = 8.5 Hz, 2H), 7.63 (ddd, *J* = 8.3, 6.8, 1.3 Hz, 2H), 7.55 – 7.47 (m, 6H), 7.29 (ddd, *J* = 8.3, 6.8, 1.3 Hz, 2H), 7.14 (d, *J* = 8.6 Hz, 2H), 6.65 (s, 2H).

^{13}C{^{1}H} NMR (151 MHz, THF) δ 159.3, 159.2, 157.5, 157.4, 146.0, 146.0, 146.0, 144.9, 144.9, 144.9, 136.0, 136.0, 135.9, 135.9, 135.8, 135.8, 135.4, 135.3, 135.3, 133.5, 133.4, 133.1, 132.8, 132.0, 131.9, 131.8, 131.8, 131.8, 131.5, 131.3, 130.5, 130.0, 128.7, 128.2, 127.7, 127.2, 127.2, 124.6, 123.9, 123.3, 123.1, 122.8, 122.5, 121.8, 121.8, 121.8, 121.4, 121.2, 120.9, 120.6, 119.7, 119.7, 119.7, 119.5, 119.3, 119.0, 119.0, 118.7, 118.6, 118.6, 118.5, 118.5, 118.4, 118.4, 118.4, 118.3, 118.3, 118.2, 118.1, 117.6, 117.4, 117.1, 116.8, 115.3, 115.2, 115.1, 115.0, 114.8, 114.7, 114.5, 114.4, 113.6, 113.5, 113.4, 113.3, 113.1, 113.0, 112.8, 112.7, 111.9, 111.8, 111.7, 111.5, 111.4, 111.3, 111.1, 111.0.

^{19}F NMR (565 MHz, THF) δ -80.85, -85.76 (dd, *J* = 26.8, 12.7 Hz), -112.75 – -116.20 (m).

^{31}P NMR (243 MHz, THF) δ -7.99.

HRMS (ESI) (m/z): calculated for $C_{82}H_{28}F_{50}N_3O_8P_2S_2$ $[M-H]^-$: 2258.00001; found: 2258.00223.

$[\alpha]_D^{25}$ = 188.8 (c = 0.50, $CHCl_3$)

(*S*,*S*)-IDPi 4.3x

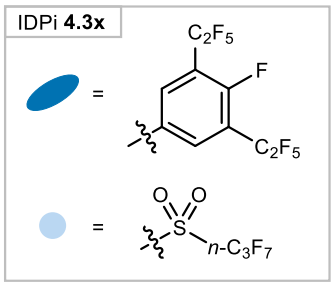

Preparation from (*S*)-3,3'-bis(4-fluoro-3,5-bis(perfluoroethyl)phenyl)-[1,1'-binaphthalene]-2,2'-diol (**4.52**, 93.0 mg, 98.3 µmol, 2.15 equiv.) and ((perfluoropropyl)sulfonyl)phosphorimidoyl trichloride (**4.40c**, 36.9 mg, 96.0 µmol, 2.10 equiv.) according to GP7 afforded the title compound as a light yellow solid (17.7 mg, 7 µmol, 16%).

^{1}H NMR (600 MHz, THF) δ 8.19 (s, 2H), 8.09 (d, *J* = 8.3 Hz, 2H), 7.94 (d, *J* = 8.6 Hz, 2H), 7.90 (d, *J* = 6.0 Hz, 4H), 7.84 (ddd, *J* = 8.1, 6.7, 1.2 Hz, 2H), 7.71 (d, *J* = 8.5 Hz, 2H), 7.62 (ddd, *J* = 8.3, 6.7, 1.3 Hz, 2H), 7.53 – 7.48 (m, 6H), 7.28 (ddd, *J* = 8.3, 6.8, 1.3 Hz, 2H), 7.11 (d, *J* = 8.6 Hz, 2H), 6.59 (s, 2H).

^{13}C{^{1}H} NMR (151 MHz, THF) δ 159.1, 157.3, 145.8, 145.8, 145.8, 144.8, 144.8, 144.8, 136.0, 135.7, 135.2, 133.3, 133.2, 133.0, 132.6, 131.9, 131.7, 131.6, 131.5, 131.2, 129.8, 129.7, 128.5, 128.4, 127.9, 127.5, 127.5, 126.9, 126.9, 124.4, 123.2, 122.9, 121.2, 121.0, 120.7, 120.5, 119.7, 119.3, 119.1, 118.8, 118.6, 118.5, 118.4, 118.3, 118.2, 118.2, 118.1, 117.8, 115.4, 114.8, 114.7, 114.6, 114.5, 113.4, 113.1, 113.0, 112.9, 112.8, 111.5, 111.2, 110.0, 109.8, 109.5, 109.3.

^{19}F NMR (565 MHz, THF) δ -82.01 (t, *J* = 9.4 Hz), -85.78 (dd, *J* = 64.3, 11.6 Hz), -112.99 – -116.41 (m), -124.49 – -126.19 (m).

^{31}P NMR (243 MHz, THF) δ -8.38.

HRMS (ESI) (m/z): calculated for $C_{86}H_{28}F_{58}N_3O_8P_2S_2$ $[M-H]^-$: 2457.987268; found: 2457.990350.

7.4. Reaction Development

Representative procedure for the optimization the olefin alkylation reaction

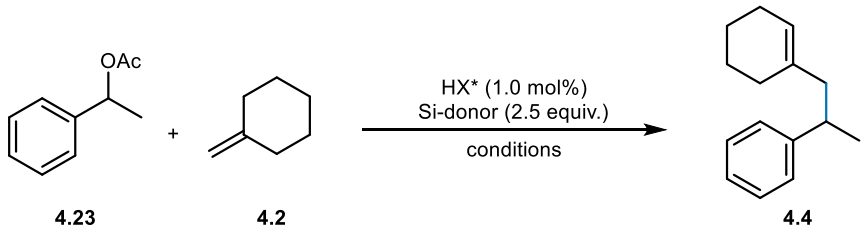

In a screw cap 1 mL glass GC vial, IDPi catalyst (**4.3a**, 0.2 µmol, 1.0 mol%) was dissolved in CyMe (0.1 mL, 0.2 M), and the reaction vessel was briefly flushed with argon and sealed. BSTFA (**4.9**, 13.2 µL, 0.05 mmol, 2.5 equiv.) and methylenecyclohexane (**4.2**, 4.8 µL, 2.0 equiv.) were sequentially added. The mixture was cooled to −60 °C, 1-phenylethyl acetate (**4.23**, 3.3 mg, 0.02 mmol, 1.0 equiv.) was added through the cap, and the cap was sealed with grease. The reaction was stirred at the same temperature for 1 d, after which it was quenched by the addition of Et_3N (1.0 µL, 7.2 µmol, 0.4 equiv.). Mesitylene (2.8 µL, 0.02 mmol, 1.0 equiv.) was added as an internal standard, and the mixture was analyzed by ^1H NMR. The mixture was filtered through a short silica plug and washed with pentane. The filtrate was subjected to GC analysis.

General procedure 8 (GP8): Asymmetric synthesis of olefin alkylation products

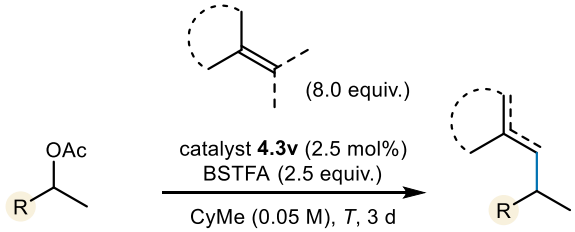

In a screw cap 10 mL glass vial under an argon atmosphere, IDPi catalyst **4.3v** (11.8 mg, 5.0 µmol, 2.5 mol%) was dissolved in CyMe (4.0 mL, 0.05 M). BSTFA (**4.9**, 132.1 µL, 0.5 mmol, 2.5 equiv.) and the respective olefin (8.0 equiv.) were sequentially added. The mixture was cooled to the appropriate reaction temperature, the respective acetate (0.2 mmol, 1.0 equiv.) was added through the cap, and the cap was sealed with grease. The reaction was stirred at the same temperature for 3 d, after which it was quenched by the addition of Et_3N (5.0 µL, 35.9 µmol,

0.2 equiv.). The crude mixture was then subjected to FCC (method and eluent indicated at respective entry) to afford the corresponding olefin alkylation products.

Synthesis of racemic reference samples

Racemic reference samples were synthesized at 0.02 mmol scale according to GP8, replacing catalyst **4.3v** with a stock solution of Tf_2NH (0.2 M in CH_2Cl_2, 5 mol%) at 25 °C, or *rac*-**4.3a** (2.5 mol%) at −40 °C (for *rac*-**4.56f**, *rac*-**4.56g**, and *rac*-**5.57h**). Racemates were prepared for chiral GC or HPLC analysis by filtration through a short silica plug and washing with pentane, or by preparative thin layer chromatography (PTLC).

7.5. Characterization of Products

(*S*)-(1-(cyclohex-1-en-1-yl)propan-2-yl)benzene (4.4)

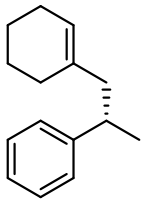

Preparation from 1-phenylethyl acetate (**4.23**, 32.8 mg, 0.20 mmol, 1.0 equiv.) and methylenecyclohexane (**4.2**, 158.9 mg, 1.60 mmol, 8.0 equiv.) at −60 °C according to GP8 afforded the title compound as a light yellow oil (30.0 mg, 0.15 mmol, 75%) after FCC (silica gel, pentane).

^{1}H NMR (501 MHz, CD_2Cl_2) δ 7.30 – 7.22 (m, 2H), 7.21 – 7.13 (m, 3H), 5.37 – 5.31 (m, 1H), 2.93 – 2.82 (m, 1H), 2.22 (dd, *J* = 13.5, 6.7 Hz, 1H), 2.12 (dd, *J* = 13.5, 8.5 Hz, 1H), 1.99 – 1.84 (m, 4H), 1.58 (dtd, *J* = 10.8, 6.0, 4.3 Hz, 2H), 1.50 (qd, *J* = 6.9, 4.9 Hz, 2H), 1.17 (d, *J* = 6.9 Hz, 3H).

^{13}C NMR (126 MHz, CD_2Cl_2) δ 148.4, 136.5, 128.5, 127.3, 126.0, 123.3, 47.7, 38.1, 28.6, 25.7, 23.4, 22.9, 21.6.

HRMS (GC-EI) (m/z): calculated for $C_{15}H_{20}$ $[M]^+$: 200.155950; found: 200.156010.

GC (30 m BGB-176, injection temperature: 220 °C, 110 °C iso 110 min, 8 °C/min, 240 °C, 0.5 bar H_2): t_{R1} = 93.6 min (major), t_{R2} = 96.1 min (minor), e.r. = 96:4 (92% e.e.).

$[\alpha]_D^{25}$ = 9.2 (c = 0.28, $CHCl_3$)

(*S*)-1-(1-(cyclohex-1-en-1-yl)propan-2-yl)-3,5-dimethylbenzene (4.54a)

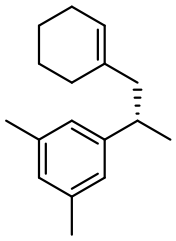

Preparation from 1-(3,5-dimethylphenyl)ethyl acetate (**4.53a**, 38.5 mg, 0.20 mmol, 1.0 equiv.) and methylenecyclohexane (**4.2**, 158.9 mg, 1.60 mmol, 8.0 equiv.) at −60 °C according to GP8 afforded the title compound as a colorless oil (43.8 mg, 0.18 mmol, 91%) after FCC (silica gel, pentane).

^{1}H NMR (501 MHz, CD_2Cl_2) δ 6.80 (s, 3H), 5.36 (p, *J* = 2.0 Hz, 1H), 2.79 (dp, *J* = 9.0, 6.8 Hz, 1H), 2.19 (dd, *J* = 13.6, 6.2 Hz, 1H), 2.07 (dd, *J* = 13.5, 8.9 Hz, 1H), 2.00 – 1.82 (m, 4H), 1.64 – 1.55 (m, 2H), 1.53 (d, *J* = 6.9 Hz, 2H), 1.14 (d, *J* = 6.9 Hz, 3H).

^{13}C NMR (126 MHz, CD_2Cl_2) δ 148.4, 137.9, 136.7, 127.6, 125.1, 123.1, 47.8, 37.9, 28.7, 25.7, 23.5, 23.0, 21.5, 21.4.

HRMS (GC-EI) (m/z): calculated for $C_{17}H_{24}$ $[M]^+$: 228.187250; found: 228.186960.

GC (24 m Cyclodextrin-H, injection temperature: 220 °C, 110 °C iso 45 min, 8 °C/min, 180 °C, 0.5 bar H_2): t_{R1} = 34.6 min (minor), t_{R2} = 36.5 min (major), e.r. = 95.5:4.5 (91% e.e.).

$[\alpha]_D^{25}$ = −9.1 (c = 0.51, $CHCl_3$)

(*S*)-1-(1-(cyclohex-1-en-1-yl)propan-2-yl)-3-methylbenzene (4.54b)

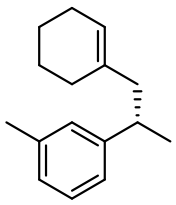

Preparation from 1-(m-tolyl)ethyl acetate (**4.53b**, 35.6 mg, 0.20 mmol, 1.0 equiv.) and methylenecyclohexane (**4.2**, 158.9 mg, 1.60 mmol, 8.0 equiv.) at −60 °C according to GP8 afforded the title compound as a colorless oil (42.9 mg, 0.20 mmol, quant.) after FCC (silica gel, pentane).

^{1}H NMR (501 MHz, CD_2Cl_2) δ 7.15 (t, *J* = 7.5 Hz, 1H), 7.03 – 6.99 (m, 1H), 6.99 – 6.96 (m, 2H), 5.38 – 5.32 (m, 1H), 2.83 (dp, *J* = 8.8, 6.8 Hz, 1H), 2.32 (s, 3H), 2.26 – 2.16 (m, 1H), 2.10 (dd, *J* = 13.4, 8.7 Hz, 1H), 2.00 – 1.82 (m, 4H), 1.65 – 1.54 (m, 2H), 1.55 – 1.48 (m, 2H), 1.16 (d, *J* = 6.9 Hz, 3H).

^{13}C NMR (126 MHz, CD_2Cl_2) δ 148.4, 138.1, 136.6, 128.4, 128.2, 126.8, 124.3, 123.2, 47.8, 38.1, 28.7, 25.7, 23.5, 23.0, 21.6, 21.5.

HRMS (APPI) (m/z): calculated for $C_{16}H_{22}$ $[M]^+$: 214.171600; found: 214.171620.

GC (25 m Lipodex-G, injection temperature: 220 °C, 80 °C iso 200 min, 8 °C/min, 220 °C, 0.6 bar H_2): t_{R1} = 171.3 min (minor), t_{R2} = 179.1 min (major), e.r. = 95.5:4.5 (91% e.e.).

$[\alpha]_D^{25}$ = −5.8 (c = 0.48, $CHCl_3$)

(*S*)-1-(1-(cyclohex-1-en-1-yl)propan-2-yl)-3-isopropylbenzene (4.54c)

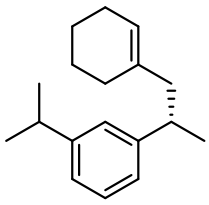

Preparation from 1-(3-isopropylphenyl)ethyl acetate (**4.53c**, 41.3 mg, 0.20 mmol, 1.0 equiv.) and methylenecyclohexane (**4.2**, 158.9 mg, 1.60 mmol, 8.0 equiv.) at −70 °C according to GP8 afforded the title compound as a colorless oil (29.0 mg, 0.12 mmol, 60%) after FCC (silica gel, pentane).

^{1}H NMR (501 MHz, $CDCl_3$) δ 7.21 (td, *J* = 7.3, 1.1 Hz, 1H), 7.07 – 6.98 (m, 3H), 5.37 – 5.31 (m, 1H), 2.94 – 2.80 (m, 2H), 2.22 (dd, *J* = 13.5, 6.3 Hz, 1H), 2.11 (dd, *J* = 13.4, 8.8 Hz, 1H), 1.98 – 1.85 (m, 4H), 1.64 – 1.55 (m, 2H), 1.54 – 1.48 (m, 2H), 1.25 (d, *J* = 6.9 Hz, 6H), 1.19 (d, *J* = 6.9 Hz, 3H).

^{13}C NMR (126 MHz, $CDCl_3$) δ 148.8, 147.9, 136.3, 128.2, 125.5, 124.3, 123.9, 123.1, 47.7, 38.0, 34.3, 28.5, 25.5, 24.2, 24.2, 23.2, 22.7, 21.3.

HRMS (GC-EI) (m/z): calculated for $C_{18}H_{26}$ $[M]^+$: 242.20290; found: 242.20307.

HPLC (150 mm Chiralcel OJ-3R column, MeCN/H_2O 65:35, 308 K, 220 nm): t_{R1} (minor) = 9.0 min, t_{R2} (major) = 10.2 min, e.r. = 96.5:3.5 (93% e.e.).

$[\alpha]_D^{25}$ = −1.3 (c = 0.47, $CHCl_3$)

(*S*)-4-(1-(cyclohex-1-en-1-yl)propan-2-yl)-1,1'-biphenyl (4.54d)

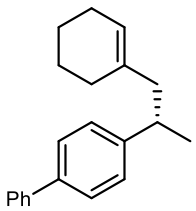

Preparation from 1-([1,1'-biphenyl]-4-yl)ethyl acetate (**4.53d**, 48.1 mg, 0.20 mmol, 1.0 equiv.) and methylenecyclohexane (**4.2**, 158.9 mg, 1.60 mmol, 8.0 equiv.) at −60 °C according to GP8 afforded the title compound as a colorless oil (27.8 mg, 0.10 mmol, 50%) after FCC (silica gel, pentane).

^{1}H NMR (501 MHz, CD_2Cl_2) δ 7.62 – 7.56 (m, 2H), 7.56 – 7.50 (m, 2H), 7.46 – 7.39 (m, 2H), 7.35 – 7.30 (m, 1H), 7.29 – 7.26 (m, 2H), 5.41 – 5.36 (m, 1H), 2.94 (dp, *J* = 8.7, 6.9 Hz, 1H),

2.30 – 2.22 (m, 1H), 2.16 (dd, *J* = 13.5, 8.5 Hz, 1H), 2.00 – 1.87 (m, 4H), 1.65 – 1.56 (m, 2H), 1.52 (d, *J* = 6.3 Hz, 2H), 1.22 (d, *J* = 6.9 Hz, 3H).

^{13}C NMR (126 MHz, CD_2Cl_2) δ 147.6, 141.5, 138.9, 136.5, 129.1, 127.8, 127.4, 127.2, 127.2, 123.4, 47.7, 37.8, 28.7, 25.7, 23.5, 23.0, 21.6.

HRMS (GC-EI) (m/z): calculated for $C_{21}H_{24}$ $[M]^+$: 276.187250; found: 276.187400.

GC (21.5 m Ivadex-5, injection temperature: 220 °C, 160 °C iso 120 min, 8 °C/min, 220 °C, 0.5 bar H_2): t_{R1} = 99.3 min (major), t_{R2} = 104.2 min (minor), e.r. = 90.5:9.5 (81% e.e.).

$[\alpha]_D^{25}$ = 8.0 (c = 0.50, $CHCl_3$)

(*S*)-1-(1-(cyclohex-1-en-1-yl)propan-2-yl)-4-(prop-1-yn-1-yl)benzene (4.54e)

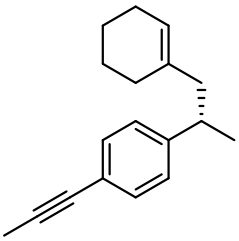

Preparation from 1-(4-(prop-1-yn-1-yl)phenyl)ethyl acetate (**4.53e**, 40.4 mg, 0.20 mmol, 1.0 equiv.) and methylenecyclohexane (**4.2**, 158.9 mg, 1.60 mmol, 8.0 equiv.) at −60 °C according to GP8 afforded the title compound as a colorless oil (23.3 mg, 0.10 mmol, 48%) after FCC (silica gel, pentane).

^{1}H NMR (501 MHz, CD_2Cl_2) δ 7.30 – 7.24 (m, 2H), 7.13 – 7.07 (m, 2H), 5.33 – 5.29 (m, 1H), 2.86 (sext, *J* = 7.1 Hz, 1H), 2.18 (dd, *J* = 13.6, 7.0 Hz, 1H), 2.11 (dd, *J* = 13.5, 8.1 Hz, 1H), 2.02 (s, 3H), 1.99 – 1.81 (m, 4H), 1.62 – 1.52 (m, 2H), 1.52 – 1.44 (m, 2H), 1.16 (d, *J* = 6.9 Hz, 3H).

^{13}C NMR (126 MHz, CD_2Cl_2) δ 148.0, 136.3, 131.6, 127.4, 123.5, 121.7, 85.3, 79.9, 47.5, 38.1, 28.7, 25.7, 23.4, 22.9, 21.4, 4.4.

HRMS (GC-EI) (m/z): calculated for $C_{18}H_{22}$ $[M]^+$: 238.171600; found: 238.171640.

GC (30 m BGB-174, injection temperature: 220 °C, 130 °C iso 250 min, 8 °C/min, 240 °C, 0.6 bar H_2): t_{R1} = 231.3 min (major), t_{R2} = 237.2 min (minor), e.r. = 95.5:4.5 (91% e.e.).

$[\alpha]_D^{25}$ = 17.7 (c = 0.44, $CHCl_3$)

(*S*)-1-(1-(cyclohex-1-en-1-yl)propan-2-yl)-3-methoxybenzene (4.54f)

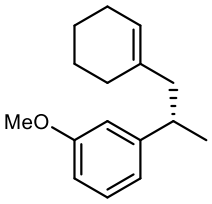

Preparation from 1-(3-methoxyphenyl)ethyl acetate (**4.53f**, 38.8 mg, 0.20 mmol, 1.0 equiv.) and methylenecyclohexane (**4.2**, 158.9 mg, 1.60 mmol, 8.0 equiv.) at −60 °C according to GP8 afforded the title compound as a colorless oil (21.1 mg, 0.09 mmol, 46%) after FCC (silica gel, pentane/Et_2O, 97:3).

^{1}H NMR (501 MHz, CD_2Cl_2) δ 7.18 (t, *J* = 7.9 Hz, 1H), 6.78 (dt, *J* = 7.6, 1.3 Hz, 1H), 6.73 (t, *J* = 2.1 Hz, 1H), 6.70 (ddd, *J* = 8.1, 2.6, 0.9 Hz, 1H), 5.36 (tt, *J* = 3.9, 1.7 Hz, 1H), 3.78 (s, 3H), 2.85 (dp, *J* = 8.7, 6.9 Hz, 1H), 2.21 (dd, *J* = 13.6, 6.6 Hz, 1H), 2.11 (dd, *J* = 13.5, 8.5 Hz, 1H), 1.99 – 1.84 (m, 4H), 1.63 – 1.54 (m, 2H), 1.54 – 1.47 (m, 2H), 1.17 (d, *J* = 6.9 Hz, 3H).

^{13}C NMR (126 MHz, CD_2Cl_2) δ 160.1, 150.1, 136.5, 129.4, 123.3, 119.7, 113.2, 111.2, 55.5, 47.6, 38.2, 28.7, 25.7, 23.5, 23.0, 21.5.

HRMS (GC-EI) (m/z): calculated for $C_{16}H_{22}O$ $[M]^+$: 230.166515; found: 230.166350.

GC (25 m Hydrodex-gamma DiMOM ID, injection temperature: 220 °C, 110 °C iso 200 min, 8 °C/min, 240 °C, 0.5 bar H_2): t_{R1} = 185.0 min (minor), t_{R2} = 190.8 min (major), e.r. = 96:4 (92% e.e.).

$[\alpha]_D^{25}$ = −1.7 (c = 0.12, $CHCl_3$)

(*S*)-4-(1-(cyclohex-1-en-1-yl)propan-2-yl)-2-methoxy-1-methylbenzene (4.54g)

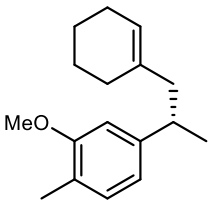

Preparation from 1-(3-methoxy-4-methylphenyl)ethyl acetate (**4.53g**, 41.7 mg, 0.20 mmol, 1.0 equiv.) and methylenecyclohexane (**4.2**, 158.9 mg, 1.60 mmol, 8.0 equiv.) at −60 °C according to GP8 afforded the title compound as a colorless oil (49.1 mg, 0.17 mmol, 83%) after FCC (silica gel, pentane/Et_2O, 97:3).

^{1}H NMR (501 MHz, $CDCl_3$) δ 7.03 (d, *J* = 7.5 Hz, 1H), 6.70 (dd, *J* = 7.6, 1.6 Hz, 1H), 6.66 (d, *J* = 1.6 Hz, 1H), 5.40 – 5.34 (m, 1H), 3.83 (s, 3H), 2.84 (dp, *J* = 8.8, 6.8 Hz, 1H), 2.23 (dd, *J* = 13.7, 6.2 Hz, 1H), 2.18 (s, 3H), 2.10 (dd, *J* = 13.5, 8.8 Hz, 1H), 1.99 – 1.84 (m, 4H), 1.65 – 1.47 (m, 4H), 1.18 (d, *J* = 6.9 Hz, 3H).

^{13}C NMR (126 MHz, $CDCl_3$) δ 157.7, 147.1, 136.3, 130.4, 123.9, 123.1, 118.7, 109.1, 55.4, 47.6, 37.9, 28.5, 25.5, 23.2, 22.7, 21.5, 16.0.

HRMS (ESI) (m/z): calculated for $C_{17}H_{24}ONa$ $[M+Na]^+$: 267.171934; found: 267.171910.

GC (21.5 m Ivadex-5, injection temperature: 220 °C, 95 °C iso 405 min, 8 °C/min, 220 °C, 0.5 bar H_2): t_{R1} = 367.1 min (major), t_{R2} = 387.4 min (minor), e.r. = 94.5:5.5 (89% e.e.).

$[\alpha]_D^{25}$ = −2.0 (c = 0.49, $CHCl_3$)

(*S*)-1-(1-(cyclohex-1-en-1-yl)propan-2-yl)-4-fluorobenzene (4.54h)

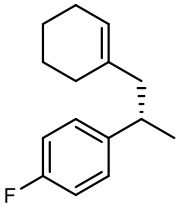

Preparation from 1-(4-fluorophenyl)ethyl acetate (**4.53h**, 36.4 mg, 0.20 mmol, 1.0 equiv.) and methylenecyclohexane (**4.2**, 158.9 mg, 1.60 mmol, 8.0 equiv.) at −70 °C according to GP8 afforded the title compound as a light yellow oil (38.1 mg, 0.18 mmol, 87%) after FCC (silica gel, pentane).

^{1}H NMR (501 MHz, $CDCl_3$) δ 7.16 – 7.08 (m, 2H), 6.99 – 6.91 (m, 2H), 5.34 – 5.28 (m, 1H), 2.86 (dt, *J* = 8.2, 6.8 Hz, 1H), 2.17 (dd, *J* = 13.2, 6.6 Hz, 1H), 2.10 (dd, *J* = 13.5, 8.2 Hz, 1H), 2.00 – 1.81 (m, 4H), 1.62 – 1.54 (m, 2H), 1.53 – 1.46 (m, 2H), 1.18 (d, *J* = 6.9 Hz, 3H).

^{13}C NMR (126 MHz, $CDCl_3$) δ 161.3 (d, *J* = 242.8 Hz), 143.5 (d, *J* = 3.2 Hz), 136.0, 128.4 (d, *J* = 7.8 Hz), 123.4, 115.0 (d, *J* = 20.7 Hz), 47.6, 37.4, 28.5, 25.4, 23.1, 22.6, 21.7.

^{19}F NMR (471 MHz, $CDCl_3$) δ -118.04.

HRMS (GC-EI) (m/z): calculated for $C_{15}H_{19}F$ $[M]^+$: 218.14653; found: 218.14669.

GC (25 m Ivadex-7, injection temperature: 220 °C, 90 °C iso 120 min, 8 °C/min, 230 °C, 0.6 bar H_2): t_{R1} = 98.5 min (major), t_{R2} = 110.0 min (minor), e.r. = 95:5 (90% e.e.).

$[\alpha]_D^{25}$ = 5.2 (c = 0.46, $CHCl_3$)

(*S*)-1-chloro-4-(1-(cyclohex-1-en-1-yl)propan-2-yl)benzene (4.54i)

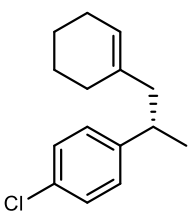

Preparation from 1-(4-chlorophenyl)ethyl acetate (**4.53i**, 39.7 mg, 0.20 mmol, 1.0 equiv.) and methylenecyclohexane (**4.2**, 158.9 mg, 1.60 mmol, 8.0 equiv.) at −60 °C according to GP8 afforded the title compound as a colorless oil (44.2 mg, 0.19 mmol, 94%) after FCC (silica gel, pentane).

^{1}H NMR (501 MHz, CD_2Cl_2) δ 7.27 – 7.21 (m, 2H), 7.17 – 7.09 (m, 2H), 5.32 – 5.30 (m, 1H), 2.87 (sext, *J* = 7.1 Hz, 1H), 2.18 (dd, *J* = 13.6, 7.1 Hz, 1H), 2.11 (dd, *J* = 13.5, 8.0 Hz, 1H), 1.99 – 1.84 (m, 4H), 1.62 – 1.52 (m, 2H), 1.51 – 1.45 (m, 2H), 1.17 (d, *J* = 6.9 Hz, 3H).

^{13}C NMR (126 MHz, CD_2Cl_2) δ 146.9, 136.2, 131.4, 128.9, 128.5, 123.6, 47.6, 37.7, 28.7, 25.7, 23.4, 22.9, 21.6.

HRMS (APPI) (m/z): calculated for $C_{15}H_{19}Cl$ $[M]^+$: 234.116978; found: 234.117020.

GC (21.5 m Ivadex-5, injection temperature: 220 °C, 110 °C iso 105 min, 8 °C/min, 220 °C, 0.5 bar H_2): t_{R1} = 91.0 min (major), t_{R2} = 99.5 min (minor), e.r. = 96:4 (92% e.e.).

$[\alpha]_D^{25}$ = 11.3 (c = 0.46, $CHCl_3$)

(*S*)-(1-(cyclopent-1-en-1-yl)propan-2-yl)benzene (4.56a)

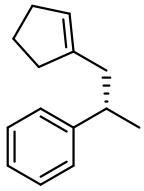

Preparation from 1-phenylethyl acetate (**4.23**, 32.8 mg, 0.20 mmol, 1.0 equiv.) and methylenecyclopentane (**4.55a**, 131.4 mg, 1.60 mmol, 8.0 equiv.) at −60 °C according to GP8 afforded the title compound as a colorless oil (21.4 mg, 0.12 mmol, 57%) after FCC (silica gel, pentane).

^{1}H NMR (501 MHz, CD_2Cl_2) δ 7.30 – 7.23 (m, 2H), 7.22 – 7.19 (m, 2H), 7.18 – 7.14 (m, 1H), 5.31 – 5.28 (m, 1H), 2.91 (sext, *J* = 7.1 Hz, 1H), 2.43 – 2.30 (m, 2H), 2.30 – 2.13 (m, 4H), 1.86 – 1.74 (m, 2H), 1.20 (d, *J* = 6.9 Hz, 3H).

^{13}C NMR (126 MHz, CD_2Cl_2) δ 148.3, 143.6, 128.6, 127.3, 126.1, 125.6, 40.4, 38.7, 35.3, 32.7, 23.9, 22.2.

HRMS (GC-EI) (m/z): calculated for $C_{14}H_{18}$ $[M]^+$: 186.140300; found: 186.140470.

GC (29.5 m BGB-178, injection temperature: 220 °C, 90 °C iso 115 min, 8 °C/min, 230 °C, 0.5 bar H_2): t_{R1} = 98.8 min (major), t_{R2} = 100.8 min (minor), e.r. = 94:6 (88% e.e.).

$[\alpha]_D^{25}$ = 6.0 (c = 0.10, $CHCl_3$)

(*S*)-1-(2-phenylpropyl)cyclohept-1-ene (4.56b)

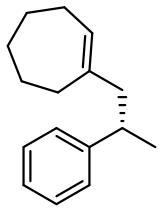

Preparation from 1-phenylethyl acetate (**4.23**, 32.8 mg, 0.20 mmol, 1.0 equiv.) and methylenecycloheptane (**4.55b**, 176.3 mg, 1.60 mmol, 8.0 equiv.) at −60 °C according to GP8 afforded the title compound as a colorless oil (31.0 mg, 0.15 mmol, 72%) after FCC (silica gel, pentane).

^{1}H NMR (501 MHz, CD_2Cl_2) δ 7.30 – 7.22 (m, 2H), 7.20 – 7.17 (m, 2H), 7.17 – 7.12 (m, 1H), 5.48 (t, *J* = 6.4 Hz, 1H), 2.84 (dp, *J* = 8.7, 6.8 Hz, 1H), 2.27 (dd, *J* = 13.1, 6.2 Hz, 1H), 2.18 – 2.09 (m, 3H), 2.09 – 1.95 (m, 2H), 1.71 (dtd, *J* = 12.1, 7.0, 4.8 Hz, 2H), 1.51 – 1.37 (m, 4H), 1.19 (d, *J* = 6.9 Hz, 3H).

^{13}C NMR (126 MHz, CD_2Cl_2) δ 148.4, 143.2, 128.5, 128.5, 127.4, 126.0, 49.9, 38.3, 33.1, 33.0, 28.7, 27.7, 27.2, 21.6.

HRMS (GC-EI) (m/z): calculated for $C_{16}H_{22}$ $[M]^+$: 214.171600; found: 214.171580.

GC (25 m Ivadex-7, injection temperature: 220 °C, 95 °C iso 140 min, 8 °C/min, 230 °C, 0.6 bar H_2): t_{R1} = 116.3 min (major), t_{R2} = 119.6 min (minor), e.r. = 95:5 (90% e.e.).

$[\alpha]_D^{25}$ = 10.1 (c = 0.53, $CHCl_3$)

(*R*)-(3,3,4-trimethylpent-4-en-2-yl)benzene (4.56c)

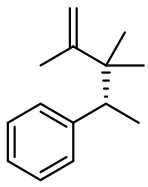

Preparation from 1-phenylethyl acetate (**4.23**, 32.8 mg, 0.20 mmol, 1.0 equiv.) and 2,3-dimethylbut-2-ene (**4.55c**, 134.7 mg, 1.60 mmol, 8.0 equiv.) at −60 °C according to GP8 afforded the title compound as a colorless oil (30.6 mg, 0.16 mmol, 81%) after FCC (silica gel, pentane).

^{1}H NMR (501 MHz, CD_2Cl_2) δ 7.28 – 7.23 (m, 2H), 7.21 – 7.15 (m, 3H), 4.78 (p, *J* = 1.5 Hz, 1H), 4.73 (d, *J* = 1.7 Hz, 1H), 2.90 (q, *J* = 7.2 Hz, 1H), 1.80 (d, *J* = 1.3 Hz, 3H), 1.14 (d, *J* = 7.2 Hz, 3H), 0.98 (s, 3H), 0.87 (s, 3H).

^{13}C NMR (126 MHz, CD_2Cl_2) δ 152.7, 144.5, 129.9, 127.7, 126.3, 110.6, 45.8, 42.6, 26.6, 21.7, 19.8, 16.1.

HRMS (GC-EI) (m/z): calculated for $C_{14}H_{20}$ $[M]^+$: 188.155950; found: 188.156080.

GC (29.5 m BGB-178, injection temperature: 220 °C, 80 °C iso 80 min, 8 °C/min, 230 °C, 0.6 bar H_2): t_{R1} = 69.7 min (major), t_{R2} = 71.2 min (minor), e.r. = 96:4 (92% e.e.).

$[\alpha]_D^{25}$ = −7.4 (c = 0.35, $CHCl_3$)

(*S*)-but-1-ene-1,1,3-triyltribenzene (4.57d)

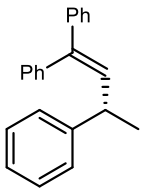

Preparation from 1-phenylethyl acetate (**4.23**, 32.8 mg, 0.20 mmol, 1.0 equiv.) and 1,1-diphenylethylene (**4.55d**, 288.4 mg, 1.60 mmol, 8.0 equiv.) at −60 °C according to GP8 afforded the title compound as a colorless oil (49.8 mg, 0.18 mmol, 88%) after FCC (silica gel, pentane).

^{1}H NMR (300 MHz, CD_2Cl_2) δ 7.46 – 7.06 (m, 15H), 6.22 (d, *J* = 10.3 Hz, 1H), 3.58 (dq, *J* = 10.5, 6.9 Hz, 1H), 1.38 (d, *J* = 6.9 Hz, 3H).

^{13}C NMR (126 MHz, CD_2Cl_2) δ 146.7, 142.9, 140.6, 140.5, 134.6, 130.2, 128.9, 128.7, 128.5, 127.6, 127.5, 127.4, 127.3, 126.4, 39.8, 22.5.

HRMS (GC-EI) (m/z): calculated for $C_{22}H_{20}$ $[M]^+$: 284.155950; found: 284.156340.

HPLC (150 mm Chiralpak IB-N3 column, MeOH/H_2O 70:30–100:0, 298 K, 220 nm): t_{R1} (minor) = 9.9 min, t_{R2} (major) = 10.2 min, e.r. = 98.5:1.5 (97% e.e.).

$[\alpha]_D^{25}$ = −9.5 (c = 0.04, $CHCl_3$)

(*S*)-(4-ethylhex-4-en-2-yl)benzene (4.56e)

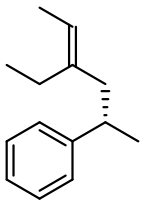

Preparation from 1-phenylethyl acetate (**4.23**, 32.8 mg, 0.20 mmol, 1.0 equiv.) and 3-methylenepentane (**4.55e**, 134.7 mg, 1.60 mmol, 8.0 equiv.) at −60 °C according to GP8 afforded the title compound as a colorless oil (15.3 mg, 0.08 mmol, 41%, *E*/*Z*≈55:45) after FCC (silica gel, pentane).

^{1}H NMR (600 MHz, CD_2Cl_2) δ 7.28 – 7.13 (m, $5H_{maj}$, $5H_{min}$), 5.24 (ddddt, *J* = 7.5, 6.8, 6.0, 1.5, 0.7 Hz, $1H_{min}$), 5.13 (dddt, *J* = 7.8, 6.8, 5.9, 1.1 Hz, $1H_{maj}$), 2.93 – 2.81 (m, $1H_{maj}$, $1H_{min}$), 2.36 – 2.30 (m, $1H_{maj}$, $1H_{min}$), 2.26 (ddt, *J* = 13.5, 7.1, 0.8 Hz, $1H_{min}$), 2.16 – 2.05 (m, $2H_{maj}$), 2.00 – 1.92 (m, $1H_{maj}$, $1H_{min}$), 1.54 (ddt, *J* = 6.8, 1.4, 0.7 Hz, $3H_{maj}$), 1.49 (dtt, *J* = 6.8, 1.3, 0.6

Hz, $3H_{min}$), 1.22 (d, J = 7.0 Hz, $3H_{min}$), 1.17 (d, J = 6.9 Hz, $3H_{maj}$), 0.96 (t, J = 7.5 Hz, $3H_{min}$), 0.95 (t, J = 7.6 Hz, $3H_{maj}$).

^{13}C NMR (151 MHz, CD_2Cl_2) δ 148.5, 148.1, 140.5, 140.4, 128.5, 128.5, 127.3, 126.2, 126.1, 120.3, 119.1, 46.0, 38.9, 38.7, 38.3, 29.9, 22.8, 21.7, 21.5, 13.5, 13.1, 13.0, 12.9.

HRMS (GC-EI) (m/z): calculated for $C_{14}H_{20}$ $[M]^+$: 188.155950; found: 188.155880.

GC (25 m Lipodex-G, injection temperature: 220 °C, 50 °C iso 330 min, 6 °C/min, 220 °C, 0.5 bar H_2): t_{R1} = 256.3 min (minor, *E*), t_{R2} = 259.8 min (major, *E*), t_{R3} = 285.6 min (minor, *Z*), t_{R4} = 290.9 min (major, *Z*), e.r.$_E$ = 95:5 (90% e.e.), e.r.$_Z$ 93:7 (86% e.e.).

$[\alpha]_D^{25}$ = 4.5 (c = 0.44, $CHCl_3$)

(*S*)-hex-4-ene-2,4-diyldibenzene (4.56f)

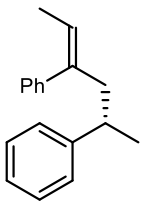

Preparation from 1-phenylethyl acetate (**4.23**, 32.8 mg, 0.20 mmol, 1.0 equiv.) and but-1-en-2-ylbenzene (**4.55f**, 211.5 mg, 1.60 mmol, 8.0 equiv.) at −60 °C according to GP8 afforded the title compound as a colorless oil (47.6 mg, 0.20 mmol, quant., *E*/*Z*≈36:64) after FCC (silica gel, pentane).

^{1}H NMR (600 MHz, CD_2Cl_2) δ 7.36 – 7.33 (m, $2H_{maj}$), 7.30 (d, J = 4.3 Hz, $4H_{min}$), 7.28 – 7.19 (m, $3H_{maj}$, $3H_{min}$), 7.17 – 7.12 (m, $3H_{maj}$, $3H_{min}$), 7.11 – 7.09 (m, $2H_{maj}$), 5.72 (qt, J = 6.9, 0.8 Hz, $1H_{min}$), 5.49 (qt, J = 6.9, 1.2 Hz, $1H_{maj}$), 2.77 (dq, J = 7.3, 0.8 Hz, $2H_{min}$), 2.73 – 2.68 (m, $1H_{maj}$, $1H_{min}$), 2.59 (dp, J = 8.6, 6.7 Hz, $1H_{maj}$), 2.52 (ddp, J = 13.4, 8.4, 0.9 Hz, $1H_{maj}$), 1.65 (dt, J = 6.9, 0.7 Hz, $3H_{min}$), 1.51 (dt, J = 6.9, 1.1 Hz, $3H_{maj}$), 1.19 (d, J = 6.9 Hz, $3H_{min}$), 1.16 (d, J = 6.8 Hz, $3H_{maj}$).

^{13}C NMR (151 MHz, CD_2Cl_2) δ 148.0, 147.7, 143.8, 141.0, 140.4, 140.0, 129.1, 128.6, 128.5, 128.5, 128.4, 127.4, 127.4, 126.9, 126.8, 126.8, 126.2, 126.1, 124.9, 123.5, 48.5, 38.7, 38.4, 38.1, 21.5, 21.0, 14.8, 14.4.

HRMS (GC-EI) (m/z): calculated for $C_{18}H_{20}$ $[M]^+$: 236.155950; found: 236.156020.

GC (21.5 m Ivadex-5, injection temperature: 220 °C, 100 °C iso 230 min, 8 °C/min, 220 °C, 0.5 bar H_2): t_{R1} = 117.7 min (major, *Z*), t_{R2} = 120.3 min (minor, *Z*), t_{R3} = 183.0 min (major, *E*), t_{R4} = 190.6 min (minor, *E*), e.r.$_Z$ = 95.5:4.5 (91% e.e.), e.r.$_E$ 90:10 (80% e.e.).

$[\alpha]_D^{25}$ = 58.1 (c = 0.59, $CHCl_3$)

(*S*)-(1-cyclohexylidenebutane-1,3-diyl)dibenzene (4.56g)

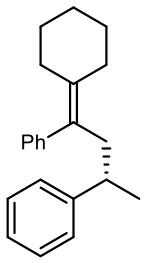

Preparation from 1-phenylethyl acetate (**4.23**, 32.8 mg, 0.20 mmol, 1.0 equiv.) and (1-cyclohexylvinyl)benzene (**4.55g**, 298.1 mg, 1.60 mmol, 8.0 equiv.) at −60 °C according to GP8 afforded the title compound and the constitutional isomer as a colorless oil (21.9 mg, 0.08 mmol, 38%, **4.56g**:**4.57g** = 20:1) after FCC (silica gel, pentane).

^{1}H NMR (600 MHz, CD_2Cl_2) δ 7.32 – 7.28 (m, 2H), 7.25 – 7.19 (m, 3H), 7.15 – 7.10 (m, 3H), 7.09 – 7.06 (m, 2H), 2.70 – 2.60 (m, 2H), 2.55 (dp, *J* = 8.2, 6.9 Hz, 1H), 2.28 – 2.22 (m, 1H), 2.22 – 2.16 (m, 1H), 1.91 (ddd, *J* = 6.8, 4.9, 1.6 Hz, 2H), 1.56 – 1.48 (m, 3H), 1.46 – 1.29 (m, 3H), 1.18 (d, *J* = 6.9 Hz, 3H).

^{13}C NMR (151 MHz, CD_2Cl_2) δ 148.0, 144.1, 137.6, 131.1, 129.6, 128.5, 128.2, 127.5, 126.2, 126.1, 42.8, 38.7, 32.7, 31.2, 29.0, 28.5, 27.3, 21.5.

HRMS (GC-EI) (m/z): calculated for $C_{22}H_{26}$ $[M]^+$: 290.202900; found: 290.202980.

HPLC (150 mm Chiralcel OJ-3R column, MeCN/H_2O 70:30, 298 K, 200 nm): t_{R1} (minor) = 10.1 min, t_{R2} (major) = 11.9 min, e.r. = 98.5:1.5 (97% e.e.).

$[\alpha]_D^{25}$ = 44.5 (c = 0.35, $CHCl_3$)

(*S*)-(4-methylpent-3-en-2-yl)benzene (4.57h) and (*S*)-(4-methylpent-4-en-2-yl)benzene (4.56h)

Preparation from 1-phenylethyl acetate (**4.23**, 40.6 mg, 0.25 mmol, 1.0 equiv.) and isobutene (**4.55h**, 1 atm., 50 mL gas condensed at −60 °C, 130.2 mg, 2.32 mmol, 9.4 equiv.) at −60 °C according to GP8 afforded the title compound, the constitutional isomer and double addition product (**7.13**) separately as colorless oils (42.9 mg, 0.19 mmol, 95%, **4.56h**:**4.57h**:**7.13** = 32:45:23) after FCC (SiO_2/$AgNO_3$, pentane/EtOAc, 100:0–95:5).

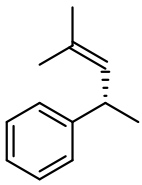

(*S*)-4.57h:

^{1}H NMR (501 MHz, CD_2Cl_2) δ 7.30 – 7.19 (m, 4H), 7.17 – 7.12 (m, 1H), 5.27 (dp, *J* = 9.3, 1.4 Hz, 1H), 3.66 (dq, *J* = 9.4, 7.0 Hz, 1H), 1.70 (d, *J* = 1.4 Hz, 3H), 1.68 (d, *J* = 1.4 Hz, 3H), 1.28 (d, *J* = 7.0 Hz, 3H).

^{13}C NMR (126 MHz, CD_2Cl_2) δ 147.8, 130.9, 130.5, 128.7, 127.2, 126.0, 38.6, 25.9, 22.6, 18.0.

HRMS (GC-EI) (m/z): calculated for $C_{12}H_{16}$ $[M]^+$: 160.124650; found: 160.124540.

GC (25 m Lipodex-G, injection temperature: 220 °C, 60 °C iso 40 min, 8 °C/min, 220 °C, 0.6 bar H_2): t_{R1} = 33.8 min (minor), t_{R2} = 34.3 min (major), e.r. = 95:5 (90% e.e.).

$[\alpha]_D^{25}$ = 105.7 (c = 0.30, $CHCl_3$)

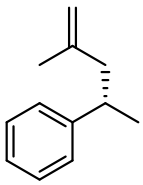

(*S*)-4.56h:

^{1}H NMR (501 MHz, CD_2Cl_2) δ 7.31 – 7.22 (m, 2H), 7.22 – 7.19 (m, 2H), 7.18 – 7.13 (m, 1H), 4.69 (p, *J* = 1.5 Hz, 1H), 4.62 (dq, *J* = 2.3, 1.1 Hz, 1H), 2.93 (h, *J* = 7.1 Hz, 1H), 2.34 (ddd, *J* = 13.8, 7.0, 1.0 Hz, 1H), 2.25 (ddd, *J* = 13.7, 8.1, 1.1 Hz, 1H), 1.69 (t, *J* = 1.2 Hz, 3H), 1.21 (d, *J* = 7.0 Hz, 3H).

^{13}C NMR (126 MHz, CD_2Cl_2) δ 147.9, 144.8, 128.6, 127.3, 126.2, 112.0, 47.1, 38.1, 30.1, 22.3, 22.0.

HRMS (GC-EI) (m/z): calculated for $C_{12}H_{16}$ $[M]^+$: 160.124650; found: 160.124650.

GC (25 m Lipodex-G, injection temperature: 220 °C, 60 °C iso 40 min, 8 °C/min, 220 °C, 0.6 bar H_2): t_{R1} = 31.0 min (minor), t_{R2} = 31.7 min (major), e.r. = 92:8 (84% e.e.).

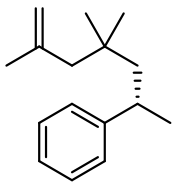

(*S*)-(4,4,6-trimethylhept-6-en-2-yl)benzene (7.13):

^{1}H NMR (501 MHz, CD_2Cl_2) δ 7.29 – 7.18 (m, 4H), 7.17 – 7.10 (m, 1H), 4.81 (dq, *J* = 2.9, 1.4 Hz, 1H), 4.59 (dq, *J* = 2.6, 0.9 Hz, 1H), 2.87 (pd, *J* = 7.1, 4.2 Hz, 1H), 1.98 – 1.92 (m, 1H), 1.91 – 1.85 (m, 1H), 1.78 – 1.74 (m, 1H), 1.74 (t, *J* = 1.1 Hz, 3H), 1.55 (dd, *J* = 14.2, 4.3 Hz, 1H), 1.21 (d, *J* = 7.0 Hz, 3H), 0.82 (s, 3H), 0.76 (s, 3H).

HRMS (GC-EI) (m/z): calculated for $C_{16}H_{24}$ $[M]^+$: 216.187250; found: 216.187240.

((2*S*,3*R*)-3,4-dimethylpent-4-en-2-yl)benzene and ((2*S*,3*S*)-3,4-dimethylpent-4-en-2-yl)benzene ((2*S*,3*R*)-4.56i, (2*S*,3*S*)-4.56i)

Preparation from 1-phenylethyl acetate (**4.23**, 32.8 mg, 0.20 mmol, 1.0 equiv.) and 2-methylbut-2-ene (**4.55i**, 112.2 mg, 1.60 mmol, 8.0 equiv.) at −60 °C according to GP8 afforded the title compounds and the constitutional isomer (**4.57i**) as colorless oils (23.2 mg, 0.13 mmol, 67%, **(2*S*,3*R*)-4.56i**:**(2*S*,3*S*)-4.56i**:**4.57i** = 48:39:13) after FCC (silica gel, pentane).

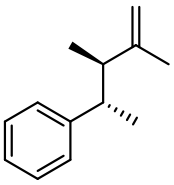

(2*S*,3*R*)-4.56i:

^{1}H NMR (600 MHz, CD_2Cl_2) δ 7.32 – 7.23 (m, 2H), 7.22 – 7.13 (m, 3H), 4.81 (dp, *J* = 2.3, 0.8 Hz, 1H), 4.77 (dq, *J* = 2.9, 1.5 Hz, 1H), 2.56 (dq, *J* = 10.5, 6.9 Hz, 1H), 2.32 (dq, *J* = 10.5, 6.9 Hz, 1H), 1.71 (dd, *J* = 1.5, 0.8 Hz, 3H), 1.13 (d, *J* = 6.9 Hz, 3H), 0.74 (d, *J* = 6.9 Hz, 3H).

^{13}C NMR (151 MHz, CD_2Cl_2) δ 149.6, 147.2, 128.6, 128.0, 126.3, 111.3, 49.1, 44.0, 21.4, 18.8, 18.2.

HRMS (GC-EI) (m/z): calculated for $C_{13}H_{18}$ $[M]^+$: 174.140300; found: 174.140220.

GC (30 m BGB-176, injection temperature: 220 °C, 90 °C iso 45 min, 8 °C/min, 240 °C, 0.6 bar H_2): t_{R1} = 28.4 min (major), t_{R2} = 29.7 min (minor), e.r. = 97.5:2.5 (95% e.e.).

$[\alpha]_D^{25}$ = −23.2 (c = 0.27, $CHCl_3$)

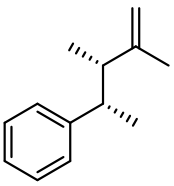

(2*S*,3*S*)-4.56i:

^{1}H NMR (600 MHz, CD_2Cl_2) δ 7.28 – 7.20 (m, 2H), 7.19 – 7.11 (m, 3H), 4.55 (dq, *J* = 2.2, 1.5 Hz, 1H), 4.54 (dp, *J* = 2.4, 0.8 Hz, 1H), 2.76 (dq, *J* = 8.9, 7.0 Hz, 1H), 2.41 (dqd, *J* = 8.8, 6.9, 0.8 Hz, 1H), 1.58 (dd, *J* = 1.5, 0.8 Hz, 3H), 1.19 (d, *J* = 7.0 Hz, 3H), 1.06 (d, *J* = 6.9 Hz, 3H).

^{13}C NMR (151 MHz, CD_2Cl_2) δ 149.8, 147.6, 128.3, 127.9, 126.0, 110.8, 47.9, 43.4, 20.0, 18.9, 16.9.

HRMS (GC-EI) (m/z): calculated for $C_{13}H_{18}$ $[M]^+$: 174.140300; found: 174.140480.

GC (30 m BGB-174, injection temperature: 220 °C, 70 °C iso 60 min, 8 °C/min, 240 °C, 0.6 bar H_2): t_{R1} = 41.9 min (major), t_{R2} = 43.1 min (minor), e.r. = 94:6 (88% e.e.).

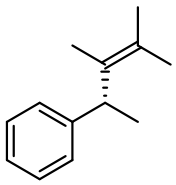

(*R*)-(3,4-dimethylpent-3-en-2-yl)benzene ((*R*)-4.57i):

^{1}H NMR (501 MHz, CD_2Cl_2) δ 7.32 – 7.11 (m, 58H), 4.13 (q, *J* = 7.1 Hz, 1H), 1.83 (q, *J* = 1.5 Hz, 3H), 1.69 (d, *J* = 1.1 Hz, 4H), 1.38 (t, *J* = 1.2 Hz, 3H), 1.32 (d, *J* = 7.1 Hz, 3H).

GC (30 m BGB-176, injection temperature: 220 °C, 90 °C iso 45 min, 8 °C/min, 240 °C, 0.6 bar H_2): t_{R1} = 39.8 min (minor), t_{R2} = 40.6 min (major), e.r. = 90:10 (80% e.e.).

((2*S*,3*R*)-3-ethyl-4-methylpent-4-en-2-yl)benzene and ((2*S*,3*S*)-3-ethyl-4-methylpent-4-en-2-yl)benzene ((2*S*,3*R*)-4.56j, (2*S*,3*S*)-4.56j)

Preparation from 1-phenylethyl acetate (**4.23**, 32.8 mg, 0.20 mmol, 1.0 equiv.) and 2-methylpent-2-ene (**4.55j**, 134.7 mg, 1.60 mmol, 8.0 equiv.) at −60 °C according to GP8 afforded the title compounds as colorless oils (25.7 mg, 0.14 mmol, 68%, **(2*S*,3*R*)-4.56j**:**(2*S*,3*S*)-4.56j** = 61:39) after FCC (silica gel, pentane).

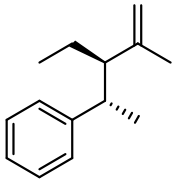

(2*S*,3*R*)-4.56j:

^{1}H NMR (501 MHz, CD_2Cl_2) δ 7.32 – 7.25 (m, 2H), 7.21 – 7.14 (m, 3H), 4.88 (dq, *J* = 2.8, 1.5 Hz, 1H), 4.82 (d, *J* = 2.6 Hz, 1H), 2.56 (dq, *J* = 10.7, 6.9 Hz, 1H), 2.05 (td, *J* = 10.5, 4.6 Hz, 1H), 1.65 (t, *J* = 1.1 Hz, 3H), 1.11 (d, *J* = 6.9 Hz, 3H), 1.06 (dtd, *J* = 11.4, 7.2, 3.3 Hz, 2H), 0.63 (t, *J* = 7.4 Hz, 3H).

^{13}C NMR (126 MHz, CD_2Cl_2) δ 147.6, 146.4, 128.6, 128.0, 126.2, 113.6, 56.9, 43.2, 24.0, 21.5, 17.8, 12.3.

HRMS (GC-EI) (m/z): calculated for $C_{14}H_{20}$ $[M]^+$: 188.155950; found: 188.155810.

GC (29.5 m BGB-178, injection temperature: 220 °C, 90 °C iso 40 min, 8 °C/min, 230 °C, 0.6 bar H_2): t_{R1} = 33.9 min (major), t_{R2} = 34.9 min (minor), e.r. = 96.5:3.5 (93% e.e.).

$[\alpha]_D^{25}$ = −47.9 (c = 0.45, $CHCl_3$)

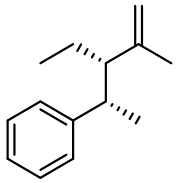

(2*S*,3*S*)-4.56j:

^{1}H NMR (501 MHz, CD_2Cl_2) δ 7.22 (dd, *J* = 8.3, 7.0 Hz, 2H), 7.16 – 7.09 (m, 3H), 4.58 (dt, *J* = 2.9, 1.5 Hz, 1H), 4.47 (d, *J* = 2.4 Hz, 1H), 2.69 (dq, *J* = 9.7, 6.9 Hz, 1H), 2.15 (ddd, *J* = 10.9, 9.6, 3.7 Hz, 1H), 1.73 (dqd, *J* = 13.5, 7.5, 3.7 Hz, 1H), 1.46 (t, *J* = 1.1 Hz, 3H), 1.31 (ddq, *J* = 14.4, 11.1, 7.3 Hz, 1H), 1.23 (d, *J* = 6.9 Hz, 3H), 0.82 (t, *J* = 7.3 Hz, 3H).

^{13}C NMR (126 MHz, CD_2Cl_2) δ 147.8, 146.5, 128.3, 128.0, 125.9, 113.0, 55.9, 43.4, 23.1, 20.6, 19.3, 12.4.

HRMS (GC-EI) (m/z): calculated for $C_{14}H_{20}$ $[M]^+$: 188.155950; found: 188.156300.

GC (29.5 m BGB-178, injection temperature: 220 °C, 90 °C iso 40 min, 8 °C/min, 230 °C, 0.6 bar H_2): t_{R1} = 31.8 min (major), t_{R2} = 32.8 min (minor), e.r. = 93:7 (86% e.e.).

((2*S*,3*R*)-3-(cyclohex-1-en-1-yl)butan-2-yl)benzene and ((2*S*,3*S*)-3-(cyclohex-1-en-1-yl)butan-2-yl)benzene ((2*S*,3*R*)-4.56k, (2*S*,3*S*)-4.56k)

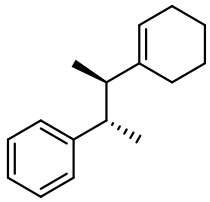

Preparation from 1-phenylethyl acetate (**4.23**, 32.8 mg, 0.20 mmol, 1.0 equiv.) and ethylidenecyclohexane (**4.55k**, 176.3 mg, 1.60 mmol, 8.0 equiv.) at −60 °C according to GP8 afforded the title compound and the diastereomer as a colorless oil (32.6 mg, 0.15 mmol, 74%, **(2*S*,3*R*)-4.56k**:**(2*S*,3*S*)-4.56k** = 60:40) after FCC (silica gel, pentane).

^{1}H NMR (600 MHz, CD_2Cl_2) δ 7.29 – 7.25 (m, $2H_{maj}$), 7.24 – 7.21 (m, $2H_{min}$), 7.19 – 7.16 (m, $3H_{maj}$), 7.15 – 7.10 (m, $3H_{min}$), 5.51 (tdd, *J* = 3.8, 1.7, 0.6 Hz, $1H_{maj}$), 5.20 (ddq, *J* = 5.3, 3.6, 1.7 Hz, $1H_{min}$), 2.75 (dq, *J* = 8.5, 7.0 Hz, $1H_{min}$), 2.56 (dq, *J* = 10.5, 6.9 Hz, $1H_{maj}$), 2.24 – 2.12 (m, $1H_{maj}$, $1H_{min}$), 2.10 – 1.96 (m, $3H_{maj}$), 1.94 – 1.81 (m, $1H_{maj}$, $2H_{min}$), 1.81 – 1.72 (m, $2H_{min}$), 1.70 – 1.55 (m, $4H_{maj}$), 1.52 – 1.46 (m, $1H_{min}$), 1.43 – 1.36 (m, $3H_{min}$), 1.19 (d, *J* = 7.0 Hz, $3H_{min}$), 1.11 (d, *J* = 6.9 Hz, $3H_{maj}$), 1.01 (d, *J* = 6.9 Hz, $3H_{min}$), 0.71 (d, *J* = 6.9 Hz, $3H_{maj}$).

^{13}C NMR (151 MHz, CD_2Cl_2) δ 147.8, 147.6, 141.3, 141.2, 128.5, 128.1, 128.0, 128.0, 126.1, 125.8, 122.4, 121.9, 49.3, 48.4, 44.1, 43.5, 26.5, 25.8, 25.6, 24.7, 23.6, 23.4, 23.3, 23.1, 21.5, 18.6, 18.4, 16.4.

HRMS (GC-CI) (m/z): calculated for $C_{17}H_{22}$ $[M+H]^+$: 215.179425; found: 215.179470.

GC (25 m Ivadex-7, injection temperature: 220 °C, 100 °C iso 75 min, 8 °C/min, 230 °C, 0.6 bar H_2): t_{R1} = 45.2 min (major, *syn*), t_{R2} = 120.3 min (minor, *syn*), t_{R3} = 183.0 min (major, *anti*), t_{R4} = 190.6 min (minor, *anti*), e.r.$_{anti}$ = 97:3 (94% e.e.), e.r.$_{syn}$ 94.5:5.5 (89% e.e.).

Note: an $[\alpha]_D^{25}$ *measurement was not obtained for the diastereomeric mixture, because the crystallized anti-product was directly used in X-ray crystallography measurements.*

(*S*)-1-bromo-4-(1-(cyclopent-1-en-1-yl)propan-2-yl)benzene (4.59a)

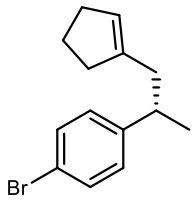

Preparation from 1-(4-bromophenyl)ethyl acetate (**4.58a**, 48.6 mg, 0.20 mmol, 1.0 equiv.) and methylenecyclopentane (**4.55a**, 131.4 mg, 1.60 mmol, 8.0 equiv.) at −60 °C according to GP8 afforded the title compound as a colorless oil (43.8 mg, 0.17 mmol, 83%) after FCC (silica gel, pentane).

^{1}H NMR (501 MHz, $CDCl_3$) δ 7.41 – 7.37 (m, 2H), 7.09 – 7.04 (m, 2H), 5.27 (p, *J* = 1.6 Hz, 1H), 2.87 (sext, *J* = 7.1 Hz, 1H), 2.39 – 2.27 (m, 2H), 2.27 – 2.19 (m, 2H), 2.18 – 2.12 (m, 2H), 1.85 – 1.75 (m, 2H), 1.19 (d, *J* = 6.9 Hz, 3H).

^{13}C NMR (126 MHz, $CDCl_3$) δ 146.8, 142.7, 131.4, 128.8, 125.8, 119.5, 40.0, 38.0, 35.1, 32.5, 23.7, 22.1.

HRMS (GC-CI) (m/z): calculated for $C_{14}H_{18}Br$ $[M+H]^+$: 282.085199; found: 282.085610.

GC (25 m Ivadex-7, injection temperature: 220 °C, 120 °C iso 60 min, 8 °C/min, 230 °C, 0.6 bar H_2): t_{R1} = 51.1 min (major), t_{R2} = 52.8 min (minor), e.r. = 93:7 (86% e.e.).

$[\alpha]_D^{25}$ = 22.5 (c = 0.62, $CHCl_3$)

(*S*)-1-(1-(cyclopent-1-en-1-yl)propan-2-yl)-4-ethynylbenzene (4.59b)

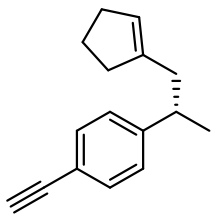

Preparation from 1-(4-ethynylphenyl)ethyl acetate (**4.58b**, 37.6 mg, 0.20 mmol, 1.0 equiv.) and methylenecyclopentane (**4.55a**, 131.4 mg, 1.60 mmol, 8.0 equiv.) at −60 °C according to GP8 afforded the title compound as a colorless oil (18.0 mg, 0.09 mmol, 43%) after FCC (silica gel, pentane).

^{1}H NMR (501 MHz, $CDCl_3$) δ 7.44 – 7.38 (m, 2H), 7.17 – 7.13 (m, 2H), 5.27 (tt, *J* = 2.4, 1.4 Hz, 1H), 3.02 (s, 1H), 2.90 (sext, *J* = 7.1 Hz, 1H), 2.40 – 2.27 (m, 2H), 2.27 – 2.19 (m, 2H), 2.18 – 2.11 (m, 2H), 1.80 (p, *J* = 7.1 Hz, 2H), 1.20 (d, *J* = 6.9 Hz, 3H).

^{13}C NMR (126 MHz, $CDCl_3$) δ 148.9, 142.7, 132.2, 127.1, 125.8, 119.5, 84.0, 76.5, 40.0, 38.5, 35.1, 32.5, 23.7, 22.0.

HRMS (APPI) (m/z): calculated for $C_{16}H_{18}$ $[M]^+$: 210.140300; found: 210.140280.

GC (25 m Ivadex-7, injection temperature: 220 °C, 120 °C iso 40 min, 8 °C/min, 230 °C, 0.6 bar H_2): t_{R1} = 35.4 min (major), t_{R2} = 36.9 min (minor), e.r. = 95:5 (90% e.e.).

$[\alpha]_D^{25}$ = 33.6 (c = 0.46, $CHCl_3$)

(*R*)-1-bromo-4-(3,3,4-trimethylpent-4-en-2-yl)benzene (4.59c)

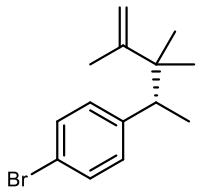

Preparation from 1-(4-bromophenyl)ethyl acetate (**4.58a**, 48.6 mg, 0.20 mmol, 1.0 equiv.) and 2,3-dimethylbut-2-ene (**4.55c**, 134.7 mg, 1.60 mmol, 8.0 equiv.) at −60 °C according to GP8 afforded the title compound as a colorless oil (31.0 mg, 0.12 mmol, 58%) after FCC (silica gel, pentane).

^{1}H NMR (501 MHz, CD_2Cl_2) δ 7.40 – 7.36 (m, 2H), 7.10 – 7.06 (m, 2H), 4.79 (p, *J* = 1.5 Hz, 1H), 4.71 (d, *J* = 1.7 Hz, 1H), 2.88 (q, *J* = 7.2 Hz, 1H), 1.78 (d, *J* = 1.3 Hz, 3H), 1.13 (d, *J* = 7.2 Hz, 3H), 0.97 (s, 3H), 0.86 (s, 3H).

^{13}C NMR (126 MHz, CD_2Cl_2) δ 152.3, 143.6, 131.7, 130.7, 119.9, 110.9, 45.4, 42.4, 26.3, 21.8, 19.8, 15.9.

HRMS (GC-CI) (m/z): calculated for $C_{14}H_{19}Br$ $[M]^+$: 266.066475; found: 266.066770.

GC (25 m Lipodex-G, injection temperature: 220 °C, 100 °C iso 80 min, 8 °C/min, 220 °C, 0.6 bar H_2): t_{R1} = 72.5 min (major), t_{R2} = 76.0 min (minor), e.r. = 97:3 (94% e.e.).

$[\alpha]_D^{25}$ = −10.2 (c = 0.41, $CHCl_3$)

(*R*)-1-((allyloxy)methyl)-3-(3,3,4-trimethylpent-4-en-2-yl)benzene (4.59d)

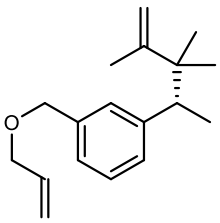

Preparation from 1-(3-((allyloxy)methyl)phenyl)ethyl acetate (**4.58d**, 46.9 mg, 0.20 mmol, 1.0 equiv.) and 2,3-dimethylbut-2-ene (**4.55c**, 134.7 mg, 1.60 mmol, 8.0 equiv.) at −60 °C according to GP8 afforded the title compound as a colorless oil (42.9 mg, 0.17 mmol, 83%) after FCC (silica gel, pentane/Et_2O, 24:1).

^{1}H NMR (501 MHz, $CDCl_3$) δ 7.24 (t, *J* = 7.4 Hz, 1H), 7.19 – 7.15 (m, 2H), 7.11 (dt, *J* = 7.6, 1.6 Hz, 1H), 5.96 (ddt, *J* = 17.2, 10.3, 5.6 Hz, 1H), 5.31 (dq, *J* = 17.2, 1.7 Hz, 1H), 5.20 (dq, *J* = 10.4, 1.3 Hz, 1H), 4.79 (p, *J* = 1.4 Hz, 1H), 4.73 (d, *J* = 1.7 Hz, 1H), 4.52 (s, 2H), 4.02 (dt, *J* = 5.6, 1.4 Hz, 2H), 2.90 (q, *J* = 7.2 Hz, 1H), 1.79 (d, *J* = 1.3 Hz, 3H), 1.15 (d, *J* = 7.2 Hz, 3H), 0.98 (s, 3H), 0.87 (s, 3H).

^{13}C NMR (151 MHz, $CDCl_3$) δ 152.2, 144.2, 137.3, 135.0, 129.2, 129.0, 127.5, 125.7, 117.2, 110.7, 72.5, 71.1, 45.6, 42.3, 26.7, 21.6, 19.8, 15.9.

HRMS (ESI) (m/z): calculated for $C_{18}H_{26}ONa$ $[M+Na]^+$: 281.187584; found: 281.187470.

GC (25 m Lipodex-G, injection temperature: 220 °C, 90 °C iso 340 min, 8 °C/min, 220 °C, 0.6 bar H_2): t_{R1} = 313.3 min (major), t_{R2} = 320.4 min (minor), e.r. = 95:5 (90% e.e.).

$[\alpha]_D^{25}$ = −8.0 (c = 0.38, $CHCl_3$)

(*S*)-4-(4,4-diphenylbut-3-en-2-yl)-2-fluoro-1,1'-biphenyl (4.60e)

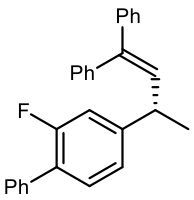

Preparation from 1-(2-fluoro-[1,1'-biphenyl]-4-yl)ethyl acetate (**4.58e**, 51.7 mg, 0.20 mmol, 1.0 equiv.) and 1,1-diphenylethylene (**4.55d**, 288.4 mg, 1.60 mmol, 8.0 equiv.) at −60 °C according to GP8 afforded the title compound as a light yellow viscous oil (46.7 mg, 0.12 mmol, 62%) after FCC (silica gel, pentane).

^{1}H NMR (501 MHz, CD_2Cl_2) δ 7.55 – 7.51 (m, 2H), 7.46 – 7.33 (m, 7H), 7.30 – 7.18 (m, 7H), 7.08 – 6.99 (m, 2H), 6.21 (d, *J* = 10.3 Hz, 1H), 3.63 (dq, *J* = 10.4, 6.8 Hz, 1H), 1.42 (d, *J* = 6.9 Hz, 3H).

^{13}C NMR (126 MHz, CD_2Cl_2) δ 160.2 (d, *J* = 246.7 Hz), 148.5 (d, *J* = 6.7 Hz), 142.7, 141.4, 140.4, 136.2, 133.6, 132.8, 131.0 (d, *J* = 3.8 Hz), 130.3, 130.1, 129.6, 129.3 (d, *J* = 2.8 Hz),

128.8 (d, *J* = 5.9 Hz), 128.7, 128.5, 127.9, 127.6, 127.5, 126.9 (d, *J* = 5.7 Hz), 123.4 (d, *J* = 3.1 Hz), 114.8 (d, *J* = 23.3 Hz), 39.3, 22.3.

^{19}F NMR (471 MHz, CD_2Cl_2) δ -118.88.

HRMS (GC-EI) (m/z): calculated for $C_{28}H_{23}F$ $[M]^+$: 378.177828; found: 378.178010.

HPLC (150 mm Chiralpak IB-N3 column, MeOH/H_2O 90:10, 298 K, 220 nm): t_{R1} (major) = 11.5 min, t_{R2} (minor) = 12.2 min, e.r. = 96:4 (92% e.e.).

$[\alpha]_D^{25}$ = 139.7 (c = 0.48, $CHCl_3$)

(*S*)-(3-(4-isobutylphenyl)but-1-ene-1,1-diyl)dibenzene (4.60f)

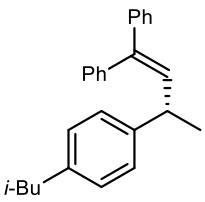

Preparation from 1-(4-isobutylphenyl)ethyl acetate (**4.58f**, 44.1 mg, 0.20 mmol, 1.0 equiv.) and 1,1-diphenylethylene (**4.55d**, 288.4 mg, 1.60 mmol, 8.0 equiv.) at −85 °C according to GP8 afforded the title compound as a colorless oil (19.1 mg, 0.06 mmol, 28%) after FCC (silica gel, pentane).

^{1}H NMR (501 MHz, $CDCl_3$) δ 7.41 – 7.36 (m, 2H), 7.36 – 7.30 (m, 1H), 7.25 – 7.18 (m, 7H), 7.11 (d, *J* = 8.1 Hz, 2H), 7.08 – 7.04 (m, 2H), 6.21 (d, *J* = 10.3 Hz, 1H), 3.57 (dq, *J* = 10.4, 6.9 Hz, 1H), 2.44 (d, *J* = 7.1 Hz, 2H), 1.84 (h, *J* = 6.8 Hz, 1H), 1.37 (d, *J* = 6.9 Hz, 3H), 0.90 (d, *J* = 6.6 Hz, 6H).

^{13}C NMR (151 MHz, $CDCl_3$) δ 143.5, 142.6, 140.3, 140.0, 139.4, 134.7, 130.0, 129.3, 128.4, 128.2, 127.4, 127.1, 127.1, 126.8, 45.2, 39.0, 30.4, 22.6, 22.4.

HRMS (GC-EI) (m/z): calculated for $C_{26}H_{28}$ $[M]^+$: 340.218550; found: 340.218530.

HPLC (150 mm Chiralpak IB-N3 column, MeOH/H_2O 85:15, 298 K, 220 nm): t_{R1} (minor) = 17.3 min, t_{R2} (major) = 18.6 min, e.r. = 95.5:4.5 (91% e.e.).

$[\alpha]_D^{25}$ = 85.9 (c = 0.32, $CHCl_3$)

(*S*,*E*)-1-(2-methylpent-3-en-1-yl)cyclohex-1-ene (4.68a)

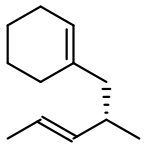

Preparation from pent-3-en-2-yl acetate (**4.67a**, 25.6 mg, 0.20 mmol, 1.0 equiv.) and methylenecyclohexane (**4.2**, 158.9 mg, 1.60 mmol, 8.0 equiv.) at −90 °C according to GP8 afforded the title compound as a colorless oil (13.0 mg, 0.07 mmol, 36%) after FCC (silica gel, pentane; followed by a short plug of SiO_2/$AgNO_3$, pentane/Et_20, 100:0–0:100).

^{1}H NMR (501 MHz, $CDCl_3$) δ 5.41 – 5.29 (m, 3H), 2.28 – 2.19 (m, 1H), 2.01 – 1.76 (m, 6H), 1.65 – 1.63 (m, 3H), 1.63 – 1.57 (m, 2H), 1.56 – 1.50 (m, 2H), 0.90 (d, *J* = 6.7 Hz, 3H).

^{13}C NMR (151 MHz, $CDCl_3$) δ 137.7, 136.5, 122.6, 122.4, 46.2, 34.5, 28.5, 25.5, 23.2, 22.8, 20.1, 18.1.

HRMS (GC-EI) (m/z): calculated for $C_{12}H_{20}$ $[M]^+$: 164.155950; found: 164.155940.

GC (29.5 m BGB-178, injection temperature: 220 °C, 70 °C iso 55 min, 8 °C/min, 230 °C, 0.6 bar H_2): t_{R1} = 45.3 min (major), t_{R2} = 48.0 min (minor), e.r. = 94.5:5.5 (89% e.e.).

$[\alpha]_D^{25}$ = −1.5 (c = 0.14, $CHCl_3$)

(*S*,*E*)-1-(2,3-dimethylpent-3-en-1-yl)cyclohex-1-ene (4.68b)

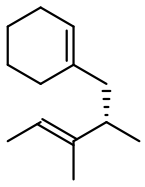

Preparation from (*E*)-3-methylpent-3-en-2-yl acetate (**4.67b**, 28.4 mg, 0.20 mmol, 1.0 equiv.) and methylenecyclohexane (**4.2**, 158.9 mg, 1.60 mmol, 8.0 equiv.) at −80 °C according to GP8 afforded the title compound as a colorless oil (32.0 mg, 0.17 mmol, 82%) after FCC (silica gel, pentane).

^{1}H NMR (501 MHz, $CDCl_3$) δ 5.37 – 5.31 (m, 1H), 5.20 (dddt, *J* = 7.7, 6.6, 5.4, 1.1 Hz, 1H), 2.25 (sext, *J* = 6.9 Hz, 1H), 2.05 – 1.93 (m, 3H), 1.92 – 1.85 (m, *J* = 2.3 Hz, 2H), 1.82 (dd, *J* = 13.4, 8.4 Hz, 1H), 1.63 – 1.47 (m, 11H), 0.91 (d, *J* = 6.9 Hz, 3H).

^{13}C NMR (126 MHz, $CDCl_3$) δ 140.5, 136.9, 122.4, 117.3, 44.5, 40.7, 28.3, 25.5, 23.2, 22.8, 19.1, 13.3, 12.6.

HRMS (APPI) (m/z): calculated for $C_{13}H_{22}$ $[M]^+$: 178.171600; found: 178.171630.

GC (25 m Ivadex-7, injection temperature: 220 °C, 80 °C iso 35 min, 8 °C/min, 230 °C, 0.6 bar H_2): t_{R1} = 26.7 min (minor), t_{R2} = 27.4 min (major), e.r. = 96:4 (92% e.e.).

$[\alpha]_D^{25}$ = −2.1 (c = 0.47, $CHCl_3$)

(*S*,*Z*)-(5-(cyclohex-1-en-1-yl)-4-methylpent-2-en-3-yl)benzene (4.68c)

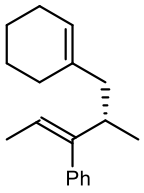

Preparation from (*E*)-3-phenylpent-3-en-2-yl acetate (**4.67c**, 40.9 mg, 0.20 mmol, 1.0 equiv.) and methylenecyclohexane (**4.2**, 158.9 mg, 1.60 mmol, 8.0 equiv.) at −85 °C according to GP8 afforded the title compound as a colorless oil (28.5 mg, 0.12 mmol, 59%) after FCC (silica gel, pentane).

^{1}H NMR (501 MHz, $CDCl_3$) δ 7.33 – 7.29 (m, 2H), 7.25 – 7.21 (m, 1H), 7.10 – 7.07 (m, 2H), 5.51 (qd, *J* = 6.8, 1.1 Hz, 1H), 5.35 (dtt, *J* = 3.8, 2.8, 1.4 Hz, 1H), 2.62 – 2.51 (m, 1H), 2.13 – 2.07 (m, 1H), 1.97 (qd, *J* = 5.7, 3.4 Hz, 2H), 1.93 – 1.85 (m, 1H), 1.77 (td, *J* = 14.5, 6.6 Hz, 2H), 1.61 – 1.49 (m, 4H), 1.46 (dd, *J* = 6.8, 0.8 Hz, 3H), 0.96 (d, *J* = 6.9 Hz, 3H).

^{13}C NMR (126 MHz, $CDCl_3$) δ 147.3, 141.4, 136.5, 129.3, 127.9, 126.3, 122.8, 119.7, 45.0, 39.2, 28.3, 25.5, 23.2, 22.7, 19.4, 14.7.

HRMS (GC-EI) (m/z): calculated for $C_{18}H_{24}$ $[M]^+$: 240.18725; found: 240.18707.

GC (25 m Ivadex-7, injection temperature: 220 °C, 100 °C iso 185 min, 8 °C/min, 230 °C, 0.6 bar H_2): t_{R1} = 169.1 min (minor), t_{R2} = 177.4 min (major), e.r. = 99.5:0.5 (99% e.e.).

$[\alpha]_D^{25}$ = −3.9 (c = 0.51, $CHCl_3$)

(*S*,*E*)-1-(2-methyl-3-vinylpent-3-en-1-yl)cyclohex-1-ene (4.68d)

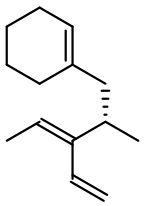

Preparation from (*E*)-3-vinylpent-3-en-2-yl acetate (**4.67d**, 30.8 mg, 0.20 mmol, 1.0 equiv.) and methylenecyclohexane (**4.2**, 158.9 mg, 1.60 mmol, 8.0 equiv.) at −50 °C according to GP8 afforded the title compound as a colorless oil (45.2 mg, 0.14 mmol, 72%) after FCC (SiO_2/$AgNO_3$, pentane/EtOAc, 100:0–95:5).

^{1}H NMR (501 MHz, $CDCl_3$) δ 6.63 (dd, *J* = 17.7, 11.2 Hz, 1H), 5.45 (qdd, *J* = 7.2, 1.6, 0.8 Hz, 1H), 5.37 (ddd, *J* = 5.1, 3.3, 1.9 Hz, 1H), 5.23 (dt, *J* = 17.6, 1.0 Hz, 1H), 5.10 (dt, *J* = 11.3, 1.7 Hz, 1H), 2.62 (dq, *J* = 13.6, 6.6 Hz, 1H), 2.21 – 2.15 (m, 1H), 2.02 – 1.93 (m, 3H), 1.89 – 1.77 (m, 2H), 1.74 (d, *J* = 7.1 Hz, 3H), 1.64 – 1.50 (m, 4H), 0.98 (d, *J* = 6.8 Hz, 3H).

^{13}C NMR (126 MHz, $CDCl_3$) δ 142.6, 136.7, 133.1, 122.6, 121.9, 112.8, 45.7, 32.6, 28.4, 25.5, 23.2, 22.8, 19.7, 13.5.

HRMS (APPI) (m/z): calculated for $C_{14}H_{22}$ $[M]^+$: 190.171600; found: 190.171640.

GC (25 m Ivadex-7, injection temperature: 220 °C, 85 °C iso 55 min, 8 °C/min, 230 °C, 0.6 bar H_2): t_{R1} = 40.3 min (minor), t_{R2} = 42.2 min (major), e.r. = 97:3 (94% e.e.).

$[\alpha]_D^{25}$ = −40.7 (c = 0.24, $CHCl_3$)

(*S*,*Z*)-1-(3-iodo-2-methylpent-3-en-1-yl)cyclohex-1-ene (4.68e)

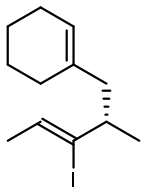

Preparation from (*Z*)-3-iodopent-3-en-2-yl acetate (**4.67e**, 50.8 mg, 0.20 mmol, 1.0 equiv.) and methylenecyclohexane (**4.2**, 158.9 mg, 1.60 mmol, 8.0 equiv.) at −60 °C according to GP8 afforded the title compound as a light pink oil (48.0 mg, 0.17 mmol, 83%) after FCC (silica gel, pentane).

^{1}H NMR (501 MHz, CD_2Cl_2) δ 5.65 (qd, *J* = 6.3, 0.7 Hz, 1H), 5.42 (dtt, *J* = 3.9, 2.8, 1.4 Hz, 1H), 2.20 – 2.05 (m, 2H), 1.96 (dtdt, *J* = 7.3, 3.7, 2.4, 1.2 Hz, 2H), 1.92 – 1.81 (m, 3H), 1.72 (d, *J* = 6.3 Hz, 3H), 1.61 – 1.49 (m, 4H), 0.97 (d, *J* = 6.5 Hz, 3H).

^{13}C NMR (126 MHz, CD_2Cl_2) δ 135.6, 128.2, 123.8, 121.9, 45.9, 44.5, 28.8, 25.7, 23.5, 23.0, 22.0, 21.5.

HRMS (APPI) (m/z): calculated for $C_{12}H_{19}I$ $[M]^+$: 290.052597; found: 290.052460.

GC (25 m Hydrodex-gamma-TBDAc, injection temperature: 220 °C, 100 °C iso 60 min, 8 °C/min, 250 °C, 0.6 bar H_2): t_{R1} = 50.6 min (minor), t_{R2} = 52.5 min (major), e.r. = 98.5:1.5 (97% e.e.).

$[\alpha]_D^{25}$ = 18.9 (c = 0.51, $CHCl_3$)

(*S*,*Z*)-1-(3-bromo-2-methylpent-3-en-1-yl)cyclohex-1-ene (4.68f)

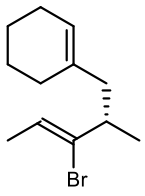

Preparation from (*Z*)-3-bromopent-3-en-2-yl acetate (**4.67f**, 41.4 mg, 0.20 mmol, 1.0 equiv.) and methylenecyclohexane (**4.2**, 158.9 mg, 1.60 mmol, 8.0 equiv.) at −50 °C according to GP8 afforded the title compound as a colorless oil (48.9 mg, 0.20 mmol, quant.) after FCC (silica gel, pentane).

^{1}H NMR (501 MHz, $CDCl_3$) δ 5.71 (q, *J* = 6.4 Hz, 1H), 5.41 (dq, *J* = 3.7, 1.8 Hz, 1H), 2.51 (sext, *J* = 6.9 Hz, 1H), 2.19 (dd, *J* = 13.6, 7.0 Hz, 1H), 2.01 – 1.95 (m, 2H), 1.93 – 1.85 (m, 3H), 1.71 (d, *J* = 6.4 Hz, 3H), 1.62 – 1.50 (m, 4H), 1.04 (d, *J* = 6.6 Hz, 3H).

^{13}C NMR (126 MHz, $CDCl_3$) δ 136.7, 135.5, 123.5, 121.6, 44.5, 42.5, 28.4, 25.5, 23.2, 22.7, 19.8, 16.7.

HRMS (APPI) (m/z): calculated for $C_{12}H_{19}Br$ $[M]^+$: 242.066475; found: 242.066380.

GC (24.5 m Ivadex-1, injection temperature: 220 °C, 100 °C iso 50 min, 8 °C/min, 230 °C, 0.6 bar H_2): t_{R1} = 36.8 min (minor), t_{R2} = 39.2 min (major), e.r. = 98.5:1.5 (97% e.e.).

$[\alpha]_D^{25}$ = 14.1 (c = 0.64, $CHCl_3$)

(*S*)-1,1'-(propane-1,2-diyl)dicyclohex-1-ene (4.68g)

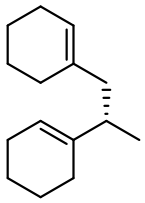

Preparation from 1-(cyclohex-1-en-1-yl)ethyl acetate (**4.67g**, 33.6 mg, 0.20 mmol, 1.0 equiv.) and methylenecyclohexane (**4.2**, 158.9 mg, 1.60 mmol, 8.0 equiv.) at −80 °C according to GP8 afforded the title compound as a colorless oil (36.5 mg, 0.17 mmol, 83%) after FCC (silica gel, pentane).

^{1}H NMR (501 MHz, $CDCl_3$) δ 5.40 – 5.32 (m, 2H), 2.17 (sext, *J* = 6.9 Hz, 1H), 2.06 – 2.00 (m, 1H), 1.97 (pd, *J* = 4.0, 2.8 Hz, 4H), 1.93 – 1.86 (m, 4H), 1.81 (dd, *J* = 13.3, 8.5 Hz, 1H), 1.65 – 1.49 (m, 8H), 0.92 (d, *J* = 6.9 Hz, 3H).

^{13}C NMR (126 MHz, $CDCl_3$) δ 142.4, 136.9, 122.4, 119.9, 44.5, 39.3, 28.3, 25.5, 25.5, 25.4, 23.3, 23.3, 23.0, 22.8, 19.0.

HRMS (APPI) (m/z): calculated for $C_{15}H_{25}$ $[M+H]^+$: 205.19508; found: 205.19502.

GC (24 m Cyclodextrin-H, injection temperature: 220 °C, 60 °C iso 345 min, 8 °C/min, 180 °C, 0.5 bar H_2): t_{R1} = 278.8 min (major), t_{R2} = 304.4 min (minor), e.r. = 97.5:2.5 (95% e.e.).

$[\alpha]_D^{25}$ = −1.8 (c = 0.55, $CHCl_3$)

(*S*,*E*)-1-(2-methylhex-3-en-1-yl)cyclohex-1-ene (4.68h)

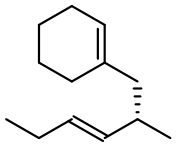

Preparation from (*E*)-hex-3-en-2-yl acetate *or* (*E*)-hex-4-en-3-yl acetate (**4.67h** *or* **4.67h'**, 28.4 mg, 0.20 mmol, 1.0 equiv.) and methylenecyclohexane (**4.2**, 158.9 mg, 1.60 mmol, 8.0 equiv.) at −80 °C according to GP8 afforded the title compound and the regioisomer as a colorless oil (34.5 mg, 0.19 mmol, 96%, r.r. = 9:1 from **4.67h**; 33.9 mg, 0.18 mmol, 91% from **4.67h'**, r.r. = 10:1) after FCC (silica gel, pentane; followed by a short plug of SiO_2/$AgNO_3$, pentane/$Et_2$0, 100:0–0:100).

^{1}H NMR (501 MHz, $CDCl_3$) δ 5.41 – 5.33 (m, 2H), 5.28 (ddt, *J* = 15.3, 7.1, 1.4 Hz, 1H), 2.23 (h, *J* = 6.6 Hz, 1H), 2.02 – 1.79 (m, 7H), 1.66 – 1.50 (m, 5H), 0.95 (t, *J* = 7.5 Hz, 3H), 0.91 (d, *J* = 6.7 Hz, 3H).

^{13}C NMR (126 MHz, $CDCl_3$) δ 136.5, 135.4, 129.8, 122.7, 46.3, 34.5, 28.5, 25.8, 25.5, 23.2, 22.8, 20.3, 14.3.

HRMS (APPI) (m/z): calculated for $C_{13}H_{22}$ $[M]^+$: 178.171600; found: 178.171660.

GC (25 m Ivadex-7, injection temperature: 220 °C, 60 °C iso 120 min, 8 °C/min, 230 °C, 0.6 bar H_2): t_{R1} = 100.0 min (major), t_{R2} = 108.8 min (minor), e.r. = 89.5:10.5 (79% e.e.).

$[\alpha]_D^{25}$ = 2.4 (c = 0.49, $CHCl_3$)

(*S*,*E*)-1-(2-methylhept-3-en-1-yl)cyclohex-1-ene (4.68i)

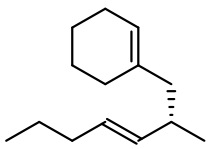

Preparation from (*E*)-hept-3-en-2-yl acetate (**4.67i**, 31.2 mg, 0.20 mmol, 1.0 equiv.) and methylenecyclohexane (**4.2**, 158.9 mg, 1.60 mmol, 8.0 equiv.) at −80 °C according to GP8 afforded the title compound and the regioisomer as a colorless oil (36.9 mg, 0.19 mmol, 96%, r.r. = 20:1) after FCC (silica gel, pentane; followed by a short plug of SiO_2/$AgNO_3$, pentane/$Et_2$0, 100:0–0:100).

^{1}H NMR (501 MHz, $CDCl_3$) δ 5.37 – 5.24 (m, 3H), 2.24 (h, *J* = 6.9 Hz, 1H), 2.01 – 1.79 (m, 7H), 1.64 – 1.49 (m, 5H), 1.35 (sextd, *J* = 7.3, 1.5 Hz, 2H), 0.91 (d, *J* = 6.7 Hz, 3H), 0.88 (t, *J* = 7.4 Hz, 3H).

^{13}C NMR (126 MHz, $CDCl_3$) δ 136.6, 136.5, 128.0, 122.6, 46.4, 34.9, 34.7, 28.5, 25.5, 23.2, 23.0, 22.8, 20.4, 13.7.

HRMS (APPI) (m/z): calculated for $C_{14}H_{24}$ $[M]^+$: 192.187250; found: 192.187380.

GC (24 m Cyclodextrin-H, injection temperature: 220 °C, 65 °C iso 55 min, 8 °C/min, 180 °C, 0.5 bar H_2): t_{R1} = 48.0 min (major), t_{R2} = 50.6 min (minor), e.r. = 88.5:11.5 (77% e.e.).

$[\alpha]_D^{25}$ = −1.2 (c = 0.51, $CHCl_3$)

(*S*,*E*)-1-(2-methyloct-3-en-1-yl)cyclohex-1-ene (4.68j)

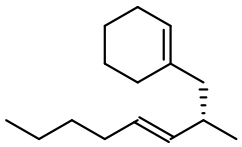

Preparation from (*E*)-oct-2-en-4-yl acetate (**4.67j'**, 34.0 mg, 0.20 mmol, 1.0 equiv.) and methylenecyclohexane (**4.2**, 158.9 mg, 1.60 mmol, 8.0 equiv.) at −80 °C according to GP8 afforded the title compound and the regioisomer as a colorless oil (43.3 mg, 0.20 mmol, 98%, r.r. = 17:1) after FCC (silica gel, pentane; followed by a short plug of SiO_2/$AgNO_3$, pentane/Et_20, 100:0–0:100).

^{1}H NMR (501 MHz, $CDCl_3$) δ 5.38 – 5.22 (m, 3H), 2.24 (h, *J* = 6.8 Hz, 1H), 2.01 – 1.77 (m, 7H), 1.65 – 1.49 (m, 5H), 1.34 – 1.23 (m, 4H), 0.93 – 0.84 (m, 6H).

^{13}C NMR (126 MHz, $CDCl_3$) δ 136.5, 136.4, 128.2, 122.6, 46.4, 34.7, 32.4, 32.0, 28.5, 25.5, 23.2, 22.8, 22.2, 20.4, 14.1.

HRMS (APPI) (m/z): calculated for $C_{15}H_{26}$ $[M]^+$: 206.202900; found: 206.202970.

GC (24 m Cyclodextrin-H, injection temperature: 220 °C, 75 °C iso 60 min, 8 °C/min, 180 °C, 0.5 bar H_2): t_{R1} = 51.2 min (major), t_{R2} = 53.9 min (minor), e.r. = 88.5:11.5 (77% e.e.).

$[\alpha]_D^{25}$ = −0.4 (c = 0.50, $CHCl_3$)

(*S*,*E*)-1-(2,3-dimethylhex-3-en-1-yl)cyclohex-1-ene (4.68k)

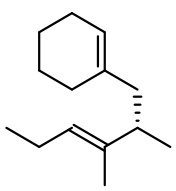

Preparation from (*E*)-4-methylhex-4-en-3-yl acetate (**4.67k'**, 31.2 mg, 0.20 mmol, 1.0 equiv.) and methylenecyclohexane (**4.2**, 158.9 mg, 1.60 mmol, 8.0 equiv.) at −80 °C according to GP8 afforded the title compound as a colorless

oil (38.6 mg, 0.19 mmol, 95%, r.r. = >20:1) after FCC (silica gel, pentane; followed by a short plug of $SiO_2/AgNO_3$, pentane/Et_20, 100:0–0:100).

^{1}H NMR (501 MHz, $CDCl_3$) δ 5.34 (ddt, *J* = 5.3, 3.7, 1.4 Hz, 1H), 5.11 (ddt, *J* = 7.0, 5.9, 1.2 Hz, 1H), 2.24 (sext, *J* = 6.7 Hz, 1H), 2.03 – 1.91 (m, 5H), 1.91 – 1.86 (m, 2H), 1.83 (dd, *J* = 13.6, 8.1 Hz, 1H), 1.62 – 1.49 (m, 7H), 0.92 (t, *J* = 7.5 Hz, 3H), 0.92 (d, *J* = 6.9 Hz, 3H).

^{13}C NMR (126 MHz, $CDCl_3$) δ 138.8, 136.9, 125.6, 122.3, 44.5, 40.7, 28.3, 25.5, 23.2, 22.8, 21.1, 19.2, 14.6, 12.6.

HRMS (APPI) (m/z): calculated for $C_{14}H_{24}$ $[M]^+$: 192.187250; found: 192.187390.

GC (25 m Ivadex-7, injection temperature: 220 °C, 80 °C iso 50 min, 8 °C/min, 230 °C, 0.6 bar H_2): t_{R1} = 41.9 min (minor), t_{R2} = 44.5 min (major), e.r. = 91.5:8.5 (83% e.e.).

$[\alpha]_D^{25}$ = −8.8 (c = 0.48, $CHCl_3$)

7.6. Two-Step, One-Pot Process

7.6.1. *Development of the Two-Step, One-Pot Process*

Screening reactions for IDPi-catalyzed acetylation

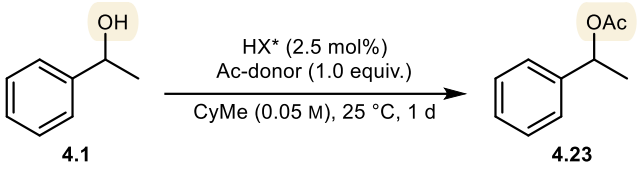

In a screw cap GC vial under an argon atmosphere, IDPi catalyst **4.3a** (5.0 µmol, 2.5 mol%) was dissolved in CyMe (0.4 mL, 0.05 M). Acyl donor (0.02 mmol, 1.0 equiv.) and 1-phenylethanol (**4.1**, 2.4 mg, 0.02 mmol, 1.0 equiv.) were added, and the reaction was stirred at 25 °C for 16 h. An aliquot of the reaction mixture was analyzed by ^{1}H NMR to determine conversion to **4.23**.

Method for the two-step, one-pot process

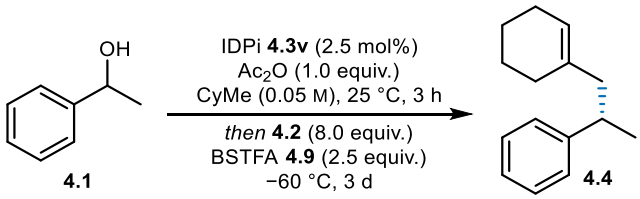

In an oven-dried screw cap GC vial under an argon atmosphere, IDPi catalyst **4.3v** (5.0 µmol, 2.5 mol%) was dissolved in CyMe (0.4 mL, 0.05 M). Ac_2O (2.04 mg, 0.02 mmol, 1.0 equiv.) and 1-phenylethanol (**4.1**, 2.4 mg, 0.02 mmol, 1.0 equiv.) were added, and the reaction was stirred at 25 °C for 3 h. The reaction was then cooled to −60 °C, and methylenecyclohexane (**4.2**, 15.4 mg, 0.16 mmol, 8.0 equiv.) and BSTFA (**4.9**, 0.05 mmol, 2.5 equiv.) were added in rapid succession through the screw cap. The cap was sealed with grease and the reaction was stirred at the same temperature for 3 d, after which it was quenched by the addition of Et_3N (1.0 µL, 7.2 µmol, 0.4 equiv.). Mesitylene (2.8 µL, 0.02 mmol, 1.0 equiv.) was added as an internal standard, and the mixture was analyzed by ^1H NMR. The mixture was filtered through a short silica plug and washed with pentane. The filtrate was subjected to GC analysis.

7.6.2. *Scale-Up of the Two-Step, One-Pot Process*

Method for the scale-up of the two-step, one-pot process

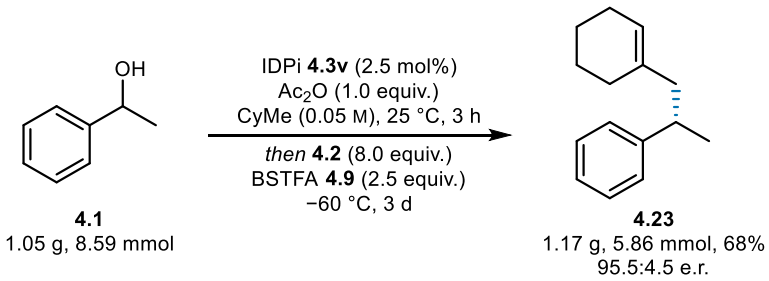

In an oven-dried, double walled Schlenk flask under an argon atmosphere connected to a cryostat, IDPi catalyst **4.3v** (506.7 mg, 0.21 mmol, 2.5 mol%) was dissolved in CyMe (172 mL). Ac_2O (0.88 g, 8.59 mmol, 1.0 equiv.) and 1-phenylethanol (**4.1**, 1.05 g, 8.59 mmol, 1.0 equiv.) were added, and the reaction was stirred at 25 °C for 2 h. The reaction was then cooled to −60 °C, after which methylenecyclohexane (**4.2**, 6.61 g, 68.70 mmol, 8.0 equiv.) and BSTFA (**4.9**, 5.53 g, 21.47 mmol, 2.5 equiv.) were added in rapid succession. The reaction was stirred at the same temperature for 3 d, after which it was quenched by the addition of Et_3N (100.0 mg,

0.99 mol, 0.08 equiv.). The crude mixture was then subjected to FCC (silica gel, pentane) to afford **4.4** as a colorless oil (1.17 g, 5.86 mmol, 68%, 95.5:4.5 e.r.).

7.7. Product Derivatization

7.7.1. *Oxidative Cleavage toward Flurbiprofen*

(*R*)-flurbiprofen (4.61)

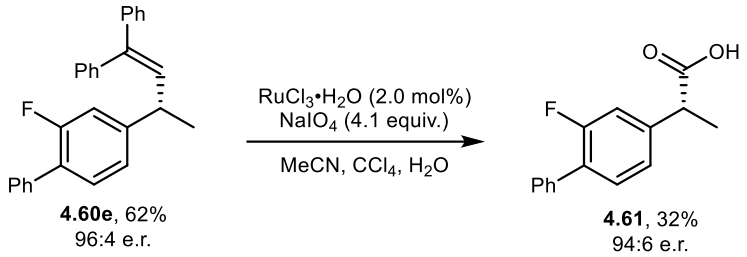

4.60e, 62%
96:4 e.r.

4.61, 32%
94:6 e.r.

Following a modified procedure by Bäckvall and coworkers.[278] Product **4.60e** (25.0 mg, 6.6 µmol, 1.0 equiv.), $RuCl_3•H_2O$ (0.27 mg, 1.3 µmol, 2.0 mol%), $NaIO_4$ (57.9 mg, 0.27 mmol, 4.1 equiv.), MeCN (0.13 mL), CCl_4 (0.13 mL), and H_2O (0.20 mL) were charged in a 25 mL round-bottom flask and stirred under ambient conditions. The reaction was followed by TLC analysis (pentane/EtOAc, 95:5). Upon completion, CH_2Cl_2 (25 mL) was added. The product was extracted with $NaHCO_3$ (3 × 20 mL). The combined aqueous phase was acidified with 2 M HCl solution until it became cloudy, and extracted again with CH_2Cl_2 (3x). The combined organic phase was dried over Na_2SO_4 and concentrated in vacuo. Benzoic acid was removed from the mixture by sublimation under high vacuum (80 °C, 3.4×10^{-2} mbar) to afford the title compound as a white solid (3.8 mg, 15.5 µmol, 23%). The spectroscopic data were in accordance with the literature.[326]

^{1}H NMR (501 MHz, CD_2Cl_2) δ 7.55 – 7.52 (m, 1H), 7.46 – 7.34 (m, 2H), 7.20 (dd, *J* = 7.9, 1.8 Hz, 1H), 7.16 (dd, *J* = 11.7, 1.8 Hz, 1H), 3.82 (q, *J* = 7.2 Hz, 1H), 1.55 (d, *J* = 7.2 Hz, 2H).

GC (24.5 m Ivadex-1, injection temperature: 220 °C, 60 °C iso 0 min, 1 °C/min, 230 °C, 0.5 bar H_2): t_{R1} = 151.4 min (minor), t_{R2} = 152.5 min (major), e.r. = 94:6 (88% e.e.).

7.7.2. *Cyclization Efforts toward Galaxolide Analogs*

Method for screening cyclization conditions using acid catalysis

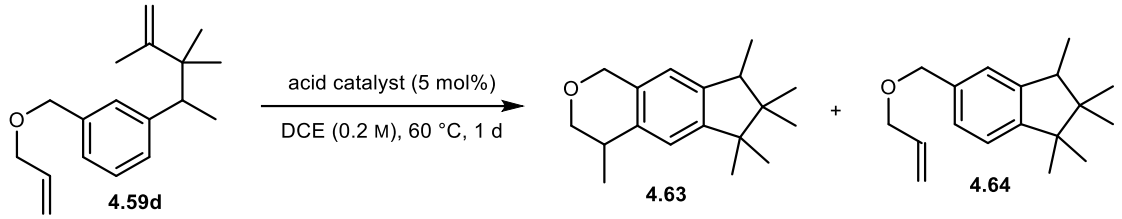

In a screw cap GC vial under an argon atmosphere, the acid catalyst (1.0 µmol, 5 mol%) and DCE (0.1 mL, 0.2 M) were added. Product **4.59d** (5.2 mg, 20.0 µmol, 1.0 equiv.) was added, and the reaction was stirred at 60 °C for 1 d. The reaction was then quenched by the addition of Et_3N (1.0 µL, 7.2 µmol, 0.4 equiv.). Mesitylene (2.8 µL, 0.02 mmol, 1.0 equiv.) was added as an internal standard, and the mixture was analyzed by ^1H NMR and GC/MS.

Method for screening cyclization conditions using Co-salen catalysis

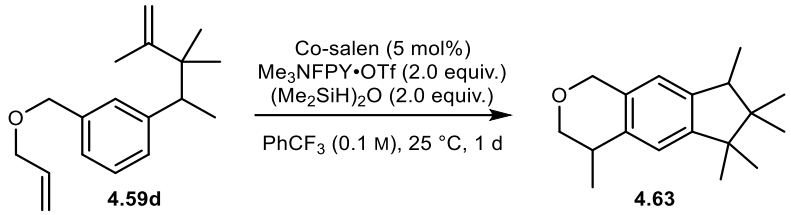

In a screw cap GC vial under an argon atmosphere, Co-salen complex (0.6 µmol, 3.0 mol%) and *N*-fluoro-2,4,6-trimethylpyridinium trifluoromethanesulfonate (11.6 mg, 40.0 µmol, 2.0 equiv.) were added. After being dried under high vacuum (3.4×10^{-2} mbar) for 30 minutes, trifluorotoluene (0.2 mL, 0.1 M) and product **4.59d** (5.2 mg, 20.0 µmol, 1.0 equiv.) were added. The solution was sparged with argon gas for 10 minutes, after which 1,1,3,3-tetramethyldisiloxane (7.1 µL, 40.0 µmol, 2.0 equiv.) was added. The resulting mixture was stirred at 25 °C for 1 d. The reaction mixture was diluted with EtOAc. The organic phase was washed with water and brine, dried over Na_2SO_4, and concentrated in vacuo. The resulting crude mixture was analyzed by ^1H NMR and GC/MS.

7.7.3. *Heck Cyclization*

Method for attempted 5-*endo* Heck cyclization

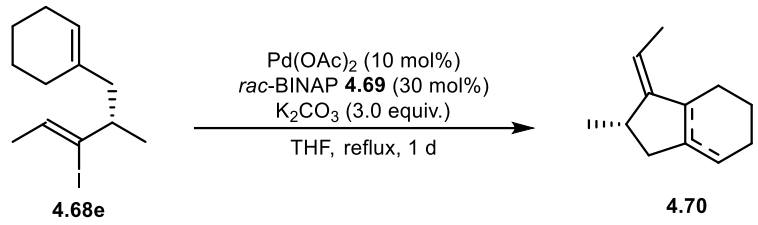

In a flame-dried Schlenk flask under an argon atmosphere, $Pd(OAc)_2$ (1.1 mg, 5.0 µmol, 10 mol%), *rac*-BINAP (9.3 mg, 15.0 µmol, 30 mol%) and product **4.68e** (14.5 mg, 50.0 µmol, 1.0 equiv.) were dissolved in degassed THF (1.0 mL), and the mixture was refluxed for 1 d. After cooling to 25 °C, the reaction was quenched by the addition of water. The mixture was transferred to an extraction funnel and extracted with Et_2O (3x). The combined organic phase was washed with brine, dried over Na_2SO_4, and concentrated in vacuo. The obtained residue was analyzed by ^1H NMR and GC/MS.

Method for screening carbonylative Heck cyclization conditions

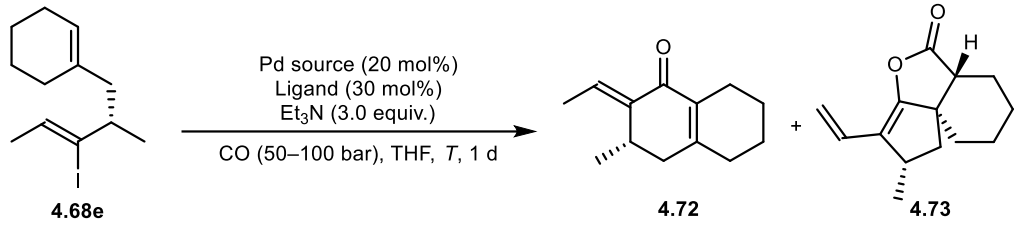

In an oven-dried screw cap vial under an argon atmosphere, the Pd source (10.0 µmol, 20 mol%), phosphine ligand (15.0 µmol, 30 mol%) and product **4.68e** (14.5 mg, 50.0 µmol, 1.0 equiv.) were dissolved in degassed THF (0.5 mL), and the mixture was refluxed for 1 d. After cooling to 25 °C, the reaction was quenched by the addition of water. The mixture was transferred to an extraction funnel and extracted with Et_2O (3x). The combined organic phase was washed with brine, dried over Na_2SO_4, and concentrated in vacuo. The obtained residue was subjected to FCC (silica gel, hexane/EtOAc, 98:2–95:5), and the obtained product mixtures were analyzed by ^1H NMR and GC/MS.

(*S*,*E*)-2-ethylidene-3-methyl-3,4,5,6,7,8-hexahydronaphthalen-1(2*H*)-one (4.72)

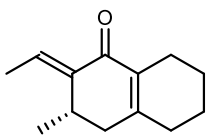

^{1}H NMR (600 MHz, $CDCl_3$) δ 6.71 (qt, *J* = 7.2, 0.7 Hz, 1H), 3.25 – 3.16 (m, 1H), 2.66 – 2.57 (m, 1H), 2.27 (q, *J* = 3.5 Hz, 2H), 2.18 – 2.13 (m, 2H), 2.01 (ddt, *J* = 17.9, 1.7, 0.9 Hz, 1H), 1.78 (d, *J* = 7.2 Hz, 3H), 1.60 – 1.49 (m, 2H), 1.06 (dd, *J* = 7.1, 0.4 Hz, 2H), 0.86 (d, *J* = 6.7 Hz, 3H).

^{13}C NMR (151 MHz, $CDCl_3$) δ 187.7, 153.5, 140.2, 132.2, 131.6, 37.9, 32.6, 29.1, 22.6, 22.4, 22.3, 20.5, 13.3.

HRMS (GC-EI) (m/z): calculated for $C_{13}H_{18}O$ $[M]^+$: 190.135215; found: 190.135480.

(2*S*,5a*R*,9a*R*)-2-methyl-3-vinyl-1,2,6,7,8,9-hexahydrocyclopenta[*c*]isobenzofuran-5(5a*H*)-one (4.73)

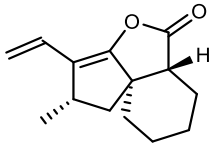

^{1}H NMR (600 MHz, $CDCl_3$) δ 6.47 (dddd, *J* = 17.5, 11.1, 0.7, 0.4 Hz, 1H), 5.13 (dd, *J* = 17.6, 1.5 Hz, 1H), 5.12 (dd, *J* = 11.0, 1.5 Hz, 1H), 3.14 (dqt, *J* = 8.7, 7.2, 0.7 Hz, 1H), 2.48 – 2.45 (m, 1H), 2.19 – 2.14 (m, 1H), 2.07 (ddd, *J* = 12.8, 9.1, 1.5 Hz, 1H), 1.82 – 1.77 (m, 1H), 1.75 (dt, *J* = 12.8, 0.5 Hz, 1H), 1.69 – 1.63 (m, 2H), 1.53 (dddd, *J* = 14.2, 13.1, 6.1, 4.6 Hz, 1H), 1.36 (tdd, *J* = 13.7, 3.0, 1.5 Hz, 1H), 1.30 (d, *J* = 7.2 Hz, 3H), 1.20 – 1.18 (m, 2H).

^{13}C NMR (151 MHz, $CDCl_3$) δ 177.9, 153.8, 127.2, 115.4, 114.5, 50.8, 49.8, 41.2, 39.0, 34.0, 22.5, 22.0, 21.5, 21.4.

HRMS (GC-EI) (m/z): calculated for $C_{14}H_{18}O_2$ $[M]^+$: 218.130130; found: 218.130360.

Note: the enantiospecificity of the reactions was not determined due to overlapping peaks of diastereomeric products in chiral GC measurements.

7.8. Mechanistic Experiments

7.8.1. *KIE Experiment*

Method for the intermolecular competition KIE experiment

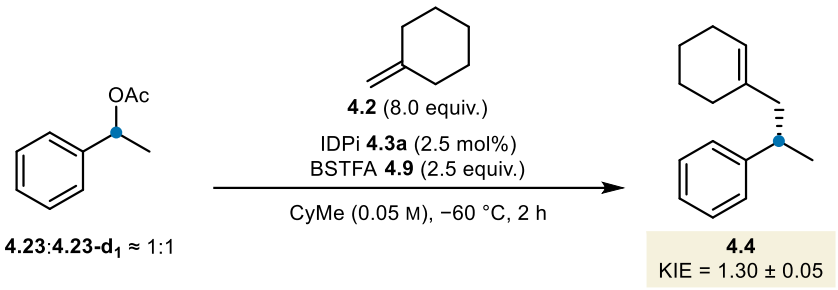

In a screw cap 10 mL glass vial, IDPi catalyst **4.3a** (4.47 mg, 2.5 µmol, 2.5 mol%) was dissolved in CyMe (2.0 mL, 0.05 M), and the reaction vessel was briefly flushed with argon and sealed. BSTFA (**4.9**, 66.1 µL, 0.25 mmol, 2.5 equiv.) and methylenecyclohexane (**4.2** 76.9 mg, 0.80 mmol, 8.0 equiv.) were sequentially added. The mixture was cooled to −60 °C, a pre-mixed ~1:1 mixture of **4.23** and **4.23-d1** (16.4 mg, 0.10 mmol, 1.0 equiv.) was added and the cap was sealed with grease. The reaction was stirred at the same temperature for 2 h, after which it was quenched by the addition of Et_3N (5.0 µL, 35.9 µmol, 0.4 equiv.). DCE (7.9 µL, 0.10 mmol, 1.0 equiv.) was added as an internal standard and an aliquot of the crude mixture was analyzed by ^1H NMR to determine conversion to the product. The crude mixture was then subjected to FCC (silica gel, pentane), and the product **4.4**/**4.4-d1**, as well as the starting mixture of **4.23**/**4.23-d1** were subjected to GC/MS to determine the isotopic ratios.

Representative NMR- and GC/MS spectra for conversion and isotope ratio analysis are shown in Figure 7.1 and Figure 7.2. Clean conversion to the product was assumed, as well as a ±2% error in the conversion.

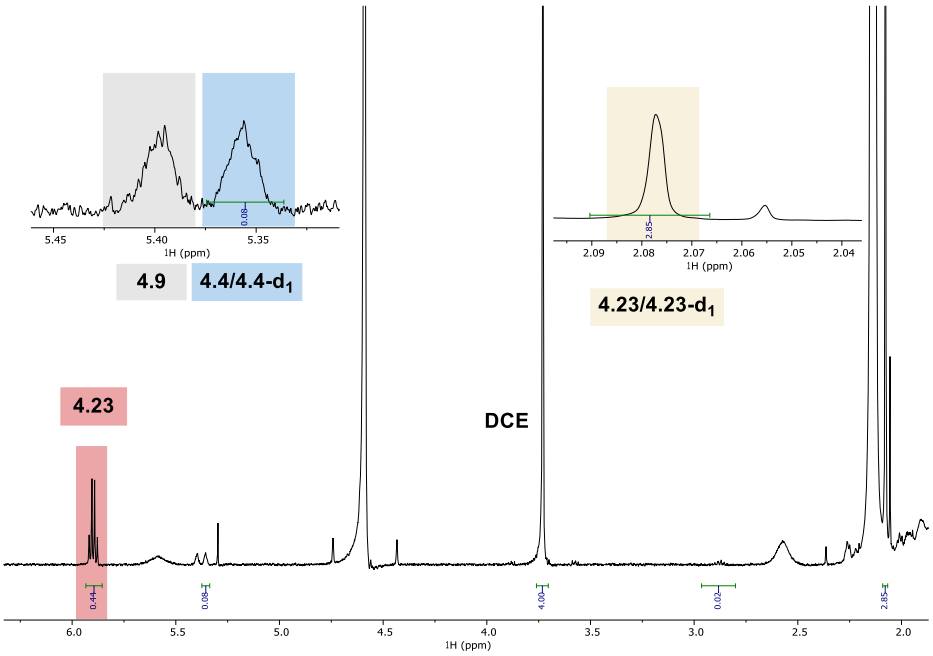

Figure 7.1 Representative ^{1}H NMR analysis of KIE experiment.

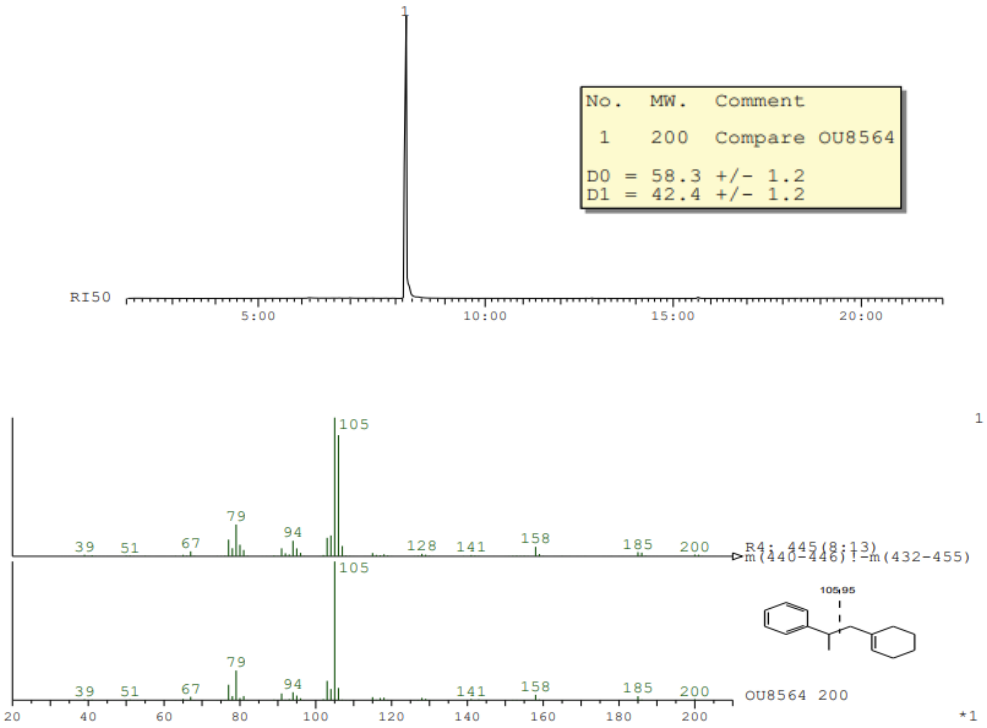

Figure 7.2 Determination of isotopic ratios of isolated **4.4** by GC/MS.

7.8.2. *Reactions with Enantiopure Acetates*

(*R*)-**4.23** and (*S*)-**4.23** were prepared from their respective alcohol precursors according to GP1. Analysis by chiral GC (Figure 7.3) revealed that the acetates were obtained in near-enantiopure form:

GC (29.5 m BGB-178, injection temperature: 220 °C, 130 °C iso 8 min, 8 °C/min, 230 °C, 0.5 bar H_2): t_{R1} = 5.8 min, t_{R2} = 6.2 min, e.r.$_{(R)}$ = 99.5:0.5 (99% e.e.), e.r.$_{(S)}$ = 99.5:0.5 (99% e.e.).

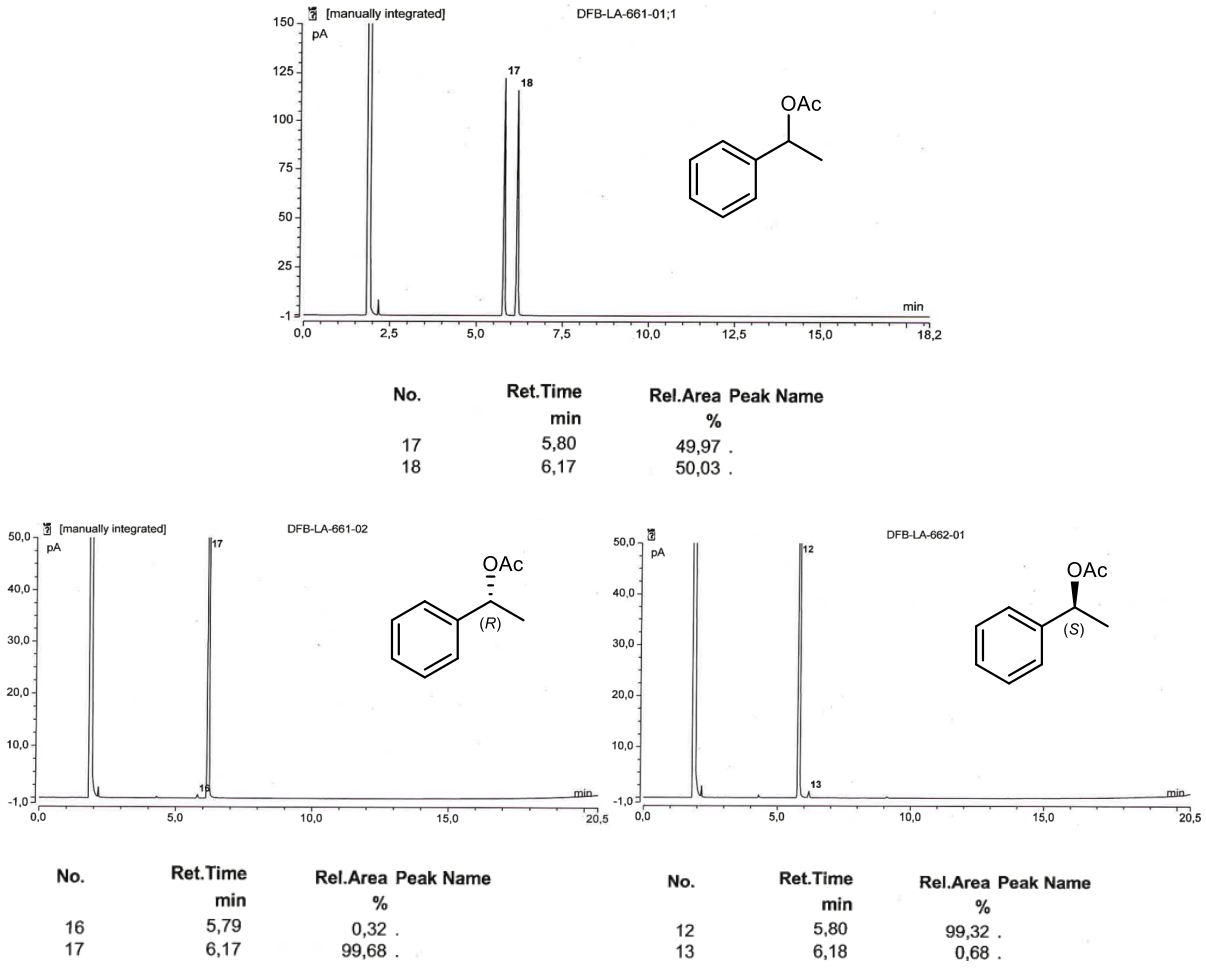

Figure 7.3 Chiral GC traces of *rac*-**4.23**, (*R*)-**4.23** and (*S*)-**4.23**.

Method for reactions with enantiopure acetates

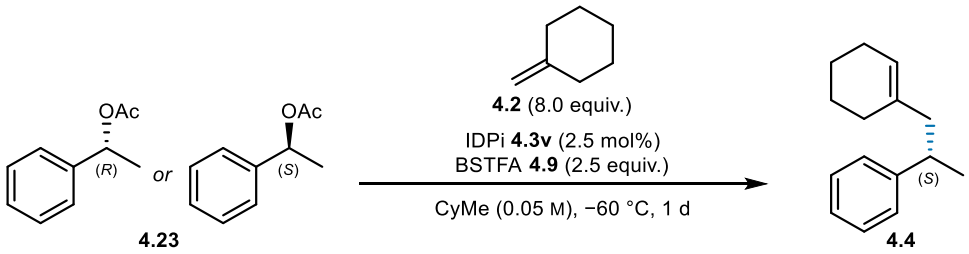

In a screw cap 1 mL glass GC vial, IDPi catalyst **4.3v** (1.18 mg, 0.5 µmol, 2.5 mol%) was dissolved in CyMe (0.4 mL, 0.05 M), and the reaction vessel was briefly flushed with argon and sealed. BSTFA (**4.9**, 13.2 µL, 0.05 mmol, 2.5 equiv.) and methylenecyclohexane (**4.2**, 15.9 mg, 0.16 mmol, 8.0 equiv.) were sequentially added. The mixture was cooled to −60 °C, the respective acetate (3.3 mg, 0.02 mmol, 1.0 equiv.) was added through the cap, and the cap was sealed with grease. The reaction was stirred at the same temperature for 1 d, after which it was quenched by the addition of Et_3N (1.0 µL, 7.2 µmol, 0.4 equiv.). Mesitylene (2.8 µL, 0.02 mmol, 1.0 equiv.) was added as an internal standard, and the mixture was analyzed by ^1H NMR spectroscopy to determine the conversion and yield of the product. The product **4.4** and starting acetate were isolated by PTLC (pentane/Et_2O, 19:1) and subjected to chiral GC analysis (Figure 7.4).

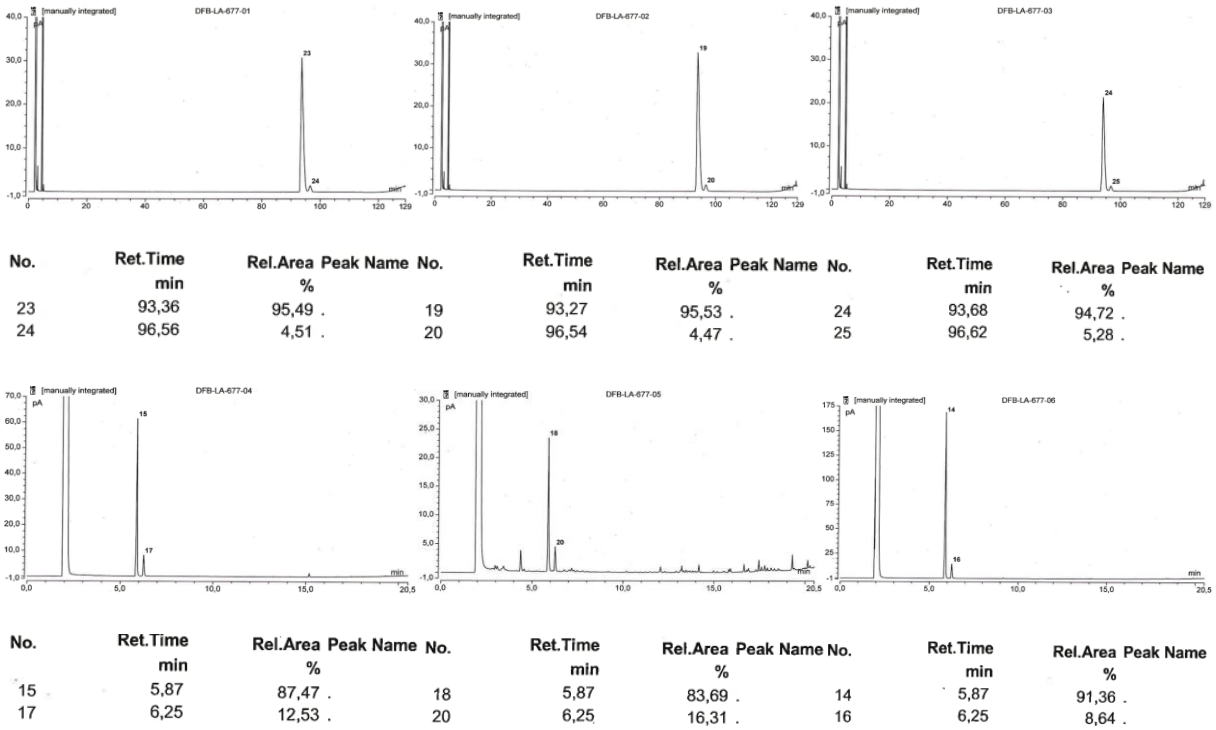

No.	Ret.Time min	Rel.Area %	Peak Name	No.	Ret.Time min	Rel.Area %	Peak Name	No.	Ret.Time min	Rel.Area %	Peak Name
23	93,36	95,49		19	93,27	95,53		24	93,68	94,72	
24	96,56	4,51		20	96,54	4,47		25	96,62	5,28	

No.	Ret.Time min	Rel.Area %	Peak Name	No.	Ret.Time min	Rel.Area %	Peak Name	No.	Ret.Time min	Rel.Area %	Peak Name
15	5,87	87,47		18	5,87	83,69		14	5,87	91,36	
17	6,25	12,53		20	6,25	16,31		16	6,25	8,64	

Figure 7.4 Chiral GC traces of reactions with *rac*-**4.23** (left), (*R*)-**4.23** (middle) or (*S*)-**4.23** (right). Top: reaction products **4.4**, bottom: starting material **4.23**.

7.8.3. *Leaving Group Scrambling Studies*

Method for the leaving group scrambling experiment

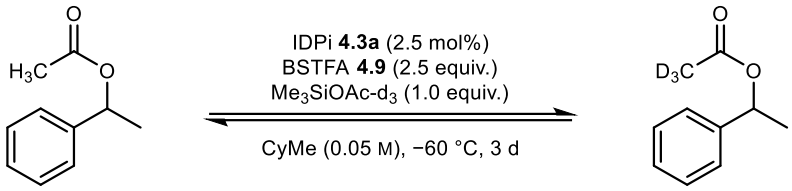

In a flame-dried Schlenk flask under an argon atmosphere, BSTFA (**4.9**, 264.3 µL, 1.00 mmol, 2.5 equiv.), DCE internal standard (31.5 µL, 0.40 mmol, 1.0 equiv.) and 1-phenylethyl acetate (**4.23**, 3.3 mg, 0.02 mmol, 1.0 equiv.) were dissolved in CyMe (8.0 mL), and the mixture was cooled to −60 °C. $Me_3SiOAc\text{-}d_3$ (60.8 µL, 0.40 mmol, 1.0 equiv.) and IDPi catalyst **4.3a** (40 mM stock solution in $CHCl_3$, 250 µL, 10 µmol, 2.5 mol%) were then added. The reaction was stirred at the same temperature for 3 d, during which 200 µL aliquots were taken with a 200 µL Gilson pipette. The aliquots were immediately quenched in a GC vial containing Et_3N (10 µL) cooled to −78 °C. The aliquots were then analyzed by ^1H NMR spectroscopy (Figure 7.5).

Representative ^1H NMR analysis of aliquots taken during the leaving group scrambling experiment is shown below.

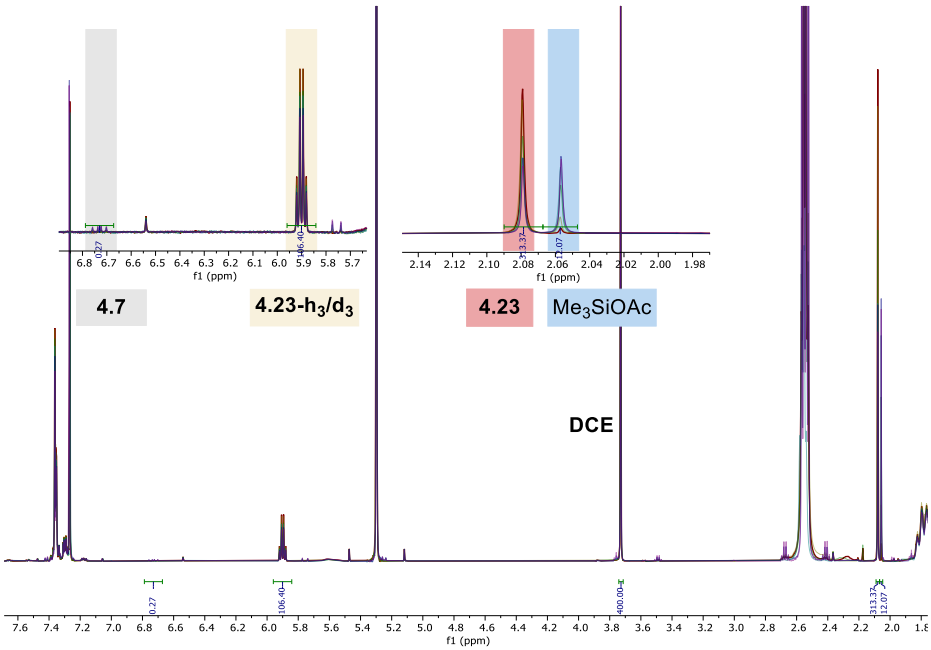

Figure 7.5 Representative ^1H NMR analysis of the leaving group scrambling experiment.

7.8.4. *Reaction Monitoring and Inhibition Studies*

Method for reaction monitoring and inhibition studies

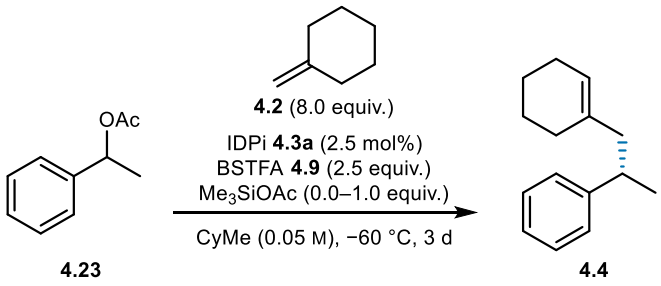

Stock solution preparation: In a flame-dried Schlenk flask under an argon atmosphere, CyMe (28.0 mL), BSTFA (**4.9**, 925.0 µL, 2.5 equiv.), methylenecyclohexane (**4.2**, 1.35 µL, 8.0 equiv.), 1-phenylethyl acetate (**4.23**, 229.9 mg, 1.0 equiv.), and DCE internal standard (110.3 µL, 1.0 equiv.) were added, and the mixture was stirred at 25 °C for 10 minutes.

In a flame-dried Schlenk flask under an argon atmosphere, 8.75 mL of the above stock solution was added, followed by Me_3SiOAc (0.0–1.0 equiv.), and the mixture was cooled to −60 °C. IDPi catalyst **4.3a** (50 mM stock solution in CH_2Cl_2, 200 µL, 10 µmol, 2.5 mol%) was then added. The reaction was stirred at the same temperature for 3 d, during which 200 µL aliquots were taken with a 200 µL Gilson pipette. The aliquots were immediately quenched in a GC vial containing Et_3N (10 µL) cooled to −78 °C. The aliquots were then analyzed by ^1H NMR spectroscopy. The e.r. of **4.4** was monitored by filtering the respective aliquots over a short plug of silica and washing (pentane/Et_2O, 19:1). The resulting filtrates were submitted to chiral GC analysis.

Representative ^1H NMR analysis of aliquots taken during reaction monitoring and inhibition studies is shown in Figure 7.6.

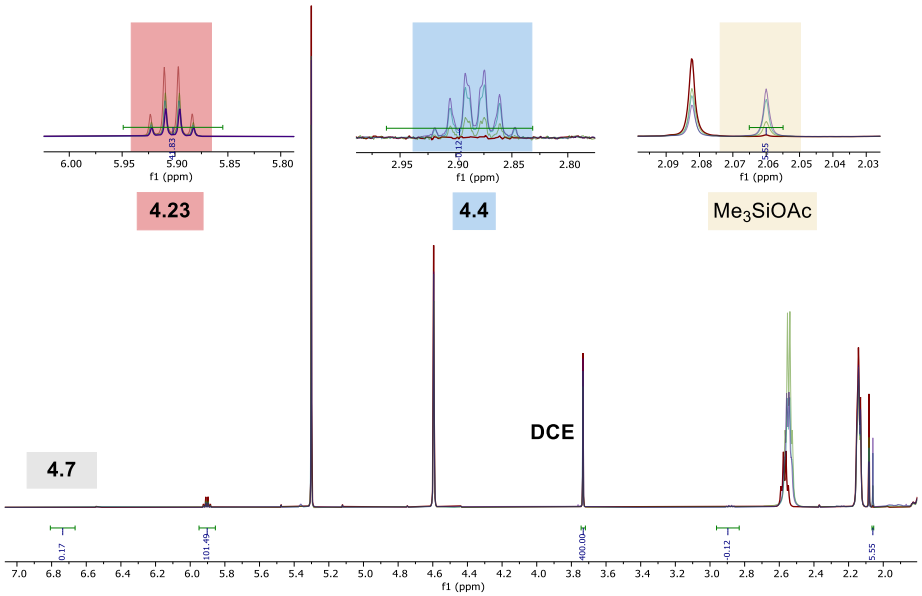

Figure 7.6 Representative ^{1}H NMR analysis of reaction monitoring and inhibition experiments.

7.9. Crystallographic Data

X-Ray data for IDPi 4.3v

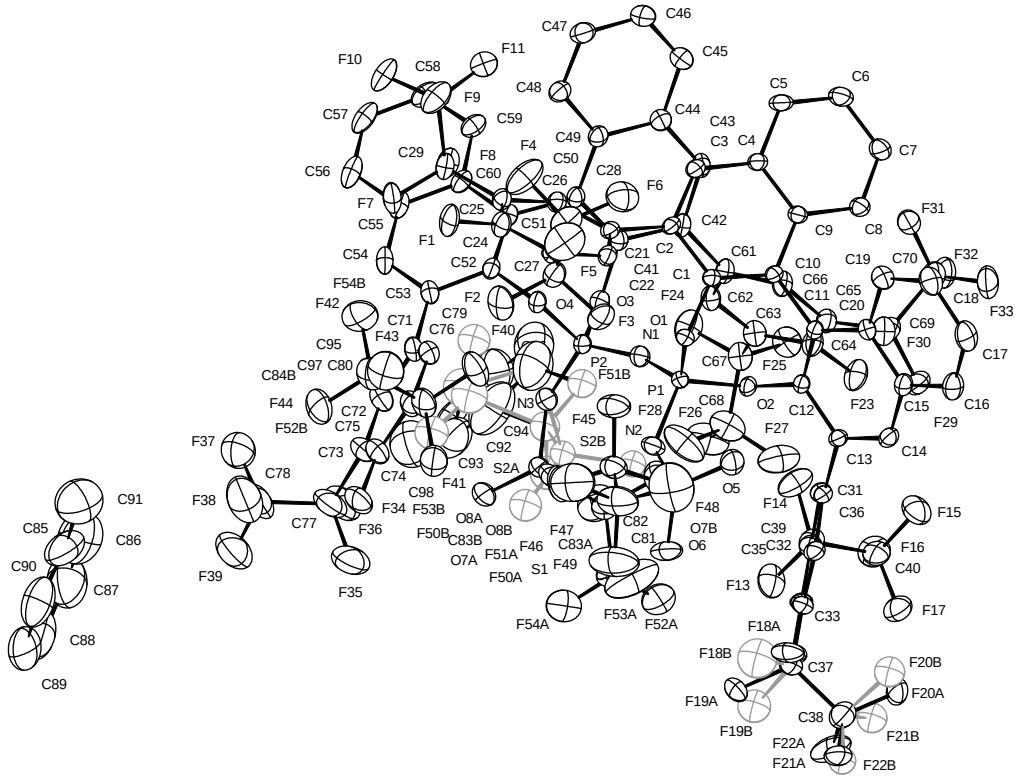

Figure 7.7 The molecular structure of IDPi **4.3v**. H atoms have been removed for clarity and disordered parts are shown in grey.

Table 7.1 Crystal data and structure refinement of IDPi **4.3v**.

Identification code	16468	
Empirical formula	$C_{98}\ H_{45}\ F_{54}\ N_3\ O_8\ P_2\ S_2$	
Color	colourless	
Formula weight	2544.43 $g \cdot mol^{-1}$	
Temperature	100(2) K	
Wavelength	0.71073 Å	
Crystal system	Orthorhombic	
Space group	$P2_12_12$, (no. 18)	
Unit cell dimensions	a = 25.4629(8) Å	α= 90°.
	b = 27.7424(9) Å	β= 90°.
	c = 14.0665(3) Å	γ = 90°.
Volume	9936.6(5) $Å^3$	
Z	4	
Density (calculated)	1.701 $Mg \cdot m^{-3}$	
Absorption coefficient	0.247 mm^{-1}	
F(000)	5064 e	
Crystal size	0.144 x 0.112 x 0.100 mm^3	
θ range for data collection	2.062 to 29.575°.	
Index ranges	$-35 \le h \le 35$, $-38 \le k \le 38$, $-17 \le l \le 19$	
Reflections collected	430656	
Independent reflections	27896 [R_{int} = 0.0558]	
Reflections with I>2σ(I)	25336	
Completeness to θ = 25.242°	99.9 %	
Absorption correction	Gaussian	
Max. and min. transmission	0.98282 and 0.97746	
Refinement method	Full-matrix least-squares on F^2	
Data / restraints / parameters	27896 / 181 / 1567	
Goodness-of-fit on F^2	1.127	
Final R indices [I>2σ(I)]	R_1 = 0.0497	wR^2 = 0.1383
R indices (all data)	R_1 = 0.0562	wR^2 = 0.1450
Absolute structure parameter	-0.010(11)	
Extinction coefficient	n/a	
Largest diff. peak and hole	0.822 and -0.630 $e \cdot Å^{-3}$	

Table 7.2 Bond lengths [Å] and angles [°] of IDPi **4.3v**.

S(1)-O(5)	1.420(3)	S(1)-O(6)	1.428(3)
S(1)-N(2)	1.623(3)	S(1)-C(81)	1.839(4)
P(1)-O(1)	1.581(2)	P(1)-O(2)	1.573(2)
P(1)-N(1)	1.523(3)	P(1)-N(2)	1.648(3)
P(2)-O(3)	1.586(2)	P(2)-O(4)	1.587(2)
P(2)-N(1)	1.555(3)	P(2)-N(3)	1.576(3)
F(1)-C(24)	1.339(3)	F(2)-C(27)	1.347(4)
F(3)-C(27)	1.362(4)	F(4)-C(28)	1.317(5)
F(5)-C(28)	1.324(4)	F(6)-C(28)	1.334(6)
F(7)-C(29)	1.350(4)	F(8)-C(29)	1.363(4)
F(9)-C(30)	1.330(4)	F(10)-C(30)	1.335(4)
F(11)-C(30)	1.321(5)	F(12)-C(34)	1.336(4)
F(13)-C(39)	1.349(4)	F(14)-C(39)	1.357(5)
F(15)-C(40)	1.328(5)	F(16)-C(40)	1.335(5)
F(17)-C(40)	1.325(5)	F(23)-C(64)	1.340(4)
F(24)-C(67)	1.358(4)	F(25)-C(67)	1.356(4)
F(26)-C(68)	1.338(5)	F(27)-C(68)	1.328(6)
F(28)-C(68)	1.315(6)	F(29)-C(69)	1.360(4)
F(30)-C(69)	1.373(4)	F(31)-C(70)	1.317(5)
F(32)-C(70)	1.321(5)	F(33)-C(70)	1.323(5)
F(34)-C(74)	1.344(5)	F(35)-C(77)	1.374(7)
F(36)-C(77)	1.356(8)	F(37)-C(78)	1.331(7)
F(38)-C(78)	1.285(10)	F(39)-C(78)	1.346(8)
F(40)-C(79)	1.351(5)	F(41)-C(79)	1.360(5)
F(42)-C(80)	1.334(6)	F(43)-C(80)	1.340(6)
F(44)-C(80)	1.330(6)	F(45)-C(81)	1.328(4)
F(46)-C(81)	1.344(6)	F(47)-C(82)	1.312(7)
F(48)-C(82)	1.327(9)	F(49)-C(82)	1.313(7)
O(1)-C(1)	1.418(3)	O(2)-C(12)	1.416(3)
O(3)-C(41)	1.403(4)	O(4)-C(52)	1.404(4)
N(2)-H(2)	0.8800	N(3)-S(2A)	1.539(3)
N(3)-S(2B)	1.475(10)	C(1)-C(2)	1.422(4)
C(1)-C(10)	1.378(4)	C(2)-C(3)	1.375(4)
C(2)-C(21)	1.489(4)	C(3)-H(3)	0.9500
C(3)-C(4)	1.416(4)	C(4)-C(5)	1.423(4)
C(4)-C(9)	1.420(4)	C(5)-H(5)	0.9500

C(5)-C(6)	1.369(5)	C(6)-H(6)	0.9500
C(6)-C(7)	1.413(5)	C(7)-H(7)	0.9500
C(7)-C(8)	1.372(4)	C(8)-H(8)	0.9500
C(8)-C(9)	1.425(4)	C(9)-C(10)	1.435(4)
C(10)-C(11)	1.489(4)	C(11)-C(12)	1.366(4)
C(11)-C(20)	1.436(4)	C(12)-C(13)	1.408(4)
C(13)-C(14)	1.371(4)	C(13)-C(31)	1.487(4)
C(14)-H(14)	0.9500	C(14)-C(15)	1.415(5)
C(15)-C(16)	1.417(4)	C(15)-C(20)	1.424(4)
C(16)-H(16)	0.9500	C(16)-C(17)	1.366(6)
C(17)-H(17)	0.9500	C(17)-C(18)	1.410(6)
C(18)-H(18)	0.9500	C(18)-C(19)	1.368(5)
C(19)-H(19)	0.9500	C(19)-C(20)	1.420(4)
C(21)-C(22)	1.394(4)	C(21)-C(26)	1.400(4)
C(22)-H(22)	0.9500	C(22)-C(23)	1.388(4)
C(23)-C(24)	1.385(5)	C(23)-C(27)	1.513(5)
C(24)-C(25)	1.393(4)	C(25)-C(26)	1.395(4)
C(25)-C(29)	1.509(4)	C(26)-H(26)	0.9500
C(27)-C(28)	1.546(6)	C(29)-C(30)	1.542(5)
C(31)-C(32)	1.396(4)	C(31)-C(36)	1.387(5)
C(32)-H(32)	0.9500	C(32)-C(33)	1.392(5)
C(33)-C(34)	1.381(6)	C(33)-C(37)	1.515(5)
C(34)-C(35)	1.400(5)	C(35)-C(36)	1.389(4)
C(35)-C(39)	1.513(5)	C(36)-H(36)	0.9500
C(37)-C(38)	1.542(6)	C(37)-F(18A)	1.394(6)
C(37)-F(19A)	1.325(5)	C(37)-F(18B)	1.05(3)
C(37)-F(19B)	1.59(2)	C(38)-F(20A)	1.275(6)
C(38)-F(21A)	1.355(6)	C(38)-F(22A)	1.331(6)
C(38)-F(20B)	1.51(2)	C(38)-F(21B)	1.387(18)
C(38)-F(22B)	1.11(2)	C(39)-C(40)	1.536(6)
C(41)-C(42)	1.423(4)	C(41)-C(50)	1.379(4)
C(42)-C(43)	1.372(5)	C(42)-C(61)	1.483(4)
C(43)-H(43)	0.9500	C(43)-C(44)	1.412(5)
C(44)-C(45)	1.417(5)	C(44)-C(49)	1.424(4)
C(45)-H(45)	0.9500	C(45)-C(46)	1.368(6)
C(46)-H(46)	0.9500	C(46)-C(47)	1.410(6)
C(47)-H(47)	0.9500	C(47)-C(48)	1.380(5)
C(48)-H(48)	0.9500	C(48)-C(49)	1.426(4)

C(49)-C(50)	1.433(4)	C(50)-C(51)	1.491(4)
C(51)-C(52)	1.376(4)	C(51)-C(60)	1.435(4)
C(52)-C(53)	1.416(4)	C(53)-C(54)	1.368(5)
C(53)-C(71)	1.491(5)	C(54)-H(54)	0.9500
C(54)-C(55)	1.424(5)	C(55)-C(56)	1.423(5)
C(55)-C(60)	1.428(5)	C(56)-H(56)	0.9500
C(56)-C(57)	1.361(7)	C(57)-H(57)	0.9500
C(57)-C(58)	1.399(6)	C(58)-H(58)	0.9500
C(58)-C(59)	1.375(5)	C(59)-H(59)	0.9500
C(59)-C(60)	1.428(5)	C(61)-C(62)	1.401(5)
C(61)-C(66)	1.385(4)	C(62)-H(62)	0.9500
C(62)-C(63)	1.396(5)	C(63)-C(64)	1.388(5)
C(63)-C(67)	1.516(5)	C(64)-C(65)	1.389(5)
C(65)-C(66)	1.397(5)	C(65)-C(69)	1.502(5)
C(66)-H(66)	0.9500	C(67)-C(68)	1.530(6)
C(69)-C(70)	1.539(5)	C(71)-C(72)	1.394(5)
C(71)-C(76)	1.389(5)	C(72)-H(72)	0.9500
C(72)-C(73)	1.399(6)	C(73)-C(74)	1.358(7)
C(73)-C(77)	1.530(7)	C(74)-C(75)	1.395(6)
C(75)-C(76)	1.398(5)	C(75)-C(79)	1.507(6)
C(76)-H(76)	0.9500	C(77)-C(78)	1.521(9)
C(79)-C(80)	1.534(7)	C(81)-C(82)	1.536(7)
S(2A)-O(7A)	1.453(4)	S(2A)-O(8A)	1.424(3)
S(2A)-C(83A)	1.849(5)	F(50A)-C(83A)	1.337(6)
F(51A)-C(83A)	1.372(7)	F(52A)-C(84A)	1.342(8)
F(53A)-C(84A)	1.288(9)	F(54A)-C(84A)	1.263(8)
C(83A)-C(84A)	1.531(8)	S(2B)-O(7B)	1.53(3)
S(2B)-O(8B)	1.38(4)	S(2B)-C(83B)	1.81(5)
F(50B)-C(83B)	1.32(6)	F(51B)-C(83B)	1.30(6)
F(52B)-C(84B)	1.50(7)	F(53B)-C(84B)	1.22(8)
F(54B)-C(84B)	1.24(7)	C(83B)-C(84B)	1.76(9)
C(92)-C(93)	1.351(11)	C(92)-C(97)	1.406(12)
C(92)-C(98)	1.499(13)	C(93)-H(93)	0.9500
C(93)-C(94)	1.417(15)	C(94)-H(94)	0.9500
C(94)-C(95)	1.316(16)	C(95)-H(95)	0.9500
C(95)-C(96)	1.420(15)	C(96)-H(96)	0.9500
C(96)-C(97)	1.334(12)	C(97)-H(97)	0.9500
C(98)-H(98A)	0.9800	C(98)-H(98B)	0.9800

C(98)-H(98C)	0.9800	C(85)-C(86)	1.376(15)
C(85)-C(90)	1.350(14)	C(85)-C(91)	1.503(12)
C(86)-H(86)	0.9500	C(86)-C(87)	1.343(16)
C(87)-H(87)	0.9500	C(87)-C(88)	1.333(17)
C(88)-H(88)	0.9500	C(88)-C(89)	1.388(15)
C(89)-H(89)	0.9500	C(89)-C(90)	1.411(13)
C(90)-H(90)	0.9500	C(91)-H(91A)	0.9800
C(91)-H(91B)	0.9800	C(91)-H(91C)	0.9800

O(5)-S(1)-O(6)	122.90(19)	O(5)-S(1)-N(2)	109.19(16)
O(5)-S(1)-C(81)	107.92(19)	O(6)-S(1)-N(2)	108.43(17)
O(6)-S(1)-C(81)	105.26(18)	N(2)-S(1)-C(81)	100.89(19)
O(1)-P(1)-N(2)	103.35(14)	O(2)-P(1)-O(1)	106.73(12)
O(2)-P(1)-N(2)	112.07(14)	N(1)-P(1)-O(1)	117.72(14)
N(1)-P(1)-O(2)	106.20(15)	N(1)-P(1)-N(2)	110.83(15)
O(4)-P(2)-O(3)	104.05(12)	N(1)-P(2)-O(3)	111.30(14)
N(1)-P(2)-O(4)	105.22(14)	N(1)-P(2)-N(3)	120.96(16)
N(3)-P(2)-O(3)	102.26(15)	N(3)-P(2)-O(4)	111.94(15)
C(1)-O(1)-P(1)	115.27(19)	C(12)-O(2)-P(1)	122.30(19)
C(41)-O(3)-P(2)	117.82(19)	C(52)-O(4)-P(2)	116.80(19)
P(1)-N(1)-P(2)	161.0(2)	S(1)-N(2)-P(1)	130.15(19)
S(1)-N(2)-H(2)	114.9	P(1)-N(2)-H(2)	114.9
S(2A)-N(3)-P(2)	129.4(2)	S(2B)-N(3)-P(2)	137.0(4)
O(1)-C(1)-C(2)	117.2(2)	C(10)-C(1)-O(1)	118.3(2)
C(10)-C(1)-C(2)	124.5(3)	C(1)-C(2)-C(21)	121.8(3)
C(3)-C(2)-C(1)	116.8(3)	C(3)-C(2)-C(21)	120.5(3)
C(2)-C(3)-H(3)	119.2	C(2)-C(3)-C(4)	121.7(3)
C(4)-C(3)-H(3)	119.2	C(3)-C(4)-C(5)	120.8(3)
C(3)-C(4)-C(9)	120.1(3)	C(9)-C(4)-C(5)	119.1(3)
C(4)-C(5)-H(5)	119.7	C(6)-C(5)-C(4)	120.7(3)
C(6)-C(5)-H(5)	119.7	C(5)-C(6)-H(6)	120.0
C(5)-C(6)-C(7)	120.1(3)	C(7)-C(6)-H(6)	120.0
C(6)-C(7)-H(7)	119.6	C(8)-C(7)-C(6)	120.8(3)
C(8)-C(7)-H(7)	119.6	C(7)-C(8)-H(8)	119.9
C(7)-C(8)-C(9)	120.3(3)	C(9)-C(8)-H(8)	119.9
C(4)-C(9)-C(10)	119.1(3)	C(8)-C(9)-C(4)	118.9(3)
C(8)-C(9)-C(10)	122.0(3)	C(1)-C(10)-C(9)	117.3(3)
C(1)-C(10)-C(11)	120.5(3)	C(9)-C(10)-C(11)	122.2(3)

C(12)-C(11)-C(10)	121.2(3)	C(12)-C(11)-C(20)	117.8(3)
C(20)-C(11)-C(10)	120.8(3)	C(11)-C(12)-O(2)	118.8(2)
C(11)-C(12)-C(13)	124.6(3)	C(13)-C(12)-O(2)	116.6(2)
C(12)-C(13)-C(31)	121.9(3)	C(14)-C(13)-C(12)	117.5(3)
C(14)-C(13)-C(31)	120.6(3)	C(13)-C(14)-H(14)	119.3
C(13)-C(14)-C(15)	121.4(3)	C(15)-C(14)-H(14)	119.3
C(14)-C(15)-C(16)	120.7(3)	C(14)-C(15)-C(20)	119.9(3)
C(16)-C(15)-C(20)	119.4(3)	C(15)-C(16)-H(16)	119.6
C(17)-C(16)-C(15)	120.8(3)	C(17)-C(16)-H(16)	119.6
C(16)-C(17)-H(17)	120.1	C(16)-C(17)-C(18)	119.8(3)
C(18)-C(17)-H(17)	120.1	C(17)-C(18)-H(18)	119.5
C(19)-C(18)-C(17)	120.9(3)	C(19)-C(18)-H(18)	119.5
C(18)-C(19)-H(19)	119.6	C(18)-C(19)-C(20)	120.8(3)
C(20)-C(19)-H(19)	119.6	C(15)-C(20)-C(11)	118.7(3)
C(19)-C(20)-C(11)	123.1(3)	C(19)-C(20)-C(15)	118.2(3)
C(22)-C(21)-C(2)	119.2(3)	C(22)-C(21)-C(26)	118.8(3)
C(26)-C(21)-C(2)	121.5(3)	C(21)-C(22)-H(22)	119.4
C(23)-C(22)-C(21)	121.3(3)	C(23)-C(22)-H(22)	119.4
C(22)-C(23)-C(27)	119.8(3)	C(24)-C(23)-C(22)	118.8(3)
C(24)-C(23)-C(27)	121.1(3)	F(1)-C(24)-C(23)	119.3(3)
F(1)-C(24)-C(25)	119.1(3)	C(23)-C(24)-C(25)	121.6(3)
C(24)-C(25)-C(26)	118.7(3)	C(24)-C(25)-C(29)	120.3(3)
C(26)-C(25)-C(29)	120.9(3)	C(21)-C(26)-H(26)	119.6
C(25)-C(26)-C(21)	120.8(3)	C(25)-C(26)-H(26)	119.6
F(2)-C(27)-F(3)	107.1(3)	F(2)-C(27)-C(23)	112.0(3)
F(2)-C(27)-C(28)	108.1(3)	F(3)-C(27)-C(23)	110.1(3)
F(3)-C(27)-C(28)	106.4(3)	C(23)-C(27)-C(28)	112.9(3)
F(4)-C(28)-F(5)	108.6(4)	F(4)-C(28)-F(6)	108.1(4)
F(4)-C(28)-C(27)	110.9(3)	F(5)-C(28)-F(6)	108.4(4)
F(5)-C(28)-C(27)	111.5(4)	F(6)-C(28)-C(27)	109.2(3)
F(7)-C(29)-F(8)	106.4(3)	F(7)-C(29)-C(25)	111.8(3)
F(7)-C(29)-C(30)	108.0(3)	F(8)-C(29)-C(25)	110.0(3)
F(8)-C(29)-C(30)	105.9(3)	C(25)-C(29)-C(30)	114.2(3)
F(9)-C(30)-F(10)	108.1(3)	F(9)-C(30)-C(29)	110.6(3)
F(10)-C(30)-C(29)	110.3(3)	F(11)-C(30)-F(9)	109.0(3)
F(11)-C(30)-F(10)	108.6(3)	F(11)-C(30)-C(29)	110.2(3)
C(32)-C(31)-C(13)	119.0(3)	C(36)-C(31)-C(13)	121.3(3)
C(36)-C(31)-C(32)	119.6(3)	C(31)-C(32)-H(32)	119.8

C(33)-C(32)-C(31)	120.5(3)	C(33)-C(32)-H(32)	119.8
C(32)-C(33)-C(37)	118.8(4)	C(34)-C(33)-C(32)	119.0(3)
C(34)-C(33)-C(37)	122.1(3)	F(12)-C(34)-C(33)	119.2(3)
F(12)-C(34)-C(35)	119.3(4)	C(33)-C(34)-C(35)	121.4(3)
C(34)-C(35)-C(39)	123.0(3)	C(36)-C(35)-C(34)	118.7(3)
C(36)-C(35)-C(39)	118.2(3)	C(31)-C(36)-C(35)	120.7(3)
C(31)-C(36)-H(36)	119.6	C(35)-C(36)-H(36)	119.6
C(33)-C(37)-C(38)	116.2(3)	C(33)-C(37)-F(19B)	102.7(8)
C(38)-C(37)-F(19B)	86.4(8)	F(18A)-C(37)-C(33)	109.2(3)
F(18A)-C(37)-C(38)	102.8(4)	F(19A)-C(37)-C(33)	112.4(4)
F(19A)-C(37)-C(38)	110.7(3)	F(19A)-C(37)-F(18A)	104.4(3)
F(18B)-C(37)-C(33)	110.6(16)	F(18B)-C(37)-C(38)	128.9(17)
F(18B)-C(37)-F(19B)	103(2)	F(20A)-C(38)-C(37)	112.8(4)
F(20A)-C(38)-F(21A)	111.0(5)	F(20A)-C(38)-F(22A)	110.4(4)
F(21A)-C(38)-C(37)	106.4(4)	F(22A)-C(38)-C(37)	111.2(4)
F(22A)-C(38)-F(21A)	104.6(4)	F(20B)-C(38)-C(37)	91.9(9)
F(21B)-C(38)-C(37)	114.2(8)	F(21B)-C(38)-F(20B)	95.6(11)
F(22B)-C(38)-C(37)	125.8(12)	F(22B)-C(38)-F(20B)	110.7(14)
F(22B)-C(38)-F(21B)	111.8(14)	F(13)-C(39)-F(14)	107.4(3)
F(13)-C(39)-C(35)	112.0(3)	F(13)-C(39)-C(40)	107.7(3)
F(14)-C(39)-C(35)	109.2(3)	F(14)-C(39)-C(40)	106.5(3)
C(35)-C(39)-C(40)	113.7(3)	F(15)-C(40)-F(16)	107.9(3)
F(15)-C(40)-C(39)	110.3(3)	F(16)-C(40)-C(39)	110.8(3)
F(17)-C(40)-F(15)	108.7(3)	F(17)-C(40)-F(16)	108.1(3)
F(17)-C(40)-C(39)	111.0(3)	O(3)-C(41)-C(42)	116.6(3)
C(50)-C(41)-O(3)	119.4(3)	C(50)-C(41)-C(42)	123.9(3)
C(41)-C(42)-C(61)	121.9(3)	C(43)-C(42)-C(41)	117.4(3)
C(43)-C(42)-C(61)	120.5(3)	C(42)-C(43)-H(43)	119.1
C(42)-C(43)-C(44)	121.8(3)	C(44)-C(43)-H(43)	119.1
C(43)-C(44)-C(45)	121.0(3)	C(43)-C(44)-C(49)	119.6(3)
C(45)-C(44)-C(49)	119.4(3)	C(44)-C(45)-H(45)	119.7
C(46)-C(45)-C(44)	120.6(3)	C(46)-C(45)-H(45)	119.7
C(45)-C(46)-H(46)	119.8	C(45)-C(46)-C(47)	120.4(3)
C(47)-C(46)-H(46)	119.8	C(46)-C(47)-H(47)	119.8
C(48)-C(47)-C(46)	120.4(4)	C(48)-C(47)-H(47)	119.8
C(47)-C(48)-H(48)	119.8	C(47)-C(48)-C(49)	120.4(3)
C(49)-C(48)-H(48)	119.8	C(44)-C(49)-C(48)	118.4(3)
C(44)-C(49)-C(50)	119.4(3)	C(48)-C(49)-C(50)	122.2(3)

C(41)-C(50)-C(49)	117.4(3)	C(41)-C(50)-C(51)	119.1(3)
C(49)-C(50)-C(51)	123.4(3)	C(52)-C(51)-C(50)	119.8(3)
C(52)-C(51)-C(60)	117.6(3)	C(60)-C(51)-C(50)	122.3(3)
O(4)-C(52)-C(53)	117.5(3)	C(51)-C(52)-O(4)	118.0(3)
C(51)-C(52)-C(53)	124.5(3)	C(52)-C(53)-C(71)	121.5(3)
C(54)-C(53)-C(52)	117.8(3)	C(54)-C(53)-C(71)	120.7(3)
C(53)-C(54)-H(54)	119.4	C(53)-C(54)-C(55)	121.1(3)
C(55)-C(54)-H(54)	119.4	C(54)-C(55)-C(56)	120.3(3)
C(54)-C(55)-C(60)	120.1(3)	C(56)-C(55)-C(60)	119.6(3)
C(55)-C(56)-H(56)	119.7	C(57)-C(56)-C(55)	120.5(4)
C(57)-C(56)-H(56)	119.7	C(56)-C(57)-H(57)	119.8
C(56)-C(57)-C(58)	120.5(3)	C(58)-C(57)-H(57)	119.8
C(57)-C(58)-H(58)	119.5	C(59)-C(58)-C(57)	121.0(4)
C(59)-C(58)-H(58)	119.5	C(58)-C(59)-H(59)	119.7
C(58)-C(59)-C(60)	120.5(4)	C(60)-C(59)-H(59)	119.7
C(55)-C(60)-C(51)	118.9(3)	C(59)-C(60)-C(51)	123.3(3)
C(59)-C(60)-C(55)	117.8(3)	C(62)-C(61)-C(42)	120.5(3)
C(66)-C(61)-C(42)	120.8(3)	C(66)-C(61)-C(62)	118.4(3)
C(61)-C(62)-H(62)	119.4	C(63)-C(62)-C(61)	121.1(3)
C(63)-C(62)-H(62)	119.4	C(62)-C(63)-C(67)	119.8(3)
C(64)-C(63)-C(62)	118.8(3)	C(64)-C(63)-C(67)	121.3(3)
F(23)-C(64)-C(63)	119.0(3)	F(23)-C(64)-C(65)	119.8(3)
C(65)-C(64)-C(63)	121.2(3)	C(64)-C(65)-C(66)	118.8(3)
C(64)-C(65)-C(69)	122.1(3)	C(66)-C(65)-C(69)	118.7(3)
C(61)-C(66)-C(65)	121.4(3)	C(61)-C(66)-H(66)	119.3
C(65)-C(66)-H(66)	119.3	F(24)-C(67)-C(63)	109.7(3)
F(24)-C(67)-C(68)	105.9(3)	F(25)-C(67)-F(24)	106.5(3)
F(25)-C(67)-C(63)	111.0(3)	F(25)-C(67)-C(68)	107.6(3)
C(63)-C(67)-C(68)	115.7(3)	F(26)-C(68)-C(67)	110.0(4)
F(27)-C(68)-F(26)	107.1(4)	F(27)-C(68)-C(67)	111.3(4)
F(28)-C(68)-F(26)	108.4(4)	F(28)-C(68)-F(27)	109.2(4)
F(28)-C(68)-C(67)	110.7(4)	F(29)-C(69)-F(30)	105.5(3)
F(29)-C(69)-C(65)	113.4(3)	F(29)-C(69)-C(70)	108.3(3)
F(30)-C(69)-C(65)	109.7(3)	F(30)-C(69)-C(70)	106.5(3)
C(65)-C(69)-C(70)	113.0(3)	F(31)-C(70)-F(32)	109.9(3)
F(31)-C(70)-F(33)	108.4(3)	F(31)-C(70)-C(69)	109.4(3)
F(32)-C(70)-F(33)	109.3(3)	F(32)-C(70)-C(69)	109.0(3)
F(33)-C(70)-C(69)	110.9(3)	C(72)-C(71)-C(53)	120.6(3)

C(76)-C(71)-C(53)	120.2(3)	C(76)-C(71)-C(72)	119.1(4)
C(71)-C(72)-H(72)	119.8	C(71)-C(72)-C(73)	120.4(4)
C(73)-C(72)-H(72)	119.8	C(72)-C(73)-C(77)	118.7(5)
C(74)-C(73)-C(72)	119.5(4)	C(74)-C(73)-C(77)	121.7(4)
F(34)-C(74)-C(73)	119.7(4)	F(34)-C(74)-C(75)	118.6(4)
C(73)-C(74)-C(75)	121.7(4)	C(74)-C(75)-C(76)	118.5(4)
C(74)-C(75)-C(79)	123.0(4)	C(76)-C(75)-C(79)	118.4(4)
C(71)-C(76)-C(75)	120.7(4)	C(71)-C(76)-H(76)	119.7
C(75)-C(76)-H(76)	119.7	F(35)-C(77)-C(73)	111.6(4)
F(35)-C(77)-C(78)	108.0(5)	F(36)-C(77)-F(35)	105.6(6)
F(36)-C(77)-C(73)	110.7(4)	F(36)-C(77)-C(78)	107.3(5)
C(78)-C(77)-C(73)	113.2(6)	F(37)-C(78)-F(39)	107.1(5)
F(37)-C(78)-C(77)	108.6(5)	F(38)-C(78)-F(37)	108.9(7)
F(38)-C(78)-F(39)	111.9(5)	F(38)-C(78)-C(77)	110.7(6)
F(39)-C(78)-C(77)	109.5(7)	F(40)-C(79)-F(41)	107.2(3)
F(40)-C(79)-C(75)	111.0(3)	F(40)-C(79)-C(80)	106.1(4)
F(41)-C(79)-C(75)	112.6(4)	F(41)-C(79)-C(80)	106.8(3)
C(75)-C(79)-C(80)	112.8(4)	F(42)-C(80)-F(43)	107.6(4)
F(42)-C(80)-C(79)	110.2(3)	F(43)-C(80)-C(79)	111.4(4)
F(44)-C(80)-F(42)	108.4(4)	F(44)-C(80)-F(43)	108.3(4)
F(44)-C(80)-C(79)	110.8(4)	F(45)-C(81)-S(1)	108.7(3)
F(45)-C(81)-F(46)	109.2(4)	F(45)-C(81)-C(82)	109.2(4)
F(46)-C(81)-S(1)	106.5(3)	F(46)-C(81)-C(82)	107.5(4)
C(82)-C(81)-S(1)	115.4(3)	F(47)-C(82)-F(48)	108.1(5)
F(47)-C(82)-C(81)	110.1(5)	F(48)-C(82)-C(81)	109.2(4)
F(49)-C(82)-F(47)	109.3(5)	F(49)-C(82)-F(48)	109.2(6)
F(49)-C(82)-C(81)	110.9(5)	N(3)-S(2A)-C(83A)	102.5(2)
O(7A)-S(2A)-N(3)	113.46(18)	O(7A)-S(2A)-C(83A)	104.6(2)
O(8A)-S(2A)-N(3)	111.38(19)	O(8A)-S(2A)-O(7A)	117.4(2)
O(8A)-S(2A)-C(83A)	105.8(2)	F(50A)-C(83A)-S(2A)	109.1(3)
F(50A)-C(83A)-F(51A)	107.7(5)	F(50A)-C(83A)-C(84A)	107.3(4)
F(51A)-C(83A)-S(2A)	109.1(4)	F(51A)-C(83A)-C(84A)	109.0(5)
C(84A)-C(83A)-S(2A)	114.4(4)	F(52A)-C(84A)-C(83A)	108.1(5)
F(53A)-C(84A)-F(52A)	106.2(6)	F(53A)-C(84A)-C(83A)	110.1(5)
F(54A)-C(84A)-F(52A)	108.8(5)	F(54A)-C(84A)-F(53A)	112.0(7)
F(54A)-C(84A)-C(83A)	111.4(5)	N(3)-S(2B)-C(83B)	103.5(16)
O(7B)-S(2B)-N(3)	113.3(13)	O(7B)-S(2B)-C(83B)	100(2)
O(8B)-S(2B)-N(3)	115.0(17)	O(8B)-S(2B)-O(7B)	117(2)

O(8B)-S(2B)-C(83B)	105(2)	F(50B)-C(83B)-S(2B)	112(3)
F(50B)-C(83B)-C(84B)	109(4)	F(51B)-C(83B)-S(2B)	114(3)
F(51B)-C(83B)-F(50B)	107(4)	F(51B)-C(83B)-C(84B)	107(4)
C(84B)-C(83B)-S(2B)	108(3)	F(52B)-C(84B)-C(83B)	97(4)
F(53B)-C(84B)-F(52B)	112(5)	F(53B)-C(84B)-C(83B)	111(5)
F(54B)-C(84B)-F(52B)	102(5)	F(54B)-C(84B)-F(53B)	124(6)
F(54B)-C(84B)-C(83B)	107(5)	C(93)-C(92)-C(97)	118.5(8)
C(93)-C(92)-C(98)	122.8(9)	C(97)-C(92)-C(98)	118.6(8)
C(92)-C(93)-H(93)	120.3	C(92)-C(93)-C(94)	119.3(9)
C(94)-C(93)-H(93)	120.3	C(93)-C(94)-H(94)	118.8
C(95)-C(94)-C(93)	122.5(9)	C(95)-C(94)-H(94)	118.8
C(94)-C(95)-H(95)	121.2	C(94)-C(95)-C(96)	117.6(10)
C(96)-C(95)-H(95)	121.2	C(95)-C(96)-H(96)	119.5
C(97)-C(96)-C(95)	120.9(10)	C(97)-C(96)-H(96)	119.5
C(92)-C(97)-H(97)	119.5	C(96)-C(97)-C(92)	120.9(8)
C(96)-C(97)-H(97)	119.5	C(92)-C(98)-H(98A)	109.5
C(92)-C(98)-H(98B)	109.5	C(92)-C(98)-H(98C)	109.5
H(98A)-C(98)-H(98B)	109.5	H(98A)-C(98)-H(98C)	109.5
H(98B)-C(98)-H(98C)	109.5	C(86)-C(85)-C(91)	121.7(10)
C(90)-C(85)-C(86)	121.9(9)	C(90)-C(85)-C(91)	116.4(9)
C(85)-C(86)-H(86)	120.5	C(87)-C(86)-C(85)	119.0(13)
C(87)-C(86)-H(86)	120.5	C(86)-C(87)-H(87)	119.6
C(88)-C(87)-C(86)	120.9(13)	C(88)-C(87)-H(87)	119.6
C(87)-C(88)-H(88)	118.8	C(87)-C(88)-C(89)	122.3(9)
C(89)-C(88)-H(88)	118.8	C(88)-C(89)-H(89)	121.6
C(88)-C(89)-C(90)	116.8(10)	C(90)-C(89)-H(89)	121.6
C(85)-C(90)-C(89)	119.2(10)	C(85)-C(90)-H(90)	120.4
C(89)-C(90)-H(90)	120.4	C(85)-C(91)-H(91A)	109.5
C(85)-C(91)-H(91B)	109.5	C(85)-C(91)-H(91C)	109.5
H(91A)-C(91)-H(91B)	109.5	H(91A)-C(91)-H(91C)	109.5
H(91B)-C(91)-H(91C)	109.5		

X-Ray data for compound 4.56k

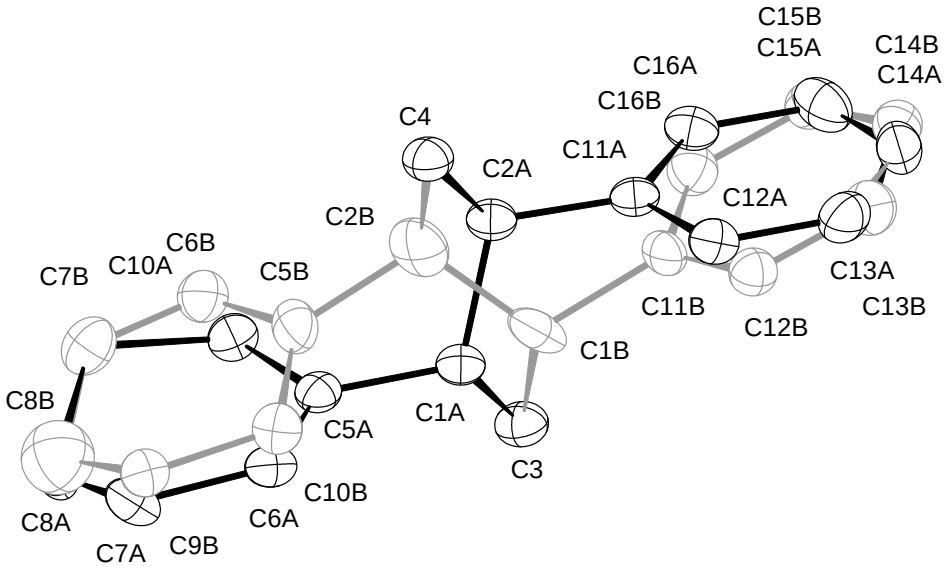

Figure 7.8 The molecular structure of **4.56k**. H atoms have been removed for clarity and disordered parts are shown in grey.

Table 7.3 Crystal data and structure refinement of **4.56k**.

Identification code	16423	
Empirical formula	$C_{16}H_{22}$	
Color	colourless	
Formula weight	214.33 $g \cdot mol^{-1}$	
Temperature	100(2) K	
Wavelength	1.54178 Å	
Crystal system	Monoclinic	
Space group	$P2_1$, (no. 4)	
Unit cell dimensions	a = 5.6970(4) Å	α= 90°.
	b = 17.3754(12) Å	β= 109.487(3)°.
	c = 6.9630(5) Å	γ = 90°.
Volume	649.77(8) $Å^3$	
Z	2	
Density (calculated)	1.096 $Mg \cdot m^{-3}$	
Absorption coefficient	0.447 mm^{-1}	
F(000)	236 e	
Crystal size	0.256 x 0.16 x 0.12 mm^3	
θ range for data collection	5.091 to 71.604°.	
Index ranges	$-6 \le h \le 6$, $-21 \le k \le 21$, $-8 \le l \le 8$	
Reflections collected	23055	

Independent reflections	2391 [R_{int} = 0.0310]	
Reflections with I>2σ(I)	2332	
Completeness to θ = 67.679°	99.8 %	
Absorption correction	Gaussian	
Max. and min. transmission	0.96736 and 0.94030	
Refinement method	Full-matrix least-squares on F^2	
Data / restraints / parameters	2391 / 49 / 253	
Goodness-of-fit on F^2	1.116	
Final R indices [I>2σ(I)]	R_1 = 0.0366	wR^2 = 0.0999
R indices (all data)	R_1 = 0.0378	wR^2 = 0.1014
Absolute structure parameter	0.2(10)	
Extinction coefficient	n/a	
Largest diff. peak and hole	0.124 and -0.151 e·$Å^{-3}$	

Table 7.4 Bond lengths [Å] and angles [°] of **4.56k**.

C(3)-H(3BE)	0.9800	C(3)-H(3BF)	0.9800
C(3)-H(3BD)	0.9800	C(3)-H(3AA)	0.9800
C(3)-H(3AC)	0.9800	C(3)-H(3AB)	0.9800
C(3)-C(1A)	1.531(3)	C(3)-C(1B)	1.606(13)
C(4)-H(4BD)	0.9800	C(4)-H(4BE)	0.9800
C(4)-H(4BF)	0.9800	C(4)-H(4AA)	0.9800
C(4)-H(4AB)	0.9800	C(4)-H(4AC)	0.9800
C(4)-C(2A)	1.551(4)	C(4)-C(2B)	1.514(15)
C(7B)-H(7BB)	0.9900	C(7B)-H(7BA)	0.9900
C(7B)-H(7BD)	0.9900	C(7B)-H(7BC)	0.9900
C(7B)-C(8A)	1.502(6)	C(7B)-C(10A)	1.548(5)
C(7B)-C(6B)	1.299(17)	C(7B)-C(8B)	1.46(4)
C(1A)-H(1A)	1.0000	C(1A)-C(2A)	1.551(4)
C(1A)-C(5A)	1.517(5)	C(2A)-H(2A)	1.0000
C(2A)-C(11A)	1.516(6)	C(5A)-C(6A)	1.338(5)
C(5A)-C(10A)	1.505(5)	C(6A)-H(6A)	0.9500
C(6A)-C(7A)	1.494(6)	C(7A)-H(7AA)	0.9900
C(7A)-H(7AB)	0.9900	C(7A)-C(8A)	1.498(8)
C(8A)-H(8AA)	0.9900	C(8A)-H(8AB)	0.9900
C(10A)-H(10A)	0.9900	C(10A)-H(10B)	0.9900
C(11A)-C(12A)	1.400(5)	C(11A)-C(16A)	1.396(5)

C(12A)-H(12A)	0.9500	C(12A)-C(13A)	1.384(8)
C(13A)-H(13A)	0.9500	C(13A)-C(14A)	1.382(7)
C(14A)-H(14A)	0.9500	C(14A)-C(15A)	1.385(8)
C(15A)-H(15A)	0.9500	C(15A)-C(16A)	1.396(7)
C(16A)-H(16A)	0.9500	C(1B)-H(1B)	1.0000
C(1B)-C(2B)	1.52(2)	C(1B)-C(11B)	1.556(19)
C(2B)-H(2B)	1.0000	C(2B)-C(5B)	1.54(2)
C(5B)-C(6B)	1.32(2)	C(5B)-C(10B)	1.47(3)
C(6B)-H(6B)	0.9500	C(8B)-H(8BA)	0.9900
C(8B)-H(8BB)	0.9900	C(8B)-C(9B)	1.49(4)
C(9B)-H(9BA)	0.9900	C(9B)-H(9BB)	0.9900
C(9B)-C(10B)	1.48(3)	C(10B)-H(10C)	0.9900
C(10B)-H(10D)	0.9900	C(13B)-H(13B)	0.9500
C(13B)-C(12B)	1.3900	C(13B)-C(14B)	1.3900
C(12B)-H(12B)	0.9500	C(12B)-C(11B)	1.3900
C(11B)-C(16B)	1.3900	C(16B)-H(16B)	0.9500
C(16B)-C(15B)	1.3900	C(15B)-H(15B)	0.9500
C(15B)-C(14B)	1.3900	C(14B)-H(14B)	0.9500

H(3BE)-C(3)-H(3BF)	109.5	H(3BE)-C(3)-H(3BD)	109.5
H(3BF)-C(3)-H(3BD)	109.5	H(3AA)-C(3)-H(3AC)	109.5
H(3AA)-C(3)-H(3AB)	109.5	H(3AC)-C(3)-H(3AB)	109.5
C(1A)-C(3)-H(3AA)	109.5	C(1A)-C(3)-H(3AC)	109.5
C(1A)-C(3)-H(3AB)	109.5	C(1B)-C(3)-H(3BE)	109.5
C(1B)-C(3)-H(3BF)	109.5	C(1B)-C(3)-H(3BD)	109.5
H(4BD)-C(4)-H(4BE)	109.5	H(4BD)-C(4)-H(4BF)	109.5
H(4BE)-C(4)-H(4BF)	109.5	H(4AA)-C(4)-H(4AB)	109.5
H(4AA)-C(4)-H(4AC)	109.5	H(4AB)-C(4)-H(4AC)	109.5
C(2A)-C(4)-H(4AA)	109.5	C(2A)-C(4)-H(4AB)	109.5
C(2A)-C(4)-H(4AC)	109.5	C(2B)-C(4)-H(4BD)	109.5
C(2B)-C(4)-H(4BE)	109.5	C(2B)-C(4)-H(4BF)	109.5
H(7BB)-C(7B)-H(7BA)	108.1	H(7BD)-C(7B)-H(7BC)	106.5
C(8A)-C(7B)-H(7BB)	109.5	C(8A)-C(7B)-H(7BA)	109.5
C(8A)-C(7B)-C(10A)	110.6(3)	C(10A)-C(7B)-H(7BB)	109.5
C(10A)-C(7B)-H(7BA)	109.5	C(6B)-C(7B)-H(7BD)	106.5
C(6B)-C(7B)-H(7BC)	106.5	C(6B)-C(7B)-C(8B)	123.3(17)
C(8B)-C(7B)-H(7BD)	106.5	C(8B)-C(7B)-H(7BC)	106.5
C(3)-C(1A)-H(1A)	107.0	C(3)-C(1A)-C(2A)	110.7(3)

C(2A)-C(1A)-H(1A)	107.0	C(5A)-C(1A)-C(3)	112.1(2)
C(5A)-C(1A)-H(1A)	107.0	C(5A)-C(1A)-C(2A)	112.8(3)
C(4)-C(2A)-H(2A)	107.7	C(1A)-C(2A)-C(4)	110.7(3)
C(1A)-C(2A)-H(2A)	107.7	C(11A)-C(2A)-C(4)	111.7(2)
C(11A)-C(2A)-C(1A)	111.1(3)	C(11A)-C(2A)-H(2A)	107.7
C(6A)-C(5A)-C(1A)	120.7(3)	C(6A)-C(5A)-C(10A)	121.2(3)
C(10A)-C(5A)-C(1A)	118.1(3)	C(5A)-C(6A)-H(6A)	118.0
C(5A)-C(6A)-C(7A)	124.0(4)	C(7A)-C(6A)-H(6A)	118.0
C(6A)-C(7A)-H(7AA)	108.9	C(6A)-C(7A)-H(7AB)	108.9
C(6A)-C(7A)-C(8A)	113.3(4)	H(7AA)-C(7A)-H(7AB)	107.7
C(8A)-C(7A)-H(7AA)	108.9	C(8A)-C(7A)-H(7AB)	108.9
C(7B)-C(8A)-H(8AA)	109.2	C(7B)-C(8A)-H(8AB)	109.2
C(7A)-C(8A)-C(7B)	111.8(4)	C(7A)-C(8A)-H(8AA)	109.2
C(7A)-C(8A)-H(8AB)	109.2	H(8AA)-C(8A)-H(8AB)	107.9
C(7B)-C(10A)-H(10A)	108.9	C(7B)-C(10A)-H(10B)	108.9
C(5A)-C(10A)-C(7B)	113.4(3)	C(5A)-C(10A)-H(10A)	108.9
C(5A)-C(10A)-H(10B)	108.9	H(10A)-C(10A)-H(10B)	107.7
C(12A)-C(11A)-C(2A)	121.4(3)	C(16A)-C(11A)-C(2A)	120.8(3)
C(16A)-C(11A)-C(12A)	117.8(3)	C(11A)-C(12A)-H(12A)	119.5
C(13A)-C(12A)-C(11A)	121.0(3)	C(13A)-C(12A)-H(12A)	119.5
C(12A)-C(13A)-H(13A)	119.7	C(14A)-C(13A)-C(12A)	120.7(3)
C(14A)-C(13A)-H(13A)	119.7	C(13A)-C(14A)-H(14A)	120.3
C(13A)-C(14A)-C(15A)	119.4(3)	C(15A)-C(14A)-H(14A)	120.3
C(14A)-C(15A)-H(15A)	119.9	C(14A)-C(15A)-C(16A)	120.2(3)
C(16A)-C(15A)-H(15A)	119.9	C(11A)-C(16A)-H(16A)	119.5
C(15A)-C(16A)-C(11A)	121.0(3)	C(15A)-C(16A)-H(16A)	119.5
C(3)-C(1B)-H(1B)	106.7	C(2B)-C(1B)-C(3)	109.1(11)
C(2B)-C(1B)-H(1B)	106.7	C(2B)-C(1B)-C(11B)	113.4(14)
C(11B)-C(1B)-C(3)	113.9(10)	C(11B)-C(1B)-H(1B)	106.7
C(4)-C(2B)-C(1B)	111.0(12)	C(4)-C(2B)-H(2B)	106.8
C(4)-C(2B)-C(5B)	112.8(11)	C(1B)-C(2B)-H(2B)	106.8
C(1B)-C(2B)-C(5B)	112.2(15)	C(5B)-C(2B)-H(2B)	106.8
C(6B)-C(5B)-C(2B)	119.7(15)	C(6B)-C(5B)-C(10B)	120.8(14)
C(10B)-C(5B)-C(2B)	119.3(14)	C(7B)-C(6B)-C(5B)	122.9(14)
C(7B)-C(6B)-H(6B)	118.6	C(5B)-C(6B)-H(6B)	118.6
C(7B)-C(8B)-H(8BA)	108.9	C(7B)-C(8B)-H(8BB)	108.9
C(7B)-C(8B)-C(9B)	113(2)	H(8BA)-C(8B)-H(8BB)	107.7
C(9B)-C(8B)-H(8BA)	108.9	C(9B)-C(8B)-H(8BB)	108.9

C(8B)-C(9B)-H(9BA)	108.7	C(8B)-C(9B)-H(9BB)	108.8
H(9BA)-C(9B)-H(9BB)	107.6	C(10B)-C(9B)-C(8B)	114(2)
C(10B)-C(9B)-H(9BA)	108.7	C(10B)-C(9B)-H(9BB)	108.7
C(5B)-C(10B)-C(9B)	116.9(17)	C(5B)-C(10B)-H(10C)	108.1
C(5B)-C(10B)-H(10D)	108.1	C(9B)-C(10B)-H(10C)	108.1
C(9B)-C(10B)-H(10D)	108.1	H(10C)-C(10B)-H(10D)	107.3
C(12B)-C(13B)-H(13B)	120.0	C(12B)-C(13B)-C(14B)	120.0
C(14B)-C(13B)-H(13B)	120.0	C(13B)-C(12B)-H(12B)	120.0
C(13B)-C(12B)-C(11B)	120.0	C(11B)-C(12B)-H(12B)	120.0
C(12B)-C(11B)-C(1B)	119.6(9)	C(12B)-C(11B)-C(16B)	120.0
C(16B)-C(11B)-C(1B)	120.3(9)	C(11B)-C(16B)-H(16B)	120.0
C(15B)-C(16B)-C(11B)	120.0	C(15B)-C(16B)-H(16B)	120.0
C(16B)-C(15B)-H(15B)	120.0	C(16B)-C(15B)-C(14B)	120.0
C(14B)-C(15B)-H(15B)	120.0	C(13B)-C(14B)-H(14B)	120.0
C(15B)-C(14B)-C(13B)	120.0	C(15B)-C(14B)-H(14B)	120.0

The crystal structure and absolute configuration of products **4.54i** and **4.68f** were determined using X-ray diffraction. As these substances are oily and/or liquid at room temperature, they cannot be accessed directly by this method.

Richert and coworkers elegantly demonstrated that TFM frequently form multicomponent crystals capable of encapsulating small molecules.[276] Compared to other crystallization methods, such as the use of crystalline sponges, the main benefit of this method is the regular and orderly incorporation of highly occupied analyte molecules.

Representative procedure for neat TFM crystallization

In a spring bottom GC vial insert with the spring removed, TFM (0.5 mg) was suspended in the analyte (5.0 µL). The insert was then placed in a GC vial and heated to 120 °C until the mixture became a homogeneous and clear solution. The heating was switched off and the mixture was allowed to slowly cool to 21 °C. After overnight incubation (or until crystal formation was observed), a suitable single crystal was selected and mounted for X-ray diffraction analysis.

X-Ray data for compound 4.54i co-crystallized with TFM

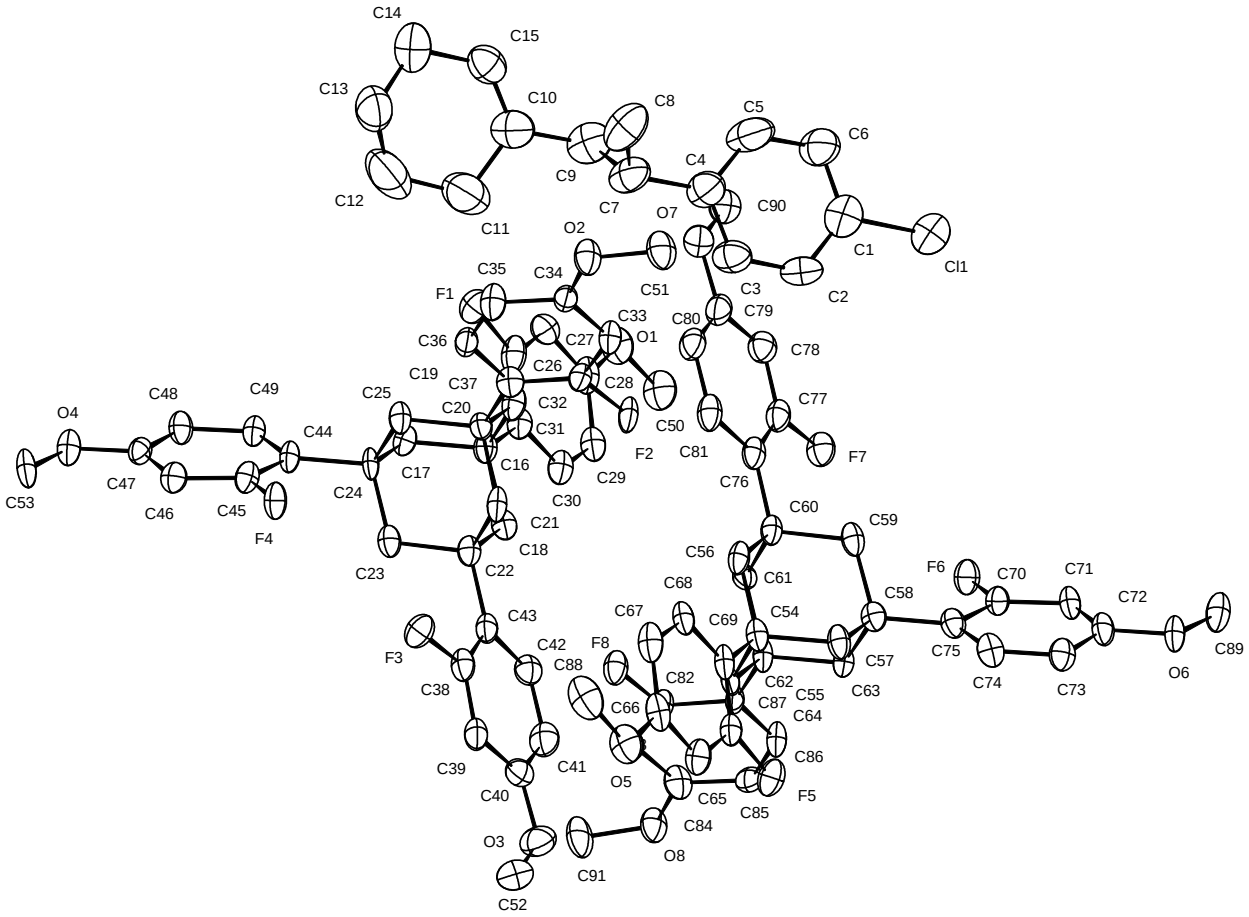

Figure 7.9 The molecular structure of **4.54i**. H atoms have been removed for clarity.

Table 7.5 Crystal data and structure refinement of **4.54i**.

Identification code	16399	
Empirical formula	$C_{91}\ H_{91}\ Cl\ F_8\ O_8$	
Color	colourless	
Formula weight	1500.08 g·mol^{-1}	
Temperature	100(2) K	
Wavelength	0.71073 Å	
Crystal system	Monoclinic	
Space group	$P2_1$, (no. 4)	
Unit cell dimensions	a = 15.1021(11) Å	α= 90°.
	b = 14.8006(11) Å	β= 111.626(5)°.
	c = 18.2175(13) Å	γ = 90°.
Volume	3785.3(5) Å^3	
Z	2	

Density (calculated)	1.316 $Mg \cdot m^{-3}$	
Absorption coefficient	0.130 mm^{-1}	
F(000)	1580 e	
Crystal size	0.417 x 0.156 x 0.060 mm^3	
θ range for data collection	1.999 to 29.129°.	
Index ranges	$-20 \leq h \leq 20$, $-20 \leq k \leq 20$, $-24 \leq l \leq 24$	
Reflections collected	93438	
Independent reflections	20351 [$R_{int} = 0.1575$]	
Reflections with I>2σ(I)	10971	
Completeness to θ = 25.242°	99.9 %	
Absorption correction	Gaussian	
Max. and min. transmission	0.99496 and 0.97704	
Refinement method	Full-matrix least-squares on F^2	
Data / restraints / parameters	20351 / 1 / 982	
Goodness-of-fit on F^2	0.977	
Final R indices [I>2σ(I)]	$R_1 = 0.0612$	$wR^2 = 0.1440$
R indices (all data)	$R_1 = 0.1312$	$wR^2 = 0.1745$
Absolute structure parameter	-0.08(6)	
Extinction coefficient	n/a	
Largest diff. peak and hole	1.348 and -0.334 $e \cdot Å^{-3}$	

Table 7.6 Bond lengths [Å] and angles [°] of **4.54i**.

F(1)-C(26)	1.363(7)	F(2)-C(32)	1.386(6)
F(3)-C(38)	1.379(6)	F(4)-C(45)	1.363(6)
O(1)-C(28)	1.365(7)	O(1)-C(50)	1.432(7)
O(2)-C(34)	1.360(6)	O(2)-C(51)	1.420(9)
O(3)-C(40)	1.360(7)	O(3)-C(52)	1.424(7)
O(4)-C(47)	1.362(8)	O(4)-C(53)	1.417(6)
C(16)-C(17)	1.534(8)	C(16)-C(18)	1.536(8)
C(16)-C(19)	1.538(7)	C(16)-C(31)	1.535(7)
C(17)-H(17A)	0.9900	C(17)-H(17B)	0.9900
C(17)-C(24)	1.531(7)	C(18)-H(18A)	0.9900
C(18)-H(18B)	0.9900	C(18)-C(22)	1.548(7)
C(19)-H(19A)	0.9900	C(19)-H(19B)	0.9900
C(19)-C(20)	1.542(7)	C(20)-C(21)	1.539(8)

C(20)-C(25)	1.550(9)	C(20)-C(37)	1.540(7)
C(21)-H(21A)	0.9900	C(21)-H(21B)	0.9900
C(21)-C(22)	1.540(7)	C(22)-C(23)	1.531(8)
C(22)-C(43)	1.530(8)	C(23)-H(23A)	0.9900
C(23)-H(23B)	0.9900	C(23)-C(24)	1.537(9)
C(24)-C(25)	1.550(7)	C(24)-C(44)	1.543(8)
C(25)-H(25A)	0.9900	C(25)-H(25B)	0.9900
C(26)-C(27)	1.386(8)	C(26)-C(31)	1.402(9)
C(27)-H(27)	0.9500	C(27)-C(28)	1.399(8)
C(28)-C(29)	1.370(9)	C(29)-H(29)	0.9500
C(29)-C(30)	1.404(8)	C(30)-H(30)	0.9500
C(30)-C(31)	1.396(8)	C(32)-C(33)	1.394(8)
C(32)-C(37)	1.364(9)	C(33)-H(33)	0.9500
C(33)-C(34)	1.381(8)	C(34)-C(35)	1.398(9)
C(35)-H(35)	0.9500	C(35)-C(36)	1.379(8)
C(36)-H(36)	0.9500	C(36)-C(37)	1.413(7)
C(38)-C(39)	1.372(9)	C(38)-C(43)	1.399(8)
C(39)-H(39)	0.9500	C(39)-C(40)	1.406(8)
C(40)-C(41)	1.383(8)	C(41)-H(41)	0.9500
C(41)-C(42)	1.379(8)	C(42)-H(42)	0.9500
C(42)-C(43)	1.399(8)	C(44)-C(45)	1.384(8)
C(44)-C(49)	1.404(7)	C(45)-C(46)	1.390(9)
C(46)-H(46)	0.9500	C(46)-C(47)	1.406(8)
C(47)-C(48)	1.383(8)	C(48)-H(48)	0.9500
C(48)-C(49)	1.392(8)	C(49)-H(49)	0.9500
C(50)-H(50A)	0.9800	C(50)-H(50B)	0.9800
C(50)-H(50C)	0.9800	C(51)-H(51A)	0.9800
C(51)-H(51B)	0.9800	C(51)-H(51C)	0.9800
C(52)-H(52A)	0.9800	C(52)-H(52B)	0.9800
C(52)-H(52C)	0.9800	C(53)-H(53A)	0.9800
C(53)-H(53B)	0.9800	C(53)-H(53C)	0.9800
F(5)-C(64)	1.378(7)	F(6)-C(70)	1.380(6)
F(7)-C(77)	1.378(6)	F(8)-C(82)	1.360(6)
O(5)-C(66)	1.385(7)	O(5)-C(88)	1.445(8)
O(6)-C(72)	1.372(8)	O(6)-C(89)	1.440(7)
O(7)-C(79)	1.369(8)	O(7)-C(90)	1.421(7)
O(8)-C(84)	1.376(6)	O(8)-C(91)	1.430(9)
C(54)-C(55)	1.551(7)	C(54)-C(56)	1.525(8)

C(54)-C(57)	1.560(9)	C(54)-C(69)	1.545(7)
C(55)-H(55A)	0.9900	C(55)-H(55B)	0.9900
C(55)-C(62)	1.553(7)	C(56)-H(56A)	0.9900
C(56)-H(56B)	0.9900	C(56)-C(60)	1.538(7)
C(57)-H(57A)	0.9900	C(57)-H(57B)	0.9900
C(57)-C(58)	1.546(7)	C(58)-C(59)	1.535(8)
C(58)-C(63)	1.551(7)	C(58)-C(75)	1.513(9)
C(59)-H(59A)	0.9900	C(59)-H(59B)	0.9900
C(59)-C(60)	1.555(8)	C(60)-C(61)	1.548(7)
C(60)-C(76)	1.528(8)	C(61)-H(61A)	0.9900
C(61)-H(61B)	0.9900	C(61)-C(62)	1.543(8)
C(62)-C(63)	1.540(8)	C(62)-C(87)	1.527(7)
C(63)-H(63A)	0.9900	C(63)-H(63B)	0.9900
C(64)-C(65)	1.385(7)	C(64)-C(69)	1.366(9)
C(65)-H(65)	0.9500	C(65)-C(66)	1.379(8)
C(66)-C(67)	1.376(10)	C(67)-H(67)	0.9500
C(67)-C(68)	1.397(7)	C(68)-H(68)	0.9500
C(68)-C(69)	1.402(8)	C(70)-C(71)	1.379(9)
C(70)-C(75)	1.399(8)	C(71)-H(71)	0.9500
C(71)-C(72)	1.375(8)	C(72)-C(73)	1.398(8)
C(73)-H(73)	0.9500	C(73)-C(74)	1.362(9)
C(74)-H(74)	0.9500	C(74)-C(75)	1.405(8)
C(76)-C(77)	1.380(8)	C(76)-C(81)	1.416(8)
C(77)-C(78)	1.372(9)	C(78)-H(78)	0.9500
C(78)-C(79)	1.385(8)	C(79)-C(80)	1.398(9)
C(80)-H(80)	0.9500	C(80)-C(81)	1.364(9)
C(81)-H(81)	0.9500	C(82)-C(83)	1.367(8)
C(82)-C(87)	1.414(8)	C(83)-H(83)	0.9500
C(83)-C(84)	1.401(8)	C(84)-C(85)	1.373(9)
C(85)-H(85)	0.9500	C(85)-C(86)	1.383(7)
C(86)-H(86)	0.9500	C(86)-C(87)	1.397(7)
C(88)-H(88A)	0.9800	C(88)-H(88B)	0.9800
C(88)-H(88C)	0.9800	C(89)-H(89A)	0.9800
C(89)-H(89B)	0.9800	C(89)-H(89C)	0.9800
C(90)-H(90A)	0.9800	C(90)-H(90B)	0.9800
C(90)-H(90C)	0.9800	C(91)-H(91A)	0.9800
C(91)-H(91B)	0.9800	C(91)-H(91C)	0.9800
Cl(1)-C(1)	1.765(7)	C(1)-C(2)	1.362(10)

C(1)-C(6)	1.385(10)	C(2)-H(2)	0.9500
C(2)-C(3)	1.394(11)	C(3)-H(3)	0.9500
C(3)-C(4)	1.366(10)	C(4)-C(5)	1.383(11)
C(4)-C(7)	1.528(12)	C(5)-H(5)	0.9500
C(5)-C(6)	1.391(11)	C(6)-H(6)	0.9500
C(7)-H(7)	1.0000	C(7)-C(8)	1.528(9)
C(7)-C(9)	1.534(8)	C(8)-H(8A)	0.9800
C(8)-H(8B)	0.9800	C(8)-H(8C)	0.9800
C(9)-H(9A)	0.9900	C(9)-H(9B)	0.9900
C(9)-C(10)	1.507(13)	C(10)-C(11)	1.519(13)
C(10)-C(15)	1.330(11)	C(11)-H(11A)	0.9900
C(11)-H(11B)	0.9900	C(11)-C(12)	1.517(15)
C(12)-H(12A)	0.9900	C(12)-H(12B)	0.9900
C(12)-C(13)	1.514(14)	C(13)-H(13A)	0.9900
C(13)-H(13B)	0.9900	C(13)-C(14)	1.489(12)
C(14)-H(14A)	0.9900	C(14)-H(14B)	0.9900
C(14)-C(15)	1.487(12)	C(15)-H(15)	0.9500

C(28)-O(1)-C(50)	117.4(5)	C(34)-O(2)-C(51)	116.8(4)
C(40)-O(3)-C(52)	118.2(5)	C(47)-O(4)-C(53)	117.3(4)
C(17)-C(16)-C(18)	109.1(5)	C(17)-C(16)-C(19)	110.1(5)
C(17)-C(16)-C(31)	110.1(5)	C(18)-C(16)-C(19)	107.1(5)
C(31)-C(16)-C(18)	110.8(5)	C(31)-C(16)-C(19)	109.5(5)
C(16)-C(17)-H(17A)	109.6	C(16)-C(17)-H(17B)	109.6
H(17A)-C(17)-H(17B)	108.1	C(24)-C(17)-C(16)	110.3(4)
C(24)-C(17)-H(17A)	109.6	C(24)-C(17)-H(17B)	109.6
C(16)-C(18)-H(18A)	109.2	C(16)-C(18)-H(18B)	109.2
C(16)-C(18)-C(22)	111.9(5)	H(18A)-C(18)-H(18B)	107.9
C(22)-C(18)-H(18A)	109.2	C(22)-C(18)-H(18B)	109.2
C(16)-C(19)-H(19A)	109.4	C(16)-C(19)-H(19B)	109.4
C(16)-C(19)-C(20)	111.2(5)	H(19A)-C(19)-H(19B)	108.0
C(20)-C(19)-H(19A)	109.4	C(20)-C(19)-H(19B)	109.4
C(19)-C(20)-C(25)	107.5(4)	C(21)-C(20)-C(19)	109.6(4)
C(21)-C(20)-C(25)	107.9(5)	C(21)-C(20)-C(37)	109.6(4)
C(37)-C(20)-C(19)	111.0(5)	C(37)-C(20)-C(25)	111.2(5)
C(20)-C(21)-H(21A)	109.4	C(20)-C(21)-H(21B)	109.4
C(20)-C(21)-C(22)	111.4(4)	H(21A)-C(21)-H(21B)	108.0
C(22)-C(21)-H(21A)	109.4	C(22)-C(21)-H(21B)	109.4

C(21)-C(22)-C(18)	107.5(5)	C(23)-C(22)-C(18)	107.7(5)
C(23)-C(22)-C(21)	109.9(5)	C(43)-C(22)-C(18)	111.2(4)
C(43)-C(22)-C(21)	110.2(5)	C(43)-C(22)-C(23)	110.3(5)
C(22)-C(23)-H(23A)	109.4	C(22)-C(23)-H(23B)	109.4
C(22)-C(23)-C(24)	111.0(5)	H(23A)-C(23)-H(23B)	108.0
C(24)-C(23)-H(23A)	109.4	C(24)-C(23)-H(23B)	109.4
C(17)-C(24)-C(23)	108.2(5)	C(17)-C(24)-C(25)	108.9(5)
C(17)-C(24)-C(44)	111.4(4)	C(23)-C(24)-C(25)	109.8(5)
C(23)-C(24)-C(44)	108.6(5)	C(44)-C(24)-C(25)	109.8(4)
C(20)-C(25)-H(25A)	109.4	C(20)-C(25)-H(25B)	109.4
C(24)-C(25)-C(20)	111.1(5)	C(24)-C(25)-H(25A)	109.4
C(24)-C(25)-H(25B)	109.4	H(25A)-C(25)-H(25B)	108.0
F(1)-C(26)-C(27)	115.3(6)	F(1)-C(26)-C(31)	119.7(5)
C(27)-C(26)-C(31)	125.0(6)	C(26)-C(27)-H(27)	120.8
C(26)-C(27)-C(28)	118.4(6)	C(28)-C(27)-H(27)	120.8
O(1)-C(28)-C(27)	114.7(6)	O(1)-C(28)-C(29)	126.0(5)
C(29)-C(28)-C(27)	119.3(5)	C(28)-C(29)-H(29)	119.9
C(28)-C(29)-C(30)	120.3(6)	C(30)-C(29)-H(29)	119.9
C(29)-C(30)-H(30)	118.4	C(31)-C(30)-C(29)	123.1(6)
C(31)-C(30)-H(30)	118.4	C(26)-C(31)-C(16)	122.5(5)
C(30)-C(31)-C(16)	123.7(6)	C(30)-C(31)-C(26)	113.8(5)
F(2)-C(32)-C(33)	114.6(5)	C(37)-C(32)-F(2)	119.4(5)
C(37)-C(32)-C(33)	126.0(5)	C(32)-C(33)-H(33)	120.9
C(34)-C(33)-C(32)	118.2(6)	C(34)-C(33)-H(33)	120.9
O(2)-C(34)-C(33)	124.3(6)	O(2)-C(34)-C(35)	117.2(5)
C(33)-C(34)-C(35)	118.5(5)	C(34)-C(35)-H(35)	119.6
C(36)-C(35)-C(34)	120.8(5)	C(36)-C(35)-H(35)	119.6
C(35)-C(36)-H(36)	118.8	C(35)-C(36)-C(37)	122.4(6)
C(37)-C(36)-H(36)	118.8	C(32)-C(37)-C(20)	123.2(5)
C(32)-C(37)-C(36)	114.0(5)	C(36)-C(37)-C(20)	122.8(6)
F(3)-C(38)-C(43)	119.0(6)	C(39)-C(38)-F(3)	114.0(5)
C(39)-C(38)-C(43)	127.0(5)	C(38)-C(39)-H(39)	121.3
C(38)-C(39)-C(40)	117.3(5)	C(40)-C(39)-H(39)	121.3
O(3)-C(40)-C(39)	123.8(5)	O(3)-C(40)-C(41)	117.8(5)
C(41)-C(40)-C(39)	118.4(6)	C(40)-C(41)-H(41)	119.3
C(42)-C(41)-C(40)	121.5(6)	C(42)-C(41)-H(41)	119.3
C(41)-C(42)-H(42)	118.5	C(41)-C(42)-C(43)	123.0(5)
C(43)-C(42)-H(42)	118.5	C(38)-C(43)-C(22)	123.2(5)

C(38)-C(43)-C(42)	112.7(6)	C(42)-C(43)-C(22)	124.1(5)
C(45)-C(44)-C(24)	121.7(5)	C(45)-C(44)-C(49)	115.6(5)
C(49)-C(44)-C(24)	122.6(4)	F(4)-C(45)-C(44)	121.2(5)
F(4)-C(45)-C(46)	114.5(5)	C(44)-C(45)-C(46)	124.3(5)
C(45)-C(46)-H(46)	120.8	C(45)-C(46)-C(47)	118.3(5)
C(47)-C(46)-H(46)	120.8	O(4)-C(47)-C(46)	124.2(5)
O(4)-C(47)-C(48)	116.8(5)	C(48)-C(47)-C(46)	119.0(6)
C(47)-C(48)-H(48)	119.6	C(47)-C(48)-C(49)	120.8(5)
C(49)-C(48)-H(48)	119.6	C(44)-C(49)-H(49)	119.1
C(48)-C(49)-C(44)	121.8(5)	C(48)-C(49)-H(49)	119.1
O(1)-C(50)-H(50A)	109.5	O(1)-C(50)-H(50B)	109.5
O(1)-C(50)-H(50C)	109.5	H(50A)-C(50)-H(50B)	109.5
H(50A)-C(50)-H(50C)	109.5	H(50B)-C(50)-H(50C)	109.5
O(2)-C(51)-H(51A)	109.5	O(2)-C(51)-H(51B)	109.5
O(2)-C(51)-H(51C)	109.5	H(51A)-C(51)-H(51B)	109.5
H(51A)-C(51)-H(51C)	109.5	H(51B)-C(51)-H(51C)	109.5
O(3)-C(52)-H(52A)	109.5	O(3)-C(52)-H(52B)	109.5
O(3)-C(52)-H(52C)	109.5	H(52A)-C(52)-H(52B)	109.5
H(52A)-C(52)-H(52C)	109.5	H(52B)-C(52)-H(52C)	109.5
O(4)-C(53)-H(53A)	109.5	O(4)-C(53)-H(53B)	109.5
O(4)-C(53)-H(53C)	109.5	H(53A)-C(53)-H(53B)	109.5
H(53A)-C(53)-H(53C)	109.5	H(53B)-C(53)-H(53C)	109.5
C(66)-O(5)-C(88)	115.5(5)	C(72)-O(6)-C(89)	117.0(4)
C(79)-O(7)-C(90)	116.9(5)	C(84)-O(8)-C(91)	117.5(5)
C(55)-C(54)-C(57)	108.3(4)	C(56)-C(54)-C(55)	109.3(4)
C(56)-C(54)-C(57)	108.4(5)	C(56)-C(54)-C(69)	112.3(5)
C(69)-C(54)-C(55)	109.2(5)	C(69)-C(54)-C(57)	109.3(5)
C(54)-C(55)-H(55A)	109.6	C(54)-C(55)-H(55B)	109.6
C(54)-C(55)-C(62)	110.2(5)	H(55A)-C(55)-H(55B)	108.1
C(62)-C(55)-H(55A)	109.6	C(62)-C(55)-H(55B)	109.6
C(54)-C(56)-H(56A)	109.0	C(54)-C(56)-H(56B)	109.0
C(54)-C(56)-C(60)	112.9(5)	H(56A)-C(56)-H(56B)	107.8
C(60)-C(56)-H(56A)	109.0	C(60)-C(56)-H(56B)	109.0
C(54)-C(57)-H(57A)	109.5	C(54)-C(57)-H(57B)	109.5
H(57A)-C(57)-H(57B)	108.1	C(58)-C(57)-C(54)	110.9(5)
C(58)-C(57)-H(57A)	109.5	C(58)-C(57)-H(57B)	109.5
C(57)-C(58)-C(63)	107.4(5)	C(59)-C(58)-C(57)	108.2(5)
C(59)-C(58)-C(63)	109.4(5)	C(75)-C(58)-C(57)	111.5(5)

C(75)-C(58)-C(59)	109.9(5)	C(75)-C(58)-C(63)	110.4(4)
C(58)-C(59)-H(59A)	109.2	C(58)-C(59)-H(59B)	109.2
C(58)-C(59)-C(60)	111.8(5)	H(59A)-C(59)-H(59B)	107.9
C(60)-C(59)-H(59A)	109.2	C(60)-C(59)-H(59B)	109.2
C(56)-C(60)-C(59)	107.3(5)	C(56)-C(60)-C(61)	108.0(5)
C(61)-C(60)-C(59)	108.6(4)	C(76)-C(60)-C(56)	112.8(4)
C(76)-C(60)-C(59)	109.6(5)	C(76)-C(60)-C(61)	110.5(4)
C(60)-C(61)-H(61A)	109.3	C(60)-C(61)-H(61B)	109.3
H(61A)-C(61)-H(61B)	108.0	C(62)-C(61)-C(60)	111.5(4)
C(62)-C(61)-H(61A)	109.3	C(62)-C(61)-H(61B)	109.3
C(61)-C(62)-C(55)	109.9(4)	C(63)-C(62)-C(55)	107.4(4)
C(63)-C(62)-C(61)	108.7(5)	C(87)-C(62)-C(55)	109.6(5)
C(87)-C(62)-C(61)	110.2(4)	C(87)-C(62)-C(63)	111.0(4)
C(58)-C(63)-H(63A)	109.2	C(58)-C(63)-H(63B)	109.2
C(62)-C(63)-C(58)	112.0(4)	C(62)-C(63)-H(63A)	109.2
C(62)-C(63)-H(63B)	109.2	H(63A)-C(63)-H(63B)	107.9
F(5)-C(64)-C(65)	115.0(6)	C(69)-C(64)-F(5)	120.1(5)
C(69)-C(64)-C(65)	124.8(5)	C(64)-C(65)-H(65)	120.9
C(66)-C(65)-C(64)	118.3(6)	C(66)-C(65)-H(65)	120.9
C(65)-C(66)-O(5)	114.2(6)	C(67)-C(66)-O(5)	125.5(5)
C(67)-C(66)-C(65)	120.3(5)	C(66)-C(67)-H(67)	120.5
C(66)-C(67)-C(68)	119.1(6)	C(68)-C(67)-H(67)	120.5
C(67)-C(68)-H(68)	118.7	C(67)-C(68)-C(69)	122.6(6)
C(69)-C(68)-H(68)	118.7	C(64)-C(69)-C(54)	123.6(5)
C(64)-C(69)-C(68)	114.9(5)	C(68)-C(69)-C(54)	121.6(6)
F(6)-C(70)-C(75)	118.3(5)	C(71)-C(70)-F(6)	115.5(5)
C(71)-C(70)-C(75)	126.1(5)	C(70)-C(71)-H(71)	121.1
C(72)-C(71)-C(70)	117.8(5)	C(72)-C(71)-H(71)	121.1
O(6)-C(72)-C(71)	124.8(5)	O(6)-C(72)-C(73)	115.8(5)
C(71)-C(72)-C(73)	119.4(6)	C(72)-C(73)-H(73)	119.9
C(74)-C(73)-C(72)	120.3(6)	C(74)-C(73)-H(73)	119.9
C(73)-C(74)-H(74)	118.2	C(73)-C(74)-C(75)	123.6(5)
C(75)-C(74)-H(74)	118.2	C(70)-C(75)-C(58)	123.0(5)
C(70)-C(75)-C(74)	112.7(6)	C(74)-C(75)-C(58)	124.3(5)
C(77)-C(76)-C(60)	123.8(5)	C(77)-C(76)-C(81)	113.0(6)
C(81)-C(76)-C(60)	123.2(5)	F(7)-C(77)-C(76)	119.0(6)
C(78)-C(77)-F(7)	114.8(5)	C(78)-C(77)-C(76)	126.1(6)
C(77)-C(78)-H(78)	120.7	C(77)-C(78)-C(79)	118.7(6)

C(79)-C(78)-H(78)	120.7	O(7)-C(79)-C(78)	124.6(6)
O(7)-C(79)-C(80)	117.1(6)	C(78)-C(79)-C(80)	118.3(6)
C(79)-C(80)-H(80)	119.7	C(81)-C(80)-C(79)	120.7(6)
C(81)-C(80)-H(80)	119.7	C(76)-C(81)-H(81)	118.4
C(80)-C(81)-C(76)	123.2(6)	C(80)-C(81)-H(81)	118.4
F(8)-C(82)-C(83)	115.7(5)	F(8)-C(82)-C(87)	119.2(5)
C(83)-C(82)-C(87)	125.1(5)	C(82)-C(83)-H(83)	121.1
C(82)-C(83)-C(84)	117.9(6)	C(84)-C(83)-H(83)	121.1
O(8)-C(84)-C(83)	122.4(6)	C(85)-C(84)-O(8)	117.4(5)
C(85)-C(84)-C(83)	120.2(5)	C(84)-C(85)-H(85)	120.2
C(84)-C(85)-C(86)	119.6(5)	C(86)-C(85)-H(85)	120.2
C(85)-C(86)-H(86)	118.2	C(85)-C(86)-C(87)	123.6(6)
C(87)-C(86)-H(86)	118.2	C(82)-C(87)-C(62)	121.6(5)
C(86)-C(87)-C(62)	124.9(5)	C(86)-C(87)-C(82)	113.5(5)
O(5)-C(88)-H(88A)	109.5	O(5)-C(88)-H(88B)	109.5
O(5)-C(88)-H(88C)	109.5	H(88A)-C(88)-H(88B)	109.5
H(88A)-C(88)-H(88C)	109.5	H(88B)-C(88)-H(88C)	109.5
O(6)-C(89)-H(89A)	109.5	O(6)-C(89)-H(89B)	109.5
O(6)-C(89)-H(89C)	109.5	H(89A)-C(89)-H(89B)	109.5
H(89A)-C(89)-H(89C)	109.5	H(89B)-C(89)-H(89C)	109.5
O(7)-C(90)-H(90A)	109.5	O(7)-C(90)-H(90B)	109.5
O(7)-C(90)-H(90C)	109.5	H(90A)-C(90)-H(90B)	109.5
H(90A)-C(90)-H(90C)	109.5	H(90B)-C(90)-H(90C)	109.5
O(8)-C(91)-H(91A)	109.5	O(8)-C(91)-H(91B)	109.5
O(8)-C(91)-H(91C)	109.5	H(91A)-C(91)-H(91B)	109.5
H(91A)-C(91)-H(91C)	109.5	H(91B)-C(91)-H(91C)	109.5
C(2)-C(1)-Cl(1)	118.9(6)	C(2)-C(1)-C(6)	122.1(7)
C(6)-C(1)-Cl(1)	119.0(6)	C(1)-C(2)-H(2)	120.9
C(1)-C(2)-C(3)	118.3(7)	C(3)-C(2)-H(2)	120.9
C(2)-C(3)-H(3)	119.1	C(4)-C(3)-C(2)	121.8(8)
C(4)-C(3)-H(3)	119.1	C(3)-C(4)-C(5)	118.5(8)
C(3)-C(4)-C(7)	120.8(8)	C(5)-C(4)-C(7)	120.7(8)
C(4)-C(5)-H(5)	119.3	C(4)-C(5)-C(6)	121.4(8)
C(6)-C(5)-H(5)	119.3	C(1)-C(6)-C(5)	117.9(7)
C(1)-C(6)-H(6)	121.1	C(5)-C(6)-H(6)	121.1
C(4)-C(7)-H(7)	108.1	C(4)-C(7)-C(8)	110.7(8)
C(4)-C(7)-C(9)	110.5(5)	C(8)-C(7)-H(7)	108.1
C(8)-C(7)-C(9)	111.1(6)	C(9)-C(7)-H(7)	108.1

C(7)-C(8)-H(8A)	109.5	C(7)-C(8)-H(8B)	109.5
C(7)-C(8)-H(8C)	109.5	H(8A)-C(8)-H(8B)	109.5
H(8A)-C(8)-H(8C)	109.5	H(8B)-C(8)-H(8C)	109.5
C(7)-C(9)-H(9A)	108.8	C(7)-C(9)-H(9B)	108.8
H(9A)-C(9)-H(9B)	107.7	C(10)-C(9)-C(7)	113.9(5)
C(10)-C(9)-H(9A)	108.8	C(10)-C(9)-H(9B)	108.8
C(9)-C(10)-C(11)	116.6(9)	C(15)-C(10)-C(9)	122.3(9)
C(15)-C(10)-C(11)	121.1(9)	C(10)-C(11)-H(11A)	109.2
C(10)-C(11)-H(11B)	109.2	H(11A)-C(11)-H(11B)	107.9
C(12)-C(11)-C(10)	112.1(9)	C(12)-C(11)-H(11A)	109.2
C(12)-C(11)-H(11B)	109.2	C(11)-C(12)-H(12A)	108.7
C(11)-C(12)-H(12B)	108.7	H(12A)-C(12)-H(12B)	107.6
C(13)-C(12)-C(11)	114.1(9)	C(13)-C(12)-H(12A)	108.7
C(13)-C(12)-H(12B)	108.7	C(12)-C(13)-H(13A)	109.8
C(12)-C(13)-H(13B)	109.8	H(13A)-C(13)-H(13B)	108.2
C(14)-C(13)-C(12)	109.5(8)	C(14)-C(13)-H(13A)	109.8
C(14)-C(13)-H(13B)	109.8	C(13)-C(14)-H(14A)	108.9
C(13)-C(14)-H(14B)	108.9	H(14A)-C(14)-H(14B)	107.7
C(15)-C(14)-C(13)	113.4(8)	C(15)-C(14)-H(14A)	108.9
C(15)-C(14)-H(14B)	108.9	C(10)-C(15)-C(14)	124.8(9)
C(10)-C(15)-H(15)	117.6	C(14)-C(15)-H(15)	117.6

X-Ray data for compound 4.68f co-crystallized with TFM

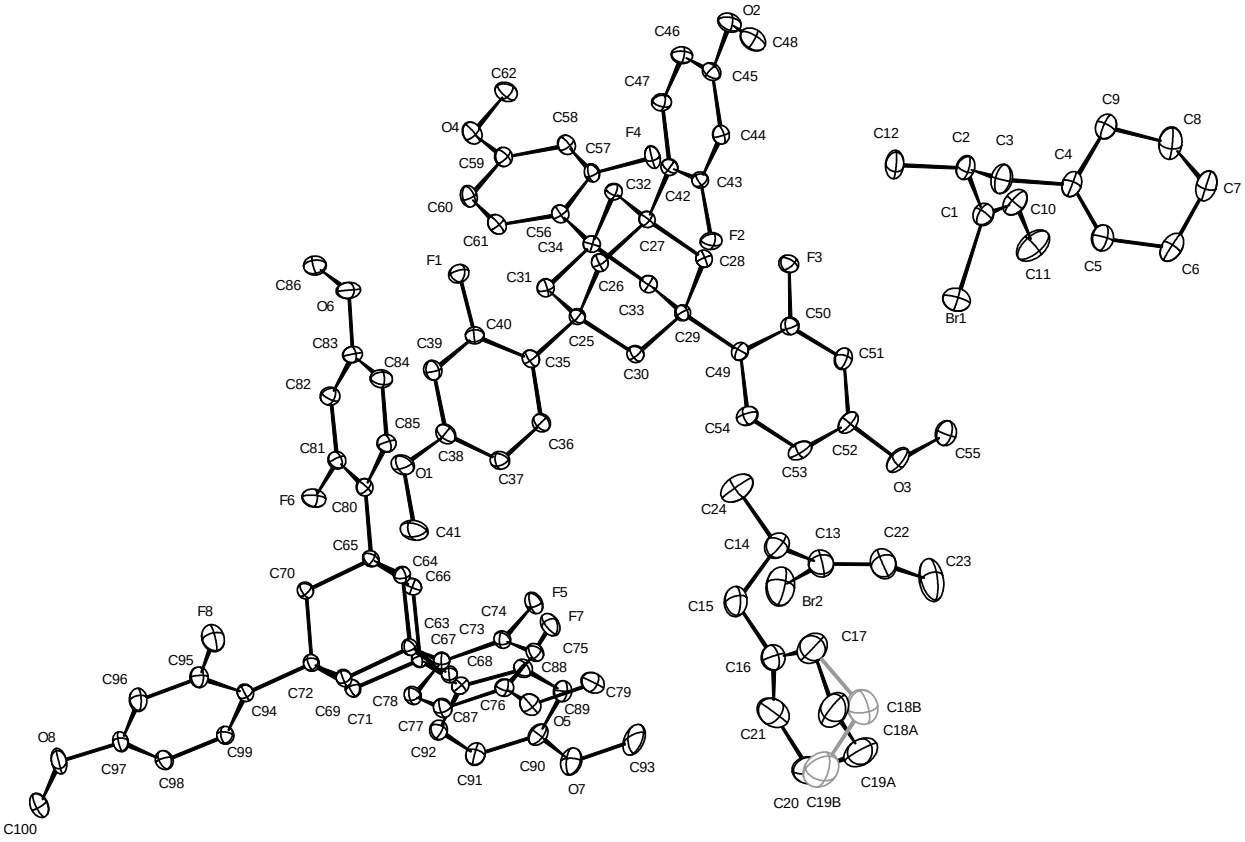

Figure 7.10 The molecular structure of **4.68f**. H atoms have been removed for clarity and disordered parts are shown in grey.

Table 7.7 Crystal data and structure refinement of **4.68f**.

Identification code	16371	
Empirical formula	C_{50} H_{55} Br F_4 O_4	
Color	colourless	
Formula weight	875.85 g·mol^{-1}	
Temperature	100(2) K	
Wavelength	0.71073 Å	
Crystal system	Monoclinic	
Space group	$P2_1$, (no. 4)	
Unit cell dimensions	a = 16.2873(6) Å	α= 90°.
	b = 14.8901(5) Å	β= 110.127(2)°.
	c = 18.5646(7) Å	γ = 90°.
Volume	4227.3(3) Å^3	
Z	4	
Density (calculated)	1.376 Mg·m^{-3}	

Absorption coefficient	1.036 mm^{-1}	
F(000)	1832 e	
Crystal size	0.125 x 0.116 x 0.034 mm^3	
θ range for data collection	1.909 to 30.506°.	
Index ranges	$-23 \leq h \leq 23$, $-21 \leq k \leq 21$, $-26 \leq l \leq 26$	
Reflections collected	819975	
Independent reflections	25784 [R_{int} = 0.1030]	
Reflections with I>2σ(I)	22952	
Completeness to θ = 25.242°	99.9 %	
Absorption correction	Gaussian	
Max. and min. transmission	0 and 0	
Refinement method	Full-matrix least-squares on F^2	
Data / restraints / parameters	25784 / 13 / 1095	
Goodness-of-fit on F^2	1.045	
Final R indices [I>2σ(I)]	R_1 = 0.0424	wR^2 = 0.1113
R indices (all data)	R_1 = 0.0502	wR^2 = 0.1172
Absolute structure parameter	0.013(5)	
Extinction coefficient	n/a	
Largest diff. peak and hole	1.072 and -0.931 e·$Å^{-3}$	

Table 7.8 Bond lengths [Å] and angles [°] of **4.68f**.

Br(1)-C(1)	1.922(3)	C(1)-C(2)	1.503(4)
C(1)-C(10)	1.323(4)	C(2)-H(2)	1.0000
C(2)-C(3)	1.547(4)	C(2)-C(12)	1.527(4)
C(3)-H(3A)	0.9900	C(3)-H(3B)	0.9900
C(3)-C(4)	1.502(4)	C(4)-C(5)	1.335(4)
C(4)-C(9)	1.512(5)	C(5)-H(5)	0.9500
C(5)-C(6)	1.497(4)	C(6)-H(6A)	0.9900
C(6)-H(6B)	0.9900	C(6)-C(7)	1.506(5)
C(7)-H(7A)	0.9900	C(7)-H(7B)	0.9900
C(7)-C(8)	1.528(5)	C(8)-H(8A)	0.9900
C(8)-H(8B)	0.9900	C(8)-C(9)	1.526(5)
C(9)-H(9A)	0.9900	C(9)-H(9B)	0.9900
C(10)-H(10)	0.9500	C(10)-C(11)	1.485(5)
C(11)-H(11A)	0.9800	C(11)-H(11B)	0.9800

C(11)-H(11C)	0.9800	C(12)-H(12A)	0.9800
C(12)-H(12B)	0.9800	C(12)-H(12C)	0.9800
Br(2)-C(13)	1.918(4)	C(13)-C(14)	1.503(5)
C(13)-C(22)	1.325(5)	C(14)-H(14)	1.0000
C(14)-C(15)	1.537(5)	C(14)-C(24)	1.520(5)
C(15)-H(15A)	0.9900	C(15)-H(15B)	0.9900
C(15)-C(16)	1.505(6)	C(16)-C(17)	1.513(7)
C(16)-C(21)	1.322(7)	C(17)-H(17A)	0.9900
C(17)-H(17B)	0.9900	C(17)-H(17C)	0.9900
C(17)-H(17D)	0.9900	C(17)-C(18A)	1.531(7)
C(17)-C(18B)	1.65(4)	C(20)-H(20A)	0.9900
C(20)-H(20B)	0.9900	C(20)-H(20C)	0.9900
C(20)-H(20D)	0.9900	C(20)-C(21)	1.498(9)
C(20)-C(19A)	1.574(12)	C(20)-C(19B)	1.29(4)
C(21)-H(21)	0.9500	C(22)-H(22)	0.9500
C(22)-C(23)	1.488(5)	C(23)-H(23A)	0.9800
C(23)-H(23B)	0.9800	C(23)-H(23C)	0.9800
C(24)-H(24A)	0.9800	C(24)-H(24B)	0.9800
C(24)-H(24C)	0.9800	C(18A)-H(18A)	0.9900
C(18A)-H(18B)	0.9900	C(18A)-C(19A)	1.493(11)
C(19A)-H(19A)	0.9900	C(19A)-H(19B)	0.9900
C(18B)-H(18C)	0.9900	C(18B)-H(18D)	0.9900
C(18B)-C(19B)	1.59(6)	C(19B)-H(19C)	0.9900
C(19B)-H(19D)	0.9900	F(1)-C(40)	1.362(3)
F(2)-C(43)	1.362(3)	F(3)-C(50)	1.365(3)
F(4)-C(57)	1.362(3)	O(1)-C(38)	1.366(3)
O(1)-C(41)	1.429(4)	O(2)-C(45)	1.366(3)
O(2)-C(48)	1.424(4)	O(3)-C(52)	1.360(3)
O(3)-C(55)	1.422(4)	O(4)-C(59)	1.365(3)
O(4)-C(62)	1.423(3)	C(25)-C(26)	1.546(3)
C(25)-C(30)	1.540(3)	C(25)-C(31)	1.548(4)
C(25)-C(35)	1.531(3)	C(26)-H(26A)	0.9900
C(26)-H(26B)	0.9900	C(26)-C(27)	1.539(3)
C(27)-C(28)	1.547(3)	C(27)-C(32)	1.538(3)
C(27)-C(42)	1.526(3)	C(28)-H(28A)	0.9900
C(28)-H(28B)	0.9900	C(28)-C(29)	1.549(3)
C(29)-C(30)	1.535(3)	C(29)-C(33)	1.543(4)
C(29)-C(49)	1.530(3)	C(30)-H(30A)	0.9900

C(30)-H(30B)	0.9900	C(31)-H(31A)	0.9900
C(31)-H(31B)	0.9900	C(31)-C(34)	1.539(3)
C(32)-H(32A)	0.9900	C(32)-H(32B)	0.9900
C(32)-C(34)	1.549(3)	C(33)-H(33A)	0.9900
C(33)-H(33B)	0.9900	C(33)-C(34)	1.542(3)
C(34)-C(56)	1.528(3)	C(35)-C(36)	1.396(3)
C(35)-C(40)	1.398(4)	C(36)-H(36)	0.9500
C(36)-C(37)	1.402(4)	C(37)-H(37)	0.9500
C(37)-C(38)	1.385(4)	C(38)-C(39)	1.397(4)
C(39)-H(39)	0.9500	C(39)-C(40)	1.373(4)
C(41)-H(41A)	0.9800	C(41)-H(41B)	0.9800
C(41)-H(41C)	0.9800	C(42)-C(43)	1.396(3)
C(42)-C(47)	1.406(3)	C(43)-C(44)	1.387(3)
C(44)-H(44)	0.9500	C(44)-C(45)	1.385(4)
C(45)-C(46)	1.393(4)	C(46)-H(46)	0.9500
C(46)-C(47)	1.390(4)	C(47)-H(47)	0.9500
C(48)-H(48A)	0.9800	C(48)-H(48B)	0.9800
C(48)-H(48C)	0.9800	C(49)-C(50)	1.391(4)
C(49)-C(54)	1.405(4)	C(50)-C(51)	1.387(4)
C(51)-H(51)	0.9500	C(51)-C(52)	1.397(4)
C(52)-C(53)	1.388(4)	C(53)-H(53)	0.9500
C(53)-C(54)	1.389(4)	C(54)-H(54)	0.9500
C(55)-H(55A)	0.9800	C(55)-H(55B)	0.9800
C(55)-H(55C)	0.9800	C(56)-C(57)	1.392(3)
C(56)-C(61)	1.402(4)	C(57)-C(58)	1.387(3)
C(58)-H(58)	0.9500	C(58)-C(59)	1.391(4)
C(59)-C(60)	1.395(4)	C(60)-H(60)	0.9500
C(60)-C(61)	1.383(4)	C(61)-H(61)	0.9500
C(62)-H(62A)	0.9800	C(62)-H(62B)	0.9800
C(62)-H(62C)	0.9800	F(5)-C(74)	1.363(3)
F(6)-C(81)	1.367(3)	F(7)-C(88)	1.371(3)
F(8)-C(95)	1.345(3)	O(5)-C(76)	1.366(3)
O(5)-C(79)	1.427(3)	O(6)-C(83)	1.362(3)
O(6)-C(86)	1.430(4)	O(7)-C(90)	1.359(3)
O(7)-C(93)	1.429(4)	O(8)-C(97)	1.370(3)
O(8)-C(100)	1.429(4)	C(63)-C(64)	1.548(3)
C(63)-C(68)	1.539(3)	C(63)-C(69)	1.542(3)
C(63)-C(73)	1.526(3)	C(64)-H(64A)	0.9900

C(64)-H(64B)	0.9900	C(64)-C(65)	1.545(3)
C(65)-C(66)	1.544(3)	C(65)-C(70)	1.542(3)
C(65)-C(80)	1.529(3)	C(66)-H(66A)	0.9900
C(66)-H(66B)	0.9900	C(66)-C(67)	1.551(3)
C(67)-C(68)	1.541(4)	C(67)-C(71)	1.540(3)
C(67)-C(87)	1.526(3)	C(68)-H(68A)	0.9900
C(68)-H(68B)	0.9900	C(69)-H(69A)	0.9900
C(69)-H(69B)	0.9900	C(69)-C(72)	1.539(4)
C(70)-H(70A)	0.9900	C(70)-H(70B)	0.9900
C(70)-C(72)	1.545(3)	C(71)-H(71A)	0.9900
C(71)-H(71B)	0.9900	C(71)-C(72)	1.539(3)
C(72)-C(94)	1.534(3)	C(73)-C(74)	1.394(3)
C(73)-C(78)	1.408(3)	C(74)-C(75)	1.387(4)
C(75)-H(75)	0.9500	C(75)-C(76)	1.393(4)
C(76)-C(77)	1.396(4)	C(77)-H(77)	0.9500
C(77)-C(78)	1.387(4)	C(78)-H(78)	0.9500
C(79)-H(79A)	0.9800	C(79)-H(79B)	0.9800
C(79)-H(79C)	0.9800	C(80)-C(81)	1.388(3)
C(80)-C(85)	1.406(3)	C(81)-C(82)	1.387(4)
C(82)-H(82)	0.9500	C(82)-C(83)	1.390(4)
C(83)-C(84)	1.400(4)	C(84)-H(84)	0.9500
C(84)-C(85)	1.385(4)	C(85)-H(85)	0.9500
C(86)-H(86A)	0.9800	C(86)-H(86B)	0.9800
C(86)-H(86C)	0.9800	C(87)-C(88)	1.395(4)
C(87)-C(92)	1.403(3)	C(88)-C(89)	1.382(4)
C(89)-H(89)	0.9500	C(89)-C(90)	1.388(4)
C(90)-C(91)	1.394(4)	C(91)-H(91)	0.9500
C(91)-C(92)	1.381(4)	C(92)-H(92)	0.9500
C(93)-H(93A)	0.9800	C(93)-H(93B)	0.9800
C(93)-H(93C)	0.9800	C(94)-C(95)	1.400(3)
C(94)-C(99)	1.393(3)	C(95)-C(96)	1.377(4)
C(96)-H(96)	0.9500	C(96)-C(97)	1.397(4)
C(97)-C(98)	1.384(4)	C(98)-H(98)	0.9500
C(98)-C(99)	1.401(4)	C(99)-H(99)	0.9500
C(100)-H(10A)	0.9800	C(100)-H(10B)	0.9800
C(100)-H(10C)	0.9800		

C(2)-C(1)-Br(1)	114.5(2)	C(10)-C(1)-Br(1)	119.3(2)

C(10)-C(1)-C(2)	126.3(3)	C(1)-C(2)-H(2)	106.8
C(1)-C(2)-C(3)	112.1(2)	C(1)-C(2)-C(12)	113.5(3)
C(3)-C(2)-H(2)	106.8	C(12)-C(2)-H(2)	106.8
C(12)-C(2)-C(3)	110.4(2)	C(2)-C(3)-H(3A)	108.8
C(2)-C(3)-H(3B)	108.8	H(3A)-C(3)-H(3B)	107.7
C(4)-C(3)-C(2)	113.9(2)	C(4)-C(3)-H(3A)	108.8
C(4)-C(3)-H(3B)	108.8	C(3)-C(4)-C(9)	117.2(3)
C(5)-C(4)-C(3)	121.5(3)	C(5)-C(4)-C(9)	121.3(3)
C(4)-C(5)-H(5)	117.7	C(4)-C(5)-C(6)	124.7(3)
C(6)-C(5)-H(5)	117.7	C(5)-C(6)-H(6A)	109.1
C(5)-C(6)-H(6B)	109.1	C(5)-C(6)-C(7)	112.4(3)
H(6A)-C(6)-H(6B)	107.9	C(7)-C(6)-H(6A)	109.1
C(7)-C(6)-H(6B)	109.1	C(6)-C(7)-H(7A)	109.4
C(6)-C(7)-H(7B)	109.4	C(6)-C(7)-C(8)	111.0(3)
H(7A)-C(7)-H(7B)	108.0	C(8)-C(7)-H(7A)	109.4
C(8)-C(7)-H(7B)	109.4	C(7)-C(8)-H(8A)	109.7
C(7)-C(8)-H(8B)	109.7	H(8A)-C(8)-H(8B)	108.2
C(9)-C(8)-C(7)	109.9(3)	C(9)-C(8)-H(8A)	109.7
C(9)-C(8)-H(8B)	109.7	C(4)-C(9)-C(8)	112.3(3)
C(4)-C(9)-H(9A)	109.1	C(4)-C(9)-H(9B)	109.1
C(8)-C(9)-H(9A)	109.1	C(8)-C(9)-H(9B)	109.1
H(9A)-C(9)-H(9B)	107.9	C(1)-C(10)-H(10)	115.4
C(1)-C(10)-C(11)	129.3(3)	C(11)-C(10)-H(10)	115.4
C(10)-C(11)-H(11A)	109.5	C(10)-C(11)-H(11B)	109.5
C(10)-C(11)-H(11C)	109.5	H(11A)-C(11)-H(11B)	109.5
H(11A)-C(11)-H(11C)	109.5	H(11B)-C(11)-H(11C)	109.5
C(2)-C(12)-H(12A)	109.5	C(2)-C(12)-H(12B)	109.5
C(2)-C(12)-H(12C)	109.5	H(12A)-C(12)-H(12B)	109.5
H(12A)-C(12)-H(12C)	109.5	H(12B)-C(12)-H(12C)	109.5
C(14)-C(13)-Br(2)	114.9(3)	C(22)-C(13)-Br(2)	120.2(3)
C(22)-C(13)-C(14)	125.0(3)	C(13)-C(14)-H(14)	106.8
C(13)-C(14)-C(15)	112.1(3)	C(13)-C(14)-C(24)	112.6(3)
C(15)-C(14)-H(14)	106.8	C(24)-C(14)-H(14)	106.8
C(24)-C(14)-C(15)	111.2(3)	C(14)-C(15)-H(15A)	108.9
C(14)-C(15)-H(15B)	108.9	H(15A)-C(15)-H(15B)	107.7
C(16)-C(15)-C(14)	113.3(3)	C(16)-C(15)-H(15A)	108.9
C(16)-C(15)-H(15B)	108.9	C(15)-C(16)-C(17)	116.8(4)
C(21)-C(16)-C(15)	123.1(5)	C(21)-C(16)-C(17)	120.1(5)

C(16)-C(17)-H(17A)	108.7	C(16)-C(17)-H(17B)	108.7
C(16)-C(17)-H(17C)	110.6	C(16)-C(17)-H(17D)	110.6
C(16)-C(17)-C(18A)	114.2(5)	C(16)-C(17)-C(18B)	105.7(14)
H(17A)-C(17)-H(17B)	107.6	H(17C)-C(17)-H(17D)	108.7
C(18A)-C(17)-H(17A)	108.7	C(18A)-C(17)-H(17B)	108.7
C(18B)-C(17)-H(17C)	110.6	C(18B)-C(17)-H(17D)	110.6
H(20A)-C(20)-H(20B)	108.1	H(20C)-C(20)-H(20D)	108.1
C(21)-C(20)-H(20A)	109.6	C(21)-C(20)-H(20B)	109.6
C(21)-C(20)-H(20C)	109.5	C(21)-C(20)-H(20D)	109.5
C(21)-C(20)-C(19A)	110.2(5)	C(19A)-C(20)-H(20A)	109.6
C(19A)-C(20)-H(20B)	109.6	C(19B)-C(20)-H(20C)	109.5
C(19B)-C(20)-H(20D)	109.5	C(19B)-C(20)-C(21)	110.8(17)
C(16)-C(21)-C(20)	126.1(7)	C(16)-C(21)-H(21)	117.0
C(20)-C(21)-H(21)	117.0	C(13)-C(22)-H(22)	115.1
C(13)-C(22)-C(23)	129.8(4)	C(23)-C(22)-H(22)	115.1
C(22)-C(23)-H(23A)	109.5	C(22)-C(23)-H(23B)	109.5
C(22)-C(23)-H(23C)	109.5	H(23A)-C(23)-H(23B)	109.5
H(23A)-C(23)-H(23C)	109.5	H(23B)-C(23)-H(23C)	109.5
C(14)-C(24)-H(24A)	109.5	C(14)-C(24)-H(24B)	109.5
C(14)-C(24)-H(24C)	109.5	H(24A)-C(24)-H(24B)	109.5
H(24A)-C(24)-H(24C)	109.5	H(24B)-C(24)-H(24C)	109.5
C(17)-C(18A)-H(18A)	109.9	C(17)-C(18A)-H(18B)	109.9
H(18A)-C(18A)-H(18B)	108.3	C(19A)-C(18A)-C(17)	108.8(6)
C(19A)-C(18A)-H(18A)	109.9	C(19A)-C(18A)-H(18B)	109.9
C(20)-C(19A)-H(19A)	109.5	C(20)-C(19A)-H(19B)	109.5
C(18A)-C(19A)-C(20)	110.9(6)	C(18A)-C(19A)-H(19A)	109.5
C(18A)-C(19A)-H(19B)	109.5	H(19A)-C(19A)-H(19B)	108.0
C(17)-C(18B)-H(18C)	110.7	C(17)-C(18B)-H(18D)	110.7
H(18C)-C(18B)-H(18D)	108.8	C(19B)-C(18B)-C(17)	105(2)
C(19B)-C(18B)-H(18C)	110.7	C(19B)-C(18B)-H(18D)	110.7
C(20)-C(19B)-C(18B)	105(3)	C(20)-C(19B)-H(19C)	110.8
C(20)-C(19B)-H(19D)	110.8	C(18B)-C(19B)-H(19C)	110.8
C(18B)-C(19B)-H(19D)	110.8	H(19C)-C(19B)-H(19D)	108.9
C(38)-O(1)-C(41)	117.3(2)	C(45)-O(2)-C(48)	116.2(2)
C(52)-O(3)-C(55)	116.9(3)	C(59)-O(4)-C(62)	117.4(2)
C(26)-C(25)-C(31)	109.52(19)	C(30)-C(25)-C(26)	107.8(2)
C(30)-C(25)-C(31)	108.3(2)	C(35)-C(25)-C(26)	109.5(2)
C(35)-C(25)-C(30)	111.2(2)	C(35)-C(25)-C(31)	110.5(2)

C(25)-C(26)-H(26A)	109.4	C(25)-C(26)-H(26B)	109.4
H(26A)-C(26)-H(26B)	108.0	C(27)-C(26)-C(25)	110.96(19)
C(27)-C(26)-H(26A)	109.4	C(27)-C(26)-H(26B)	109.4
C(26)-C(27)-C(28)	109.8(2)	C(32)-C(27)-C(26)	107.7(2)
C(32)-C(27)-C(28)	108.3(2)	C(42)-C(27)-C(26)	110.2(2)
C(42)-C(27)-C(28)	109.79(19)	C(42)-C(27)-C(32)	111.0(2)
C(27)-C(28)-H(28A)	109.5	C(27)-C(28)-H(28B)	109.5
C(27)-C(28)-C(29)	110.92(19)	H(28A)-C(28)-H(28B)	108.0
C(29)-C(28)-H(28A)	109.5	C(29)-C(28)-H(28B)	109.5
C(30)-C(29)-C(28)	107.9(2)	C(30)-C(29)-C(33)	108.4(2)
C(33)-C(29)-C(28)	109.08(19)	C(49)-C(29)-C(28)	109.5(2)
C(49)-C(29)-C(30)	111.0(2)	C(49)-C(29)-C(33)	110.9(2)
C(25)-C(30)-H(30A)	109.2	C(25)-C(30)-H(30B)	109.2
C(29)-C(30)-C(25)	112.2(2)	C(29)-C(30)-H(30A)	109.2
C(29)-C(30)-H(30B)	109.2	H(30A)-C(30)-H(30B)	107.9
C(25)-C(31)-H(31A)	109.5	C(25)-C(31)-H(31B)	109.5
H(31A)-C(31)-H(31B)	108.1	C(34)-C(31)-C(25)	110.7(2)
C(34)-C(31)-H(31A)	109.5	C(34)-C(31)-H(31B)	109.5
C(27)-C(32)-H(32A)	109.3	C(27)-C(32)-H(32B)	109.3
C(27)-C(32)-C(34)	111.8(2)	H(32A)-C(32)-H(32B)	107.9
C(34)-C(32)-H(32A)	109.3	C(34)-C(32)-H(32B)	109.3
C(29)-C(33)-H(33A)	109.4	C(29)-C(33)-H(33B)	109.4
H(33A)-C(33)-H(33B)	108.0	C(34)-C(33)-C(29)	111.1(2)
C(34)-C(33)-H(33A)	109.4	C(34)-C(33)-H(33B)	109.4
C(31)-C(34)-C(32)	108.54(19)	C(31)-C(34)-C(33)	107.90(19)
C(33)-C(34)-C(32)	109.43(19)	C(56)-C(34)-C(31)	111.1(2)
C(56)-C(34)-C(32)	109.5(2)	C(56)-C(34)-C(33)	110.2(2)
C(36)-C(35)-C(25)	123.6(2)	C(36)-C(35)-C(40)	114.1(2)
C(40)-C(35)-C(25)	122.2(2)	C(35)-C(36)-H(36)	118.3
C(35)-C(36)-C(37)	123.4(2)	C(37)-C(36)-H(36)	118.3
C(36)-C(37)-H(37)	120.4	C(38)-C(37)-C(36)	119.3(2)
C(38)-C(37)-H(37)	120.4	O(1)-C(38)-C(37)	124.9(2)
O(1)-C(38)-C(39)	115.7(2)	C(37)-C(38)-C(39)	119.4(2)
C(38)-C(39)-H(39)	120.5	C(40)-C(39)-C(38)	118.9(2)
C(40)-C(39)-H(39)	120.5	F(1)-C(40)-C(35)	119.6(2)
F(1)-C(40)-C(39)	115.5(2)	C(39)-C(40)-C(35)	124.8(2)
O(1)-C(41)-H(41A)	109.5	O(1)-C(41)-H(41B)	109.5
O(1)-C(41)-H(41C)	109.5	H(41A)-C(41)-H(41B)	109.5

H(41A)-C(41)-H(41C)	109.5	H(41B)-C(41)-H(41C)	109.5
C(43)-C(42)-C(27)	122.2(2)	C(43)-C(42)-C(47)	114.2(2)
C(47)-C(42)-C(27)	123.6(2)	F(2)-C(43)-C(42)	119.7(2)
F(2)-C(43)-C(44)	115.2(2)	C(44)-C(43)-C(42)	125.1(2)
C(43)-C(44)-H(44)	120.9	C(45)-C(44)-C(43)	118.2(2)
C(45)-C(44)-H(44)	120.9	O(2)-C(45)-C(44)	123.9(2)
O(2)-C(45)-C(46)	116.4(2)	C(44)-C(45)-C(46)	119.8(2)
C(45)-C(46)-H(46)	120.1	C(47)-C(46)-C(45)	119.9(2)
C(47)-C(46)-H(46)	120.1	C(42)-C(47)-H(47)	118.6
C(46)-C(47)-C(42)	122.8(2)	C(46)-C(47)-H(47)	118.6
O(2)-C(48)-H(48A)	109.5	O(2)-C(48)-H(48B)	109.5
O(2)-C(48)-H(48C)	109.5	H(48A)-C(48)-H(48B)	109.5
H(48A)-C(48)-H(48C)	109.5	H(48B)-C(48)-H(48C)	109.5
C(50)-C(49)-C(29)	123.3(2)	C(50)-C(49)-C(54)	113.9(2)
C(54)-C(49)-C(29)	122.8(2)	F(3)-C(50)-C(49)	119.6(2)
F(3)-C(50)-C(51)	114.8(2)	C(51)-C(50)-C(49)	125.6(3)
C(50)-C(51)-H(51)	121.0	C(50)-C(51)-C(52)	118.0(3)
C(52)-C(51)-H(51)	121.0	O(3)-C(52)-C(51)	124.5(3)
O(3)-C(52)-C(53)	116.3(3)	C(53)-C(52)-C(51)	119.2(2)
C(52)-C(53)-H(53)	119.8	C(52)-C(53)-C(54)	120.4(3)
C(54)-C(53)-H(53)	119.8	C(49)-C(54)-H(54)	118.5
C(53)-C(54)-C(49)	122.9(3)	C(53)-C(54)-H(54)	118.5
O(3)-C(55)-H(55A)	109.5	O(3)-C(55)-H(55B)	109.5
O(3)-C(55)-H(55C)	109.5	H(55A)-C(55)-H(55B)	109.5
H(55A)-C(55)-H(55C)	109.5	H(55B)-C(55)-H(55C)	109.5
C(57)-C(56)-C(34)	122.6(2)	C(57)-C(56)-C(61)	114.3(2)
C(61)-C(56)-C(34)	123.1(2)	F(4)-C(57)-C(56)	119.2(2)
F(4)-C(57)-C(58)	115.4(2)	C(58)-C(57)-C(56)	125.3(2)
C(57)-C(58)-H(58)	121.0	C(57)-C(58)-C(59)	118.0(2)
C(59)-C(58)-H(58)	121.0	O(4)-C(59)-C(58)	124.6(2)
O(4)-C(59)-C(60)	116.2(2)	C(58)-C(59)-C(60)	119.2(2)
C(59)-C(60)-H(60)	119.8	C(61)-C(60)-C(59)	120.5(2)
C(61)-C(60)-H(60)	119.8	C(56)-C(61)-H(61)	118.7
C(60)-C(61)-C(56)	122.7(2)	C(60)-C(61)-H(61)	118.7
O(4)-C(62)-H(62A)	109.5	O(4)-C(62)-H(62B)	109.5
O(4)-C(62)-H(62C)	109.5	H(62A)-C(62)-H(62B)	109.5
H(62A)-C(62)-H(62C)	109.5	H(62B)-C(62)-H(62C)	109.5
C(76)-O(5)-C(79)	117.2(2)	C(83)-O(6)-C(86)	116.8(2)

C(90)-O(7)-C(93)	116.6(2)	C(97)-O(8)-C(100)	117.1(2)
C(68)-C(63)-C(64)	109.62(19)	C(68)-C(63)-C(69)	107.8(2)
C(69)-C(63)-C(64)	108.5(2)	C(73)-C(63)-C(64)	109.8(2)
C(73)-C(63)-C(68)	110.0(2)	C(73)-C(63)-C(69)	111.1(2)
C(63)-C(64)-H(64A)	109.3	C(63)-C(64)-H(64B)	109.3
H(64A)-C(64)-H(64B)	107.9	C(65)-C(64)-C(63)	111.7(2)
C(65)-C(64)-H(64A)	109.3	C(65)-C(64)-H(64B)	109.3
C(66)-C(65)-C(64)	108.1(2)	C(70)-C(65)-C(64)	107.8(2)
C(70)-C(65)-C(66)	109.4(2)	C(80)-C(65)-C(64)	110.9(2)
C(80)-C(65)-C(66)	110.0(2)	C(80)-C(65)-C(70)	110.5(2)
C(65)-C(66)-H(66A)	109.4	C(65)-C(66)-H(66B)	109.4
C(65)-C(66)-C(67)	111.3(2)	H(66A)-C(66)-H(66B)	108.0
C(67)-C(66)-H(66A)	109.4	C(67)-C(66)-H(66B)	109.4
C(68)-C(67)-C(66)	109.4(2)	C(71)-C(67)-C(66)	107.7(2)
C(71)-C(67)-C(68)	108.2(2)	C(87)-C(67)-C(66)	110.3(2)
C(87)-C(67)-C(68)	110.0(2)	C(87)-C(67)-C(71)	111.2(2)
C(63)-C(68)-C(67)	111.0(2)	C(63)-C(68)-H(68A)	109.4
C(63)-C(68)-H(68B)	109.4	C(67)-C(68)-H(68A)	109.4
C(67)-C(68)-H(68B)	109.4	H(68A)-C(68)-H(68B)	108.0
C(63)-C(69)-H(69A)	109.5	C(63)-C(69)-H(69B)	109.5
H(69A)-C(69)-H(69B)	108.0	C(72)-C(69)-C(63)	110.9(2)
C(72)-C(69)-H(69A)	109.5	C(72)-C(69)-H(69B)	109.5
C(65)-C(70)-H(70A)	109.5	C(65)-C(70)-H(70B)	109.5
C(65)-C(70)-C(72)	110.9(2)	H(70A)-C(70)-H(70B)	108.0
C(72)-C(70)-H(70A)	109.5	C(72)-C(70)-H(70B)	109.5
C(67)-C(71)-H(71A)	109.2	C(67)-C(71)-H(71B)	109.2
H(71A)-C(71)-H(71B)	107.9	C(72)-C(71)-C(67)	111.9(2)
C(72)-C(71)-H(71A)	109.2	C(72)-C(71)-H(71B)	109.2
C(69)-C(72)-C(70)	109.7(2)	C(69)-C(72)-C(71)	108.3(2)
C(71)-C(72)-C(70)	108.1(2)	C(94)-C(72)-C(69)	110.3(2)
C(94)-C(72)-C(70)	109.4(2)	C(94)-C(72)-C(71)	111.0(2)
C(74)-C(73)-C(63)	122.5(2)	C(74)-C(73)-C(78)	114.4(2)
C(78)-C(73)-C(63)	123.0(2)	F(5)-C(74)-C(73)	119.6(2)
F(5)-C(74)-C(75)	115.2(2)	C(75)-C(74)-C(73)	125.3(2)
C(74)-C(75)-H(75)	121.0	C(74)-C(75)-C(76)	118.1(2)
C(76)-C(75)-H(75)	121.0	O(5)-C(76)-C(75)	124.9(2)
O(5)-C(76)-C(77)	115.7(2)	C(75)-C(76)-C(77)	119.4(2)
C(76)-C(77)-H(77)	119.8	C(78)-C(77)-C(76)	120.4(2)

C(78)-C(77)-H(77)	119.8	C(73)-C(78)-H(78)	118.8
C(77)-C(78)-C(73)	122.5(2)	C(77)-C(78)-H(78)	118.8
O(5)-C(79)-H(79A)	109.5	O(5)-C(79)-H(79B)	109.5
O(5)-C(79)-H(79C)	109.5	H(79A)-C(79)-H(79B)	109.5
H(79A)-C(79)-H(79C)	109.5	H(79B)-C(79)-H(79C)	109.5
C(81)-C(80)-C(65)	122.5(2)	C(81)-C(80)-C(85)	114.1(2)
C(85)-C(80)-C(65)	123.3(2)	F(6)-C(81)-C(80)	119.7(2)
F(6)-C(81)-C(82)	114.9(2)	C(82)-C(81)-C(80)	125.4(2)
C(81)-C(82)-H(82)	120.9	C(81)-C(82)-C(83)	118.3(2)
C(83)-C(82)-H(82)	120.9	O(6)-C(83)-C(82)	124.3(2)
O(6)-C(83)-C(84)	116.6(2)	C(82)-C(83)-C(84)	119.2(2)
C(83)-C(84)-H(84)	120.0	C(85)-C(84)-C(83)	120.0(2)
C(85)-C(84)-H(84)	120.0	C(80)-C(85)-H(85)	118.5
C(84)-C(85)-C(80)	123.0(2)	C(84)-C(85)-H(85)	118.5
O(6)-C(86)-H(86A)	109.5	O(6)-C(86)-H(86B)	109.5
O(6)-C(86)-H(86C)	109.5	H(86A)-C(86)-H(86B)	109.5
H(86A)-C(86)-H(86C)	109.5	H(86B)-C(86)-H(86C)	109.5
C(88)-C(87)-C(67)	123.4(2)	C(88)-C(87)-C(92)	113.4(2)
C(92)-C(87)-C(67)	123.3(2)	F(7)-C(88)-C(87)	119.4(2)
F(7)-C(88)-C(89)	114.7(2)	C(89)-C(88)-C(87)	125.9(2)
C(88)-C(89)-H(89)	121.0	C(88)-C(89)-C(90)	117.9(2)
C(90)-C(89)-H(89)	121.0	O(7)-C(90)-C(89)	124.5(3)
O(7)-C(90)-C(91)	116.2(3)	C(89)-C(90)-C(91)	119.3(2)
C(90)-C(91)-H(91)	119.9	C(92)-C(91)-C(90)	120.2(3)
C(92)-C(91)-H(91)	119.9	C(87)-C(92)-H(92)	118.4
C(91)-C(92)-C(87)	123.3(2)	C(91)-C(92)-H(92)	118.4
O(7)-C(93)-H(93A)	109.5	O(7)-C(93)-H(93B)	109.5
O(7)-C(93)-H(93C)	109.5	H(93A)-C(93)-H(93B)	109.5
H(93A)-C(93)-H(93C)	109.5	H(93B)-C(93)-H(93C)	109.5
C(95)-C(94)-C(72)	121.7(2)	C(99)-C(94)-C(72)	124.2(2)
C(99)-C(94)-C(95)	114.1(2)	F(8)-C(95)-C(94)	119.9(2)
F(8)-C(95)-C(96)	115.1(2)	C(96)-C(95)-C(94)	125.0(2)
C(95)-C(96)-H(96)	120.8	C(95)-C(96)-C(97)	118.4(2)
C(97)-C(96)-H(96)	120.8	O(8)-C(97)-C(96)	115.1(3)
O(8)-C(97)-C(98)	125.0(3)	C(98)-C(97)-C(96)	120.0(2)
C(97)-C(98)-H(98)	120.5	C(97)-C(98)-C(99)	119.0(2)
C(99)-C(98)-H(98)	120.5	C(94)-C(99)-C(98)	123.7(2)
C(94)-C(99)-H(99)	118.2	C(98)-C(99)-H(99)	118.2

O(8)-C(100)-H(10A)	109.5	O(8)-C(100)-H(10B)	109.5
O(8)-C(100)-H(10C)	109.5	H(10A)-C(100)-H(10B)	109.5
H(10A)-C(100)-H(10C)	109.5	H(10B)-C(100)-H(10C)	109.5

8. REFERENCES

[1] M. Enquist, A. Arak *Nature* **1994**, *372*, 169–172.

[2] E. Petrakou, "Supersymmetry's Long Fall from Grace," can be found under https://www.scientificamerican.com/article/supersymmetrys-long-fall-from-grace/(accessed 16 August 2025), **2025**.

[3] D. G. Blackmond *Cold Spring Harb. Perspect. Biol.* **2019**, *11*, a032540.

[4] F. G. Riddell, M. J. T. Robinson *Tetrahedron* **1974**, *30*, 2001–2007.

[5] D. R. Brocks *Biopharm. Drug Dispos.* **2006**, *27*, 387–406.

[6] T. Bugg, *Introduction to Enzyme and Coenzyme Chemistry*, Blackwell Publishing, Oxford, **2004**.

[7] G. Bredig, P. S. Fiske *Biochem. Z.* **1912**, *687*, 7–23.

[8] K. C. Nicolaou, E. J. Sorensen, *Classics in Total Synthesis*, Wiley-VCH, Weinheim, **1996**.

[9] B. List, R. A. Lerner, C. F. Barbas *J. Am. Chem. Soc.* **2000**, *122*, 2395–2396.

[10] K. A. Ahrendt, C. J. Borths, D. W. C. MacMillan *J. Am. Chem. Soc.* **2000**, *122*, 4243–4244.

[11] B. M. Trost *Science* **1991**, *254*, 1471–1477.

[12] E. Oldfield, F. Y. Lin *Angew. Chem., Int. Ed.* **2012**, *51*, 1124–1137.

[13] A. G. M. Barrett, T. K. Ma, T. Mies *Synthesis* **2019**, *51*, 67–82.

[14] E. Fulhame in *An Essay on Combustion: With a View to a New Art of Dying and Painting*, Cooper, J., London, **1794**, pp. 166–177.

[15] J. W. Mellor *J. Phys. Chem.* **2002**, *7*, 557–567.

[16] J. Berzelius in *Årsberättelse Om Fram. i Fys. Och Kemi*, P.A. Norstedt & Söner, Kongl. Boktrykare, Stockholm, **1835**, pp. 245–246.

[17], "DeepL Translate: The world's most accurate translator," can be found under https://www.deepl.com/en/translator(accessed 27 October 2025), **2017**.

[18] J. Carrière, *Berzelius und Liebig – Ihre Briefe von 1831-1845 mit erläuternden Einschaltungen aus gleichzeitigen Briefen von Liebig und Wöhler*, J. F. Lehmann, München, **1898**.

[19] J. Van Houten *J. Chem. Educ.* **2002**, *79*, 146.

[20] F. E. Wall *J. Chem. Educ.* **1948**, *25*, 2–10.

[21] W. Ostwald, *PROCESS OF MANUFACTURING NITRIC ACID*, **1907**, 858,904.

[22] R. Bentley *Chem. Rev.* **2006**, *106*, 4099–4112.

[23] O. García Mancheño, M. Waser *Eur. J. Org. Chem.* **2023**, *26*, e202200950.

[24] W. Ostwald *Zeitschrift für phys. Chemie* **1900**, *34*, 508–512.

[25] J. von Liebig *Justus Liebigs Ann. Chem.* **1860**, *113*, 246–247.

[26] W. Langenbeck *Justus Liebigs Ann. Chem.* **1929**, *469*, 16–25.

[27] W. Langenbeck *Angew. Chem.* **1928**, *41*, 740–745.

[28] E. Knoevenagel *Ber. dtsch. Chem. Ges.* **1896**, *29*, 172–174.

[29] U. Eder, G. Sauer, R. Wiechert *Angew. Chem., Int. Ed.* **1971**, *10*, 496–497.

[30] Z. G. Hajos, D. R. Parrish *J. Org. Chem.* **1974**, *39*, 1615–1621.

[31] B. Bradshaw, J. Bonjoch *Synlett* **2012**, *2012*, 337–356.

[32] S. Bahmanyar, K. N. Houk *J. Am. Chem. Soc.* **2001**, *123*, 11273–11283.

[33] S. Bahmanyar, K. N. Houk *J. Am. Chem. Soc.* **2001**, *123*, 12911–12912.

[34] B. List, L. Hoang, H. J. Martin *Proc. Natl. Acad. Sci. U. S. A.* **2004**, *101*, 5839–5842.

[35] S. Mukherjee, J. W. Yang, S. Hoffmann, B. List *Chem. Rev.* **2007**, *107*, 5471–5569.

[36] A. Erkkilä, I. Majander, P. M. Pihko *Chem. Rev.* **2007**, *107*, 5416–5470.

[37] S. Bertelsen, K. A. Jørgensen *Chem. Soc. Rev.* **2009**, *38*, 2178–2189.

[38] I. Seayad, B. List *Org. Biomol. Chem.* **2005**, *3*, 719–724.

[39] R. B. Sunoj in *Comprehensive Enantioselective Organocatalysis* (Ed.: P.I. Dalko), Wiley-VCH, Weinheim, **2013**, pp. 463–494.

[40] Y. E. Türkmen, Y. Zhu, V. H. Rawal in *Comprehensive Enantioselective Organocatalysis* (Ed.: P.I. Dalko), Wiley-VCH, Weinheim, **2013**, pp. 239–288.

[41] T. Heckel, R. Wilhelm in *Comprehensive Enantioselective Organocatalysis* (Ed.: P.I. Dalko), Wiley-VCH, Weinheim, **2013**, pp. 431–459.

[42] B. List, "Benjamin List – Nobel Prize lecture - NobelPrize.org," can be found under https://www.nobelprize.org/prizes/chemistry/2021/list/lecture/(accessed 20 August 2025), **2021**.

[43] D. McNaught, A. Wilkinson, *The IUPAC Compendium of Chemical Terminology, 2nd ed.*, Blackwell Scientific Publications, Oxford, **1997**.

[44] E. V. Anslyn, D. A. Dougherty in *Modern Physical Organic Chemistry*, University Science Books, Sausalito, California, **2006**, p. 507—522.

[45] E. E. Kwan *J. Chem. Educ.* **2005**, *82*, 1026–1030.

[46] A. Ault *J. Chem. Educ.* **2007**, *84*, 38–39.

[47] W. P. Jencks *Acc. Chem. Res.* **1976**, *9*, 425–432.

[48] M. Fleischmann, D. Drettwan, E. Sugiono, M. Rueping, R. M. Gschwind *Angew. Chem., Int. Ed.* **2011**, *50*, 6364–6369.

[49] T. Akiyama, J. Itoh, K. Fuchibe *Adv. Synth. Catal.* **2006**, *348*, 999–1010.

[50] M. S. Sigman, E. N. Jacobsen *J. Am. Chem. Soc.* **1998**, *120*, 4901–4902.

[51] Y. Huang, A. K. Unni, A. N. Thadani, V. H. Rawal *Nature* **2003**, *424*, 146.

[52] N. T. McDougal, S. E. Schaus *J. Am. Chem. Soc.* **2003**, *125*, 12094–12095.

[53] B. M. Nugent, R. A. Yoder, J. N. Johnston *J. Am. Chem. Soc.* **2004**, *126*, 3418–3419.

[54] J. P. Malerich, K. Hagihara, V. H. Rawal *J. Am. Chem. Soc.* **2008**, *130*, 14416–14417.

[55] A. G. Doyle, E. N. Jacobsen *Chem. Rev.* **2007**, *107*, 5713–5743.

[56] S. Vera, A. García-Urricelqui, A. Mielgo, M. Oiarbide *Eur. J. Org. Chem.* **2023**, *26*, e202201254.

[57] H. M. L. Davies, R. E. J. Beckwith *Chem. Rev.* **2003**, *103*, 2861–2903.

[58] H. Furuno, T. Hayano, T. Kambara, Y. Sugimoto, T. Hanamoto, Y. Tanaka, Y. Z. Jin, T. Kagawa, J. Inanaga *Tetrahedron* **2003**, *59*, 10509–10523.

[59] H. Furuno, T. Hanamoto, Y. Sugimoto, J. Inanaga *Org. Lett.* **2000**, *2*, 49–52.

[60] M. C. Pirrung, J. Zhang *Tetrahedron Lett.* **1992**, *33*, 5987–5990.

[61] N. McCarthy, M. A. McKervey, T. Ye, M. McCann, E. Murphy, M. P. Doyle *Tetrahedron Lett.* **1992**, *33*, 5983–5986.

[62] T. Akiyama, J. Itoh, K. Yokota, K. Fuchibe *Angew. Chem., Int. Ed.* **2004**, *43*, 1566–1568.

[63] D. Uraguchi, M. Terada *J. Am. Chem. Soc.* **2004**, *126*, 5356–5357.

[64] M. Hatano, K. Moriyama, T. Maki, K. Ishihara *Angew. Chem., Int. Ed.* **2010**, *49*, 3823–3826.

[65] M. Terada *Synthesis* **2010**, *2010*, 1929–1982.

[66] S. Hoffmann, A. M. Seayad, B. List *Angew. Chem., Int. Ed.* **2005**, *44*, 7424–7427.

[67] X. del Corte, E. Martínez de Marigorta, F. Palacios, J. Vicario, A. Maestro *Org. Chem. Front.* **2022**, *9*, 6331–6399.

[68] I. O. Betinol, Y. Kuang, B. P. Mulley, J. P. Reid *Chem. Rev.* **2025**, *125*, 4184–4286.

[69] D. Parmar, E. Sugiono, S. Raja, M. Rueping *Chem. Rev.* **2014**, *114*, 9047–9153.

[70] K. Kaupmees, N. Tolstoluzhsky, S. Raja, M. Rueping, I. Leito *Angew. Chem., Int. Ed.* **2013**, *52*, 11569–11572.

[71] M. Hatano, Y. Goto, A. Izumiseki, M. Akakura, K. Ishihara *J. Am. Chem. Soc.* **2015**, *137*, 13472–13475.

[72] J. Wang, Q. Zhang, Y. Li, X. Liu, X. Li, J. P. Cheng *Chem. Commun.* **2019**, *56*, 261–264.

[73] Y. L. Pan, H. L. Zheng, J. Wang, C. Yang, X. Li, J. P. Cheng *ACS Catal.* **2020**, *10*, 8069–8076.

[74] Q. X. Zhang, Y. Li, J. Wang, C. Yang, C. J. Liu, X. Li, J. P. Cheng *Angew. Chem., Int. Ed.* **2020**, *59*, 4550–4556.

[75] G. P. Wang, M. Q. Chen, S. F. Zhu, Q. L. Zhou *Chem. Sci.* **2017**, *8*, 7197–7202.

[76] L. Zhang, J. Zhang, J. Ma, D. J. Cheng, B. Tan *J. Am. Chem. Soc.* **2017**, *139*, 1714–1717.

[77] C. D. Gheewala, B. E. Collins, T. H. Lambert *Science* **2016**, *351*, 961–965.

[78] I. A. Koppel, J. Koppel, I. Leito, I. Koppel, M. Mishima, L. M. Yagupolskii *J. Chem. Soc., Perkin Trans. 2* **2001**, 229–232.

[79] L. M. Yagupolskii, V. N. Petrik, N. V. Kondratenko, L. Sooväli, I. Kaljurand, I. Leito, I. A. Koppel *J. Chem. Soc., Perkin Trans. 2* **2002**, *2*, 1950–1955.

[80] F. G. Bordwell, D. Algrim *J. Org. Chem.* **1976**, *41*, 2507–2508.

[81] G. A. Olah, G. K. S. Prakash, J. Sommer, A. Molnar in *Superacid Chemistry*, Wiley-VCH Verlag GmbH, Weinheim, **2009**, pp. 1–34.

[82] A. Kütt, S. Tshepelevitsh, J. Saame, M. Lõkov, I. Kaljurand, S. Selberg, I. Leito *Eur. J. Org. Chem.* **2021**, *2021*, 1407–1419.

[83] A. Kütt, T. Rodima, J. Saame, E. Raamat, V. Mäemets, I. Kaljurand, I. A. Koppel, R. Y. Garlyauskayte, Y. L. Yagupolskii, L. M. Yagupolskii, E. Bernhardt, H. Willner, I. Leito *J. Org. Chem.* **2011**, *76*, 391–395.

[84] B. Peng, J. Ma, J. Guo, Y. Gong, R. Wang, Y. Zhang, J. Zeng, W. W. Chen, K. Ding, B. Zhao *J. Am. Chem. Soc.* **2022**, *144*, 2853–2860.

[85] D. Nakashima, H. Yamamoto *J. Am. Chem. Soc.* **2006**, *128*, 9626–9627.

[86] P. S. J. Kaib, B. List *Synlett* **2016**, *27*, 156–158.

[87] G. Pousse, A. Devineau, V. Dalla, L. Humphreys, M. C. Lasne, J. Rouden, J. Blanchet *Tetrahedron* **2009**, *65*, 10617–10622.

[88] N. D. Shapiro, V. Rauniyar, G. L. Hamilton, J. Wu, F. D. Toste *Nature* **2011**, *470*, 245–250.

[89] H. C. Cheol, H. Yamamoto *J. Am. Chem. Soc.* **2008**, *130*, 9246–9247.

[90] S. C. Pan, B. List *Chem. Asian J.* **2008**, *3*, 430–437.

[91] M. Hatano, T. Maki, K. Moriyama, M. Arinobe, K. Ishihara *J. Am. Chem. Soc.* **2008**, *130*, 16858–16860.

[92] M. Hatano, K. Ishihara *Asian J. Org. Chem.* **2014**, *3*, 352–365.

[93] H. Y. Bae, D. Höfler, P. S. J. Kaib, P. Kasaplar, C. K. De, A. Döhring, S. Lee, K. Kaupmees, I. Leito, B. List *Nat. Chem.* **2018**, *10*, 888–894.

[94] P. Garcia-Garcia, F. Lay, P. Garcia-Garcia, C. Rabalakos, B. List *Angew. Chem., Int. Ed.* **2009**, *48*, 4363–4366.

[95] M. Treskow, J. Neudörfl, R. Giernoth *Eur. J. Org. Chem.* **2009**, *2009*, 3693–3697.

[96] M. C. Benda, S. France *Org. Biomol. Chem.* **2020**, *18*, 7485–7513.

[97] B. Mathieu, L. Ghosez *Tetrahedron* **2002**, *58*, 8219–8226.

[98] M. Mahlau, B. List *Angew. Chem., Int. Ed.* **2013**, *52*, 518–533.

[99] T. James, M. Van Gemmeren, B. List *Chem. Rev.* **2015**, *115*, 9388–9409.

[100] E. B. Rowland, G. B. Rowland, E. Rivera-Otero, J. C. Antilla *J. Am. Chem. Soc.* **2007**, *129*, 12084–12085.

[101] G. Della Sala, A. Lattanzi *Org. Lett.* **2009**, *11*, 3330–3333.

[102] S. Ni, V. Ramesh Naidu, J. Franzén *Eur. J. Org. Chem.* **2016**, *2016*, 1708–1713.

[103] R. E. Shelton, S. Sezer, D. M. Hodgson *Tetrahedron* **2020**, *76*, 131701.

[104] T. Gatzenmeier, M. Van Gemmeren, Y. Xie, D. Höfler, M. Leutzsch, B. List *Science* **2016**, *351*, 949–952.

[105] A. Hasegawa, K. Ishihara, H. Yamamoto *Angew. Chem., Int. Ed.* **2003**, *42*, 5731–5733.

[106] D. Höfler, M. van Gemmeren, P. Wedemann, K. Kaupmees, I. Leito, M. Leutzsch, J. B. Lingnau, B. List *Angew. Chem., Int. Ed.* **2017**, *56*, 1411–1415.

[107] S. Vellalath, I. Čorić, B. List *Angew. Chem., Int. Ed.* **2010**, *49*, 9749–9752.

[108] L. Schreyer, R. Properzi, B. List *Angew. Chem., Int. Ed.* **2019**, *58*, 12761–12777.

[109] I. Čorić, B. List *Nature* **2012**, *483*, 315–319.

[110] L. Liu, P. S. J. Kaib, A. Tap, B. List *J. Am. Chem. Soc.* **2016**, *138*, 10822–10825.

[111] P. S. J. Kaib, L. Schreyer, S. Lee, R. Properzi, B. List *Angew. Chem., Int. Ed.* **2016**, *55*, 13200–13203.

[112] M. J. Scharf, N. Tsuji, M. M. Lindner, M. Leutzsch, M. Lõkov, E. Parman, I. Leito, B. List *J. Am. Chem. Soc.* **2024**, *146*, 28339–28349.

[113] J. P. Handjaya, N. Patankar, J. P. Reid *Chem. Eur. J.* **2024**, *30*, e202400921.

[114] A. Kütt, I. Leito, I. Kaljurand, L. Sooväli, V. M. Vlasov, L. M. Yagupolskii, I. A. Koppel *J. Org. Chem.* **2006**, *71*, 2829–2838.

[115] C. D. Diáz-Oviedo, R. Maji, B. List *J. Am. Chem. Soc.* **2021**, *143*, 20598–20604.

[116] J. A. A. Grimm, H. Zhou, R. Properzi, M. Leutzsch, G. Bistoni, J. Nienhaus, B. List *Nature* **2023**, *615*, 634–639.

[117] J. Lai, B. List, J. P. Reid *Nat. Commun.* **2025**, *16*, 1–10.

[118] S. A. Schwengers, C. K. De, O. Grossmann, J. A. A. Grimm, N. R. Sadlowski, G. G. Gerosa, B. List *J. Am. Chem. Soc.* **2021**, *143*, 14835–14844.

[119] K. Brak, E. N. Jacobsen *Angew. Chem., Int. Ed.* **2013**, *52*, 534–561.

[120] S. Mayer, B. List *Angew. Chem., Int. Ed.* **2006**, *45*, 4193–4195.

[121] G. L. Hamilton, J. K. Eun, M. Mba, F. D. Toste *Science* **2007**, *317*, 496–499.

[122] L.-M. Entgelmeier, O. G. Mancheño *Synthesis* **2022**, *54*, 3907–3927.

[123] M. S. Taylor, E. N. Jacobsen *J. Am. Chem. Soc.* **2004**, *126*, 10558–10559.

[124] C. Cimino, O. M. Maurel, T. Musumeci, A. Bonaccorso, F. Drago, E. M. B. Souto, R. Pignatello, C. Carbone *Pharmaceutics* **2021**, *13*, 327.

[125] J. Hasserodt, K. D. Janda, R. A. Lerner *J. Am. Chem. Soc.* **1996**, *118*, 11654–11655.

[126] D. W. Christianson *Chem. Rev.* **2006**, *106*, 3412–3442.

[127] F. H. Arnold *Angew. Chem., Int. Ed.* **2018**, *57*, 4143–4148.

[128] A. M. F. Phillips, L. M. Ferreira, P. S. Branco, A. Lourenço *Asian J. Org. Chem.* **2025**, *14*, e202500229.

[129] A. Kekulé in *Lehrbuch Der Organischen Chemie*, Ferdinand Enke, Erlangen, **1866**, pp. 464–465.

[130] M. Eggersdorfer in *Ullmann's Encyclopedia of Industrial Chemistry*, John Wiley & Sons, Ltd, **2000**.

[131] S. Dev in *Natural Products of Woody Plants* (Ed.: J.W. Rowe), Springer-Verlag Berlin, Heidelberg, **1989**, pp. 691–808.

[132] G. P. Moss, P. A. S. Smith, D. Tavernier *Pure Appl. Chem.* **1995**, *67*, 1307–1375.

[133] K.-H. Ernst *Chimia* **2018**, *72*, 399–403.

[134] O. Wallach, *Terpene und Campher: Zusammenfassung eigener Untersuchungen auf dem Gebiet der alicyclischen Kohlenstoffverbindungen*, Verlag Von Veit & Comp., Leipzig, **1914**.

[135] O. Wallach *Justus Liebigs Ann. Chem.* **1887**, *238*, 78–89.

[136] L. Ruzicka *J. Chem. Soc.* **1932**, 1582–1597.

[137] L. Ruzicka *Experientia* **1953**, *9*, 357–367.

[138] J. C. Gray *Adv. Bot. Res.* **1988**, *14*, 25–91.

[139] S. G. Hillier, R. Lathe *J. Endocrinol.* **2019**, *242*, R9–R22.

[140] K. Bloch *Steroids* **1992**, *57*, 378–383.

[141] M. Rohmer *Nat. Prod. Rep.* **1999**, *16*, 565–574.

[142] A. Frank, M. Groll *Chem. Rev.* **2017**, *117*, 5675–5703.

[143] D. W. Christianson *Chem. Rev.* **2017**, *117*, 11570–11648.

[144] F. Lynen, H. Eggerer, U. Henning, I. Kessel *Angew. Chem.* **1958**, *70*, 738–742.

[145] F. Lynen, B. W. Agranoff, H. Eggerer, U. Henning, E. M. Möslein *Angew. Chem.* **1959**, *71*, 657–663.

[146] P. H. Liang, T. P. Ko, A. H. J. Wang *Eur. J. Biochem.* **2002**, *269*, 3339–3354.

[147] J. W. Cornforth *Angew. Chem., Int. Ed.* **1968**, *7*, 903–911.

[148] H. Y. Chang, T. H. Cheng, A. H. J. Wang *IUBMB Life* **2021**, *73*, 40–63.

[149] K. Ogura, T. Koyama, H. Sagami in *Sub-Cellular Biochemistry*, Springer, Boston, MA, **1997**, pp. 57–87.

[150] S. Y. Chang, T. P. Ko, P. H. Liang, A. H. J. Wang *J. Biol. Chem.* **2003**, *278*, 29298–29307.

[151] P. H. Liang *Biochemistry* **2009**, *48*, 6562–6570.

[152] D. J. Tantillo *Nat. Prod. Rep.* **2011**, *28*, 1035–1053.

[153] D. J. Tantillo *Chem. Soc. Rev.* **2010**, *39*, 2847–2854.

[154] M. Seemann, G. Zhai, J. W. De Kraker, C. M. Paschall, D. W. Christianson, D. E. Cane *J. Am. Chem. Soc.* **2002**, *124*, 7681–7689.

[155] R. Croteau *Chem. Rev.* **1987**, *87*, 929–954.

[156] R. B. Croteau, J. J. Shaskus, B. Renstrom, N. M. Felton, D. E. Cane, A. Saito, C. Chang *Biochemistry* **1985**, *24*, 7077–7085.

[157] R. Croteau, D. M. Satterwhite, D. E. Cane, C. C. Chang *J. Biol. Chem.* **1988**, *263*, 10063–10071.

[158] J. A. Faraldos, P. E. O'Maille, N. Dellas, J. P. Noel, R. M. Coates *J. Am. Chem. Soc.* **2010**, *132*, 4281–4289.

[159] M. B. Jarstfer, B. S. J. Blagg, D. H. Rogers, C. D. Poulter *J. Am. Chem. Soc.* **1996**, *118*, 13089–13090.

[160] B. S. J. Blagg, M. B. Jarstfer, D. H. Rogers, C. D. Poulter *J. Am. Chem. Soc.* **2002**, *124*, 8846–8853.

[161] J. Pandit, D. E. Danley, G. K. Schulte, S. Mazzalupo, T. A. Pauly, C. M. Hayward, E. S. Hamanaka, J. F. Thompson, H. J. Harwood *J. Biol. Chem.* **2000**, *275*, 30610–30617.

[162] E. Beytia, A. A. Qureshi, J. W. Porter *J. Biol. Chem.* **1973**, *248*, 1856–1867.

[163] N. K. Chua, H. W. Coates, A. J. Brown *Prog. Lipid Res.* **2020**, *79*, 101033.

[164] K. Takahashi, Y. Sasaki, T. Hoshino *Eur. J. Org. Chem.* **2018**, *2018*, 1477–1490.

[165] T. Hoshino, S. I. Nakano, T. Kondo, T. Sato, A. Miyoshi *Org. Biomol. Chem.* **2004**, *2*, 1456–1470.

[166] T. Sato, T. Hoshino *Biosci., Biotechnol., Biochem.* **1999**, *63*, 2189–2198.

[167] P. O. Syrén, S. Henche, A. Eichler, B. M. Nestl, B. Hauer *Curr. Opin. Struct. Biol.* **2016**, *41*, 73–82.

[168] H. Mayr, W. Striepe *J. Org. Chem.* **1983**, *48*, 1159–1165.

[169] S. C. Eyley in *Comprehensive Organic Synthesis, Vol. 2*, Elsevier, Amsterdam, **1991**, pp. 707–731.

[170] J. F. Norris, W. W. Sanders *Am. Chem. J.* **1901**, *25*, 54–62.

[171] J. F. Norris *Am. Chem. J.* **1901**, *25*, 117–122.

[172] M. Gomberg *Am. Chem. J.* **1901**, *25*, 317–335.

[173] F. Kehrmann, F. Wentzel *Ber. dtsch. Chem. Ges.* **1901**, *34*, 3815–3819.

[174] H. Meerwein, K. van Emster *Ber. dtsch. Chem. Ges. A/B* **1922**, *55*, 2500–2528.

[175] C. K. Ingold, E. Rothstein *J. Chem. Soc.* **1928**, 1217–1221.

[176] F. C. Whitmore *J. Am. Chem. Soc.* **1932**, *54*, 3274–3283.

[177] F. C. Whitmore *Ind. Eng. Chem.* **1934**, *26*, 94–95.

[178] G. A. Olah, G. K. S. Prakash, *Carbocation chemistry*, Wiley, Hoboken, NJ, **2004**.

[179] E. Bernoud, C. Lepori, M. Mellah, E. Schulz, J. Hannedouche *Catal. Sci. Technol.* **2015**, *5*, 2017–2037.

[180] N. Tsuji, J. L. Kennemur, T. Buyck, S. Lee, S. Prévost, P. S. J. Kaib, D. Bykov, C. Farès, B. List *Science* **2018**, *359*, 1501–1505.

[181] L. Ackermann, A. Althammer *Synlett* **2008**, *2008*, 995–998.

[182] P. Zhang, N. Tsuji, J. Ouyang, B. List *J. Am. Chem. Soc.* **2021**, *143*, 675–680.

[183] C. Laurence, J.-F. Gal in *Lewis Basicity and Affinity Scales: Data and Measurement*, John Wiley & Sons Ltd, Chichester, UK, **2010**, pp. 111–227.

[184] S. Aoshima, S. Kanaoka *Chem. Rev.* **2009**, *109*, 5245–5287.

[185] A. Fürstner, P. W. Davies *Angew. Chem., Int. Ed.* **2007**, *46*, 3410–3449.

[186] Y. Yamamoto *J. Org. Chem.* **2007**, *72*, 7817–7831.

[187] D. H. Aue, M. T. Bowers in *Gas Phase Ion Chemistry*, Academic Press, New York, NY, **1979**, pp. 1–51.

[188] A. Budakoti, P. K. Mondal, P. Verma, J. Khamrai *Beilstein J. Org. Chem.* **2021**, *17*, 932–963.

[189] E. Reyes, L. Prieto, U. Uria, L. Carrillo, J. L. Vicario *ACS Omega* **2022**, *7*, 31621–31627.

[190] M. L. Clarke, M. B. France *Tetrahedron* **2008**, *64*, 9003–9031.

[191] B. B. Snider in *Comprehensive Organic Synthesis*, Elsevier, **2014**, pp. 148–191.

[192] L. Shi, N. Tsuji, C. Zhu, M. Leutzsch, J. A. A. Grimm, B. List *J. Am. Chem. Soc.* **2025**, *147*, 34225–34230.

[193] M. G. Vinogradov, O. V. Turova, S. G. Zlotin *Adv. Synth. Catal.* **2021**, *363*, 1466–1526.

[194] L. Zeng, S. Liu, Y. Lan, L. Gao *Nat. Commun.* **2023**, *14*, 3511.

[195] H. Albright, A. J. Davis, J. L. Gomez-Lopez, H. L. Vonesh, P. K. Quach, T. H. Lambert, C. S. Schindler *Chem. Rev.* **2021**, *121*, 9359–9406.

[196] S. A. Chernyak, M. Corda, J. P. Dath, V. V. Ordomsky, A. Y. Khodakov *Chem. Soc. Rev.* **2022**, *51*, 7994–8044.

[197] G. Lopez, D. Keiner, M. Fasihi, T. Koiranen, C. Breyer *Energy Environ. Sci.* **2023**, *16*, 2879–2909.

[198] H. Mayr, A. R. Ofial, H. Schimmel *Macromolecules* **2004**, *38*, 33–40.

[199] H. Mayr, T. Bug, M. F. Gotta, N. Hering, B. Irrgang, B. Janker, B. Kempf, R. Loos, A. R. Ofial, G. Remennikov, H. Schimmel *J. Am. Chem. Soc.* **2001**, *123*, 9500–9512.

[200] J. Ammer, C. Nolte, H. Mayr *J. Am. Chem. Soc.* **2012**, *134*, 13902–13911.

[201] J. A. Cella *J. Org. Chem.* **1982**, *47*, 2125–2130.

[202] M. Murakami, T. Kato, T. Mukaiyama *Chem. Lett.* **1987**, *16*, 1167–1170.

[203] G. Kaur, M. Kaushik, S. Trehan *Tetrahedron Lett.* **1997**, *38*, 2521–2524.

[204] M. Rubin, V. Gevorgyan *Org. Lett.* **2001**, *3*, 2705–2707.

[205] S. K. De, R. A. Gibbs *Tetrahedron Lett.* **2005**, *46*, 8345–8350.

[206] T. Saito, Y. Nishimoto, M. Yasuda, A. Baba *J. Org. Chem.* **2006**, *71*, 8516–8522.

[207] T. Saito, Y. Nishimoto, M. Yasuda, A. Baba *J. Org. Chem.* **2007**, *72*, 8588–8590.

[208] G. Onodera, E. Yamamoto, S. Tonegawa, M. Iezumi, R. Takeuchi *Adv. Synth. Catal.* **2011**, *353*, 2013–2021.

[209] X. Fan, X. M. Cui, Y. H. Guan, L. A. Fu, H. Lv, K. Guo, H. B. Zhu *Eur. J. Org. Chem.* **2014**, *2014*, 498–501.

[210] Y. Sawama, R. Goto, S. Nagata, Y. Shishido, Y. Monguchi, H. Sajiki *Chem. Eur. J.* **2014**, *20*, 2631–2636.

[211] M. Braun, W. Kotter *Angew. Chem., Int. Ed.* **2004**, *43*, 514–517.

[212] J. Y. Hamilton, N. Hauser, D. Sarlah, E. M. Carreira *Angew. Chem., Int. Ed.* **2014**, *53*, 10759–10762.

[213] A. E. Wendlandt, P. Vangal, E. N. Jacobsen *Nature* **2018**, *556*, 447–451.

[214] E. F. Flegeau, U. Schneider, S. Kobayashi *Chem. Eur. J.* **2009**, *15*, 12247–12254.

[215] H. Thanh Dao, U. Schneider, S. Kobayashi *Chem. Commun.* **2010**, *47*, 692–694.

[216] A. Jiménez-Aquino, E. Ferrer Flegeau, U. Schneider, S. Kobayashi *Chem. Commun.* **2011**, *47*, 9456–9458.

[217] P. Zhang, L. A. Brozek, J. P. Morken *J. Am. Chem. Soc.* **2010**, *132*, 10686–10688.

[218] P. Zhang, H. Le, R. E. Kyne, J. P. Morken *J. Am. Chem. Soc.* **2011**, *133*, 9716–9719.

[219] Y. R. Gao, D. Y. Wang, Y. Q. Wang *Org. Lett.* **2017**, *19*, 3516–3519.

[220] X. Wang, X. Wang, Z. Han, Z. Wang, K. Ding *Angew. Chem., Int. Ed.* **2017**, *56*, 1116–1119.

[221] Y. Zheng, B. B. Yue, K. Wei, Y. R. Yang *Org. Lett.* **2018**, *20*, 8035–8038.

[222] H. Le, A. Batten, J. P. Morken *Org. Lett.* **2014**, *16*, 2096–2099.

[223] C. García-Ruiz, J. L. Y. Chen, C. Sandford, K. Feeney, P. Lorenzo, G. Berionni, H. Mayr, V. K. Aggarwal *J. Am. Chem. Soc.* **2017**, *139*, 15324–15327.

[224] A. Yanagisawa, N. Nomura, H. Yamamoto *Tetrahedron* **1994**, *50*, 6017–6028.

[225] A. Sofia, E. Karlström, J.-E. Bäckvall *Chem. Eur. J.* **2001**, *7*, 1981–1989.

[226] V. Hornillos, M. Pérez, M. Fañanás-Mastral, B. L. Feringa *J. Am. Chem. Soc.* **2013**,

135, 2140–2143.

[227] Y. Sumida, S. Hayashi, K. Hirano, H. Yorimitsu, K. Oshima *Org. Lett.* **2008**, *10*, 1629–1632.

[228] J. Tsuji, H. Takahashi, M. Morikawa *Tetrahedron Lett.* **1965**, *6*, 4387–4388.

[229] B. M. Trost, T. J. Fullerton *J. Am. Chem. Soc.* **1973**, *95*, 292–294.

[230] J. Tsuji in *Organic Synthesis with Palladium Compounds*, Springer, Berlin, **1980**, pp. 125–132.

[231] J. Tsuji *Tetrahedron* **1986**, *42*, 4361–4401.

[232] B. M. Trost, D. L. Van Vranken *Chem. Rev.* **1996**, *96*, 395–422.

[233] O. Pàmies, J. Margalef, S. Cañellas, J. James, E. Judge, P. J. Guiry, C. Moberg, J. E. Bäckvall, A. Pfaltz, M. A. Pericàs, M. Diéguez *Chem. Rev.* **2021**, *121*, 4373–4505.

[234] C. S. Cerione, F. A. Moghadam, B. M. Stoltz *J. Am. Chem. Soc.* **2025**, *147*, 35185–35191.

[235] X. Yan, Z. Zhang, Z. Wu, F. Wu, X. Feng, Y. Liu *J. Am. Chem. Soc.* **2025**, *147*, 34869–34880.

[236] F. Mühlthau, O. Schuster, T. Bach *J. Am. Chem. Soc.* **2005**, *127*, 9348–9349.

[237] M. Yasuda, T. Somyo, A. Baba *Angew. Chem., Int. Ed.* **2006**, *45*, 793–796.

[238] V. K. Singh, C. Zhu, C. K. De, M. Leutzsch, L. Baldinelli, R. Mitra, G. Bistoni, B. List *Science* **2023**, *382*, 325–329.

[239] W. S. Johnson, M. F. Semmelhack, M. U. S. Sultanbawa, L. A. Dolak *J. Am. Chem. Soc.* **1968**, *90*, 2994–2996.

[240] F. Z. Zhang, Y. Tian, G. X. Li, J. Qu *J. Org. Chem.* **2014**, *80*, 1107–1115.

[241] A. M. Camelio, T. C. Johnson, D. Siegel *J. Am. Chem. Soc.* **2015**, *137*, 11864–11867.

[242] M. A. Schafroth, D. Sarlah, S. Krautwald, E. M. Carreira *J. Am. Chem. Soc.* **2012**, *134*, 20276–20278.

[243] O. F. Jeker, A. G. Kravina, E. M. Carreira *Angew. Chem., Int. Ed.* **2013**, *52*, 12166–12169.

[244] J. Deng, S. Zhou, W. Zhang, J. Li, R. Li, A. Li *J. Am. Chem. Soc.* **2014**, *136*, 8185–8188.

[245] S. Zhou, H. Chen, Y. Luo, W. Zhang, A. Li *Angew. Chem., Int. Ed.* **2015**, *54*, 6878–6882.

[246] E. E. van Tamelen *Acc. Chem. Res.* **1968**, *1*, 111–120.

[247] E. J. Corey, J. Lee *J. Am. Chem. Soc.* **1993**, *115*, 8873–8874.

[248] E. J. Corey, S. Lin *J. Am. Chem. Soc.* **1996**, *118*, 8765–8766.

[249] E. J. Corey, G. Luo, L. S. Lin *J. Am. Chem. Soc.* **1997**, *119*, 9927–9928.

[250] E. J. Corey, G. Luo, L. S. Lin *Angew. Chem., Int. Ed.* **1998**, *37*, 1126–1128.

[251] A. X. Huang, Z. Xiong, E. J. Corey *J. Am. Chem. Soc.* **1999**, *121*, 9999–10003.

[252] K. Surendra, Z. J. Corey *J. Am. Chem. Soc.* **2008**, *130*, 8865–8869.

[253] Y. Mi, J. V. Schreiber, E. J. Corey *J. Am. Chem. Soc.* **2002**, *124*, 11290–11291.

[254] S. V. Pronin, R. A. Shenvi *Nat. Chem.* **2012**, *4*, 915–920.

[255] Q. Zhang, J. Rinkel, B. Goldfuss, J. S. Dickschat, K. Tiefenbacher *Nat. Catal.* **2018**, *1*, 609–615.

[256] I. Cornu, L. D. Syntrivanis, K. Tiefenbacher *Nat. Protoc.* **2024**, *19*, 313–339.

[257] D. Sokolova, G. M. Piccini, K. Tiefenbacher *Angew. Chem., Int. Ed.* **2022**, *61*, e202203384.

[258] N. Luo, M. Turberg, M. Leutzsch, B. Mitschke, S. Brunen, V. N. Wakchaure, N. Nöthling, M. Schelwies, R. Pelzer, B. List *Nature* **2024**, *632*, 795–801.

[259] D. Wilcke, E. Herdtweck, T. Bach *Synlett* **2011**, *2011*, 1235–1238.

[260] S. G. Wang, L. Han, M. Zeng, F. L. Sun, W. Zhang, S. L. You *Org. Biomol. Chem.* **2012**, *10*, 3202–3209.

[261] W. Zhao, Z. Wang, B. Chu, J. Sun *Angew. Chem., Int. Ed.* **2015**, *54*, 1910–1913.

[262] Z. Wang, F. Ai, Z. Wang, W. Zhao, G. Zhu, Z. Lin, J. Sun *J. Am. Chem. Soc.* **2015**, *137*, 383–389.

[263] Z. Wang, Y. F. Wong, J. Sun *Angew. Chem., Int. Ed.* **2015**, *54*, 13711–13714.

[264] X. Li, M. Duan, Z. Deng, Q. Shao, M. Chen, G. Zhu, K. N. Houk, J. Sun *Nat. Catal.* **2020**, *3*, 1010–1019.

[265] N. Tsukada, T. Sato, Y. Inoue *Chem. Commun.* **2001**, 237–238.

[266] R. Matsubara, T. F. Jamison *J. Am. Chem. Soc.* **2010**, *132*, 6880–6881.

[267] R. Matsubara, T. F. Jamison *Chem. Asian J.* **2011**, *6*, 1860–1875.

[268] Y. Gumrukcu, B. De Bruin, J. N. H. Reek *Chem. Eur. J.* **2014**, *20*, 10905–10909.

[269] J. Y. Hamilton, D. Sarlah, E. M. Carreira *J. Am. Chem. Soc.* **2014**, *136*, 3006–3009.

[270] K. Tanaka, M. Kishimoto, Y. Hoshino, K. Honda *Tetrahedron Lett.* **2018**, *59*, 1841–1845.

[271] S. Ghosh, S. Das, C. K. De, D. Yepes, F. Neese, G. Bistoni, M. Leutzsch, B. List *Angew. Chem., Int. Ed.* **2020**, *59*, 12347–12351.

[272] S. Ghosh, J. E. Erchinger, R. Maji, B. List *J. Am. Chem. Soc.* **2022**, *2022*, 6703–6708.

[273] J. S. Fritz, G. H. Schenk *Anal. Chem.* **1959**, *31*, 1808–1812.

[274] S. Brunen, B. Mitschke, M. Leutzsch, B. List *J. Am. Chem. Soc.* **2023**, *145*, 15708–15713.

[275] C. Y. He, J. W. Gu, X. Zhang *Tetrahedron Lett.* **2017**, *58*, 3939–3941.

[276] T. Berking, J. Hartenfels, C. Lenczyk, G. Santiso-Quinones, W. Frey, C. Richert

Angew. Chem., Int. Ed. **2024**, *63*, e202402976.

[277] M. Lee, D. H. Kim *Bioorg. Med. Chem.* **2000**, *8*, 815–823.

[278] L. K. Thalén, A. Sumic, K. Bogár, J. Norinder, A. K. . Persson, J. E. Bäckvall *J. Org. Chem.* **2010**, *75*, 6842–6847.

[279] United States Environmental Protection Agency, "TSCA Work Plan Chemical Risk Assessment HHCB 1,3,4,6,7,8-Hexahydro-4,6,6,7,8,8-hexamethylcyclopenta-g-2-benzopyran," can be found under https://www.epa.gov/assessing-and-managing-chemicals-under-tsca/tsca-work-plan-chemical-risk-assessment-hhcb-134678(accessed 12 October 2025), **2014**.

[280] F. Elterlein, N. Bugdahn, P. Kraft *Chem. Eur. J.* **2024**, *30*, e202400006.

[281] G. Fráter, U. Müller, P. Kraft *Helv. Chim. Acta* **1999**, *82*, 1656–1665.

[282] A. Ciappa, U. Matteoli, A. Scrivanti *Tetrahedron: Asymmetry* **2002**, *13*, 2193–2195.

[283] S. W. Youn, S. J. Pastine, D. Sames *Org. Lett.* **2004**, *6*, 581–584.

[284] B. Cacciuttolo, S. Poulain-Martini, F. Fontaine-Vive, M. A. H. Abdo, H. El-Kashef, E. Duñach *Eur. J. Org. Chem.* **2014**, *2014*, 7458–7468.

[285] S. A. Bonderoff, F. G. West, M. Tremblay *Tetrahedron Lett.* **2012**, *53*, 4600–4603.

[286] H. Shigehisa, T. Ano, H. Honma, K. Ebisawa, K. Hiroya *Org. Lett.* **2016**, *18*, 3622–3625.

[287] J. J. A. Garwood, A. D. Chen, D. A. Nagib *J. Am. Chem. Soc.* **2024**, *146*, 28034–28059.

[288] A. Ruffoni, R. C. Mykura, M. Bietti, D. Leonori *Nat. Synth.* **2022**, *1*, 682–695.

[289] G. Zhao, A. Khosravi, S. Sharma, D. G. Musaev, M. Y. Ngai *J. Am. Chem. Soc.* **2024**, *146*, 31391–31399.

[290] Y. N. Yin, H. Y. Liu, D. C. Ouyang, Q. Zhang, R. Zhu *Green Synth. Catal.* **2023**, *4*, 64–66.

[291] H. Zhou, Y. Zhou, H. Y. Bae, M. Leutzsch, Y. Li, C. K. De, G. J. Cheng, B. List *Nature* **2022**, *605*, 84–89.

[292] Z. Li, T. Bally, K. N. Houk, W. T. Borden *J. Org. Chem.* **2016**, *81*, 9576–9584.

[293] P. Vital, P. O. Norrby, D. Tanner *Synlett* **2006**, *2006*, 3140–3144.

[294] T. Gatzenmeier, M. Turberg, D. Yepes, Y. Xie, F. Neese, G. Bistoni, B. List *J. Am. Chem. Soc.* **2018**, *140*, 12671–12676.

[295] J. Burés *Angew. Chem., Int. Ed.* **2016**, *55*, 16084–16087.

[296] E. Vedejs, M. Jure, E. Vedejs, M. Jure *Angew. Chem., Int. Ed.* **2005**, *44*, 3974–4001.

[297] E. M. Simmons, J. F. Hartwig *Angew. Chem., Int. Ed.* **2012**, *51*, 3066–3072.

[298] H. Gu, S. Zhang *Molecules* **2013**, *18*, 9278–9292.

[299] C. Colletto, D. Whitaker, I. Larrosa *Top. Catal.* **2017**, *60*, 589–593.

[300] D. A. Singleton, A. A. Thomas *J. Am. Chem. Soc.* **1995**, *117*, 9357–9358.

[301] E. V. Anslyn, D. A. Dougherty in *Modern Physical Organic Chemistry*, University Science Books, Sausalito, California, **2004**, pp. 428–441.

[302] K. C. Westaway *Adv. Phys. Org. Chem.* **2006**, *41*, 217–273.

[303] L. Gilles, S. Antoniotti *ChemPlusChem* **2022**, *87*, e202200227.

[304] N. Millius, G. Lapointe, P. Renaud *Molecules* **2019**, *24*, 4184.

[305] J. J. Molloy, J. B. Metternich, C. G. Daniliuc, A. J. B. Watson, R. Gilmour *Angew. Chem., Int. Ed.* **2018**, *57*, 3168–3172.

[306] Y. Wang, L. Deng, H. Mei, B. Du, J. Han, Y. Pan *Green Chem.* **2018**, *20*, 3444–3449.

[307] C. Zhang, G. Zhang, S. Luo, C. Wang, H. Li *Org. Biomol. Chem.* **2018**, *16*, 8467–8471.

[308] P. Yu, X. Huang, D. Wang, H. Yi, C. Song, J. Li *Chem. Eur. J.* **2024**, *30*, e202402124.

[309] H. S. Hwang, E. J. Cho *Adv. Synth. Catal.* **2025**, *367*, e202401334.

[310] K. Yamada, Y. Nomura, D. Citterio, N. Iwasawa, K. Suzuki *J. Am. Chem. Soc.* **2005**, *127*, 6956–6957.

[311] M. Huai, L. Chen, W. Dong, W. Wang, Z. Qin, K. Dai, Y. Li, X. Zhang, C. Tao *Org. Biomol. Chem.* **2024**, *22*, 5385–5392.

[312] M. Yagoubi, A. C. F. Cruz, P. L. Nichols, R. L. Elliott, M. C. Willis *Angew. Chem., Int. Ed.* **2010**, *49*, 7958–7962.

[313] Y. L. Chow, B. H. Bakker *Can. J. Chem.* **1982**, *60*, 2268–2273.

[314] D. J. Pasto, K. D. Sugi *J. Org. Chem.* **1991**, *56*, 4157–4160.

[315] M. E. Krafft, J. W. Cran *Synlett* **2005**, *2005*, 1263–1266.

[316] P. Bovonsombat, G. J. Angara, E. Mc Nelis *Tetrahedron Lett.* **1994**, *35*, 6787–6790.

[317] T. W. Funk, J. Efskind, R. H. Grubbs *Org. Lett.* **2005**, *7*, 187–190.

[318] M. Beckmann, H. Hildebrandt, E. Winterfeldt *Tetrahedron: Asymmetry* **1990**, *1*, 335–345.

[319] R. L. Danheiser, D. J. Carini, D. M. Fink, A. Basak *Tetrahedron* **1983**, *39*, 935–947.

[320] V. Cadierno, S. E. García-Garrido, J. Gimeno *Adv. Synth. Catal.* **2006**, *348*, 101–110.

[321] H. Zhou, P. Zhang, B. List *Synlett* **2021**, *32*, 1953–1956.

[322] L. Liu, H. Kim, Y. Xie, C. Fares, P. S. J. Kaib, R. Goddard, B. List *J. Am. Chem. Soc.* **2017**, *139*, 13656–13659.

[323] Y. He, Z. Bian, C. Kang, L. Gao *Chem. Commun.* **2010**, *46*, 5695–5697.

[324] A. Bähr, A. S. Droz, M. Püntener, U. Neidlein, S. Anderson, P. Seiler, F. Diederich *Helv. Chim. Acta* **1998**, *81*, 1931–1963.

[325] C. Y. He, J. W. Gu, X. Zhang *Tetrahedron Lett.* **2017**, *58*, 3939–3941.

[326] T. Knecht, T. Pinkert, T. Dalton, A. Lerchen, F. Glorius *ACS Catal.* **2018**, *9*, 1253–1257.